National Research Council Canada

Conseil national de recherches Canada

NRC·CNRC

Canadian Journal of Fisheries and Aquatic Sciences

Journal canadien des sciences halieutiques et aquatiques

http://www.nrc.ca/cisti/journals

ISSN 0706-652X / CJFSDX 56(6) 907–1142 (1999)

The *Canadian Journal of Fisheries and Aquatic Sciences*, previously published as *Contributions to Canadian Biology* 1901–1925, *Contributions to Canadian Biology and Fisheries* 1926–1934, *Journal of the Biological Board of Canada* 1934–1937, and *Journal of the Fisheries Research Board of Canada* 1938–1979, is issued monthly to form annual volumes of 12 numbers plus supplements.

Editorial policy: The Journal publishes original research articles, perspectives (syntheses, critiques, re-evaluations), discussions (comment and reply), and rapid communications. Manuscripts may concern cells, organisms, populations, communities, ecosystems, or processes that affect aquatic systems. They may cover a range of disciplines including biology and ecology of marine and freshwater organisms, limnology, oceanography, physiology, toxicology, genetics, economics, disease, and management. Preference will be given to manuscripts that emphasize understanding of observed phenomena and interpretation of experimental results. The Journal encourages papers that lead from clearly stated purpose or rationale and from testable hypotheses, concepts, or questions to identifiable conclusions or syntheses. Such papers may amplify, modify, question, or redirect accumulated knowledge embodied in contemporary perceptions of a particular state of aquatic sciences. The Journal discourages papers that are essentially descriptive, except in emerging disciplines; have only site-specific or local applications (a certain year, place, taxon, chemical compound, etc.); only confirm previously established principles; or apply standard techniques without breaking new methodological ground.

Manuscripts for publication should be submitted to the Editors, Canadian Journal of Fisheries and Aquatic Sciences, Department of Zoology, University of Guelph, Guelph, ON N1G 2W1, Canada (519-824-4120 ext. 2646; fax: 519-767-9798; e-mail: cjfas@uoguelph.ca).

Submissions in either English or French are acceptable. The information must be original, that is, not copyrighted, published, or submitted elsewhere except in abstract form or unless by written consent of the Editor. NRC accepts no responsibility for statements or opinions expressed by a contributor. Acceptance of an advertisement, announcement, or other material does not imply endorsement by either the *Journal*'s Editors or NRC. The use of proprietary names does not imply endorsement of the product or company.

Correspondence concerning accepted manuscripts and corrected proofs should be sent to NRC Research Press, National Research Council of Canada, Ottawa, ON K1A 0R6, Canada.

Instructions to Authors are published once a year in the first issue of each volume. Copies are available from NRC Research Press or from our Web site. The **Publication Policy** of NRC Research Press is also available at our Web site:
http://www.nrc.ca/cisti/journals/rj.html

Microfilm: Issues from 1934 through the current volume can be purchased on 16- or 35-mm microfilm. Photocopies of individual articles or issues can be purchased from University Microfilms International, 330 North Zeeb Road, Ann Arbor, MI 48106, U.S.A.

U.S. periodical postage paid at Champlain, N.Y., and at additional mailing offices. Attention U.S. POSTMASTER: Send address changes to **Canadian Journal of Fisheries and Aquatic Sciences**, c/o USACAN Media Distribution Center, P.O. Box 2888, Plattsburg, NY 12901, U.S.A.

Publié sans interruption depuis 1901, le *Journal canadien des sciences halieutiques et aquatiques* a paru sous plusieurs titres : *Contributions to Canadian Biology* 1901–1925, *Contributions to Canadian Biology and Fisheries* 1926–1934, *Journal of the Biological Board of Canada* 1934–1937, et *Journal of the Fisheries Research Board of Canada* 1938–1979. Le *Journal* paraît tous les mois, formant ainsi un volume de 12 numéros, et offre en plus jusqu'à deux suppléments par année.

Politique éditoriale : On publie, dans le Journal, des articles rendant compte de recherche originale, des perspectives (synthèses, critiques et réévaluations), des discussions (commentaires et réponses) et des communications rapides. Les documents peuvent porter sur les cellules, organismes, populations, communautés, écosystèmes ou processus qui affectent les systèmes aquatiques. Ils peuvent relever de divers domaines y compris la biologie et l'écologie des organismes marins et d'eau douce, la limnologie, l'océanographie, la physiologie, la toxicologie, la génétique, l'économie, la pathologie et la gestion. On accorde la préséance aux articles qui contribuent à la compréhension de phénomènes observés et à l'interprétation de résultats expérimentaux. On invite les auteurs à soumettre des articles ayant des objectifs précis ou relevant d'hypothèses, de concepts ou de questions vérifiables et se terminant par de solides conclusions ou d'utiles synthèses. Ces articles enrichissent, changent, mettent en question ou réorientent les connaissances acquises sur divers aspects des sciences aquatiques. On décourage toutefois la soumission d'articles simplement descriptifs (à moins qu'il ne s'agisse de nouvelles disciplines), d'application très limitée (applicables à une seule année, une seule région ou un seul taxon, portant sur un unique composé chimique, etc.); d'articles qui ne font que reprendre les principes énoncés dans des articles précédents; et d'articles rendant compte de l'application de normes sans gain de méthodologie.

Les auteurs voudront adresser leurs **manuscrits** aux directeurs scientifiques, Journal canadien des sciences halieutiques et aquatiques, Département de Zoologie, University of Guelph, Guelph, ON N1G 2W1, Canada (519-824-4120 poste. 2646; télécopieur : 519-767-9798; adresse électronique : cjfas@uoguelph.ca).

Les contributions peuvent être en anglais ou en français. Elles doivent être originales, c.-à.-d. qu'elles ne doivent pas avoir fait l'objet d'un copyright, avoir été publiées ou soumises ailleurs, sauf sous forme abrégée ou avec le consentement du rédacteur. Le CNRC ne se tient en aucune façon responsable des opinions exprimées par un collaborateur ou des déclarations qui pourrait faire ce dernier. La publication d'annonces publicitaires, d'avis et autres n'implique pas l'endossement de leur contenu par les directeurs du *Journal* ou du CNRC. L'utilisation des noms de marques de commerce ne signifie aucunement une sanction du produit en question ou de la compagnie qui le fabrique.

La correspondance ayant trait aux manuscrits acceptés et les **épreuves corrigés** doivent être envoyées aux Presses scientifiques du CNRC, Conseil national de recherches du Canada, Ottawa, ON K1A 0R6, Canada.

Recommandations aux auteurs sont publiés une fois par année dans le premier numéro de chaque volume. Des copies, ainsi que la **Politique de publication**, sont disponibles auprès des Presses scientifiques du CNRC ou au site Web :
http://www.nrc.ca/cisti/journals/rj.html

Microfilms : On peut acheter sur microfilms de 16 ou 35 mm tous les numéros depuis 1934. Des photocopies d'articles ou de numéros individuels sont aussi en vente auprès de University Microfilms International, 330 North Zeeb Road, Ann Arbor, MI 48106, É.-U.

This journal is indexed or abstracted in / Ce journal est signalé ou résumé dans
Aquatic Sciences and Fisheries Abstracts, Biological & Agricultural Index, CAB Abstracts (Centre for Agriculture and Biosciences), Chemical Abstracts, Current Awareness in Biological Sciences, Current Contents, FAO Freshwater and Aquaculture Contents Tables, FAO Marine Science Contents Tables, GEOBASE – Geo Abstracts, Meteorological and Geoastrophysical Abstracts, Oceanic Abstracts, Science Citation Index, Biological Abstracts, Environment Abstracts, Environmental Periodicals Bibliography, GEOREF, Life Sciences Collection, ABSEARCH, and PASCAL Database

Volume 56, Number 6, June 1999

Canadian Journal of Fisheries and Aquatic Sciences

Published by the National Research Council of Canada

Volume 56, numéro 6, juin 1999

Journal canadien des sciences halieutiques et aquatiques

Publié par le Conseil national de recherches du Canada

Editors / directeurs scientifiques John C. Roff and Moira M. Ferguson

Assistant to the Editors / adjointe aux directeurs scientifiques **Holly Foster**

Associate Editors / directeurs scientifique associés

D. Boisclair, *Université de Montréal*
U. Borgmann, *Environment Canada, Burlington*
S.E. Campana, *DFO/MPO, Dartmouth*
D.G. Dixon, *University of Waterloo*
A.E. Dizon, *National Marine Fisheries Service, La Jolla, Calif.*
J.J. Dodson, *Université Laval*
J.A. Downing, *Iowa State University*
K.T. Frank, *DFO/MPO, Dartmouth*
D.F. Houlihan, *University of Aberdeen, Aberdeen, Scotland*
F.A. Huntingford, *University of Glasgow*
J.A. Hutchings, *Dalhousie University*
G.S. Jamieson, *DFO/MPO, Nanaimo*
B. Jonsson, *Norwegian Institute for Nature Research, Oslo, Norway*
L. Legendre, *Université Laval*
D.M. Mason, *Purdue University, West Lafayette, Ind.*
A. Mazumder, *Université de Montréal*
D.L. Parrish, *Vermont Cooperative Fish and Wildlife Research Unit (USGS/BRD), University of Vermont*
P. Pepin, *DFO/MPO, St. John's*
R.M. Peterman, *Simon Fraser University*
E.E. Prepas, *University of Alberta*
T.M. Powell, *University of California, Berkeley, Calif.*
T.J. Quinn II, *University of Alaska–Fairbanks, Juneau, Alaska*
T.P. Quinn, *University of Washington*
R.D. Robarts, *Environment Canada, Saskatoon*
B. Sainte-Marie, *DFO/MPO, Mont-Joli*
P.F. Sale, *University of Windsor*
D.W. Schindler, *University of Alberta*
S.J. Smith, *DFO/MPO, Dartmouth*
W.G. Sprules, *University of Toronto*
R.J. Thompson, *Memorial University of Newfoundland*
C.J. Walters, *University of British Columbia*
R.D. Ward, *CSIRO Division of Fisheries, Australia*
C.M. Wood, *McMaster University*
B. de Young, *Memorial University of Newfoundland*

NRC Research Press / Presses scientifiques du CNRC

Editor-in-chief / directeur général **Bruce P. Dancik**

Assistant Editor-in-chief / directeur général adjoint **Iain E.P. Taylor**

Journals Program / Programme des revues

(Fax / télécopieur : 613-952-7656; e-mail / adresse électronique : research.journals@nrc.ca;
URL: http://www.nrc.ca/cisti/journals/)

Director / directrice **Aldyth Holmes**

Business Manager / gestionnaire des affaires **Paul McClymont**

Managing Editor / rédactrice administrative **Cecily M. Pearson (613-993-9099)**

Publication Officer / agente de publication **Jennifer McColl**

Advertising / annonces publicitaires **Judy Heyman (613-993-0151)**

Reprints / tirés à part **Roxanne Landriault (613-990-2254)**

Subscriptions / abonnements **Helen Goulet (613-993-9084)**

© National Research Council of Canada 1999. World rights reserved.
No part of this publication may be reproduced, stored, or transmitted in any form or by any means, without the written permission of the publisher, except as stated below.

The National Research Council of Canada grants **permission*** to individuals to make single copies of articles for personal use. Any person may reproduce short excerpts from articles in the journal for any purpose that respects the moral rights of authors, provided that the source is fully acknowledged. As a courtesy, the consent of authors of such material should be obtained directly from the author.

Authorization to reproduce items for other than personal use, as stated above, is granted by the National Research Council of Canada provided that the copyright fee of $7.00 per copy is paid directly to the Copyright Clearance Center (CCC) Transactional Reporting Service, 222 Rosewood Drive, Danvers, MA 01923, U.S.A. 0706-652X/99 $7.00.

*The above permission does not extend to other kinds of copying, such as copying for general distribution, for advertising, or promotional purposes, for creating new collective works, or for resale. For such copying, arrangements must be made with the publisher, National Research Council of Canada, Ottawa, ON K1A 0R6, Canada.

© Conseil national de recherches du Canada 1999. Tous droits réservés.
Il est interdit de reproduire, de sauvegarder ou de transmettre quelque partie de la présente publication dans quelque format ou de quelque façon sans le consentement écrit de l'éditeur, à l'exception des conditions suivantes.

Le Conseil national de recherches du Canada accorde aux particuliers le droit de faire des copies individuelles pour leur usage personnel. Toute personne peut reproduire de courts extraits des articles de la Revue pour autant que les droits moraux de l'auteur soient respectés et que la mention de provenance soit clairement indiquée. Il est de convenance de demander le consentement de l'auteur avant de faire mention de son travail.

On obtiendra l'autorisation de reproduire des articles à d'autres fins que l'usage personnel (tel qu'on l'a décrit ci-dessus) auprès du Conseil national de recherches du Canada pour autant que des redevances de droits d'auteurs de 7,00 $/copie soient versées au Copyright Clearance Center (CCC) Transactional Reporting Service, 222 Rosewood Drive, Danvers, MA 01923, U.S.A. 0706-652X/99 7,00 $.

*La permission ci-dessus ne s'applique pas à la reproduction à grande échelle, telle que la reproduction aux fins de distribution générale, publicitaire ou promotionnelle, de compilation de nouveaux ouvrages collectifs ou de revente. Dans de tels cas, il faudra ratifier une entente particulière avec l'éditeur, le Conseil national de recherches du Canada, Ottawa, ON K1A 0R6, Canada.

Subscription information

The *Canadian Journal of Fisheries and Aquatic Sciences* (ISSN 0706-652X) is published monthly by the National Research Council of Canada. 1999 annual subscription rates (second class postage) for Canada are $578CAN institutional and $182CAN personal, for US & foreign $578US institutional and $182US personal. For air mail add $150US to foreign rate. Canadian customers please include 7% GST (business no. 12149 1807 RT 0275). Subscriptions are entered for the calendar year. Remittances should be made payable to the Receiver General for Canada credit NRC. Price for regular single issues: institutional, $75.00; personal, $25.00. Supplements will be priced separately. Special rates apply to members of Canadian scientific and engineering societies if they subscribe through their respective societies.

There are no refunds on cancelled subscriptions once delivery has begun. Claims for missing issues should be made within four months (N. America) or six months (outside N. America) following the date of publication. The publisher expects to supply missing issues only when losses have occurred in transit and when the reserve stock will permit. For change of address and subscription enquiries: Subscription Office, NRC Research Press, National Research Council of Canada, Ottawa, ON K1A 0R6, Canada; tel: 613-993-9084; fax: 613-952-7656; e-mail: research.journals@nrc.ca.

Microform backfiles are available from UMI, P.O. Box 1346, Ann Arbor, MI 48106-1346, U.S.A., and Micromedia Ltd., 20 Victoria St., Toronto, ON M5C 2N8, Canada.

The 1999 issues of the *Canadian Journal of Fisheries and Aquatic Sciences* are available on the Web. Pricing information can be found at

http://www.nrc.ca/cisti/journals/

Renseignements sur l'abonnement

Journal canadien des sciences halieutiques et aquatiques (ISSN 0706-652X) est une publication mensuelle du Conseil national de recherches du Canada. Le prix de l'abonnement annuel au Canada (courrier de deuxième classe) est de 578 $CAN pour les organismes et de 182 $CAN pour les particuliers. À l'étranger (y compris les É.-U.), le prix de l'abonnement est de 578 $US pour les organismes et de 182 $US pour les particuliers. L'expédition par avion exige des frais de 150 $US en sus du prix d'abonnement à l'étranger. Les clients du Canada doivent ajouter la TPS de 7% (numéro d'entreprise 12149 1807 RT 0275). Les abonnements sont pour l'année civile. Tout paiement doit être adressé au Receveur général du Canada, crédit du CNRC. Le prix par numéro est de 75 $ pour les organismes et de 25 $ pour les particuliers. Le prix des hors-série varie. Les membres des sociétés canadiennes de sciences et de génie bénéficient de taux préférentiels en s'abonnant via leurs sociétés respectives.

Aucun remboursement ne sera accordé ni aucune annulation acceptée une fois que les livraisons auront commencé. Les réclamations de numéros manquants devront être soumises dans les quatre mois (Amérique du Nord) ou dans les six mois (à l'extérieur de l'Amérique du Nord) suivant la date de publication. L'éditeur ne fournira de numéros manquants que si le document a été perdu pendant l'expédition et que si le stock le permet. Adressez tout changement d'adresse ou toute question quant à l'abonnement au : Bureau des abonnements, Presses scientifiques du CNRC, Conseil national de recherches Canada, Ottawa, ON K1A 0R6, Canada; téléphone : 613-993-9084; télécopieur : 613-952-7656; adresse électronique : research.journals@nrc.ca.

On peut obtenir les fichiers rétrospectifs sur **microforme** auprès de UMI, P.O. Box 1346, Ann Arbor, MI 48106-1346, É.-U., et auprès de Micromedia Ltée, 20 rue Victoria, Toronto, ON M5C 2N8, Canada.

Les numéros de 1999 de *Journal canadien des sciences halieutiques et aquatiques* sont accessibles sur le Web. On trouvera des renseignements sur les tarifs à

http://www.nrc.ca/cisti/journals/rjfr.html

Spatial distribution of sardine (*Sardinops sagax*) eggs and larvae: an application of geostatistics and resampling to survey data

W.J. Fletcher and Neil R. Sumner

Abstract: The abundance of eggs and larvae of sardine (pilchard) (*Sardinops sagax*) off the south coast of Western Australia was investigated using geostatistical and bootstrap resampling techniques. A two-dimensional correlogram showed that the patch of newly spawned pilchard eggs had dimensions of 8 nautical miles (M) in diameter in the offshore direction and 10 M in the alongshore direction. For older stages, the size of the patch tended to increase and the level of cohesion decrease. It was more difficult to determine the size of the patch from directional variograms. The abundance of 1- and 2-day-old eggs in the study area was estimated using ordinary kriging. A bootstrapping analysis suggested that the optimal sampling design for day 1 eggs should use 4 × 10 M grids, an increase in intensity on the 5 × 15 M grids used in previous surveys.

Résumé : On a étudié l'abondance des oeufs et des larves de la sardine (*Sardinops sagax*) au large de la côte sud de l'ouest de l'Australie au moyen de techniques géostatistiques et bootstrap de rééchantillonnage. Un corrélogramme bidimensionnel a montré que le groupe d'oeufs fraîchement pondus s'étendaient sur une distance de 8 milles marins (M) vers le large et de 10 M parallèlement à la côte. Pour les oeufs plus âgés, la taille du groupe d'oeufs tendait à s'accroître, et son niveau de cohésion était inférieur. Il était plus difficile de déterminer la taille du groupe à partir de variogrammes directionnels. On a estimé l'abondance des oeufs de 1 et 2 jours dans l'aire de l'étude au moyen du krigeage ordinaire. Selon une analyse bootstrap, on obtiendrait un échantillonnage optimal des oeufs d'un jour en utilisant des grilles de 4 × 10 M, ce qui représente une résolution plus fine que celle des études antérieures qui utilisaient des grilles de 5 × 15 M.

[Traduit par la Rédaction]

Introduction

The spatial distribution of organisms has a significant impact on the sampling scheme that will be appropriate to accurately estimate their abundance. Knowledge of the spatial distribution is important if these data are to be used for computing estimates for stock assessment purposes. While fisheries scientists have been concerned with the spatial variation of samples that they obtain from the oceans for many years, it is only recently that satisfactory means have become available for describing the observed variation quantitatively through the study of geostatistics.

Geostatistical techniques originated in the mining industry for the analysis of ore samples (Matheron 1965, 1971). Within the marine science area, these tools could be used in the design of optimal sampling schemes and the spatial prediction of abundances (Petitgas 1993; Maravelias and Haralabous 1995; Murray 1996). A number of fishery resource assessment techniques rely upon spatially separated samples. For example, the daily egg production method (DEPM) depends on using the abundance of eggs collected by numerous plankton hauls to estimate the extent and density of eggs over large areas (for details, see Lasker 1985; Fletcher et al. 1996*a*). Plankton studies, however, often produce highly variable data due to the very patchy distributions of eggs and larvae. Hence, prior knowledge of the nature and scale of this variability will help in designing the most efficient survey in terms of cost and information provided.

Few studies have investigated the fine-scale spatial arrangement of fish eggs collected by plankton tows. Most of these have only examined relatively small-scale variability by collecting samples at the same locations a number of times (e.g., Silliman 1946; Smith and Hewitt 1985). None have directly determined what is the most efficient sampling distance between stations for sardine (pilchard) (*Sardinops sagax*) for the completion of a DEPM survey despite the now wide usage of this technique (Alheit 1993). In this study, we use data obtained from plankton tows that were conducted on a fine-scale grid basis to investigate the variability in abundance of pilchard eggs and larvae over the range from a few centimetres to tens of kilometres.

The data will be analysed using variograms that spatially represent the levels of relatedness of samples at increasing distances apart. Furthermore, a correlogram will be used to determine the level of autocorrelation among samples at varying distances. This is one of the first times such techniques have been used on plankton data (but see Petitgas

Received April 2, 1998. Accepted December 16, 1998.
J14534

W.J. Fletcher[1] and N.R. Sumner. Western Australian Marine Research Laboratories, P.O. Box 20, North Beach, Western Australia 6020, Australia.

[1]Author to whom all correspondence should be addressed. Present address and address for correspondence: New South Wales Fisheries Research Institute, P.O. Box 21, Cronulla, New South Wales 2230, Australia.
e-mail: fletcher@fisheries.nsw.gov.au

© 1999 NRC Canada

1997). Finally, bootstrapping and jackknifing will be used to examine the potential variation in abundance estimates that could result from a number of different sampling intensities. From these analyses, the preferred sampling scheme for future plankton surveys involving pilchards will be determined.

Methods

Plankton sampling

Approximately 50 vertical plankton tows were completed within a relatively small region (400 nautical miles $(M)^2$) of the south coast of Western Australia near Albany (32°S, 118°E) in January 1994. Stations were sampled on a grid basis with varying intervening distances of 1, 2, or 4 M apart. Furthermore, more than one plankton haul was often made at the same stations to investigate variations at the scale of a few metres. Finally, at most sites, each net on the bongo frame was analysed separately to gauge the fine-scale (centimetres) variations in abundance.

Two vessels were used simultaneously between 07:00 and 15:00. Both vessels had a global positioning system and used a frame holding two 60-cm-diameter bongo nets. Both nets had 500-μm mesh or one had 300-μm mesh and the other 500-μm mesh; both mesh sizes retain all pilchard eggs (Fletcher et al. 1996*b*). Analyses of larvae were restricted to the 300-μm-mesh samples, since substantial extrusion of early-stage larvae is known to occur in the coarser mesh (Fletcher et al. 1996*b*). At the sites where two hauls were completed, two separate sampling units were used to avoid any potential contamination. Where each net was assessed separately, a General Oceanics flowmeter was located in the mouth of each net. For tows where the samples were combined, only a single flowmeter was used.

Samples were sorted by the removal of all pilchard material (eggs and larvae), which was staged according to the methods detailed by White and Fletcher (1997). The resultant data were analysed using the relative indices of abundance per 200 m^3 calculated separately for day 1 (0–24 h) and day 2 eggs (24 h to hatching) and the three larval stages (yolk-sac larvae, early postlarvae, and late postlarvae).

Spatial analysis

The level of autocorrelation between samples provides useful information on the nature of the spatial structure. It is of interest whether the approximate value of a variable at point B can be estimated on the basis of the value obtained at point A. If the two stations are within the zone of spatial influence of the underlying ecological phenomenon, the value of the variable at B will be related to the value of the same variable at A. Therefore, autocorrelation generally depends on the distance between the two sampling points, with positive values corresponding to short distances and values close to zero corresponding to larger distances.

Correlogram

Spatial structure can be represented graphically by plotting autocorrelation against distance. For these correlograms, the distance may be in one direction or, in the case of the all-directional correlogram, in all directions. The all-directional correlogram and omnidirectional variogram (see below) make the assumption that the spatial structure is isotropic; autocorrelation is the same regardless of the direction being considered. When the autocorrelation is a function of both distance and direction, the structure is anisotropic and should be looked at in one direction at a time.

Sample variogram

Another measure of spatial structure, the variogram, describes spatial variation quantitatively in terms of distance and direction and in a way that facilitates our understanding of spatial patterns and processes. The variogram is central to techniques for spatial prediction such as kriging (Matheron 1971). Given values for a variable, Z_t are the realisation of a random function $\{Z_t;\ t \in R^2\}$ observed at certain points $\{t_i\}$ of a region R^2. The variogram is a function of distance and can be estimated from the data Z_{t_i}, $i = 1,\ldots, n$, as follows:

$$(1)\qquad \gamma(h) = \frac{1}{2N_h}\sum_{i=1}^{N_h}(Z_{t_i+h} - Z_{t_i})^2, \quad h = h(1), h(2), \ldots, h(k)$$

where $h(1), h(2),\ldots, h(k)$ are discrete lags and N_h is the number of pairs of data samples separated at distance h. Before using the variogram, one must assume that the data are second-order stationary (the expected value of Z_t is constant for all points in the study area and that observations the same distance apart have the same covariance); otherwise, trends (i.e., drift) in the data will need to be removed (Cressie 1991). The variogram values, lags, and number of lag h differences for the omnidirectional variograms of day 1 and day 2 pilchard eggs were computed using Geo-eas (Englund and Sparks 1991).

Modelling the sample variogram

Many geostatistical studies require estimation of the variogram from the data. A theoretical variogram (model) is fitted to the experimental variogram so the variogram values may be readily estimated for any distance within the range of the data.

The important features of the variogram need to be estimated. The sill (C) is the maximum variance, the range (a) is the distance at which the variance stops increasing and the sill is achieved, and the nugget effect (C_0) is the distance between the origin and the value of the variogram, at extremely small separation distances, due to sampling error and small-scale heterogeneity.

The variogram may be fitted by one or a combination of several variogram models by estimating $\theta = [a, C_0, C]^T$. The spherical, exponential, and Gaussian models (Isaaks and Srivastava 1989) were investigated using a Mathcad (Mathsoft 1995) worksheet developed by the authors. The worksheet provides a convenient means to compare the fit of three variogram models both graphically and in terms of the residual sum of squares (alternatively, many nonlinear regression programs will suffice; see Gotway 1991). Weighted least squares as suggested by Cressie (1985, 1991) was used to fit a model to the experimental variogram by finding the value of θ that minimises eq. 2:

$$(2)\qquad S(\theta) = \sum_{j=1}^{k}\frac{N_{h(j)}}{(\hat{\gamma}(h(j);\theta))^2}\left\{\gamma(h(j)) - \hat{\gamma}(h(j);\theta)\right\}^2$$

where $\gamma(h(j))$, $j = 1,\ldots, k$, are the experimental variogram values and $\gamma(h(j);\ \theta)$, $j = 1,\ldots, k$, the modelled variogram. The objective function places more emphasis on the small lags with a larger number of pairs near the origin. This is desirable, since when the variogram model is used for kriging, the fit near the origin is more important than the fit at larger lags.

Spatial prediction

Kriging is a linear unbiased interpolation method. The observations are weighted using the distance–variance relationship from the variogram in a way that minimises the estimation variance. Kriging can estimate the value for a point from surrounding observations within the range of spatial influence. Kriging is often used to generate a three-dimensional mesh of x–y coordinates and pre-

© 1999 NRC Canada

Fig. 1. Relative concentrations (no./200 m^3) of the pilchard egg and larval stages collected during the intensive survey off southern Australia in January 1994.

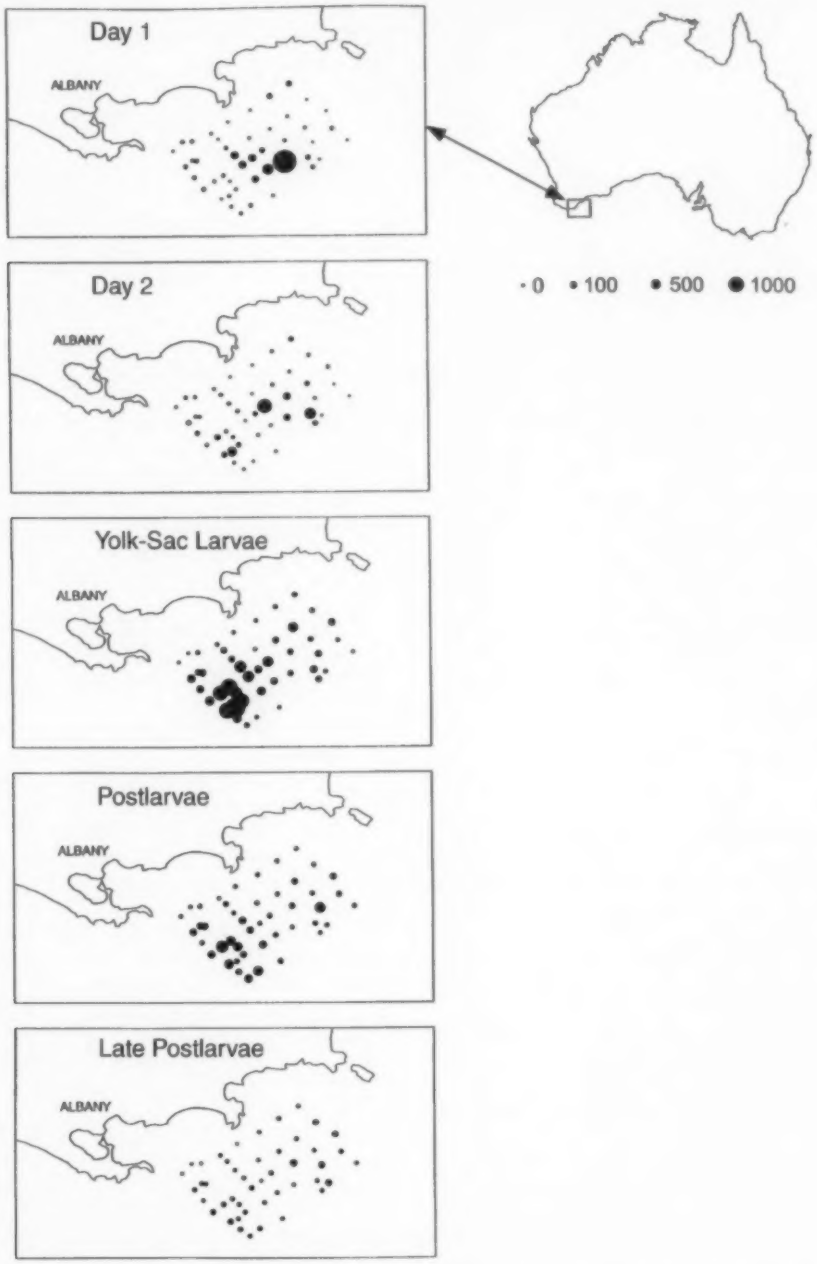

dicted values that, when displayed as contours or a three-dimensional surface, enhances our understanding of any spatial relationships in the data.

Kriging does not require a random sampling approach for the estimation of abundance. The technique is well suited to systematic designs and zigzag transects where the sampling scheme is not performed randomly and consecutive observations are not independent and may be correlated. A model of the spatial correlation structure via the variogram of the region is used to weight data values according to their location. The kriged estimate is optimal provided the structural model is a reasonable approximation.

Resampling

The data for the survey were subjected to a jackknifing analysis. The region was divided into six subareas, each of which had be-

© 1999 NRC Canada

Fig. 2. Correlogram for day 1 pilchard eggs off southern Australia.

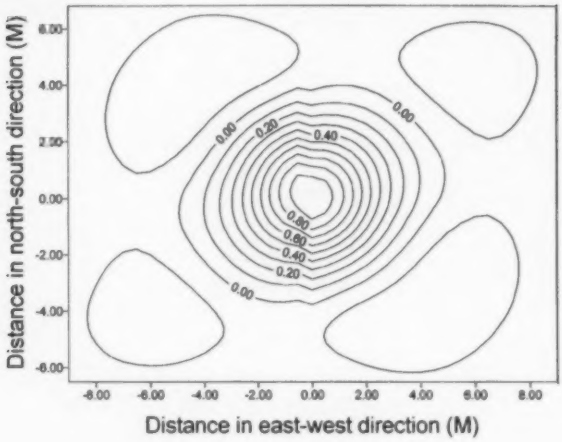

tween six and nine representative tows. From each of these six subareas, a subsample of one, two, or three tows was selected randomly (without replacement) and combined to calculate an estimate of the population mean value and its sampling distribution. This resampling was completed a total of 1000 times.

Both the raw and kriged data were subjected to a bootstrapping exercise. Random samples of between two and 100 selections were made 1000 times with the mean values calculated. The 90% confidence intervals for the kriged means were obtained from the sampling distribution directly.

Results

Spatial analysis

Considerable spatial variability in the indices of abundance for pilchard eggs and larvae was evident in samples collected (Fig. 1). Large numbers of pilchard eggs and larvae were collected with a total mean abundance of 359 and 915/200 m^3, respectively.

The spatial structure of the abundance of day 1 pilchard eggs was investigated using a two-dimensional correlogram (Fig. 2). This shows the spatial structure as a function of distance with contours depicting the autocorrelation values. The resultant pattern is symmetrical, since the autocorrelation is the same regardless of whether one is travelling from east to west or from west to east. The zone of spatial influence (taken as the distance from the centre of the graph to the zero contour line) is slightly greater in the alongshore direction than in the inshore–offshore direction. Since a single elliptical-shaped patch of eggs is represented, the distance from the zero contour across the centre of the figure to the opposite zero contour corresponds approximately to the diameter of the patch in that direction. Using this technique, the size of the patch of day 1 eggs during January 1994 was estimated to be 8 M across in the inshore–offshore direction (minor diameter) and 10 M across in the alongshore direction (major diameter).

The spherical model (eq. 3) was selected, since it gave the best fit to the variogram with the lowest residual sum of squares value:

$$(3)\qquad \gamma(h;\theta) = \begin{cases} C_0 + C\left(\dfrac{3h}{2a} - \left(\dfrac{h^3}{2a^3}\right)\right) & H < a \\ C_0 + C & H \geq a \end{cases}$$

The variograms of the egg and larval stages show the structure of the patches following spawning (Fig. 3). Samples (tows) that were spatially close were similar, with an associated small variance. The nugget values particularly for day 1 and day 2 eggs were small. Samples that were farther apart were less similar and consequently had a larger variance that increased with increasing distance between a pair of sample points until the sill is achieved. The maximum variance in a patch will be attained at a distance equal to the radius of an aggregation, since at this distance, high abundance samples in the centre of the aggregation are being paired with low abundance samples on the edge. Normally the variance remains constant as the lag is increased further; however, at larger lags, edge effects come into play. Due to the limited area sampled, fewer pairs of points are available and the comparisons tend to be from one side of the survey area to the other, missing the patch of eggs in the middle. This causes points at a large lag to have a small variance, as evident in Fig. 3. These values were considered to be an artifact of the sampling method and were not used when fitting the modelled variograms.

For the spherical model fitted to day 1 eggs, $a = 0.12°$ (7.2 M), $C = 4.7 \times 10^5$, and $C_0 = 4.3 \times 10^4$ (Fig. 3*a*). For day 2 eggs, $a = 0.042°$ (2.5 M), $C = 1.3 \times 10^5$, and $C_0 = 3.0 \times 10^4$ (Fig. 3*b*). However, the range for day 2 eggs may have been underestimated, since the largest variance was attained at a distance of 6.8 M. Because of the importance of day 1 eggs in the DEPM method, these data were examined separately for variation in the east–west and north–south directions (Figs. 3*c* and 3*d*). The range in the east–west direction appears to be larger than in the north–south direction, suggesting the presence of geometric anisotropy. This is consistent with the correlogram and adds support to the presence of an elliptical-shaped patch of eggs with a larger zone of influence in the alongshore direction than in the inshore–offshore direction. However, these directional variograms were not used for kriging, since due to the smaller number of pairs available the spatial structure was not as clear as the omnidirectional variogram, particularly in the north–south direction. For simplicity, we assumed that the structure is isotrophic and used the omnidirectional variogram.

Yolk-sac larvae also had a large degree of spatial cohesion with increasing levels of variance in samples up to 8 M apart (Fig. 3*e*). For both of the postlarval stages, however, the spatial structure had altered such that there was a high level of variance even in close samples with patch sizes greater than 12 M (Figs. 3*f* and 3*g*).

Ordinary kriging was used to estimate the abundance of 1- and 2-day-old pilchard eggs in the study area as shown (Fig. 4). The distribution of eggs is obviously not homogenous, but rather is clustered in patches. We cannot assume that the population is distributed either uniformly or randomly in space. This has implications for selecting an appropriate sampling strategy that takes account of the heterogeneous spatial distribution. The kriged mean abundance of

© 1999 NRC Canada

Fig. 3. Variograms of stages of pilchard material collected. (*a*) Day 1 eggs; (*b*) day 2 eggs; (*c*) day 1 eggs in an east–west direction; (*d*) day 1 eggs in a north–south direction; (*e*) yolk-sac larvae; (*f*) early postlarvae; (*g*) late postlarvae.

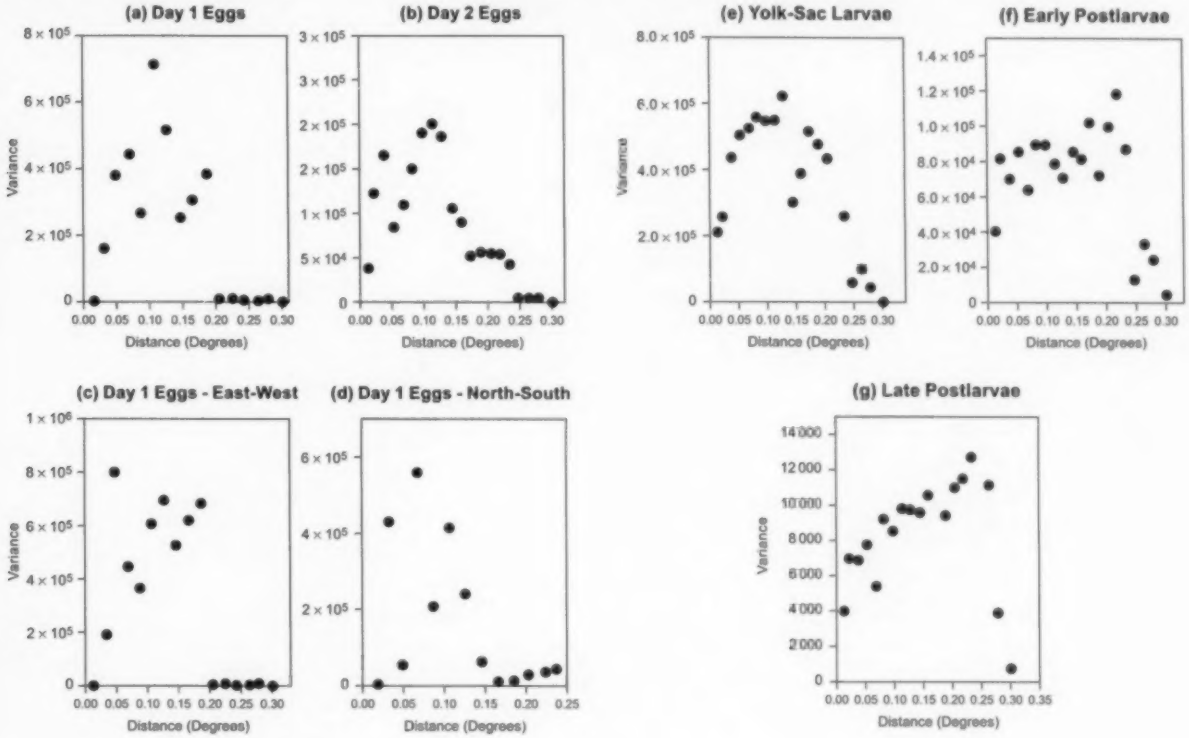

Fig. 4. Kriged abundances of (*a*) day 1 and (*b*) day 2 pilchard eggs off southern Australia.

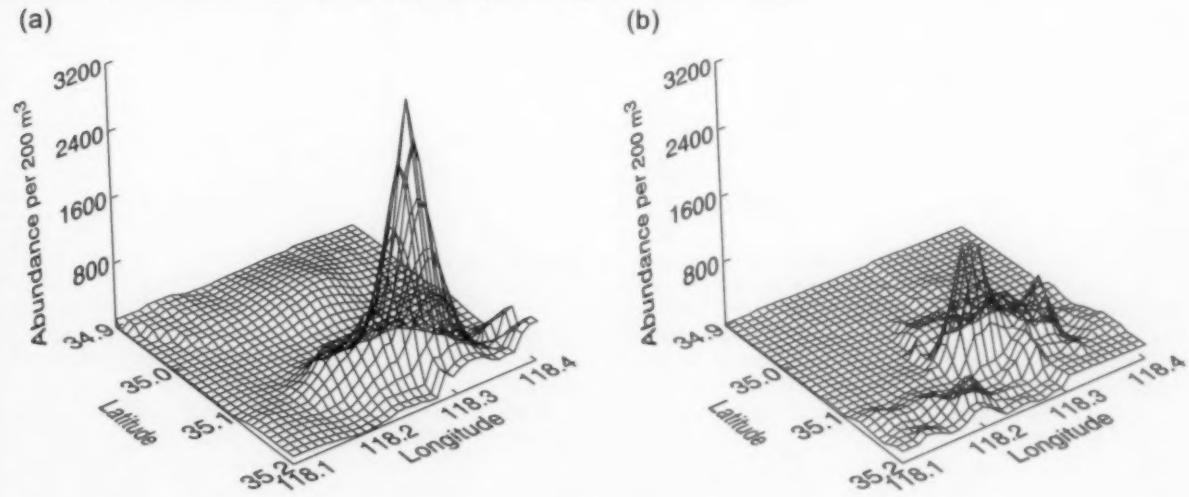

day 1 eggs for the area is 201/200m^3. The kriged mean is slightly smaller than the simple sample arithmetic mean abundance of 208/200m^3. The kriged mean is more precise, since it is an optimal estimate. The variances for the kriged and sample data were 129 826 and 331 179, respectively.

Resampling

The jackknife population mean for day 1 eggs (using only one sample per site) for all 48 sites was 198. The distribution of means calculated using one sample per zone (six in total), however, varied from 30 to 900; the sample standard

© 1999 NRC Canada

Fig. 5. Distribution of jackknife means and standard deviations for day 1 pilchard eggs using one, two, or three samples per zone (six zones in total). The arrows indicate population values.

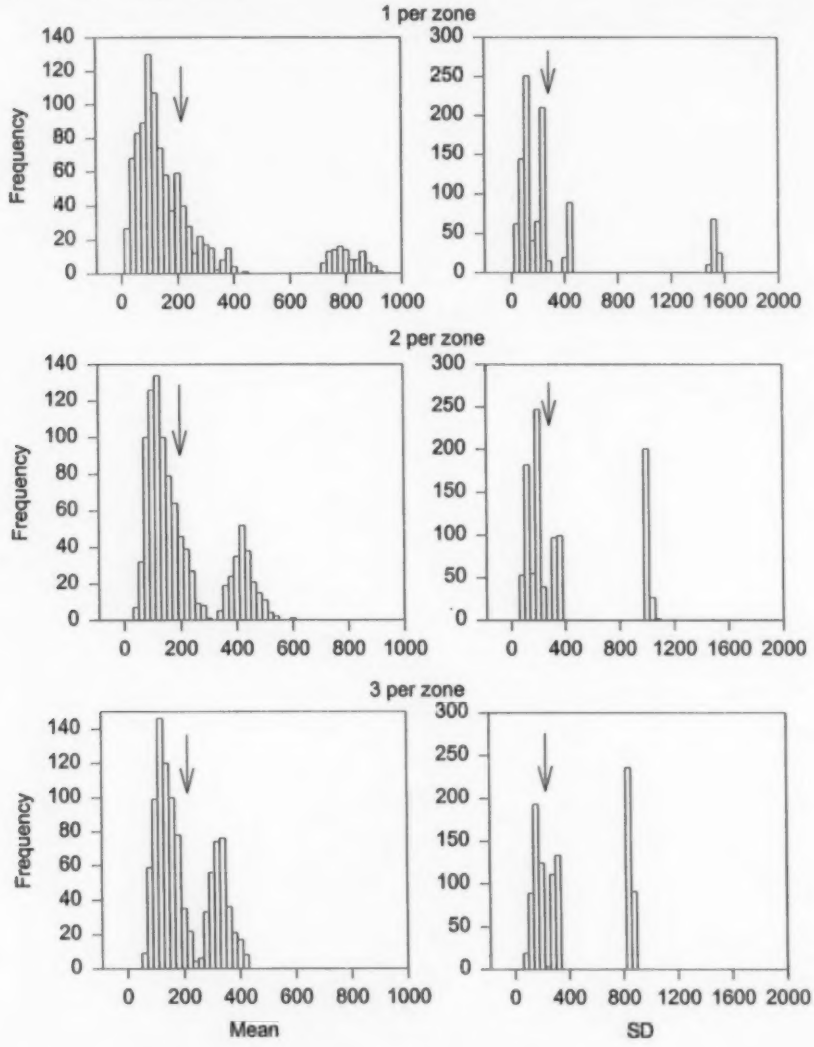

deviation also varied (Fig. 5). The majority (90%) were, nonetheless, between 50 and 300. The bimodal nature of the distribution resulted from the impact of one large influential area of eggs being either present or absent in the random samples. By increasing the number of samples to calculate the mean, the total range of means declined but the range for 90% limits did not decrease greatly with two or even three samples per sector.

The standard deviation of the 1000 bootstrapped means was large at small sample sizes but dropped rapidly to a plateau beyond 20 samples (Fig. 6). Similarly, the 90% confidence limits on the kriged data declined from a range between 50 and 500 when only two samples were taken to only 100–350 when 12 samples were taken. Increases beyond 24 samples yielded little further reduction in these limits (Fig. 6).

Discussion

The results of this and other studies (e.g., Barange and Hampton 1997) indicate that pilchard eggs have a patchy distribution that reflects upon the spawning behaviour of the adults. Thus, the spatial structure for newly spawned eggs adds support to the concept that pilchards spawn in discrete schools, and given the similarity with eggs greater than 1 day old, the general location of spawning may remain similar for at least two consecutive nights.

We found a large degree of concordance, as evidenced by the small nugget values, between the numbers of each of the pilchard egg and early larval stages collected by replicate tows taken at the same sites. This, together with the similarity found from separate nets on the one frame (Fletcher et al. 1996*a*) and in other paired tow comparisons (Fletcher et al.

© 1999 NRC Canada

Fig. 6. Bootstrap (*a*) standard deviation for estimates of pilchard egg abundance using kriged (solid circles) and raw (open squares) data and (*b*) 90% confidence limits calculated using kriged data; the mean abundance is shown in Fig. 6*b* as a solid line.

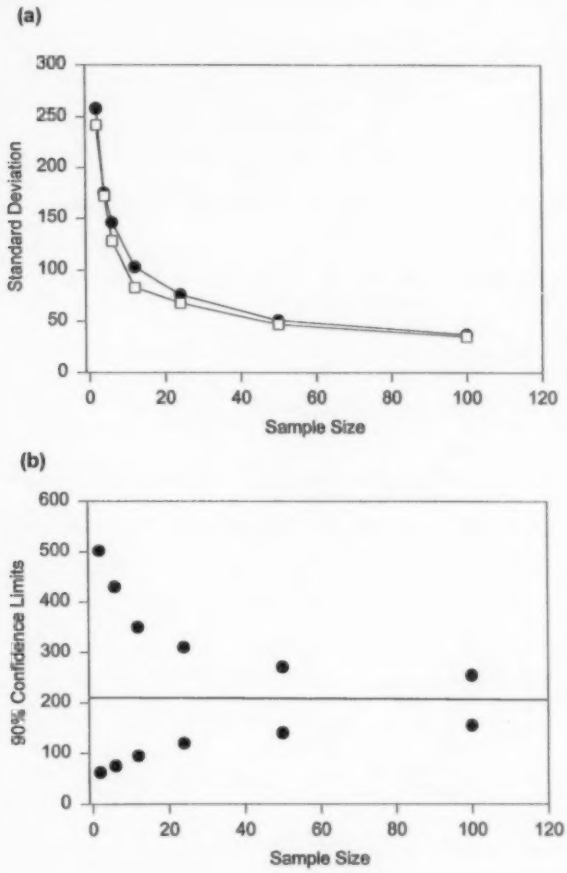

1994), supports the use of plankton sampling as an accurate, quantitative method of estimating egg abundance. The similarity of samples taken at the same location in quick succession has also been investigated by Silliman (1946) who, from replicate tows at a number of sites, concluded that 90% of the variability in abundances of *Sardinops* eggs off California was due to differences amongst sites with only 10% due to sampling variability. Similarly, Smith and Hewitt (1985) found that there were strong similarities in the numbers of day 1 to day 3 anchovy eggs within the eight samples they took at each site. From this, they concluded that nearly uniform results would have been obtained irrespective of which of the replicates had been used.

The number of spatial scales sampled in this study allowed the determination of the zone of spatial influence. The level of autocorrelation for the abundance of eggs between samples declined steadily with increasing distance for most stages. Similarly, the variance increased with increasing distance between samples. The distance from the centre of the correlogram to the zero contour line is analogous to the range of the variogram for the same direction. For day 1 eggs, size of the patch is estimated at 8 M in the inshore–offshore direction and 10 M in the alongshore direction. A patch size of less than 10 M was also determined for pilchards off South Africa using geostatisitcs based on acoustic data (Barange and Hampton 1997). Likewise, results from a study on anchovy eggs off California have revealed very similar patterns and patch dimensions (N.C-H. Lo, personal communication).

In order to detect a patch, the sampling interval should be smaller than its diameter to ensure that the patches are sampled at least once. If the sampling interval is too large compared with patch size, entire patches may be overlooked. The data from the present study suggest that to representatively sample pilchard eggs, samples should be no greater than 8–10 M apart; otherwise, it is likely that patches of eggs will be missed completely.

The results suggest that as the eggs develop from day 1 to day 2 and through the larval stages, the size of patch increases and the level of cohesion decreases. The kriged data demonstrated the change from a highly peaked distribution for day 1 eggs to a more spread distribution for day 2 eggs. For anchovies, N.C-H. Lo (personal communication) also found a strong trend of increasing patch size for older egg stages. Barange and Hampton (1997) speculated that having stations greater than 5 M apart and combining all ages of eggs was a major contributor to the lack of structure in their analyses of pilchard eggs.

Changes in patch size related to the age of the stage examined are to be expected due to the dispersal of the egg and larval stages that will follow spawning by schooling fish in a discrete area. For the later larval stages, which are capable of movement, the degeneration in cohesion is likely to be greater. Thus the correlogram and variograms provided valuable insight into the nature of the spatial structure for eggs and larvae.

Kriging provided both estimates of day 1 and day 2 egg abundance and an expanded population of values from which to determine the most efficient sampling regime for future surveys. Bootstrapping of both raw and kriged values indicates that the sampling intensity would need to increase from the three or four samples per 5 × 15 M sector previously used (Fletcher et al. 1996*a*) to obtain more precise egg abundance estimates. Increasing the intensity to six samples within each of these areas could potentially reduce the standard deviation and the confidence limits of estimates by almost 50%. Such a reduction should result in a major decrease in the uncertainly surrounding any biomass estimate that would result from these surveys.

To achieve a 50% reduction in variance, the distance between samples will need to be reduced such that they are only 4 M apart in an offshore direction and about 10 M in the alongshore direction. Such distances are consistent with the sizes of the patches of eggs determined by the spatial analyses. Further examination of these analyses suggests that the increases in sampling time required to significantly enhance the sampling frequency beyond a 4 × 10 M grid would be prohibitive and probably not cost effective. Further reductions in variance may, however, be achieved if extra tows could be completed on an opportunistic basis using

© 1999 NRC Canada

adaptive sampling methods during surveys. Thus, when large numbers of eggs are observed, the sampling intensity in these areas could be increased (Barange and Hampton 1997). Such a plan could utilise techniques, such as kriging or adaptive sampling, that are suitable for calculating mean abundances when the sampling is not homogenous and sample points may be clustered.

The approach used in this study has demonstrated the value of determining the proper nature of the spatial structure and in particular the utility of geostatistics for the analysis of plankton data. The data obtained will be invaluable for future sampling of pilchard eggs off southern Australia.

Acknowledgments

We would like to thank Mr. Peter Kerr and Mr. Gary Peters for the use of their fishing vessels during the January 1994 sampling trip. Stuart Blight, Rob Tregonning, Elizabeth Hayes, Dan Gaughan, and Ken White assisted in obtaining the plankton samples. Ken White and Richard Mijat sorted the pilchard eggs and larvae. The analyses and text were commented upon by Geoff Gordon, Mike Moran, Dan Gaughan, and Jim Penn. We would also like to thank the two anonymous referees for their constructive comments, which led to significant improvements in the final manuscript. This study was partly funded by the Fisheries Research and Development Corporation, project No. 92/025.

References

Alheit, J. 1993. Use of the daily egg production method for estimating biomass of clupeoid fishes: a review and evaluation. Bull. Mar. Sci. **53**: 750–767.

Barange, M., and Hampton, I. 1997. Spatial structure of co-occurring anchovy and sardine populations from acoustic data: implications for survey design. Fish. Oceanogr. **6**: 94–108.

Cressie, N. 1985. Fitting variogram models by weighted least squares. Math. Geol. **17**: 563–586.

Cressie, N. 1991. Statistics for spatial data. John Wiley & Sons, New York.

Englund, E., and Sparks, A. 1991. Geo-eas 1.2.1 geostatistical environmental assessment software user's guide. U.S. Environmental Protection Agency, Las Vegas, Nev.

Fletcher, W.J., Tregonning, R.J., and Sant, G.J. 1994. Interseasonal variation in the transport of pilchard eggs and larvae off southern Western Australia. Mar. Ecol. Prog. Ser. **111**: 209–224.

Fletcher, W.J., Lo, N.C-H., Hayes, E.A., Tregonning, R.J., and Blight, S.J. 1996*a*. Use of the daily egg production method to estimate the stock size of Western Australian sardines (*Sardinops sagax neopilchardus*). Mar. Freshwater Res. **47**: 819–825.

Fletcher, W.J., White, K.V., Gaughan, D.J., and Sumner, N.R. 1996*b*. Analysis of the distribution of pilchard eggs off Western Australia to determine stock identity and monitor stock size. Project 92/25. Final Report. Fisheries Research and Development Corporation, Canberra, Australia.

Gotway, C. 1991. Fitting semivariogram models by weighted least squares. Comp. Geosci. **17**: 171–172.

Isaaks, E.H., and Srivastava, R.M. 1989. Applied geostatistics. Oxford University Press, New York.

Lasker, R. (*Editor*). 1985. An egg production method for estimating spawning biomass of pelagic fish: an application to the northern anchovy, *Engraulis mordax*. NOAA Tech. Rep. NMFS 36.

Maravelias, C.D., and Haralabous, J. 1995. Spatial distribution of herring in the Orkney/Shetland area (northern north sea): a geostatistical analysis. Neth. J. Sea Res. **34**: 319–329.

Matheron, G. 1965. Les variables régionalisées et leur estimation. Masson, Paris.

Matheron, G. 1971. The theory of regionalized variables and its applications. Cah. Cent. Morphol. Math. Fountainbleau No. 5.

Mathsoft. 1995. Mathcad user's manual Mathcad plus 6.0. Mathsoft Inc., Cambridge, Mass.

Murray, A.W.A. 1996. Comparison of geostatistical and random sample survey analyses of Antarctic krill acoustic data. ICES J. Mar. Sci. **53**: 415–421.

Petitgas, P. 1993. Geostatistics for fish stock assessments: a review and acoustic application. ICES J. Mar. Sci. **50**: 285–298.

Petitgas, P. 1997. Sole egg distributions in space and time characterised by a geostatistical model and its estimated variance. ICES J. Mar. Sci. **54**: 213–225.

Silliman, R.P. 1946. A study of variability in plankton tow-net catches of Pacific pilchard (*Sardinops caerulea*) eggs. J. Mar. Res. **6**: 74–83.

Smith, P.E., and Hewitt, R.P. 1985. Anchovy egg dispersal and mortality as inferred from close-interval observations. Calif. Coop. Oceanic Fish. Invest. Rep. **26**: 97–109.

White, K.V., and Fletcher, W.J. 1997. Identifying the developmental stages for eggs of the Australian pilchard, *Sardinops sagax*. Fish. Res. Rep. West. Aust. **103**: 1–21.

© 1999 NRC Canada

Large woody debris in bull trout (*Salvelinus confluentus*) spawning streams of logged and wilderness watersheds in northwest Montana

F. Richard Hauer, Geoffrey C. Poole, John T. Gangemi, and Colden V. Baxter

Abstract: We measured large woody debris (LWD) in 20 known bull trout (*Salvelinus confluentus*) spawning stream reaches from logged and wilderness watersheds in northwestern Montana. Mean bankfull width of stream reaches was 14.1 m ranging from 3.9 to 36.7 m. Streams were large enough to move LWD and form aggregates. We determined the characteristics of individual pieces of LWD that were interactive with the stream channel. Large, short pieces of LWD attached to the stream bank were the most likely to be positioned perpendicular to stream flow, while large, long pieces either tended to be parallel to the flow or, when attached, were most apt to extend across the channel thalweg. Observations indicated that the majority of pools were formed as scour pools by either very large LWD pieces that were perpendicular to the stream or multipiece LWD aggregates. Among reaches in wilderness watersheds, ratios of large to small LWD, attached to unattached LWD, and with and without rootwads were relatively consistent. However, among reaches with logging in the watershed, these ratios varied substantially. These results suggest that logging can alter the complex balance of delivery, storage, and transport of LWD in northern Rocky Mountain streams, and therefore, the likely substantive change in stream habitats.

Résumé : Nous avons mesuré les gros débris ligneux (GDL) dans 20 tronçons de cours d'eau servant de frayères à l'omble à tête plate dans des bassins exploités par l'industrie forestière et des bassins sauvages du nord-ouest du Montana. La largeur moyenne des tronçons à pleins bords était de 14,1 m, avec une fourchette de 3,9 m à 36,7 m. Les cours d'eau étaient assez larges pour que les GDL se déplacent et forment des agrégats. Nous avons déterminé les caractéristiques des morceaux de GDL qui interagissaient avec le chenal. Les morceaux gros et courts attachés à la berge étaient les plus susceptibles de se positionner perpendiculairement au courant, tandis que les morceaux gros et longs se plaçaient parallèlement au courant ou, s'ils étaient attachés, étaient les plus susceptibles de se placer en travers du thalweg du chenal. Les observations ont montré que la majorité des fosses sont le résultat de l'affouillement causé soit par de très gros morceaux de GDL perpendiculaires au courant, soit par des agrégats composés de plusieurs morceaux de GDL. Parmi les tronçons des bassins sauvages, les rapports des gros aux petits GDL, des GDL attachés aux GDL non attachés, des GDL avec et sans attaches racinaires, étaient relativement constants, alors qu'ils variaient considérablement parmi les tronçons des bassins soumis à l'exploitation forestière. Ces résultats permettent de penser que l'exploitation forestière peut altérer l'équilibre complexe de l'apport, de l'installation et du transport des GDL dans les cours d'eau du nord des Montagnes Rocheuses, et donc occasionner des modifications potentiellement importantes des habitats lotiques.

[Traduit par la Rédaction]

Introduction

Large woody debris (LWD) plays numerous roles in the structure and function of stream ecosystems (Gregory et al. 1991). Riparian forests contribute LWD to a channel network, directly affecting both large- and small-scale stream morphology, hydrologic processes, and stream biota (Abbe and Montgomery 1996; Bisson and Montgomery 1996). Large wood accumulations influence the dissipation of stream energy and thus the ability of the stream to transport material. For example, LWD has been associated with channel avulsion, floodplain formation, and island development (Abbe and Montgomery 1996; Nanson and Knighton 1996). LWD also plays an important role in localized modification of streambed morphology (Bisson et al. 1987; Ralph et al. 1994) and pool frequency and channel geometry (Beschta and Platts 1986; Fausch and Northcote 1992; Richmond and Fausch 1995). The orientation and position of LWD in streams affect storage of organic and inorganic matter (Bilby and Ward 1989; Nakamura and Swanson 1993). Likewise, wood serves as trophic support of stream biota by providing organic matter for stream invertebrates and substratum for attachment and growth (Angermeier and Karr 1984; Benke et al. 1985; Hauer and Benke 1991).

The factors that directly affect introduction, stability, or character of stream LWD have a potentially significant influence on native fish populations that utilize streams for spawning, rearing, or growth and completion of life histories

Received August 7, 1998. Accepted January 6, 1999.
J14737

F.R. Hauer,[1] G.C. Poole,[2] J.T. Gangemi, and C.V. Baxter. Flathead Lake Biological Station, University of Montana, 311 BioStation Lane, Polson, MT 59860-9659, U.S.A.

[1]Author to whom all correspondence should be addressed. e-mail: rhauer@selway.umt.edu
[2]Present address: U.S. EPA, OEA-095, 1200 6th Avenue, Seattle, WA 98101, U.S.A.

© 1999 NRC Canada

(Andrus et al. 1988). Stream characteristics affected by LWD and its implications on salmonid populations have been the focus of numerous studies (e.g., Marcus et al. 1990; Ralph et al. 1994; Riley and Fausch 1995). A species of particular concern is the bull trout (*Salvelinus confluentus*), which has been in decline throughout the Pacific Northwest and was recently (1998) listed as a threatened species under the U.S Endangered Species Act. Numerous explanations for its decline have been offered, including habitat degradation (Fraley and Shepard 1989), overharvest (Rieman and McIntyre 1996), and displacement by exotic species (Leary et al. 1993).

Despite a generally ubiquitous trend of decline, the bull trout populations of the Flathead Basin in northwest Montana were considered relatively healthy, until recently. Strong spawning populations from Flathead Lake, Swan Lake, and Hungry Horse Reservoir have been an important part of the native fish fauna and an important sport fishery. In the past several years, however, the frequency of bull trout spawning in tributaries of the North and Middle forks of the Flathead River (i.e., the Flathead Lake population) has seriously declined (Rieman and Myers 1997). Overfishing, competitive interactions, predation of juveniles, food web alterations in Flathead Lake, and loss of habitat for spawning and rearing have all been suggested as causes for this decline. It is likely, however, that no single factor can be isolated as the overriding ecological bottleneck. Rather, all these factors influence the Flathead Lake population. For example, inundation of spawning gravels with fine sediments or changes in channel form and complexity may be major factors affecting the decline in bull trout spawning in the tributary drainages of the North and Middle forks of the Flathead River (Weaver and Fraley 1991). Low frequencies of spawning in some of the tributaries of the Swan River have been associated with the presence of logging roads (Baxter et al. 1999). Although the mechanisms that may be leading to the observed decline in bull trout are unclear, either on the landscape or in specific streams, hydrologic and vegetative changes associated with land use clearly play an important role. We suggest that a significant part of that role may be the result of change in the frequency, character, and distribution of in-stream LWD.

Although LWD plays an important role among streams in forested watersheds of the Pacific Northwest Coastal and Cascade Mountains (e.g., Nakamura and Swanson 1993; Ralph et al. 1994) and in the central Rocky Mountains (e.g., Fausch and Northcote 1992; Richmond and Fausch 1995), little information is available regarding the character or function of LWD in forested streams of the northern Rocky Mountains. The processes that have been documented among Washington and Oregon streams or streams in Colorado might not be seamlessly applicable in western Montana. Differences in climatic regime, landscape geomorphology, hydrologic regime, and the size, density, and longevity of dominant riparian species among these regions will have direct bearing on the interactive relationship between stream structure and function and LWD.

Regardless of the potential causes of bull trout population declines or the current cumulative effects impinging on the health and long-term viability of bull trout populations in western Montana, the maintenance of productive spawning and rearing habitat will be critical to the long-term sustainability or recovery of bull trout (see Fausch and Northcote 1992). As the recent changes in the food web of Flathead Lake come to some new quasi-equilibrium, with its cascading effects on higher trophic levels (Spencer et al. 1991), population restoration for bull trout will be strongly affected by reproductive success and juvenile survivorship. LWD may play a critical role in maintaining appropriate stream habitat and thus affect the long-term sustainability of bull trout populations in the Flathead Basin.

The purpose of this study is to describe the characteristics and selected functions of LWD among an array of historical bull trout spawning streams in the Flathead Basin. Although in several instances, redds occurred within a study reach, it was not our intention to specifically locate bull trout redds or covariation of redds and LWD. We selected streams from each of the four major tributaries in the drainage: the North and Middle forks of the Flathead River (Flathead Lake bull trout population), the South Fork of the Flathead River (Hungry Horse Reservoir population), and the Swan River drainage (Swan Lake population). We also chose streams that represented different types and levels of land use. Streams in the North Fork and Swan River include tributary drainages with extensive logging and riparian clearcuts. Streams in the Middle and South forks were within Glacier National Park or designated wilderness, respectively. The primary objectives of the research were to (*i*) characterize LWD in known bull trout spawning streams of the Flathead Basin, (*ii*) examine relationships of LWD size, position, and orientation across an array of stream sizes, (*iii*) examine the role of LWD in affecting local-scale bedform and stream morphology, and (*iv*) examine the potential effect of land use and (or) riparian logging on the size frequency structure, orientation, and decay relationships of LWD.

Materials and methods

Study area

This study was conducted in the Flathead Basin, a 22 241-km^2 drainage in northwestern Montana and southeastern British Columbia, along the west slope of the Continental Divide and within the belt series of the northern Rocky Mountains (Fig. 1). Sedimentary bedrock from the late Paleogene to the Proterozoic underlies the region and has been affected by low-grade metamorphosis. These mountain ranges are part of the Rocky Mountain Belt Supergroup and consist of argillites, siltites, and carbonates with a maximum stratigraphic thickness of 5200 m (Whipple et al. 1984). Colluvium and glacial till mantle the heavily forested valleys. During the height of the last major glaciation, about 20 000 years ago, the Flathead Basin was covered by glacial ice. The main glacial advance flowed from the cordilleran ice sheet down the Rocky Mountain Trench. Smaller valley glaciers flowed from the Livingston, Whitefish, Swan, Flathead, and Mission ranges to merge along the valley floors, forming trunk glaciers as much as 1000 m thick. Alluvial valley segments of tributary drainages formed with faulting and local accumulations of valley fill from alluvial and glacial sources.

Twenty stream reaches were selected from a stratified random design for study from eight streams distributed around the basin (Fig. 1). All reaches were in third- or fourth-order segments. We consulted the Montana Department of Fish, Wildlife, and Parks

© 1999 NRC Canada

Fig. 1. Map of the Flathead Basin and northern Continental Divide region of northwest Montana showing the names of major river drainages and study stream reaches in unlogged wilderness watersheds (open circles), logged watersheds with unlogged riparian (encircled dots), and logged watersheds with logged riparian (solid circles).

and selected study reaches within known bull trout spawning tributaries. We selected study streams within watersheds that had a land use history of either logging or wilderness management. Additionally, we selected specific study reaches within streams based on prevalent streamside management within the watershed. In some cases, as in Red Meadow Creek, the selected reaches flowed through riparian clearcuts, which occur commonly along that stream's length. Among other streams, such as Ole Creek in Glacier National Park, the riparian zone along the study reach was in an unaltered condition.

The substratum of each study reach was similar, generally composed of gravel and cobble, although occasionally, larger boulders (50–100 cm) were also present. The drainage area above the study reaches varied from 23 290 ha on Young's Creek to 1610 ha on Red Meadow Creek (Table 1).

Stream channel

Stream cross-sectional profiles, sinuosity, and gradient were measured at each stream reach using an Abney level, a Sonin® electronic distance measurer, and a leveling rod. Eleven transects (A–K) were taken across each stream reach at 10-m intervals covering a total reach length of 100 m. Each transect consisted of channel profiles measured perpendicular to the stream thalweg and to the top of the bankfull channel on both sides of the stream. Typically, 8–12 measures were taken to develop the cross-sectional profile at each transect. The profile data included all major breaks in elevation, the wetted channel width, water depth at the thalweg (at the time of measure), and height of the average bankfull channel. The change in bed height and water depth between each transect profile was measured using the Abney level, electronic distance measurer, and leveling rod. The 10-m intervals between each transect were identified as a stream section and referenced to the downstream transect.

LWD measurements

Measures of LWD were made within each 10-m stream section between each transect. LWD was defined as logs ≥10 cm in diameter and ≥1 m in length. Although there are no standard criteria established as to the minimum size that constitutes LWD, the criteria used here are the same as used in research at other locations (Andrus et al. 1988; Fausch and Northcote 1992; Richmond and Fausch 1995). Each piece of wood meeting the LWD criteria was measured if any part occurred within or was suspended above the bankfull stream channel. The diameter was measured at each end of the LWD piece with a 1-m caliper. The length of each piece was measured with the electronic distance measurer if the length was >2 m or with the caliper for shorter pieces. Piece volume was calculated as a tapered cylinder (Lienkaemper and Swanson 1987). All large rootwads were considered LWD regardless of length. Stumped rootwads with a length <1 m were common among streams with logged riparian areas. Volume of rootwads was estimated by measuring the diameter of the root structure across the dominant mass as one end of the cylinder, the bole of the tree stump above the root structure as the other end of the cylinder, and the distance between these measurements as the tapered cylinder length. The position and orientation of LWD to the channel were determined for each LWD piece. Piece position was recorded as one of three possibilities: (*i*) no contact with either bank, (*ii*) contacting either the left or right bank, or (*iii*) contacting both banks. In addition to simply contacting a bank, many pieces were strongly "attached" to one or, rarely, both banks. We classified an LWD piece as being attached if either or both ends were anchored into the stream bank.

Orientation of LWD is known to affect stream flow and bed morphology (Robison and Beschta 1990). Likewise, stream power affects piece orientation because hydraulic forces move unattached ends in a downstream direction (Nakamura and Swanson 1994). Piece orientation was divided into three categories: (*i*) at an about 0° angle (parallel) to the channel, (*ii*) at an about 45° angle to the channel, and (*iii*) at an about 90° angle (perpendicular) to the channel. We also noted whether an LWD piece had a rootwad attached to the bole, since this plays an important function in the attachment, orientation, and distribution dynamics of the piece.

The relative age of each piece was assessed using a modification of the Grette (1985) decay classification procedure, which divided LWD into four decay classes: (1) bark and branches attached, (2) bark and branches missing; wood solid with evidence of decay restricted to the outer perimeter, (3) wood showing significant signs of decay to at least depths of 5–10 cm, and (4) wood soft and decayed nearly or completely to the center of the piece. We later combined categories 3 and 4 for our analysis because of the infrequency of observing type 4 decay class LWD. We believe that the scarcity of decay class 4 wood is due to the rapidity of final decay and disappearance once a piece undergoes a transition from decay class 3 to class 4.

Data analyses

We conducted a variety of statistical analyses including χ^2, correlation analysis, ANOVA, and MANOVA using the statistical analysis software SPSS for Windows by SPSS, Inc. We considered test results to be significant at $\alpha = 0.95$.

© 1999 NRC Canada

Table 1. River drainage, stream name, watershed area above study reaches, number of pieces in aggregates or not in aggregates, and other characteristics of LWD.

Flathead River drainage	Stream Name	Drainage area (ha)	Reach and logging condition	LWD aggregate (no.)	LWD nonaggregate (no.)	LWD volume (m^3)	LWD attachment	
							Attached	Unattached
Middle Fork	Ole Creek	10 295	A[a]	0	13	8.8	5	8
			B[a]	18	11	7.4	17	12
			C[a]	0	32	30.8	7	25
	Nyack Creek	22 005	A[a]	0	7	0.4	1	6
			B[a]	0	5	3.0	2	3
North Fork	Red Meadow Creek	1 612	A[c]	10	41	35.9	35	16
			B[c]	53	70	73.3	95	28
	Whale Creek	9 836	A[b]	0	56	14.3	26	30
			B[b]	0	87	19.4	37	50
			C[b]	39	52	58.9	59	32
	Coal Creek	12 113	A[b]	51	72	33.3	57	66
			B[b]	11	25	19.8	19	17
South Fork	Young's Creek	23 289	A[a]	145	39	73.2	90	94
			B[a]	49	28	18.6	49	28
			C[a]	0	37	10.1	17	20
Swan River	Jim Creek	3 705	A[c]	71	46	65.2	72	45
			B[c]	0	46	10.9	35	11
	Goat Creek	5 602	A[b]	16	45	18.1	31	30
			B[b]	35	35	20.4	49	21
			C[c]	27	48	56.7	54	21

Note: Diameter class: 1 = 10–19 cm; 2 = 20–29 cm; 3 = 30–39 cm; 4 = 40 cm.
[a]Reach in unlogged wilderness watershed.
[b]Reach in logged watershed with unlogged riparian.
[c]Reach in logged watershed with logged riparian.

Results and discussion

General characteristics of study reaches

Mean (±SD) bankfull widths among all stream reaches combined were 14.2 ± 6.6 m with a range of 3.9–36.7 m across all transects. Study reaches were variable, both between and within streams. Stream gradients among all reaches were moderate (mean 1.0%, maximum 2.6%) but again highly variable. The thalweg bed elevation of some downstream transects was higher than that of upstream transects, clearly illustrating streambed complexity.

Five of the 20 study reaches had one or more side channels. In cases where side channels were present, there was always one dominant channel. The side channels were always small with only minor flow. Side channels in two stream reaches contained a high density of LWD and likely were abandoned main channels.

Thalweg stream depths across all transects ranged from a minimum of 0.15 m in Ole Creek reach A to a maximum of 1.33 m in Young's Creek reach C. An examination of the relationship between drainage area and stream depth showed a significantly, positive correlation (p = 0.016) with stream maximum depths; however, neither mean nor minimum stream depth was significantly correlated with basin size (Fig. 2).

General characterization of LWD

A total of 1320 pieces of LWD were counted and measured among all study reaches. The number of pieces and volume of LWD across all reaches were highly variable (Table 1). For example, reach A on Young's Creek had 184 pieces, while, in contrast, reach B on Nyack Creek had only five pieces of LWD.

Across all stream reaches, the size of the LWD was also extremely variable. About 70% of all LWD was in the smaller two diameter classes (10–19 cm: >35%; 20–29 cm: >30%) (Fig. 3A) and >50% of the LWD was between 1 and 4 m in length (Fig. 3B). Size frequency of diameter measures and tree length measures demonstrated a decreasing exponential curve with increasing piece size. Together, <50% of the LWD across all stream reaches consisted of pieces >30 cm in diameter and >4 m in length. However, as in other studies (e.g., Abbe and Montgomery 1996), we found that the larger LWD pieces played the primary role in streambed configuration and the formation of aggregates (see data analysis below). LWD pieces that had been moved by the stream into large debris jams, or aggregates, often spanned the stream channel and were extremely stable, owing to their mass and configuration with the stream banks and the LWD pieces within the jam.

Other studies have found that LWD attachment to one or both banks and (or) the presence of the tree's rootwad are important factors influencing the stability (i.e., the resistance to being moved during flood) and orientation of the LWD piece (Beschta and Platts 1986; Richmond and Fausch 1995). Among nonaggregated LWD, we found attachment to one or both banks and the number of pieces that had rootwads to be highly variable, commensurate with the high variation in LWD occurrence between stream reaches (Table 1). However, we did find statistically significant relation-

© 1999 NRC Canada

0° by diameter class				45° by diameter class				90° by diameter class				Rootwad	
1	2	3	4	1	2	3	4	1	2	3	4	With	Without
1	0	1	0	2	3	1	4	1	0	0	0	6	7
4	3	0	1	4	3	2	3	4	2	1	2	2	27
4	6	3	4	3	4	1	1	1	1	0	4	7	25
2	0	0	0	3	1	0	0	0	0	0	0	0	7
2	1	1	0	0	0	0	0	0	0	0	1	1	4
2	4	5	4	3	3	2	4	3	10	3	8	9	42
3	7	1	4	5	18	9	12	8	15	13	28	8	115
13	19	3	1	10	2	2	2	4	0	0	0	1	55
19	14	6	3	18	13	6	1	2	3	2	0	0	87
13	14	14	5	11	13	3	1	5	7	0	5	17	74
33	20	3	4	17	17	6	6	10	6	1	0	4	119
7	2	2	3	5	2	0	1	5	4	3	2	2	34
16	16	8	5	43	29	20	9	12	10	5	9	27	157
11	7	2	1	20	9	3	10	4	4	2	3	15	62
6	4	0	4	9	4	4	0	3	2	0	1	5	32
9	8	2	3	19	19	8	8	7	14	9	11	18	99
7	3	0	2	13	7	1	2	5	0	3	2	2	44
6	7	1	2	6	2	2	1	9	13	4	8	8	53
15	5	3	3	9	7	1	4	7	9	1	6	6	64
4	5	2	4	7	3	4	8	9	9	4	16	20	55

ships between the orientation of the LWD piece, the attachment of the piece to the bank, and both the volume and the length of the LWD piece. Using χ^2 analysis, we found that LWD tends to be significantly shorter among those pieces that are perpendicular to the stream flow (orientation 90°) than among those that are parallel (orientation 0°) to stream flow (Table 2). This is likely due to longer pieces being subject to rotation around an anchor point, such as a bank attachment, during flooding when stream power and floatation of the LWD are at their highest (Nakamura and Swanson 1994). We found a similar significant relationship of increased LWD piece diameter associated with pieces that were perpendicular to the channel compared with those parallel to the channel (Table 2). We also observed that bank attachment often extended a considerable distance onto the bank and back into the riparian vegetation. These pieces were often the most stable and demonstrated resistance to change in orientation.

In addition to girth and length influencing stream LWD position, we also examined the affect of LWD attachment on orientation. A χ^2 analysis revealed that LWD pieces that were perpendicular to the current had a significantly higher frequency of bank attachment (Table 3). We found these features to be particularly important, since perpendicular pieces were the most interactive with the stream channel in that they were often most responsible for change in streambed morphology and complexity (see LWD influence on streambed morphology below). We also examined LWD wood decay (Table 1). We found that among all stream reaches, most LWD was in decay class 2, i.e., most pieces had been stripped of their bark and branches and showed only the earliest signs of rotting at the surface. This finding has the following implications: (*i*) most of the wood has been in the stream for at least several years, long enough to loose the outer bark and limbs, but not so long as to enter advanced decay stages and (*ii*) the paucity of decay classes 3 and 4 suggests that once an LWD piece enters the latter stages of decay, decomposition processes occur rapidly. The latter stages of decay may be strongly enhanced during spring runoff as increased stream power causes decomposing logs to break apart. We did not conduct tests to directly determine the rate of LWD decomposition; however, based on our knowledge of aggregate accumulations at sites that we have visited regularly since the mid-1970's, we know that LWD can remain >20 years with no signs of surface decomposition. Thus, it appears that LWD probably remains in these streams for periods exceeding 50 years (sensu Andrus et al. 1988). To summarize, those pieces that were perpendicular to the flow tended to be attached to the stream bank, large in diameter, and short. This finding corroborates Nakamura and Swanson (1994).

LWD influence on streambed morphology

An important feature of stream habitat structure is the development and stability of streambed morphology. Streams that alternate between riffles, pools, and runs provide complex habitats that support high biodiversity, biomass, and secondary production of aquatic insects and fish. Complex

© 1999 NRC Canada

Fig. 2. Maximum, mean, and minimum thalweg depths among all transects for each stream reach regressed against the drainage area of each watershed above the study area. The maximum thalweg depth to basin area correlation coefficient ($r = 0.51$) is significant at the 0.05 level. Correlations between mean and minimum thalweg depths and basin area were nonsignificant.

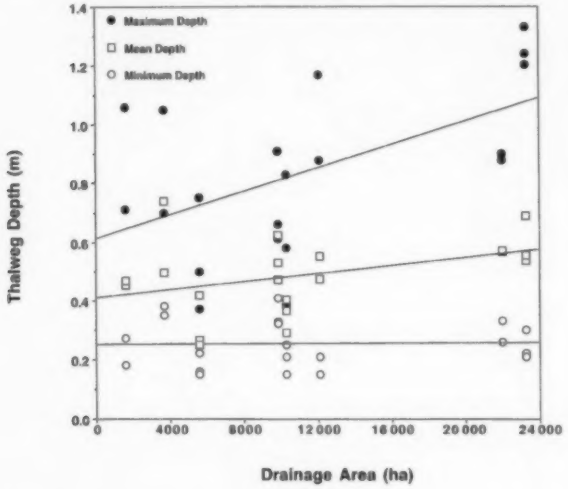

Fig. 3. Percentage of LWD in each of (A) eight bole diameter classes and (B) 11 length classes.

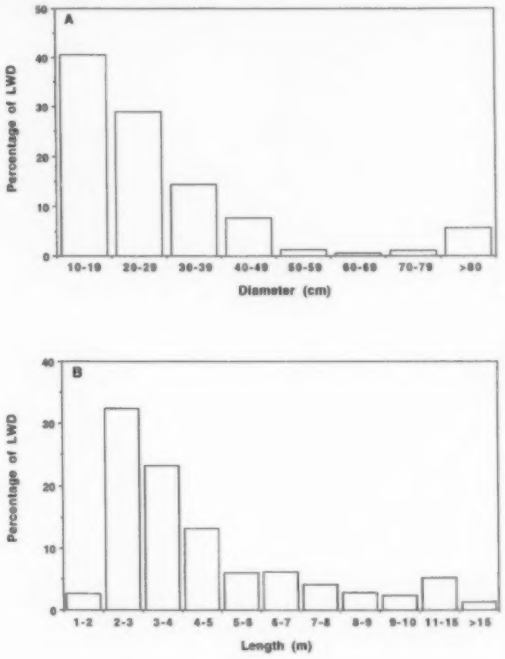

variation in stream habitat and streambed morphology is frequently required for different species to coexist (sensu Connell 1980).

Using correlation analysis, we examined the role of LWD and its influence on streambed morphology. We found that as the number of pieces of LWD and the volume of LWD increased within a stream section, there was a corresponding increase in the bedslope of the section immediately downstream (Fig. 4). The steepest bedslopes were all associated with upstream aggregates, large snags with rootwads, or large-diameter LWD oriented perpendicular to the stream thalweg. Each of these LWD structures performs important bed-forming functions, e.g., the retention of gravel on the upstream side of the structure and (or) the focus of stream flow and thus stream power and scour on the downstream bed material forming pools. Both of these factors lead to the aggradation of upstream gravel and cobble and the downstream degradation of bed material. These correlations between increased LWD piece frequency and volume and bedslope underscore the importance of LWD aggregates in stabilizing bedload, capturing gravel, and promoting pool formation.

Land use influence on LWD

Three of the eight watersheds (eight of 20 study reaches) examined were located within Glacier Park or the Bob Marshall Wilderness. These three watersheds are managed as wilderness and have never been logged or roaded. The other five watersheds are in the North Fork or the Swan River drainages and flow through lands managed for multiple use, but primarily for timber harvest.

We found a tight correlation ($r = 0.99$) between the frequency of large LWD (≥30 cm in diameter) and the frequency of small LWD (<30 cm in diameter) among the reaches draining wilderness areas (Fig. 5). In contrast, among reaches in watersheds with upstream logging, the large to small LWD relationship was poorly correlated ($r = 0.18$). These data suggest that even though variation in number of pieces of LWD among stream reaches may be high, there is a consistent and highly predictable relationship between the frequency of large-diameter trees and small-diameter trees in the LWD pool in wilderness watersheds that was not present in logged watersheds. In addition to the cross-watershed comparison of LWD size ratios, we further compared streams flowing through logged riparian zones with those flowing through unlogged riparian zones, but in logged watersheds. Among the logged watersheds, we found that streams flowing through logged riparian zones tended to have a higher large LWD to small LWD ratio than streams flowing from wilderness areas, while streams flowing from logged watersheds, but with unlogged riparian zones, usually had smaller ratios (Fig. 5).

We also examined the relationship of attachment of LWD to the stream bank. Again, we found that among wilderness watersheds, there was a relatively tight correlation ($r = 0.94$) between the frequency of attached LWD and the frequency of unattached LWD and a poorly correlated relationship ($r = 0.30$) among logged watersheds (Fig. 6). Additionally, we examined the relationship between the frequency of LWD pieces with rootwads and the frequency of those without rootwads. Again, among reaches in wilderness watersheds, there was a high correlation ($r = 0.96$) between LWD pieces with rootwads and those without rootwads, but among logged watersheds, this relationship was poorly correlated ($r = 0.13$) (Fig. 7).

© 1999 NRC Canada

Table 2. Chi square analysis of length and bole diameter versus attachment and orientation characteristics of nonaggregate LWD among all stream study reaches.

	Attachment characteristic			Orientation characteristic			
LWD characteristic	Attached	Unattached	Pearson χ^2	0°	45°	90°	Pearson χ^2
Length <4 m	219	155	0.05 ($p = 0.82$)	108	150	116	38.0 ($p < 0.00$)
Length ≥4 m	184	135		153	121	45	
Diameter <30 cm	236	232	35.4 ($p < 0.00$)	190	191	87	17.7 ($p < 0.00$)
Diameter ≥30 cm	167	58		71	80	74	

Table 3. Chi square analysis of attachment and orientation characteristics of nonaggregate LWD among all stream study reaches.

Attachment	Orientation characteristic			
characteristic	0°	45°	90°	Pearson χ^2
Attached	127	156	120	27.5 ($p < 0.00$)
Unattached	134	115	41	

Among all watersheds, there was high variance in the frequency of LWD. Furthermore, LWD is not evenly distributed at the stream reach (100 m) spatial scale. However, the ratio of large to small LWD, the ratio of attached to unattached LWD, and the ratio of LWD with and without rootwads were relatively consistent across stream reaches in wilderness areas. However, among stream reaches in logged watersheds, these relationships were highly variable. These data suggest that logging or associated land use activities within a watershed may result in an alteration in the balance of delivery, storage, and transport of stream LWD, which in turn would have strong implications regarding effects on material transport and stream habitats.

It would require additional, focused study to determine the cause and effect relationship between size, attachment, and rootwad frequencies of stream LWD and specific logging practices. However, regardless of whether increased variance in size frequency is the result of direct actions that alter LWD input to the stream (e.g., cutting of large-diameter riparian trees) or indirect forces (e.g., postlogging blowdown), they may contribute to LWD characteristics that depart from relationships among streams in unlogged watersheds. Such departures may result in substantive habitat alteration and adverse effects on species dependent on habitats affected by stream LWD structure and function, such as pool size and frequency, surface/ground water exchange, and complex channel morphology.

Implications for watershed and streamside management

We found a close association between LWD and streambed morphology. For example, the steepest bedslopes were all associated with upstream aggregates of LWD. Among nonaggregated LWD, we found large pieces attached to stream banks and oriented perpendicular to the thalweg to be more closely associated with pool formation than parallel or unattached pieces. Among LWD pieces that were oriented perpendicular to stream flow and crossed the stream thalweg, there was a statistically significant higher frequency of long pieces (i.e., ≥4 m in length), a nearly significant proportion of large pieces (i.e., ≥30 cm in diameter),

Fig. 4. (A) Number of LWD pieces and (B) volume of LWD in the upstream 10-m stream section and the corresponding downstream bedslope.

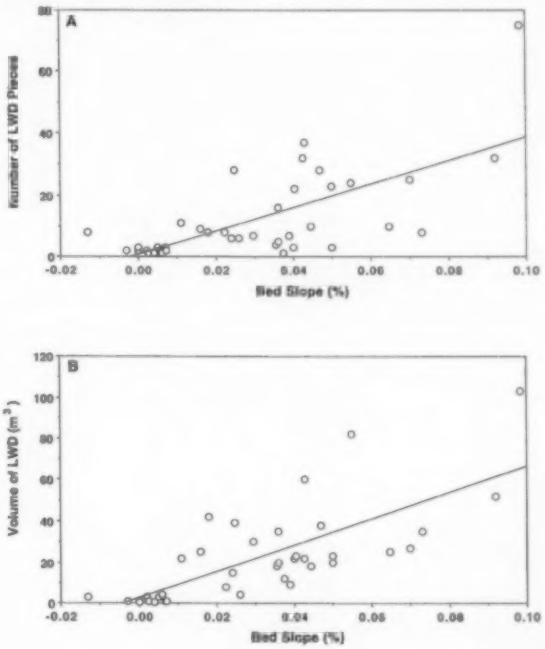

and a statistically significant higher frequency of LWD pieces attached to the stream bank (Table 4). These field observations suggest that LWD pieces that are perpendicular to the stream channel and engage the stream thalweg are the primary influence promoting pool formation. Field measurements further indicate that of the perpendicular LWD pieces, large-diameter pieces that are long and attached to the stream bank are the most stable (e.g., best able to resist reorientation and movement once in the channel). Grette (1985) and Richmond and Fausch (1995) also reported a significant positive relationship between LWD and the abundance of pools, as well as the importance of relatively few, stable LWD pieces that accounted for most of the pool formation.

Wohl et al. (1993) reported that stream depth, gradient, stream power, and the resistance of bed and bank materials to erosion were important determinants of pool size. We observed a similar relationship in which the streams of the larger drainages had the deepest pools, even though drainage size had no significant effect on mean or minimum thalweg

© 1999 NRC Canada

Fig. 5. Frequency of large-diameter (≤30 cm) versus small-diameter (<30 cm) LWD among study stream reaches in wilderness watersheds (solid circles) and in logged watersheds (open circles). Arrows denote study stream reaches with logged riparian areas. The trend line is for wilderness watersheds. Correlation coefficients are given in the text.

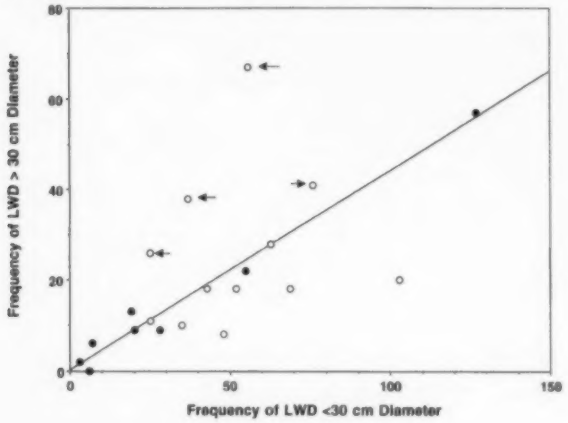

Fig. 6. Frequency of unattached versus attached LWD among study stream reaches in wilderness watersheds (solid circles) and in logged watersheds (open circles). The trend line is for wilderness watersheds. Correlation coefficients are given in the text.

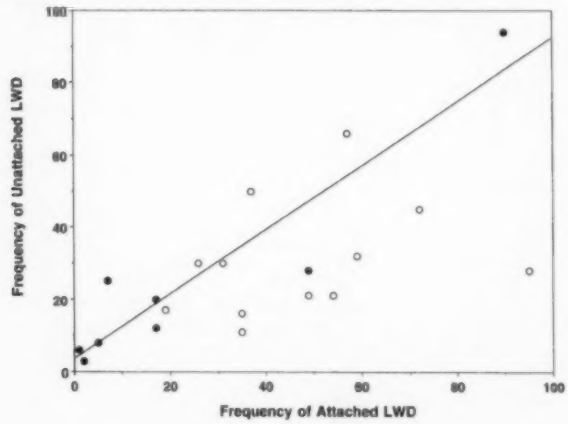

depth. Other researchers have suggested that for large streams and rivers, LWD generally has a limited effect on gradient, stream power, maximum stream width, and maximum bankfull depth (Andrus et al. 1988; Evans et al. 1993). Our results support this suggestion, since within the largest watershed streams, such as Young's Creek, pool-forming LWD pieces occurred almost exclusively as aggregates (Table 1). In other words, as a stream gets larger, exemplified by Young's Creek in our study, stream power becomes sufficient to move virtually all wood that enters the channel. However, this does not mean that as stream size increases, LWD becomes of little consequence but rather that the role of LWD may change as aggregates interact with the dynamics of flood waters affecting anabranching and (or) avulsion behavior (e.g., Nanson and Knighton 1996).

Fig. 7. Frequency of LWD with rootwad versus without rootwad among study stream reaches in wilderness watersheds (solid circles) and in logged watersheds (open circles). The trend line is for wilderness watersheds. Correlation coefficients are given in the text.

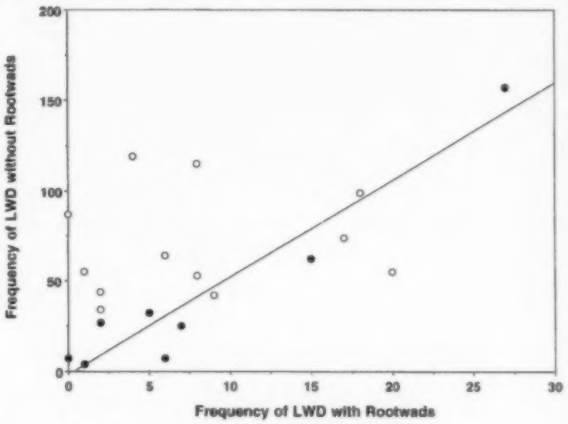

Table 4. Chi square analysis of length, bole diameter, and attachment characteristics of nonaggregate LWD crossing the stream channel and engaging the stream thalweg versus LWD within the bankfull channel but not engaging the stream thalweg.

	Crossing characteristic		
LWD characteristic	Across thalweg	Not across thalweg	Pearson χ^2
Length <4 m	40	321	6.64 (p = 0.01)
Length ≥4 m	56	254	
Diameter <30 cm	57	396	3.38 (p = 0.07)
Diameter ≥30 cm	39	179	
Attached	66	324	5.20 (p = 0.02)
Unattached	30	251	

Robison and Beschta (1990) and Richmond and Fausch (1995) showed that changing relationships between LWD and stream flow influenced pool types and that the majority of pools were formed by LWD spanning the channel perpendicular to flow. Richmond and Fausch (1995) found plunge and dammed pools to be the most prevalent pool type in the small subalpine streams of Colorado. Bilby and Ward (1989) found a similar pool type in smaller streams (<7 m wide) in southwestern Washington, but mainly scour pools in large streams (Bilby and Ward 1991). We observed similar situations among streams in the Flathead Basin where pools in the smaller streams (e.g., Goat Creek, Red Meadow Creek) were primarily associated with plunging or dammed water around LWD and with scour pools around aggregates in the largest streams (e.g., Young's Creek, Coal Creek).

In forested watersheds, LWD is an essential component in the formation of stream morphology and provides habitat for aquatic insects and fish. However, the relationship between stream size and power and the position and role played by LWD in the modification of bedform and channel develop-

© 1999 NRC Canada

ment is a changing one. It is apparent from this study that large-diameter, shorter pieces of LWD attached to the stream bank have a higher frequency of perpendicular orientation and that larger, longer pieces attached to the bank tend to interact with the channel, as represented by those logs that cross the thalweg. Thus, a greater degree of pool-forming interaction with stream flows is represented by large, long pieces of LWD attached to the stream bank. Likewise, as the stream size increases, a concurrent increase in the size of LWD comprising an aggregate is needed to remain stable and interactive with the channel. Thus, the interaction of stream power, bed characteristics, and LWD piece diameter, length, and position largely determines the structure and function of stream LWD. The distribution of LWD among size classes, and attachment and orientation categories appears relatively consistent across streams in unlogged watersheds but becomes less predictable in streams that have been influenced by logging. A detailed investigation into the specifics of various logging histories would be necessary to determine how specific site prescriptions affect the outcome of LWD relationships associated with forest streams.

The implications of this study for forest managers are twofold: (*i*) with riparian logging comes increased unpredictability in the frequency of size, attachment, and stability of the LWD and (*ii*) maintaining the appropriate ratios of size frequency, orientation, and bank attachment, as well as rate of delivery, storage, and transport of LWD to streams, is essential to maintaining historic LWD characteristics and dynamics. Our data suggest that exclusion of logging from riparian zones may be necessary to maintain natural stream morphology and habitat features. Likewise, careful upland management is also necessary to prevent cumulative effects that result in altered water flow regimes and sediment delivery regimes. While not specifically evaluated in this study, in general, it appears that patterns of upland logging over space *and* time may have cumulative effects that could additionally alter the balance of LWD delivery, storage, and transport in fluvial systems. These issues will be critical for forest managers attempting to prevent future detrimental environmental change or setting restoration goals for degraded bull trout spawning streams (cf. Reeves et al. 1991).

Acknowledgements

We thank the Montana Department of Fish, Wildlife, and Parks for its financial support of this research. We also thank the two anonymous reviewers for their helpful suggestions that improved this paper.

References

Abbe, T.B., and Montgomery, D.R. 1996. Large woody debris jams, channel hydraulics and habitat formation in large rivers. Regul. Rivers, **12**: 201–221.

Andrus, C.W., Long, B.A., and Froehlich, H.A. 1988. Woody debris and its contribution to pool formation in a coastal stream 50 years after logging. Can. J. Fish. Aquat. Sci. **45**: 2080–2086.

Angermeier, P.L., and Karr, J.R. 1984. Relationship between woody debris and fish habitat in a small warmwater stream. Trans. Am. Fish. Soc. **113**: 716–726.

Baxter, C.V., Frissell, C.A., and Hauer, F.R. 1999. Geomorphology, logging roads and the distribution of bull trout (*Salvelinus confluentus*) spawning in a forested river basin: implications for management and conservation. Trans. Am. Fish. Soc.

Benke, A.C., Henry, R.L., III, Gillespie, D.M., and Hunter, R.J. 1985. Importance of snag habitat for animal production in southeastern streams. Fisheries (Bethesda), **10**: 8–13.

Beschta, R.L., and Platts, W.S. 1986. Morphological features of small streams: significance and function. Water Resour. Bull. **22**: 369–379.

Bilby, R.E., and Ward, J.W. 1989. Changes in characteristics and function of woody debris with increasing size of streams in western Washington. Trans. Am. Fish. Soc. **118**: 368–378.

Bilby, R.E., and Ward, J.W. 1991. Characteristics and function of large woody debris in streams draining old-growth, clear-cut, and second-growth forests in southwestern Washington. Can. J. Fish. Aquat. Sci. **48**: 2499–2508.

Bisson, P.A., and Montgomery, D.R. 1996. Valley segments, stream reaches, and channel units. *In* Methods in stream ecology. *Edited by* F.R. Hauer and G.A. Lamberti. Academic Press, New York. pp. 23–52.

Bisson, P.A., Bilby, R.E., Bryant, M.D., Dolloff, C.A., Grette, G.B., House, R.A., Murphy, M.L., Koski, K V., and Sedell, J.R. 1987. Large woody debris in forested streams in the Pacific Northwest: past, present, and future. *In* Proceedings of the Symposium on Forest Hydrology and Watershed Management. *Edited by* E.O. Salo and T.W. Cundy. Publ. 167. International Association of Hydrologic Sciences, Wallingford, Oxfordshire. pp. 191–198.

Connell, J.H. 1980. Diversity and the coevolution of competitors, or the ghost of competition past. Oikos, **35**: 131–138.

Evans, B.F., Townsend, C.R., and Crowl, T.A. 1993. Distribution and abundance of coarse woody debris in some southern New Zealand streams from contrasting forest catchments. N.Z. J. Mar. Freshwater Res. **27**: 227–239.

Fausch, K.D., and Northcote, T.G. 1992. Large woody debris and salmonid habitat in a small coastal British Columbia stream. Can. J. Fish. Aquat. Sci. **49**: 682–693.

Fraley, J., and Shepard, B. 1989. Life history, ecology and population status of migratory bull trout (*Salvelinus confluentus*) in the Flathead Lake and River system, Montana. Northwest Sci. **63**: 133–143.

Gregory, S.V., Swanson, F.J., McKee, W.A., and Cummins, K.W. 1991. An ecosystem perspective of riparian zones. BioScience, **41**: 540–551.

Grette, G.B. 1985. The role of large organic debris in juvenile salmonid rearing habitat in small streams. M.S. thesis, University of Washington, Seattle, Wash.

Hauer, F.R., and Benke, A.C. 1991. Rapid growth of snag-dwelling chironomids in a blackwater river: the influence of temperature and discharge. J. North Am. Benthol. Soc. **10**: 154–164.

Leary, R.F., Allendorf, F.W., and Forbes, S.H. 1993. Conservation genetics of bull trout in the Columbia and Klamath River drainages. Conserv. Biol. **7**: 856–865.

Lienkaemper, G.W., and Swanson, F.J. 1987. Dynamics of large woody debris in stream in old-growth Douglas-fir forests. Can. J. For. Res. **17**: 150–156.

Marcus, M.D., Noel, L.E., and Young, M.K. 1990. Rating salmonid habitat research needs in the central Rocky Mountains. Fisheries (Bethesda), **15**: 14–18.

Nakamura, F., and Swanson, F.J. 1993. Effects of coarse woody debris on morphology and sediment storage of a mountain stream system in western Oregon. Earth Surf. Processes Landforms, **18**: 43–61.

Nakamura, F., and Swanson, F.J. 1994. Distribution of coarse

© 1999 NRC Canada

woody debris in a mountain stream, western Cascade Range, Oregon. Can. J. For. Res. **24**: 2395–2403.

Nanson, G.C., and Knighton, A.D. 1996. Anabranching rivers: their cause, character and classification. Earth Surf. Processes Landforms, **21**: 217–239.

Ralph, S.C., Poole, G.C., Conquest, L.L., and Naiman, J.R. 1994. Stream channel morphology and woody debris in logged and unlogged basins of western Washington. Can. J. Fish. Aquat. Sci. **51**: 37–51.

Reeves, G.H., Hall, J.D., Roelofs, T.D., Hickman, T.L., and Baker, C.O. 1991. Rehabilitating and modifying stream habitats. Am. Fish. Soc. Spec. Publ. **19**: 519–557.

Richmond, A.D., and Fausch, K.D. 1995. Character and function of large woody debris in subalpine Rocky Mountain streams in northern Colorado. Can. J. Fish. Aquat. Sci. **52**: 1789–1802.

Rieman, B.E., and McIntyre, J.D. 1996. Spatial and temporal variability in bull trout redd counts. N. Am. J. Fish. Manage. **16**: 132–141.

Rieman, B.E., and Myers, D.L. 1997. Use of redd counts to detect trends in bull trout (*Salvelinus confluentus*) populations. Conserv. Biol. **11**: 1015–1018.

Riley, S.C., and Fausch, K.D. 1995. Trout population response to habitat enhancement in six northern Colorado streams. Can. J. Fish. Aquat. Sci. **52**: 34–53.

Robison, E.G., and Beschta, R.L. 1990. Coarse woody debris and channel morphology interactions for undisturbed streams in southeast Alaska, U.S.A. Earth Surf. Processes Landforms, **15**: 149–156.

Spencer, C.N., McClelland, B.R., and Stanford, J.A. 1991. Shrimp stocking, salmon collapse and eagle displacement: cascading interactions in the food web of a large aquatic ecosystem. BioScience, **41**: 14–21.

Weaver, T.M., and Fraley, J. 1991. Fisheries habitat and fish populations. Flathead basin forest practices, water quality and fisheries cooperative program. Flathead Basin Commission, Kalispell, Mont.

Whipple, J.W., Connor, J.J., Raup, O.B., and McGimsey, R.G. 1984. Preliminary report on the stratigraphy of the Belt Supergroup, Glacier National Park and the adjacent Whitefish Range, Montana. *In* Northwestern Montana and adjacent Canada. *Edited by* J.D. McBride and P.B. Garrison. Mont. Geol. Soc. Field Conf. Guideb. Montana Geological Society, Billings, Mont. pp. 33–50.

Wohl, E.E., Vincent, K.R., and Merritts, D.J. 1993. Pool and riffle characteristics in relation to channel gradient. Geomorphology, **6**: 99–110.

© 1999 NRC Canada

An advection–diffusion–reaction model for the estimation of fish movement parameters from tagging data, with application to skipjack tuna (*Katsuwonus pelamis*)

John R. Sibert, John Hampton, David A. Fournier, and Peter J. Bills

Abstract: The mobility of fish populations is often ignored in population dynamics models. However, in many cases (with tunas being a prime example), movement and spatial heterogeneity may be striking features of the fish populations and their exploitation. We describe a general quantitative framework to estimate movement and mortality of fish populations from tagging data. Movement is represented by an advection–diffusion process, which is the population equivalent of individual movement based on a biased random walk. Finite difference approximations for solving the partial differential equation are provided. The model is parameterized by assuming that movement parameters are homogeneous within specified geographical regions and seasons, that fishing mortality is proportional to fishing effort, and that natural mortality is constant over area and time. All model parameters are estimated simultaneously by maximum likelihood. The method is illustrated by application to skipjack tuna (*Katsuwonus pelamis*) in the western Pacific Ocean. Skipjack movement is shown to be highly variable at both seasonal and interannual time scales. Comparison with the results of a spatially aggregated analysis of the same data reveals that the spatial model provides a much better fit to the data and, unlike the spatially aggregated model, enables estimation of the natural mortality rate free of the effects of movement within the model domain.

Résumé : La mobilité des populations de poisson est souvent ignorée dans les modèles de dynamique des populations. Cependant, dans de nombreux cas (celui des thons au premier chef), les déplacements et l'hétérogénéité spatiale peuvent être des caractéristiques marquantes des populations de poisson et de leur exploitation. Nous décrivons un cadre quantitatif général permettant d'estimer les déplacements et la mortalité des populations de poisson à partir de données de marquage. Les déplacements sont représentés par un processus d'advection et de diffusion, qui est, pour une population, l'équivalent des déplacements aléatoires biaisés d'un individu. Nous fournissons les approximations en différences finies nécessaires pour résoudre l'équation différentielle partielle. Nous avons paramétré le modèle en supposant que les paramètres des déplacements sont homogènes dans les régions et saisons spécifiées, que la mortalité par pêche est proportionnelle à l'effort de pêche et que la mortalité naturelle est constante dans l'espace et dans le temps. Tous les paramètres du modèle sont estimés simultanément selon le maximum de vraisemblance. Nous avons appliqué notre méthode à la bonite à ventre rayé (*Katsuwonus pelamis*) de l'ouest du Pacifique. Nous avons montré que les déplacements de ce poisson sont très variables d'une saison et d'une année à l'autre. La comparaison avec les résultats d'une analyse spatialement agrégée des mêmes données montre que le modèle spatial donne un bien meilleur ajustement aux données et, à la différence du modèle spatialement agrégé, permet d'estimer le taux de mortalité naturelle sans qu'interviennent les effets des déplacements dans le domaine du modèle.

[Traduit par la Rédaction]

Introduction

Although fish are mobile, the explicit effects of mobility on fisheries management policies are usually neglected. In cases where fishing is distributed uniformly over the range of the exploited fish species, movement may not be relevant in models of population dynamics (Beverton and Holt 1957). For tunas, however, fishing is certainly not uniform and is often restricted to a fraction of the range of the exploited species. Therefore, neglecting movement may lead to errors in estimates of exploitation rates (Laloë 1989; Die et al. 1990).

Tuna movements have been the subject of many field studies that depend on a variety of tagging and tracking techniques (see review by Hunter et al. 1986), and extensive collections of tag release and recapture data are maintained by various organizations dedicated to the scientific analysis of tuna populations. These data have yielded important insights into the exploitation and population dynamics of tunas (e.g., Bayliff 1971; Kleiber et al. 1987).

Received February 24, 1998. Accepted December 15, 1998. J14457

J.R. Sibert[1] **and P.J. Bills.** Pelagic Fisheries Research Program, Joint Institute of Marine and Atmospheric Research, University of Hawaii, Honolulu, HI 96822, U.S.A.
J. Hampton. Oceanic Fisheries Programme, Secretariat of the Pacific Community, B.P. D5, Noumea Cedex, New Caledonia.
D.A. Fournier. Otter Research Ltd., P.O. Box 2040, Sidney, BC V8L 3S3, Canada.

[1]Author to whom all correspondence should be addressed.
e-mail: jsibert@soest.hawaii.edu

© 1999 NRC Canada

Quantitative analyses of tuna movement have been slower to develop, with treatment often confined to drawing arrows on maps to represent the long-range movement of a few tagged individuals. In fact, several general classes of models can be applied to the quantitative analysis of fish movement. Bulk transfer models, where exchange rates between large regions are characterized by transfer coefficients, were first outlined by Beverton and Holt (1957). Models of this type have been applied to yellowfin tuna (*Thunnus albacares*) in the eastern Pacific (Ishii 1979*a*, 1979*b*), to skipjack tuna (*Katsuwonus pelamis*) in the western Pacific (Sibert 1984; Hilborn 1990), and to southern bluefin tuna (*Thunnus maccoyii*) (Hampton 1991). In some cases, these models have closed-form solutions, are easily implemented in computer code, and have parameters that can be estimated statistically from tagging data. Although bulk transfer models can predict changes in population size in arbitrary regions, they cannot be used to predict the changes in population density at an arbitrary point within a region because they are not continuous in space.

Models based on diffusion concepts are continuous in both space and time. These models have a long history in animal ecology (Skellam 1951), and their potential application to fisheries population modeling dates back at least to Beverton and Holt (1957) and Jones (1959). Although the diffusion concept suggests that the population moves at random, it does not require that individual fish move randomly. The small-scale movements of individuals, which are surely nonrandom, may, in a large population, produce a net distribution that gives the appearance of being the result of random movements. Because purely diffusive movement will ultimately produce a uniform distribution of the population at equilibrium, other factors such as directional movement or spatial variability in recruitment, mortality, or population growth rate (Mullen 1989; MacCall 1990) are required to maintain persistent gradients in population density. Directional movements are easily incorporated into a diffusion model by introducing "advective" terms. Okubo (1980) presented an insightful derivation of the advection–diffusion equation as the limiting form of a biased random walk. Thus, the advection–diffusion model can be viewed as being equivalent to the individual-based modeling approach (Tyler and Rose 1994; Porch 1995) in the same sense that Eulerian and Lagrangian approaches are complementary views of fluid movement. Further discussion of the theoretical basis for the use of diffusion models in the analysis of fish movement is presented in Appendix A.

The application of advection–diffusion models to fish population dynamics has grown recently. MacCall (1990) developed an elegant theory relating movement, population growth, and habitat selection that, to a large extent, is based on an advection–diffusion model. Deriso et al. (1991) applied a Markovian transition matrix approach to estimating diffusion and advection parameters for eastern Pacific yellowfin tuna. Kleiber and Hampton (1994) applied an advection–diffusion model to the analysis of tagged skipjack tuna movements in relation to fish-aggregating devices.

The present paper extends previous work by providing a formal derivation of a general advection–diffusion–reaction model for the analysis of tagged fish movement. We provide a flexible means of parameterizing movement through grouping of parameters by geographical regions and seasons and describe the maximum likelihood estimation of parameters from tagging data. We apply the model to the analysis of variability in skipjack tuna movement in the western Pacific Ocean, using tag release and recapture data from the 1977–1982 South Pacific Commission Skipjack Survey and Assessment Programme (SSAP) (Kearney 1982*a*, 1983). These results are contrasted with analysis of the same data using a spatially aggregated model.

The model

An advection–diffusion–reaction model is used to describe the movement and mortality of tagged skipjack tuna. Let $\tilde{N}_{xytc}$ symbolize the density of tagged tunas (numbers of tagged fish per unit of surface area) at point (x,y) in the ocean at time t of tag release cohort c. The aggregate density of tagged tunas (or simply, tags) from all cohorts released up to time t is given by

$$(1) \qquad N_{xyt} = \sum_{c=1}^{C_t} \tilde{N}_{xytc} .$$

Assuming that the tag cohorts move independently, the aggregate tag density satisfies the following partial differential equation:

$$(2) \qquad \frac{\partial N}{\partial t} = \frac{\partial}{\partial x}\left(D\frac{\partial N}{\partial x}\right) + \frac{\partial}{\partial y}\left(D\frac{\partial N}{\partial y}\right) - \frac{\partial}{\partial x}(uN) - \frac{\partial}{\partial y}(vN) - ZN.$$

Equation 2 partitions the local rate of change of tag density at point (x,y) into "dispersive" movements, "directed" movements, and mortality. The first two terms on the right-hand side of eq. 2 characterize dispersive movements in terms of a "diffusion" parameter D. The next two terms in eq. 2 characterize directed movements in terms of two "advection" parameters (u,v) that describe east–west (positive toward the east) and north–south (positive toward the north) movements. Note that the movement parameters u, v, and D may vary in space and time. The final term in eq. 2, the "reaction" term, describes the loss of tagged fish due to mortality from all sources. Since movement is explicit in this model, the mortality term does not include local losses due to emigration away from the fishing grounds.

Solution of the partial differential equation

Equation 2 is solved using a finite difference method on a regular grid with a spatial resolution of 60 nautical miles (Nmi), i.e., $\Delta x = \Delta x = 60$ (60 Nmi = 111.12 km), and a discrete time step. The numerical solution of eq. 2 is used in a numerical function minimization procedure to obtain estimates of model parameters. Therefore, the solution method must be fast because the partial differential equation (PDE) will be solved hundreds of time, and it must also be robust because function minimization algorithms may test parameter values that are not necessarily conducive to numerical stability. These two criteria are often conflicting. Speed is

© 1999 NRC Canada

Fig. 1. Cross section of a computational grid showing grid point labels and closed boundaries.

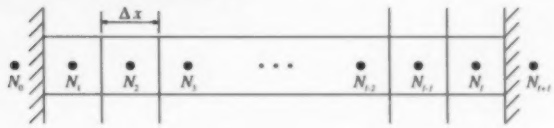

achieved by using large time and space steps, while stability is often achieved by using small time and space steps.

The finite difference approximation used for the time derivative is

$$(3)\qquad \left.\frac{\partial N}{\partial t}\right|_{i,j}^{n+1} \simeq \frac{N_{i,j}^{n+1} - N_{i,j}^{n}}{\Delta t}.$$

The subscripts i, j denote the spatial location of a grid point with position $(i\Delta x, j\Delta y)$; superscript n refers to time level $n\,\Delta t$.

Two schemes for the approximation of the first derivatives in the directed movement terms were considered: approximation by two-point "backward" differences, a scheme known as "upwind" or "upstream" differencing (Roache 1972; Press et al. 1988), and approximation by two-point centered-space differences.

Upwind differencing is very robust, but contributes numerical (i.e., nonbiological) diffusion to the solution field, which may confound estimation of the actual (i.e., biological) random movement parameter values for tagged tuna (O'Brien 1986). Upwind differencing of the directed movement terms at time level n takes the form

$$(4)\qquad \left.\frac{\partial uN}{\partial x}\right|_{i,j}^{n} \simeq \begin{cases} \dfrac{u_{i,j}N_{i,j}^{n} - u_{i-1,j}N_{i-1,j}^{n}}{\Delta x}, & u_{i,j} > 0 \\ \dfrac{u_{i+1,j}N_{i+1,j}^{n} - u_{i,j}N_{i,j}^{n}}{\Delta x}, & u_{i,j} < 0 \end{cases}$$

$$\left.\frac{\partial vN}{\partial y}\right|_{i,j}^{n} \simeq \begin{cases} \dfrac{v_{i,j}N_{i,j}^{n} - v_{i,j-1}N_{i,j-1}^{n}}{\Delta y}, & v_{i,j} > 0 \\ \dfrac{v_{i,j+1}N_{i,j+1}^{n} - v_{i,j}N_{i,j}^{n}}{\Delta y}, & v_{i,j} < 0. \end{cases}$$

Centered-space differencing is a nondispersive alternative approximation to upwind differencing but introduces grid-scale oscillations into the solution field if advective terms are large relative to diffusive terms (Price et al. 1966; Roache 1972; Leonard 1979; Neuman 1981; Abbott and Basco 1989). In preliminary tests, such oscillations were large enough to cause negative values for tag density, and the parameter estimation procedure (see below) did not converge. All subsequent analysis was done using upwind differencing.

The second derivatives in the random movement terms are approximated using three-point finite differences as follows:

$$(5)\qquad \left.\frac{\partial}{\partial x}\left(D\frac{\partial N}{\partial x}\right)\right|_{i,j}^{n} \simeq N_{i-1,j}^{n}\frac{D_{i-1,j} + D_{i,j}}{2(\Delta x)^2} - N_{i,j}^{n}\frac{D_{i-1,j} + 2D_{i,j} + D_{i+1,j}}{2(\Delta x)^2} + N_{i+1,j}^{n}\frac{D_{i,j} + D_{i+1,j}}{2(\Delta x)^2}$$

$$\left.\frac{\partial}{\partial y}\left(D\frac{\partial N}{\partial y}\right)\right|_{i,j}^{n} \simeq N_{i,j-1}^{n}\frac{D_{i,j} + D_{i,j-1}}{2(\Delta y)^2} - N_{i,j}^{n}\frac{D_{i,j-1} + 2D_{i,j} + D_{i,j+1}}{2(\Delta y)^2} + N_{i,j+1}^{n}\frac{D_{i,j+1} + D_{i,j}}{2(\Delta y)^2}.$$

Boundary conditions must be specified in order to solve the PDE. Closed boundaries occur naturally around islands and along continental coastlines. Either closed or open boundaries may be applied to the edges of the model region. Closed boundary conditions are appropriate where the model region encompasses a large proportion of the tagged fish distribution. For closed boundaries, a simple reflection condition on N and an impermeability condition on the normally directed component of movement are used. Thus:

$$(6)\qquad \frac{\partial N}{\partial x} = 0 \quad \text{and } u = 0$$

on eastern and western closed boundaries

$$\frac{\partial N}{\partial y} = 0 \quad \text{and } v = 0$$

on northern and southern closed boundaries.

These conditions ensure that tagged tuna numbers are conserved in the model when both natural and fishing mortality are zero.

In the one-dimensional grid point lattice in Fig. 1, the reflection conditions on N at each boundary have the numerical counterparts in the x direction:

$$(7)\qquad N_0 = N_1 \text{ and } N_{I+1} = N_I$$

and guarantees tag conservation in the absence of mortality. A more complete discussion of boundary conditions can be found in Bills and Sibert (1997).

The obvious initial condition for N is

$$(8)\qquad N_{xy0} = \begin{cases} \displaystyle\sum_{c} \tilde{N}_{x_c, y_c, 0c}, & \text{over all tag release sites} \\ 0, & \text{elsewhere} \end{cases}$$

where $\tilde{N}_{x_c, y_c, 0c}$ is the number of tagged skipjack released at point (x_c, y_c) at time 0 in tag cohort c. In the case of a cohort release s at a subsequent time t_s and at position (x_s, y_s), the density of tags at that point is reassigned the sum of its present value and the cohort value, viz.:

$$(9)\qquad N(x_s, y_s, t_s) \leftarrow N(x_s, y_s, t_s) + \tilde{N}(x_s, y_s, t_s).$$

The complete numerical approximation to the PDE is given by substituting finite difference approximations for the movement terms taken at appropriate time levels into the right-hand side of eq. 2. A combination of time levels n + 1/2 and n + 1 leads to the well-known alternating direction

© 1999 NRC Canada

Table 1. Values of bounds applied to parameter estimates and tag density in the penalty functions.

Parameter	Lower bound	Upper bound
M	0	0.5
Q_f	0	0.1
u	−1 500	1 500
v	−1 500	1 500
D	0	500 000
N_{ij}	0	None

implicit (ADI) method. This method is robust and converges to a solution unconditionally for all step sizes (Carnahan et al. 1969; Press et al. 1988).

Reparameterization

All of the solutions of the PDE described above require specification of each model parameter at every grid point. The 60 × 35 grid used in the present example requires values of each parameter u, v, D, and Z in eq. 2 to be specified at each time step at each of the 2100 grid points, a total of 8400 parameter values per time step. Direct estimation of so many parameters is impractical, and some means of reducing the number of parameters is required.

Tuna movement patterns are frequently represented by arrows on maps, often with months or seasons specified, to suggest the general trend of population movement at different times and places (e.g., see Kearney 1982*b*; Hunter et al. 1986). This point of view implies that fish movement may be time and site specific. Consistent with this possibility, "regions" are defined as subdivisions of the model domain over which the movement parameters u, v, and D are constant, and "seasons" are defined as periods of time during which the parameters within a region are constant. Let R_{ij} be a matrix that contains the region number for each model cell indexed by (i, j) and S^n be a vector that contains the season for each time step indexed by n. In other words, R_{ij} maps the model domain into specified regions and S^n maps calendar time to seasons. The model parameters are specified at each grid point by the following equations:

$$(10)\quad [u_{ij}^n] = \mathbf{u}_{R_{ij}S^n}$$
$$[v_{ij}^n] = \mathbf{v}_{R_{ij}S^n}$$
$$[D_{ij}^n] = \mathbf{D}_{R_{ij}S^n}$$

where **u**, **v**, and **D** are matrices of parameters to be estimated. For a model with 10 regions and two seasons, **u**, **v**, and **D** are 2 × 10 matrices containing the 60 movement parameters required to specify values for **u**, **v**, and **D** at the 2100 points in the model domain used in the present analysis. The matrices **u**, **v**, and **D** are collectively referred to as movement "patterns" or "hypotheses" below.

Total mortality Z is separated into two components in a conventional manner by

$$(11)\quad Z_{ij}^n = M + \sum_f F_{ijf}^n$$

where F_{ijf}^n is the mortality due to fishing by fishing fleet f operating in computational element (i, j) during time step n and M is mortality due to other causes or "natural" mortality. Natural mortality is assumed to be constant at all places, over the period of time that the tagged fish are at liberty. Fishing mortality is assumed to be a simple function of observed fishing effort:

$$(12)\quad F_{ijf}^n = Q_f \times E_{ijf}^n$$

where E_{ijf}^n is the observed fishing effort of fleet f operating in element (i, j) during time step n and Q_f is a fleet-specific proportionality constant or "catchability coefficient". This parameterization enables the specification of mortality at all grid points in terms of a small number of parameters of direct relevance to the dynamics of exploited populations.

Parameter estimation

The predicted number of skipjack tags returned during 1 month is given by

$$(13)\quad \hat{C}_{ijf}^n = \beta_f \frac{F_{ijf}^n}{Z_{ij}^n}(1 - e^{-Z_{ij}^n})N_{ij}^n$$

where β_f is the reporting rate, i.e., the proportion of tags captured by fleet f returned with usable recapture information, and N_{ij}^n satisfies eq. 2 for time step n. For the example presented here, β_f is assumed to be 1.0 for all fleets.

Observed numbers of tag returns, C_{ijf}^n, are related to predicted numbers of tag returns, $\hat{C}_{ijf}^n$, by a Poisson likelihood function:

$$(14)\quad L(\mathbf{u}, \mathbf{v}, \mathbf{D}, Q, M | C_{ijf}^n, E_{ijf}^n) = \prod_{ijnf}\left[\frac{(\hat{C}_{ijf}^n)^{C_{ijf}^n} e^{-\hat{C}_{ijf}^n}}{C_{ijf}^n!}\right].$$

This function assumes that the predicted number of tag returns in each cell during 1 month is the expected value of a random variable with a Poisson distribution. This distribution is appropriate for an observation of a rare event such as the radioactive decay of an atom (Feller 1968) or the recapture and return of a tagged skipjack. Maximum likelihood parameter estimates are obtained by finding the values of the parameters that maximize eq. 14. The maximization is accomplished by minimizing the negative log of eq. 14 using a quasi-Newton numerical function minimizer, which, in turn, depends on the gradient of partial derivatives computed using adjoint functions (Griewank and Corliss 1991).

Additional information is provided to the function minimizer through the use of penalty functions (Bard 1974). These functions are continuous functions of the upper and lower bounds of the parameters and are interpreted as prior probability distribution functions added to the likelihood function. Penalty functions also restrict the minimization process to a region constrained by feasible parameter values. The net effect of the penalty functions is a more efficient minimization process. The values of the upper and lower bounds used in the penalty functions are given in Table 1. Certain combinations of parameter values will produce grid-scale oscillations in the solution of eq. 2. If these oscillations are large, the local tag density may take on negative values. A penalty function is therefore added to the likelihood function to prevent the function minimizer from seeking parameters that destabilize the numerical approximation of eq. 2. This penalty is equal to the sum of the squares of the local negative tag densities.

© 1999 NRC Canada

Fig. 2. Map of the southwest Pacific Ocean showing the location of the 10-region model area used for the skipjack tuna analysis.

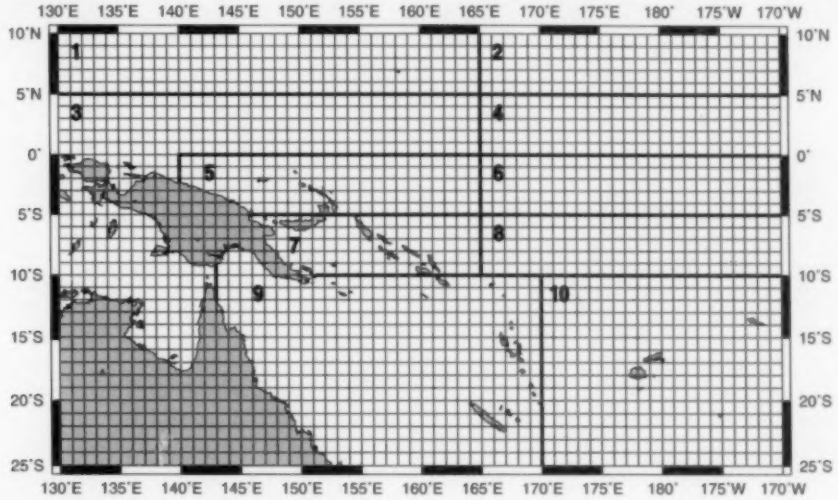

Simulations have shown that parameter estimates for region × season strata for which few tag returns were observed may be inaccurate (Sibert and Fournier 1994; Bills and Sibert 1997). The (spatial) gradients of the movement parameters are therefore constrained to be small by imposing a small penalty on the curvature of the movement field. That is, penalties are applied to $\frac{\partial^2 u}{\partial x^2}$, $\frac{\partial^2 v}{\partial y^2}$, $\frac{\partial^2 D}{\partial x^2}$, and $\frac{\partial^2 D}{\partial y^2}$. These penalties help to ensure that estimates of movement parameters in regions with few tag returns will be similar to estimates in neighboring regions.

Estimates of the variance of the parameter estimates are computed from the Hessian matrix, **H**, the elements of which are

$$(15) \quad H_{ij} = \frac{\partial^2(-\log L)}{\partial\theta_i \partial\theta_j}$$

where θ_i and θ_j are any two model parameters. The approximate covariance matrix, **V**, is given by the inverse of the Hessian matrix $\mathbf{V} = \mathbf{H}^{-1}$ (Bard 1974). This procedure provides other useful information about the minimum attained by the function minimizer. If **H** is not positive definite, the minimizer has found a saddle point or has not converged. Such a condition occurs when the minimum is not well determined by the data, as may occur when the likelihood function is dominated by constraints on parameter ranges or by various penalties.

Application to western Pacific skipjack tuna

Data sources and treatment

Skipjack tag releases within the model area (Fig. 2) during the period 1 October 1977 to 31 August 1980 were selected from the SSAP database. The selected data set comprised 94 430 releases and 5319 reported recaptures. Of these recaptures, 92 occurred outside the model area and were excluded from the analysis. The model considers tag returns by the five main fishing fleets active in the area at the time: the Japan pole-and-line, Japan purse seine, Fiji pole-and-line, Papua New Guinea pole-and-line, and Solomon Islands pole-and-line fleets. Tag returns by other fleets (188 recaptures) were excluded from the analysis. Tag releases and returns were stratified by release "cohorts", each consisting of releases in a one-degree geographic area during a calendar month. Returns from each cohort were further stratified by one-degree area, calendar month, and recapture fleet. Recaptures that could not be so stratified (828 recaptures) because of missing or inaccurate data were also excluded from the analysis. The tag recapture period used in the model extended until 31 August 1983, which encompassed all observed tag recaptures. The final data set analyzed therefore consisted of 4211 returns, or 79% of the total reported recaptures. The rejection of recaptures from the analysis effectively contributes to nonreporting and therefore could be explicitly included in the analysis by adjustment of β_j in eq. 13. We have opted not to do so in the present analysis because the other sources of nonreporting cannot be quantified.

Fishing effort data, stratified by one-degree area, calendar month, and recapture fleet, for the period 1 October 1997 to 31 August 1993 were compiled from South Pacific Commission databases.

The model regions and computational grid are shown on the map in Fig. 2. The boundaries of the model domain were assumed to be closed. Representations of coastlines and islands at a resolution of one degree (about 60 Nmi) inevitably cause errors in the locations of fishing events (tag release, tag recapture, fishing) that occur within 60 Nmi of a shoreline. In some cases, fishing events may appear on land when mapped at one-degree resolution. Such events were arbitrarily shifted to an adjacent one-degree area. Tag releases, recaptures, and fishing effort positions that appeared on land at one-degree resolution were all shifted consistently.

Results

Interaction between the solution of the PDE and the function minimizer should be considered before the results of the

© 1999 NRC Canada

Fig. 3. Effects of time step size on the value of the negative log likelihood function at convergence (solid line, solid circles) and the number of evaluations of eq. 15 required for the function minimizer to converge (broken line, open circles).

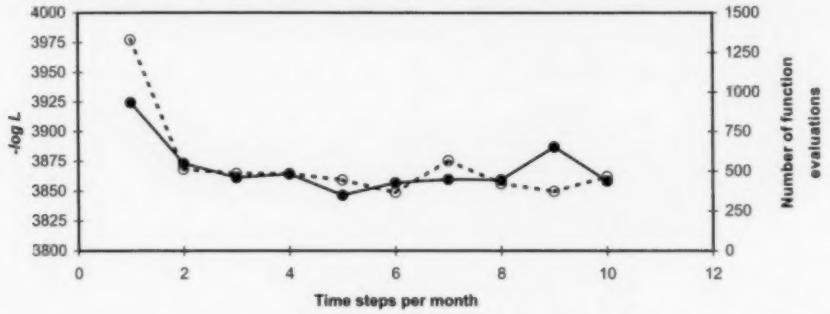

Fig. 4. Effect of length of recapture period (time since last tag release) on estimation of natural mortality rate (solid circles). Also shown is the value of the negative log likelihood function at convergence (triangles) and the predicted number of recaptures (open circles).

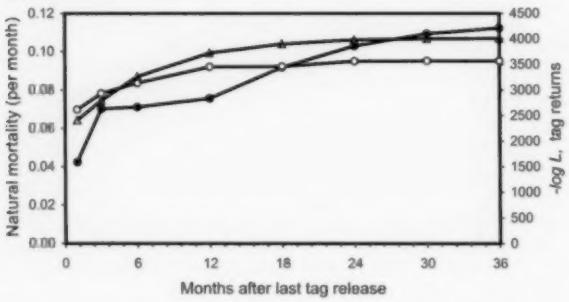

parameter estimation are presented. Solutions to eq. 2 using different approximations and different time steps are in effect different models from the standpoint of maximizing eq. 14. The effects of step size on the function minimization process are shown in Fig. 3 for the upwind approximation. Similar solutions were reached at most time steps. Six time steps per month is the method used unless otherwise noted.

The estimate of M is dependent on the time elapsed since the last release of tagged fish. Figure 4 shows the change in likelihood and change in the estimated value of M as the time since the last release is increased. It appears that it necessary to wait at least 2 years after all tags have been released before a reliable estimate of M can be obtained. A 36-month recapture period was routinely used for the results that follow.

Variability of movement was explored by comparing models with different numbers of "seasons". The single-season model with 10 regions (Fig. 2) has 36 estimated parameters: three movement parameters for each of the 10 regions, one catchability coefficient (Q_f) for each of the five fleets, and one natural mortality coefficient (M). All possible models with two seasons of 6-month duration were estimated. The two seasons per year models each have 66 parameters: three movement parameters for each of the 10 regions for each of the two seasons in addition to the six parameters for M and Q_f. Table 2 shows the values of the likelihood function for these models. The best fit is obtained for a model in which the seasons start in March and September. Other two-season models are possible, but only those with seasons of 6-month duration were tested.

The best two-season model (model 2) can be compared with the single-season model. The single-season model has 36 estimated parameters with a negative log likelihood value of 4214.79. In contrast, the best two-season model has 66 estimated parameters with a negative log likelihood value of 4007.71. The significance of the improvement in fit of the two-season model over the one-season model can be tested using a likelihood ratio test (Brownlee 1965) in which twice the difference between the negative log likelihood for the two models is interpreted as a χ^2 variable with degrees of freedom equal to the difference in numbers of parameters estimated in the two models. In this case, the χ^2 value is 414.16 with 30 df, and the difference is significant with $P < 0.001$. A two-season hypothesis is therefore more consistent with the observed tag returns than is a single-season hypothesis.

The preceding process was extended to compare all possible models with four seasons of 3-month duration. These results are also presented in Table 2. The increase to four seasons produces a significant improvement in fit, with the best fit occurring for a seasonal pattern with seasons beginning in March, June, September, and December. The negative log likelihood decreases from 4007.71 (66) to 3854.56 (126) or $\chi^2(60) = 306.30$, again significant with $P < 0.001$.

Increasing the number of strata always increases the possibility that some strata will not contain any observations. Bills and Sibert (1997) showed that parameters for season × region strata with low numbers of tag returns are not estimated accurately in simulations. Some of the strata in the four-season models had no observations, as indicated in Table 2. Therefore, no movement hypotheses with more than four seasons were tested.

Variability in movement was further tested by dividing the data into two periods spanning the early and late parts of the SSAP study. The tag release interval for the first period was October 1977 through December 1979 with recaptures through January 1980. The tag release interval for the second period was February 1980 through August 1980 with recaptures through August 1982. The M and Q_f were fixed at the estimates for the two-season model (see discussion on effects of the length of the recovery period on estimates of mortality). The results are presented in Table 3. The aggre-

© 1999 NRC Canada

Table 2. Hypothesis tests for increasing the number of "seasons" per year.

	Starting month	–log L	Empty strata
Model 1. Single season (n = 36)		4214.79	
Model 2. Two seasons (n = 66)	1, 7	4056.46	
	2, 8	4020.03	
	3, 9	4007.71	
	4, 10	4059.42	
	5, 11	4092.81	
	6, 12	4100.96	
	7, 1	4019.84	
Model 4. Four seasons (n = 126)	1, 4, 7, 10	3886.39	2
	2, 5, 8, 11	3961.92	3
	3, 6, 9, 12	3854.56	1
	4, 7, 10, 1	3881.38	2

Note: The movement hypotheses are identified by the number of seasons per year (single, two, or four), number of parameters estimated (n), and the starting month of each season in the hypothesis. The underlined likehood values indicate the best fit to the data within each model. The number of season × region strata with no reported recaptures is given for the four-season hypotheses. No emply strata occurred in the single- and two-season models.

Table 3. Hypothesis testing for dividing the SSAP tagging study into two periods.

	Model 2 Two seasons	Model 2A Period I	Model 2B Period II	Model 2C Aggregate
Cohorts	159	124	35	159
Tags released	94 430	64 186	30 244	94 430
Tags recaptured	4 211	2 495	1 716	4 211
–log L	4 007.71	1 726.49	1 767.67	3 494.16
Parameters	66	66	66	132
Empty strata	0	0	1	1

Note: "Aggregate" is the sum of periods I and II. The underlined likehood value indicates the best fit to the data.

gate likelihood for the two periods is 3561.51 and the χ^2 value is 1027.10, a significant improvement in fit at $P < 0.001$. The hypothesis in which the seasonal movements vary among years is more consistent with the observed tag returns than is a hypothesis in which the same pattern of movement repeats each year.

Spatially resolved models predict both temporal and spatial distributions of tag recaptures. Figure 5 displays the aggregate distribution of observed and predicted tag returns from model 2 summed over the entire period of the analysis. Agreement is generally good, particularly for grid cells with large numbers of returns. Figure 6 shows the total observed and predicted returns from model 2 summed over the entire model domain plotted by calendar month. Sharp peaks in tag returns occur immediately following releases of large tag cohorts. These large numbers of returns are predicted fairly well by the model. Figure 7 shows observed and predicted returns summed over the entire model domain as a function of the time that the tagged fish were at liberty. Again, agreement in time of recapture between observed and predicted is good even for short times at liberty.

Table 4. Comparison of tropical (regions 1–8) and subtropical (regions 9 and 10) movement parameters for model 2 and division of the study into two periods.

Season	Region	$\|u\|$	$\|v\|$	$\bar{D}$
March–August (cool)	Tropical	120.9	99.6	7 504.3
	Subtropical	101.7	100.21	845.7
September–February (warm)	Tropical	132.6	50.5	24 376.5
	Subtropical	0.4	38.3	29.2

Note: $|u|$ and $|v|$ are the root mean squared averages of u and v, respectively, and $\bar{D}$ is the arithmetic mean of the estimates of D over the indicated region.

The estimated movement pattern for the two-season, 10-region model (model 2) shows considerable spatial variability in both directed and random components of movement, but with suggestions of large-scale spatial consistency (Fig. 8). There is consistent eastward and southward directed movement in regions 3, 5, 6, 7, and 8 during the September–February season. Directed movements in region 10 are northward in the March–August season and southward in the September–February season. Seasonal differences are more pronounced when the tropical (regions 1–8) and subtropical (regions 9 and 10) model regions are compared (Table 4). During the March–August period (the Southern Hemisphere cold season), the zonal and meridional components of directed movement are of about equal magnitude in both tropical and subtropical regions; diffusive movement is greater in tropical than in subtropical regions. In contrast, during the September–February period (the Southern Hemisphere warm season), the zonal component of directed movement is much greater than the meridional component in the tropical region, whereas the reverse is true in the subtropical region; diffusive movement is much greater in the tropical than in the subtropical region.

Estimates of all parameters and approximate coefficients of variation for the two-season fit (model 2) are tabulated in Appendix B for reference.

Discussion

Accurate finite difference approximation of the advective terms in eq. 2 is a well-known problem in numerical analysis. The upwind difference approximation introduces "numerical viscosity" into the solution that stabilizes the numerical solution, but may also introduce bias in the estimates of the diffusion coefficients, D. Low estimates of D are evident in some of the region × season strata shown in Fig. 8. Nevertheless, the model appears to give accurate predictions of both the temporal and spatial distribution of tag returns. This result and the results reported by Bills and Sibert (1997) show that introduction of numerical viscosity is probably not important as long as the parameter values estimated using the upwind approximation are used in prediction algorithms that also use upwind approximations. In this sense, the computer program (approximation method, time step, spatial resolution, and boundary conditions) rather than

© 1999 NRC Canada

Fig. 5. Spatial distribution of observed and predicted (model 2) skipjack tuna tag returns summed over time. Each one-degree area of the model region is divided into two triangles, the northwest triangle representing the observed and the southeast triangle representing the predicted tag returns. The color of the triangles represents the number of returns on a logarithmic scale. Two triangles forming a square of uniform color indicate close agreement between observed and predicted recaptures in a one-degree geographic area. Geographic boundaries are the same as in Fig. 2.

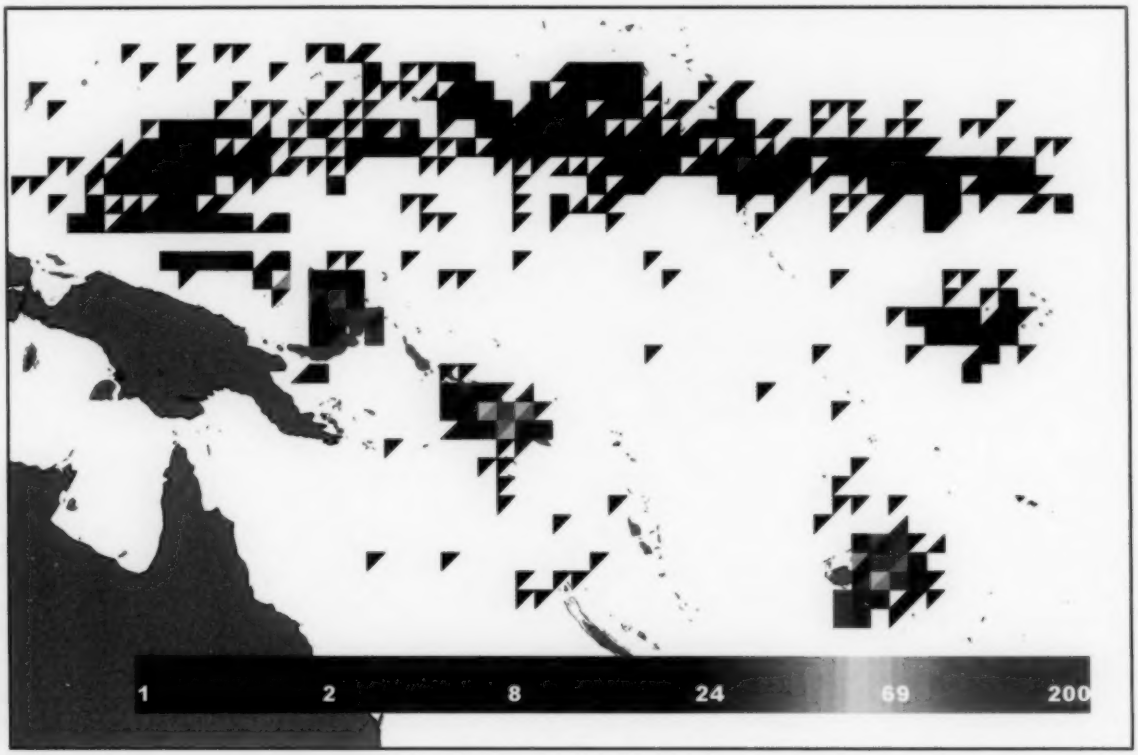

the PDE is the model. Discrepancies might occur if specific numerical values of the diffusion parameters were of interest. For example, if comparison of estimates of movement parameters between species or computation of movement parameters from environmental information were of interest, alternative approximations to the advective terms might be more appropriate. Less dispersive approximations are available in the numerical methods literature (e.g., Leonard 1979; Roe 1996), but they tend to be more difficult to implement and require more computational steps. These methods are currently under investigation for use in tuna movement analysis. In the meantime, O'Brien's (1986) criticism of the use of upwind differencing in fluid dynamics models suggests a potentially useful method to approximate the amount of numerical dispersion introduced by upwind differencing. A derivation of the correction is given in Appendix C, and "corrected" diffusion estimates based on it are included in Appendix B.

The model presented in this paper introduces a quantitative framework for expressing the movement of tagged fish and, perhaps more importantly, introduces means to objectively test alternative movement hypotheses. Statistically significant differences in skipjack movement patterns are detectable in the SSAP data, and movement appears to be highly variable in time and space. There is, however, some degree of spatial consistency in the estimated patterns. The north–south movements noted in region 10 were previously noted in the context of exchange of fish between Fiji and New Zealand (Kearney 1982; Argue and Kearney 1983) and in the context of interaction between widely separated fisheries (Kleiber et al. 1984). Whether this particular movement represents a response to seasonal changes in habitat quality or to trophic and spawning taxes is a matter for speculation (Gauldie and Sharp 1996). Variability in movement on annual or longer time scales is not surprising given the likely response of tuna populations to environmental variation, such as that mediated by the El Niño – Southern Oscillation (Lehodey et al. 1997).

In general, agreement in both time and place of predicted and observed tag returns is excellent. Sporadic, isolated single returns are not well predicted, which should not be surprising. More importantly, the agreement between observed and predicted tag recaptures for short times at liberty in the aggregate attrition curve (Fig. 7) is very encouraging. This result represents a substantial improvement over previous analyses of these data using a spatially aggregated model in which the data for short periods at liberty were excluded from the analysis (Kleiber et al. 1987). Spatially aggregegated models make the implicit assumption that tagged fish mix instantaneously through the population in a very large

© 1999 NRC Canada

Fig. 6. Observed (solid circles) and predicted (solid line) tag returns over the time course of the tagging study summed over the model area. The broken line indicates the predicted tag returns from the spatially aggregated model.

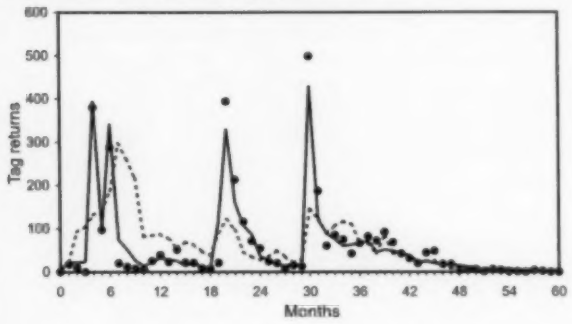

Fig. 7. Observed (solid circles) and predicted (solid line) tag returns over the life of each tag release cohort summed over the model area. The broken line indicates the predicted tag returns from the spatially aggregated model.

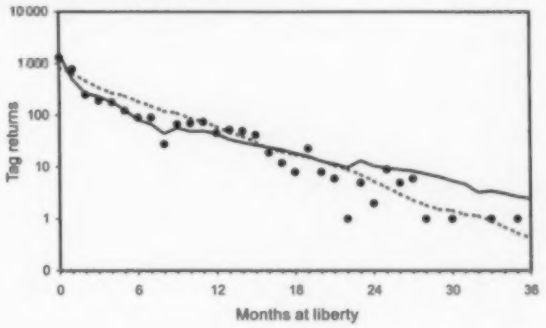

Fig. 8. Estimated movement pattern for model 2. The length of the arrows is proportional to the resultant directed movement component (u, v), and the areas of the circles are proportional to the random movement component (D). The arrow in the legend inset represents directed movement of 100 Nmi·month^{-1}; the circle represents random movement of 3000 Nmi^2·month^{-1}. Geographic coordinates are the same as in Fig. 2.

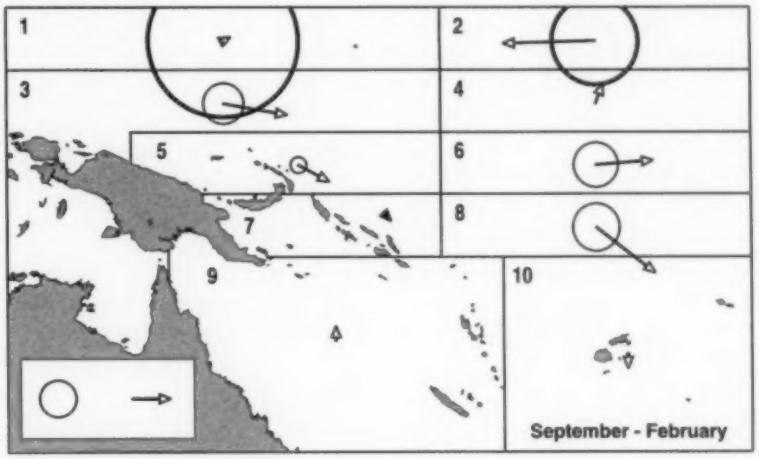

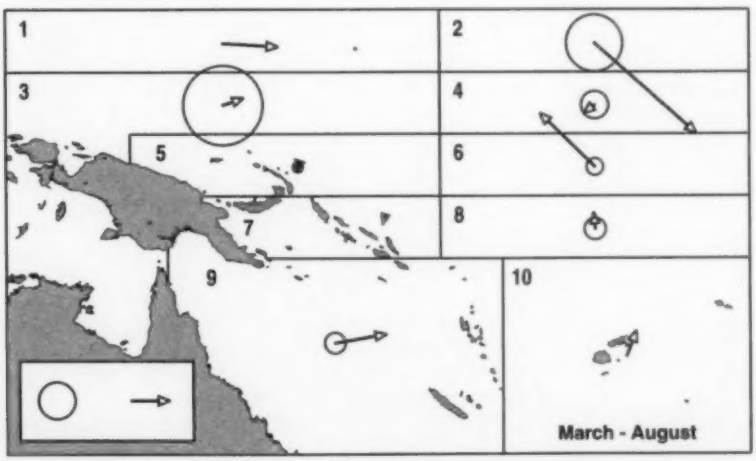

© 1999 NRC Canada

and undefined area. The model presented here makes the assumption that mixing of tags occurs within a single computational element of 60 × 60 Nmi, a much weaker assumption.

We fitted a model similar to that of Kleiber et al. (1987) to the same data used in the present analysis, obtaining estimates of m and q_f as the spatially aggregated analogs of natural mortality and catchability coefficients. This six-parameter model has a negative log likelihood function value of 5023.04. The likelihood ratio comparison with model 2 is 2030.66 with 60 df, significant with $P < 0.001$. The predicted tag returns from the aggregated model are also shown in Figs. 6 and 7 and demonstrate clearly the lack of fit at short times at liberty.

The spatially resolved estimate of natural mortality is about one half of the analogous estimate from the spatially aggregated model. The usual interpretation of "natural" mortality includes losses from the tag population that cannot be attributed to the recapture of tagged fish. Therefore, M is like fishing mortality for a fishing fleet that never reports catches. This distinction is important because the catchability coefficients, Q_f, are closely related to the predicted recaptures, whereas M is a "residual" mortality related to tagged fish that were never recaptured or were recaptured outside the model domain. In the spatially resolved model, the model domain is precisely defined, and movement of tagged fish within the model domain is explicitly parameterized. In a spatially aggregated model, the model domain is not well defined, and emigration of tagged fish from the fishing grounds could be a major component of natural mortality. The extent to which such movement is explicitly captured by the spatially resolved model depends on the size of the model domain in relation to the distribution of the tagged population and whether closed or open boundaries are specified. In the present analysis, using open boundaries or increasing the size of the model domain had little effect on the estimate of M, indicating that emigration from the model domain is probably not a major component of the estimated M.

Estimates of skipjack natural mortality from spatially aggretated analyses are known to be size dependent, with highest mortality at smallest and largest sizes (South Pacific Commission 1996). However, since most of the fish tagged by the SSAP were greater than 40 cm fork length, the assumption of constant M is justified for most of the period at liberty. The overestimation of recaptures at times at liberty greater than 18 months (Fig. 7) could be attributed to increasing natural mortality for these older fish. Age- or size-structured versions of the diffusion model are possible, requiring solutions of eq. 2 for each age or size cohort. Such models are probably feasible with the current generation of personal computers.

Interpretations of the estimates of M and Q_f are complicated by nonreporting of tag recaptures. Our analysis assumes complete reporting; failure of this assumption would tend to cause overestimates of M and underestimates of Q_f. If the numerical values of these parameters are of interest, accurate estimates of tag-reporting rates are required (Hampton 1997).

Tuna populations often span entire ocean basins. They are not uniformly distributed within their range, and the fisheries that exploit them are also not uniformly distributed. Inclusion of movement in assessment models for such widely distributed and mobile resources would seem essential. The diffusion equation appears to be well suited to describe the dynamics of tag movement, and using modern computer hardware and efficient estimation algorithms, it is possible to estimate movement parameters from tagging data. The diffusion equation may thus be a useful framework for quantitatively considering spatial heterogeneity when devising precautionary policies for "management...of highly migratory fish stocks *in their entirety*" (Lévy and Schram 1996, emphasis added).

Work is in progress to improve the approximation of the directed movement terms and to apply the model to other large-scale tagging data, including data for other species. Future work will be directed to inclusion of size-related natural mortality and selectivity, environmentally mediated movement (Bertignac et al. 1999), and estimation of movement in circumstances where extensive tagging data are not available.

Acknowledgments

The work described in this paper was initiated under the project Cooperative Research on Interaction in Pacific Tuna Fisheries administered by the Food and Agriculture Organization (FAO) of the United Nations. Subsequent work was sponsored by the University of Hawaii Pelagic Fisheries Research Program under Cooperative Agreement Nos. NA37RJ0199 and NA67RJ0154 from the National Oceanic and Atmospheric Administration (NOAA). The views expressed herein are those of the authors and do not necessarily reflect the views of FAO or NOAA or any of their subagencies. We are grateful to Mr. Peter Williams for assistance in preparation of the skipjack tagging data and the fisheries data used in this analysis.

References

Abbott, M.B., and Basco, D.R. 1989. Computational fluid dynamics: an introduction for engineers. Longman Scientific and Technical, Essex, U.K.

Argue, A.W., and Kearney, R.E. 1983. An assessment of the skipjack and baitfish resources of New Zealand. Skipjack Survey and Assessment Programme Final Country Rep. No. 6. South Pacific Commission, Noumea, New Caledonia.

Bard, Y. 1974. Nonlinear parameter estimation. Academic Press, New York.

Bayliff, W.H. 1971. Estimates of the rates of mortality of yellowfin tuna in the eastern Pacific Ocean derived from tagging experiments. Inter-Am. Trop. Tuna Comm. Bull. **15**: 379–436.

Bertignac, M., Lehodey, P., Hampton, J., and Andre, J.M. 1999. A spatial population dynamics simulation model of tropical tunas using a habitat index based on environmental parameters. Fish. Oceanogr. In press.

Beverton, R.J.H., and Holt, S.J. 1957. On the dynamics of exploited fish populations. Fish. Invest. Ser. II. Mar. Fish. G.B. Minist. Agric. Fish. Food, **19**.

Bills, P.J., and Sibert, J.R. 1997. Design of tag–recapture experiments for estimating yellowfin tuna stock dynamics, mortality and fishery interaction. Joint Inst. Mar. Atmos. Res. Tech. Rep. No. 97-313.

© 1999 NRC Canada

Brownlee, K.A. 1965. Statistical theory and methodology. John Wiley & Sons, New York.

Carnahan, B., Luther, H.A., and Wilkes, J.O. 1969. Applied numerical methods. John Wiley & Sons, New York.

Deriso, R.B., Punsly, R.G., and Bayliff, W. 1991. A Markov movement model of yellowfin tuna in the eastern Pacific Ocean and some analyses for international management. Fish. Res. **11**: 375–395.

Die, D.J., Restrepo, V.R., and Fox, W.W. 1990. Equilibrium production models that incorporate fished area. Trans. Am. Fish. Soc. **119**: 445–454.

Feller, W. 1968. An introduction to probability theory and its applications. Vol. I. 3rd ed. John Wiley & Sons, New York.

Gauldie, R.W., and Sharp, G.D. 1996. Skipjack velocity, dwell time and migration. Fish. Oceanogr. **5**: 100–113.

Griewank, A., and Corliss, G.F. 1991. Automatic differentiation of algorithms: theory, practice and application. SIAM, Philadelphia, Pa.

Hampton, J. 1991. Estimation of southern bluefin tuna *Thunnus maccoyii* mortality and movement rates from tagging experiments. Fish. Bull. U.S. **89**: 591–610.

Hampton, J. 1997. Estimates of tag-reporting and tag-shedding rates in a large-scale tuna tagging experiment in the western tropical Pacific Ocean. Fish. Bull. U.S. **95**: 68–79.

Hilborn, R. 1990. Determination of fish movement patterns from tag recoveries using maximum likelihood estimators. Can. J. Fish. Aquat. Sci. **47**: 635–643.

Hunter, J.R., Argue, A.W., Bayliff, W.H., Dizon, A.E., Fonteneau, A., Goodman, D., and Seckel, G. 1986. The dynamics of tuna movements: an evaluation of past and future research. FAO Fish. Tech. Pap. No. 227.

Ishii, T. 1979*a*. Estimating parameters of a fish population supplied by sequential recruitment. Invest. Pesq. **43**: 123–137.

Ishii, T. 1979*b*. Attempt to estimate migration of fish population with survival parameters from tagging experiment data by the simulation method. Invest. Pesq. **43**: 301–317.

Jones, R. 1959. A method of analysis of some tagged haddock returns. J. Cons. Cons. Int. Explor. Mer, **25**: 58–72.

Kearney, R.E. (*Editor*). 1982*a*. Methods used by the South Pacific Commission for the survey and assessment of skipjack and baitfish resources. Tuna and Billfish Assessment Programme Tech. Rep. No. 7. South Pacific Commission, Noumea, New Caledonia.

Kearney, R.E. 1982*b*. An assessment of the skipjack and baitfish resources of Fiji. Skipjack Survey and Assessment Programme Final Country Rep. No. 1. South Pacific Commission, Noumea, New Caledonia.

Kearney, R.E. 1983. Assessment of the skipjack and baitfish resources in the central and western tropical Pacific Ocean: a summary of the Skipjack Survey and Assessment Programme. South Pacific Commission, Noumea, New Caledonia.

Kleiber, P., and Hampton, J. 1994. Modeling effects of FADs and islands on movement of skipjack tuna (*Katsuwonus pelamis*): estimating parameters from tagging data. Can. J. Fish. Aquat. Sci. **51**: 2642–2653.

Kleiber, P., Argue, A.W., Sibert, J.R., and Hammond, L.S. 1984. A parameter for estimating potential interaction between fisheries for skipjack tuna (*Katsuwonus pelamis*) in the western Pacific. Tuna and Billfish Assessment Programme Tech. Rep. No. 12. South Pacific Commission, Noumea, New Caledonia.

Kleiber, P., Argue, A.W., and Kearney, R.E. 1987. Assessment of Pacific skipjack tuna (*Katsuwonus pelamis*) resources by estimating standing stock and components of population turnover from tagging data. Can. J. Fish. Aquat. Sci. **44**: 1122–1134.

Laloë, F. 1989. Un modèle global avec quantité de biomass inacessable dépendant de la surface de pêche. Application aux données de la pêche d'albacores (*Thunnus albacares*) de l'Atlantique est. Aquat. Living Resour. **2**: 231–239.

Lehodey, P., Bertignac, M., Hampton, J., Lewis, A., and Picaut, J. 1997. El Niño Southern Oscillation and tuna in the western Pacific. Nature (Lond.), **389**: 715–718.

Leonard, B.P. 1979. A stable and accurate convective modeling procedure based on quadratic upstream differencing. Comput. Methods Appl. Mech. Eng. **19**: 59–98.

Lévy, J., and Schram, G.G. 1996. United nations conference on straddling fish stocks and highly migratory fish stocks. Selected documents. Martinus Nijhoff, The Hague, The Netherlands.

MacCall, A.D. 1990. Dynamic geography of marine fish populations. University of Washington Press, Seattle, Wash.

Mullen, A.J. 1989. Aggregation of fish through variable diffusivity. Fish. Bull. U.S. **87**: 353–362.

Neuman, S.P. 1981. An Eulerian–Lagrangian scheme for the dispersion–convection equation using conjugate space–time grids. J. Comp. Physiol. **41**: 270–294.

O'Brien, J.J. 1986. The hyperbolic problem. *In* Advanced physical oceanographic numerical modeling. *Edited by* J.J. O'Brien. D. Reidel, Dordrecht, The Netherlands.

Okubo, A. 1980. Diffusion and ecological problems: mathematical models. Springer, New York.

Porch, C.E. 1995. Trajectory-based approaches to estimating velocity and diffusion from tagging data. Fish. Bull. U.S. **93**: 694–709.

Press, W.H., Flannery, B.P., Teukolsky, S.A., and Vetterling, W.T. 1988. Numerical recipes in C. Cambridge University Press, New York.

Price, H.S., Varga, R.S., and Warren, J.E. 1966. Application of oscillation matrices to diffusion–convection equations. J. Math. Phys. **XLV**: 301–311.

Roache, P.J. 1972. Computational fluid dynamics. Hermosa Publishers, Albuquerque, N. Mex.

Roe, P. 1996. Upwinding without dissipation. *In* Advances in computational fluid dynamics. *Edited by* C. Liu and Z. Liu. Louisiana Tech University, Ruston, La.

Sibert, J.R. 1984. A two-fishery tag attrition model for the analysis of mortality, recruitment, and fishery interaction. Tuna and Billfish Assessment Programme Tech. Rep. No. 13. South Pacific Commission, Noumea, New Caledonia.

Sibert, J.R., and Fournier, D.A. 1994. Evaluation of advection–diffusion equations for estimation of movement patterns from tag recapture data. *In* Proceedings of the First FAO Expert Consultation on Interactions of Pacific Ocean Tuna Fisheries, 3–11 December 1991, Noumea, New Caldeonia. Vol. 1. Summary report and papers on interaction. *Edited by* R. Shomura, J. Majkowski, and S. Langi. FAO Fish. Tech. Pap. **336/1**: 108–121.

Skellam, J.G. 1951. Random dispersal in theoretical populations. Biometrika, **38**: 196–218.

South Pacific Commission. 1996. Status of tuna stocks in the western and central Pacific Ocean. Working Pap. 3. Ninth Standing Committee on Tuna and Billfish Meeting, 22–23 July 1996. South Pacific Commission, Noumea, New Caledonia.

Tyler, J.A., and Rose, K.A. 1994. Individual variability and spatial heterogeneity in fish population models. Rev. Fish Biol. Fish. **4**: 91–123.

© 1999 NRC Canada

Appendix A. Applicability of diffusion models to fish movement

The applicability of diffusion models to fisheries in general and to skipjack tuna in particular has been criticized recently (Gauldie and Sharp 1996). These criticisms are based on common misconceptions about diffusion models. We present some general material that we hope will clarify diffusion models and correct some erroneous interpretations. The following presentation is based loosely on material presented by Okubo (1980) and Feller (1966, 1968). Readers requiring more detail and complete mathematical derivations are referred to these references.

The diffusion equation can be derived from the concept of a simple random walk in which an animal is assumed to move a constant small distance, λ, in a constant small interval of time, τ, as shown schematically below in one dimension:

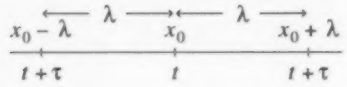

At time 0, the animal is at position x_0 and can move either to the right with probability P_1 or to the left with probability P_2. At time $t + \tau$, the animal is at position $x_0 + \lambda$ with probability P_1 or at position $x_0 - \lambda$ with probability P_2. The difference in probability of moving to the left or to the right is $\varepsilon = P_1 - P_2$, or bias.

Okubo (1980) showed that

$$\text{(A1)} \quad \lim_{\lambda,\tau,\varepsilon \to 0} \varepsilon\ (\lambda/\tau) = u \qquad \lim_{\lambda,\tau \to 0} \lambda\ (\lambda/\tau) = \frac{D}{2}$$

and that the rate of change in density of animals at a point can be expressed as

$$\text{(A2)} \quad \frac{\partial N}{\partial t} = -u\frac{\partial N}{\partial x} + \frac{D}{2}\frac{\partial^2 N}{\partial x^2}.$$

This equation is the special case of eq. 2 in one dimension without mortality and gradients in u and D. The quantity λ/τ has the dimensions of speed. The constant movement implied by this quantity is characteristic of obligate swimmers such as tunas, and the presence of such a quantity in the derivation of the diffusion equation argues strongly for its applicability to skipjack. There is no direction implied by λ/τ. Direction is given to movement by the bias, ε. Thus, it is possible for the directed movement term, u, to be zero without implying that the animals are immobile. Rather, $u = 0$ because there is no preferred direction to their movements. The quantity λ/τ also appears in the diffusion parameter D and can be interpreted as a "characteristic speed" parameter.

The model presented in this paper implicitly interprets ε and λ, and hence u and D, to be determined by time and place (i.e., season and region) as might be appropriate for an animal with well-defined seasonal migratory pathways. In principal, it is equally possible to parameterize ε and λ in terms of gradients in environmental variables such as sea surface temperature, depth of the oxycline, or forage (Bertignac et al. 1999). The result would be a model in which all movement is determined by features of the environment.

The diffusion equation is closely related to the normal probability distribution. Feller (1968) showed that if the probability of observing an animal at point x at time t is given as a normal probability density function

$$\text{(A3)} \quad p(t,x)\frac{1}{\sqrt{2\pi Dt}}e^{-\frac{1}{2}\frac{(x-ut)^2}{Dt}}$$

the function p uniquely satisfies eq. A2. In other words, if animals are dispersing according to eq. A2, after a period of time t, their mean position will be given by ut and the variance of their position will be Dt. Thus, u can be considered to be the average rate of displacement (which may be zero) and D a measure of the rate at which the variance of the displacement increases with time, or spreading rate (Feller 1966).

Simple diffusion models are not very interesting without augmentation. If $u = 0$ in eq. A2, the equilibrium condition is achieved when all horizontal gradients in population density vanish, i.e., no spatial heterogeneity, $\partial N/\partial x = 0$. This case is, of course, the "heat equation" used to describe the distribution of heat in a uniform plate. Various authors who have used diffusion models to describe spatial heterogeneity have introduced additional structure into the diffusion framework. For instance, MacCall (1990) introduced spatially variable logistic population growth and linked the advective parameter u to the instantaneous growth rate. Similarly, Mullen (1989) also introduced spatially variable logistic population growth, but linked the diffusive parameter to local carrying capacity.

Spatial heterogeneity can also be achieved using a diffusion model in which there are spatial gradients in the advective terms, i.e., $\partial u/\partial x \neq 0$. Such variability can be introduced explicitly as in eq. 2 with the term $(\partial/\partial x)(uN)$. Alternatively, the diffusive term can be expressed as $(\partial^2/\partial x^2)(DN)$, which introduces "implicit" advection equal to $\partial D/\partial x$ (which has the same units as velocity). This parameterization may be preferable in some situations (Okubo 1980) but limits the amount of advection that can be expressed by the model.

The diffusion model presented in eq. 2 is one of a large class of models that can be applied to the analysis of spatial variation in ecology and fisheries. Other models can be derived by making alternative assumptions about the underlying process,

© 1999 NRC Canada

e.g., random walks where the step size is not uniform (Schlesinger and Klafter 1985) or correlated (Okubo 1980). The challenge for fisheries is not whether the diffusion framework is suitable, but rather to explicitly include population movement and spatial structure in stock assessment models. Diffusion models are one class of models that appear to work.

References

Feller, W. 1966. An introduction to probability theory and its applications. Vol. II. John Wiley & Sons, New York.

Schlesinger, M.F., and Klafter, J. 1985. Levy walks versus Levy flights. *In* On growth and form. *Edited by* H. Stanley and N. Ostrowski. Martinus Nijhof Rub, Amsterdam, The Netherlands.

Appendix B. Numerical values of all estimated model parameters with coefficients of variation

Table B1. Estimates and coefficients of variation (CV) of natural mortality, M, and catchability coefficients, Q_f, for the best two-season × 6-month model (2).

	Estimate	CV	Estimate from aggregated model
M (month^{-1})	0.11	0.013	0.20
Q_f of fleet			
Pole-and-line, Papua New Guinea	0.00041	0.0016	0.0000052
Pole-and-line, Solomon Islands	0.00040	0.0025	0.00000029
Pole-and-line, Fiji	0.0046	0.0040	0.0000080
Pole-and-line, Japan	0.00083	0.0058	0.000000094
Purse seine, Japan	0.0057	0.018	0.0000032

Table B2. Estimated movement parameters with approximate coefficients of variation given in parentheses.

Season	Region	Tag returns	u (Nmi·day^{-1})	v (Nmi·day^{-1})	D (Nmi^2·month^{-1})	$D + \tilde{D}$ (Nmi^2·month^{-1})
1	1	30	4.9 (0.021)	–0.30 (0.0013)	0.047 (0.021)	4 600 (0.020)
	2	2	8.9 (0.057)	–7.9 (0.043)	17 000 (0.23)	32 000 (0.11)
	3	73	1.8 (0.017)	0.64 (0.0057)	34 000 (0.093)	36 000 (0.087)
	4	238	–1.0 (0.0074)	–0.75 (0.0030)	4 100 (0.027)	5 700 (0.019)
	5	779	–0.14 (0.0010)	–0.41 (0.0012)	510 (0.0026)	999 (0.0015)
	6	3	–4.8 (0.027)	4.7 (0.017)	1 600 (0.079)	10 000 (0.018)
	7	285	–0.20 (0.0010)	–0.70 (0.0016)	110 (0.0095)	920 (0.0020)
	8	2	–0.14 (0.0065)	1.4 (0.0097)	2 400 (0.042)	3 900 (0.025)
	9	2	4.5 (0.0067)	0.78 (0.0023)	2 400 (0.013)	7 100 (0.0051)
	10	1309	0.87 (0.0011)	2.2 (0.0016)	8.5×10^{-5} (0.0087)	2 800 (0.0012)
2	1	114	0.68 (0.021)	0.34 (0.018)	120 000 (0.012)	120 000 (0.012)
	2	47	–8.1 (0.031)	–0.22 (0.0085)	40 000 (0.12)	47 000 (0.10)
	3	125	5.6 (0.020)	–0.989 (0.0069)	8 900 (0.048)	15 000 (0.028)
	4	251	0.67 (0.0059)	1.7 (0.0039)	3.0 (0.055)	2 200 (0.0031)
	5	137	2.7 (0.0048)	–1.5 (0.0047)	1 400 (0.015)	5 200 (0.0043)
	6	35	5.0 (0.033)	0.40 (0.0070)	11 000 (0.10)	16 000 (0.074)
	7	259	0.49 (0.0016)	–0.56 (0.0019)	41 (0.017)	990 (0.0016)
	8	11	5.1 (0.036)	–4.0 (0.016)	12 000 (0.0540	20 000 (0.035)
	9	20	0.017 (0.0082)	1.3 (0.0037)	2.9×10^{-3} (0.034)	1 200 (0.0036)
	10	490	0.0021 (0.0016)	–1.2 (0.0014)	58 (0.0088)	1 200 (0.0015)

Note: $D + \tilde{D}$ is the "corrected" estimate of total diffusive movement based on the derivation presented in Appendix C.

Appendix C. Approximating numerical dispersion

O'Brien's (1986) criticism of the use of upwind differencing in fluid dynamics simulations suggests a potentially useful method to approximate the amount of numerical dispersion introduced by upwind differencing. It is necessary to assume that there are no spatial gradients in the movement parameters to apply this correction, i.e., to assume that $\frac{\partial u}{\partial x} = \frac{\partial v}{\partial y} = \frac{\partial D}{\partial x} = \frac{\partial D}{\partial y} = 0$. Under these assumptions the upwind difference approximation, eq. 4, of the directed movement term for $u_{ij} > 0$ is

$$\text{(C1)} \quad u_{ij}\frac{\partial N}{\partial x} \simeq u_{ij}\frac{N_i - N_{i-1}}{\Delta x} = 2u_{ij}\frac{N_i - N_{i-1}}{2\Delta x}.$$

© 1999 NRC Canada

Adding a very particular zero, the approximation becomes

$$\text{(C2)} \quad u_{ij}\frac{\partial N}{\partial x} \simeq 2u_{ij}\frac{N_i - N_{i-1}}{2\Delta x} + 2u_{ij}\frac{N_{i+1} - N_{i+1}}{2\Delta x}$$

which upon rearrangement yields

$$\text{(C3)} \quad u_{ij}\frac{\partial N}{\partial x} \simeq u_{ij}\left(\frac{\Delta x}{2}\right)\frac{N_{i-1} - 2N_i + N_{i+1}}{(\Delta x)^2} + u_{ij}\frac{N_{i+1} - N_{i-1}}{2\Delta x}.$$

The right-hand term in eq. C3 is the centered-space approximation of the directed movement term, appropriate when $\frac{\partial u}{\partial x} = 0$. The left-hand term is a finite difference approximation for a second partial derivative in the x direction used for the random movement term appropriate when $\frac{\partial D}{\partial x} = 0$. The numerical dispersion introduced by upwind differencing is approximately $u_{ij}\left(\frac{\Delta x}{2}\right)$ for $u_{ij} > 0$. Similar derivations apply for $u_{ij} < 0$ as well as for the terms involving v_{ij}. The approximate amount of numerical dispersion is thus

$$\text{(C4)} \quad \tilde{D} = \frac{1}{2}\left(\Delta x|u| + \Delta y|v|\right).$$

Equation C4 approximates the bias introduced into the estimates of the random movement parameter by the use of upwind differencing in areas of the model domain where gradients in the movement parameters (u, v, D) are small, such as the interior parts of regions.

© 1999 NRC Canada

Emigration of age-0 chinook salmon (*Oncorhynchus tshawytscha*) smolts from the upper South Umpqua River basin, Oregon, U.S.A.

Brett B. Roper and Dennis L. Scarnecchia

Abstract: Two rotating smolt traps were used through 4 consecutive years to monitor emigrations of age-0 chinook salmon (*Oncorhynchus tshawytscha*) from two watersheds of the upper South Umpqua River basin, Oregon, U.S.A. The number of wild smolts moving past the mainstem South Umpqua River trap ranged from 26 455 in 1991 to less than 5000 in 1993. The number of wild smolts passing the Jackson Creek trap ranged from 13 345 in 1991 to 0 in 1993. Higher numbers of wild smolts were significantly ($P = 0.003$) correlated with higher numbers of prespawning adults counted in index reaches the preceding year. Timing of emigration of smolts was found to be significantly related to stream temperature ($P < 0.05$) and phase of the lunar cycle ($P < 0.05$) but not related to changes in discharge ($P > 0.05$). Median emigration dates, which varied over 9 weeks, were earlier when spring water temperatures were higher. On average, two thirds of yearly smolt runs occurred when the moon was either waning or new, even though these moon phases were present only about half of the time. Significantly ($P < 0.05$) more fish than expected emigrated past both traps when day length was increasing.

Résumé : On a utilisé deux pièges à smolts rotatifs durant 4 années consécutives pour surveiller l'émigration des quinnats (*Oncorhynchus tshawytscha*) d'âge 0 depuis deux sous-bassins du cours supérieur de la South Umpqua, en Oregon (É.-U.). Le nombre de smolts sauvages qui ont été dénombrés dans le piège du cours principal de la South Umpqua se situait entre 26 455 en 1991 et moins de 5 000 en 1993, et le nombre de ceux qui ont été recensés dans le piège du ruisseau Jackson, entre 13 345 en 1991 et 0 en 1993. Les effectifs élevés de smolts sauvages étaient corrélés significativement ($P = 0{,}003$) avec les effectifs élevés d'adultes dénombrés avant la fraye dans des tronçons témoins l'année précédente. On a observé que le moment de l'émigration des smolts était relié à la température de l'eau ($P < 0{,}05$) et à la phase du cycle lunaire ($P < 0{,}05$), mais n'était pas relié aux variations du débit ($P > 0{,}05$). Les dates médianes d'émigration, qui ont varié sur 9 semaines, étaient plus hâtives quand les températures printanières de l'eau étaient plus élevées. En moyenne, les deux tiers des smolts d'une année étaient en dévalaison quand la lune était déclinante ou nouvelle, même si ces phases de la lune n'étaient présentes que la moitié du temps. Un nombre de poissons significativement ($P < 0{,}05$) plus important que prévu sont passés par les deux pièges quand le jour allongeait.

[Traduit par la Rédaction]

Introduction

Chinook salmon (*Oncorhynchus tshawytscha*) smolts typically emigrate seaward from rivers in either their first or second spring following emergence (Gilbert 1913). The age at which seaward migration occurs is influenced by both genetic (Taylor 1990) and environmentally mediated developmental processes (Thorpe 1989). In general, smolts of stocks from more southern and coastal areas emigrate during their first spring, whereas smolts of stocks from more northern, inland areas emigrate at an older age (Carl and Healey 1983).

Received April 23, 1996. Accepted December 22, 1998. J13428

B.B. Roper[1] **and D.L. Scarnecchia.**[2] Department of Fish and Wildlife Resources, University of Idaho, Moscow, ID 83844-1136, U.S.A.

[1]Current address: Idaho Panhandle National Forest, 3815 Schreiber Way, Coeur d'Alene, ID 83814, U.S.A.
[2]Author to whom all correspondence should be addressed. e-mail: scar@uidaho.edu

Although considerable research has focused on understanding the physiological and genetic aspects of chinook salmon smolt emigrations (Carl and Healey 1983; Taylor 1988, 1990), much less information exists on the factors affecting the timing of these migrations (Nicholas and Hankin 1989). Overall, the timing and variation of smolt movements probably reflect past selection processes that have minimized mortality risk while maximizing growth (Riddell and Leggett 1981; Holtby et al. 1989).

Variation in the magnitude and timing of salmonid emigrations is influenced by a variety of factors including species (Groot and Margolis 1991), adult escapement, rearing history (Bilby and Bisson 1987), and size of juvenile fish (Ewing et al. 1984; Irvine and Ward 1989) as well as environmental factors such as stream temperature (Morrill 1972; Holtby et al. 1989), stream discharge magnitude and changes (Bjornn 1971), lunar cycle (Grau et al. 1981), and photoperiod (Wagner 1974; Zaugg et al. 1986). The importance of these factors on emigration magnitude and timing may vary greatly among years. To compound the difficulty of understanding emigration and its causes, the shape of the emigration curve may be influenced by the location within the

© 1999 NRC Canada

Fig. 1. Location of the two smolt traps within the South Umpqua River basin.

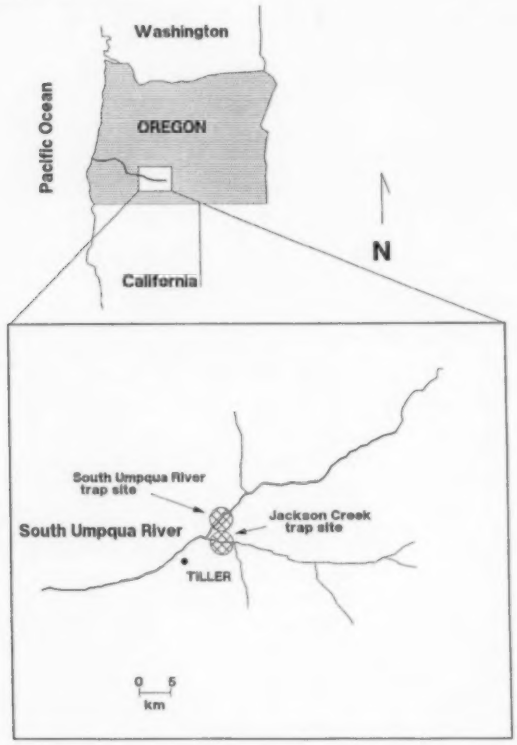

watershed where smolts are enumerated (Irvine and Ward 1989).

Understanding factors affecting the magnitude and timing of smolt emigrations is important for stock restoration and management. The objectives of this paper were to (*i*) characterize the magnitude and timing of age-0 chinook salmon emigrations from two adjacent basins in a southwestern Oregon, U.S.A., river system and (*ii*) relate the timing of these emigrations to adult escapement and four environmental factors: stream temperature, changes in stream discharge, lunar cycle, and photoperiod. For adult escapement, our null hypothesis was that the magnitude of smolt emigrations was unrelated to the number of adult fish returning to spawn the previous year. For environmental factors, our null hypotheses were that percentages of the total smolt emigrations would occur in proportion to the frequencies of occurrence, during the emigration period, of specific stream temperatures, daily changes in discharge, phases of the lunar cycle, and photoperiod.

Materials and methods

Study site

The study was conducted in two large drainages of the upper South Umpqua River basin, Oregon, U.S.A. (Fig. 1): the mainstem South Umpqua River drainage basin (area 78 567 ha) and the Jackson Creek drainage basin (area 37 297 ha). Stream width at the study sites during low flows was 20 m in the mainstem and 15 m at Jackson Creek. Discharge, riparian zone vegetation, and land use practices are described in Roper (1995).

Table 1. Percentage of age-0 chinook salmon populations emigrating between 15 April and 31 August estimated to have been missed due to trap malfunctions or traps not being deployed.

		Run missed due to trap malfunction, %	
Year	Rearing history	South Umpqua River	Jackson Creek
1991	Wild	2.9 (26 455)	4.2 (13 345)
	Hatchery	—	0.5 (47 453)
1992	Wild	14.8 (14 689)	0.0 (1635)
	Hatchery	0.0 (82 031)	—
1993	Wild	16.1 (4978)	0.0 (0)
	Hatchery	12.7 (85 537)	—
1994	Wild	0.1 (15 665)	0.0 (7394)
	Hatchery	—	—

Note: Run strength when traps were not operating was estimated using regression methods. Numbers in parentheses are the estimated total run size. Dashed indicate no hatchery fish released.

The stock of chinook salmon is small, averaging less than 300 returning adults annually (Oregon Department of Fish and Wildlife, Roseburg, Oreg.) and has a low probability of remaining viable through the next 100 years (Ratner et al. 1999). Surveys conducted for adult chinook salmon indicated that spawning occurred upstream from the confluence of the mainstem and Jackson Creek. For the entire distance between the ocean and the confluence of these rivers (314 km), no dams impede salmon migration.

Smolt trapping and population estimation

Traps

Age-0 chinook salmon were sampled and enumerated in the spring and summer, from 1991 to 1994, with two rotating smolt traps. The larger trap (2.44-m orifice) was located in the mainstem South Umpqua River 2 km upstream from its confluence with Jackson Creek; the smaller trap (1.52-m orifice) was located in Jackson Creek 1 km upstream from its mouth (Fig. 1). Cabling systems on both traps permitted operation in the area of greatest water velocity. Thedinga et al. (1994) described operation of traps of this design.

Traps were deployed in April or early May and removed in mid-October. Both traps were fished continuously, barring malfunctions, until the end of July. From August until mid-October, they were operated intermittently, typically 5 days out of 7. This April–October time period encompassed the period during which most of the age-0 smolts emigrated from the South Umpqua River watershed (Table 1). All captured fish were measured for fork length or randomly sampled for lengths if catches were large.

Population estimation

Trap efficiencies were determined by marking captured fish with one of four caudal fin marks and then transporting the marked fish 400 m above the trap site and releasing them into the stream so that they were available for recapture as they moved past the trap a second time. Four unique caudal marks were used because 99% of the recaptures from bimonthly releases at the Jackson Creek trap site in 1990 were subsequently recaptured within 4 days. The percentage of the marked fish recaptured was used to estimate trap efficiency (Seelbach et al. 1985). Trap efficiencies were determined independently at each trap site. Confidence intervals (CI) for trap efficiencies were calculated directly from the binomial distribution (Seber 1973; Dowdy and Wearden 1983). Trap efficiency averaged about 15% at both traps throughout the study.

© 1999 NRC Canada

Population estimates were determined by multiplying the number of unmarked fish captured in the trap by the inverse of the trap efficiency (Ricker 1975; Seelbach et al. 1985). For example, if trap efficiency was 20% and 100 unmarked fish were captured, then the estimate of that day's emigration was 500 fish ((1/0.2) × 100).

Daily population estimates were based on daily estimates of trap efficiency when the total number of recaptures from a daily release group exceeded seven. Because mark–recapture estimates are biased when recaptures are few (Robson and Regier 1964; Seber 1973; Jensen 1981), we combined several days' data (between 2 and 30 days) to estimate smolt populations over those days when the number of recaptures from a release group was less than seven.

On the few days when a trap either malfunctioned or was not operated, we used regression methods and the number of smolts emigrating before and after to estimate the number of smolts leaving when the trap was inactive (Seelbach 1993). For a more complete description of the methods used to estimate smolt populations, see Roper (1995) and Roper and Scarnecchia (1996).

In addition to wild fish, estimates of recently released hatchery-reared age-0 chinook salmon were made during those periods when hatchery fish were present. Hatchery fish were released into Jackson Creek during the spring of 1991 and into the mainstem during the springs of 1992 and 1993. In both rivers the releases occurred 20–30 km above the trap sites during the last week of May. Hatchery-reared fish were identifiable by the absence of an adipose fin. In 1992 and 1993, more than 98% of these fish were marked, whereas in 1991, only 52% were marked. Estimates of hatchery-reared smolts leaving Jackson Creek in 1991 were based on a near doubling of the counts of marked fish. The number of wild fish was then estimated as the total catch minus the estimated number of hatchery-reared fish. All future discussions and analyses in this paper refer strictly to wild fish unless stated otherwise.

Smolt emigrations

Magnitude

The total annual emigration was estimated as the sum of daily estimates between 15 April and 31 August. Differences in magnitude among years were examined with pairwise comparisons. Variations in the magnitude of annual smolt emigrations from the mainstem and Jackson Creek were assessed using the coefficient of variation.

Adult escapement

Indexes of adult salmon abundance in both the mainstem and Jackson Creek were based on the number of adults counted in selected large pools just prior to spawning (Oregon Department of Fish and Wildlife, Roseburg, Oreg.). Counts in index pools accounted for about 50% of the total number of adults within the basin (B.B. Roper, personal observation). Regression methods were used to relate an index of numbers of adults the previous fall in each of the two rivers to the number of smolts emigrating the following spring.

Timing

The timing of the smolt emigrations (both wild and hatchery reared) was characterized by the date of peak emigration (mode) and the date when half of the estimated total smolt emigration had occurred (median emigration date).

Environmental factors

For stream temperatures, we recorded daily values at midmorning (08:30–10:30) at both trap sites. We calculated the percentages of the observed emigration that occurred in six temperature ranges: <10, 10 to <12.5, 12.5 to <15, 15 to <17.5, 17.5 to <20, and ≥20°C. Under the null hypothesis, the percentage of the total emigration within each temperature range would not differ from the percentage of the trapping season within that temperature range. For example, if stream temperatures of less than 10°C were encountered during 10% of the trapping season, one would expect 10% of the total smolt run to have occurred within this temperature range. Deviations from the null hypothesis were evaluated using the χ^2 goodness-of-fit test. Because the large number of smolts leaving the basin would have resulted in extremely high statistical power (i.e., significant differences in cases when deviations from the null hypothesis were small), we standardized the total number of smolts (yearly) to 100 when making all goodness-of-fit comparisons (Gorman 1988; Roper et al. 1994). Linear regression methods were used to compare the day of year of median emigration (dependent variable) with average midmorning water temperatures from 1 May to 15 June.

For changes in discharge, we obtained daily mean discharges of the South Umpqua River basin from a permanent gauging station located at Tiller, Oreg. (United States Geological Survey gauge 1430800). Its location 8 km downstream from the confluence of the mainstem and Jackson Creek represented the summed discharge of the two rivers. We characterized changes in discharge as (*i*) rapidly decreasing: discharge was more than 10% lower than that of the previous day, (*ii*) slowly decreasing: discharge was >1 to 10% lower than that of the previous day, (*iii*) no perceptible change: discharge was within 1% if the previous day's discharge, (*iv*) slowly increasing: discharge was from >1 to 10% higher than that of the previous day, and (*v*) rapidly increasing: discharge was more than 10% higher than that of the previous day. Under the null hypothesis, if flow was slowly increasing 25% of the time that the traps were operating, we would have expected 25% of the fish to have emigrated under these conditions. Departure from the null hypothesis was assessed with a χ^2 goodness-of-fit test.

For lunar cycle, we calculated the percentage of fish emigrating at each of four moon phases: new moon, waxing towards a full moon, full moon, and waning toward a new moon (Moore 1990). For fish to have been considered to be emigrating during either the new or full moon phase, they had to have been captured during the 7 days nearest either the new or full moon. Fish captured on the days between the new and full moon were considered to be emigrating as the moon was waxing towards full; those fish captured in the days between a full and new moon were considered to be emigrating as the moon was waxing towards new. Under the null hypothesis, we expected about 25% of the fish to leave at each moon phase. Departure from the null hypothesis was tested with a χ^2 goodness-of-fit test.

For photoperiod, we assessed what portion of the total emigration was completed during the period of increasing day length (i.e., prior to 21 June). If a majority of the fish emigrated as day length increased, and timing of emigration was consistent among years, the hypothesis of emigration timing being related to photoperiod was supported.

Results

Smolt migrations

Magnitude

The number of wild age-0 spring chinook salmon emigrating varied significantly among years and between the two sites. For the South Umpqua River the number of smolts ranged from a high of 26 455 (95% CI = 19 073 – 50 658) in 1991 to a low of 4978 (95% CI = 3137 – 13 975) in 1993. The number of smolts leaving the Jackson Creek basin ranged from a high of 13 345 (95% CI = 8616 – 33 243) in 1991 to a low of 0 in 1993. In both rivers the number of

© 1999 NRC Canada

Fig. 2. Relationship between index of adult escapement (1990–1993) and smolt emigration the following spring (1991–1994) for the mainstem South Umpqua River (■) and Jackson Creek (Δ).

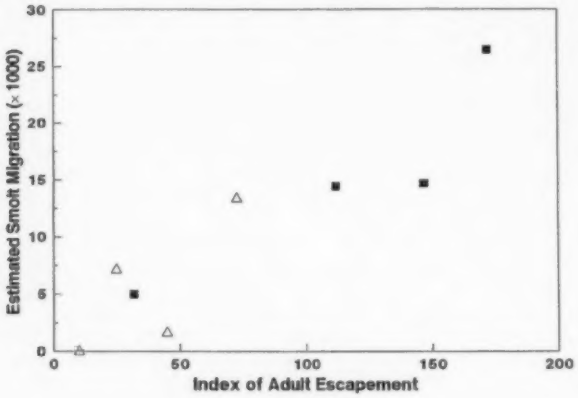

smolts decreased from 1991 to 1993 and then increased slightly in 1994.

The number of smolts leaving the mainstem was larger and more stable than in Jackson Creek. Although annual emigration from the mainstem averaged 15 456 fish, roughly three times that of Jackson Creek (5593), the coefficient of variation in the mainstem (57) was essentially half that of Jackson Creek (108).

During the period 1991–1993 the number of hatchery-reared age-0 chinook salmon emigrating from the upper South Umpqua River basin ranged from 47 453 to 85 537 (mean = 71 674). Hatchery-reared smolts constituted a progressively larger portion of the total emigration from 1991 to 1993: 75% in Jackson Creek in 1991, 80% in the mainstem run in 1992, and 93% in the mainstem run in 1993. Hatchery-reared fish accounted for more than 50% of the total age-0 chinook salmon emigration from the basin in all years that they were present. Because no fish, wild or hatchery reared, emigrated from Jackson Creek in 1993, hatchery-reared fish constituted more than 90% of the juvenile chinook salmon emigrating from the entire upper basin that year. Because the fraction of smolts that were hatchery reared was high from 1991 to 1993, discernment of emigration patterns of wild fish was dependent on hatchery-reared fish being marked.

Adult escapement

The number of wild smolts leaving each river was positively related to higher numbers of spawning adults the previous fall (South Umpqua, $r^2 = 0.67$, $P > 0.05$; Jackson Creek, $r^2 = 0.61$, $P > 0.05$; combined, $r^2 = 0.80$, $P = 0.003$) (Fig. 2). Counts of adult fish in the mainstem (112) were nearly three times higher than in Jackson Creek (38), whereas the coefficient of variation of adult counts was lower in the mainstem (50) than in Jackson Creek (71). Both the magnitude and variation in the number of adults were thus closely related to the magnitude and variation in the number of smolts.

Timing

Peak (modal) times of emigration varied up to 2.5 months among years of this study. In the mainstem, emigration peaked on 11 June in 1991, 29 April in 1992, 23 June in 1993, and 1 June in 1994. In Jackson Creek, emigration peaked on 11 July in 1991, 24 May in 1992, and 25 May in 1994.

The median emigration date of wild smolts (i.e., date by which half had emigrated) also differed between rivers and among years. In most cases, median emigration date occurred from 22 May to 11 June (Table 2) but occurred on 11 July in Jackson Creek in 1991 and on 8 May in the mainstem in 1992. In every case, peak emigration occurred within 2 weeks of, and usually within days of, the median emigration date (Table 2).

The emigration timing of hatchery-reared and wild smolts differed in the upper basin. In all three years, emigration of hatchery-reared fish peaked within 2 days of their release, and at least 10% of the total emigration occurred on a single day. In 1992, almost half of the hatchery fish emigrated on a single day. The date of median emigration for hatchery-reared fish occurred within 8 days of release in 1991, within 3 days of release in 1992, and within 20 days of release in 1993.

Smolt length

Although the dates when wild smolts first reached 50 mm in length varied among years by nearly a month (Table 3), lengths at emigration showed an interannual consistency. Nearly half (44%) of the annual emigrants from the mainstem from 1991 to 1994 were between 50 and 59.9 mm in length (Table 4). Less than 10% of the fish emigrated before they reached 50 mm or after they had reached 80 mm. A similar tendency for emigration at these lengths (50–59 mm) was found in Jackson Creek, but inadequate length data in 1991–1993 precluded firmer conclusions.

Environmental factors

Stream temperature

Higher average spring temperatures at the trap sites were associated with an earlier median emigration date of wild smolts ($r^2 = 0.78$, $P = 0.01$) (Fig. 3). Smolt emigrations past both traps began once stream temperature exceeded 10°C, were greatest when temperatures were between 12.5 and 15°C, and were nearly complete by the time stream temperatures exceeded 20°C (Table 5). Although stream temperatures in the mainstem ranged between 12.5 and 15°C on only 74 (13%) of the 556 days from 15 April to 31 August 1991–1994, on average, 50% of the annual emigration of wild age-0 chinook salmon occurred between these temperatures. In contrast, when temperatures were below 10°C (on 106, or 19%, of 556 days) and above 20°C (on 137, or 25%, of 556 days), less than 10% of the total wild smolt emigration occurred.

Movement of smolts through the Jackson Creek trap occurred at higher temperatures than the emigration through the mainstem trap. The largest percentage (43%) of the Jackson Creek fish left when stream temperatures were between 12.5 and 15°C, even though these temperatures were encountered only 9% of the time the traps were in operation. The year 1993 was excluded because no fish were captured that year. Deviations from the null hypothesis that emigration of smolts was equally likely at all stream temperatures

© 1999 NRC Canada

Table 2. Peak emigration dates and first emigration quartile (25%), median emigration quartile (50%), and third emigration quartile (75%) of age-0 chinook salmon emigrating from the South Umpqua River and Jackson Creek.

		Emigration quartile		
	Peak emigration	25%	50%	75%
South Umpqua River				
1991	11 June	8 June	11 June	22 June
1992	29 April	29 April	8 May	26 May
1993	23 June	4 June	19 June	2 July
1994	1 June	19 May	4 June	22 June
Jackson Creek				
1991	11 July	22 June	10 July	12 July
1992	24 May	21 May	25 May	28 May
1994	25 May	19 May	28 May	8 June

Table 3. Dates when age-0 chinook salmon smolt sizes (lower tail of a 95% CI) first exceeded 50, 60, and 70 mm.

	Fish size		
	50 mm	60 mm	70 mm
South Umpqua River			
1991	16 May	14 June	27 June
1992	29 April	15 June	14 June
1993	23 May	17 June	30 June
1994	14 May	5 June	16 June
Jackson Creek			
1994	16 May	7 June	21 June

Table 4. Percentage of total spring emigrations of age-0 chinook salmon within six length categories.

	Length category				
	<50 mm	50 to <60 mm	60 to <70 mm	70 to <80 mm	≥80 mm
South Umpqua River					
1991	2	58	20	16	4
1992	15	44	35	6	0
1993	8	37	21	26	8
1994	14	37	14	34	1
Average	10	44	22	21	3
Jackson Creek					
1994	13	52	19	16	0

were large and significant ($P < 0.01$) in both rivers and for all years.

Changes in discharge

For more than 60% of the days when traps were in operation, discharges were slowly decreasing, i.e., from >0 to 10% less below the previous day's flow. Nearly 70% of the smolts emigrated during these days. Deviations from the null hypothesis that emigration was proportional to the number of days in each of the five discharge categories were small and nonsignificant ($P > 0.05$). Wild smolts were evidently not relying on changes in discharge as an emigration cue.

Lunar cycle

Although smolts emigrated during all four lunar phases, in five of the seven monitored emigrations (mainstem, 1991, 1992, and 1994; Jackson Creek, 1991 and 1992), smolts were significantly ($P < 0.05$) more likely to have moved during the waning and new moon phases rather than during the waxing and full moon phases. On average, for all seven smolt runs, 66% of the smolts emigrated during the waxing and new moon phases, even though these phases constituted only half the emigration period.

Photoperiod

Significantly more fish than expected ($P < 0.05$) emigrated past both traps when day length was increasing. In six of the monitored emigrations (mainstem, 1991–1994; Jackson Creek, 1992 and 1994), at least 75% of the total spring emigration was completed prior to the summer solstice, whereas slightly less than 50% of the capture season occurred prior to this day. In only one case (Jackson Creek, 1991) did a majority of fish leave when day length was decreasing. The variation in annual emigration timing provides evidence that photoperiod (or a correlated variable) was a migratory cue.

Discussion

The strongly positive relationship between the number of adult chinook salmon in the upper South Umpqua River basin and the number of emigrating smolts the following year indicates the importance of adult escapement to smolt production, especially when adult escapement is low (Ricker 1975). The mere presence of adult salmon, however, did not guarantee smolt production the next year. Jackson Creek produced no juvenile chinook salmon in 1993, even though adults were seen in this creek the previous fall. It is thus important to estimate both juvenile and adult numbers, especially when populations are small.

Whereas the magnitude of annual smolt emigrations was consistently explained with just one variable, adult escapement, the timing of annual spring emigrations was more difficult to attribute to one environmental factor. Of the four environmental factors considered, stream temperature, changes in discharge, lunar cycle, and photoperiod, three, stream temperature, lunar cycle, and photoperiod, were significantly related to emigration timing. A central problem in interpreting this result is the confounding effect resulting from correlation among environmental variables.

© 1999 NRC Canada

Table 5. Percentage of total spring age-0 chinook salmon emigrations within six temperature categories.

	Temperature category					
	<10°C	10 to <12.5°C	12.5 to <15°C	15 to <17.5°C	17.5 to <20°C	>20°C
South Umpqua River						
1991	5 (33)	19 (9)	53 (11)	2 (5)	8 (13)	13 (29)
1992	<1 (1)	1 (9)	67 (19)	18 (22)	7 (18)	7 (31)
1993	6 (26)	42 (20)	18 (8)	21 (21)	14 (22)	1 (3)
1994	3 (17)	4 (12)	59 (15)	17 (9)	16 (12)	3 (35)
Average	3 (19)	17 (13)	49 (13)	15 (14)	11 (16)	6 (25)
Jackson Creek						
1991	5 (35)	3 (11)	11 (8)	18 (11)	54 (21)	9 (14)
1992	<1 (1)	<1 (9)	47 (19)	37 (23)	12 (34)	3 (14)
1994	<1 (17)	5 (16)	72 (12)	17 (11)	4 (18)	2 (26)
Average	2 (18)	3 (12)	43 (13)	24 (15)	23 (24)	5 (18)

Note: Numbers in parentheses are the percentage of the total trap season (15 April to 30 August) within each temperature category.

Fig. 3. Relationship between average spring temperature and median emigration date of age-0 chinook salmon from the South Umpqua River (■) and Jackson Creek (Δ).

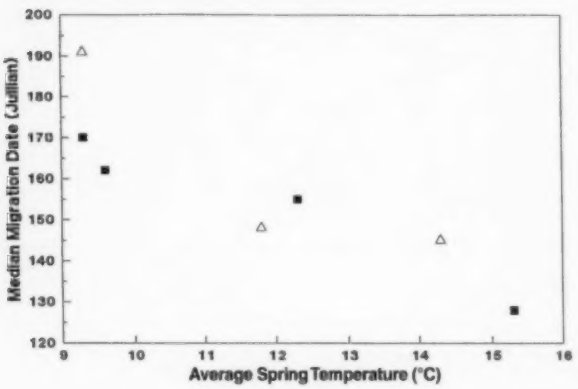

Of these three environmental factors, stream temperature explained the most variation in timing. An earlier median emigration date was consistently associated with higher average spring stream temperatures, and smolts emigrated within a narrow temperature range of 12.5–15°C. Timing of age-0 chinook salmon migrations was also related to temperature in a stream in British Columbia (Holtby et al. 1989). These authors and Rombough (1985) have suggested that the timing of emigration in age-0 smolts is influenced by stream temperature through controls on the rate of juvenile development. Cooler stream temperatures during winter and spring slow growth so that fish emerge and migrate later. In contrast, warmer stream temperatures accelerate juvenile development and hasten emigration in the spring. The idea that warmer water temperatures in spring could increase growth rates is supported by our data. Higher stream temperature were positively related to fish length within the South Umpqua River basin ($r^2 = 0.54$, $P \leq 0.001$; Roper 1995).

Although the positive relationship between stream temperature, fish size, and photoperiod (prior to 21 June) makes it difficult to distinguish their roles in controlling the emigration timing of wild smolts, water temperature rather than fish size or photoperiod evidently cued hatchery-reared fish. In 1992 and 1993 in the mainstem, when sizes of released hatchery fish were similar (85.1 and 83.3 mm) and releases occurred at nearly the same day length (30 May versus 26 May), the number of days after release when median emigration occurred was substantially different (3 versus 20 days). In 1992, when average spring water temperatures were 15.3°C, the median emigration occurred 17 days sooner than in 1993, when average stream temperatures were 9.9°C. This difference suggests that even large fish may emigrate later when water temperatures are low (Ewing et al. 1984).

The greater tendency for smolts to emigrate during the new and waning moon phases in this study is consistent with other research relating moon phase to smolt emigrations (Grau et al. 1981). Because wild smolts in the South Umpqua River basin emigrate primarily at night (Roper and Scarnecchia 1996), movements during dark moon phases may be an adaptation to minimize predation risk.

We found little evidence that changes in discharge cued smolt emigrations, even though this factor has been shown to be important in other salmonid stocks in different basins (Folmar and Dickoff 1980).

Our conclusion is that these factors, temperature, lunar cycle, and photoperiod, interacted to influence emigration timing. The exact nature of their interaction is probably influenced by other factors as well.

For example, the trapping location may also affect the observed relationship between smolt emigrations and abiotic variables (Irvine and Ward 1989). Both traps within the South Umpqua River basin were more than 300 km from the ocean. If the traps had been closer to the ocean, the relationships between stream temperature or moon phase and smolt emigrations may not have been evident as a result of the increased travel time or the addition of smolts from other streams within the basin. Relationships between the magnitude and timing of smolt emigrations and other biotic and abiotic factors must therefore be investigated with reference to the location and scale of monitoring (McArdle et al. 1990).

Inasmuch as our research supports the idea that the timing of age-0 smolt emigrations is temperature dependent (Hartman et al. 1982; Rombough 1985; Holtby et al. 1989), land management activities that warm stream temperatures (Brown and Krygier 1970; Hostetler 1991) will probably affect emigration timing (Holtby et al. 1989) and alter life his-

© 1999 NRC Canada

tory characteristics (Lichatowich et al. 1995) as well as affect the ultimate survival of smolts (Bilton et al. 1982). Because land management activities have already simplified many of the streams within the upper South Umpqua River basin (Dose and Roper 1994), future land use within this basin must be undertaken with regard to potential effects on smolt emigration and survival.

Acknowledgments

We thank L. Kruzic and S. Sundancer for help with field work and J. Dose for logistical support. We also thank J.C. Scrivener, T.G. Brown, and an anonymous reviewer for their helpful comments. Financial support for this research was provided by the U.S. Forest Service through the Umpqua National Forest, Roseburg, Oreg.

References

Bilby, R.E., and Bisson, P.A. 1987. Emigration and production of hatchery coho salmon (*Oncorhynchus kisutch*) stocked in streams draining an old-growth and a clear-cut watershed. Can. J. Fish. Aquat. Sci. **44**: 1397–1407.

Bilton, H.T., Alderdice, D.F., and Murray, C.B. 1982. Influence of time and size at release of juvenile coho salmon (*Oncorhynchus kisutch*) in returns at maturity. Can. J. Fish. Aquat. Sci. **39**: 426–447.

Bjornn, T.C. 1971. Trout and salmon movements in two Idaho streams as related to temperature, food, stream flow, cover and population density. Trans. Am. Fish. Soc. **100**: 423–438.

Brown, G.W., and Krygier, J.T. 1970. Effects of clear-cutting on stream temperatures. Water Resour. Res. **6**: 1133–1139.

Carl, L.M., and Healey, M.C. 1983. Coastwide distribution and ocean migration patterns of stream-type and ocean-type chinook salmon (*Oncorhynchus tshawytscha*). Can. Field-Nat. **97**: 427–433.

Dose, J.J., and Roper, B.B. 1994. Long-term changes in low-flow channel widths within the South Umpqua watershed, Oregon. Water Resour. Bull. **36**: 993–1000.

Dowdy, S., and Wearden, S. 1983. Statistics for research. John Wiley & Sons, New York.

Ewing, R.D., Hart, C.E., Fustish, C.A., and Concannon, G. 1984. Effects of size and time of release on seaward migration of spring chinook salmon, *Oncorhynchus tshawytscha*. Fish. Bull. U.S. **82**: 157–164.

Folmar, L.C., and Dickoff, W.W. 1980. The parr–smolt transformation (smoltification) and seawater adaptation in salmonids. A review of selected literature. Aquaculture, **21**: 1–37.

Gilbert, C.H. 1913. Age of maturity of the Pacific salmon *Oncorhynchus*. Bull. U.S. Bur. Fish. **32**: 1–22.

Gorman, O.T. 1988. The dynamics of habitat use in a guild of Ozark minnows. Ecol. Monogr. **58**: 1–18.

Grau, E.G., Nishioka, R.S., Bern, H.A., and Folmar, L.C. 1981. Lunar phasing of the thyroxine surge preparatory to seaward migration of salmonid fishes. Science (Washington, D.C.), **211**: 607–609.

Groot, C., and Margolis, L. 1991. Pacific salmon life histories. University of British Columbia Press, Vancouver, B.C.

Hartman, G.F., Anderson, B.C, and Scrivener, J.C. 1982. Seaward movement of coho salmon (*Oncorhynchus kisutch*) fry in Carnation Creek, an unstable coastal stream in British Columbia. Can. J. Fish. Aquat. Sci. **39**: 588–597.

Holtby, L.B., McMahon, T.E., and Scrivener, J.C. 1989. Stream temperatures and inter-annual variability of coho salmon (*Oncorhynchus kisutch*) smolts and fry and chum salmon (*O. keta*) fry from Carnation Creek, British Columbia. Can. J. Fish. Aquat. Sci. **46**: 1396–1405.

Hostetler, S.W. 1991. Analysis and modeling of long-term stream temperatures on the Steamboat Creek basin, Oregon: implication for land use and fish habitat. Water Resour. Bull. **27**: 637–647.

Irvine, J.R., and Ward, B.R. 1989. Patterns of timing and size of wild coho salmon (*Oncorhynchus kisutch*) smolts migrating from the Keogh River watershed on northern Vancouver Island. Can. J. Fish. Aquat. Sci. **46**: 1086–1094.

Jensen, A.L. 1981. Sample sizes for single mark and recapture experiments. Trans. Am. Fish. Soc. **110**: 455–458.

Lichatowich, J., Morbrand, L., Lestelle, L., and Vogel, T. 1995. An approach to the diagnosis and treatment of depleted Pacific salmon populations in Pacific Northwest watershed. Fisheries (Bethesda), **20**: 10–18.

McArdle, B.H., Gaston, K.J., and Lawton, J.H. 1990. Variation in the size of animal populations: patterns, problems and artifacts. J. Anim. Ecol. **59**: 439–454.

Moore, P.M. 1990. The amateur astronomer. W.W. Norton and Company, New York.

Morrill, C.F. 1972. Migration response of juvenile chinook salmon to substrates and temperature. M.S. thesis, University of Idaho, Moscow, Idaho.

Nicholas, J.W., and Hankin, D.G. 1989. Chinook salmon populations in Oregon coastal river basins: description of life histories and assessment of recent trends in run strengths. Oregon State University Press, Corvallis, Oreg.

Ratner, S., Lande, R., and Roper, B.B. 1999. Population viability of spring chinook salmon in the South Umpqua River. Conserv. Biol.

Ricker, W.E. 1975. Computation and interpretation of biological statistics of fish populations. Bull. Fish. Res. Board Can. No. 191.

Riddell, B.E., and Leggett, W.C. 1981. Evidence of an adaptive basis for geographic variation in body morphology and time of downstream migration of juvenile Atlantic salmon (*Salmo salar*). Can. J. Fish. Aquat. Sci. **38**: 308–320.

Robson, D.S., and Regier, H.A. 1964. Sample size in Petersen mark–recapture experiments. Trans. Am. Fish. Soc. **93**: 215–226.

Rombough, P.J. 1985. Initial egg weight, time to maximum alevin weight, and optimal ponding times for chinook salmon (*Oncorhynchus tshawytscha*). Can. J. Fish. Aquat. Sci. **42**: 287–291.

Roper, B.B. 1995. Ecology of anadromous salmonids within the upper South Umpqua basin, Oregon. Doctoral dissertation, University of Idaho, Moscow, Idaho.

Roper, B.B., and Scarnecchia, D.L. 1996. A comparison of trap efficiencies for wild and hatchery age-0 chinook salmon. N. Am. J. Fish. Manage. **16**.

Roper, B.B., Scarnecchia, D.L., and La Marr, T.J. 1994. Summer distribution of and habitat use by chinook salmon and steelhead within a major basin of the South Umpqua River, Oregon. Trans. Am. Fish. Soc. **123**: 298–308.

Seber, G.A.F. 1973. The estimation of animal abundance and related parameters. Charles Griffin and Company Limited, London, England.

Seelbach, P.W. 1993. Population biology of steelhead in a stable-flow, low-gradient tributary of Lake Michigan. Trans. Am. Fish. Soc. **122**: 179–198.

Seelbach, P.W., Lockwood, R.N., and Alexander, G.R. 1985. A modified inclined-screen trap for catching salmonid smolts in large rivers. N. Am. J. Fish. Manage. **5**: 494–498.

Taylor, E.B. 1988. Adaptive variation in rheotatic and agonistic be-

© 1999 NRC Canada

havior in newly emerged fry of chinook salmon, *Oncorhynchus tshawytscha*, for ocean- and stream-type populations. Can. J. Fish. Aquat. Sci. **45**: 237–243.

Taylor, E.B. 1990. Phenotypic correlates of life-history variation in juvenile chinook salmon, *Oncorhynchus tshawytscha*. J. Anim. Ecol. **59**: 455–468.

Thedinga, J.F., Murphy, M.L., Johnson, S.W., Lorenz, J.M., and Koski, K V. 1994. Determination of salmonid yield with rotary-screw traps in the Situk River, Alaska, to predict effects of glacial flooding. N. Am. J. Fish. Manage. **14**: 837–851.

Thorpe, J.E. 1989. Developmental variation in salmonid populations. J. Fish Biol. **35**(A): 295–303.

Wagner, H.H. 1974. Photoperiod and temperature regulation of smolting steelhead trout (*Salmo gairdneri*). Can. J. Zool. **52**: 219–234.

Zaugg, W.S., Bodle, J.E., Manning, J.E., and Wold, E. 1986. Smolt transformation and seaward migration in 0-age progeny of adult spring chinook salmon (*Oncorhynchus tshawytscha*) matured early with photoperiod control. Can. J. Fish. Aquat. Sci. **43**: 885–888.

© 1999 NRC Canada

Infection with low numbers of the sea louse *Lepeophtheirus salmonis* induces stress-related effects in postsmolt Atlantic salmon (*Salmo salar*)

D.T. Nolan, P. Reilly, and S.E. Wendelaar Bonga

Abstract: Infection of postsmolt Atlantic salmon (*Salmo salar*) with three, six, or 10 preadult and adult sea lice (*Lepeophtheirus salmonis*) per fish resulted in changes to epithelial structure and at sites in the skin and gill, distant from lice attachment and feeding. In the skin, increased apoptosis and necrosis occurred in the superficial epithelial cells and numbers of mucous cells decreased. In the gill, where no lice were found, uplifting of the epithelium, intercellular swelling, and infiltration by leukocytes occurred in filaments and lamellae. High cell turnover of chloride cells was associated with significantly elevated gill Na^+/K^+-ATPase activities. Serum chloride levels were elevated in the 3 and 6 lice/fish groups, and the serum Na to Cl ratio was lower in all parasitized groups at 5 days. The results indicate that infection with low numbers of the preadult and adult parasite induced changes characteristic of a stress response. In the low- and medium-infested groups, homeostatic recovery had occurred by 10 days, but recovery was incomplete in the highly infected group. Thus, 10 lice per fish, which is a low infestation level in nature, is stressful and creates a long period during which the overall condition of the skin and gill epithelia may render the fish susceptible to secondary infections.

Résumé : L'infection de post-smolts de saumon atlantique (*Salmo salar*) par trois, six ou 10 poux de poisson (*Lepeophtheirus salmonis*) pré-adultes et adultes par poisson a donné lieu à des changements dans la structure épithéliale et en des endroits sur la peau et les branchies éloignés du site de fixation et d'alimentation des poux. Sur la peau, on a observé un accroissement d'apoptose et de nécrose dans les cellules épithéliales superficielles, ainsi qu'une réduction du nombre de cellules muqueuses. Dans les branchies, où aucun pou n'était présent, on a observé un soulèvement de l'épithélium, un oedème intercellulaire et une infiltration de leucocytes dans les filaments et les lamelles. On a aussi observé un fort taux de renouvellement des cellules à chlorures, associé à des activités significativement élevées de la Na^+/K^+-ATPase branchiale. Les niveaux de chlorure sérique étaient élevés chez les poissons infectés par trois ou six poux, et le ratio Na à Cl dans le sérum était réduit chez tous les groupes parasités après 5 jours. Les résultats montrent que l'infection par un petit nombre de parasites pré-adultes et adultes induit des changements caractéristiques d'une réponse à un stress. Dans les groupes faiblement et moyennement infectés, la récupération homéostatique s'est produite après 10 jours, mais la récupération a été incomplète dans le groupe fortement infecté. Ainsi, un parasitisme de 10 poux par poisson, qui représente un faible niveau d'infestation dans la nature, constitue un stress important qui affecte la condition générale des épithéliums de la peau et des branchies durant une longue période et rend ainsi le poisson vulnérable à des infections secondaires.

[Traduit par la Rédaction]

Introduction

The sea louse *Lepeophtheirus salmonis* is a caligid copepod that is an ectoparasite of salmonids in seawater. This species is an economically important parasite of sea-farmed salmonids that frequently causes serious disease throughout the Northern Hemisphere (Wootten et al. 1982; Pike 1989). In wild stocks, this species is normally present in low numbers (i.e., from 10 parasites/fish upwards) on wild fish (Berland 1993; Holst et al. 1993); however, under certain conditions, epizootics can occur (Wootten et al. 1982; Tully et al. 1993; Johnson et al. 1996).

Lepeophtheirus salmonis has a direct life cycle (i.e., no intermediate host) consisting of 10 stages. These include two planktonic naupliar stages, one infectious copepodid stage, and seven on-host stages (four chalimus, two preadult, and one adult) (Wootten et al. 1982; Johnson and Albright 1991*b*). Numerous studies have investigated aspects of the life cycle, population dynamics, and ecology of *L. salmonis* in relation to environmental factors (Ritchie et al. 1993; Heuch et al. 1995; Johnson et al. 1996). However, remarkably fewer studies have examined the nature of the host–parasite relationship. Tissue responses at the site of attachment and feeding, as well as copepodid distribution and load

Received June 17, 1998. Accepted January 22, 1999.
J14655

D.T. Nolan[1] **and S.E. Wendelaar Bonga.** Department of Animal Physiology, University of Nijmegen, 6500 GL Nijmegen, The Netherlands.
P. Reilly. Aquaculture Development Center, University College Cork, Lee Maltings, Cork, Ireland.

[1]Author to whom all correspondence should be addressed.
e-mail: dnolan@sci.kun.nl

© 1999 NRC Canada

Fig. 1. (A) SEM of the head skin of control *S. salar* uninfected with *L. salmonis*. The individual pavement cells form a continuous sheet. Occasional pores are the site of mucous cell discharge (arrows). Scale bar = 100 μm. (B) SEM of head skin of *S. salar* at site where *L. salmonis* was attached. The pavement cells are mechanically damaged by the activities of the parasite and much residual mucus is visible around the lesion (asterisks). Many pores from discharging mucous cells can be seen (arrows). Scale bar = 100 μm. (C) SEM of head skin of *S. salar* at 1 DPI with *L. salmonis* (6 parasites/fish) taken from an area where there was no parasite attachment. Although there are no direct signs of parasite feeding activity, swollen pavement cells can be seen sloughing off (asterisks), many mucous pores are visible, and the integrity of the pavement cell layer is disrupted. Scale bar = 50 μm. (D) SEM of a mucous cell lined duct from the head of control *S. salar*. Scale bar = 50 μm. (E) Light microscopy view through the scaleless skin from the head of control *S. salar*. The stain is Alcian blue (pH 2.5) to demonstrate mucous cells in the epithelium (e) and the mucous cells lining a mucous cell duct (d). p, pigment cells; m, muscular tissue. Scale bar = 100 μm.

on the body of the fish, have been investigated (Jones et al. 1990; Johnson and Albright 1992*a*; Jonsdottir et al. 1992). Physiological effects following experimental infection of postsmolt Atlantic salmon (*Salmo salar*) with large numbers of *L. salmonis* have only recently been reported (Grimnes and Jakobsen 1996), and these effects include disturbance of hydromineral balance and mortality attributed to the development of subadult and adult stages of the lice.

One key factor that can affect the health status of fish and increase susceptibility to disease is stress (Pickering et al. 1989; Wedemeyer 1997). While the topic of stress in fish is complex and many of the mechanisms involved are not yet fully understood, cortisol and the catecholamines are crucial in mediating the integrated stress response (see review by Wendelaar Bonga 1997). Salmonids intensively raised in aquaculture are known to have high stress levels, and these can be compounded by aquaculture practices such as transport, grading, and routine maintenance (Barton and Iwama 1991), increasing susceptibility to disease, including ectoparasites. Johnson and Albright (1992*b*) have shown that intraperitoneal administration of cortisol influenced the salmonid host–parasite interaction and increased susceptibility of coho salmon (*Oncorhynchus kisutch*) to experimental infection with *L. salmonis* by suppressing inflammatory response and epithelial hyperplasia in skin and gills.

The skin and gills of a fish are covered by complex epithelia comprising several layers of living cells that are continuous over the body surface (Iger et al. 1995; Nolan et al. 1998). They form the first barrier between the external and the internal environment and are protected with a chemically and functionally complex mucus coat that is discharged by specialized mucous cells in the epidermis (Shephard 1994). The teleostean epidermis is apparently influenced by a number of endocrine factors (Pottinger and Pickering 1985; Iger et al. 1995) and shows characteristic changes in fish exposed to stressors. It has been proposed that salmonids probably die from osmoregulatory problems caused by adult lice mechanically disrupting the skin (Wootten et al. 1982). Recently, osmoregulatory failure and mortality by developing adult stages have been demonstrated in Atlantic salmon (Grimnes and Jakobsen 1996), yet possible indirect effects of the parasite on the epithelia have not been examined. Such effects will become expressed at locations distant from the feeding and attachment areas and may also affect osmoregulation adversely.

The skin epithelium of fish responds strongly to stressors (Iger et al. 1995; Nolan et al. 1998) and offers good possibilities for evaluating indirect stress effects of ectoparasites on the host fish. Several responses, such as increased apoptosis of branchial chloride cells and the pavement cells of the skin, have been shown to be under control of the stress hormone cortisol and will therefore also occur in areas not affected directly by the parasites, including the gills. These stress parameters also allow any relationship between the effects of sea lice and susceptibility to secondary infection to be established through examination of the skin and gill epithelia. The direct tissue damage caused by parasite grazing and indirect epithelial effects and immunosuppression offer opportunities for invasion by secondary pathogens if the overall integrity of the epithelia is compromised during, or remains compromised beyond, this period. These effects may disrupt hydromineral balance and can be assessed by measuring blood ion levels and the activity of key ionoregulatory Na^+/K^+-ATPases, such as in the gill.

The objective of the present study was to determine whether infection with low numbers of adult and preadult *L. salmonis* induced a stress response in the Atlantic salmon. We studied parameters in the skin and gill (ultrastructure through light and electron microscopy, as well as gill Na^+/K^+-ATPase) coupled with blood parameters (serum sodium, chloride, calcium, protein, and urea), to reveal the presence of a stress response.

Materials and methods

Experimental setup

Four groups of 40 seawater-adapted Atlantic salmon (200–250 g body weight) were placed in 400-L circular green plastic holding tanks at the Bantry research facility of the National Aquaculture Development Centre, Cork, Ireland. The tanks were provided with a constant supply of temperature-controlled seawater at 15°C under a 12 h light :12 h dark photoperiod. After 3 weeks of acclimation, three groups were infected with 120, 240, or 400 subadult and adult *L. salmonis* of both sexes to achieve initial infection levels of 3, 6, and 10 lice/fish. Infection was carried out in the evening by pouring seawater containing the parasites into each tank. Seawater only was poured into the control tank. Seven fish from each group were sampled at 24 h, 5 days, and 10 days postinfection (1, 5, and 10 DPI).

Sampling procedure

All fish were killed by concussion at the dorsal part of the head. Blood was collected by needle from the caudal blood vessels, allowed to clot for 24 h at 4°C, and centrifuged to obtain serum. Samples of skin from the rostral part of the head above the nostrils and small pieces from the second gill arches were fixed in Bouin's fixative for light microscopy and 3% glutaraldehyde buffered in sodium cacodylate (0.09 M, pH 7.3) with postfixation in 1% osmium tetroxide in the same buffer for electron microscopy (Iger et al. 1995). The samples were taken from areas where the parasites were not attached or where no indications of previous feeding activity could be observed. Another series of head skin samples were

© 1999 NRC Canada

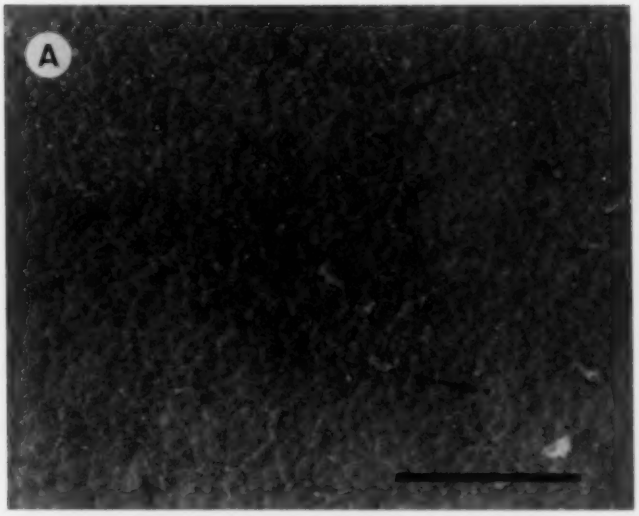

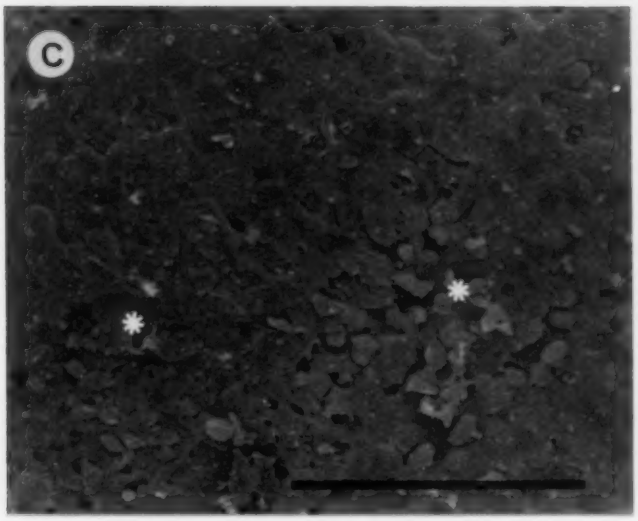

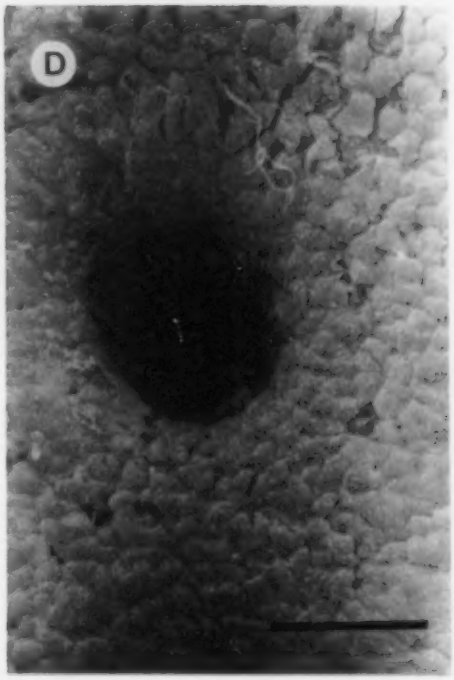

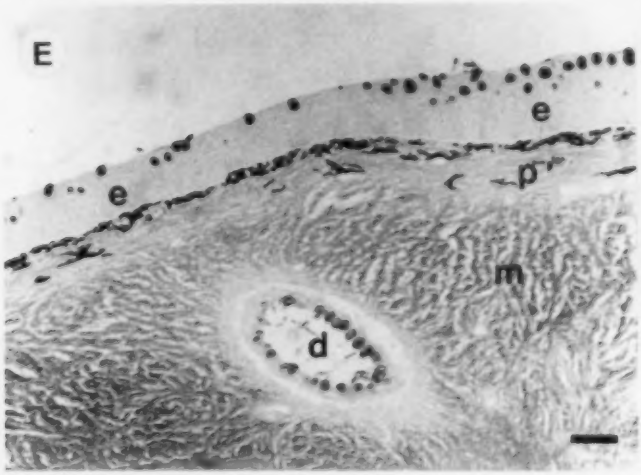

© 1999 NRC Canada

Fig. 2. (A) Upper epidermis of skin from control *S. salar*. The pavement cells (p), showing microridges at the upper cell limits (arrows), form the interface with the water. Little intercellular spacing occurs and the epithelium has good structural integrity. m, mucous cell. Scale bar = 5 μm. (B) Upper epidermis of skin from *S. salar* at 1 DPI with *L. salmonis* (3 parasites/fish) taken from an area where there was no parasite attachment. Intercellular spaces are visible (asterisks) and the integrity of the epithelium is disrupted. A discharging mucous cell (m) can be seen. Scale bar = 5 μm. (C) Upper epidermis of skin from *S. salar* at 5 DPI with 3 parasites/fish taken from an area where there was no parasite attachment. Intercellular spaces are not present and the integrity of the epithelium is good. Considerable numbers of electron-dense desmosomes (arrows) are seen at the borders of the filament cells. Scale bar = 5 μm. (D) Upper epidermis of the skin from *S. salar* at 1 DPI with 6 parasites/fish taken from an area where there was no parasite attachment. Many necrotic pavement cells (n) can be seen and intercellular spaces are present (asterisks). Many predischarge mature mucous cells (m) can be seen close to the surface. Scale bar = 5 μm.

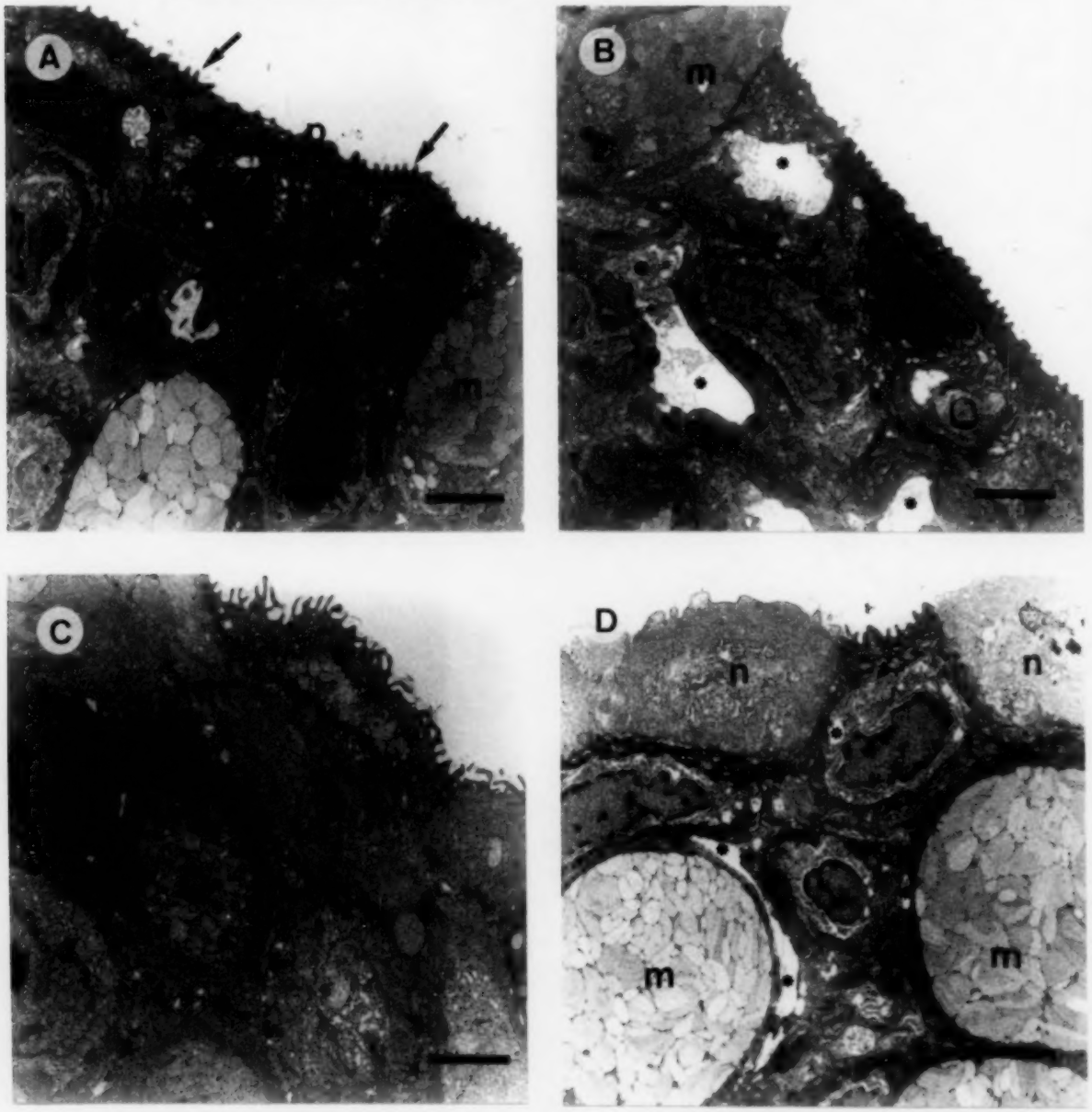

© 1999 NRC Canada

taken at locations where parasites were observed and fixed for electron microscopy in the same way. The remaining gills were dissected and the filaments trimmed from the gill arch, placed in 1 mL of ice-cold buffer (0.3 M sucrose, 20 mM Na_2EDTA, 0.1 mM imidazole, pH 7.1 with HCl), and immediately frozen for measurement of Na^+/K^+-ATPase activity.

Sample processing

For quantification of mucous cells, Bouin-fixed skin samples from each fish were processed into paraffin blocks and 5-μm sections were cut perpendicular to the plane of the epidermis. Replicate series of sections were stained with periodic acid – Schiff's (PAS) stain to identify total mucous cells and with the Alcian blue (pH 2.5) method to identify acidophilic mucous cells (Blackstock and Pickering 1982). Total numbers of mucous cells were counted in 10 independent 300-μm views from each sample using a calibrated micrometer in the ocular lens of a light microscope, averaged for each fish, and the mean number of cells per millimetre of transverse epidermal section calculated. Gill samples from each fish were processed by sectioning perpendicular to the plane of the lamellae, stained with haematoxylin and eosin, and examined for general morphology by light microscopy.

For transmission electron microscopy (TEM), one replicate set of fixed skin and gill samples from four fish was stained for 2 h in 2% uranyl acetate, dehydrated through an ethanol series, and embedded in Spurr's resin. Ultrathin sections were cut by diamond knife, collected on 150-mesh copper grids, and contrasted with lead citrate before viewing in a Philips EM 300 transmission electron microscope at 40 kV. For skin, the overall ultrastructure was observed and attention was focused on cellular necrosis (characterized by nuclei with aggregations of chromatin, swelling of the cytoplasmic compartment, and loss of apical microridges) and apoptosis (characterized by progressive densification of the nucleus, organelles, and cytoplasm, leading to shrinkage and loss of contacts with surrounding cells), leukocyte infiltration, and epithelial integrity (evaluated by intercellular swelling and cell–cell contacts). For gills, the overall ultrastructure and the appearance of the respiratory lamellae were observed. In addition, the interlamellar chloride cell populations were studied and necrosis (defined above), apoptosis (characterized for chloride cells by progressive densification of the mitochondria, nucleus, and cytoplasm, as well as dilation of the tubular system), and leukocyte infiltration evaluated. From micrographs, the epithelia were evaluated and scored semiquantitatively against control using a graded evaluation system (–, +, ++, +++, ++++), representing parameter unaffected (–) to strongly affected (++++).

A second replicate set of skin and gill samples was examined by scanning electron microscopy (SEM). These samples were dehydrated through an ethanol series, critical point dried under liquid carbon dioxide, gold sputtered in a Balzers coating unit (CPD 020, Balzers, Switzerland), and viewed in a Jeol-JSM T 300 scanning electron microscope.

The sera were analyzed for sodium and chloride indirectly using ion-specific electrodes, calcium using *o*-cresolphthalein complexone, and urea using urease and glutamate dehydrogenase. Total protein was measured with the biuret reagent. All determinations were carried out on a Hitachi 747 automatic analyzer. The assay of Na^+/K^+-ATPase activity in the gill tissue was carried out on first homogenates according to the method of Flik et al. (1984).

Statistical analysis

Data are expressed as means ± SE of seven fish for each treatment at each timepoint. Differences between control groups over experimental time were assessed by ANOVA of log-transformed data (except for the Na to Cl ratio (Na:Cl)). Data sets for each timepoint (except Na:Cl) were log transformed, analyzed by ANOVA, and significance between treatments assessed using the Bonferroni multiple comparisons test. For Na:Cl, data were tested using the Mann–Whitney *U* nonparametric test. Statistical significance was accepted at $P < 0.05$.

Results

Skin

Ultrastructure of head skin from control salmon by SEM showed the surface to be a continuous sheet of pavement cells (Fig. 1A). Examination by TEM at 1, 5, and 10 DPI revealed several distinct cell populations (Fig. 2A). The most numerous cell type is the filament cell, which is characterized by numbers of perinuclear microfilaments. The uppermost layer of cells is differentiated into specialized pavement cells that have apical microridges (Fig. 2A). Cell–cell contacts between pavement cells and filament cells are maintained by tight junctions and desmosomes. Little intercellular spacing occurs in the epithelium (Fig. 2A). Mucous cells differentiate in the middle layers of the epidermis and migrate through to the upper layer where they discharge their contents onto the body surface. Low numbers of leukocytes are also present (Table 1).

The skin ultrastructure from the head of parasitized fish by SEM in areas distant from the feeding sites of the parasites showed marked epithelial changes (Fig. 1C) compared with control fish (Fig. 1A), including swelling and shedding of the pavement cells (Fig. 1C). At sites of copepod feeding, gross damage was visible as lesions of disrupted and swollen pavement cells (Fig. 1B). In all fish examined, lines of ducts were observed in the scaleless region of the head (Fig. 1D) and, when examined by light microscopy, these ducts were richly lined with mucous cells (Fig. 1E).

There was no statistical difference between the counts of cells stained with PAS or with the Alcian blue (pH 2.5) method at any sample point; therefore the total numbers of cells counted from PAS staining are given. There were significantly fewer mucous cells in the nonfeeding areas of the epidermis of infected fish when compared with controls at 1, 5, and 10 DPI (see Table 3).

There were strong effects in the epidermis of fish infected with 3 parasites/fish at nonfeeding sites at 1 DPI (Fig. 2B). Necrotic pavement cells were commonly observed. Increased intercellular spaces and increased incidence of heavily stained desmosomes were typical (Table 1; Fig. 2B). Leukocytes were seen throughout the epidermis and within the intercellular spaces. At 5 DPI, heavily stained desmosomes were very abundant (Fig. 2C). Apoptotic cells were occasionally encountered, but necrosis in the pavement cell layer was reduced. At 10 DPI, the condition of the skin of these fish was slightly recovered compared with 5 DPI (Table 1).

At 1 DPI, the epidermal condition of fish infected with 6 parasites/fish was similar to that of the group infected with 3 parasites/fish (Table 1; Fig. 2D). However, necrosis in the pavement cell layer was more severe, disruption of the underlying cell layers was greater and many predischarge mucous cells were located in the upper epidermis (Fig. 2D). At 5 DPI, there was an increase in the staining intensity of the desmosomes and the intercellular spacing was reduced (Table 1; Fig. 3A). Various stages of filament cell apoptosis

© 1999 NRC Canada

Fig. 3. (A) Upper epidermis of skin from *S. salar* at 5 DPI with *L. salmonis* (6 parasites/fish) taken from an area where there was no parasite attachment. A macrophage (asterisk) engulfs an apoptotic filament cell. Intercellular spaces are absent and numbers of electron-dense desmosomes (arrows) are visible at the filament cell borders. Scale bar = 5 μm. (B) Upper epidermis of skin from *S. salar* at 1 DPI with 10 parasites/fish taken from an area where there was no parasite attachment. Many necrotic pavement cells (n) can be seen and intercellular spaces are present (asterisks). Numbers of electron-dense desmosomes (arrows) are visible at the filament cell borders and a mature predischarge mucous cell (m) can be seen. Scale bar = 5 μm. (C) Upper epidermis of skin from *S. salar* at 5 DPI with 10 parasites/fish taken from an area where there was no parasite attachment. Necrotic pavement cells and intercellular spaces (asterisks) still occur. A lymphocyte (l) is present in the pavement cell layer. Numbers of electron-dense desmosomes are visible and a discharging immature mucous cell can be seen. Scale bar = 5 μm. (D) Upper epidermis of skin from *S. salar* at 10 DPI with 10 parasites/fish taken from an area where there was no parasite attachment. The integrity of the epithelium is restored in this fish. Few electron-dense desmosomes (arrows) are visible. Scale bar = 5 μm.

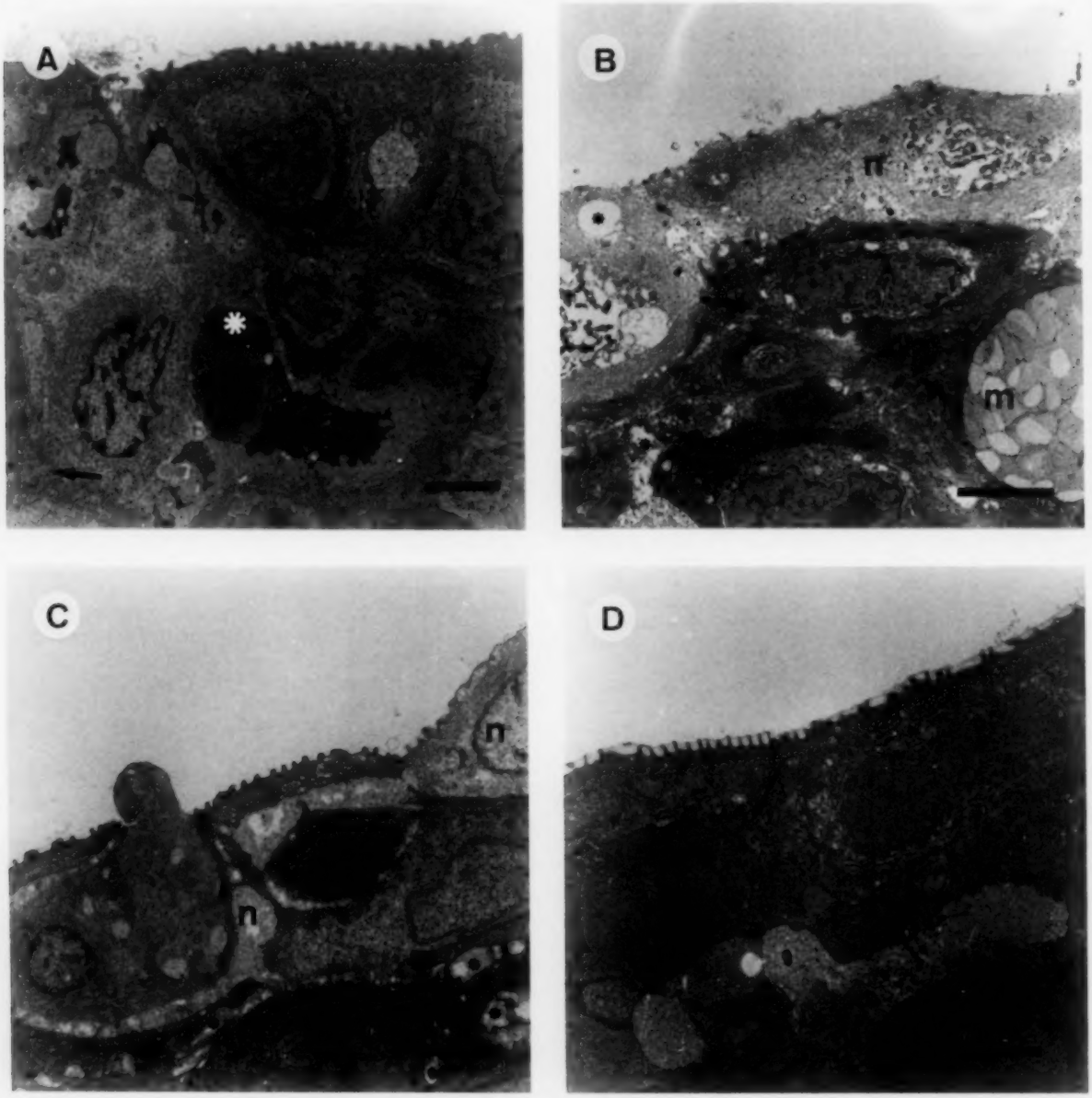

© 1999 NRC Canada

Table 1. Semiquantitative evaluation of the epidermal responses of head skin of postsmolt *S. salar* to three infection levels of preadult and adult *L. salmonis*.

Skin parameter	Control	3 lice/ fish	6 lice/ fish	10 lice/ fish
1 and 5 DPI				
Pavement cell necrosis	–	++	+++	++++
Heavily stained desmosomes	–	+++	+++	++++
Intercellular space	–	+++	+++	++++
Mucous cell discharge	–	+++	+++	+++
Apoptotic cells	–	++	+++	+++
Leukocyte infiltration	–	++	++	++
10 DPI				
Pavement cell necrosis	–	–	++	+++/+
Heavily stained desmosomes	–	++	++	+++
Intercellular spaces	–	+	++++	+++/+
Mucous cell discharge	–	++	++	++
Apoptotic cells	–	+	++	++
Leukocyte infiltration	–	++	++	+++/+

Note: The samples are taken away from areas of parasite attachment and feeding. – = unaffected to ++++ = strongly affected.

Table 2. Semiquantitative evaluation of the responses of the gill of postsmolt *S. salar* to three infection levels of preadult and adult *L. salmonis*.

Gill parameter	Control	3 lice /fish	6 lice/ fish	10 lice/ fish
1 and 5 DPI				
Lamellar swelling	–	+++	+++	+++
Chloride cells: dilated tubular system	–	+++	+++	++++
Chloride cells: apoptosis	–	+++	+++	++++
Gill Na^+/K^+-ATPase	–	+++	+++	+++
Leukocytes	–	++	+++	+++
10 DPI				
Lamellar swelling	–	–	+	+++/+
Chloride cells: dilated tubular system	–	+	+	+++/+
Chloride cells: apoptosis	–	+	+	+++/+
Gill Na^+/K^+-ATPase	–	+	+	+++
Leukocytes	–	++	++	+++/+

Note: – = unaffected to ++++ = strongly affected.

were observed (Fig. 3A). At 10 DPI, the overall situation was comparable with 5 DPI, with the exception that intercellular spaces were more extensive and necrosis of the pavement cell layer was reduced (Table 1).

The 10 parasites/fish group showed the strongest epidermal effects at all samplings (Table 1). At 1 DPI, there was extensive necrosis of the pavement cell layer, heavily stained desmosomes, and intercellular spaces present (Fig. 3B). At 5 DPI, immature mucous cells could be seen discharging at the surface, and apoptosis and necrosis of the pavement cell were common (Fig. 3C). At 10 DPI, there was some variation in the condition of the epidermis of individual fish. Some individuals still had extensive pavement cell necrosis and intercellular swelling, while others showed good recovery with a well-differentiated and active pavement cell layer and good epithelial integrity (Fig. 3D).

Gill

The external gill structure of uninfected salmon inspected by SEM and TEM was typical for salmonids that we have sampled from aquaculture conditions (personal observation). The filaments had leaflike lamellae arranged alternately on both sides (Fig. 4A). The respiratory epithelium was one cell thick and leukocytes were commonly in the intercellular spaces (Fig. 4B). In the interlamellar areas, populations of mitochondria-rich chloride cells and mucous cells were present (Fig. 4E). Apoptotic chloride cells were seen occasionally, whereas apoptosis and necrosis were uncommon in other cell types (Table 2). The epithelium of the filaments, with the exception of the interlamellar areas, resembled that of the skin, being composed of filament cells, mucous cells, leukocytes, and an apical pavement cell layer with microridges.

In lice-infected groups, SEM observations showed that the lamellae were swollen and wrinkled (Table 2; Fig. 4C). In TEM observations, the lamellar respiratory epithelium was uplifted and detached from the endothelium of the central blood sinus in many places (Fig. 4D). Both mucous and chloride cells were found on the filaments, as well as on the lamellae. In lice-infected fish, the chloride cells showed an extensive dilated tubular system (Fig. 4F) not observed in control fish (Fig. 4E; Table 2).

At 1 DPI, the lamellae of fish infected with 3 parasites/fish were swollen (Table 2). Mucus discharge was stimulated in the filament, and apoptotic chloride cells were frequently seen in the interlamellar area (Table 2). Apoptotic chloride cells in the interlamellar lost apical contact with the water and were apparently replaced by neighboring new chloride cells. At 5 DPI, apoptotic bodies, the last stage of apoptotic chloride cells, could be observed (Fig. 5A) in addition to other apoptotic stages (Fig. 5B).

The lamellae sampled from fish infected with 6 parasites/fish at 1 DPI were comparable with those of the 3 lice/fish group (Table 2). Mucus discharge was stimulated in the filament epithelium, and intercellular spaces occurred with heavy leukocyte infiltration (Fig. 5C). The chloride cell population and pavement cells in the interlamellar area were also strongly affected, as desmosomes were reduced and apoptotic cells atrophied (Fig. 5D). At 10 DPI, the gill structure in this group was comparable with the 3 lice/fish group, with the exception of lamellar swelling, which still occurred (Table 2).

The group infected with 10 parasites/fish showed the strongest lamellar effects (Table 2). Cellular shrinkage and swelling of the lamellar respiratory epithelium were severe (Fig. 5E). At 1 DPI, newly differentiated cells could be seen at the base of the lamella (Fig. 5F). At 5 DPI, many macrophages containing cellular debris (composed mainly of apoptotic bodies) were observed. The high turnover of chloride cells was continuous and observed at 5 and 10 DPI in most fish examined, although there was some variation between individuals at 10 DPI (Table 2).

Blood parameters

Compared with control values, serum sodium was signifi-

© 1999 NRC Canada

Fig. 4. (A) Representative SEM of gill from control *S. salar* uninfected with *L. salmonis*. The filament (f) and lamellae (arrows) are clearly seen. Scale bar = 100 μm. (B) TEM view of the lamellae of control *S. salar* gills. The blood space (b) and the water (w) are separated by a thin respiratory epithelium that is one cell layer thick. Leukocytes (l) can be seen in the intercellular spaces of this epithelium. Scale bar = 5 μm. (C) SEM view of the gills of *S. salar* at 1 DPI with 10 lice/fish. The lamellae are wrinkled and swollen (arrows). Scale bar = 50 μm. (D) Lamellae of gill from *S. salar* at 1 DPI with 6 lice/fish. The distance between the blood space and the water is increased by epithelial uplifting. Numbers of leukocytes can be seen in the epithelial intercellular spaces (asterisks). Mucous cells (m) and chloride cells (lc) are present on the lamella. Scale bar = 5 μm. (E) Representative TEM of the interlamellar region of gill from control *S. salar* uninfected with lice. Many mitochondria-rich chloride cells (c) are present here, as well as mucous cells (m). There are few enlarged intercellular spaces, epithelial integrity is good, and some leukocytes (arrows) and mast cells (mc) can be seen. Scale bar = 10 μm. (F) TEM view of the interlamellar region of gill from *S. salar* at 1 DPI with 10 lice/fish. The tubular systems of the chloride cells are dilated (arrows) and apoptotic chloride cells (a) are present. Scale bar = 5 μm.

cantly lower in the 10 lice/fish group sampled at 1 DPI and serum chloride significantly higher at 5 DPI in both the 3 and 6 lice/fish groups (Table 3). Although the serum sodium and chloride levels did not differ significantly in any other group at any other time, the serum Na:Cl in all lice-infected groups was significantly reduced at 5 DPI (Table 3). Serum total calcium levels, protein, and urea were significantly elevated in the 10 lice/fish group sampled at 1 DPI (Table 4) but not at any other time point or in any of the other groups.

Gill Na^+/K^+-ATPase

The gill Na^+/K^+-ATPase activity was significantly higher in all infected fish at 5 DPI and remained elevated in the 10 lice/fish group sampled at 10 DPI (Table 3).

Discussion

Infection with low numbers of preadult and adult *L. salmonis* had a marked effect on the integrity of the skin and gill epithelia of the Atlantic salmon. This is an indirect effect of the parasite, as it is reported from areas of epithelia where there was no obvious evidence of prior parasite attachment. The results of this study lead to the conclusion that many of the epithelial changes reported are similar to those described for stressors in general (Wendelaar Bonga 1997), including toxic agents (chemical stressors), handling, and a submissive position in hierarchy. These effects are likely hormone mediated, as a consequence of the infection causing an integrated stress response in the fish, resulting in increased levels of circulating cortisol and catecholamines. These results demonstrate that the effects of infection with *L. salmonis* can be divided into two distinct categories. The first is a direct effect of parasite attachment and feeding on the body surface, as reported by others (Jones et al. 1990; Johnson and Albright 1992*a*; Jonsdottir et al. 1992; MacKinnon 1993) and confirmed in this study, i.e., direct damage caused by parasite feeding, etc. The second is the indirect effect of the integrated stress response on the integrity of the skin and gill epithelia, including the osmoregulatory consequences in terms of gill Na^+/K^+-ATPase, as reported here for the first time.

At nonfeeding sites, infestation with *L. salmonis* caused necrosis in the pavement cells of the skin, increased apoptosis in the inner cell layers of the epidermis, and stimulated mucus discharge. Necrosis is a form of cellular death directly caused by toxic factors and other damaging agents. Pavement cell necrosis has been reported for a number of toxic chemicals in freshwater (Nolan et al. 1998) and also during seawater adaptation (Wendelaar Bonga and van der Meij 1989; Uchida et al. 1996) and water acidification (Wendelaar Bonga et al. 1990). The necrotic cells were restricted to the pavement cell layer of parasitized salmon, suggesting that a change in the protective role of the mucus layer may have been a contributing factor, possibly by reduced protection as a result of a reduction in either total mucus coat or a change in mucus composition. The function of the mucus layer on the body surface of the fish and its components and composition have been reviewed, although there is still uncertainty about the involvement of mucus in ionoregulation in fishes (Shephard 1994). Increased mucus secretion in the present study was indicated by the numbers of discharging and predischarge mucous cells seen in TEM and reduced total numbers of epidermal mucous cells in infested fish. Ectoparasites have been shown to reduce numbers of mucous cells in brown trout (*Salmo trutta*) epidermis (Pottinger et al. 1984), and stimulation of mucus discharge is a cortisol-mediated effect in rainbow trout (*Oncorhynchus mykiss*) (Iger et al. 1995).

The deletion of cells from a tissue is achieved by apoptosis, a physiologically controlled process that activates a genetically programmed mechanism that induces death and elimination of a cell. The stimulation of apoptosis in the skin and gill of parasitized fish is typical of the general epithelial response reported in many fishes (Wendelaar Bonga and van der Meij 1989; Nolan et al. 1998) and indicates increased aging, and therefore increased cell turnover, within these epithelia (Wendelaar Bonga 1997). The mechanisms controlling this process are not fully elucidated, but recently, it has been shown in vivo (Iger et al. 1995) and in vitro (Bury et al. 1997) that cortisol promotes apoptosis. The increased apoptosis in skin and gill epithelia of the sea lice infested fish in the present study may result from elevated circulating cortisol levels.

The overall structural integrity of the epithelia was disrupted, as indicated by the presence of widened intercellular spaces. These spaces are believed to be caused by hydrostatic pressure and osmotic forces and are prominent during periods of epithelial cell elimination through necrosis and apoptosis and increased mucus discharge. As numbers of cells are eliminated, the contacts between the remaining cells are reduced and the spaces become infiltrated with leukocytes. The stimulation of leukocyte infiltration and increased epithelial permeability are probably catecholamine-mediated effects (see review by Wendelaar Bonga 1997). The increase in electron density of the desmosomes connecting the epithelial cells of the skin was correlated with parasite infestation. These desmosomes may fortify the epidermis and reduce intercellular swelling. Heavily stained

© 1999 NRC Canada

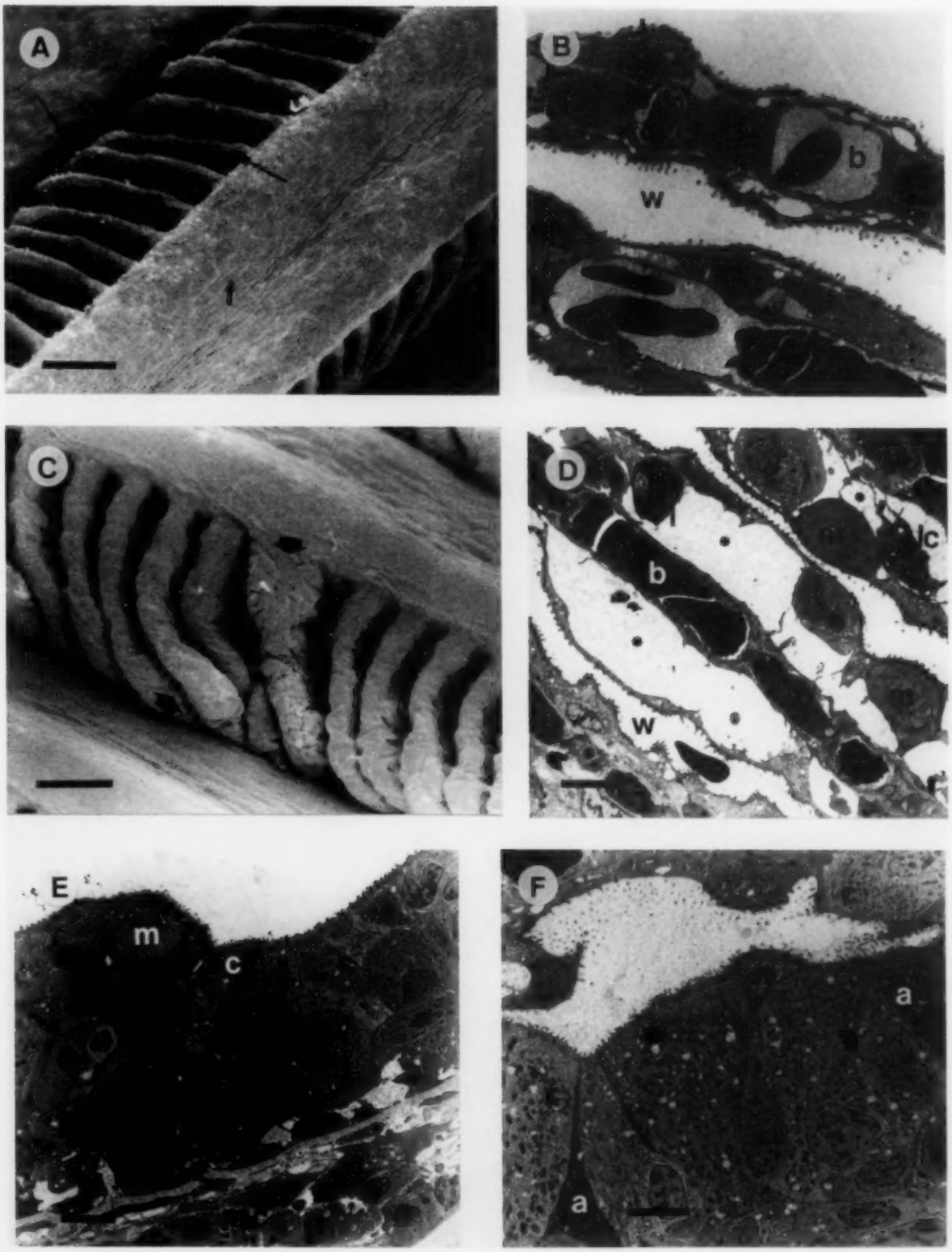

© 1999 NRC Canada

Fig. 5. (A) Interlamellar region of gill from *S. salar* at 5 DPI with *L. salmonis* (3 lice/fish). Late-stage apoptotic chloride cells (a) are present as condensed apoptotic bodies located in a macrophage (MP), and electron-dense earlier stages in the chloride cell apoptotic pathway with dilated tubular systems can be seen (asterisks). Scale bar = 5 μm. (B) Interlamellar region of gill from *S. salar* at 5 DPI with 3 lice/fish. Apoptotic chloride cells will be replaced at the original location by newly differentiated replacement chloride cells (asterisk). Scale bar = 5 μm. (C) Primary filament epithelium of gill from *S. salar* at 5 DPI with 6 lice/fish. The normal epithelial structure is completely disrupted and the intercellular spaces (asterisks) are massively infiltrated by leukocytes (l); m, mucous cell. Scale bar = 10 μm. (D) Chloride cells in the interlamellar region of gill from *S. salar* at 5 DPI with 6 lice/fish. Late-stage (la) and earlier-stage apoptotic chloride cells (ea) can be seen; asterisks, intercellular spaces. Scale bar = 5 μm. (E) Gill lamellae from *S. salar* at 1 DPI with 10 lice/fish. The micrograph illustrates the disruption of the respiratory epithelium that underlies the wrinkling observed in the SEM views. The individual cells are shrunken and intercellular spaces are present (arrows). A shrunken chloride cell (c) is present on the lamella; e, erythrocyte; w, water. Scale bar = 5 μm. (F) Chloride cells on the gill lamella of *S. salar* at 1 DPI with 10 lice/fish. Apoptotic chloride cells occur in the inner layers of the epithelium, while numbers of newly differentiating chloride cells are present also (asterisks). Leukocytes (l) are in the upper layer. p, pillar cell. Scale bar = 5 μm.

Table 3. Parameters investigated in *S. salar* infected with numbers of preadult and adult *L. salmonis*.

Parameter	Control	3 lice/fish	6 lice/fish	10 lice/fish
1 DPI				
Sodium	170±2.5	164±3.1	167±2.6	159±2.2*
Chloride	141±4.5	136±2.6	142±4.2	134±2.2
Na:Cl	1.20±.02	1.20±.02	1.18±.02	1.19±.01
Gill Na^+/K^+-ATPase	8.2±0.97	8.3±0.41	8.7±.0.38	9.7±0.41
Epidermal mucous cells	91.9±6.2	63.5±16.9**	66.3±6.1**	65.1±8.1**
5 DPI				
Sodium	166±1.1	169±3.0	168±1.4	162±2.4
Chloride	132±1.5	143±3.7*	142±1.9*	137±2.4
Na:Cl	1.26±.01	1.19±.01***	1.18±.01***	1.20±.02**
Gill Na^+/K^+-ATPase	8.9±0.82	14.43±1.04**	15.88±1.30**	15.0±0.67***
Epidermal mucous cells	91.3±4.6	62.3±3.7**	65.4±7.4**	64.4±4.5**
10 DPI				
Sodium	169±1.1	171±2.4	170±1.7	171±1.3
Chloride	137±1.6	136±1.9	142±1.8	135±1.0
Na:Cl	1.24±.02	1.27±.01	1.20±.01	1.26±.01
Gill Na^+/K^+-ATPase	7.0±0.27	7.9±1.42	7.8±1.04	13.3±0.70**
Epidermal mucous cells	90.8±6.2	54.2±8.2**	57.6±11.6**	50.0±6.5***

Note: Data for serum sodium and chloride values are mmol/L), gill Na^+/K^+-ATPase activity is mmol ATP·mg $protein^{-1}·h^{-1}$, and total numbers of mucous cells are per millimetre of skin epidermis. Data are expressed as means ± SE for $n = 7$. $*P < 0.05$, $**P < 0.01$, and $***P < 0.001$ compared with control values.

Table 4. Serum protein, urea, and total calcium of *S. salar* at 1 DPI with numbers of preadult and adult *L. salmonis*.

Serum parameter	Control	3 lice/fish	6 lice/fish	10 lice/fish
Protein (mg/dL)	28.7±6	42.3±5	42.0±5	50.7±2*
Urea (mmol/L)	2.3±0.2	2.2±0.1	2.3±0.2	3.0±0.1*
Total calcium (mmol/L)	2.7±0.2	3.1±0.2	3.3±0.2	3.6±0.1**

Note: Data are expressed as means ± SE for $n = 7$. $*P < 0.05$ and $**P < 0.01$ compared with control values.

desmosomes in the present study were observed predominantly in the epidermis of fish that had relatively high levels of damage. In a study of sea lice effects on skin of Atlantic salmon, electron-dense desmosomes between cells have also been shown in the skin of control fish. However, a different tissue fixative for TEM analysis was used (MacKinnon 1993).

In the gill, catecholamine action also increases branchial blood flow, resulting in increased gill perfusion and blood pressure (Satchell 1991; Wendelaar Bonga 1997). The lamellar swelling reported in the present study in parasitized fish may reflect the action of high levels of catecholamines released as a result of parasite-induced stress. We are confident that the effects we report in the gills do not result from any direct action of the parasite, as we infected our fish with preadult and adult parasites, while only the copepodid and chalimus stages have been reported to attach to the gills (Johnson and Albright 1992*a*, 1992*b*). Inspection of the gills from our infected fish by light microscopy and SEM revealed no parasites or parasite damage to the gills. In addition, at the water temperature in our experiment (15°C), the generation time from egg to infective stage is estimated at 7.4 days (Johnson and Albright 1991*a*), so if successful reproduction had occurred, the infective stages would have been active shortly before the 10 DPI sample point. This was when the 3 and 6 lice/fish groups (but not 10 lice/fish group) showed recovery.

Infestation with sea lice increased gill Na^+/K^+-ATPase activity and induced chloride cell apoptosis without greatly disrupting hydromineral balance. Elevated cortisol levels in fish stimulate chloride cell differentiation in vitro (McCormick 1995) and improve hypoosmoregulation in vivo

© 1999 NRC Canada

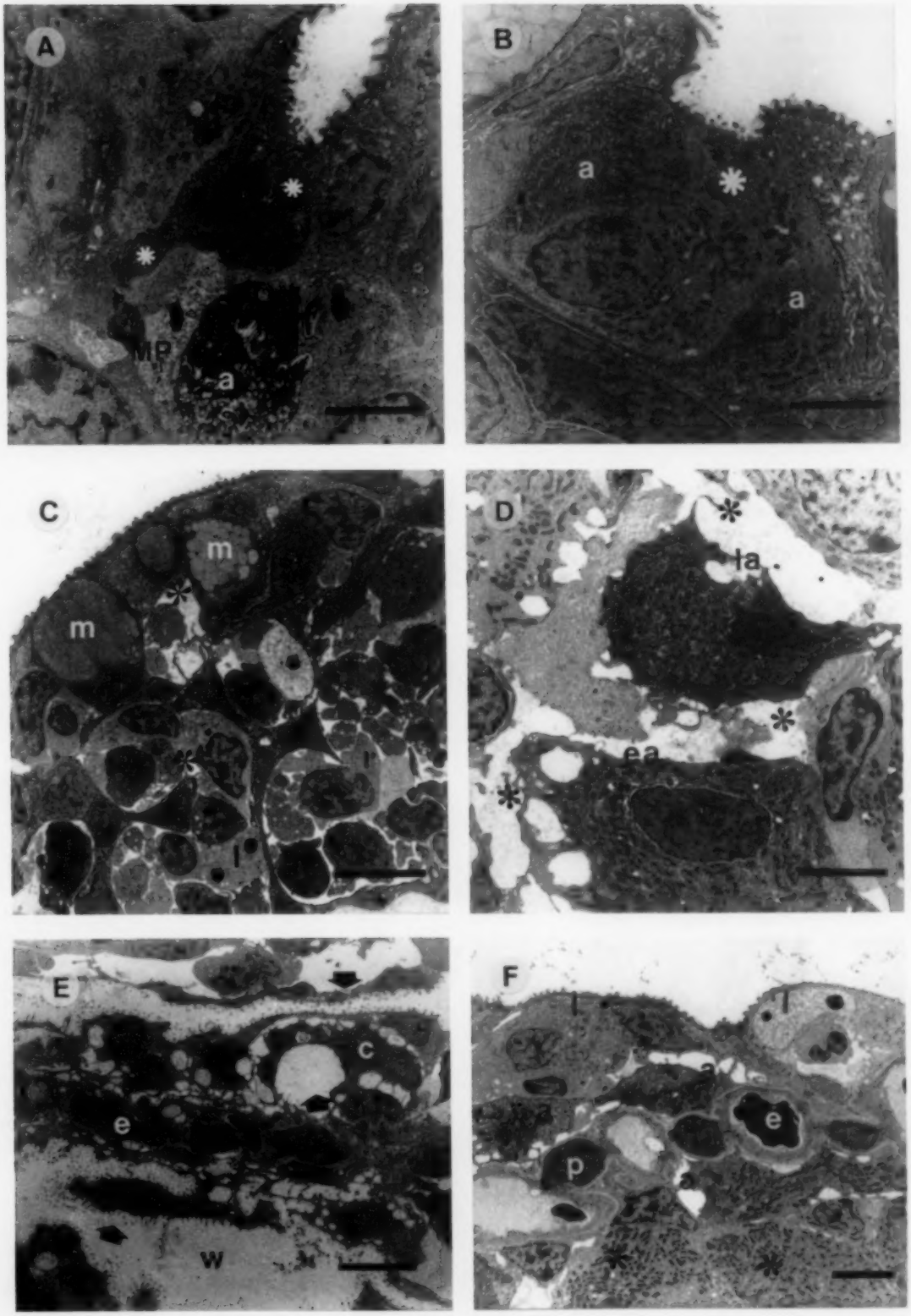

© 1999 NRC Canada

(Madsen 1990; Cornell et al. 1994), as well as inducing chloride cell apoptosis in vitro (Bury et al. 1997). Cortisol is a pluripotent hormone whose effects can be advantageous at moderately elevated levels and deleterious at highly elevated levels (Wendelaar Bonga 1997). In parasitized fish in the present study, the infection increased gill Na^+/K^+-ATPase activity at 5 DPI in all groups, increased aging of the mature chloride cells, and stimulated differentiation of a new chloride cell population, and these responses may have contributed to the maintenance or restoration of hydromineral balance. At 10 DPI, gill Na^+/K^+-ATPase activity and chloride cell apoptosis had returned to control levels in the 3 and 6 lice/fish groups. However, Na^+/K^+-ATPase activity and chloride cell apoptosis in the 10 lice/fish group remained above control levels, indicating that recovery was incomplete and that the stress was greater at this infestation level.

The effects on the chloride cells of the 10 lice/fish group were the strongest. These were correlated functionally at 1 DPI with decreased serum sodium and increased urea, total calcium, and protein in this group. Teleosts are ammoniotelic and excrete most nitrogenous waste through the gill as ammonium (NH_4^+). This occurs through the chloride cells, and elevated levels of urea in the blood are indicative of a rise in the production of nitrogenous waste products, as is typical for stressed fish (Wendelaar Bonga 1997), and may reflect impaired excretion of these products as a result of disrupted gill function. This is further supported by the decreased sodium and increased calcium levels. The former reflects the activity of increased gill Na^+/K^+-ATPase activity to eliminate excess sodium influx and (or) effects of reduced drinking rate, while the latter cannot be explained. Another study has reported increased plasma chloride and decreased serum total protein in Atlantic salmon infested with adult *L. salmonis* (Grimnes and Jakobsen 1996). This contrasts with the present study where we report an increase in serum protein, no increase in serum sodium, and a small increase in serum chloride at 5 DPI in the 3 and 6 lice/fish groups. However, the study of Grimnes and Jakobsen (1996) involved much higher infestation levels on considerably smaller fish (median infestation intensity 64 lice/fish at 11 days and 42 lice/fish at 31 days following infection with 86–176 infective copepodids/40-g fish) and these numbers of lice caused osmoregulatory failure.

The results of this study are based on single groups of fish for each experimental treatment. Although several replicate tanks per treatment are preferable, this was not possible. However, we are confident that the effects we report here are representative, as we have carried out later experiments infecting groups of salmonids with the crustacean ectoparasite *Argulus foliaceus*. Here, using a similar methodology and replicate treatment tanks, no differences were noted between replicate tanks for any treatment group at any time (Ruane et al. 1999).

We report here the presence of mucous cell lined ducts in the head region of Atlantic salmon. These ducts have not been reported previously, to the best of our knowledge, and we have confirmed the presence of these ducts in other salmonids (*S. trutta* and *O. mykiss*). We propose that, under normal circumstances, these ducts provide a rich supply of mucus to flow back over the body surface. Sea lice infestation of the scaleless head region can be severe (Pike 1989). The parasites may find this area attractive because the mucus provides a rich food source and preferentially gather there during heavy infestation, when competition between parasites for feeding resources may be high.

In conclusion, infection of postsmolt Atlantic salmon with low numbers of the sea louse *L. salmonis* has marked effects on the epithelia of the skin and gills, both locally in the skin as a result of parasite attachment and feeding (a direct effect) and overall as a result of the stress response of the fish to infection (an indirect effect). Hydromineral balance in the blood is not greatly affected, but increased gill Na^+/K^+-ATPase activity indicates that while the epithelial integrity is compromised, a high rate of sodium turnover occurs. The fish could apparently adapt to an initial infection level of 3–6 lice/fish within 10 days, but not to 10 lice/fish. Thus, infestation is stressful and at higher infection levels creates a prolonged period during which the overall compromised integrity of the skin and gill epithelia, as well as stress-related immunosuppression, may render the fish susceptible to secondary infections.

Acknowledgments

The excellent technical assistance of J.C.A. van der Meij (transmission electron microscopy) and H.P.M. Geurts (scanning electron microscopy) is gratefully acknowledged. This work was supported by a grant from the Graduate School M&T to D.T.N.

References

Barton, B.A., and Iwama, G.K. 1991. Physiological changes in fish from stress in aquaculture with emphasis on the response and effects of corticosteroids. Annu. Rev. Fish Dis. **1**: 3–26.

Berland, B. 1993. Salmon lice on wild salmon (*Salmo salar* L.) in western Norway. *In* Pathogens of wild and farmed fish: sea lice. *Edited by* G.A. Boxshall and D. Defaye. Ellis Horwood Limited, London, U.K. pp. 179–187.

Blackstock, N., and Pickering, A.D. 1982. Acidophilic granular cells in the epidermis of the brown trout, *Salmo trutta* L. Cell Tissue Res. **210**: 259–269.

Bury, N.R., Li, J., Lock, R.A.C., and Wendelaar Bonga, S.E. 1997. Cortisol protects against copper induced necrosis and promotes apoptosis in fish gill chloride cells *in vitro*. Aquat. Toxicol. **40**: 193–202.

Cornell, S.C., Portesi, D.M., Veillette, P.A., Sundell, K., and Speckler, J.L. 1994. Cortisol stimulates intestinal fluid uptake in Atlantic salmon (*Salmo salar*) in the post-smolt stage. Fish Physiol. Biochem. **13**: 183–190.

Flik, G., Wendelaar Bonga, S.E., and Fenwick, J.C. 1984. Ca^{2+}-dependent phosphatase and Ca^{2+}-dependent ATPase activities in plasma membranes of eel gill epithelium. III. Stimulation of branchial high-affinity Ca^{2+}-ATPase activity during prolactin-induced hypercalcemia in American eels. Comp. Biochem. Physiol. B. Comp. Biochem. **79**: 521–524.

Grimnes, A., and Jakobsen, P.J. 1996. The physiological effects of salmon lice infection on post-smolt of Atlantic salmon. J. Fish Biol. **48**: 1179–1194.

Heuch, P.A., Parsons, A., and Boxaspen, K. 1995. Diel vertical migration: a possible host-finding mechanism in salmon louse (*Lepeophtheirus salmonis*) copepodids? Can. J. Fish. Aquat. Sci. **52**: 681–689.

© 1999 NRC Canada

Holst, J.C., Nilsen, F., Hodneland, K., and Nylund, A. 1993. Observations of the biology and parasites of postsmolt Atlantic salmon, *Salmo salar*, from the Norwegian Sea. J. Fish Biol. **42**: 962–966.

Iger, Y., Balm, P.H.M., Jenner, H.A., and Wendelaar Bonga, S.E. 1995. Cortisol induced stress-related changes in the skin of rainbow trout (*Oncorhynchus mykiss*). Gen. Comp. Endocrinol. **97**: 188–198.

Johnson, S.C., and Albright, L.J. 1991*a*. Development, growth, and survival of *Lepeophtheirus salmonis* (Copepoda: Caligidae) under laboratory conditions. J. Mar. Biol. Assoc. U.K. **71**: 425–436.

Johnson, S.C., and Albright, L.J. 1991*b*. The developmental stages of *Lepeophtheirus salmonis* (Krøyer, 1837) (Copepoda: Caligidae). Can. J. Zool. **69**: 929–950.

Johnson, S.C., and Albright, L.J. 1992*a*. Comparative susceptibility and histopathology of the response of naive Atlantic, chinook and coho salmon to experimental infection with *Lepeophtheirus salmonis* (Copepoda: Caligidae). Dis. Aquat. Org. **14**: 179–193.

Johnson, S.C., and Albright L.J. 1992*b*. Effects of cortisol implants on the susceptibility and the histopathology of the responses of naive coho salmon *Oncorhynchus kisutch* to experimental infection with *Lepeophtheirus salmonis* (Copepoda: Caligidae). Dis. Aquat. Org. **14**: 195–205.

Johnson, S.C., Blaylock, R.B., Elphick, J., and Hyatt, K.D. 1996. Disease induced by the sea louse (*Lepophtheirus salmonis*) (Copepoda: Caligidae) in wild sockeye salmon (*Oncorhynchus nerka*) stocks of Alberni Inlet, British Colombia. Can. J. Fish. Aquat. Sci. **53**: 2888–2897.

Jones, M.W., Sommerville, C., and Bron, J. 1990. The histopathology associated with the juvenile stages of *Lepeophtheirus salmonis* on the Atlantic salmon, *Salmo salar* L. J. Fish Dis. **13**: 303–310.

Jonsdottir, H., Bron, J.E., Wootten, R., and Turnbull, J.F. 1992. The histopathology associated with the pre-adult and adult stages of *Lepeophtheirus salmonis* on the Atlantic salmon, *Salmo salar* L. J. Fish Dis. **15**: 521–527.

MacKinnon, B.M. 1993. Host response of Atlantic salmon (*Salmo salar*) to infection by sea lice (*Caligus elongatus*). Can. J. Fish. Aquat. Sci. **50**: 789–792.

Madsen, S. 1990. The role of cortisol and growth hormone in seawater adaptation and development of hypoosmoregulatory mechanisms in sea trout parr (*Salmo trutta trutta*). Gen. Comp. Endocrinol. **79**: 1–11.

McCormick, S.D. 1995. Hormonal control of gill Na^+,K^+-ATPase and chloride cell function. *In* Cellular and molecular approaches to fish ionic regulation. *Edited by* C.M. Wood and T.J. Shuttleworth. Academic Press Inc., San Diego, Calif. pp. 285–315.

Nolan, D.T., Hadderingh, R.H., Jenner, H.A., and Wendelaar Bonga, S.E. 1998. The effects of exposure to Rhine water on the sea trout smolt (*Salmo trutta trutta* L.): an ultrastructural and physiological study. *In* New concepts for sustainable management of river basins. *Edited by* P.H. Nienhuis, R.S.E.W. Leuven and A.M.J. Ragas. Backhuys Publishers, Leiden. pp. 261–271.

Pickering, A.D., Pottinger, T.G., and Carragher, J.F. 1989. Differences in the sensitivity of brown trout, *Salmo trutta* L., and rainbow trout, *Salmo gairdneri* Richardson, to physiological doses of cortisol. J. Fish Biol. **34**: 757–768.

Pike, A.W. 1989. Sea lice — major pathogens of farmed Atlantic salmon. Parasitol. Today, **5**: 291–297.

Pottinger, T.G., and Pickering, A.D. 1985. The effects of 11-ketotestosterone and testosterone on the skin structure of brown trout, *Salmo trutta* L. Gen. Comp. Endocrinol. **59**: 335–342.

Pottinger, T.G., Pickering, A.D., and Blackstock, N. 1984. Ectoparasite induced changes in epidermal mucification of the brown trout, *Salmo trutta* L. J. Fish Biol. **25**: 123–128.

Ritchie, G., Mordue, A.J., Pike, A.W., and Rae, G.H. 1993. The reproductive output of *Lepeophtheirus salmonis* adult females in relation to temperature and photoperiod. *In* Pathogens of wild and farmed fish: sea lice. *Edited by* G.A. Boxshall and D. Defaye. Ellis Horwood Limited, London, U.K. pp. 153–165.

Ruane, N.M., Nolan, D.T., Rotllant, J., Tort, L., Balm, P.H.M., and Wendelaar Bonga, S.E. 1999. Modulation of the response of rainbow trout (*Oncorhynchus mykiss* Walbaum) to confinement by an ectoparasitic (*Argulus foliaceus* L.) infestation and cortisol feeding. Fish Physiol. Biochem. **20**: 43–51.

Satchell, G.H. 1991. Physiology and form of fish circulation. Cambridge University Press, Cambridge, U.K.

Shephard, K.L. 1994. Functions for fish mucus. Rev. Fish Biol. Fish. **4**: 401–429.

Tully, O., Poole, W.R., and Whelan, K.F. 1993. Infestation parameters for *Lepeophtheirus salmonis* (Krøyer) (Copepoda: Caligidae) parasitic on sea trout, *Salmo trutta* L., off the west coast of Ireland during 1990 and 1991. Aquacult. Fish. Manage. **24**: 545–555.

Uchida, K., Kaneko, T., Yamauchi, K., and Hirano, T. 1996. Morphometrical analysis of chloride cell activity in the gill filaments and lamellae and changes in Na^+,K^+-ATPase activity during seawater adaptation in chum salmon fry. J. Exp. Zool. **276**: 193–200.

Wedemeyer, G.A. 1997. Effects of rearing conditions on the health and physiological quality of fish in intensive culture. *In* Fish stress and health in aquaculture. *Edited by* G.K. Iwama, A.D. Pickering, J.P. Sumpter, and C.B. Schreck. Cambridge University Press, Cambridge, U.K. pp. 35–71.

Wendelaar Bonga, S.E. 1997. The stress response in fish. Physiol. Rev. **77**: 591–625.

Wendelaar Bonga, S.E., and van der Meij, J.C.A. 1989. Degeneration and death, by apoptosis and necrosis, of the pavement and chloride cells in the gills of the teleost *Oreochromis mossambicus*. Cell Tissue Res. **255**: 235–243.

Wendelaar Bonga, S.E., Flik, G., Balm, P.H.M., and van der Meij, J.C.A. 1990. The ultrastructure of chloride cells in the gills of the teleost *Oreochromis mossambicus* during exposure to acidified water. Cell Tissue Res. **259**: 575–585.

Wootten, R., Smith, J.W., and Needham, E.A. 1982. Aspects of the biology of the parasitic copepods *Lepeophtheirus salmonis* and *Caligus elongatus* on farmed salmonids, and their treatment. Proc. R. Soc. Edinb. Sect. B (Biol. Sci.), **81**: 185–197.

© 1999 NRC Canada

A probabilistic analysis of decision-making about trip duration by Strait of Georgia sport anglers

Barry D. Smith

Abstract: Since 1984, an access-point creel survey of the Strait of Georgia, British Columbia, sport fishery has generated data on catch, effort, and attributes of effort from thousands of interviews of salmon anglers completing a daily boat-trip. I present a maximum-likelihood model for this daily bag limit (DBL) constrained fishery that estimates catch rate and variance for various angling fleets (as defined by boat-trip attributes such as the number of angling lines), estimates the probability that a boat-trip ends after a certain number of hours angling, and measures how angling success influences that probability. Most anglers targeting either chinook salmon (*Oncorhynchus tshawytscha*) or coho salmon (*Oncorhynchus kisutch*) became more likely to end a boat-trip in response to angling success, i.e., they were satiated by angling success before reaching a DBL. However, autumn and winter chinook salmon anglers tended to extend a boat-trip in response to angling success, i.e., they were motivated by angling success. Variability in angling success could not be attributed to variability in angler skill. Coho salmon catch rates increased by about 42% with each additional angling line per boat-trip up to three. The model can be used to judge the effectiveness of a DBL in reducing daily catch.

Résumé : Depuis 1984, une enquête menée aux points d'accès auprès des pêcheurs sportifs dans le détroit de Géorgie (Colombie-Britannique), a fourni des données sur les prises, l'effort de pêche et les attributs de ce dernier. Des milliers d'entrevues de pêcheurs sportifs de saumon effectuant des sorties en bateau d'une journée ont été réalisées. Je présente un modèle fondé sur le maximum de vraisemblance pour cette pêche restreinte par des limites quotidiennes de prises, modèle qui estime le taux de capture et la variance des captures pour diverses flottilles (définies selon les attributs des sorties, comme le nombre de lignes) et la probabilité qu'une sortie se termine après un certain nombre d'heures de pêche, et qui mesure comment le succès de la pêche influe sur cette probabilité. Chez la plupart des pêcheurs de quinnat (*Oncorhynchus tshawytscha*) ou de coho (*O. kisutch*), le succès de la pêche tend à motiver l'arrêt de la sortie, c'est-à-dire que ces pêcheurs se jugent satisfaits avant d'atteindre la limite quotidienne de prises. Cependant, le succès de la pêche tend à motiver les pêcheurs de quinnat d'automne et de printemps à prolonger leur sortie. La variabilité du succès de la pêche ne pouvait pas être attribuée à la variabilité de l'habileté des pêcheurs. Pour chaque ligne additionnelle par sortie, et jusqu'à trois lignes, les taux de capture du coho augmentaient d'environ 42 %. Le modèle peut être utilisé pour juger l'efficacité des limites quotidiennes de prises pour réduire les captures quotidiennes.

[Traduit par la Rédaction]

Introduction

One view of fisheries science sees fishers and fish as defining a predator–prey system. This paradigm can be useful in that it facilitates the testing of ecological models for evaluating fishers' behaviour and foraging success. Two prominent ecological models concern a predator's functional and numerical responses to prey abundance. However, for several reasons, there are few studies of fishers as predators (Hilborn and Ledbetter 1979, 1985; Peterman and Steer 1981). Perhaps the main reason that studies of the predatory behaviour of fishers are rare is that fishers are highly constrained predators. Complex management regimes that include quotas, area and seasonal closures, size limits, bag limits, etc., preclude the testing of simple hypotheses concerning the behaviour of fishers as freely foraging and competitive predators. Different designs and powers of fishing gear also complicate the calibration of the predatory skills of any one fisher or fishing vessel (Hilborn and Ledbetter 1985).

On the other hand, the information requirements of managing fisheries for conservation and allocation have led to large expenditures to measure the parameters of some fisheries. The large-scale access-point creel survey (Pollock et al. 1994, 1997) ongoing in the Strait of Georgia, British Columbia, is motivated by the need for estimates of the total number of five species of salmon and some groundfish caught by the sport fishery (e.g., Collicutt and Shardlow 1992). Those totals form a component of a Canadian Department of Fisheries and Oceans (DFO) stock assessment program whose mandate is to provide quantitative information central to the harvest management of salmon and groundfish and to assure that salmon escapement goals are achieved. Confidence in estimates of the total number of fish caught and kept, or caught and released, comes from appropriately designed and executed statistical surveys of fishing activities and out-

Received January 12, 1998. Accepted February 10, 1999.
J14386

B.D. Smith. Environment Canada, Canadian Wildlife Service, Pacific Wildlife Research Centre, 5421 Robertson Road, Delta, BC V4K 3N2, Canada. e-mail: barry.smith@ec.gc.ca

© 1999 NRC Canada

Table 1. Annual sport angling regulations directly or indirectly affecting the retainable daily catch by a licensed angler who targeted and caught exclusively either chinook salmon or coho salmon in the Strait of Georgia from 1984 to 1993.

	Chinook salmon				Coho salmon			
Year	DBL	Minimum retainable size (cm)	Annual bag limit	% released	DBL	Minimum retainable size (cm)	Annual bag limit	% released
1984	4, 2[a]	45	30	25	4	30.5	None	23
1985	2	45	20	17	4	30.5	None	16
1986	2	45	20	17	4	30.5	None	4
1987	2	45	20	14	4	30.5	None	15
1988	2	62[b]	8	37	4	30.5	None	16
1989	2	62	15	50	4	30.5	None	15
1990	2	62	15	53	4	30.5	None	24
1991	2	62	15	52	4	30.5	None	7
1992	2	62	15	49	4	30.5	None	28
1993	2	62	15	52	4	30.5	None	26

Note: The DBL for the total of all salmon species caught is four fish. The percentage of chinook salmon or coho salmon caught and subsequently released by anglers targeting each species is also tabled.

[a]Only for 1 December until 31 March or within Howe Sound.

[b]Introduced 1 December 1988.

comes. The Strait of Georgia creel survey was designed to estimate, with 95% confidence, catch and effort within 20% of their true values by sampling at least 5% of boat-trips.

By the end of 1993, the Strait of Georgia creel survey database contained several hundred thousand records of access-point interviews of sport anglers. These interviews were conducted by posing questions to anglers at an access point (e.g., a launch ramp) regarding the number of salmon and groundfish they caught (then either kept or released), their effort (in hours spent angling), and some attributes of effort for their just completed boat-trip. The angling power of a daily boat-trip can be defined by measured attributes of effort such as the number of licensed anglers or the number of angling lines. This allows subsets of boat-trips to be segregated into specific angling fleets defined by those attributes shared by all boats in that fleet.

The Strait of Georgia sport fishery for chinook salmon (*Oncorhynchus tshawytscha*) and coho salmon (*Oncorhynchus kisutch*) is a year-round saltwater fishery prosecuted by anglers who fish from shore or a boat. Both serious and casual anglers participate in this fishery because of its adjacency to the urbanised lower mainland of British Columbia (greater Vancouver) and southern Vancouver Island. Anglers are also entitled to catch sockeye salmon (*Oncorhynchus nerka*), pink salmon (*Oncorhynchus gorbusha*), chum salmon (*Oncorhynchus keta*), as well as groundfish. For management purposes the daily bag limits (DBL's) for the salmon species differ, e.g., four for all salmon except chinook salmon, two chinook salmon, and no more than four salmon in total (Table 1). In this study of decision-making by salmon sport anglers, I eliminated the analytical complication associated with calculating various DBL combinations that would arise from anglers catching more than one species of salmon by dealing with only those two species preferred by sport anglers, chinook salmon and coho salmon.

Motivated in part by Hilborn (1985), I address both conceptual and practical considerations related to the angling success of fleets of anglers targeting exclusively either chinook salmon or coho salmon. For various angling fleets defined by their attributes, I (1) define a unit of effort for an angling fleet given the attributes (e.g., number of angling lines, number of licensed anglers) of the boats in the fleet, (2) estimate catch rates, their variance, and the rate at which boats of an angling fleet quit a daily boat-trip, (3) question if angling success affects the length of a daily boat-trip, (4) question if angler skill affects angling success, and (5) evaluate the effectiveness of DBL's in reducing total catch per daily boat-trip. These considerations deal with the functional response of anglers to angling success (Peterman and Steer 1981). That is, once having made the decision to take a sport angling boat-trip, how is a decision to continue the boat-trip affected by angling success? By modelling the probability of catching a certain number of fish after a certain number of hours angling, and the probability of a boat ending its angling trip as a function of time and angling success, I produce bivariate probability mass distributions for the proportion of boats in an angling fleet that quit angling as a function of catch and effort. These probabilities indicate if angling success tends to encourage or discourage continuation of a boat-trip. They are also informative of how often achieving the DBL affects the length of a boat-trip and how daily catch rates are affected by the DBL. These probabilities can also be indicative of how variability in angler skill contributes to observed variability in angler success. I test, using a general linear model (GLM), if the number of anglers per boat, or the number of angling lines per boat, affects angling success and anglers' tendencies to either extend or shorten a boat-trip in response to their angling success.

Analytical model

Model development

I developed a model that captures the dynamics of a fleet of boats making daily angling trips that conforms to the following considerations: (1) only one species is targeted and caught during the boat-trip, (2) total catch for a boat-trip can be constrained by a DBL rule, (3) all boat-trips end, but after variable amounts of time angling, (4) the length of a boat-

© 1999 NRC Canada

trip can be a function of angling success (i.e., anglers quit angling because they are (dis)satisfied with the number of fish they have caught), and (5) the expected mean hourly catch rate and catch rate variance can (*i*) remain constant for a fleet ($\rho = 0$), (*ii*) be determined by the catch rate of those anglers still angling ($\rho = 1$), or (*iii*) be a function of both hypotheses ($0 < \rho < 1$). These considerations led to the conceptualisation of a bivariate probability mass distribution describing the probability that a boat-trip will end after a certain number of hours angling, and with a certain total catch. Specifically, the probability mass for each cell of the distribution can be described by

$$(1) \qquad p[Q_{C,h}] = p[C_h] \times p[E_h | S_{h-1}]$$

which reads as follows. The probability that a boat-trip will end in hour h with catch C ($p[Q_{C,h}]$) equals the probability that C fish were caught after h hours of angling ($p[C_h]$) times the probability that the boat-trip will end in hour h on the condition that the boat-trip lasted at least $h - 1$ hours ($p[E_h|S_{h-1}]$). Given models for calculating $p[C_h]$ and $p[E_h|S_{h-1}]$, their parameters can be adjusted to fit the observed data for a particular angling fleet using a criterion such as maximum-likelihood.

Useful parametric models exist for defining $p[C_1]$, $p[E_h|S_{h-1}]$ and, as a consequence, $p[C_h]$. If angling success, when measured as total catch after 1 h of angling (C_1), is treated as a discrete random variable with its variance attributable to random sampling error plus other sources of random variability (e.g., variability in fish distribution or in angler skill), then $p[C_1]$ can be modelled using the negative binomial distribution (Mood et al. 1985) with $r = \dfrac{\mu_1^2}{\sigma_1^2 - \mu_1}$ and $q = \dfrac{\mu_1}{\sigma_1^2}$, where μ_1 and σ_1 represent the mean and SD of the hourly catch rate, respectively:

$$(2a) \qquad p[C_*] = \frac{(r + C - 1)!}{C!(r-1)!} q^r (1-q)^C \quad \text{when } C < \text{DBL}$$

$$(2b) \qquad p[C_*] = 1 - \sum_{X=0}^{\text{DBL}-1} p[X_*] \quad \text{when } C = \text{DBL}$$

where the asterisk helps to conceptually distinguish hourly catch rate probabilities from the probable catches after 1 h of angling ($h = 1$), although $p[C_1] = p[C_*]$ in eq. 2. This hypothesis of a constant mean hourly catch rate and catch rate variance (i.e., $\rho = 0$) is premised upon catch rate being proportional to fish abundance and fish abundance not changing perceptibly during a boat-trip.

I base the parametric model for $p[E_h|S_{h-1}]$ on the attenuated Weibull probability distribution with parameters $\alpha > 0$ and $\beta > 0$:

$$(3) \qquad p[S_h] = e^{-\alpha h^\beta}.$$

The Weibull distribution has its genesis in failure analysis (Walpole et al. 1998) and is well suited to model the probability of a boat-trip ending as a function of time. Here, I modify the Weibull distribution to render an attenuated distribution that can be used to describe the probability of a boat-trip ending as a function of both time (h) and total catch (C):

$$(4) \qquad p[S_h] = e^{-\alpha h^{\beta(C+1)^\zeta}}.$$

The ζ in eq. 4 is a dimensionless parameter that modifies the influence of discrete catches $C = 0, 1, 2, \ldots,$ DBL on the rate of attenuation. This modified distribution is still Weibull in form with a new parameter $\beta' = \beta^{(C+1)^\zeta}$ for fixed values of C and ζ. If $\zeta = 0$, then $\beta' = \beta$ and it can be said that the probability of a boat-trip ending is independent of total catch.

Using eq. 4, I define the probability of a boat-trip ending in hour h conditional on the boat-trip having lasted at least $h - 1$ hours and as a function of total catch C, $p[E_h|S_{h-1}]$, as

$$(5a) \qquad p[E_h | S_{h-1}] = \frac{e^{-\alpha(h-1)^{\beta(C+1)^\zeta}} - e^{-\alpha h^{\beta(C+1)^\zeta}}}{e^{-\alpha(h-1)^{\beta(C+1)^\zeta}}} \quad \text{when } C < \text{DBL}$$

$$(5b) \qquad p[E_h | S_{h-1}] = 1 \quad \text{when } C = \text{DBL}$$

starting with $p[S_0] = 1$.

In practice, an analyst must choose a maximum value for h that is greater than the length of most, if not all, boat-trips. For this final hour, which I designate by h_f:

$$(5c) \qquad p[E_{h_f} | S_{h_f - 1}] = 1.$$

I used $h_f = 10$ h for the analyses presented in this paper.

The models for $p[C_1]$ and $p[E_h|S_{h-1}]$ allow the probable catches in any hour h ($p[C_h]$ in eq. 1) to be calculated sequentially in time by convolving ($\otimes$) the probable catches of boat-trips that lasted $h - 1$ hours with the negative binomial distribution of probable catch rates in hour h ($p[C_*]$), i.e.:

$$(6) \qquad p[C_h] = (p[C_{h-1}] \times (1 - p[E_{h-1} | S_{h-2}])) \otimes p[C_*]$$

using the moments μ_* and σ_*^2 where

$$(7a) \qquad \mu_* = \rho \mu_{h-1} + (1 - \rho) \mu_1$$

$$(7b) \qquad \sigma_*^2 = \rho^2 \sigma_{h-1}^2 + (1 - \rho)^2 \sigma_1^2$$

subject to the constraint that $\sigma_*^2 \geq \mu_*$. In eq. 7, μ_{h-1} and σ_{h-1}^2 refer to the mean hourly catch rate and catch rate variance, respectively, for those boats still angling after $h - 1$ hours. The ρ estimates the proportion of the hourly catch rate distribution attributable to the competing hypotheses of a constant hourly catch rate and a catch rate determined by the angling success of those anglers still angling.

The model is now fully stated. One way to conceptualize this model is to view Fig. 1, which demonstrates how different values for ζ (–0.5, 0, 0.5) influence the appearance of ideal (i.e., no sampling error) bivariate probability mass distributions. The mean hour of a boat-trip ending is independent of catch when $\zeta = 0$ (Fig. 1*b*). If $\zeta < 0$, then angling success tends to lengthen a boat-trip (Fig. 1*a*), while if $\zeta > 0$, then angling success tends to shorten a boat-trip (Fig. 1*c*).

The magnitude of estimated values for ζ is inherently scaled to the catch expectations of a particular fleet. To allow comparisons of values for ζ among fleets, I scaled ζ in

© 1999 NRC Canada

Fig. 1. Simulated bivariate distributions of the number of boats ending a daily boat-trip as a function of catch (C) and hours of angling (h) and for three values of ζ: (*a*) –0.5, (*b*) 0, and (*c*) 0.5. Expected distributions are shown for a mean hourly catch rate (μ_1) of 0.5 fish·h^{-1}, an SD of hourly catch rates (σ_1) of 1.0 fish·h^{-1}, a mean trip length (when $\zeta = 0$) of 4.0 h, an SD in trip length (when $\zeta = 0$) of 2.0 h, $h_t = 10$ h, $\rho = 0$, and the three values of ζ. The fleet size (N) is 400 boats and the DBL for a boat-trip is eight fish.

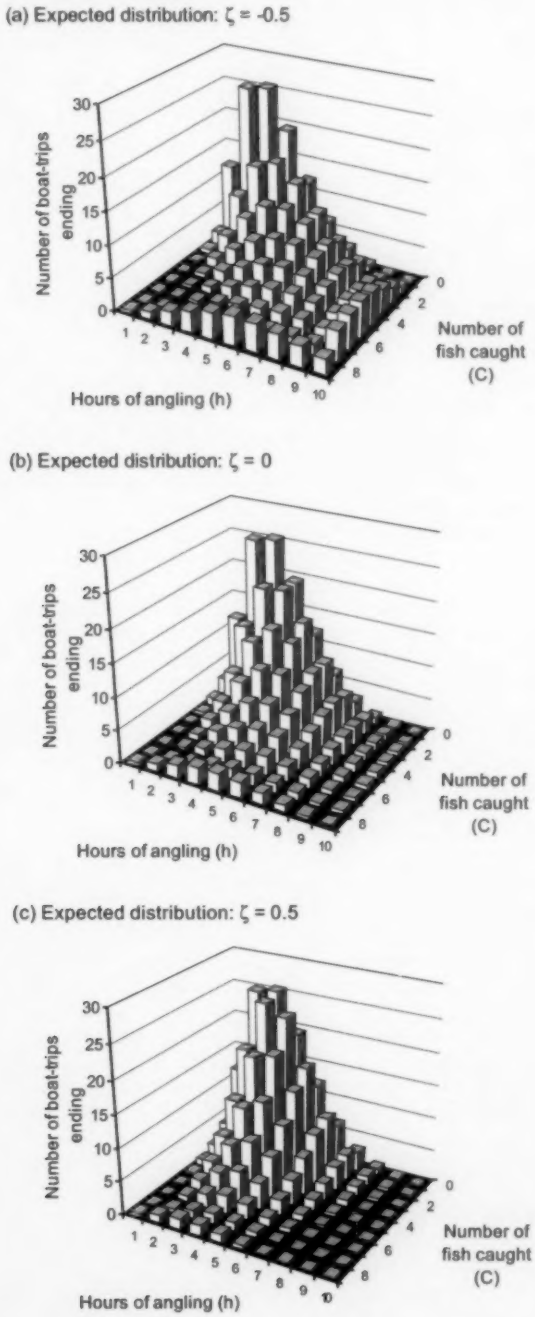
(a) Expected distribution: ζ = -0.5
Number of boat-trips ending
Hours of angling (h)
Number of fish caught (C)
(b) Expected distribution: ζ = 0
Number of boat-trips ending
Hours of angling (h)
Number of fish caught (C)
(c) Expected distribution: ζ = 0.5
Number of boat-trips ending
Hours of angling (h)
Number of fish caught (C)

order to express it relative to the catch expectation of a reference fleet ($\overline{C_R}$). I chose the fleet composed of two licensed anglers and two angling lines (2-A, 2-L) predominant in all years as the reference fleet. Scaling sets $e^{\alpha_h \beta^{(\overline{C_R}+1)}\zeta'}$ (eq. 4) equivalent to $e^{\alpha_h \beta^{(\overline{C_F}+1)}\zeta}$ such that scaled values (ζ') are defined by

$$(8) \qquad \zeta' = \zeta\left(\frac{\ln(\overline{C_F}+1)}{\ln(\overline{C_R}+1)}\right)$$

where the catch expectation of each fleet is defined as $\overline{C_F} = \mu_1 \bar{h}$, $\bar{h}$ being the expected mean trip length (hours) when $\zeta = 0$. Scaling does not change the sign of ζ.

Data preparation

I had available for analysis data from the Strait of Georgia creel survey for the years 1984–1993. One important detail of these data is that the total number of chinook salmon or coho salmon caught and retained, or caught and released, by anglers on a daily boat-trip was assigned to the boat-trip, not to individual anglers. Therefore, the DBL applicable to any boat-trip is the single angler regulatory DBL times the number of licensed anglers. This implicitly assumes that licensed anglers made only one boat-trip per day.

Anglers may have caught and released other salmon and groundfish species while targeting either chinook salmon or coho salmon. I did not investigate any possible effect of the number of chinook salmon or coho salmon caught and released on an angler's perception of his or her angling success because the release of salmon smaller than a minimum legal size limit is mandated by sport angling regulations and is not a decision made by the angler (Table 1). A change in a DBL regulation might also influence the length of a daily boat-trip or an angler's perception of his or her angling success. The DBL's for both chinook salmon and coho salmon remained unchanged during this study after 1984 (Table 1), eliminating this concern.

I organized individual boat-trips into fleets where exclusively either chinook salmon (26 687 records) or coho salmon (27 361 records) was both the target species and the only species caught, subject to some other data-refining criteria. Thus, for each species, a single data record corresponding to one daily boat-trip was accepted for analysis if and only if (1) the targeted and caught species was exclusively either chinook salmon or coho salmon, (2) the number of licensed anglers was three or fewer, (3) the number of angling lines was three or fewer, (4) the anglers were residents of British Columbia, (5) the boat-trip was not guided, (6) the number of chinook salmon or coho salmon caught and retained did not exceed the DBL for the species and corresponding fleet definition, and (7) the time targeting exclusively either chinook salmon or coho salmon (measured to the nearest 0.5 h) was no more than 10 h. The first three define categorical data that facilitate the definition of an angling fleet (e.g., all boat-trips where only one angling line was used). This definition can be extended to time periods (e.g., all boat-trips in a particular year or month). Only the last two refer to the data required to evaluate the dynamics

© 1999 NRC Canada

Fig. 2. (*a*) Observed and (*b*) estimated bivariate frequency distributions of the number of boats ending a daily boat-trip as a function of catch (C) and hours of angling (h) for the most well sampled (N = 344) monthly chinook salmon angling fleet (two licensed anglers and two angling lines (2-A, 2-L) in June 1990). For this example, μ_1 = 0.12 fish·h^{-1}, σ_1 = 0.16 fish·h^{-1}, $\bar{h}$ = 3.8 h, $\overline{C_F}$ = 0.44 fish, ζ = 0.12, and ρ = 0 (p = 0.05).

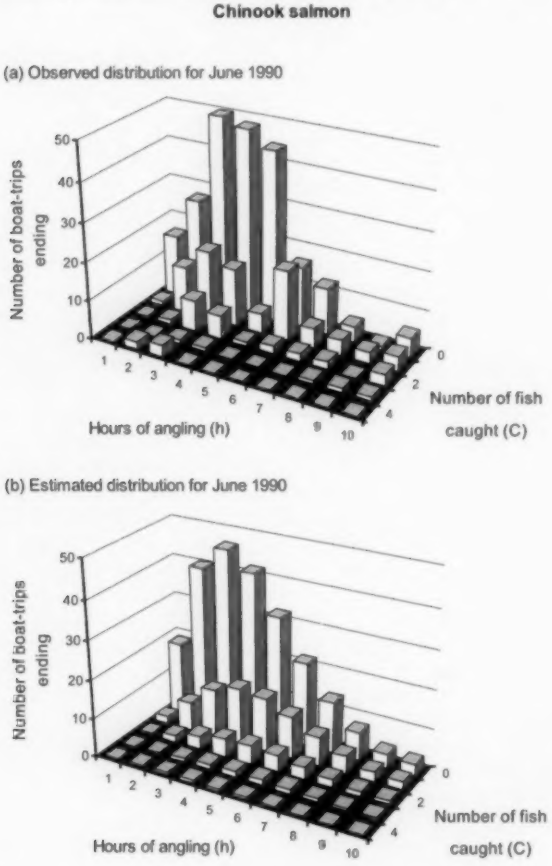
Chinook salmon
(a) Observed distribution for June 1990
Number of boat-trips ending
Hours of angling (h)
Number of fish caught (C)
(b) Estimated distribution for June 1990
Number of boat-trips ending
Hours of angling (h)
Number of fish caught (C)

of catch rate and the decision of anglers to continue or discontinue a boat-trip, i.e., total catch and total hours spent angling.

One deficiency of the data concerns the type of angling gear and bait. The former is particularly relevant to chinook salmon angling, since some anglers would have chosen to use downriggers (Argue et al. 1983) with one or more of their lines. The use of downriggers allows an angler to precisely choose an angling depth. Any difference in catch rate between lines with and without downriggers will contribute to variance in catch rates. The influences of tides, currents, time of day, fish distribution, and choice of bait can also contribute to overall variability in angling success (see Holtby et al. 1992), but these specific factors are not investigated in this paper.

Parameter estimation

Fitting the model to the data organized for this study requires that values be estimated for the six parameters introduced in eq. 2 (μ_1, σ_1), eq. 4 (α, β, ζ), and eq. 7 (ρ). Maximum-likelihood estimates for these parameters are those obtained by maximising Θ_1:

$$(9)\qquad \Theta_1(\mu_1, \sigma_1, \alpha, \beta, \zeta, \rho) = \prod_{h=1}^{h_L} \prod_{C=0}^{\mathrm{DBL}} p[Q_{C,h}]^{n_{C,h}}$$

where $n_{C,h}$ is the number of boat-trips ending with catch C in hour h. The total number of boats in the fleet, N, is

$$(10)\qquad N = \sum_{h=1}^{h_L} \sum_{C=0}^{\mathrm{DBL}} n_{C,h}.$$

I found it more expedient to minimise the following separation statistic:

$$(11)\qquad \Theta_2(\mu_1, \sigma_1, \alpha, \beta, \zeta, \rho) = 2\sum_{h=1}^{h_L} \sum_{C=0}^{\mathrm{DBL}} O_{C,h} \ln\left[\frac{O_{C,h}}{P_{C,h}}\right] \text{ for all } O_{C,h} > 0$$

(Schnute and Fournier 1980) rather than maximise eq. 9 to obtain maximum-likelihood estimates, although both Θ_1 and Θ_2 lead to identical estimates and their SE's. Equation 11 measures the discrepancy between the observed ($O_{C,h}$) and predicted ($P_{C,h}$) number of boat-trips ending within each frequency cell defined by C and h. The objective function Θ_2 is twice the negative ln-likelihood for a multinomial distribution, without the additive constant. The value for Θ_2 at the maximum-likelihood estimates is always zero or positive, is conveniently zero only when $P_{C,h} = O_{C,h}$ in all cells, and approximates the χ^2 statistic when N is large and the fit is good.

I used the software of Mittertreiner and Schnute (1985) to minimise Θ_2. SE's of the maximum-likelihood parameter estimates were calculated using their numerical method. The quality of model fit was diagnosed based on χ^2 probabilities (p) precisely calculated using simulation (Roff and Bentzen 1989). The χ^2 diagnostic evaluates the probability of the observed data given the model and parameter estimates; thus, higher values of p will be associated with more likely models. This diagnosis is the antithesis to null hypothesis testing where one generally tests to reject the null model.

Parameter estimates and their SE's for μ_1, σ_1, α, β, ζ, and ρ were obtained from nearly 420 analyses of various chinook salmon and coho salmon angling fleets (three anglers (A) × three lines (L) × 10 years plus the predominant "2-A, 2-L" fleet × 12 months × 10 years) where there were sufficient data. I judged a fleet to have sufficient data if N exceeded 50 boats (maximum N = 1811 for chinook salmon and N = 2862 for coho salmon). Typical chinook salmon and coho salmon data sets, and the maximum-likelihood fits to these data, are illustrated in Figs. 2 and 3, respectively. The maximum-likelihood estimate for ρ was zero in 90 and 81% of the analyses of chinook salmon and coho salmon fleets, respectively. On the basis of this strong statistical support for ρ = 0 and the simulations reported below, all analyses were redone with ρ fixed at zero.

Parameter accuracy and precision

One concern I had was that the intrinsic nonlinearity (Ratkowsky 1983; Bates and Watts 1988) of eq. 4 in particular

© 1999 NRC Canada

Fig. 3. (*a*) Observed and (*b*) estimated bivariate frequency distributions of the number of boats ending a boat-trip as a function of catch (*C*) and hours of angling (*h*) for the most well sampled (N = 796) monthly coho salmon angling fleet (two licensed anglers and two angling lines (2-A, 2-L) in June 1992). For this example, μ_1 = 1.09 fish·h^{-1}, σ_1 = 3.62 fish·h^{-1}, $\bar{h}$ = 2.9 h, $\overline{C_F}$ = 3.21 fish, ζ = 0.10, and ρ = 0 (p = 0.133).

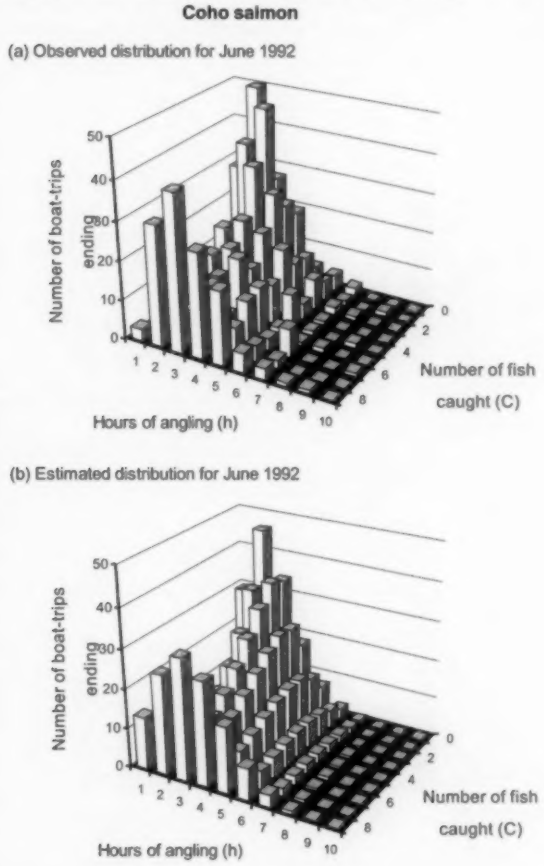
Coho salmon
(a) Observed distribution for June 1992
Number of boat-trips ending
Hours of angling (h)
Number of fish caught (C)
(b) Estimated distribution for June 1992
Number of boat-trips ending
Hours of angling (h)
Number of fish caught (C)

Fig. 4. Percent and mean trip lengths of boat-trips targeting (*a*) chinook salmon (N = 26 687, overall mean trip length is 3.7 h) or (*b*) coho salmon (N = 27 361, overall mean trip length is 3.2 h) for all years from 1984 to 1993 and according to fleet. A fleet is defined by the number of licensed anglers (A) and the number of angling lines (L).

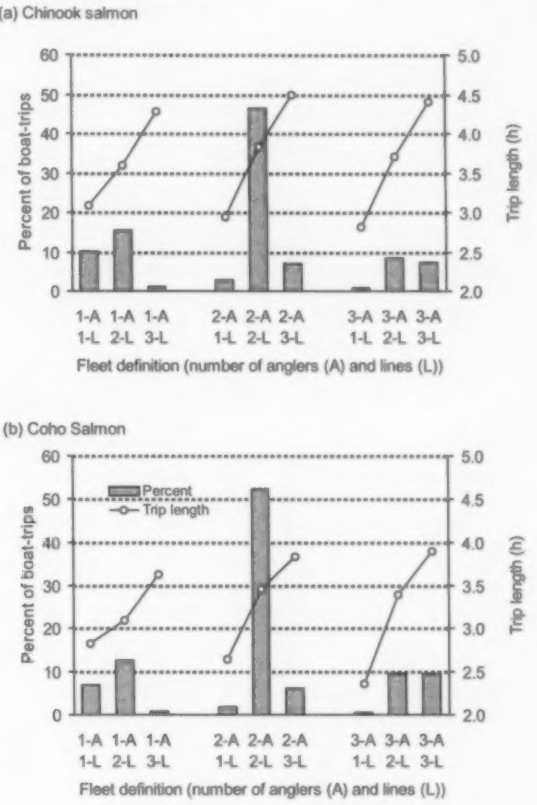
(a) Chinook salmon
Percent of boat-trips
Trip length (h)
1-A 1-A 1-A 2-A 2-A 2-A 3-A 3-A 3-A
1-L 2-L 3-L 1-L 2-L 3-L 1-L 2-L 3-L
Fleet definition (number of anglers (A) and lines (L))
(b) Coho Salmon
Percent
Trip length
Percent of boat-trips
Trip length (h)
Fleet definition (number of anglers (A) and lines (L))

could lead to seriously biased parameter estimates and their SE's, particularly for ζ. Such bias could result in parameter values that badly misrepresent fleet dynamics and lead to incorrect qualitative conclusions of fleet behaviour. To address these concerns, I performed an extensive set of analyses of data simulated using values for the six model parameters. These simulated values were generated by randomly sampling Gaussian distributions whose means and SD's were calculated using the approximately 420 parameter estimates (for ζ), or the natural logarithm of parameter estimates (for μ_1, σ_1, α, and β) obtained by analysing the chinook salmon or coho salmon angling data of this study. Natural logarithms of μ_1, σ_1, α, and β were taken to accommodate the skewness in their sample distributions, which, by definition, is always positive. Sequential predictive regressions (i.e., $\ln[\sigma_1]$ regressed on $\ln[\mu_1]$, then $\ln[\alpha]$ regressed on $\ln[\sigma_1]$, etc.) among the parameter domains were used to assure that the correlations among the simulated parameter values represented the correlations among the parameter estimates obtained from real data. Since the maximum-likelihood estimate for ρ was zero for nearly all analyses, the simulated values for ρ were obtained by randomly sampling the uniform distribution 0–1.

Simulations were performed for fleet sizes (N) of 30, 60, 120, 240, 480, and 960 boats and for DBL's of two, four, and six fish, using parameters values typical of the chinook salmon fleet, and four, eight, and 12 fish, using parameters values typical of the coho salmon fleet (Table 1). Sixty replicates for each of these simulations were performed. The parameter values estimated from these simulated fleets had undetectable bias. Mittertreiner and Schnute's (1985) numerical method usually produced reliable SE's for those estimates, with the exception of the estimates for ρ. The SE's were statistically indistinguishable from the SD's of the parameter estimates of the 60 replicates for each simulation when samples sizes were judged to be adequate (N > 50). These very acceptable results are due to the high ratio of data to parameters resulting in the model's behaviour being close to linear (Ratkowsky 1983; Bates and Watts 1988) at the maximum-likelihood parameter estimates. The simulations revealed that sample sizes greater 480 boats were re-

© 1999 NRC Canada

Fig. 5. Annual patterns in anomalies from mean trip length and ζ' for (*a*) chinook salmon and (*b*) coho salmon angling trips with two licensed anglers and two angling lines (2-A, 2-L). Error bars indicate 1 SE. Note that the minimum retainable size for chinook salmon was increased from 45 to 62 cm in December 1988 (Table 1). For chinook salmon, mean trip length is 3.8 h and N = 12 411; for coho salmon, mean trip length is 3.5 h and N = 14 304.

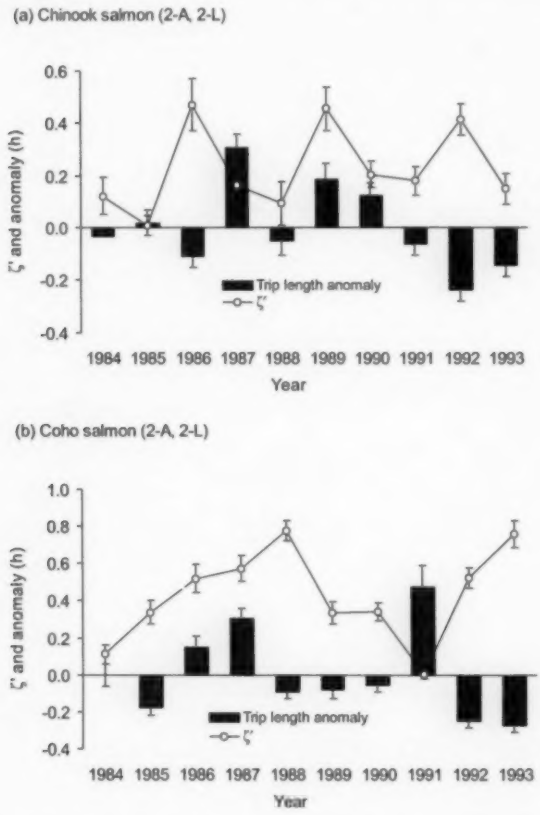

Fig. 6. Annual patterns in (*a*) chinook salmon (N = 12 411) and (*b*) coho salmon (N = 14 304) mean hourly catch rate (μ_1) and the percentage of boat-trips ending at, and due to, the DBL for angling trips with two licensed anglers and two angling lines (2-A, 2-L). Error bars indicate 1 SE. The percentage of boat-trips ending due to the DBL is that percentage of trips where the expected catch would have exceeded the DBL. Note that the minimum retainable size for chinook salmon was increased from 45 to 62 cm in December 1988 (Table 1).

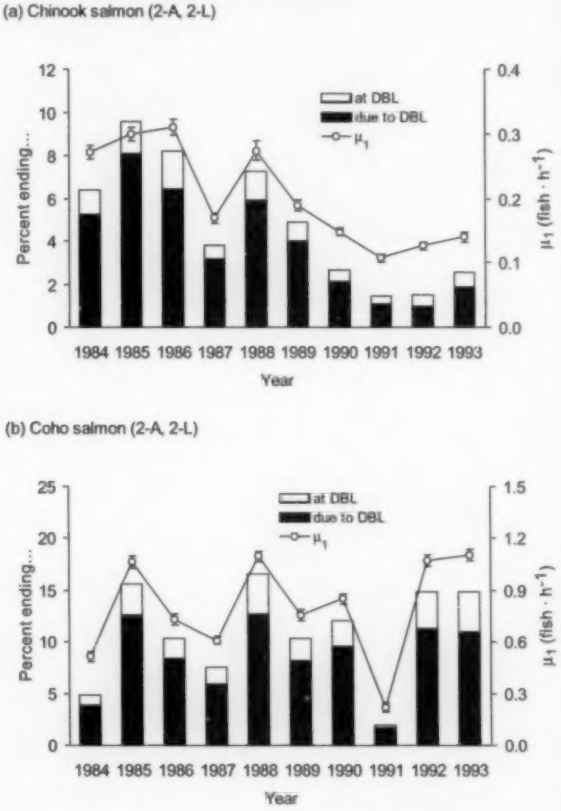

quired to obtain estimates of ρ whose 95% confidence interval excluded the extreme hypotheses ρ = 0 and ρ = 1 when ρ = 0.5. Thus, precise values for ρ could not be estimated in most analyses, and the hypothesis ρ = 0 upon which all analyses were conditioned could not be rejected.

Results

The fleet most characteristic of Strait of Georgia chinook salmon and coho salmon anglers from 1984 to 1993 was composed of two licensed anglers and two angling lines (2-A, 2-L, Fig. 4). Anglers of this fleet who targeted chinook salmon invested significantly ($p < 0.0001$) more time angling (3.8 h) than did coho salmon anglers (3.5 h), likely reflecting the generally lower catch rate for chinook salmon (see Fig. 6). For anglers targeting either species, the number of angling lines significantly influenced the length of a boat-trip, whereas the number of anglers onboard did not. Each additional angling line tended to increase the length of a boat-trip by 30–45 min. The shortest trips occurred for the most ill-equipped fleet, i.e., three anglers and one line (3-A, 1-L).

Trips targeting both chinook salmon and coho salmon varied in length according to year (Fig. 5). Although mean annual chinook salmon catch rates (Fig. 6*a*) for years before 1988 are not directly comparable with those after 1988 because of a dramatic increase in the minimum retainable size from 45 to 62 cm in 1988 (Table 1), the following interpretation can be made. Before 1988, a poor annual catch rate tended to increase the length of a boat-trip (Fig. 5*a*), whereas poorer annual catch rates in the latter years correspond to shorter trip lengths and fewer trips ending due to anglers having reached the DBL (Fig. 6*a*). An almost threefold increase in the percentage of chinook salmon caught and released after 1988 (Table 1) suggests that the catch rate for chinook salmon 45 cm and larger after 1988 might have been somewhat higher than the rate for fish 62 cm and larger. Poorer annual catch rates for coho salmon generally

© 1999 NRC Canada

Fig. 7. Monthly patterns in anomalies from mean trip length and ζ' for (*a*) chinook salmon and (*b*) coho salmon angling trips with two licensed anglers and two angling lines (2-A, 2-L). Error bars indicate 1 SE. For chinook salmon, mean trip length is 3.8 h and N = 12 374; for coho salmon, mean trip length is 3.3 h and N = 14 256. Insufficient data are available to confidently estimate ζ' for chinook salmon in October and for coho salmon during November through February.

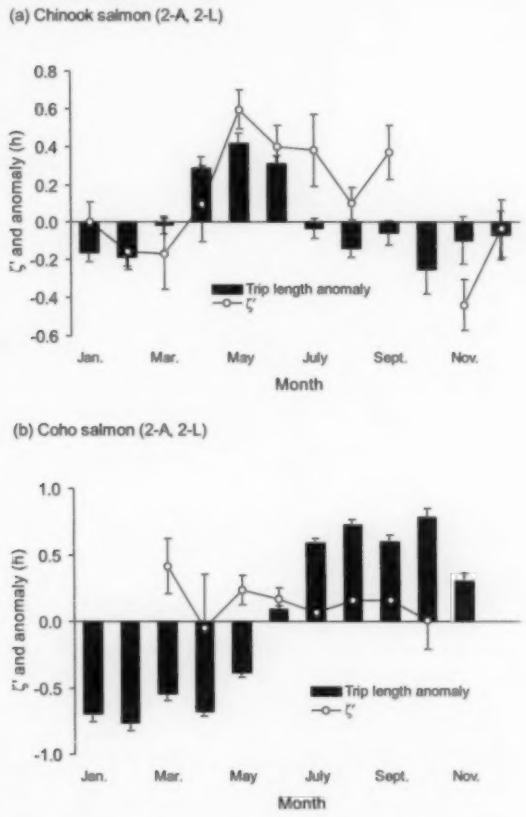

Fig. 8. Monthly patterns in (*a*) chinook salmon (N = 12 374) and (*b*) coho salmon (N = 14 256) mean hourly catch rate (μ_1) and the percentage of boat-trips ending at, and due to, the DBL for angling trips with two licensed anglers and two angling lines (2-A, 2-L). Error bars indicate 1 SE. The percentage of boat-trips ending due to the DBL is that percentage of trips where the expected catch would have exceeded the DBL. Insufficient data are available to confidently estimate μ_1 for chinook salmon in October and for coho salmon during November through February.

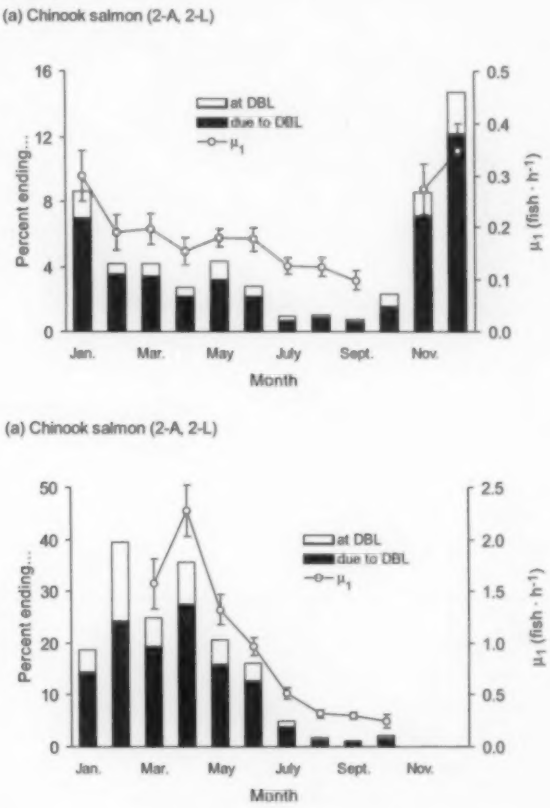

resulted in longer trip lengths (Fig. 5*b*) and fewer trips ending due to anglers having reached the DBL (Fig. 6*b*).

Monthly trip lengths for both chinook salmon and coho salmon vary with the season, the longer trips tending to occur in the more pleasant spring (chinook salmon) and summer (coho salmon) months (Fig. 7). The highest seasonal catch rates for chinook salmon occurred in the autumn and winter months (Fig. 8*a*) when the mean sizes of ocean-age-2 and ocean-age-3 fish (Argue et al. 1983) surpass the minimum retainable sizes of 45 and 62 cm, respectively (Table 1). The highest seasonal catch rates for coho salmon occurred in the spring months (Fig. 8*b*) when growth is rapid (Groot and Margolis 1991) and the mean size of ocean-age-2 fish rapidly surpasses the minimum retainable size of 30.5 cm (Argue et al. 1983).

The positive values for ζ' for all years (except 1991 for coho salmon, Fig. 5) indicate that anglers targeting chinook salmon or coho salmon tend to shorten their boat-trips as a result of angling success. Notwithstanding 1991, a year of particular low coho salmon abundance, there is a slight tendency for ζ' to increase over the years, but unexplained high interannual variability is a dominant feature. Figure 7 illustrates that interpretation of ζ' is independent of mean trip length; summer boat-trips targeting chinook salmon are about an hour longer than autumn and winter boat-trips, yet summer trips tend to be shortened by angling success, while autumn and winter trips are lengthened. Arguably, chinook salmon anglers who brave uncomfortable autumn and winter conditions are keen anglers who are motivated to continue angling when they have some angling success. The high catch rate of coho salmon in the spring (Fig. 8*b*) results in rapid angling success and correspondingly shorter trip lengths (Fig. 7*b*) as anglers are satisfied, reach their DBL (Fig. 8*b*), or find spring weather less comfortable than summer weather.

Using a GLM, I found the mean hourly catch rate (μ_1) of boat-trips targeting chinook salmon to be dependent on the number of anglers, with boat-trips having two and three an-

© 1999 NRC Canada

Table 2. GLM ($\ln[\mu_{ijy}] = \gamma_i + \kappa_j + \lambda_y + \varepsilon_{ijy}$) of $\ln[\mu_{ijy}$, fish·h^{-1}] for chinook salmon and coho salmon (Fig. 6) as a function of the number of angling lines (i = 1,..., 3), the number of licensed anglers (j = 1,..., 3), and the year (y = 1984,..., 1993).

Chinook salmon (n = 69, error df = 55, r^2 = 0.83, $p < 0.0001$)

No. of lines (i)	1	2	3
γ_i	0.000	0.045	–0.059
SE of γ_i	—	0.056	0.067

No. of anglers (j)	1	2	3
κ_j	0.000	0.358*	0.442*
SE of κ_j	—	0.056	0.066

Year (y)	1984	1985	1986	1987	1988	1989	1990	1991	1992	1993
λ_y	–1.671*	–1.511*	–1.660*	–2.151	–1.752*	–2.087	–2.067	–2.347*	–2.423*	–2.329*
SE of λ_y	0.081	0.081	0.081	0.081	0.081	0.081	0.081	0.081	0.081	0.087

Coho salmon[a] (n = 62, error df = 48, r^2 = 0.85, $p < 0.0001$)

No. of lines (i)	1	2	3
γ_i	0.000	0.374*	0.603*
SE of γ_i	—	0.065	0.079

No. of anglers (j)	1	2	3
κ_j	0.000	–0.027	0.037
SE of κ_j	—	0.062	0.072

Year (y)	1984	1985	1986	1987	1988	1989	1990	1991	1992	1993
λ_y	–1.017*	–0.475*	–0.679	–0.896	–0.433*	–0.819	–0.629	–1.728*	–0.288*	–0.321*
SE of λ_y	0.091	0.085	0.091	0.085	0.085	0.085	0.085	0.122	0.091	0.091

Note: The model uses fewer than 90 observations (see Fig. 9) because the analyses were restricted to estimates of μ_{ijy} based on fleets with more than 50 boat-trips to assure that the variance was normal and homogeneous. Reconstructing the relationship $\overline{\mu_{ijy}} = e^{\gamma_i + \kappa_j + \lambda_y}$ allows multiplicative comparisons of mean hourly catch rates ($\overline{\mu_{ijy}}$) according to the number of angling lines, the number of anglers, or the year. Asterisks within the number of lines or number of anglers classes indicate values statistically different from the value for one line or one angler, respectively ($p < 0.05$). Asterisks within the year-class indicate values statistically different from the mean value for all years.

[a]For coho salmon the estimated hourly catch rate ($\overline{\mu_{ijy}}$) of two lines is 1.45 (e^{γ_2}) times that of one line, while the hourly catch rate of three lines is 1.83 (e^{γ_3}) times that of one line. These differences in hourly catch rates are strongly statistically significant ($p < 0.0001$) (Fig. 9).

glers onboard tending to be more successful regardless of the number of angling lines (Table 2; Fig. 9*a*). Having more anglers onboard would allow more attention to be paid to each line, with perhaps more success in landing a chinook salmon attracted to a line. Angling success was equal regardless of the number of lines used, suggesting that one, two, or three lines have essentially the same effective area fished relative to the distribution and effective foraging area of chinook salmon (Shardlow 1993). This occurs despite that many boat-trips with two or three lines would have used lines with and without downriggers to angle the extensive depth range of chinook salmon (Orsi and Wertheimer 1995; Candy et al. 1996). On the other hand, there was no difference in mean hourly catch rate (μ_1) of coho salmon for boat-trips with one, two, or three anglers onboard (Table 2; Fig. 9*b*). However, the estimated hourly catch rate of two lines is 1.45 times that of one line, while the hourly catch rate of three lines is 1.83 times that of one line. This suggests that more lines result in a larger effective area fished relative to the distribution and effective foraging area of coho salmon (Shardlow 1993).

A GLM also revealed that boat-trips targeting coho salmon tended toward smaller, but positive, values of ζ' as the number of anglers onboard increased (Table 3; Fig. 10*b*). This result is intuitive in that with more anglers onboard, the focus of a boat-trip could be distracted from angling to include other social considerations such as camaraderie (Holland and Ditton 1992; Spencer 1993; Fisher 1997). Also, the need to accommodate the personal and domestic responsibilities of each angler means that it becomes more likely that a boat-trip will end for reasons independent of angling success as the number of anglers increases. The potential catch of a boat-trip with two or three anglers exceeds that of one angler, since the DBL would be double or triple that for a single angler. This increased catch potential would tend to lengthen boat-trips using two or three lines, while ill-equipped boat-

© 1999 NRC Canada

Fig. 9. Means for all years from 1984 to 1993, mean annual values, and means predicted by a GLM (Table 2) for hourly catch rates (μ_1) of (*a*) chinook salmon and (*b*) coho salmon. Annual means are shown for fleets of more than 50 boat-trips. A fleet is defined by the number of licensed anglers (A) and the number of angling lines (L). There were 50 or fewer boat-trips of the fleets 1-A, 3-L and 3-A, 1-L in all years; ergo, no annual mean values for μ_1 were available for analysis from these two categories.

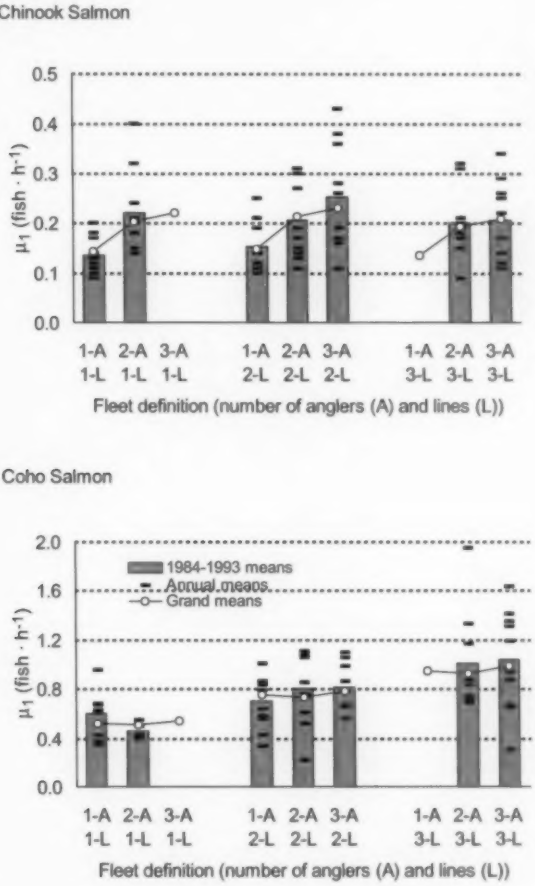

trips, e.g., three anglers and one line (3-A, 1-L), would tend to be shortened when a DBL constrains catch (Fig. 4*b*).

As the number of lines for boat-trips targeting coho salmon increases from one to three, the values of ζ' also tend to increase (Table 3; Fig. 10*b*). This could be a result of the increased catch rate of coho salmon for two and three lines, relative to one line (Fig. 9*b*), leading to boat-trips ending earlier than they would have otherwise ended. Notwithstanding this dynamic, and further illustrating that ζ' is independent of mean trip length, boat-trips targeting coho salmon tended to increase in length as the number of lines increased (Fig. 4*b*). This implies that anglers using more lines are prepared to commit relatively more time to angling.

Boat-trips targeting chinook salmon may have similar dynamics for ζ' in relation to the number of anglers and number of lines, but this dynamic is not clearly revealed in the data that I analysed (Table 3; Fig. 10*a*). However, as for coho salmon, boat-trips with three lines had the highest values for ζ'. It might be that the smaller DBL for chinook salmon and an hourly catch rate generally only 20–25% of that for coho salmon preclude the statistical identification of such a dynamic, given the relatively low sample sizes for those fleets other than the 2-A, 2-L fleet (Fig. 4*a*). Consider also that the chinook salmon DBL for a single angler is two fish and that the low hourly catch rate for chinook salmon (Figs. 6*a* and 8*a*) means most anglers will be unsuccessful. This results in bivariate probability mass distributions that lack enough information to precisely determine the value of ζ (compare Figs. 2 and 3).

Discussion

The results presented address both conceptual and practical considerations of fisheries managers. The concept that time invested in angling is influenced by angling success is intuitive to biologists and managers of recreational fisheries. Although the functional response of anglers to the abundance of their prey is often measured by creel survey methodology, to my knowledge, no study has quantitatively measured anglers' response, in terms of time invested in angling, to angling success. On the other hand, sociological studies, usually based on questionnaire methods (Duttweiler 1976), suggest that anglers appreciate the angling experience for "fun" and "relaxation" values (Smith 1980). They are said to be less interested in actual angling success, although they are no doubt partly motivated by anticipation of successful angling (Fisher 1997).

My analyses refine these qualitative interpretations in that I show quantitatively that anglers can react in two ways to angling success. Anglers in the majority of fleets tended to use angling success to shorten an angling trip ($\zeta > 0$). An exception was autumn and winter chinook salmon anglers who seem to use angling success to lengthen a boat-trip ($\zeta < 0$, Fig. 7*a*). Holland and Ditton (1992) used sociological terminology to categorize certain aspects of angler behaviour. They defined seven categories of anglers, and among them, they included a group of anglers who rate angling success as an important component of their angling experience. These anglers need to be aroused/excited by angling success and need to have a sense of competency as anglers. My results suggest that anglers can be further categorized as anglers that are either motivated (i.e., I am catching fish, so I will keep angling) or satiated (i.e., I caught fish, so I will go home now) by their angling success. Neither behaviour contradicts the qualitative interpretations of Smith (1980) or Fisher (1997) mentioned above, but with most fleets tending to shorten a boat-trip as a result of angling success, it seems that anglers generally want to be rewarded with fish and will increase angling time to achieve that reward.

If the assumptions of the model developed here are judged appropriate for a fishery, then it can be used by a fishery manager to estimate catch rate and its variance and measure the feedback of angling success on angling effort. If, as was typical of the data that I analysed, anglers tend to end a boat-trip as a result of angling success ($\zeta > 0$), then longer boat-trips will be associated with less successful anglers who will disproportionately contribute to total effort. Ratios

© 1999 NRC Canada

Table 3. GLM ($\zeta'_{ijy} = \gamma_i + \kappa_j + \lambda_y + \varepsilon_{ijy}$) of ζ' for chinook salmon and coho salmon (Fig. 5) as a function of the number of angling lines (i = 1,..., 3), the number of licensed anglers (j = 1,..., 3), and the year (y = 1984,..., 1993).

Chinook salmon (n = 69, error df = 55, r^2 = 0.38, p = 0.011)										
No. of lines (i)	1	2	3							
γ_i	0.000	–0.018	0.314*							
SE of γ_i	—	0.098	0.118							
No. of anglers (j)	1	2	3							
κ_j	0.000	0.126	–0.119							
SE of κ_j	—	0.098	0.115							
Year (y)	1984	1985	1986	1987	1988	1989	1990	1991	1992	1993
λ_y	0.101	0.291	–0.071*	0.175	0.366	0.272	0.324	0.162	0.198	0.437
SE of λ_y	0.142	0.142	0.142	0.142	0.142	0.142	0.142	0.142	0.142	0.152
Coho salmon (n = 62, error df = 48, r^2 = 0.49, p = 0.001)										
No. of lines (i)	1	2	3							
γ_i	0.000	0.375*	0.583*							
SE of γ_i	—	0.121	0.146							
No. of anglers (j)	1	2	3							
κ_j	0.000	–0.148	–0.342*							
SE of κ_j	—	0.116	0.132							
Year (y)	1984	1985	1986	1987	1988	1989	1990	1991	1992	1993
λ_y	–0.014	0.228	0.333	0.387	0.690*	0.316	0.304	–0.431*	0.586	0.412
SE of λ_y	0.168	0.156	0.168	0.156	0.156	0.156	0.156	0.226	0.168	0.168

Note: The model uses fewer than 90 observations (see Fig. 10) because the analyses were restricted to estimates of ζ' based on fleets with more than 50 boat-trips to assure that the variance was normal and homogeneous. Asterisks within the number of lines or number of anglers classes indicate values statistically different from the value for one line or one angler, respectively ($p < 0.05$). Asterisks within the year-class indicate values statistically different from the mean value for all years.

of variance to mean greater than 1 for the fleets targeting chinook salmon (≈1.8) and coho salmon (≈4.6) confirm that variability in angling success is due to factors in addition to sampling variability. However, despite successful anglers tending to quit angling after having had some angling success, this decision alone will not bias appropriate sample statistics used to estimate hourly catch rate. The reason for this is that all anglers, whether successful or not, have the same expected hourly catch rate (μ_1). So although a boat-trip may have ended because the anglers were successful, their success cannot be attributed to them being better anglers, given the strong statistical support for $\rho = 0$ (eq. 7). This is not to say that there is no variation in skill among anglers, rather that angler skill is not a factor required to explain catch rate and catch rate variance for this fishery. The statistical conclusion of a constant mean hourly catch rate and catch rate variance ($\rho = 0$) seems reasonable for this easy-access open-water fishery where information on fish location, abundance, bait effectiveness, etc., moves rapidly among anglers.

Unlike the model estimators for mean hourly catch rate (μ_1) and catch rate variance (σ_1^2), the simulations showed that the unbiased stratified sample statistics

$$(12)\quad \mu_1' = \frac{1}{N}\sum_{h=1}^{h_t}\frac{1}{h}\sum_{i=1}^{N_h} C_i = \frac{1}{N}\sum_{i=1}^{N}\frac{C_i}{h_i}$$

$$(13)\quad \sigma_1'^2 = \frac{1}{N}\sum_{h=1}^{h_t}\frac{1}{h(N_h-1)}\left(\sum_{i=1}^{N_h} N_h C_i^2 - \left(\sum_{i=1}^{N_h} C_i\right)^2\right)$$

tended to underestimate their true values as DBL's were lowered, thus forcing more boats to quit angling at that lower DBL. Also, true catch rate variance tended to be underestimated when true $\zeta \neq 0$. These tendencies are probably partly due to these two estimators being more sensitive to a loss of resolution associated with time being measured in discrete units than were their corresponding model estimators. Short boat-trips with low catches provide poor information for accurately calculating catch rates and their variances using sample statistics. Note that these two estimators (eqs. 12 and 13) treat hours (h) as strata, since, if unfettered, cumulative catch should progress as a Poisson ($\mu_1 = \sigma_1^2$) or negative binomial ($\sigma_1^2 > \mu_1$) process where both catch rate

© 1999 NRC Canada

Fig. 10. Means for all years from 1984 to 1993, mean annual values, and means predicted by a GLM (Table 3) for ζ'. Annual means are shown for fleets of more than 50 boat-trips targeting (*a*) chinook salmon or (*b*) coho salmon. A fleet is defined by the number of licensed anglers (A) and the number of angling lines (L). There were 50 or fewer boat-trips of the fleets 1-A, 3-L and 3-A, 1-L in all years; ergo, no annual mean values for ζ' were available for analysis from these two categories.

(a) Chinook Salmon

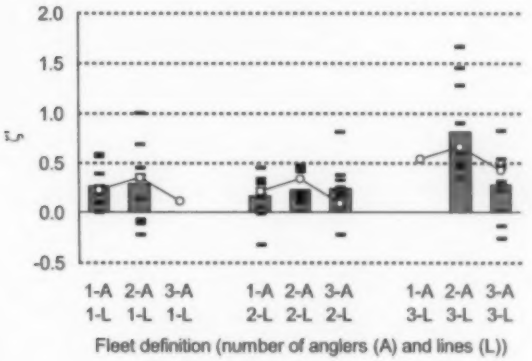

(b) Coho Salmon

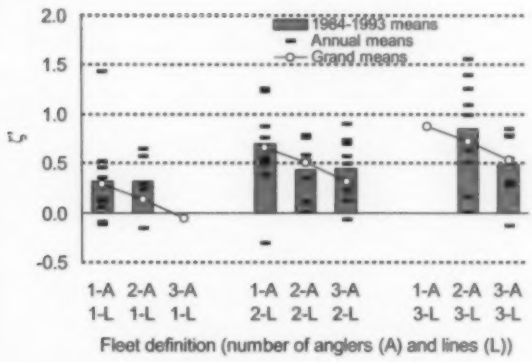

and catch rate variance increase in proportion to the number of hours angled.

I caution that the estimator of mean catch rate (μ_1) introduced in this paper and those of Pollock et al. (1994, 1997) could be seriously biased indices of fish abundance if an important amount of variability in angling success was due to variability in angler skill, this difference affected trip lengths, and there is no statistical mechanism to account for this variability. Consequently, variability in fleet dynamics from time to time or place to place could invalidate the use of mean hourly catch rate as an index to compare fish abundance among those times and places. On the basis of χ^2 goodness-of-fit ($\alpha = 0.05$), the hypothesis that all anglers have the same catch expectation ($\rho = 0$) was sufficient to explain the observed bivariate distributions for 79% of chinook salmon fleets and 75% of coho salmon fleets in the Strait of Georgia. The χ^2 diagnostic tended to fail for the largest fleet sizes, since sample distributions are rarely as ideal as predicted distributions. Goodness-of-fit tests are pessimistic in that they assume that the only source of random variability in an observed distribution is sampling error; thus, outliers can be heavily penalized in a χ^2 calculation for observed data.

The effectiveness of a DBL in reducing daily catch of one boat-trip can also be evaluated with this model structure. For example, I show in Fig. 6*a* that the chinook salmon DBL has become steadily less effective over time. In 1984, about 6% of boat-trips ended due to the DBL, while in 1993, only about 2% of boat-trips ended due to the DBL. Once model parameters are estimated for a particular fleet, then those parameter values can be used to project total effort and total catch for different DBL scenarios, thereby assisting a manager to judge the potential effectiveness of a DBL. These projections would of course be conditional on the debatable assumption that the parameters describing a fleet remain relatively unchanged in the face of changing DBL regulations (see Porch and Fox 1991). Careful use of the model to evaluate DBL effectiveness would include a sensitivity analysis of the model's parameters to such changes and of the impact of changing catch rates on the abundance of the targeted population.

Consider the following examples for the well-sampled two-angler and two-angling-line (2-A, 2-L) fleets targeting chinook salmon and coho salmon in 1990. For chinook salmon the predicted catch of those boats interviewed (N = 1811) was 1027 fish with the current DBL of four fish (two licensed anglers × a DBL of two fish per angler). Without that DBL rule the projected catch would have been 1063 fish. The DBL thus reduces the daily catch only by about 4%. About 3% of boats ended their trip due to the DBL. With the parameter values estimated for that chinook salmon fishery ($\mu_1 = 0.15$ fish·h^{-1}, $\sigma_1 = 0.52$ fish·h^{-1}, $\bar{h} = 3.9$ h, $\overline{C_F} = 0.58$ fish, $\zeta = 0.29$, $\rho = 0$), a new, lower DBL of one fish per angler would achieve about a 15% reduction in daily catch. The equivalent result for coho salmon (N = 1977) at the current DBL of four fish per angler is a 16% reduction in catch with 12% of boats ending their trip due to the DBL. With the parameter values estimated for that coho salmon fishery ($\mu_1 = 0.85$ fish·h^{-1}, $\sigma_1 = 2.23$ fish·h^{-1}, $\bar{h} = 3.5$ h, $\overline{C_F} = 2.95$ fish, $\zeta = 0.31$, $\rho = 0$), a new, lower DBL of two fish per angler would achieve about a 23% reduction in daily catch. For these two examples the values for ζ of about 0.3 indicate reductions in the mean length of boat-trips targeting chinook salmon and coho salmon of about 11 and 32%, respectively, relative to $\zeta = 0$.

The above calculations would be less tractable for fleets that targeted and (or) caught both chinook salmon and coho salmon, or the other salmon species, because of complications in calculating the DBL's. Nevertheless, the results for this subset of the Strait of Georgia sport angling community imply that only modest reductions in the daily catch by individual boats might be achieved by DBL rules because too few anglers achieve the DBL. Given these particular catch rate and effort dynamics, it would appear that dramatic reductions in total harvest can only be achieved by reducing the number of anglers. My suspicion for this fishery is that a

© 1999 NRC Canada

DBL might be more effective in reducing the number of anglers than it is in reducing the daily catch of a boat-trip. This could occur because anglers feel that their opportunity for a satisfying angling experience has been compromised or they may have been made more conscientious of a conservation concern by the imposition of a more restrictive DBL regulation.

In support of my suspicion, I am aware that in 1995, DFO decreased the summer DBL for chinook salmon in the tidal waters of Barkley Sound (DFO Statistical Area 23B on the west coast of Vancouver Island) from four fish per day to one fish per day for conservation reasons. The number of boat-trips by anglers targeting either chinook salmon or coho salmon in 1995 was estimated at 36 500, down from a mean of 49 600 (range 43 100 to 58 200) for the preceding 5 years, 1990–1994 (DFO, unpublished data). More generally, the relative importance of the functional and numerical responses of anglers to angling success will depend on the characteristics of particular fisheries, the magnitude of the DBL's, and anglers' propensities to reach the DBL. A satisfactory understanding of sport angler dynamics for a particular fishery will require that both numerical and functional responses to angling success be studied and then evaluated in the context of the impact of angling on the targeted population (Porch and Fox 1991).

Acknowledgments

I thank Sandy Argue, Ron Kadowaki, Wilf Luedke, and Brian Riddell of the Canadian Department of Fisheries and Oceans for informative discussions of the Strait of Georgia sport fishery in the context of the analyses presented in this article. The manuscript was improved in content and presentation thanks to constructive criticisms from Wilf Luedke, Doug Bertram, and Sean Boyd prior to submission and from two astute and conscientious formal reviewers.

References

Argue, A.W., Hilborn, R., Peterman, R.M., Staley, M.J., and Walters, C.J. 1983. Strait of Georgia chinook and coho fishery. Can. Bull. Fish. Aquat. Sci. No. 211.

Bates, D.M., and Watts, D.G. 1988. Nonlinear regression analysis and its application. John Wiley & Sons, Inc., New York.

Candy, J.R., Carter, E.W., Quinn, T.P., and Riddell, B.E. 1996. Adult chinook salmon behavior and survival after catch and release from purse-seine vessels in Johnstone Strait, British Columbia. N. Am. J. Fish. Manage. **16**: 521–529.

Collicutt, L.D., and, Shardlow, T.F. 1992. Strait of Georgia sport fishery creel survey statistics for salmon and groundfish, 1990. Can. MS Rep. Fish. Aquat. Sci. No. 2109.

Duttweiler, M.W. 1976. Use of questionnaire surveys in forming fishery management policy. Trans. Am. Fish. Soc. **105**: 232–239.

Fisher, M.R. 1997. Segmentation of angler population by catch preference, participation, and experience: a management-oriented application of recreation specialization. N. Am. J. Fish. Manage. **17**: 1–10.

Groot, C., and, Margolis, L. 1991. Pacific salmon life histories. University of British Columbia Press, Vancouver, B.C.

Hilborn, R. 1985. Fleet dynamics and individual variation: why some people catch more fish than others. Can. J. Fish. Aquat. Sci. **42**: 2–13.

Hilborn, R., and Ledbetter, M. 1979. Analysis of the British Columbia salmon purse-seine fleet: dynamics of movement. J. Fish. Res. Board Can. **36**: 384–391.

Hilborn, R., and Ledbetter, M. 1985. Determinants of catching power in the British Columbia salmon purse seine fleet. Can. J. Fish. Aquat. Sci. **42**: 51–56.

Holland, S.M., and Ditton, R.B. 1992. Fishing trip satisfaction. A typology of anglers. N. Am. J. Fish. Manage. **12**: 28–33.

Holtby, L.B., Kadowaki, R.K., and Simpson, K.S. 1992. Factors affecting the vulnerability of juvenile coho (*Oncorhynchus kisutch*) and chinook salmon (*O. tshawytscha*) in a saltwater sport fishery. Can. J. Fish. Aquat. Sci. **49**: 2164–2178.

Mittertreiner, A., and Schnute, J. 1985. Simplex: a manual and software package for easy nonlinear parameter estimation and interpretation in fishery research. Can. Tech. Rep. Fish. Aquat. Sci. No. 1384.

Mood, A.M., Graybill, F.A., and Boes, D.C. 1985. Introduction to the theory of statistics. 3rd ed. McGraw-Hill, New York.

Orsi, J.A., and Wertheimer, A.C. 1995. Marine vertical distribution of juvenile chinook and coho salmon in southeastern Alaska. Trans. Am. Fish. Soc. **124**: 159–169.

Peterman, R.M., and Steer, G.J. 1981. Relation between sport-fishing catchability coefficients and salmon abundance. Trans. Am. Fish. Soc. **110**: 585–593.

Pollock, K.H., Jones, C.M., and Brown, T.L. 1994. Angler survey methods and their applications in fisheries management. Am. Fish. Soc. Spec. Publ. No. 25.

Pollock, K.H., Hoenig, J.M., Jones, C.M., Robson, D.S., and Greene, C. 1997. Catch rate estimation for roving and access point surveys of anglers. N. Am. J. Fish. Manage. **17**: 11–19.

Porch, C.E, and Fox, W.W., Jr. 1991. Evaluating the potential effects of a daily bag limit from the observed frequency distribution of catch per fisher. Am. Fish. Soc. Symp. **12**: 435–456.

Ratkowsky, D.A. 1983. Nonlinear regression modelling: a unified practical approach. Statistics: Textbooks and Monographs. Vol. 48. Marcel Dekker, Inc. New York.

Roff, D.A., and Bentzen, P. 1989. The statistical analysis of mitochondrial DNA polymorphisms: χ^2 and the problem of small samples. Mol. Biol. Evol. **6**: 539–545.

Schnute, J., and Fournier, D.A. 1980. A new approach to length frequency analysis: growth structure. Can. J. Fish. Aquat. Sci. **37**: 1337–1351.

Shardlow, T.F. 1993. Components analysis of a density-dependent catchability coefficient in a salmon hook and line fishery. Can. J. Fish. Aquat. Sci. **50**: 513–520.

Smith, C.L. 1980. Attitudes about the value of steelhead and salmon angling. Trans. Am. Fish. Soc. **109**: 272–281.

Spencer, P.D. 1993. Factors influencing satisfaction of anglers on Lake Miltona, Minnesota. N. Am. J. Fish. Manage. **13**: 201–209.

Walpole, R.E., Myers, R.H., and Myers, S. 1998. Probability and statistics for engineers and scientists. 6th ed. Prentice Hall Press, Englewood Cliffs, N.J.

© 1999 NRC Canada

Population decline of the Japanese sardine, *Sardinops melanostictus*, in relation to sea surface temperature in the Kuroshio Extension

Masayuki Noto and Ichiro Yasuda

Abstract: The relationship between the population size of the Japanese sardine, *Sardinops melanostictus*, and sea surface temperature (SST) from 1979 to 1994 was studied. Significant positive correlations were found between the natural mortality coefficient during the period from the postlarval stage to age 1 and winter–spring SST in the Kuroshio Extension and its southern recirculation area (30–35°N, 145–180°E). That is, higher (lower) SST over the possible migration route corresponded to higher (lower) mortality rate. This result is consistent with the high mortality and low population size for the high-SST period of the 1950's and 1960's and the population increase during the low-SST period of the 1970's and 1980's due to a decrease in mortality. The population decline after 1988 possibly occurred as a result of the abrupt increase in SST since 1988 in the Kuroshio Extension region and suggests a close relationship between interdecadal climate–ocean variability and sardine population size. This may also explain the relationship between biomass size and distribution area.

Résumé : On a étudié la relation entre la taille de la population de pilchard du Japon, *Sardinops melanostictus*, et la température de surface de la mer de 1979 à 1994. On a observé des corrélations positives significatives entre le coefficient de mortalité naturelle depuis le stade de post-larve jusqu'à l'âge 1 et la température de la surface de la mer à l'hiver et au printemps dans l'extension du Kuroshio et sa zone méridionale de recirculation (30–35°N, 145–180°E). C'est-à-dire que les températures élevées de la surface de la mer dans la voie migratoire possible entraînaient un taux de mortalité élevé, et les basses températures s'accompagnaient d'un faible taux de mortalité. On avait de la même manière observé une forte mortalité et une faible population durant la période de températures élevées de la surface de la mer des années 50 et 60, ainsi qu'un accroissement de la population durant la période de basses températures de la surface de la mer des années 70 et 80 lié à une baisse de la mortalité. Le déclin de la population après 1988 est peut-être lié à la hausse abrupte des températures de la surface de la mer depuis 1988 dans la région de l'extension du Kuroshio, et laisse penser qu'il y a une relation étroite entre la variabilité climatique et océanique interdécennale et la taille de la population de pilchard. Cela pourrait aussi expliquer la relation entre la biomasse et l'aire de distribution.

[Traduit par la Rédaction]

Introduction

The population size of the Japanese sardine, *Sardinops melanostictus*, is known to fluctuate drastically on interdecadal time scales (Ito 1961; Kuroda 1991). The large and rapid changes have great social and economic impacts; therefore, a large number of studies have been made on the fluctuation of the Japanese sardine population. The fluctuations may be related to several factors including predation, species replacement, density effects, and the physical and biological oceanographic environments. This paper will focus on aspects of the physical oceanographic environment of the Japanese sardine.

There have been many previous studies that examined relationship between the population of the Japanese sardine and physical oceanographic conditions in the northwestern Pacific Ocean (e.g., Fukushima and Ogawa 1988; Tomosada 1988; Kawasaki 1991; Kodama et al. 1995; Kasai et al. 1997; Yasuda et al. 1999); however, they are not sufficient for understanding the sardine variations. For the population decline after 1988, Watanabe et al. (1995) attributed the cause to high larval mortality between the end of the first-feeding stage and recruitment at age 1, based on data from the 1978–1992 year-classes. This suggests that the period from post-first-feeding larvae in winter to juveniles in summer is quite important in determining sardine recruitment. However, since there is no commercial fishing in the period from spring to summer, statistical data are not available for the stage from postlarvae, "whitebait" ("shirasu" in Japanese), to age 1. Therefore, the ecology of the Japanese sardine during this stage has not been clearly defined, and mechanisms that control the population are still far from clear. In the present study, we examined the relationship between the oceanic environment and sardine mortality to clar-

Received May 28, 1998. Accepted January 27, 1999.
J14607

M. Noto. Division of Ocean and Atmospheric Science, Graduate School of Environmental Earth Science, Hokkaido University W.5, N.10, Kita-ku, Sapporo, 060-0810, Japan.
I. Yasuda.[1] Department of Earth and Planetary Physics, Graduate School of Science, University of Tokyo 7-3-1, Hongo, Bunkyo-ku, Tokyo, 113-0033, Japan.

[1]Author to whom all correspondence should be addressed.
e-mail: ichiro@geoph.s.u-tokyo.ac.jp

© 1999 NRC Canada

Fig. 1. Monthly correlation maps between SST's and relative abundances of the 1979–1994 year-classes in (A) January, (B) February, and (C) March. The light (dark) shaded areas are the regions where the correlation exceeds the 90% (95%) significant level by t test (df = 14). The contour interval is 0.25 and negative contours are dashed.

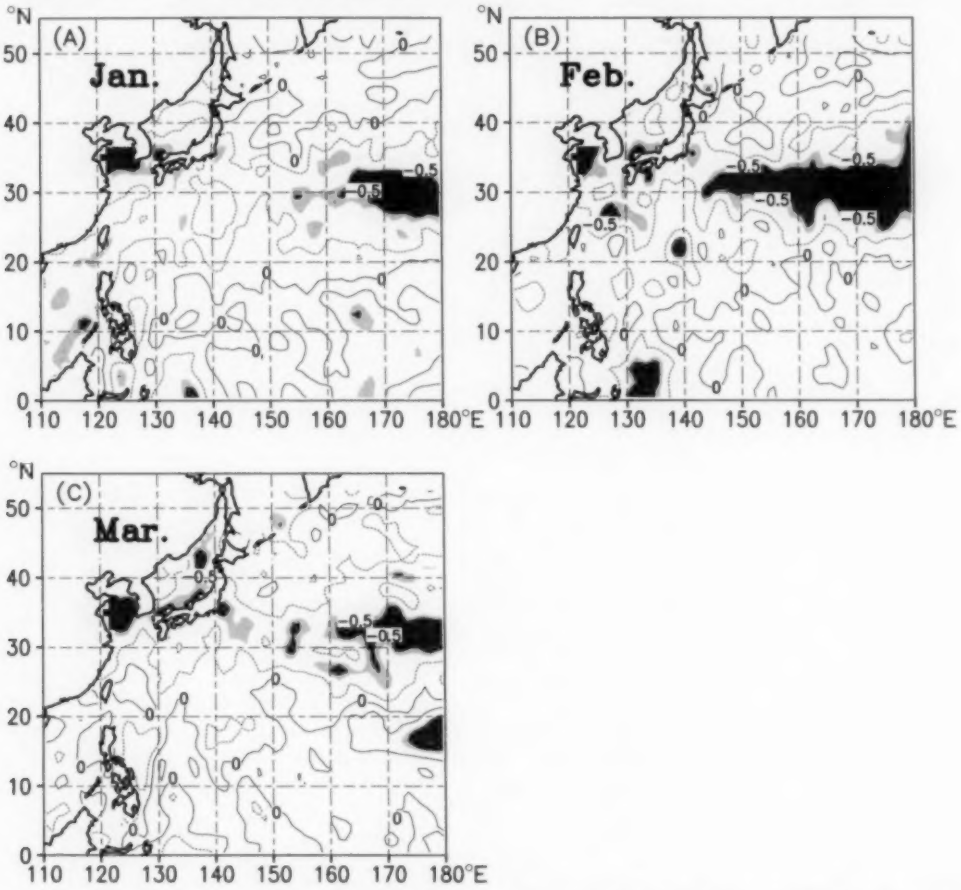

ify which area, period, and stage contribute to the Japanese sardine population.

Materials and methods

Japanese sardine and ocean data

The data used here include relative abundances of eggs, post-first-feeding larvae, postlarvae, and older year-classes of Japanese sardine in the northwestern Pacific. The annual egg production data were originally collected by two National Fisheries Research Institutes and 15 Prefectural Fisheries Experimental Stations from Kagoshima to Fukushima. Surveys were collected in the winter of each year (for technical methods, see Nakai and Hattori 1962) because most sardines spawn from December to April in the south of Japan (Ito 1961; Kuroda 1991; Watanabe et al. 1995). The surveys covered the inshore and offshore waters from Kyushu to Tohoku (northeastern Japan) along the Pacific coast during the period from 1978 to 1990 (Japan Fisheries Agency 1988, 1990, 1992); the egg data from 1991 to 1993 were censused by four National Fisheries Research Institutes and 30 Prefectural Fisheries Experimental Stations (National Research Institute of Fisheries Science 1995*a*). We used the egg data for the period from 1979 to 1993.

The post-first-feeding larva is defined as starting from the end of the first-feeding stage at 6.0–7.9 mm total length. The annual abundance of larvae was estimated by Watanabe et al. (1995). The original data were collected by two National Fisheries Research Institutes and 15 Prefectural Fisheries Experimental Stations located on the Pacific coast between Kagoshima and Fukushima (Japan Fisheries Agency 1988, 1990, 1992). We used the same data as Watanabe et al. (1995) from 1979 to 1990 and henceforth refer to larvae at the end of post-first-feeding stage as "early larvae".

The postlarvae, shirasu, were caught by shirasu boats during seine fisheries in Enshunada and its adjacent waters near the coast of Shizuoka and Aichi prefectures in springtime. The data were compiled by Kishida et al. (1994), who estimated relative abundance of the whole shirasu stock off the Pacific coast of Japan using a relationship between the location of the Kuroshio axis and an index of immigration rate of postlarvae. We used the data for the period from 1979 to 1994.

The relative abundance of the 1979–1990 year-classes was estimated by Kishida and Matsuda (1993) and Kishida et al. (1994), based on the catch in the southeastern area off Hokkaido in summer–fall from 1976 to 1990. The catch data were collected by Hokkaido Kushiro Fisheries Experimental Station. Kishida and Matsuda (1993) showed that their estimates were highly correlated (r = 0.94) with year-class estimates by Wada (1983) from 1976 to

© 1999 NRC Canada

Fig. 2. Monthly correlation maps between SST's and natural mortality coefficients (A) from egg to early larva in February, (B) from early larva to postlarva in April, and (C) from postlarva to age 1 in January and in (D) February, (E) March, and (F) April. The light (dark) shaded areas are the regions where the correlation exceeds the 90% (95%) significance level (Figs. 2A and 2B, df = 10; Figs. 2C–2F, df = 14). The contour interval is 0.25 and negative contours are dashed.

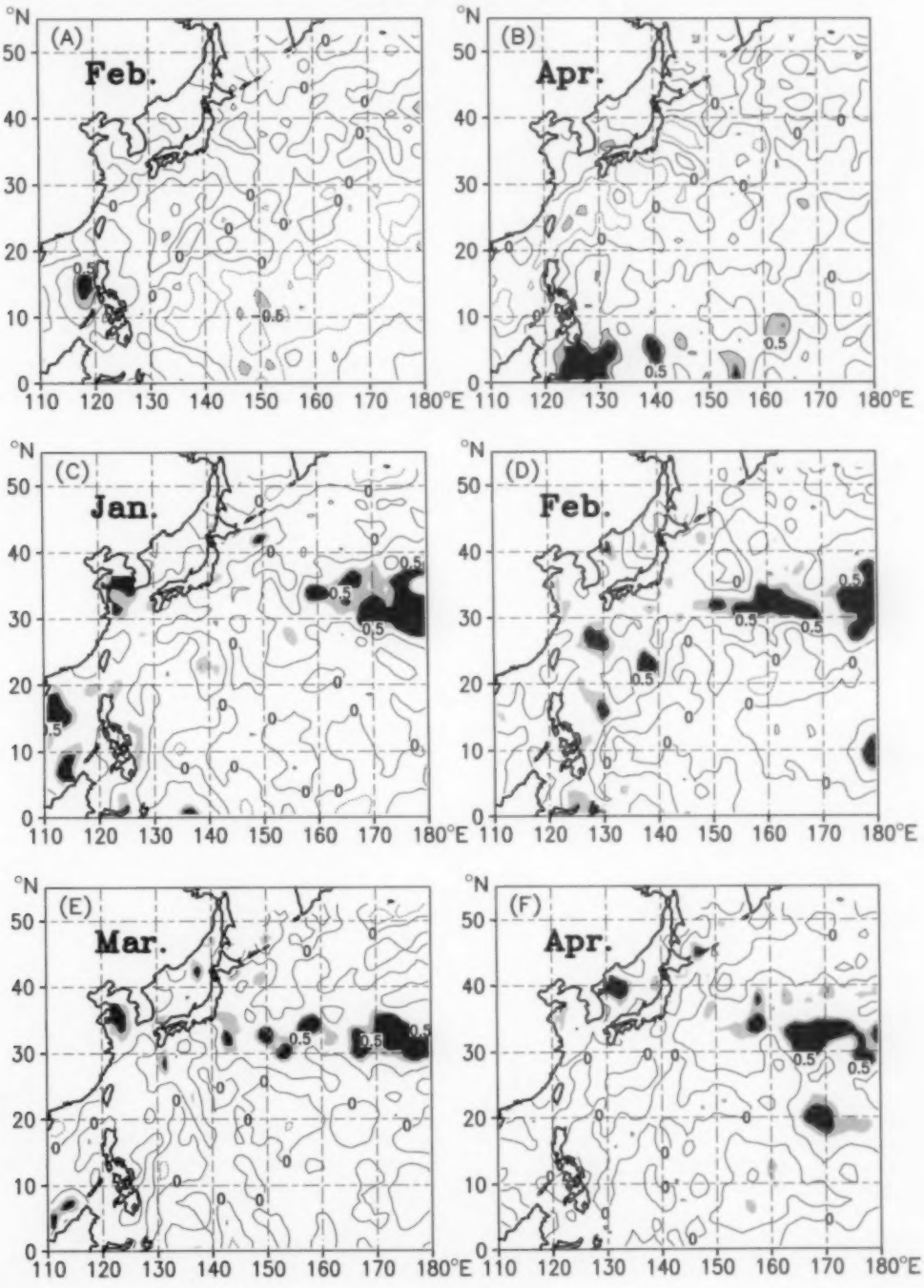

© 1999 NRC Canada

Fig. 3. Monthly correlation maps between SST's and natural mortality coefficients (A) from egg to age 1 in February and (B) from early larva to age 1 in February. The light (dark) shaded areas are the regions where the correlation exceeds the 90% (95%) significance level (Fig. 3A, df = 13; Fig. 3B, df = 10). The contour interval is 0.25 and negative contours are dashed.

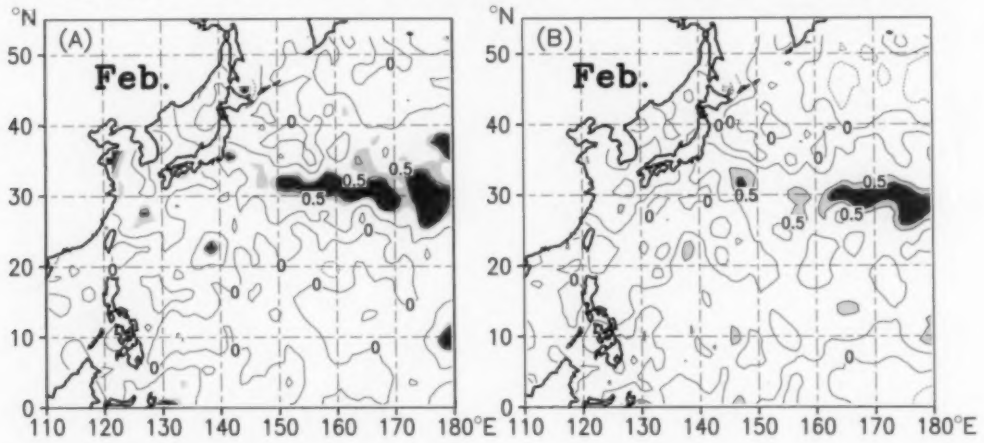

Fig. 4. Scatterplot of February SST averaged in the KESA and natural mortality coefficient anomaly from postlarva to age 1 from 1979 to 1994. The regression is represented by a solid line: $Y = -24.88 + 1.44X$, $r = 0.68$, df = 14, $P < 0.01$; $\bar{T}$ is the mean February SST in the KESA.

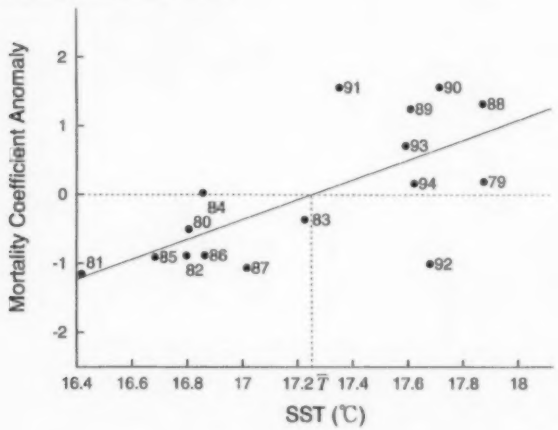

Fig. 5. Temporal variations of the February SST anomaly averaged in the KESA from 1950 to 1994 (broken line) and natural mortality coefficient anomaly during the period from postlarva to age 1 from 1979 to 1994 (thick solid line with solid circles).

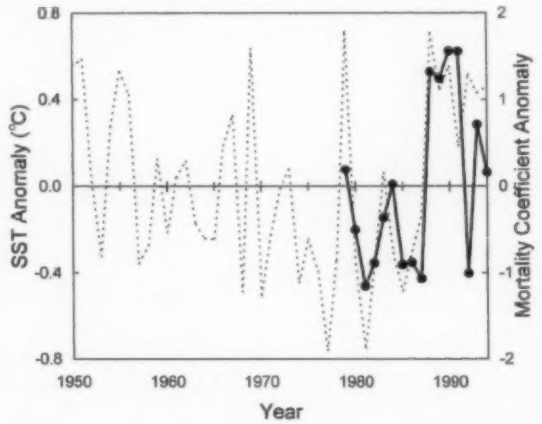

1981. In addition, we used the index of the relative abundance of year-classes from 1985 to 1994, using cohort analysis (National Research Institute of Fisheries Science 1995*b*). To obtain the relative abundance from 1979 to 1994, we adjusted these two data sets, multiplying a linear regression coefficient for the data after 1985 because the correlation in the overlapping period from 1985 to 1990 was high and significant ($r = 0.97$).

We used a sea surface temperature (SST) data set for the northwestern Pacific provided by the Oceanographical Division of the Japan Meteorological Agency to perform correlation analyses with sardine abundance and mortalities. The full data set is made up of 10-day-averaged SST's on a 1° grid over the northwestern Pacific from 110 to 180°E between the equator and 53°N for the period from 1950 to 1994. In this study, we used monthly mean SST data from January 1950 to December 1994, where we calculated monthly averages from the original 10-day means.

Geosat altimetry data were used to detect the Kuroshio Extension, which turns out to be an important area for determining survival rates in the present study. We used data on the mean flow and its temporal and spatial variations in the Kuroshio Extension along 140–180°E and 30–40°N for the 2.5-year period from November 1986 to April 1989 from the Geosat Exact Repeat Mission. The data set was obtained from Qiu et al. (1991). We calculated geostrophic flow in each 30′-interval of longitude and regard the location of maximum geostrophic flow as the Kuroshio Extension axis.

Mortality coefficient

To examine which stage contributed the most to mortality until recruitment at age 1, we analyzed relationships between SST and stage-specific natural mortality coefficients from January to June, when sardines are in the stages from egg to juvenile (Ivanov 1992; Watanabe et al. 1995; Sugisaki 1996). We estimated the natural mortality coefficients M^n in year n, assuming $N^n = N_0^n \times e^{-M^n}$,

© 1999 NRC Canada

Fig. 6. Relative abundance of the 1979–1994 year-classes. Open circles, observations; solid circles, modeled values.

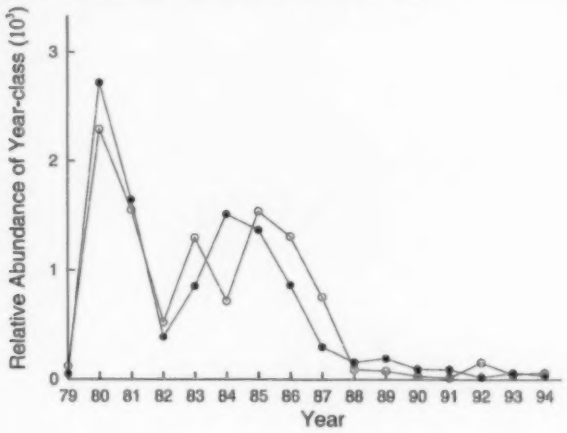

where N^n and N_0^n are final and starting abundance of each stage, respectively. The survival rate is defined as $S^n = N^n/N_0^n = e^{-M^n}$ and therefore, $-\log_e S^n = M^n$. The mortality coefficient anomaly, which is normalized by the standard deviation, is defined by the deviation from the mean value of M^n.

Results

Relationship between SST and year-class abundance

We examined the correlations in the first half of the year between SST's and relative abundances of the 1979–1994 year-classes. Our focus is on the whole northwestern Pacific because Japanese sardines can be broadly distributed in the North Pacific (Kuroda 1991; Ivanov 1992; Sugisaki 1996). Significant negative correlations, implying that high SST leads to low abundance, were found between year-class abundance and SST in the Kuroshio Extension and its southern recirculation area (henceforth, KESA: 30–35°N, 145–180°E) from January to March (Fig. 1). The correlations ($r \leq -0.50$) exceeded the 95% significant level by Student's t test. The month with the highest value and widest area of significant correlation was February (Fig. 1B). The correlation coefficient between the February SST averaged in the KESA and year-class abundance was –0.80, significant at greater than the 99.9% level. The results suggest that the winter–spring SST in the KESA is a controlling factor that determines the strength of the year-class. Significant negative correlations exceeding the 90% significant level ($r \leq -0.43$) were also seen in the Japan Sea and the Yellow Sea from January to June.

Relationship between SST and stage-specific mortality

To examine which stage contributed the most to mortality, we analyzed correlations between SST's in the first half of the year and stage-specific natural mortality coefficients from egg to early larva, from early larva to postlarva, and from postlarva to age 1. From egg to early larva, positive correlations, implying that high SST leads to high mortality, were observed in the spawning grounds around the Kuroshio from January to March when sardines spawn and hatch, but the correlations were not significant. Figure 2A shows the correlation map in February when most sardines spawn and hatch. From early larva to postlarva, negative correlations were observed along the Kuroshio from January to June, although the correlations were also not significant. Figure 2B shows the correlation map in April when sardine larvae are distributed near the Pacific coast of Japan. From postlarva to age 1, positive correlations exceeding 95% significance ($r \geq 0.50$) were observed in the KESA from January to April (Figs. 2C–2F), and the highest correlations and greatest geographic area occurred in February (Fig. 2D). The correlation coefficient between the February SST averaged in the KESA and the natural mortality coefficient from 1979 to 1994 was 0.68, significant at greater than the 99% level.

We also examined another two cases: from egg to age 1 and from early larva to age 1. In both cases, high positive correlations exceeding 95% significance were observed in the KESA from January to April, and the highest correlations and greatest geographic area occurred in February (Fig. 3). The results suggested that the survival during the period from postlarva to age 1 in the KESA mostly determines the strength of the year-class. A scatterplot (Fig. 4) shows that higher February SST's corresponded to higher mortalities during the period from postlarva to age 1 and the range of SST's during the period of lower year-class abundance from 1988 to 1994 (e.g., see Fig. 6). The SST's ranged from 16.4 to 17.9°C with a mean SST ($\overline{T}$) close to 17.2°C; however, almost all of the observations fall into two groups at higher or lower than the mean.

Temporal variations of SST in the Kuroshio Extension and population fluctuations of the Japanese sardine

When we compared the time series of the February SST anomaly averaged in the KESA and the natural mortality coefficient anomaly from postlarva to age 1, a clear relationship could be seen between the two variables (Fig. 5). In years when the SST was low (high), the mortality was low (high), which is the year-to-year relationship. On a longer time scale from 1950 to 1994 (Fig. 5), the February SST anomaly in the KESA was positive until the late 1950's and had been around zero or slightly negative in the 1960's. The SST anomaly became well below average around 1970 when the Japanese sardine catches started increasing. Low SST's continued until 1987; they then abruptly increased in 1988 and remained high until at least 1994.

Assuming that the relationship between the natural mortality coefficient and the SST in the KESA observed from 1979 to 1994 can be extended to the period from 1950 to 1978, then the low sardine population level from 1950 to 1970 may be due to higher mortalities in the earlier period of high SST. Conversely, the population increase during the low-SST period in the 1970's and 1980's could be ascribed to lower mortalities.

The mortality variations can be reproduced using the relationship between the natural mortality coefficients from postlarva to age 1, M^n, in year n and the February SST's in the KESA from 1979 to 1994 (Fig. 6). The form of the function is the linear regression $M^n = -30.95 + 1.83 \times \mathrm{SST}^n_{\mathrm{KESA}}$ and $N^n = N_0^n \times e^{-M^n}$, where N_0^n and N^n are the relative abundance of postlarval and 1-year-old sardines, respectively. The modeled abundance agrees well with the observations (Fig. 6).

© 1999 NRC Canada

Fig. 7. Ten-year average February SST anomalies (°C) for the years (A) 1950–1959, (B) 1960–1969, (C) 1970–1979, (D) 1980–1987, and (E) 1988–1994. The shade interval is 0.25 and zero is represented by the solid contour line.

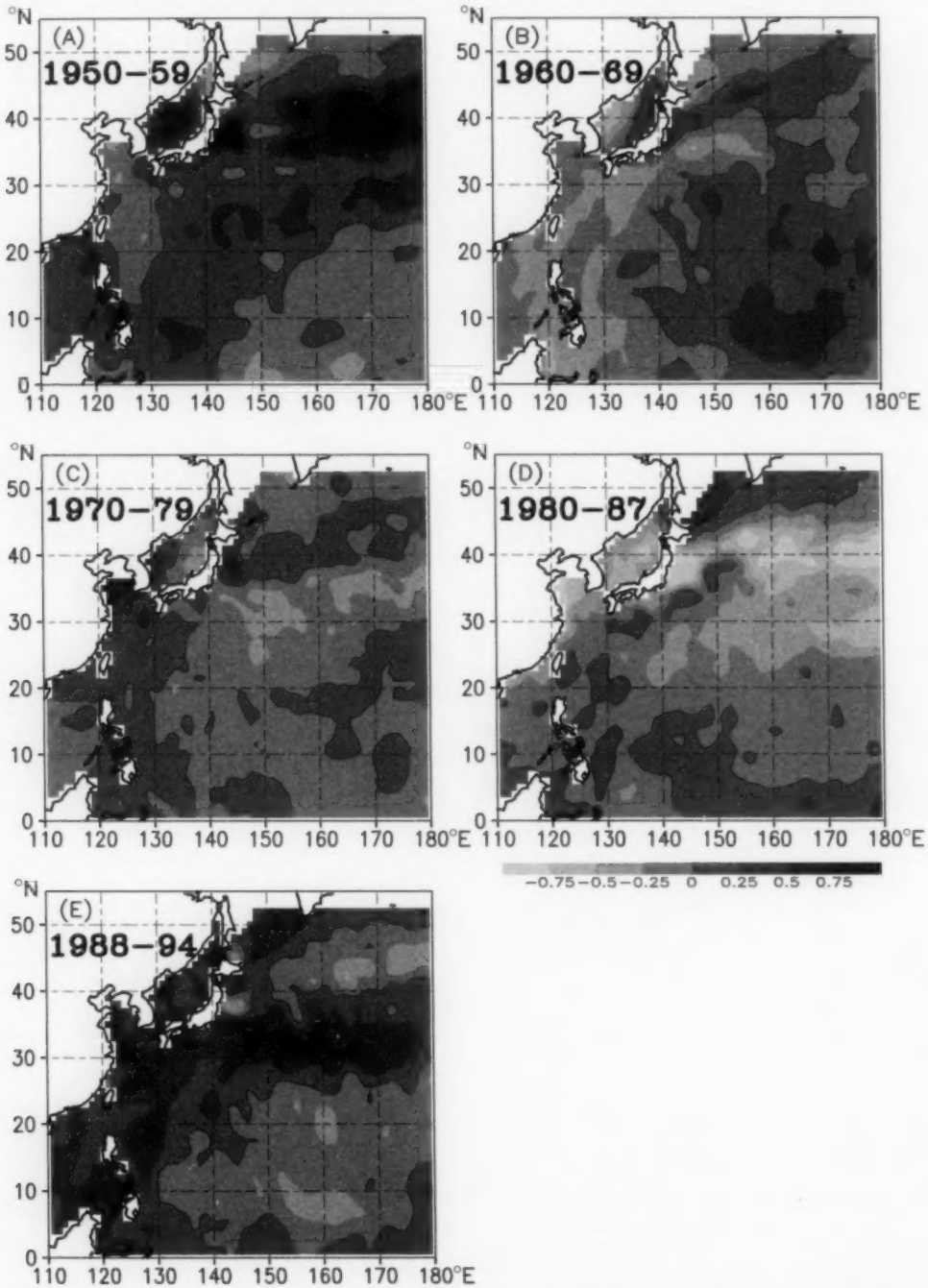

Interdecadal SST variability in the northwestern Pacific

The winter SST anomalies around the Kuroshio Extension where sardines possibly migrate changed from negative to positive in 1988 (Fig. 5). Ten-year composite February SST anomalies in the northwestern Pacific during the five periods of the 1950's, 1960's, 1970's, 1980–1987, and 1988–1994 are helpful to sketch out the spatial difference in the SST variability (Fig. 7).

Figure 7 shows that the February SST anomalies differ between the KESA and the Kuroshio–Oyashio transition

© 1999 NRC Canada

Fig. 8. Monthly latitude, velocity, and SST along the Kuroshio Extension axis where maximum geostrophic flow was detected in each 30′ of longitude in the region of 30–40°N and 140–180°E and SST anomaly in the KESA from January 1987 to December 1988. The first three variables are the monthly mean values averaged in the region of 30–40°N and 140–180°E.

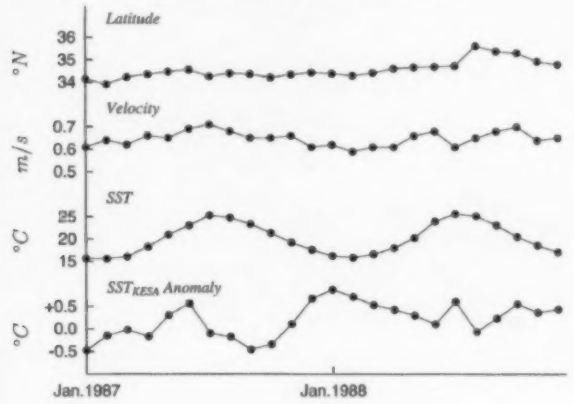

region (henceforth, KOTR: 35–45°N, 145–180°E). In the 1950's, positive SST anomalies were seen in the KESA, and the most intense positive anomalies were observed in the KOTR (Fig. 7A). In the 1960's, SST anomalies weakened in both areas, with anomalies in the KESA becoming slightly negative whereas slightly positive SST anomalies were observed in the KOTR (Fig. 7B). Negative SST anomalies in the KESA continued during the 1970's whereas positive SST anomalies were still observed in the KOTR (Fig. 7C). Negative SST anomalies were distributed in both regions from 1980 to 1987 (Fig. 7D). During the period from 1988 to 1994, SST anomalies around the KESA became highly positive, while anomalies in the KOTR remained negative (Fig. 7E). Thus the SST increase occurred only in the KESA during the period of low year-class abundance from 1988 to 1994. These results indicate that changes occurring in the Kuroshio Extension region can be related to changes in the survival of the Japanese sardines but that this is not true of temperature changes in the KOTR.

Variations in the Kuroshio Extension from 1987 to 1988

We now examine the variability of the Kuroshio Extension, where Japanese sardine larvae and juveniles could be transported, and SST from January 1987 to December 1988, the period when the abrupt SST increase was observed and the population decline of the sardine began.

The monthly mean latitude, velocity, and SST along the Kuroshio Extension axis and the SST anomaly averaged in the KESA are shown in Fig. 8. Winter-averaged (January–March) latitudes of the Kuroshio Extension axis were 34.05°N in 1987 and 34.38°N in 1988, respectively. The Kuroshio Extension axis thus shifted northward about 0.3° from 1987 to 1988, as was also shown by Qiu et al. (1991). The velocity of the Kuroshio Extension fluctuated annually; however, a significant velocity jump was not detected during winter 1988. The winter-averaged SST's along the Kuroshio Extension axis were 15.92 and 16.57°C, respectively.

The SST's along the axis increased about 0.6°C from the winter of 1987 to that of 1988, despite the position of the axis having been shifted northwards where more cooling is usually expected. These results indicate that the SST jump that occurred in winter 1988 was caused not only by the northward shift of the Kuroshio Extension axis but also by an increase in the Kuroshio Extension SST.

The SST anomaly in the KESA changed from negative to positive in November 1987 (Fig. 8). The high SST anomaly continued at least until December 1988. From December 1987 to February 1988, intense positive SST anomalies were observed in the KESA.

Figure 9 shows the Kuroshio Extension axis superimposed on the SST anomalies over the northwestern Pacific from February 1987 to May 1988. The February SST anomalies in 1987 during the period of low mortality were negative along the Kuroshio Extension axis except for the region from 150 to 160°E (Fig. 9A). Negative anomalies were remarkable in the areas of 142–147°E and east of 155°E on the northern side of the Kuroshio Extension axis. In contrast, in February 1988 the SST anomalies were positive along the Kuroshio Extension axis and its southern areas (i.e., KESA) (Fig. 9E). These results clearly show that the SST in the KESA increased in 1988 whereas the winter–spring SST anomaly on the northern side of the Kuroshio Extension axis was still negative.

In November 1987, the SST anomalies became highly positive in the Kuroshio area south of Japan and upstream of the Kuroshio Extension areas (20–33°N, 120–150°E) (Fig. 9D). The positive anomaly appeared to propagate northeastward during the period from November 1987 to May 1988 and continued until at least May 1988 (Figs. 9D–9F).

Discussion

We have studied the relationship between the Japanese sardine population and SST. In particular, to examine which life stage contributed the most to mortality until recruitment at age 1, we compared the natural mortality coefficients between various stages and January–June SST's. Significant negative correlations were found between SST and year-class abundance (high SST's leading to low abundances) in the KESA from January to March. Positive correlations were observed between the mortality coefficients for the postlarva to age 1 period and the SST's in the KESA from January to April. On the other hand, the correlations between the mortality coefficients in the early developmental stages and the SST's in the KESA were not significant, although significant positive correlations between the mortality coefficients from these early stages until age 1 were observed from January to April. These results and the belief that eggs and early stage larvae are distributed mainly around the Kuroshio south of Japan and not in the KESA in winter–spring (Ito 1961; Kuroda 1991) lead to the conclusion that mortality from postlarva to age 1 in the Kuroshio Extension region contributes most to determine the abundance of recruits on the year-to-year basis. This is consistent with the suggestion of Watanabe et al. (1995) that mortality after the end of the first-feeding stage controls the subsequent strength of the

© 1999 NRC Canada

Fig. 9. Variations in SST anomalies (°C) with the axis of the Kuroshio Extension (white dots) from February 1987 to May 1988 at 3-month intervals in the northwestern Pacific in (A) February 1987, (B) May 1987, (C) August 1987, (D) November 1987, (E) February 1988, and (F) May 1988. The shade interval is 0.5 and zero is represented by the solid contour line.

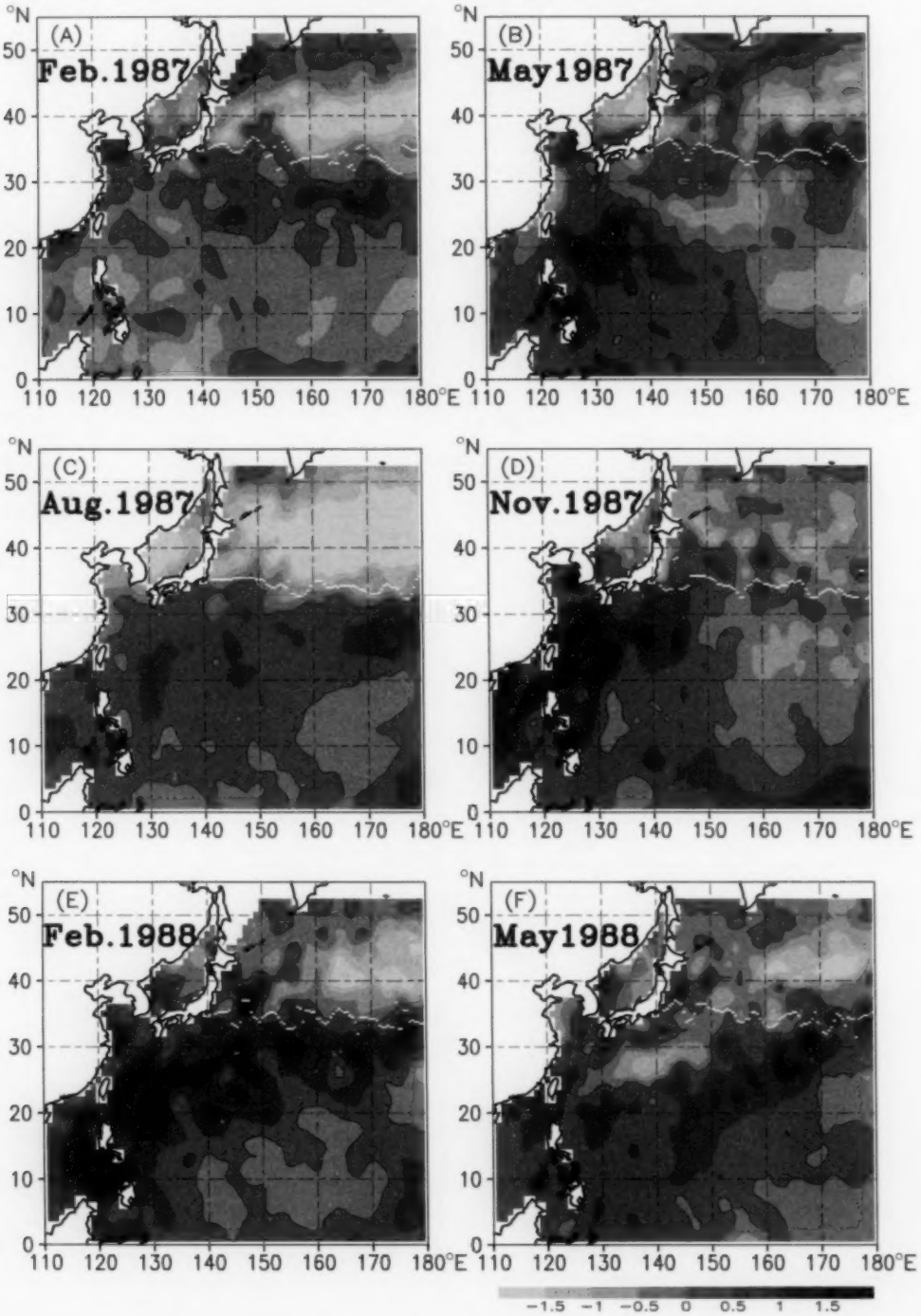

© 1999 NRC Canada

Fig. 10. Schematic illustration of the possible migration route of the Japanese sardine (broken curves) and winter atmosphere–ocean conditions. Sg, spawning grounds; Fg; feeding grounds; AL, Aleutian Low. $N = kg \cdot m \cdot s^{-2}$.

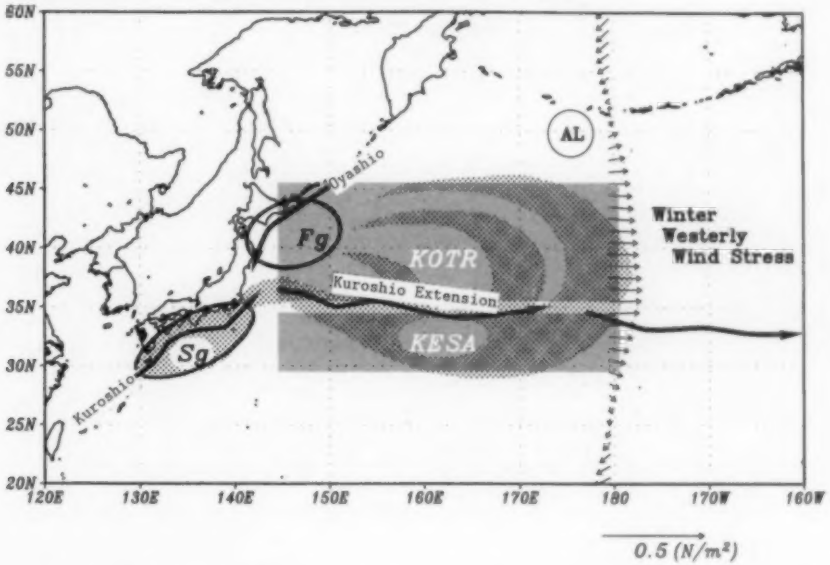

year-class. The present study further limited life stage and area that control year-class abundance.

The first question that arises is whether Japanese sardine larvae and (or) juveniles really do go to the KESA region in winter–spring. If we consider that adult sardines spawn in the Kuroshio area south of Kyushu, for example, around 130°E and 30°N in January, and that sardine eggs and larvae are transported at typical speeds for the Kuroshio and the Kuroshio Extension (about 1 m/s), the young sardines can be advected to 160°E 1 month later (February). Even if young sardines are transported at 0.2 m/s, as has been observed near the edge of the Kuroshio and the Kuroshio Extension, they reach 150°E by June. Heath et al. (1998) indeed showed that sardine larvae are transported to the Kuroshio Extension region in 2 weeks from spawning grounds using the observed velocity field data. Thus, if we assume that larvae and (or) juveniles are transported passively with the surface water, the sardines can reach the KESA region because the Ekman transport due to the westerly wind moves the surface water in the southward direction (Fig. 10). Note that this is different from Kodama et al. (1995) and Kasai et al. (1997) who showed a relationship among the coastal SST at Miyagi (38°N, 140°E), the southern limit of the Oyashio coastal intrusion, and sardine survival. However, sardine larvae and (or) juveniles are not distributed in the coastal Oyashio regions according to a recent survey (Sugisaki 1996). The present result is also different from Fukushima and Ogawa (1988), Tomosada (1988), and Yasuda et al. (1999) who suggested a relationship between the sardine catch and the SST in the area north of Kuroshio Extension (KOTR), where the SST was still negative since 1988 when the sardine recruitment failed (Figs. 7 and 9).

The well-known relationship between biomass and distribution area of the Japanese sardine (Nakai 1962; Watanabe et al. 1979; Kuroda 1991) can be explained if sardine survival in the Kuroshio Extension determines the year-class abundance through the relationship with the SST. When winter–spring SST in the Kuroshio Extension region is low, as observed in the 1970's and 1980's, sardines can survive in the Kuroshio Extension and can expand their distribution because of strong transport in the Kuroshio and the Kuroshio Extension. At such times, sardines can utilize broader areas for nursery grounds. During the low-SST period, sardines can thus increase both their biomass and their nursery area while keeping food density almost constant. When the winter–spring SST anomaly in the Kuroshio Extension region becomes positive and high SST's continue, as observed in the 1950's and from 1988 to 1994, recruitment in the Kuroshio Extension could fail. If such poor conditions continue for more than 7 years (life span of the Japanese sardine), the population that migrates over a wide area using the Kuroshio current system should collapse. It is then expected that sardines would only be distributed near the coast of Japan where the carrying capacity is limited, as observed during the 1950's, 1960's, and 1990's.

In previous studies, the Kuroshio Extension region was believed to be an area of poor survival of Japanese sardine (Ito 1961; Kuroda 1991). However, in the KESA and the KOTR, there have been no reports on the occurrence of larvae and juveniles during the high-population period in the 1980's except for Ivanov (1992). Ivanov (1992) reported that the abundance of sardine juveniles caught in summer in the area within 40–46°N and 146–160°E was well correlated with subsequent recruitment, but the study was conducted over a short period (from 1985 to 1989) and the juvenile data were collected during summer when sardines can swim by themselves and might migrate from the KESA. Sugisaki (1996) reported on recent surveys that indicated that sardine larvae and juveniles were broadly distributed around the Kuroshio Extension, in particular near its northern edge and around the edge of warm-core rings over a wide area east of Japan from April to June; however, the observations were

© 1999 NRC Canada

conducted from 1990 to 1996 during the period of low abundance and high SST in the KESA. Hence the observations might represent the distribution after sardines had disappeared from the Kuroshio Extension region because of the high mortality rate. Further investigations are needed on survival during the migration around the Kuroshio Extension region in winter–spring.

The question that we must consider next is why the SST in the KESA from winter to early spring has a significant correlation with mortality. For this question, there is no direct evidence. A possible mechanism is that survival rates in the KESA are related to the food environment. Winter SST can be used as an index of the thickness of the surface mixed layer.

In the subtropical North Pacific, the lower the winter SST, the thicker the mixed layer (Polovina et al. 1995), and therefore the higher the nutrient levels in the spring. Polovina et al. (1995) showed that in the central Pacific the mixed layer depth was thicker in 1977–1988 than in 1960–1976, consistent with the phytoplankton difference found by Venrick et al. (1987), which suggests that lower SST in the KESA should have given a better food environment in the 1970's and 1980's.

We have shown that negative correlations were observed between SST's around the Kuroshio south of Japan and mortality coefficients from early larvae to postlarvae stages (Fig. 2B). This is consistent with Tomosada's (1988) findings that the Japanese sardine population increased and had a peak in the period of high SST in the area south of Japan. The significant correlations observed in the Japan Sea and the Yellow Sea (Fig. 1) imply the possibility of coherent fluctuations of sardines in the Japan Sea with those in the Pacific, although further studies are necessary.

The scatterplot between mortality coefficients and SST's (Fig. 4) might give an impression of a "regime shift", since the data are divided into two groups and there are no data between the two. This is simply because the studied period is before and after the SST jump and only a few SST's were available near the mean temperature. Although further considerations of the application of linear regression approaches are needed, we would like to emphasize that the year-to-year variations in mortality correspond well to SST, especially in the low-SST period (1979–1987) as shown in Fig. 5. The year-to-year relationship is new in the present study in contrast with Tomosada (1988), Kawasaki (1991), and Yasuda et al. (1999), who only discussed long-term tendencies. The simple model developed in the present study, with mortality parameterized from year-to-year variations in SST, can be used to predict sardine biomass about 1 year in advance, if this relationship holds in future (Fig. 6).

Acknowledgments

We wish to thank Y. Watanabe, Y. Oozeki, H. Sugisaki, T. Kishida, and T. Wada for their helpful comments and Y. Watanabe, T. Kishida, T. Wada, and B. Qiu for providing data. Special thanks are extended to Drs. I. Perry and D. Welch for improving our manuscript. This work was partially supported by grants from the Ministry of Education, Culture and Science and from the BIOCOSMOS project of the Japan Ministry of Agriculture, Forestry and Fisheries. We used the Grid Analysis and Display System (GrADS) routines.

References

Fukushima, S., and Ogawa, Y. 1988. Changes in catch composition of coastal pelagic fishes in relation to long-term fluctuations in oceanographic condition of the northwestern Pacific Ocean. Bull. Tohoku Reg. Fish. Res. Lab. **50**: 67–95. (In Japanese with English abstract.)

Heath, M., Zenitani, H., Watanabe, Y., Kimura, R., and Ishida, M. 1998. Modeling the dispersal of larval Japanese sardine, *Sardinops melanostictus*, by the Kuroshio current in 1993 and 1994. Fish. Oceanogr. **7**: 335–346.

Ito, S. 1961. Fishery biology of the sardine, *Sardinops melanosticta* (T. & S.), in the waters around Japan. Bull. Jpn. Sea Natl. Fish. Res. Lab. **9**. (In Japanese with English abstract.)

Ivanov, A. N. 1992. Raspregelenie i otzenka chislennoisti seboletkov sarkinui v 1989g. Prog. Rep. 22th. Meet. Jpn. Russia Joint Res. Saury, Mackerel, Sardine, Squid and Pollack. Japan Fisheries Agency, Tokyo. pp. 399–408. (In Russian with Japanese translation.)

Japan Fisheries Agency. 1988. Monthly egg productions of the Japanese sardine, anchovy, and mackerels off the southern coast of Japan by egg censuses: January, 1978 through December, 1986. *Edited by* K. Mori, K. Kuroda, and Y. Konishi. Tokai Regional Fisheries Research Laboratory, Tokyo.

Japan Fisheries Agency. 1990. Monthly egg productions of the Japanese sardine, anchovy, and mackerels off the southern coast of Japan by egg censuses: January, 1987 through December, 1988. *Edited by* H. Kikuchi and Y. Konishi. National Research Institute of Fisheries Science, Tokyo.

Japan Fisheries Agency. 1992. Monthly egg productions of the Japanese sardine, anchovy, and mackerels off the southern coast of Japan by egg censuses: January, 1989 through December, 1990. *Edited by* M. Ishida and H. Kikuchi. National Research Institute of Fisheries Science, Tokyo.

Kasai, A., Sugimoto, T., and Nakata, H. 1997. The dependence of yearly recruitment of Japanese sardine *Sardinops melanostictus* on survival in the Kuroshio–Oyashio transition region. Fish. Sci. **63**: 372–377.

Kawasaki, T. 1991. Effects of global climatic change on marine ecosystems and fisheries. *In* Climatic change: science, impacts and policy. Proceedings of the Second World Climate Conference. *Edited by* J. Jäger and H.L. Ferguson. Cambridge University Press, Cambridge, U.K.. pp. 291–299.

Kishida, T., and Matsuda, H. 1993. Statistical analyses of intra- and interspecific density effects on recruitment of chub mackerel and sardine in Japan. Fish. Oceanogr. **2**: 278–287.

Kishida, T., Katsumata, Y., Nakamura, M., Yanagibashi, S., and Funakoshi, S. 1994. An attempt for assessment on relative abundance of shirasu, larval Japanese sardine, off the Pacific coast of Japan. Bull. Natl. Res. Inst. Fish. Sci. **6**: 57–66. (In Japanese with English abstract.)

Kodama, J., Nagashima, H., and Izumi, Y. 1995. Long-term variations in the "mangoku herring", *Clupea pallasi valenciennes*, resources in relation to the ocean environments in the waters off Sanriku and Joban. Bull. Miyagi Pref. Fish. Res. Dev. Cent. **14**: 17–36. (In Japanese.)

Kuroda, K. 1991. Studies on the recruitment process focusing on the early life history of the Japanese sardine, *Sardinops melanostictus* (Schlegel). Bull. Natl. Res. Inst. Fish. Sci. **3**: 25–278. (In Japanese with English abstract.)

© 1999 NRC Canada

Nakai, Z. 1962. Studies relevant to mechanisms underlying the fluctuation in the catch of the Japanese sardine, *Sardinops melanosticta* (T. & S.). Jpn. J. Ichthyol. **9**.

Nakai, Z., and Hattori, S. 1962. Quantitative distribution of eggs and larvae of the Japanese sardine by year, 1949 through 1951. Bull. Tokai Reg. Fish. Res. Lab. **9**: 23–60. (In Japanese.)

National Research Institute of Fisheries Science. 1995*a*. Distributions of eggs and larvae of Japanese sardine, Japanese anchovy, mackerels, round herring, Japanese horse mackerel, and Japanese common squid in the waters around Japan, 1991 through 1993. *Edited by* H. Zenitani, M. Ishida, Y. Konishi, T. Goto, Y. Watanabe, and R. Kimura. National Research Institute of Fisheries Science, Tokyo.

National Research Institute of Fisheries Science. 1995*b*. Long-term forecasting on the distribution and abundance of the important fishery resources and the related oceanographic conditions in the Sea of Tohoku and Chuo Blocs. National Research Institute of Fisheries Science, Tokyo.

Polovina, J.J., Mitchum, G., and Evans, G.T. 1995. Decadal and basin-scale variation in mixed layer depth and the impact on biological production in the Central and North Pacific, 1960–88. Deep-Sea Res. **42**: 1701–1716.

Qiu, B., Kelly, K.A., and Joyce, T.M. 1991. Mean flow and variability in the Kuroshio Extension from Geosat altimetry data. J. Geophys. Res. **96**(C10): 18 491 – 18 507.

Sugisaki, H. 1996. Distribution of larval and juvenile Japanese sardine (*Sardinops melanostictus*) in the western North Pacific and its relevance to predation on these stages. *In* Survival strategies in early life stages of marine resources. *Edited by* Y. Watanabe, Y. Yamashita, and Y. Oozeki. A.A. Balkema, Rotterdam, The Netherlands. pp. 261–270.

Tomosada, A. 1988. Long-term variations in sea surface temperature and Japanese sardine catch. Bull. Tokai Reg. Fish. Res. Lab. **126**: 1–9. (In Japanese.)

Venrick, E.L., McGowan, J.A., Cayan, D.R., and Hayward, T.L. 1987. Climate and chlorophyll *a*: long-term trends in the central North Pacific Ocean. Science (Washington, D.C.), **238**: 70–72.

Wada, T. 1983. On the sardine stock off southeastern Hokkaido. Rep. Pelagic Fish Sect. Jpn. Sci. Counc. Fish. Resour. **15**: 39–55. (In Japanese.)

Watanabe, T., Honjo, K., and Okutani, T. 1979. Fluctuation of population size of the Japanese sardine, *Sardinops melanosticta* (T. & S.), and the Kuroshio. The Kuroshio IV. Proceedings of the Fourth CSK Symposium, Tokyo. Japan Ocean Data Center, Tokyo. pp. 830–848.

Watanabe, Y., Zenitani, H., and Kimura, R. 1995. Population decline of the Japanese sardine *Sardinops melanostictus* owing to recruitment failures. Can. J. Fish. Aquat. Sci. **52**: 1609–1616.

Yasuda, I., Sugisaki, H., Watanabe, Y., Minobe, S., and Oozeki, Y. 1999. Inter-decadal variations in Japanese sardine and ocean/climate. Fish. Oceanogr. **8**: 18–24.

© 1999 NRC Canada

Tropical tuna associated with floating objects: a simulation study of the meeting point hypothesis

Laurent Dagorn and Pierre Fréon

Abstract: Among the different assumptions proposed to explain why tropical tuna aggregate around floating objects ("logs"), one of the most recent is that floating objects may represent meeting points for tuna. This "meeting point hypothesis" proposes that tuna can use these floating objects to form larger schools after school fission or dispersion. The influence of meeting points on tuna school sizes is explored through different individual-based models that consider a single fusion rule and a variety of fission rules based on energetic considerations, the role of school size on school cohesion, predator attacks, and dispersion during the night. Results are first analyzed using an averaging approach to study the overall mean school size in habitats having different floating object densities. Second, a dynamic approach is used to compare the temporal dynamics of associated and free-swimming school sizes. The averaging approach indicates that in all the models (except those based on energetics), floating objects increase school size, at least up to a certain object density. The dynamic approach clearly illustrates different dynamics in the school size of associated and free-swimming schools. Most of our models show that tuna associated with logs resume schooling in larger schools after fission events.

Résumé : Parmi les différentes hypothèses proposées pour expliquer pourquoi les thons tropicaux s'agglomèrent autour d'objets flottants (« billots »), l'une des plus récentes est que les objets flottants pourraient représenter des points de rencontre. Selon cette hypothèse du « point de rencontre », les thons pourraient utiliser ces objets flottants pour former de plus grands bancs après division ou dispersion des bancs. L'influence des points de rencontre sur les tailles des bancs de thons est examinée au moyen de modèles fondés sur les individus qui utilisent une règle de fusion unique et diverses règles de division fondées sur des considérations énergétiques, le rôle de la taille du banc dans sa cohésion, les attaques des prédateurs et la dispersion nocturne. On analyse d'abord les résultats suivant une méthode d'établissement de moyennes pour étudier la taille moyenne globale des bancs dans des habitats où l'on trouve diverses densités d'objets flottants. Deuxièmement, on applique une méthode dynamique pour comparer les dynamiques temporelles des tailles des bancs associés et libres. La méthode des moyennes montre que, suivant tous les modèles (sauf ceux basés sur l'énergétique), les objets flottants accroissent la taille des bancs, au moins jusqu'à une certaine densité d'objets. La méthode dynamique, quant à elle, révèle clairement que les dynamiques de la taille des bancs associés et libres sont différentes. La plupart de nos modèles montrent que les thons associés aux billots reforment de plus grands bancs après les divisions de bancs.

[Traduit par la Rédaction]

Introduction

Tropical and subtropical fish aggregate around floating objects of various kinds (Gooding and Magnuson 1967; Hunter and Mitchell 1967; Fonteneau 1993). This phenomenon has taken on great importance in tuna fisheries. Fishers search for floating objects (and also construct and release artificial ones) because they know that finding these objects will increase their chances of finding and catching tuna. Catches ranging from a few hundred kilograms to several hundred tons of tuna are taken from under logs or floating objects such as timber, kelp, branches, or debris. In recent years, most of the world catch of tropical tuna has been taken under floating objects (Fonteneau 1993). Tuna caught near floating objects are generally smaller than those not associated with objects, particularly in the case of yellowfin tuna (*Thunnus albacares*). The net result of this has been an increase in the proportion of juvenile fish in the total catches. Consequently, fishers voluntarily decided to prohibit tuna catches under floating objects in the eastern Atlantic Ocean for a period of 3 months beginning November 1, 1997.

Tuna aggregations around logs (the terms "log" and "floating object" will be used interchangeably) has become a fundamental issue in tuna biology and tuna fisheries. Why tuna associate with floating objects is still unknown. Ultrasonic tagging studies have contributed to an improved understanding of the effects of anchored fish-aggregating devices (FAD's) on spatial behavior of yellowfin, skipjack (*Katsuwonus pelamis*), and bigeye tuna (*Thunnus obesus*) (Cayré and Chabanne 1986; Holland et al. 1990; Cayré

Received May 27, 1998. Accepted December 1, 1998.
J14610

L. Dagorn.[1] ORSTOM, BP 529, Papeete, French Polynesia.
P. Fréon. ORSTOM/SFRIM, Private Bag X2, Rogge Bay 8012, Cape Town, South Africa.

[1]Author to whom all correspondence should be addressed.
e-mail: dagorn@orstom.fr

© 1999 NRC Canada

Fig. 1. Artificial habitat (30 × 30) with a random distribution of 10 floating objects (circles).

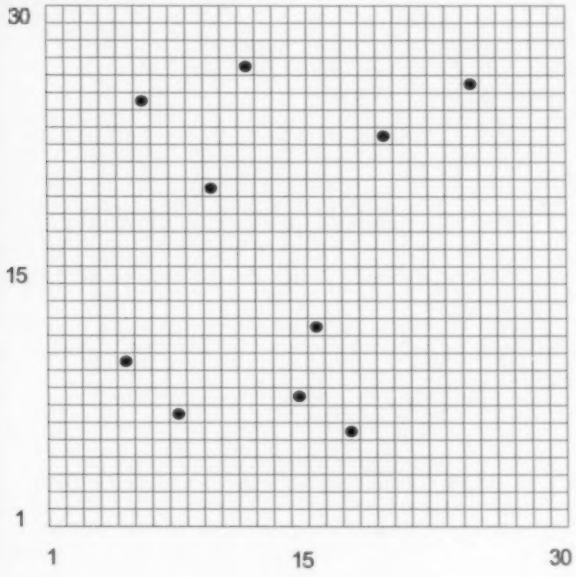

1991; Bach et al. 1998; Josse et al. 1998; Marsac and Cayré 1998) but have not determined why these fish aggregate around FAD's. In contrast with the study of anchored FAD's, few ultrasonic tagging experiments have been performed on fish around drifting logs in the open ocean (except for one study by Yonemori (1982) with inconclusive data concerning horizontal movements) or on the behavior of tuna schools around such objects. Therefore, we have to rely on fisheries' data and fishers' observations for developing hypotheses.

Fréon and Misund (1998) reviewed the different hypotheses proposed to explain the association of tuna with logs. These include hypotheses of the concentration of food supply (Kojima 1956), schooling companion (Hunter and Mitchell 1967), substitute environment (Hunter and Mitchell 1967), cleaning station (Gooding and Magnuson 1967), shelter from predator (Gooding and Magnuson 1967), spatial references (Klima and Wickham 1971), and comfortability stipulation (Batalyants 1992). Two promising hypotheses have been proposed recently: the generic log hypothesis (and related hypotheses, Hall 1992) and the meeting point hypothesis (Soria and Dagorn 1992; Fréon and Misund 1998). This paper explores the meeting point hypothesis, which proposes enhancement of fish aggregation by floating objects through improving the encounter rate between small schools or between isolated individuals or both. We think that logs can help tuna to form larger schools, as suggested by fisheries statistics, and we will test the following null hypothesis: the presence of logs does not increase school size.

Log-associated schools are usually larger than free-swimming schools, especially in the eastern Atlantic (Fonteneau 1993), assuming that catches in a purse-seine set reflect relative school sizes. This is a relatively common assumption in fisheries science in the absence of precise studies on the quantification of different biases (such as net saturation for large schools or overlooking small schools). Being a member of a large school is believed to provide many advantages to schooling fish in general. Fish foraging in schools gain benefits through faster location of food, more time for feeding, more effective sampling, information transfer, and opportunity for learning by social facilitation and can perform a repertoire of antipredator behaviors that reduce the risk of predation (Pitcher and Parrish 1993).

The aim of this study is to evaluate the effects of logs on school sizes on the basis of different assumptions about tuna behavior. Since it is difficult to design in situ experiments on tuna aggregations around logs, computer models are used to explore the meeting point hypothesis. To the best of our knowledge, this is the first attempt to study the impact of floating objects on school sizes. The models used belong to the family of individual-based models that have been applied to terrestrial ecology (see Huston et al. 1988; Hogeweg and Hesper 1990) and fish ecology (Tyler and Rose 1994). Scheffer et al. (1995) listed the main advantages of this approach: (*i*) input parameters in such models are similar to those measured by experimental biologists, (*ii*) model behavior is often robust to variations in formulation of the processes, and (*iii*) individuals are taken as natural units, which is realistic and intuitively straightforward.

Our initial intention was to model the individual behavior of a large number of fish. However, in order to simulate the behavior of several schools, it was necessary to model thousands or millions of individuals. Scheffer et al. (1995) experienced similar problems and proposed the concept of superindividuals in order to represent a population by a smaller number of units. Superindividuals are classes of individuals for which parameters in the model (e.g., energetic state) are identical. We used the same concept to simplify the computation in our models. The elementary unit of the models is therefore not a single fish but a small group of fish (composed of s individuals), and several units (N) can merge to form a larger school (composed of N units, i.e., Ns individuals). The aim here is not to study the organization of fish within schools but the organization of schools in relation to floating objects. All fish are assumed to be identical in terms of size and species. Five different models (models 0–IV) are used to test hypotheses of tuna behavior.

Material and methods

Modeling tuna habitat

In the models the habitat is defined as a lattice (30 × 30) composed of 900 small squares that are our basic space units. The opposite ends of the lattice are joined to form a torus (so that fish never leave the modeled habitat). The distribution of floating objects within this artificial habitat is random (Fig. 1). Where prey are included, we distribute them homogeneously throughout the habitat (model I), an acceptable simplification already suggested by Duffy and Wissel (1988), and predators (model III) can attack tuna schools anywhere in the habitat.

Time, space, and population scales considered in the model

The dimension of a square in the habitat corresponds to the dimension of the area of action of a floating object. From ultrasonic tagging studies on individuals around anchored FAD's (Cayré and Chabanne 1986; Holland et al. 1990; Cayré 1991; Marsac and

© 1999 NRC Canada

Cayré 1998) and from models (Hilborn and Medley 1989; Kleiber and Hampton 1994), the radius of an area over which a floating object has an effect is estimated to be 7–13 km (4–7 nautical miles). We decided to use the lower value of this action range (7 km) for the dimensions of the squares. The lattice of 30 × 30 = 900 squares that represents the tuna habitat therefore corresponds to a 210 × 210 = 44 100 km^2 area, or a 2 × 2° area, and is consistent with estimates of sizes of areas occupied by yellowfin tuna concentrations in the Atlantic Ocean (Fonteneau 1985).

Different studies on tuna behavior around FAD's (Cayré and Chabanne 1986; Holland et al. 1990; Cayré 1991; Marsac and Cayré 1998) indicate swimming speeds between 0.5 and 2 m·s^{-1} (1–4 knots). Considering the length of one square in the modeled habitat (7 km) and in order to match in situ swimming speed estimates, it was decided to set the time step to 2 h (time for a tuna to cross one square). One day is therefore equivalent to 12 time steps and each simulation lasts 360 time steps (1 month).

About 135 000 tuna are caught in a typical tuna concentration, and the smallest sets made on such concentrations are composed of about 150 individuals (Fonteneau 1985). Although smaller schools can exist, they are not likely to be worth fishing on. A reasonable size for our elementary group unit s could be 50 individuals. Combining Fonteneau's (1985) estimates and 50 individuals as the group unit, we decided to test 2500 and 500 basic group units as the size of local tuna populations. These numbers of units represent, respectively, the typical exploited concentration (2500 × 50 = 125 000 individuals) and less dense concentrations (500 × 50 = 25 000 individuals).

In our models, only one log can occupy one square (49 km^2). Logs must be separated by at least two squares to avoid overlapping of attraction areas (Fig. 1). The only available data on the frequency of logs in the open ocean come from observers from the Inter-American Tropical Tuna Commission onboard fishing vessels. It appears that the presence of floating objects is very patchy and very seasonal. From 1992 to 1994, the estimated modal density of logs observed per 3-month period fluctuated between 5 and 15 logs per 1° square (R. Solana-Sansores, Inter-American Tropical Tuna Commission, Scripps Institution of Oceanography, La Jolla, CA 92037-1508, U.S.A., personal communication). These densities correspond to 20–60 logs in our 2 × 2° artificial habitat. We then tested all the models in habitats with a total of 0, 10, 20, 30, 40, 50, and 60 logs.

Modeling tuna behavior

We consider any floating object as a potential "meeting point" where tuna schools can converge, find other schools, and merge with them. The rule implemented in the models is basic: when a school is in the range of attraction of a floating object, it simply converges to it. When a school is in the vicinity of a floating object, it does not move from there until a perturbation occurs (see below for explanations of a perturbation). If no floating object is detected, the school randomly moves to one of the four adjacent squares (random walk model, at a regular speed of one square per time step).

Tuna schools either join together to form larger schools or break up into smaller schools depending on the prevalent behavior (avoiding predation, feeding, etc.). This can be achieved by setting positive and negative rules (or attraction and repulsion rules, fusion and fission rules), which is usual in schooling models (Aoki 1982; Huth and Wissel 1992) or in more general grouping models (Gueron and Levin 1995).

In all the models (except model IV during nighttime), gregarious behavior is an obligate behavior, regardless of the values of other parameters. Hence, when two or more schools are located in the same square at the end of a time step, they are supposed to encounter each other, mix, and form only one school. In the absence of any documented observation on processes of splitting of tuna schools, different fission rules derived from studies on other species will be considered in this work. In models I and III, schools may suffer perturbations that make them increase their speed to two squares per time step. We assume that these accelerations result in splitting of the school. In model II, large schools have greater probabilities of breaking up than small schools, and swimming speed of the resulting new schools is increased. This last rule allows us to keep the fission events between the models (models I–III) consistent and ensures that associated schools can leave floating objects. In these models, the number of new schools resulting from a fission event is limited to two, and these two schools have a random size, the sum of which equals the size of the original school. When a perturbation affects an associated school, it results in the emergence of two nonassociated schools located two squares away from the floating object. In model IV, schools split into elementary units at night.

A common assumption in all these models is that floating objects are easier for tuna to locate than are conspecifics (tuna can detect conspecifics during a time step only when they are located in the same square). Some ultrasonic studies (Holland et al. 1990; Cayré 1991; Bach et al. 1998; Josse et al. 1998; Marsac and Cayré 1998) have shown that tuna are able to return directly to a FAD from distances up to 13 km (7 nautical miles) away. Nevertheless, it is still unclear whether tuna are able to sense stimuli generated by a floating object at this distance or whether they navigate after memorizing its geographical position. No study has yet provided similar observations of direct routes for the location of distant schools, even for other pelagic schooling species. Fréon and Misund (1998) discussed the learning capabilities of fish and the senses (auditory, chemotaxis, and vision) that tuna are most likely to use to locate floating objects over longer distances than the schools.

In this study, five different models were used to test hypothesis of tuna behavior. Table 1 summarizes the different assumptions used in each model.

Model 0 (no fission)

This basic model does not include a fission rule. We simply consider the attraction rule and the meeting point hypothesis. The aim of this oversimplified model is to quantify the influence of logs on school sizes without any perturbation due to fission. The other models are derived from this basic model by adding different fission rules.

Model I (energetic)

This model is based on energetic considerations and the incorporation of artificial prey units in the habitat. Despite the benefits gained by increasing school size in terms of predator avoidance and foraging, some costs such as competition can also increase with school size. This suggests the existence of a trade-off and a critical school size where benefits equal or exceed costs (Pitcher and Parrish 1993). In this model, at the end of each time step and for a given square, n individual schools i of size $N_i s$ will merge in a single tuna school of size $Ns = \Sigma_n N_i s$, and the fish in this resulting school will have consumed $N = \Sigma_n N_i$ units of energy per time step (one unit of energy per group unit). Let us define P as the amount of prey that is located in the same square. If $P \geq N$, the number of prey left after the consumption by all the tuna in a given square during one time step is $P - N$, and these tuna schools have a positive energetic balance for this step. If $P < N$, there are no more prey left and those schools have a negative energetic balance. When a tuna school has a positive energetic balance, it keeps its internal structure and its swimming speed of one square per time step. However, when the tuna school has a negative energetic balance, the swimming speed increases from one to two squares per time step and this school will split in two. Indeed, as suggested by Atema (1980) for tuna and observed for many terrestrial species

© 1999 NRC Canada

Table 1. Description of the different models with their corresponding assumptions.

Model	Meeting point hypothesis	Fusion rule	Fission rule
0 (test)	At each time step, schools converge to any floating object detected in one of the four adjacent squares	At each time step, all group units located in the same spatial unit aggregate in a single school	No fission rule
I (energetic)	As above	As above	At the end of each time step, if $P \geq N$ in a square, the school splits into two schools of random size
II (school size)	As above	As above	At each time step, each school can split into two schools of random size (with a probability proportional to its size Ns)
III (predation)	As above	As above	After each of 12 time steps (on average), schools split into two schools of random size
IV (night dispersion)	Only during daytime steps, schools converge to any floating object detected in one of the four adjacent squares	Only during daytime steps, all group units located in the same spatial unit aggregate in a single school	Every 12 time steps and during six time steps (night), all schools of size $Ns > s$ split into N schools of size s

Note: s = elementary school unit = 50 individuals, N = number of elementary school units in a given school, P = amount of prey required by an elementary school, and n = number of schools in the same square, before fusion.

(reviewed by Benhamou 1992), a common reaction in low prey density areas is to speed up in order to vacate the area and thereby increase the chance of encountering new prey.

Two different processes for supplying prey have been considered in this model. In the first case (model I*a*), prey appear at a regular rate in each square during the first half of the simulation (180 steps), representing an enrichment process. For the two simulated tuna populations of 500 and 2500 group units, eight and 34 prey units, respectively, appear every six time steps in each square. During the second half of the simulation, no more prey are incorporated in order to simulate an impoverishment process. In the second case (model I*b*), prey are renewed at a regular rate during the entire simulation: four and 17 prey units, respectively, appear every six time steps in each square for tuna populations of 500 and 2500 group units. The total quantity of prey injected into the habitat at the end of a simulation is then identical in both cases. It corresponds approximately to the quantity needed by the tuna population to meet its metabolic requirements according to our initial assumption.

Model II (school size)

In model II, we consider that the probability of school fission is proportional to school size, a reasonable hypothesis often used in group models (Anderson 1981; Bakun 1989; Gueron and Levin 1995). This probability varies linearly between 0 ($N = 1$) and 1 ($N \geq 500$). We assume that large schools are more likely to break up because of increased difficulties in maintaining their internal structures.

Model III (predation)

At each time step in the model, each school can be attacked by a predator or a school of predators according to a fixed probability of attack. This probability has been set to 1/12, which corresponds to about one attack per day. When a school is attacked, it splits into two schools of random size.

Model IV (day/night)

In other models (models I–III), we ignored situations where tuna schools form loose structures or are dispersed during nighttime, as is typical of many other schooling fish (Blaxter and Hunter 1982), because this behavior is not documented in tuna. In model IV, we assume that convergence around floating objects can help tuna resume schooling in larger schools than if there were no meeting points. The bulk of log school fishing occurs early in the morning, which suggests that tuna tend to leave log areas when the sun rises and to gather under logs during the night (Hallier and Parajua 1992). This circadian behavior is opposite to the circadian behavior observed by ultrasonic tagging experiments performed on tuna associated with anchored objects (Cayré and Chabanne 1986; Holland et al. 1990; Cayré 1991; Marsac and Cayré 1998).

In this model, every 12 time steps (at the beginning of each night), each school of size Ns splits into N schools of size s. This rule implies that from the beginning of the night and all night long (six steps), the number of schools in the habitat equals the size of the population expressed in the number of group units, and the school size is equal to one unit. In this model, we assume that group units are able to merge or to aggregate under floating objects only during daytime steps.

Quantification of the effects of association with logs

Comparisons between the sizes of free-swimming schools and the sizes of associated schools are not sufficient to study of the effect of association with logs on tuna. A free-swimming school could have been previously associated with an object and therefore could have already benefited from it by increasing its size. As a result, we have identified two complementary approaches for assessing the impact of logs on school size: (*i*) an averaging approach, which compares the overall mean school size (of both associated and free-swimming schools) in habitats having different densities of floating objects, including zero, and (*ii*) a dynamic approach, which simultaneously compares the temporal evolution of school size of associated and free-swimming schools. Assuming that these two types of schools live in the same environment and interact with each other, we cannot ignore their simultaneous temporal dynamics.

In the averaging approach, 50 simulations of 360 steps each (30 days) were performed to obtain overall mean school sizes for each model and each set of parameters (0, 10, 20, 30, 40, 50, or 60 logs and 500 or 2500 group units). Model IV was treated differently because of its fission rule, and only the school sizes at the

© 1999 NRC Canada

end of each day in the simulation (every 12 time steps) were analyzed. In the dynamic approach, we only analyzed a selection of typical time series from 50 simulations with 50 logs and 2500 group units. We compare the speed of school rebuilding after fission events in associated schools versus free-swimming schools.

Results

Averaging approach

First, for any of the tested models, an increase in the size of the population from 500 to 2500 group units does not change the shape of the relationship between the number of floating objects and the school size but only increases the overall mean school size. The influence of an increase in floating object density on the overall mean school size varies among the different models (Fig. 2). In models 0 and I, the addition of floating objects in the habitat tends to decrease the school size, except in model 0 where this decrease only starts at 10 logs (the difference in school size between 0 and 10 is not significant, $p = 0.9$). For more than 10 logs in the habitat of model 0, school size decreases exponentially (slope of the exponential regression significantly different from zero, $p < 0.001$), resulting from the competition between floating objects for aggregating the whole population in the absence of any fission rule. In model 0, the mean school size in 60-log habitats is three times smaller than the mean school size in 0- or 10-log habitats. In model I*a*, and especially in model I*b*, the decrease in mean school size is slower than that in model 0. Nevertheless, the slope of the exponential regression is highly significant in both models I*a* and I*b* ($p < 0.001$).

In contrast with these first three models, the addition of up to 30 floating objects in the habitat of models II and III results in a significant increase in the mean school size (slopes of the linear regressions differ significantly from zero, $p < 0.001$, and our null hypothesis is rejected). For more than 30 floating objects, mean school sizes decrease significantly ($p < 0.001$). In model IV, a significant increase in mean school size is observed when log density is increased (slope of the linear regression differs significantly from zero, $p < 0.001$), despite a slowing down of this increase at a density of 30 logs.

Temporal dynamics of log and free-swimming schools

Figure 3 presents time series of school size for the different models in 50-log habitats and 2500 group units. Typical examples of the results obtained from single runs of 30 days are displayed for the different models (5 days for model IV) because average values over many runs would have resulted in a smoothing of the time series. A common result of many of these models (except for models 0, I*a*, and, to a lesser extent, II when log density is high) is that free-swimming schools in habitats with logs exhibit temporal size dynamics similar to those of schools in habitats without logs (Figs. 3*b*–3*f*). This result suggests that the addition of floating objects to an area does not strongly impact upon the size of free-swimming schools. Another common result is that the dynamic pattern of school size is not affected by an increase in the population size (only the school size is increased). We therefore restrict our discussion and figures to the 2500 group units.

In model 0 (no fission rule), when there are no logs in the habitat, the whole simulated population tends to aggregate as the number of time steps approaches infinity. This is illustrated in Fig. 3*a* by the constant increase in school sizes in the zero-log habitat. A comparison of the changes in school sizes in associated and free-swimming schools during the first time steps clearly shows the advantage of using logs to form large schools rapidly from a dispersed population. Associated schools are always larger than free-swimming schools (regardless of the number of logs in the area; results not shown). In this first model, a school located under a floating object cannot abandon it, due to the absence of any fission or departing rule and a constant aggregative behavior. Therefore, the logs continuously aggregate all the free-swimming schools. When all tuna are associated with logs, the mean size of associated schools logically corresponds to the total size of the population divided by the number of logs. It follows that mean sizes of associated schools decrease when the number of logs in the area is increased, due to competition between logs to attract free-swimming schools. The subsequent models indicate what happens when realistic fission rules are added to this basic model.

In model I*a*, where prey are input during the first half of the simulation, schools in zero-log habitat logically increase their size during the enrichment phase (Fig. 3*b*). When no more prey are added to the habitat (second half of the simulation), the mean school size decreases. Associated schools and free-swimming schools follow the same pattern, but variability is greater in associated schools. In the first half of the simulation (enrichment process), log schools are smaller than zero-log habitat schools, but at the end of the impoverishment process, the three types of schools display similar sizes. Figure 3*b* shows an interesting feature. During the last half of the impoverishment process (from step 271 to 360), associated schools are larger than free-swimming schools and zero-log habitat schools for 82 and 79% of the time, respectively. This result suggests that logs contribute to the formation of larger tuna schools, despite the high variability. Model I*b* shows a stable distribution of school sizes over time (Fig. 3*c*) because of the constant replacement rate of prey. In addition, associated schools and free-swimming schools have similar sizes. A comparison of the results from the two submodels that include processes of input (models I*a* and I*b*) indicates that the mean school sizes of the different school types reach similar values towards the end of each simulation, but, as expected, the dynamics of school size in each model are different. Towards the end of each simulation, associated schools are slightly larger than free-swimming schools in model I*a* (enrichment and then impoverishment, which seems to be the more realistic) compared with model I*b* (regular renewal rate).

In model II (school size), log schools are often slightly larger than free-swimming schools (Fig. 3*d*), especially when log density and fish density are high. This result was even more pronounced for the case of low log density and fish density (10 logs and 500 groups; not shown).

In model III (predation), the presence of logs results in very large schools compared with free-swimming schools and schools in zero-log habitats (Fig. 3*e*). If large schools are assumed to be effective for reducing predation, then logs can be considered as efficient antipredator tools.

© 1999 NRC Canada

Fig. 2. Overall mean size (± 1 SD) of free-swimming and associated schools in habitats with different numbers of logs for the six models. Large and small circles correspond to simulations of population sizes of 2500 and 500 elementary units, respectively.

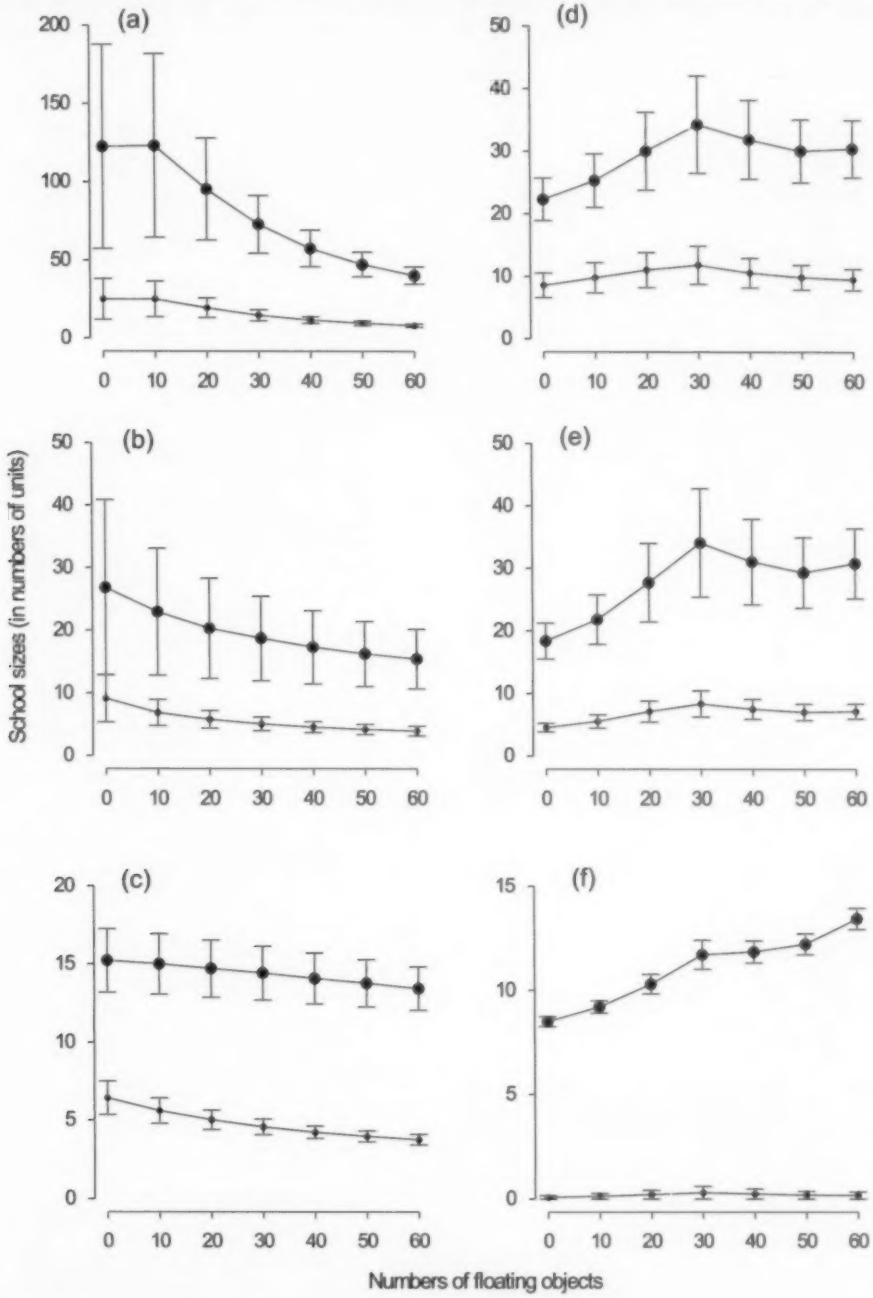

The advantages provided by logs in promoting the formation of large schools are obvious in model IV (day/night). Log schools are larger than free-swimming schools during daytime (Fig. 3*f*). At night, tuna disperse so that school sizes are minimal. During the day, tuna associated with logs aggregate rapidly at the start of each day and school size increases continuously throughout the day.

Discussion

The meeting point hypothesis assumes that fish use logs as spatial cues where they can converge and find conspecifics in order to form larger schools. In the wild, log-associated schools appear, on average, to be larger than free-swimming schools (Hall 1992; Fonteneau 1993). However,

© 1999 NRC Canada

Fig. 3. Temporal changes in the school sizes of tuna in habitats without logs (broken line), of free-swimming schools (solid thin line), and of schools associated with logs (solid thick line) in 50 log habitats. Results are shown for a local population size of 2500 group units during 360 time steps (except model IV, 60 time steps). (*a*) Model 0 (no fission rule); (*b*) model I*a* (energetic, enrichment and then impoverishment processes); (*c*) model I*b* (energetic, constant replenishment rate); (*d*) model II (school size); (*e*) model III (predators); (*f*) model IV (day/night).

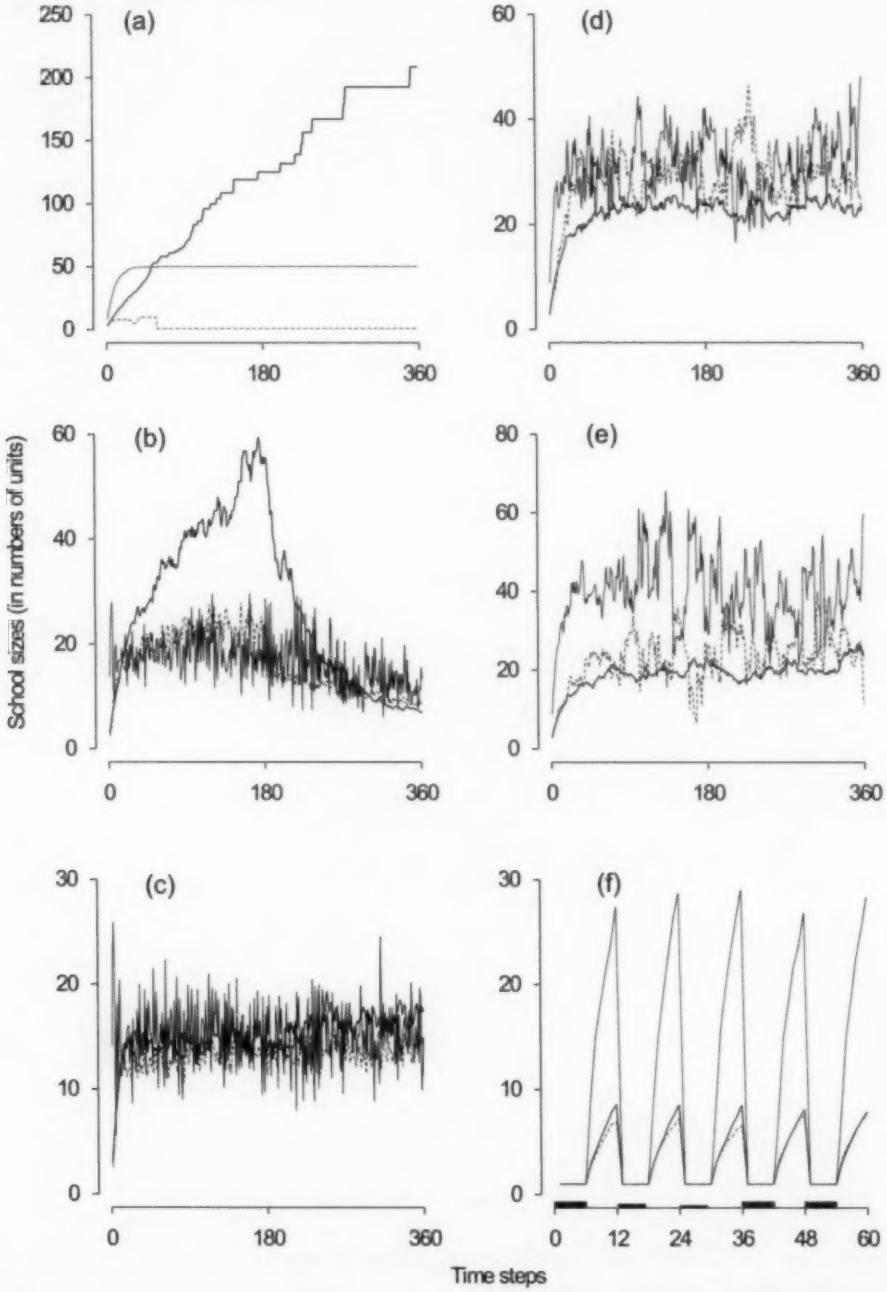

the comparison between the mean sizes of associated and free-swimming schools can be misleading because a free-swimming school could have been associated with an object previously and therefore may already have benefited from it by increasing its size. We believe that the role of logs in school sizes should be studied in two different ways: (*i*) using an averaging approach and (*ii*) using a dynamic approach, where time series of associated and free-swimming

© 1999 NRC Canada

Table 2. Changes in school size (associated and free-swimming schools) in different models according to two criteria: (*i*) number of logs (averaging approach; +, increase; –, decrease) and (*ii*) time (temporal dynamics; <, =, and >, mean log school size smaller than, equal to, or larger than swimming school size, respectively). *f*( ): criterion.

Model	Averaging approach *f* (number of logs)	Temporal dynamics *f* (time)
0	– – –	> > >
I*a*	– –	< then = (10 logs) = then > (50 logs)
I*b*	–	> then =
II	+ + then –	= or > or > >
III	+ + then –	> >
IV	+ + then +	> > >

schools are compared. The first approach is related to the whole simulated population and deals with long-term benefits, whereas the second approach represents individual school behavior and short-term benefits. The results are summarized in Table 2, which shows that in all models, it is always advantageous, in either the long term or the short term, or both, for fish to use floating objects as meeting points to form larger schools. Models III, IV, and, to a lesser extent, II clearly show the advantage of using moderate density of logs for meeting, in both the short and long term.

The basic model 0, which is the least realistic model due to the absence of any fission rule, clearly illustrates the fact that logs act as foci ("wells") that concentrate schools until perturbations occur. When many floating objects attract tuna schools, the tuna population is shared among them and the mean school size is reduced. Adding fission rules to this basic model sometimes disturbs this behavior in a way that was not easy to predict before performing the simulations; this suggests that our models are not tautological.

In model I (energetic), irrespective of the enrichment processes, increased log densities tend to reduce the overall mean school size. Because we did not fix any spatial relationships between prey and floating objects, the attraction of tuna to logs resulted in reduced abundance of prey near these floating objects (Fig. 4), even if the prey were initially homogeneously distributed in the habitat. This reduction, in turn, results in negative energy balances for tuna schools, which affect both the time of residence of schools around logs and their size. This result is supported by observations of the condition of skipjack tuna caught under floating objects by the Japanese fleet. These fish are leaner than skipjack tuna caught from free-swimming schools and therefore sell at higher prices on the Japanese markets for Katsuobushi ingredients (a popular Japanese dish) (Z. Suzuki, National Research Institute of Far Seas Fisheries, 5-7-1, Orido, Shimizu 424, Shizuoka, Japan, personal communication). However, in the wild, many different mechanisms can contribute towards a reversal of the simulated impoverishment around floating objects: higher concentrations of prey in the vicinity of floating objects if prey and object are trapped in the same retention area by hydrodynamic processes, activity of tuna when associated with a log (e.g., absence of any feeding motivation), a patchy distribution of log, prey, or tuna, different regeneration processes, etc. Additional scientific data, especially condition or fatness indices per species and per school type, are needed to support this result.

The dynamic patterns of model I show interesting details that cannot be deduced from the averaging approach, e.g., the large sizes of associated schools during a food-depletion process. In the other models (school size, predation, day/night), schools are always significantly larger when logs are present in the habitat. Moreover, the very first steps of each simulation of each model effectively indicate that logs help tuna to form larger schools rapidly when the starting point is assumed to be a complete dispersion of the population. Results from models I (energetic), II (school size), and III (predation) are not as clear as those obtained from model IV in this respect. This is because events responsible for fissions in these earlier models occur at the school level and affect schools at different time steps, whereas in model IV, diurnal rhythms affect schools simultaneously.

Too many logs in the area do not always increase the school size, even in models II–IV. Models II and III show that competition between logs for aggregating tuna can balance their effect on increased school sizes. Above a certain threshold of log density, school size will not continue increasing. This finding is not influenced by the splitting rule, as the school sizes are far beyond the threshold set for obligatory splitting (N = 500). This result is important for understanding fisheries catch statistics. Fishers construct and deposit artificial objects to increase their chances of finding and subsequently catching tuna. Since the beginning of the 1990's, tuna purse seiners have been using drifting FAD's, which are labeled, easy to locate (e.g., radar reflectors, radio beacons), and frequently retrieved and redeployed elsewhere to enhance catches. Some FAD's are equipped with echosounders that automatically transmit data to fishing vessels by radio. We can speculate from our models that deployment of too many floating objects in an area would decrease the school size. This phenomenon may lead to unexpected consequences such as schools being reduced to such small sizes that they are not worth fishing.

The results of the models indicate that the effects of floating objects on school sizes (in an averaging and a dynamic approach) depend on the fission rules (Table 2). In this paper, we have designed models with specific fission rules, but in the wild, it is likely that many types of perturbations that are not yet identified are responsible for school fission. A limitation of our simulations is that after 2 h, no more than one school per square (49 km^2) can be observed, which is not realistic. This oversimplification should not affect the trends observed in the simulations. Another limitation is that attraction areas of floating objects do not overlap in our artificial habitat. This assumption follows Holland et al. (1990) and Cayré (1991) who recommended that the minimum separation between adjacent anchored FAD's should be about 20 km so that their fields of influence do not overlap. However, for high densities of floating objects such as 15 logs in a 1° area (60-log habitats), this rule implies that a third of the habitat attracts tuna, which appears to be unrealistic. In the wild, many drifting objects can aggregate in a small area, overlapping their fields of influence and consequently reducing the total attraction area in the habitat. It would then be necessary to compare the role of the spatial distribution of logs in tuna behavior. The conclusions of this study sup-

© 1999 NRC Canada

Fig. 4. Contoured snapshot of model I*a* during a simulation showing the spatial distribution of prey. The different grayscale levels correspond to different numbers of prey per square. The white crosses indicate floating objects.

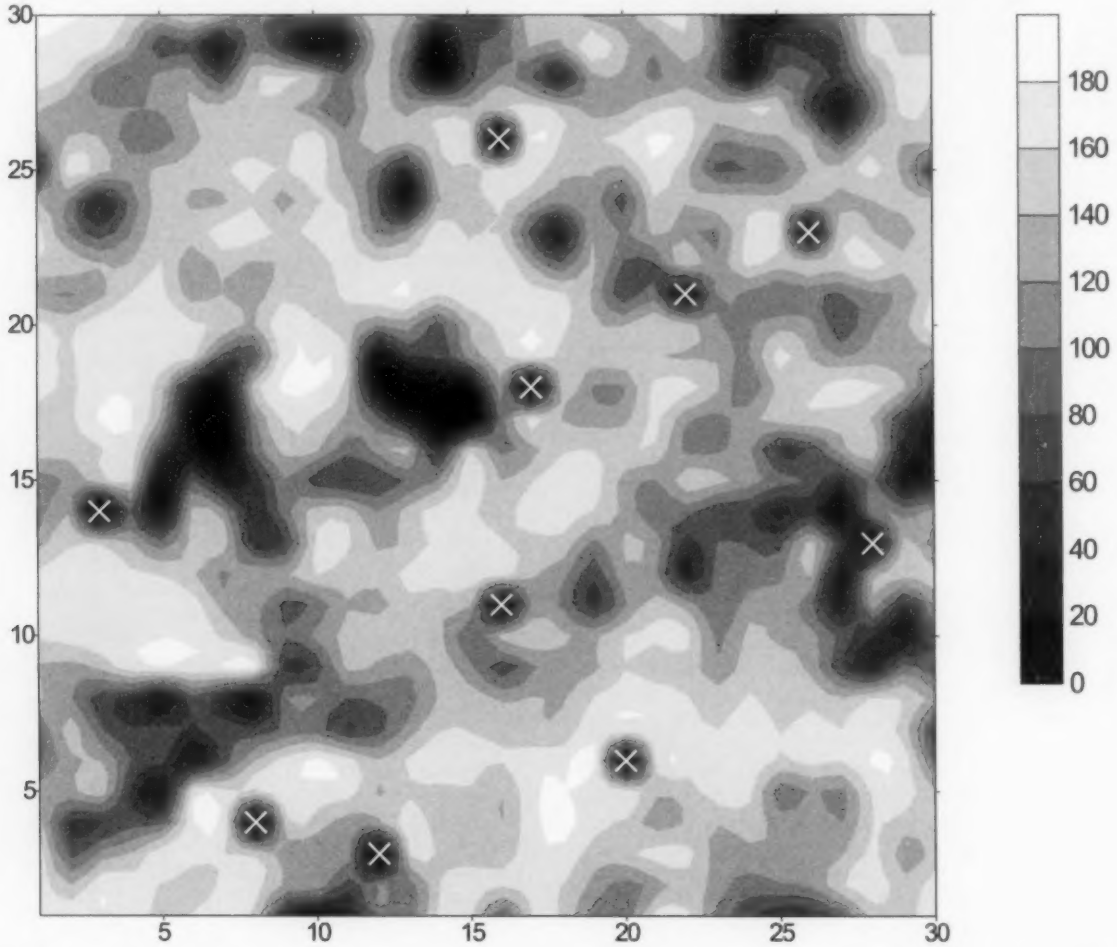

port the contention that more information on school dynamics (fidelity to floating objects, fission and fusion, etc.) is required in order to better understand the impact of logs on tuna school sizes.

In conclusion, from our simulations, we can recommend two complementary approaches to in situ studies of the association of tuna with floating objects: (*i*) a comparison of mean school size of all the schools in habitats with different densities of floating objects and (*ii*) a simultaneous comparison of the dynamics of associated and free-swimming schools in the same area. In addition, in situ tuna tracking should be performed around logs. At present, we can only speculate on the evolutionary advantage of associative behavior. Model III shows that the use of logs after school dispersal following predatory attacks helps the fish to form larger schools. However, in this model, we did not consider the fact that the predators (marlins, sharks, killer whales, etc.) might also be attracted by floating objects because predators and tuna have been coevolving with floating objects in their habitat. In this kind of situation, the advantage of large schools associated with logs should be balanced by the disadvantage of being more easily located by predators. An important issue is that fishers have now detected the associative behavior of tuna and have quickly adapted their fishing strategy accordingly. They now behave as evolved predators and, consequently, they have substantially increased their tuna catches. It will probably take several decades (by learning and learning transmission), if not centuries (evolutionary process), for tuna to modify their behavior. If fishers keep exploiting this association and if tuna do not rapidly adapt to this particular type of predation, tuna populations may become endangered, especially skipjack tuna.

Acknowledgments

We sincerely thank Pascal Bach, Philippe Cury, Alain Fonteneau, François Gerlotto, Francis Marsac, Michel Potier, and Marc Soria for their helpful suggestions in early versions of this work. We are also grateful to Suzanne Painting, Coleen Moloney, and Gary Melvin who improved the English of this text.

© 1999 NRC Canada

References

Anderson, J.J. 1981. A stochastic model for the size of fish schools. Fish. Bull. U.S. **78**: 315–323.

Aoki, I. 1982. A simulation study on the schooling mechanisms in fish. Bull. Jpn. Soc. Sci. Fish. **48**: 1081–1088.

Atema, J. 1980. Chemical senses, chemical signals, and feeding behavior in fishes. *In* Fish behavior and its use in the capture and culture of fishes. Proceedings of the Conference on the Physiological and Behavioral Manipulation of Food Fish as Production and Management Tools, Bellagio, Italy, 3–8 November 1977. *Edited by* J.E. Bardach, J.J. Magnuson, R.C. May, and J.M. Reinhart. ICLARM Conference Proceedings (Manille). pp. 57–101.

Bach, P., Dagorn, L., Josse, E., Bard, F.-X., Abbes, R., Bertrand, A., and Misselis, C. 1998. Experimental research and fish aggregating devices (FADs) in French Polynesia. SPC FAD Inf. Bull. **3**: 3–19.

Bakun, A. 1989. Mechanisms for density-dependent growth in Peruvian anchoveta: alternatives to impact on the regional-scale food supply. *In* The Peruvian upwelling ecosystem: dynamics and interactions. *Edited by* D. Pauly, P. Muck, J. Mendo, and I. Tsukayama. ICLARM Conference Proceedings 18. pp. 235–243.

Batalyants, K.Y. 1992. On the hypothesis of comfortability stipulation of tuna association with natural and artificial floating objects. ICCAT Coll. Vol. Sci. Pap. **40**: 447–453.

Benhamou, S. 1992. Efficiency of area-concentrated searching behaviour in a continuous patchy environment. J. Theor. Biol. **159**: 67–81.

Blaxter, J.H.S., and Hunter, J.R. 1982. The biology of clupeoid fishes. Adv. Mar. Biol. **20**: 1–223.

Cayré, P. 1991. Behaviour of yellowfin tuna (*Thunnus albacares*) and skipjack tuna (*Katsuwonus pelamis*) around fish aggregating devices (FADs) in the Comoros Islands as determined by ultrasonic tagging. Aquat. Living Resour. **4**: 1–12.

Cayré, P., and Chabanne, J. 1986. Marquage acoustique et comportement de thons tropicaux (albacore et listao) au voisinage d'un dispositif concentrateur de poissons. Océanogr. Trop. **21**: 167–183.

Duffy, D.C., and Wissel, C. 1988. Models of fish school size in relation to environmental productivity. Ecol. Model. **40**: 201–211.

Fonteneau, A. 1985. Analyse de l'exploitation de quelques concentrations d'albacore par les senneurs durant la période 1980–1983, dans l'Atlantique Est. ICCAT Coll. Vol. Sci. Pap. **32**: 81–98.

Fonteneau, A. 1993. Pêche thonière et objets flottants: situation mondiale et perspectives. ICCAT Coll. Vol. Sci. Pap. **40**: 459–472.

Fréon, P., and Misund, O.A. 1998. Dynamics of pelagic fish distribution and behaviour: effects on fisheries and stock assessment. Fishing News Books, Blackwell, Oxford, U.K.

Gooding, R.M., and Magnuson, J.J. 1967. Significance of a drifting object to pelagic fishes. Pac. Sci. **21**: 486–497.

Gueron, S., and Levin, S.A. 1995. The dynamics of group formation. Mathematical Biosciences, **128**: 243–264.

Hall, M. 1992. The association of tunas with floating objects and dolphins in the eastern Pacific Ocean. VII. Some hypotheses on the mechanisms governing the association of tunas with floating objects and dolphins. *In* International Workshop on the Ecology and Fisheries for Tunas Associated with Floating Objects and on Assessment Issues Arising from the Association of Tunas with Floating Objects. *Edited by* M. Hall. Internal Rep., Inter-American Tropical Tuna Commission, San Diego, Calif.

Hallier, J.-P., and Parajua, J.I. 1992. Review of tuna fisheries on floating objects in the Indian ocean. International Workshop on Fishing Tunas Associated with Floating Objects. *In* International Workshop on the Ecology and Fisheries for Tunas Associated with Floating Objects and on Assessment Issues Arising from the Association of Tunas with Floating Objects. *Edited by* M. Hall. Internal Rep., Inter-American Tropical Tuna Commission, San Diego, Calif.

Hilborn, R., and Medley, P. 1989. Tuna purse-seine fishing with fish-aggregating devices (FAD): models of tuna FAD interactions. Can. J. Fish. Aquat. Sci. **46**: 28–32.

Hogeweg, P., and Hesper, B. 1990. Individual-oriented modeling in ecology. Math. Comput. Model. **13**: 83–90.

Holland, K.N., Brill, R.W., and Chang, R.K.C. 1990. Horizontal and vertical movements of yellowfin and bigeye tuna associated with fish aggregating devices. Fish. Bull. U.S. **88**: 493–507.

Hunter, J.R., and Mitchell, C.T. 1967. Association of fishes with flotsam in the offshore waters of central America. Fish. Bull. U.S. **66**: 13–29.

Huston, M., DeAngelis, D.L., and Post, W. 1988. New computer models unify ecological theory. BioScience, **38**: 682–691.

Huth, A., and Wissel, C. 1992. The simulation of the movement of fish schools. J. Theor. Biol. **156**: 365–385.

Josse, E., Bach, P., and Dagorn, L. 1998. Simultaneous observations of tuna movements and their prey by sonic tracking and acoustic surveys. *In* Advances in invertebrates and fish telemetry. *Edited by* J.P. Lagardère, M-L. Bégout-Anras, and G. Claireaux. Hydrobiologia, **371/372**: 61–69.

Kleiber, P., and Hampton, J. 1994. Modeling effects of FADs and islands on movement of skipjack tuna (*Katsuwonus pelamis*): estimating parameters from tagging data. Can. J. Fish. Aquat. Sci. **51**: 2642–2653.

Klima, E.F., and Wickham, D.A. 1971. Attraction of coastal pelagic fishes with artificial structures. Trans. Am. Fish. Soc. **1**: 86–99.

Kojima, S. 1956. Fishings for dolphins in the western part of the Japan Sea. II. Why do the fish take shelter under floating materials? Bull. Jpn. Soc. Sci. Fish. **21**: 1049–1052.

Marsac, F., and Cayré, P. 1998. Telemetry applied to behaviour analysis of yellowfin tuna (*Thunnus albacares*, Bonnaterre, 1788) movements in a network of fish aggregating devices. *In* Advances in invertebrates and fish telemetry. *Edited by* J.P. Lagardère, M-L. Bégout-Anras, and G. Claireaux. Hydrobiologia, **371/372**: 155–171.

Pitcher, T.J., and Parrish, J.K. 1993. Functions of shoaling behaviour in teleosts. *In* The behaviour of teleost fishes. 2nd ed. *Edited by* T.J. Pitcher. Croom Helm, London. pp. 363–439.

Scheffer, M., Baveco, J.M., DeAngelis, D.L., Rose, K.A., and van Nes, E.H. 1995. Super-individuals a simple solution for modeling large populations on an individual basis. Ecol. Model. **80**: 161–170.

Soria, M., and Dagorn, L. 1992. Rappels sur le comportement grégaire. *In* Action Incitative Comportement Agrégatif (AICA), Montpellier, June 1992. *Edited by* J.-M. Stretta. Doc. Int. Cent. ORSTOM, Montpellier. pp. 5–9.

Tyler, J.A., and Rose, K.A. 1994. Individual variability and spatial heterogeneity in fish population models. Rev. Fish Biol. Fish. **4**: 91–123.

Yonemori, T. 1982. Study of tuna behavior, particularly their swimming depths, by the use of sonic tags. Far Seas Fish. Res. Lab. (Shimizu) Newslett. **44**: 1–5.

© 1999 NRC Canada

Growth modelling in accordance with daily water temperature in European grayling (*Thymallus thymallus* L.)

J.P. Mallet, S. Charles, H. Persat, and P. Auger

Abstract: The model of von Bertalanffy has been and is still widely used to model fish growth, mainly because of its good description of annual growth over the whole life span. However, it does not take into account a seasonal variability in growth rate, an important phenomenon that appears quite well correlated with water temperature fluctuations in temperate climates. In the present study, we demonstrated that it was possible to model such variations by including daily water temperature in the von Bertalanffy growth formula owing to the correlation between the growth coefficient k and water temperature. The model we chose to describe such a correlation includes parameters with obvious biological significance and is mathematically well structured, which allowed an extensive use of our growth model. Hence, we use our new model to describe annual variability in the growth of European grayling (*Thymallus thymallus* L.) in a river section where water temperature could rise up to the thermal tolerance limit for this species, inducing reduced growth rates and severe mortality events. Finally, we were able to explain the growth rate variability from one year to the next by interannual water temperature fluctuations.

Résumé : Le modèle de von Bertalanffy a été et reste encore largement utilisé pour modéliser la croissance des poissons, notamment parce qu'il permet de bien décrire ce phénomène sur toute la durée de vie des individus. Cependant, ce modèle ne prend pas en compte la variabilité saisonnière du taux de croissance, un phénomène important sous les climats tempérés, et qui apparaît assez bien corrélé aux fluctuations de la température de l'eau. Dans cette étude, nous démontrons qu'il est possible de modéliser de telles variations à l'aide des températures journalières, en reliant le coefficient de croissance k de l'équation de von Bertalanffy et la température. Le modèle retenu pour décrire une telle corrélation fait intervenir des paramètres ayant tous une signification biologique évidente, et est de plus bien structuré mathématiquement, ce qui devrait permettre d'étendre le champ d'application de notre modèle de croissance. En utilisant ce dernier, nous avons pu décrire la croissance de l'ombre commun européen (*Thymallus thymallus* L.) dans un secteur de rivière où la température de l'eau peut dépasser le seuil de tolérance de l'espèce, entraînant la réduction des taux de croissance ainsi que d'importantes mortalités. Finalement, nous montrons qu'il est possible d'expliquer la variabilité du taux de croissance d'une année sur l'autre par les fluctuations interannuelles de la température de l'eau.

Introduction

Previous work (Pitcher and MacDonald 1973; Pauly and David 1981) has pointed out that the seasonal variability of growth rate could be taken into account in the von Bertalanffy (1960) model, which could improve growth description, particularly that of fishes. Water temperature is the factor most often introduced to account for such a variability in the von Bertalanffy growth formula (VBGF); growth rate fluctuations are in fact quite well correlated with temperature, at least in temperate climates. But, surprisingly, the description of these variations was generally cursory (in most cases, authors used the sine function in the exponent part of the VBGF), probably because of the lack of reliable temperature data recorded on a sufficient short time scale.

The aim of the present study was to develop a new model incorporating daily temperatures in the VBGF in order to significantly improve the description of critical thermal peri-

Received June 9, 1998. Accepted February 5, 1999.
J14644

J.P. Mallet.[1] Association Rhône-Alpes de Laboratoires pour l'Étude des Problèmes Biologiques de la Pêche (ARALEPBP), 43, boul. du 11 novembre 1918, F-69622 Villeurbanne, Cedex, France.
S. Charles and P. Auger. Laboratoire de Biométrie-Génétique et Biologie des Populations, UMR CNRS 5558, Université Lyon 1, 43, boul. du 11 novembre 1918, F-69622 Villeurbanne, Cedex, France.
H. Persat. Laboratoire d'Écologie des Eaux Douces et des Grands Fleuves, E.S.A CNRS 5023, Université Lyon 1, 43, boul. du 11 novembre 1918, F-69622 Villeurbanne, Cedex, France.

[1]Author to whom all correspondence should be addressed. Present address: Laboratoire d'Écologie des Eaux Douces et des Grands Fleuves, E.S.A CNRS 5023, Université Lyon 1, 43, boul. du 11 novembre 1918, F-69622 Villeurbanne, Cedex, France.
e-mail: mallet@cismsun.univ-lyon1.fr

© 1999 NRC Canada

Fig. 1. The Ain River in France and the study site location.

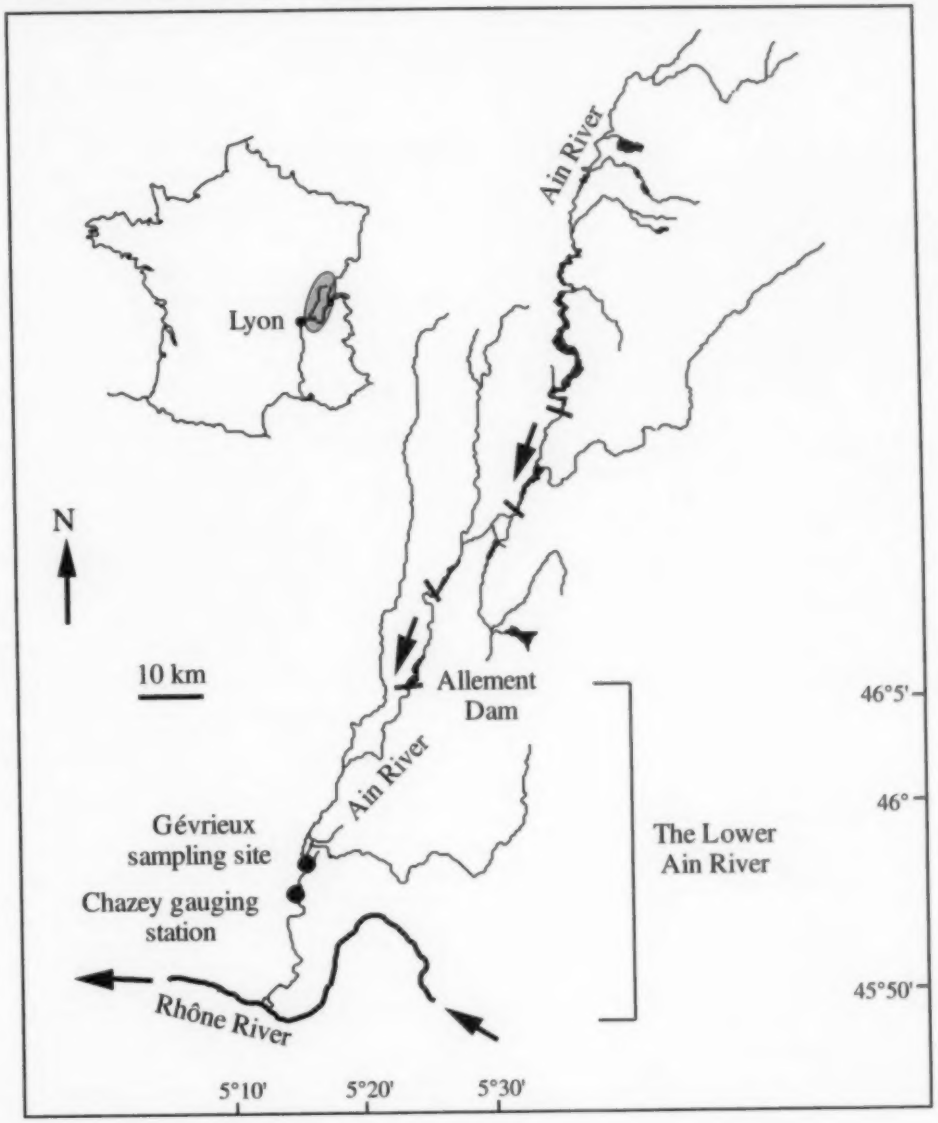

ods for fish. Our approach makes use of the relationship between the VBGF growth coefficient, k, and temperature, mentioned earlier by Taylor (1960) and Fontoura and Agostinho (1996).

We then use our model to describe the growth of European grayling (*Thymallus thymallus* L.) in the Lower Ain River, a large tributary of the Rhône River, in order to determine whether the growth rate decreases observed in some cohorts could be related to water temperature changes. Temperature is assumed to be an important factor controlling grayling growth (Persat and Pattee 1981; Nagy 1984), like in other salmonids (Elliott 1995), but some factors such as fish density or food abundance (Hellawell 1969; Woolland and Jones 1975) can interact.

Materials and methods

Study area

The Ain River is a large (>190 km) tributary of the Rhône River, entering it 20 km upstream of Lyon (Fig. 1). The mean slope of the river is 3.06 $m \cdot km^{-1}$ and the catchment area is around 3700 km^2. The study area extends about 40 km from the foot of the last hydroelectric dam (Allement Dam) to the confluence with the Rhône River. This braided section flowing through a large floodplain is commonly called the Lower Ain River.

The natural hydrological pattern shows high flows during winter and low flows during summer months and is characterised by frequent, sudden flood events due to heavy rains or melting snow. Since the early 1960's, dams have greatly regulated this natural pattern; the minimum discharge downstream from Allement Dam

© 1999 NRC Canada

Fig. 2. Average annual water temperatures (bars) and air temperatures (diamonds) recorded at the gauging station of Pont de Chazey and the Météo-France station of Ambérieu.

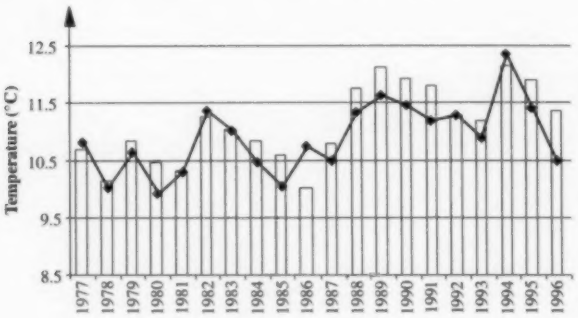

is 12 $m^3 \cdot s^{-1}$ between June and November, but since 1992, it has been increased to 28 $m^3 \cdot s^{-1}$ during winter and early spring in order to protect the spawning of trout and grayling.

Temperature and discharge volumes are permanently recorded in several places in the Lower Ain River by Electricité De France, and we have chosen to use data from the gauging station of Pont de Chazey (Fig. 1) because of its central location on this stretch. At this station, the catchment area is 3630 km^2, the average annual discharge is about 120 $m^3 \cdot s^{-1}$ (1961–1993), and the average annual water temperature is 11.2°C (the average maximum daily temperature is 22.4°C and the minimum is 1.7°C (1975–1996)). Annual water and air temperatures are shown in Fig. 2.

Data acquisition

The main characteristics of the grayling population of the Gévrieux site (Fig. 1) were monitored over two periods, 1978–1985 (cohorts, 1977–1981) and from 1993 on (cohorts, 1992–1997). Important differences were observed between these two periods and in particular a large reduction in densities. Grayling were collected by electrofishing (Persat 1988) during periods of low water discharge several times a year during the years of study. Further collections were made on spawning grounds to provide larger sample sizes of large individuals. All grayling were measured (total length to the nearest millimetre) and scale samples were collected for age determination and back-calculation of length-at-age before their release back into the capture zone.

For each date of the electrofishing survey, we were thus able to calculate the average length of individuals in each cohort. The extensive data collected during the first period (1978–1985), called DataF, were used to estimate various parameters of the model. Data obtained during the second period (1992–1997), called DataS, were used to test predictions of the model and to validate the growth curve simulations.

A survey of the grayling reproduction in the Ain River and its main tributaries was carried out over a period of several years (Persat 1988; Mallet 1997). As a rule, the spawning period starts with the increase of water temperature over 8°C; this is in agreement with observations by Poncin (1996) in the Ourthe, a large tributary of the Meuse River. Spawning lasts about 4 weeks, provided water temperatures do not drop below 7°C. Incubation time is around 210 degree-days (D'Hulstere and Philippart 1982; Jungwirth and Winkler 1984; Bardonnet and Gaudin 1990), and emergence occurs some days later (10 days at 10°C, D'Hulstere and Philippart 1982; Bardonnet and Gaudin 1990). This yields a total time between fertilisation and emergence of about 310 degree-days. Finally, we were able to define for each cohort, from direct field observations and (or) daily water temperature data, an initial time, t_{init}, that corresponds to the median emergence time for grayling fry.

Growth model

The VBGF, which is generally given in an integrated form (eq. 1), describes rate of change in length (L_t) of an organism such as fish with time (t). It is based on the assumption that fish growth is limited (i.e., growth rate decreases with fish size), which can be modelled conveniently by asymptotic regression models (Ricker 1979, p. 715):

$$(1) \qquad L_t = L_\infty(1 - e^{-k(t-t_0)})$$

where k is the growth coefficient, L_∞ is the asymptotic length, L_t is the length at age t, and t_0 the age at which the length of a fish is theoretically equal to zero. For each cohort, t_{init} corresponds to $t = 0$ in eq. 1.

Effect of temperature on the growth coefficient

A seasonal variability can be included in the VBGF through a relationship between the growth coefficient and water temperature, the control factor that seems to best describe this seasonality. The existence of such a relationship, with k assimilated to a growth rate, has been demonstrated at multipopulation levels in Taylor (1960). Fontoura and Agostinho (1996) successfully used it to describe the growth of two freshwater fishes (sculpin (*Cottus gobio*) and stone loach (*Barbatula barbatula*)).

According to these authors, the relationship between the growth coefficient k and temperature is not linear. In fact, k is equal to 0 if the temperature is lower or equal to the minimal growth temperature T_{min}; it increases with temperature up to an optimum k_{opt} at the optimal growth temperature T_{opt}. If temperature continues to increase, the growth coefficient k rapidly decreases down to 0 at the maximal growth temperature T_{max}.

To model this relationship, we used the formula proposed by Rosso et al. (1995) to describe bacterial growth versus a pH increase, since it includes these four parameters (the cardinal temperatures T_{min}, T_{opt}, T_{max}, and k_{opt}), which have an obvious biological meaning. We chose the cardinal pH model of Rosso et al. (1995) rather than the temperature one because the shape of the relationship between growth rate and pH more closely resembles the shape of the curves between growth rate and temperature obtained by Elliott (1995) for brown trout (*Salmo trutta*). This relationship is expressed as follows:

$$(2) \qquad k = k_{opt} \frac{(T - T_{min})(T - T_{max})}{(T - T_{min})(T - T_{max}) - (T - T_{opt})^2}.$$

Figure 3 shows the shape of the relationship between k and temperature T and the graphical meaning of the four parameters.

We used DataF to determine the relationship between k and temperature for the European grayling. For each time interval $[t_{init}; t]$, it was possible to calculate an average temperature $\bar{T}$ (considering t_0 equal to 0 as a first approximation). All parameters can theoretically be estimated using a nonlinear regression analysis based on the VBGF (Smith et al. 1997):

$$(3) \qquad L_t = L_\infty(1 - e^{-\bar{k}(t-t_0)})$$

where $\bar{k}$ is function of the average temperature $\bar{T}$ according to eq. 2.

In fact, it was not possible to achieve this analysis because the range of observed values of $\bar{T}$ fall in a too narrow a range (below T_{opt}) and all the more close to the average annual temperature (11.2°C for the Lower Ain River) as time interval $[t_{init}; t]$ increases; this problem has previously been identified by Fontoura and Agostinho (1996). If we try to specify a value for T_{opt} or T_{max} (e.g., from the literature), the calculation leads to the same estima-

© 1999 NRC Canada

Table 1. Values of the parameters of the growth model including water temperature variations.

Parameter	Estimation	95% CI	Origin
L_∞ (cm)	45.492	44.741; 46.244	Estimated from data
t_0 (days)	–13.08	–21.44; –4.71	Estimated from data
k_{opt} (day^{-1})	0.002699	0.002634; 0.002764	Estimated from data
T_{min} (°C)	4.5	—	Expert opinion
T_{opt} (°C)	17.3	—	Expert opinion
T_{max} (°C)	21	—	Expert opinion

Fig. 3. Shape of the relationship between the growth coefficient and water temperature. T_{min}, minimal growth temperature; T_{opt}, optimal growth temperature; T_{max}, maximal growth temperature; k_{opt}, optimal growth coefficient at T_{opt}.

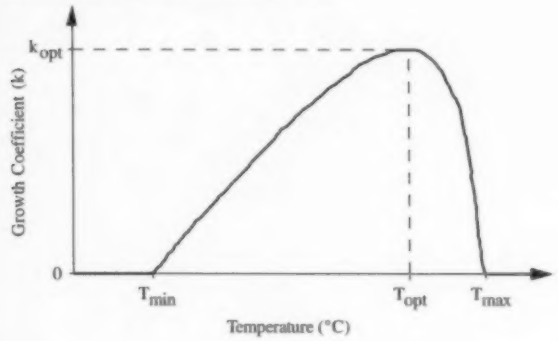

tion for both parameters (i.e., $T_{opt} = T_{max}$), as no measured values of $\bar{T}$ fall within the interval $[T_{opt}; T_{max}]$.

For this reason, and in order to use homogeneous values, we obtained cardinal temperatures from the literature and our personal observations. For T_{opt}, we had two references suggesting 17°C (Persat and Pattee 1981; J. Cerny, unpublished data) and one suggesting 18°C (Coutant 1977, cited in Northcote 1995), so we decided to use the average of these three values (17.3°C). The T_{min} and T_{max} values generally found in the literature concerned lethal levels (Kraiem and Pattee 1980), i.e., far from the temperature limits for growth. The range of viable temperatures "in which feeding occurs and where there are no external signs of abnormal behaviour" is 4–18°C for grayling (Elliott 1981, cited in Crisp 1996), but according to our observations, it seems slightly broader; we finally settled on 4.5°C for T_{min} and 21°C for T_{max} (Table 1).

Daily water temperatures were then transformed into a coefficient of temperature (X_T) defined as follows:

$$(4) \qquad X_T = \frac{(T - T_{min})(T - T_{max})}{(T - T_{min})(T - T_{max}) - (T - T_{opt})^2}.$$

This procedure appears superior to the model described previously (eqs. 2 and 3), as the effects of daily temperature are more precisely taken into account. In the former, temperature values above T_{max} have a positive contribution to the final growth as they increase $\bar{T}$ towards T_{opt}, whereas in reality, these high daily temperatures have a negative impact on k, as described previously.

It was thus possible to calculate an average coefficient of temperature $\bar{X}_T$ in the time interval $[t_{init}; t]$ and to estimate the remaining parameters (L_∞, t_0, and k_{opt}) by nonlinear regression analysis through eq. 3 with

$$(5) \qquad \bar{k} = \bar{k}_{opt}\bar{X}_T.$$

Theoretically, the $\bar{X}_T$ values would have been calculated on the interval $[t_0; t]$, as grayling growth starts at t_0. Nevertheless, the difference between t_0 and t_{init} is small (less than 2 weeks, see Table 1), and daily temperatures during this period are quite similar from year to year (because t_{init} is related to water temperature); thus, we decided not to correct $\bar{X}_T$ values.

Testing the growth model

To test the growth model, we compared the growth curves predicted by the model with actual growth curves of the six cohorts observed between 1992 and 1997 (DataS). To model the fluctuations of the coefficient of temperature during each year, we used an interpolation spline function (a local polynomial regression of degree 3). The interpolation function was computed with the Interpolation routine of Mathematica 3.0™ software and allowed us to express X_T as a function of time:

$$(6) \qquad X_T = f_{interpol}(t).$$

Then, the VBGF was processed as a standard differential equation:

$$(7) \qquad \frac{dL_t}{dt} = \bar{k}(L_\infty - L_t)$$

where the growth coefficient $\bar{k}$ was a function of the "temperature" X_T (eq. 5), itself a function of time t (eq. 6).

Solutions of eq. 7 were calculated with the NDSolve routine of Mathematica 3.0™ software and L_t was expressed as a function of time. It was then possible to plot simulated growth curves and to superimpose them on experimental data. The accuracy of grayling growth curve simulations was estimated by calculating the sum of unexplained residual variations between observed and simulated length for each cohort of both data sets (DataF and DataS) through the following equation:

$$(8) \qquad SCE_Y = \frac{1}{n}\sum_{i=1}^{n}\frac{(L_{predicted_i} - L_{observed_i})^2}{L_{predicted_i}}$$

where n is the number of average lengths observed for cohort Y (Y = 1977 to 1981 for DataF and Y = 1992 to 1997 for DataS).

In order to compare the growth of the various cohorts, the time required to reach a size of 25 cm (t_c) was calculated with a simple program that will not be detailed here.

Results

Parameter values are given in Table 1. Simulated growth curves are shown in Fig. 4. The times t_c and the sum of unexplained residuals values (SCE_Y) calculated for each cohort of the two periods are provided in Table 2. No t_c value could be calculated for the 1997 year-class, as this cohort was not to reach 25 cm until 1998.

© 1999 NRC Canada

Table 2. Values of t_c and SCE calculated from our model including daily water temperature variations for 10 and 11 cohorts, respectively, of European grayling from the Lower Ain River.

Cohort	1977	1978	1979	1980	1981	1992	1993	1994	1995	1996	1997
t_c[a]	482.5	466.1	460.5	484.7	460.8	452.1	438.4	507.3	487.7	432.0	—
SCE[b]	0.095	0.135	0.192	0.092	0.239	0.135	0.143	0.199	0.284	0.031	0.007

[a]Estimation of the number of days (since t_{init}) required to reach a size of 25 cm
[b]Estimation of the residual unexplained variation (see eq. 8).

Fig. 4. Simulated growth curves superimposed on observed data. Circles represent the average total lengths (±95% CI). For each cohort, t_{init} corresponds to the median emergence time (arrows) for European grayling fry; day 0 corresponds to the t_{init} of the first cohort of each period (i.e., 1977 and 1992). (*a*) Growth curves corresponding to DataF; (*b*) Growth curves corresponding to DataS and simulated with parameters estimated from DataF.

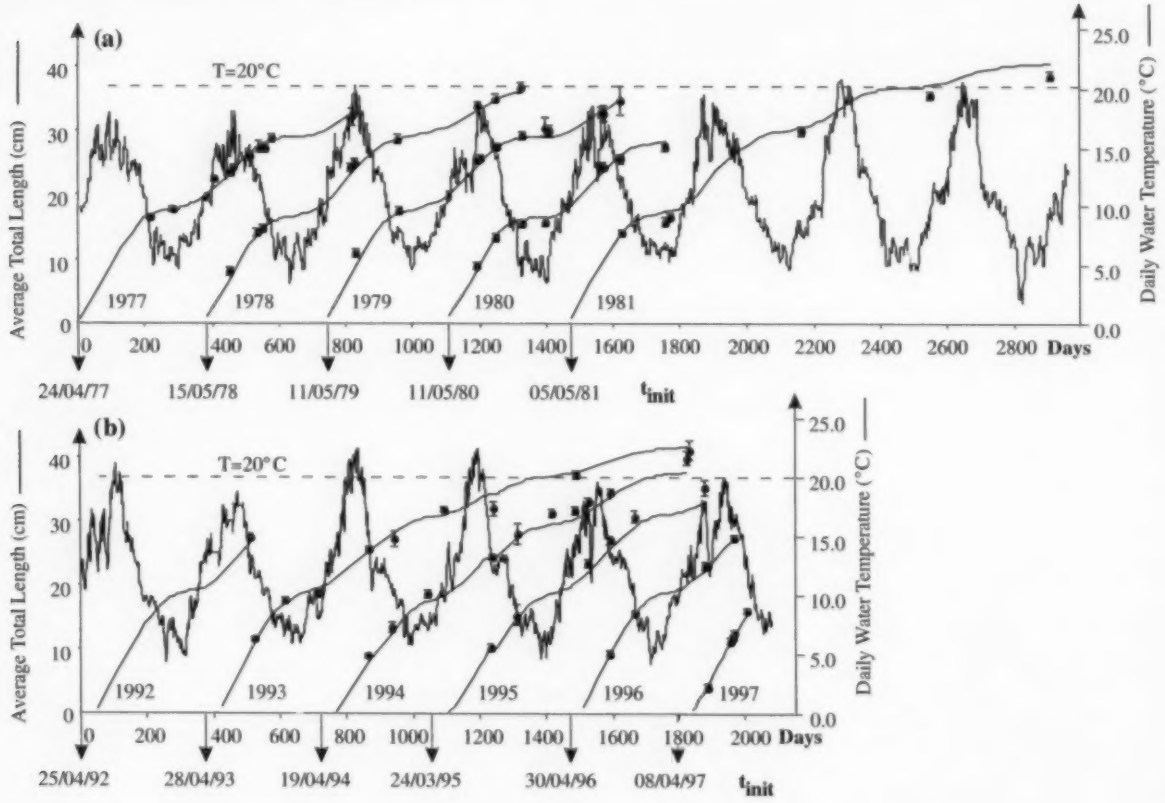

Discussion

The description and the prediction of European grayling growth in the Lower Ain River with our model appeared quite precise. For 11 annual cohorts of this population, the error term on average length was almost always less than 1 cm. Growth curves for cohorts of the second survey period (1992–1997) provided results as positive as those obtained with the first-period cohorts (Table 2).

However, some differences may be found between periods, as well as between years within each period (mainly concerning growth rates and densities). Thus, changes in growth rates (modification of $\bar{k}$) can influence t_0 and L_∞ values; e.g., a negative correlation between $\bar{k}$ and L_∞ has been underlined (Pauly 1987; Charnov 1993). The estimations of parameters t_0 and L_∞ as well as $\bar{k}$ values might then be quite different if calculated from DataS. In spite of these differences, the validation of a priori growth predictions confirms the choice of the model (eqs. 1 and 2) and underlines the importance of water temperature variations in order to explain the interannual modifications of grayling growth rate.

Moreover, the observation of temperature fluctuations shows an increase in the annual average temperature since 1987 (Fig. 2). Grayling growth was thus globally faster over the 1992–1997 period than over the 1977–1985 period (Fig. 4), apart from 1994 and 1995 where water temperature exceeded the maximal growth temperature (21°C) for long periods. This phenomenon is also highlighted by t_c values, which are the smallest in 1992, 1993, and 1996 (Table 2). Hence, the slowest growth observed for the 1994 cohort (un-

© 1999 NRC Canada

derlined by the largest t_c value equal to 507 days) seems to be well explained by the fact that during its first two summers (1994 and 1995), this cohort faced long periods (4 weeks each year) during which water temperatures exceeded 20°C.

In the Lower Ain River, factors potentially involved in the reduction of grayling densities are numerous and the phenomenon is not recent. The increase in water temperature up to T_{opt} seems to enhance grayling growth rates and might then reduce underyearling mortality, which is assumed to be size selective, as mentioned for young-of-the-year of many species (Backiel and Le Cren 1978; Elliott 1994). However, the detrimental effect of water temperature maxima exceeding the upper thermal tolerance limit for all stages causes both a reduction in growth and some severe mortality events. In fact, significant correlation between air and water temperatures suggests that global climate warming is largely involved in the succession of warm years since 1987 and consequently in the modification of grayling growth.

From the calculated residual analysis, it seems that the real growth is sometimes overestimated (residuals are almost all negative, e.g., 1980; Fig. 4). This could be due either to the model chosen (eq. 2) or to factors other than the temperature that might be involved in the growth process. According to Elliott (1994, p. 69) and others (Wootton 1990; Jobling 1994), the three main parameters that can influence fish growth are water temperature, fish size, and level of energy intake. In fact, as grayling mainly feed on drifting macroinvertebrates (Hellawell 1971; Nagy 1984; Sempeski et al. 1995), reduction of discharge during dry summers might decrease prey availability. Quantitative or qualitative modifications of food supply could then explain the further slow down of growth during this season. Our model already takes into account the first two factors (temperature and reduction of growth rate with size through VBGF), but it could be enhanced, for example, by including a food dependence in the expression of the average growth rate.

Further development of our model could be considered. As mentioned earlier, it was sometimes difficult to estimate the biological parameters, especially t_0 and L_∞, but above all the three cardinal temperatures (T_{min}, T_{opt}, and T_{max}) because of the lack of relevant experimental data. To solve these difficulties, it is possible to replace the numerical value of one or more parameters by a variation interval (with lower and upper limits and a most probable value) and to include it directly in the growth model. The extent of variation intervals is a function of parameter uncertainty, and we will no longer simulate a single growth curve, but a growth band instead. This method, based on the risk analysis principle, allows one to identify those parameters having the greatest influence on grayling growth and to estimate not only a single value for t_c but also a variation interval. By considering this interval as a confidence interval, it will be possible to compare t_c values between cohorts.

Our study demonstrated that the grayling growth in the Ain River can be accurately predicted from a knowledge of water temperature and that warming of the water could lead to a possible extinction of the fish population. Our model seems to be a good descriptor of the biological phenomenon and might be validated by application to other populations in other rivers.

Acknowledgements

This research was a part of a larger study funded in part by Electricité De France, the Association Rhône-Alpes de Laboratoires Pour l'Étude des Problèmes Biologiques de la Pêche, and the Conseil Supérieur de la Pêche for the first data series. All water temperatures were recorded by Electricité De France. The local angler societies (Union des Pêcheurs de la Rivière d'Ain and the Angler Society of Pont d'Ain) allowed us to collect grayling. We greatly appreciated the field assistance of many students and anglers with fish collection. We are also grateful to Dr. M.L. Delignette-Muller and two referees for their critical reading.

References

Backiel, T., and Le Cren, E.D. 1978. Some density relationships for fish population parameters. *In* Ecology of freshwater fish production. *Edited by* S.D. Gerking. Blackwell Scientific Publications, Oxford, U.K. pp. 279–302.

Bardonnet, A., and Gaudin, P. 1990. Diel pattern of emergence in grayling (*Thymallus thymallus*). Can. J. Zool. **68**: 465–469.

Charnov, E.L. 1993. Life history invariants: some explorations of symmetry in evolutionary ecology. Oxford University Press, Oxford, U.K.

Crisp, D.T. 1996. Environmental requirements of common riverine european salmonid fish species in fresh water with particular references to physical and chemical aspects. Hydrobiologia, **323**: 201–221.

D'Hulstere, D., and Philippart, J.C. 1982. Observations sur le comportement d'éclosion et de post-éclosion chez l'ombre commun, *Thymallus thymallus* L. Cah. Ethol. Appl. **2**: 63–80.

Elliott, J.M. 1994. Quantitative ecology and the brown trout. Oxford University Press, Oxford, U.K.

Elliott, J.M. 1995. A new, improved growth model for brown trout, *Salmo trutta*. Funct. Ecol. **9**: 290–298.

Fontoura, N.F., and Agostinho, A.A. 1996. Growth with seasonally varying temperatures: an expansion of the von Bertalanffy growth model. J. Fish Biol. **48**: 569–584.

Hellawell, J.M. 1969. Age determination and growth of the grayling *Thymallus thymallus* (L.) of the River Lugg, Herefordshire. J. Fish Biol. **1**: 373–382.

Hellawell, J.M. 1971. The food of the grayling *Thymallus thymallus* (L.) of the River Lugg, Herefordshire. J. Fish Biol. **3**: 187–197.

Jobling, M. 1994. Fish bioenergetics. Fish and Fisheries Series. Vol. 13. Chapman and Hall, London, U.K.

Jungwirth, M., and Winkler, H. 1984. The temperature dependence of embryonic development of grayling (*Thymallus thymallus*), danube salmon (*Hucho hucho*), Arctic char (*Salvelinus alpinus*) and brown trout (*Salmo trutta fario*). Aquaculture, **38**: 315–327.

Kraiem, M., and Pattee, E. 1980. La tolérance à la température et au déficit en oxygène chez le barbeau (*Barbus barbus* L.) et d'autres espèces provenant des zones piscicoles voisines. Arch. Hydrobiol. **88**: 250–261.

Mallet, J.P. 1997. Études du peuplement piscicole et de la dynamique des populations d'ombres communs (*Thymallus thymallus* L.) de la Basse Rivière d'Ain. Tech. Rep. ARALEPBP, Université Lyon 1, France.

Nagy, S. 1984. Alter, Wachstum und Nahrung der Äsche (*Thymallus thymallus*, L.) im Fluss Bela. Pr. Lab. Ryb. Hydrobiol. Bratisl. **4**: 301–326.

© 1999 NRC Canada

Northcote, T.G. 1995. Comparative biology and management of Arctic and European grayling (Salmonidae, *Thymallus*). Rev. Fish Biol. Fish. **5**: 141–194.

Pauly, D. 1987. On the interelationships between natural mortality, growth parameters, and mean environmental temperature in 175 fish stocks. J. Cons. Int. Explor. Mer, **39**: 175–192.

Pauly, D., and David, N. 1981. ELEFAN I, a basic program for the objective extraction of growth parameters from length–frequency data. Meeresforschung, **28**: 205–211.

Persat, H. 1988. De la biologie des populations de l'ombre commun *Thymallus thymallus* (L. 1758) à la dynamique des communautés dans un hydrosystème fluvial aménagé, le Haut Rhône français. Eléments pour un changement d'échelles. State thesis, Université Lyon 1, France.

Persat, H., and Pattee, E. 1981. The growth rate of young grayling in some French rivers. Verh. Int. Ver. Limnol. **21**: 1270–1275.

Pitcher, T.J., and MacDonald, P.D.M. 1973. Two models for seasonal growth in fishes. J. Appl. Ecol. **10**: 599–606.

Poncin, P. 1996. Reproduction chez nos poissons. Le pêcheur Belge. Fédération Sportive des Pêcheurs Francophones de Belgique, Belgique.

Ricker, W.E. 1979. Growth rates and models. *In* Fish physiology. Vol. 8. *Edited by* W.S. Hoar, D.J. Randall, and J.R. Brett. Academic Press, New York. pp. 677–743.

Rosso, L., Lobry, J.R., Bajard, S., and Flandrois, J.P. 1995. Convenient model to describe the combined effects of temperature and pH on microbial growth. Appl. Environ. Microbiol. **61**: 610–616.

Sempeski, P., Gaudin, P., Persat, H., and Grolet, O. 1995. Diet selection in early-life stages of grayling (*Thymallus thymallus*). Arch. Hydrobiol. **132**: 437–452.

Smith, E.B., Williams, F.M., and Fisher, C.R. 1997. Effects on intrapopulation variability on von Bertalanffy growth parameter estimates from equal mark–recapture intervals. Can. J. Fish. Aquat. Sci. **54**: 2025–2032.

Taylor, C.C. 1960. Temperature, growth and mortality – the Pacific cockle. J. Cons. **26**: 117–124.

von Bertalanffy, L. 1960. Principles and theory of growth. *In* Fundamental aspects of normal and malignant growth. *Edited by* W.W. Nowinski. Elsevier, Amsterdam, The Netherlands. pp. 137–259.

Woolland, J.V., and Jones, J.W. 1975. Studies on grayling, *Thymallus thymallus* L., in Llyn Tegid and the upper River Dee, North Wales. I. Age and growth. J. Fish Biol. **7**: 749–773.

Wootton, R.J. 1990. Ecology of teleost fishes. Chapman and Hall, London, U.K

© 1999 NRC Canada

Organic matter and pigments in surface sediments: possible mechanisms of their horizontal distributions in a stratified lake

I. Ostrovsky and Y.Z. Yacobi

Abstract: The analysis of spatial changes of organic matter and pigments (chlorophyll *a*, chlorophyll *b*, bacteriochlorophyll *e*, and phaeophytin *a*) in the uppermost bottom sediments was used to distinguish between sources of settled material in Lake Kinneret (Israel) during thermal stratification. The proportion of phytobenthic chlorophyll *a* decreased relatively to total chlorophyll *a* down to zero at 17 m. Bacteriochlorophyll *e*, derived from *Chlorobium phaeobacteroides*, was the most abundant pigment below the thermocline. Organic matter content in the sand-free sediment fraction and chlorophyll *a* to organic matter ratio were the lowest in the bottom area most extensively affected by shoaling internal seiches and where resuspension occurred. The proportion of resuspended matter sharply decreased with bottom depth in the hypolimnion. The importance of degraded materials of planktonic origin apparently increased towards the lake center. These distribution patterns could be achieved by dispersion of the rapidly sinking resuspended particles with fast metalimnetic jets and by focusing of the lighter planktonic particles by water motions in the turbulent benthic boundary layer. Our study showed that analysis of distribution of freshly settled organic components on the bottom may be a useful tool for understanding particle transport mechanisms in lakes.

Résumé : L'analyse des variations spatiales de la matière organique et des pigments (chlorophylle *a*, chlorophylle *b*, bactériochlorophylle *e* et phéophytine *a*) dans la couche supérieure des sédiments du fond a été utilisée pour distinguer les sources des matières déposées dans le lac Kinneret (Israël) durant la stratification thermique. La proportion de chlorophylle *a* phytobenthique diminuait relativement à la chlorophylle *a* totale pour devenir nulle à 17 m. La bactériochlorophylle *e*, issue de *Chlorobium phaeobacteroides*, était le pigment le plus abondant sous la thermocline. La teneur en matière organique dans la fraction de sédiments exempte de sable et le ratio chlorophylle *a* à matière organique étaient les plus faibles dans la région du fond la plus touchée par les seiches internes qui balayent les hauts fonds et là où se produisait une remise en suspension. La proportion de matière remise en suspension diminuait abruptement en raison directe de la profondeur du fond dans l'hypolimnion. La quantité de matières dégradées d'origine planctonique s'accroissait apparemment vers le centre du lac. Ces profils de distribution pourraient être attribuables à la dispersion par des jets métalimnétiques rapides des particules remises en suspension qui descendent rapidement et à la concentration des particules planctoniques plus légères par les mouvements de l'eau dans la couche limite benthique turbulente. Notre étude a montré que la distribution des composantes organiques fraîchement déposées sur le fond peut aider à comprendre les mécanismes de transport des particules dans les lacs.

[Traduit par la Rédaction]

Introduction

The uppermost layer of bottom sediments (ULBS) is continually formed by addition of newly settled particles and by subsequent degradation of the accumulated material, its removal by resuspension processes, and its relocation (e.g., Hakanson and Jansson 1983; Bloesch 1995). The structure and composition of ULBS record information about recent events occurring in aquatic ecosystems and thus may be used for assessing the relative importance of mechanisms determining spatial distribution of particles. Spatial heterogeneity may be induced by localized factors, e.g., production and degradation, but to a large extent may be formed by vertical and lateral transport of particles, which is facilitated by several mechanisms of water motions. Recent hydrophysical studies show that internal seiche-related motions are a major factor in inducing material transport and in redistributing particles in stratified lakes. The release of seiche-induced kinetic energy drives a flux in the benthic boundary layer (BBL), producing turbulent mixing and other nearshore phenomena (Garrett and Gilbert 1988; Imberger 1994). Past investigations suggest that internal seiche-initiated motions are responsible for resuspension in lakes (e.g., Chambers and Eadie 1981; Gloor et al. 1994; Ostrovsky et al. 1996). In addition, particle sorting and focusing are important phenomena affecting the heterogeneity of material deposition (Hakanson and Jansson 1983; Bloesch 1995). The actual role of different processes in particle migration and bottom sediment formation is not well known and is a subject of interest in many current investigations.

Pigment analysis has been used in numerous studies of aquatic ecosystems to characterize the composition of photo-

Received June 17, 1998. Accepted February 5, 1999.
J14657

I. Ostrovsky[1] and Y.Z. Yacobi. Israel Oceanographic & Limnological Research, Yigal Allon Kinneret Limnological Laboratory, P.O. Box 345, Tiberias 14102, Israel.

[1]Author to whom all correspondence should be addressed.
e-mail: ostrovsky@ocean.org.il

© 1999 NRC Canada

synthetic populations and (or) to follow changes in the physiological status of phototrophic populations (e.g., Gieskes and Kraay 1986). Tracing algal particles in bottom sediments is, however, more complicated than tracing them in the water column. The pigment suite found in bottom sediment records the phytoplankton dynamics in an incomplete and biased way, due to differential degradation of the various chlorophylls and carotenoids (Hurley and Armstrong 1990). For instance, the signature of *Peridinium* pigments is virtually lost 3–4 months after an intensive bloom of that species, while pigments representing minor populations can be abundant (Yacobi et al. 1991). The tendency to modify settled material increases as sampling is performed in deeper (i.e., older) parts of the sediment core. Fresh sediments, however, convey information about the recent history of sinking phytoplankton and may be used to study the distribution of settled matter in bottom sediments (Hurley and Armstrong 1990; Ostrovsky et al. 1997).

The goal of this study was to determine the sources of particles forming bottom sediments and to consider possible mechanisms mediating the spatial distribution of these particles. Distribution of sedimentary components was analyzed and compared with the composition of tripton and material accumulated in 24-h sedimentation traps. Organic matter (OM) and pigments were used as tracers over a period of thermal and chemical stratification in the subtropical Lake Kinneret.

The lake

Lake Kinneret is monomictic and warm, with a surface area of 168 km^2. Its average and maximum depths are 23 and 43 m, respectively. Homothermy usually occurs between December and March. During stratification (April–December) the thermocline deepens from 10 m in May to 25 m in October–November. Wind speeds are maximal from July through August and are lowest in October and November. During the stratification period, wind-induced internal seiches are a recurrent phenomenon (Serruya 1975). The epilimnion is characterized by relatively high pH (8.2–9.6) and dissolved oxygen, whereas the hypolimnion is anoxic and H_2S enriched and has lower pH (7.3–8.0). The metalimnion is well developed from June to November–December (Serruya 1978). The internal seiche activity generates a thick (up to 8–10 m wide) turbulent BBL (Imberger 1998; Lemckert and Imberger 1998).

The Jordan River is the major inflow, and water pumped into the National Water Carrier constitutes the main outflow. Particles of allochthonous origin are variable, depending on hydrological conditions in the watershed. However, even during the peak of inflows to the lake during the winter, the allochthonous load does not exceed (by mass) 14% of the particles found in the lake (A.S. Parparov and Y.Z. Yacobi, unpublished data). The allochthonous input of algal cells is relatively even less important than the bulk of other matter imported to the lake.

The average primary productivity is about 600 g $C \cdot m^{-2} \cdot year^{-1}$ (Berman et al. 1995). Planktonic algae inhabiting the highly productive epilimnion are the major producers of OM and (or) pigments in Lake Kinneret. Benthic algae occupying the euphotic littoral and photosynthetic bacteria colonizing the metalimnion and metalimnion–sediment interface are relatively minor contributors to primary productivity (Butow and Bergstein-Ben Dan 1992).

The dominant phytoplankton from February through May is usually the dinoflagellate *Peridinium gatunense* Nygaard, which forms thick blooms and comprises more than 90% of the algal biomass during the bloom and 59–90% on an annual basis (Berman et al. 1995). In 1996, however, this bloom did not occur and other algae were prominent in the phytoplankton assemblage, e.g., *Microcystis*, *Ankistrodesmus*, and *Carteria*. Nanoplanktonic forms of chlorophytes, diatoms, cyanophytes, and dinoflagellates normally dominate the assemblage from June through January in Lake Kinneret. Another feature of the phototrophic population of this lake is the bloom of the green sulfur bacterium *Chlorobium phaeobacteroides* Pfennig (Chlorobiaceae) in the metalimnion between July and October (Bergstein et al. 1979).

The degradation products of OM (e.g., ammonium and dissolved phosphorus) accumulate in the hypolimnion. Bulk sedimentation rates vary from relatively high values (10–20 $kg \cdot m^{-2} \cdot year^{-1}$) in the littoral zone to lower values (about 1 $kg \cdot m^{-2} \cdot year^{-1}$) in the pelagic zone (Nishri and Koren 1993) where sediment is mainly clay or silt–clay. Depending on location, the upper 0.5–2 cm of the sediment layer is composed of fluffy material, while the underlying sediments are more compact. Bottom sediments are formed mainly from autochthonous material (Koren 1993). The bottom area affected most by the seiche activity is defined as the washing zone (WZ) where epilimnetic and hypolimnetic waters exchange with each other during a seiche cycle (Ostrovsky et al. 1996). For a more detailed description of the lake, see Serruya (1978).

Materials and methods

Duplicate sediment samples were collected by SCUBA divers along a transect from the littoral (6 m) on the northwestern shore of Lake Kinneret to the deepest point (40 m) from October 24 to November 10, 1996. Each sampling day, bottom sediment was randomly collected at either one deep or two to four shallow stations. Our study showed that during a 3-week period in the summer–fall, ULBS composition did not change remarkably (Ostrovsky 1998). Location of the transect on the lake's lee side guaranteed that surface waves did not influence bottom sediments. The transect crossed the thermocline at about 18 m and had a slope similar to the lake's average slope. Sampling stations located deeper than 19 m (i.e., below the seasonal thermocline) were overlain by deoxygenated water. A SCUBA diver collected samples from a large bottom area (0.5–1 m^2) to diminish the effect of patchy distribution. The SCUBA sampling method allowed collection of ULBS with high reproducibility (variation between subsamples was <10%). Precautions were taken to prevent resuspension during collection by skimming the topmost sediment layer (as thinly as possible) directly into a plastic box. The SCUBA sampling allowed us to collect a higher proportion of fresh ULBS than that collected with an ordinary sediment gravity corer (Ostrovsky 1998).

The collected material was transferred to plastic opaque containers and kept on ice until arrival at the laboratory (within 1–2 h), where subsamples were stored at –18°C before further processing for pigment analysis. Other subsamples were processed immediately as follows. To remove water, which inevitably accompanied ULBS collection, a teaspoon of wet sediment was placed on a tilted glass surface for 10 min. Excessive drops of water were removed from the sediment knoll side with a filter paper. A portion

© 1999 NRC Canada

(2–5 g) of wet sediment was weighed with a precision of ± 0.1 mg, dried at 80°C for 24 h, and then reweighed. Water content (WC) of sediment was calculated as loss on drying and expressed on a weight per weight basis. A small portion (about 0.1–0.3 g) of the oven-dried matter was weighed with a precision of ± 10 µg, ignited in a muffle furnace at 550°C for 4 h, and then reweighed. The losses on ignition, equivalent to the OM content, were calculated from the difference in dried and combusted weight of the samples. Grain size composition was estimated using a standard hydrometric method (Buchanan and Kain 1971).

Sediment traps were positioned about 2 m above the bottom at the lake center on November 3, 1996. During the next 24 h, sinking material was collected. Eight cylinders with a diameter of 5 cm and a length of 50 cm were used. Subsamples of several hundred millilitres were filtered onto GF/C filters under subdued light and stored at –20°C in the dark until processing within 1 week of the time of collection. The content of particulate matter and its OM content were measured in duplicate, as described above for bottom sediment samples.

Water samples were withdrawn from the hypolimnion 2 m above the bottom with a 5-L Aberg-Rodhe sampler at the time of sediment trap installation. Collected water samples were preserved in opaque plastic carboys until processing in the laboratory 1–2 h after collection. Subsamples of 1 L were filtered onto GF/C filters and processed the same way as the sediment trap samples.

For pigment analysis, duplicate subsamples of sediment (about 20–100 mg) were extracted in 1 mL of 100% acetone, vortexed, and centrifuged. The supernatant was transferred to a dark test tube and kept at 4°C, and the pellet was resuspended in 2 mL of 90% acetone, vortexed, and centrifuged. The supernatant was pooled with the first extract and the treatment repeated until a colorless supernatant was formed. The clear supernatant was discarded and the pellet was oven-dried for determination of dry matter (DM). The acetone extract was filtered onto a GF/F filter and then injected into the high-performance liquid chromatography (HPLC) system. Pigment concentrations were normalized to sediment DM. Such normalization to lipid-free DM did not bias the results, since the difference between total DM and lipid-free DM did not surpass 5%.

The reverse-phase HPLC system used in this study is described elsewhere in detail (Yacobi et al. 1996). Many carotenoids showed on the chromatograms when the detector was tuned to 436 nm but overlapped some chlorophyllous pigments, thus rendering both pigment classes inappropriate for quantitative analysis. In the current study the detector was tuned to 640 nm. This enabled simultaneous detection of algal and bacterial chloropigments and concealed the presence of carotenoids. Peak identification was facilitated by comparison with (*i*) chromatograms from pure cultures of phytoplankton species isolated from Lake Kinneret and (*ii*) purified pigments (Yacobi et al. 1996). Bacteriochlorophyll *e* (Bchl *e*) was isolated from monoalgal culture extracts of *Chlorobium phaeobacteroides* on the HPLC system (Yacobi et al. 1990). The spectral characteristics of the purified pigments in the HPLC eluent were examined using a spectrophotometer and the optical density determined. The concentration of the pigments was calculated using published extinction coefficients (Stal et al. 1984; Rowan 1989). The quantification of the chromatograms was facilitated by injection of known pigment concentrations into the HPLC system and calculating the response factor based on the area under the peak. All calculations of pigment concentration are presented as the mean of duplicate measurements. Individual measurements did not differ by more than 10%.

The proportion of the resuspended fraction, R, at different bottom locations was calculated using the following well-known formula (e.g., Bloesh 1995):

$$(1a) \quad R = (f'_i - f'_{nr})(f_r - f'_{nr})^{-1}$$

where f'_i is the concentration of a trace substance in bottom sediments at a given location and f_r and f'_{nr} are the concentrations of a trace substance in resuspended and nonresuspended fractions in bottom sediments, respectively. The f_r was assumed to be invariable and derived from the concentration of the tracer at the WZ, where resuspension occurred (see Discussion). The concentration of a trace substance in the nonresuspended fraction of bottom sediments was estimated specifically for the location of trap deployment by using a modified version of eq. (1*a*):

$$(1b) \quad f'_{nr} = (f'_i - R_T f_r)(1 - R_T)^{-1}$$

where R_T is the proportion of resuspended matter in near-bottom trap sediments. This formula suggests that resuspended material contributes equally to bottom and trap sediments, i.e., $R_T = R$. This is appropriate in the case of the deep hypolimnion of Lake Kinneret because no resuspension takes place there during a stratified period (see Discussion). The R_T was calculated using eq. 1*a*, where the concentration of a tracer in tripton (f_{nr}) and in trap material (f_i) stood for f'_{nr} and f'_i, respectively. The use of tripton for characterization of the nonresuspended fraction of the trap material is based on the assumption that resuspended particles comprise an insignificant fraction of the total suspended material in the water column. The latter is valid when the sinking velocity of resuspended particles is much higher than the sinking velocity of nonresuspended (newly produced) particles, which is normally the case. However, if the actual f_{nr} is higher than the concentration of a tracer in tripton, R_T will be underestimated.

The portion of the tracer being decomposed in the nonresuspended fraction of the ULBS (D, percent) during the period of its accumulation was estimated as follows:

$$(2) \quad D = 100 - (f'_{nr}\ f_{nr}^{-1})100$$

Wind velocity and direction were measured hourly with a Yonng anemometer located about 50 m from the western edge of our transect and positioned 6 m above the water level.

Results

The velocity of westerly winds prevailing in the lake area showed a linear declining trend from July until November. During this period the weekly average velocity decreased from 2.9–3.6 to 1.2 $m \cdot s^{-1}$. The observed wind changes followed the general pattern recorded during summer–fall in previous years (Serruya 1975). In July–August the number of hours of strong winds (>6 $m \cdot s^{-1}$) was usually very high and varied between 20 and 43 $h \cdot week^{-1}$. At the end of August, there was a marked decline, and after mid-September, strong winds were rare (0–10 $h \cdot week^{-1}$). The seasonal change in wind regime apparently affects the pattern of displacements of metalimnetic isotherms. During June–July, the 20°C metalimnetic isotherm is displaced 5–10 m over 24 h, whereas between the end of September and the end of October, the displacement is reduced to 1–3.5 m (Serruya 1975; cf. Bergstein et al. 1979).

Granulometric analysis showed that the sand fraction was abundant up to a depth of 8 m, where it comprised >80% of the DM but was virtually absent at depths below 17 m (Fig. 1*a*). The combined silt plus clay fraction obviously provided an inverse picture to that of the sand fraction.

The WC of the ULBS increased steadily from shallow waters towards the lake center (Fig. 1*b*). The increase of WC with depth was abrupt (from 40 to 75%) between 6 and 12 m and then increased at a much slower rate. In the littoral

© 1999 NRC Canada

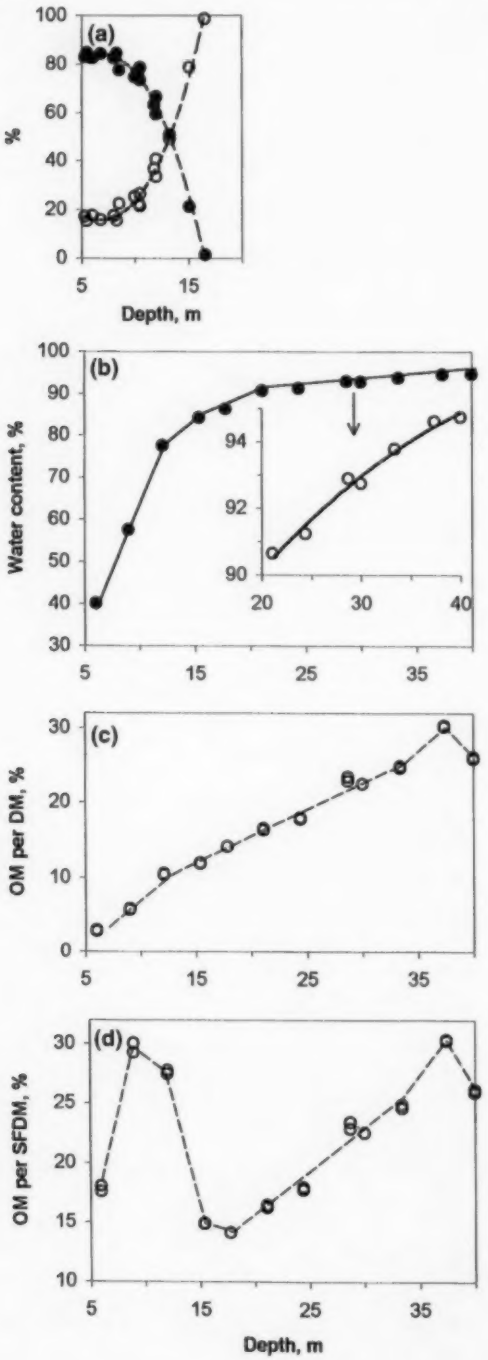

Fig. 1. Characteristics of the ULBS sampled in Lake Kinneret in October–November 1996. (*a*) Texture of the sediments (●, sand; ○, silt plus clay); (*b*) WC (the inset displays the WC of the sediments located below the thermocline); (*c*) OM content expressed relatively to DM; (*d*) OM content expressed relatively to SFDM.

area the WC increased with a decrease in the sand fraction. In the sediments located below the thermocline, between 21 and 39 m, the change in WC was from 90 to 95%, but the change was consistent and statistically significant ($P < 0.01$) (Fig. 1*b*, inset).

At 40 m, where WC was 94.7%, a millimetre of sediment layer contained $(1 - 0.947) \times 10^3 \times 1.034 \approx 55$ g DM·m^{-2}, where 1.034 is the specific gravity of the sediment with that given WC. In the shallower part of the hypolimnetic zone (21 m depth), where WC was 90.6% (specific gravity 1.062), a millimetre of sediment layer contained 100 g DM·m^{-2}, i.e., about twice as high as at the deepest location. Since the sedimentation rate at the lake periphery is higher than at the lake center by a factor of 1.5–2.5 (Serruya 1977; Koren 1993), a sediment layer of comparable thickness would be accumulated during a similar time span at both sites.

The proportion of OM (expressed on a DM basis) in the ULBS increased steadily from 6 to 37 m and then declined slightly (Fig. 1*c*). The OM calculated on the basis of sand-free dry mass (SFDM) of the bottom sediments (i.e., silt plus clay) showed a minimum between 15.4 and 17.8 m and showed a maximum in shallow (between 9 and 12 m) and deep (37 m) parts of the bottom (Fig. 1*d*).

Pigment concentrations, normalized on the basis of OM and SFDM, showed that chlorophyll *a* (Chl *a*) assumed a different pattern of depth distribution than the other pigments (Fig. 2). Chl *a* displayed a consistent decline from the shallowest station down to a depth of 12–18 m and then a sharp increase between 18 and 33 m. All other pigments indicated a conspicuous increase in concentration from 15–18 to 24 –29 m, i.e., a sharp change with the transition from sediments overlain by oxygenated water to sediments residing below the thermocline.

Relative pigment concentrations, normalized to the concentration at the geometrical lake center, allowed us to compare their spatial changes (Fig. 3). Bchl *e* showed the most drastic exponential increase from the lakeshore towards 18 m depth. Within the same depth range, changes in chlorophyll *b* (Chl *b*) and phaeophytin *a* (Phaeo *a*) concentrations showed a slighter slope of increase. Chl *a* displayed the most gradual alterations in that area. The relative changes in OM and pigment concentrations below the thermocline clearly indicated an existence of two different areas in that part of the bottom. Within the peripheral area (between 21 and about 25–28 m depth), concentrations of various pigments decreased towards the shoreline faster than the OM did, while within the central area (below 25–28 m), relative changes in OM and pigments were comparable, such that the pigment to OM ratios were about constant. The proportion between major photopigments showed regular changes below the thermocline (Fig. 4). Chl *a* : Chl *b* and Chl *a* : Phaeo *a* gradually decreased in the bottom sediments located from 21 m depth to the lake center (34–37 m). Chl *b* : Bchl *e* decreased gradually from 21 m depth to the deepest station.

Pigment concentrations in the pelagic water (Table 1) were within the range found in October–November (Yacobi et al. 1996). The sedimented material in the traps bares closer resemblance to water column tripton than to the material found in bottom sediments. The most prominent difference was in the concentration of Bchl *e* (normalized to OM),

© 1999 NRC Canada

Fig. 2. Concentration of chlorophyllous pigments in the uppermost layer of bottom sediments sampled in Lake Kinneret in October–November 1996. (*a–d*) Concentration relative to OM; (*e–h*) concentration relative to SFDM. Pigment concentrations normalized to SFDM are displayed on a logarithmic scale to enhance the differences between samples taken from shallow stations.

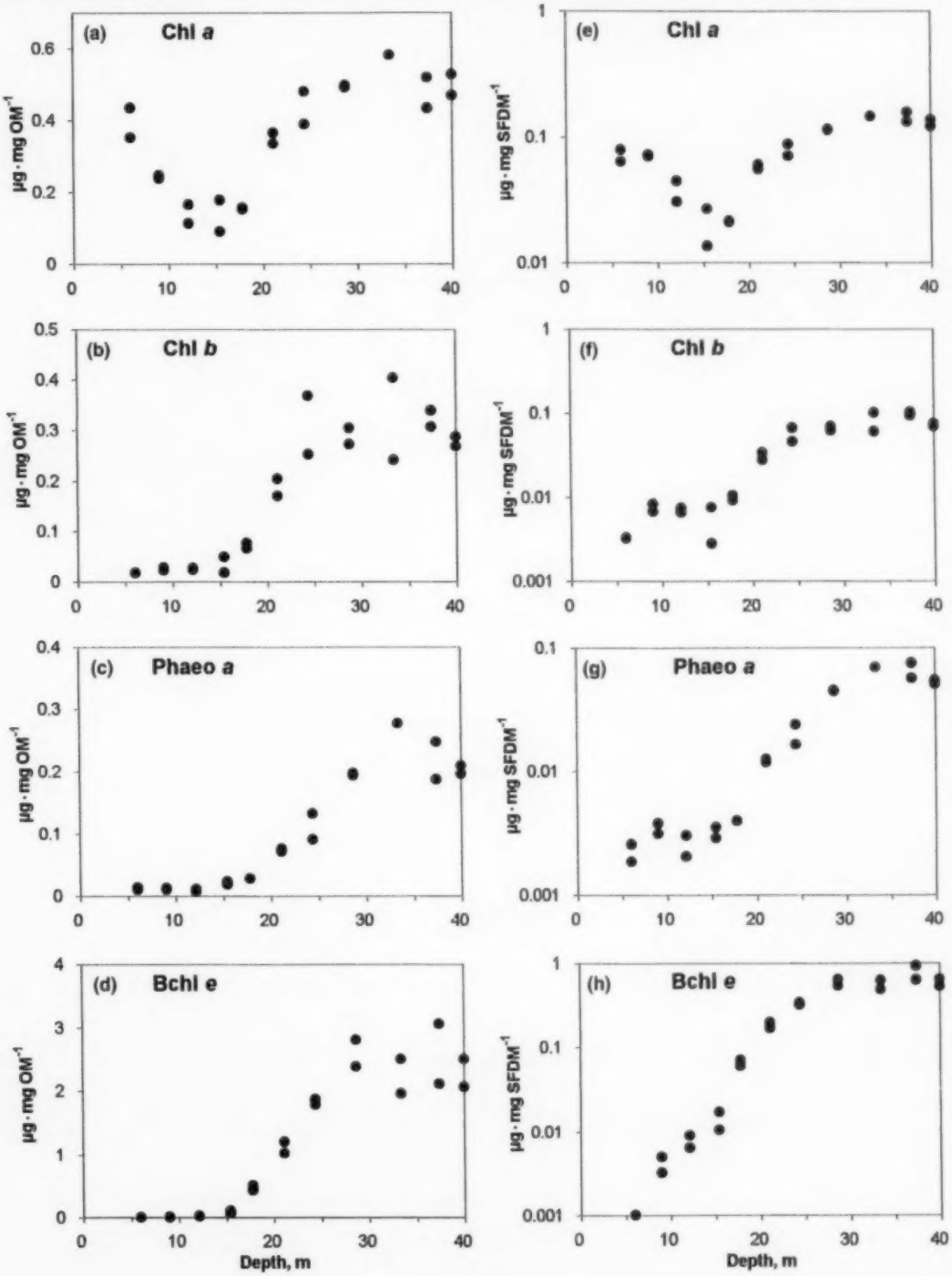

© 1999 NRC Canada

Fig. 3. Depth-related trends of OM and pigment concentrations expressed relative to their concentration at the lake geometric central station of 37 m depth. ●, OM content; △, Chl *a*; □, Chl *b*; ▲, Paeo *a*; ○, Bchl *e*.

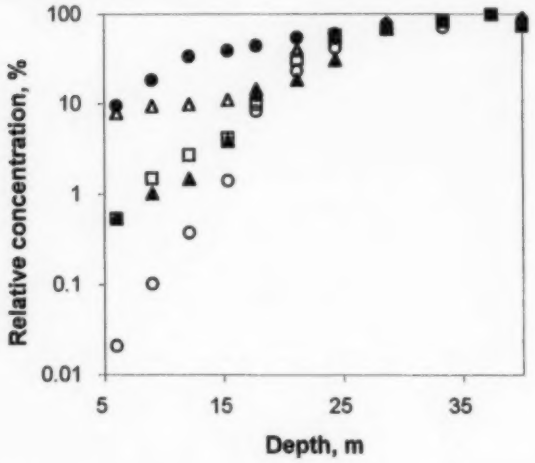

which was almost eight times higher in the bottom sediments than in the other samples. There was relative enrichment of Chl *b* containing particles in the trap material and even more prominent enrichment in the bottom sediment.

The proportion of resuspended material in the sediment trap (R_T) varied at the lake center between 18.2 and 23.2% for different tracers. The values of R_T were not very sensitive to f_r, as a variation of 50% in f_r altered R_T by only 15%. If the real zone from where the sediments were resuspended was wider, R_T could be slightly underestimated because concentrations of OM and Chl *a* per silt plus clay base (the fraction being potentially resuspended) were minimal at 15–18 m depth.

The tracer concentration of the newly produced component in the ULBS was estimated (using eq. 1*b*) in the deepest station as 33.9% for OM, 0.172 μg Chl *a*·mg DM^{-1}, 0.118 μg Chl *b*·mg DM^{-1}, and 0.951 μg Bchl *e*·mg DM^{-1}. The proportion of decomposed matter during ULBS accumulation was calculated (using eq. 2) as 46% for OM and 49% for Chl *a*. The resulting magnitude of OM degradation under anoxic conditions was typical for decomposition of freshly settled detritus (e.g., Hertzig et al. 1981; Hurley and Armstrong 1990).

Different tracers indicate an essential decrease in the proportion of resuspended material in bottom sediments (R) from the peripheral zone of the hypolimnion toward the lake geometrical center (Fig. 5). The difference in R between the 21- and 40-m stations (about twofold) using OM and pigment tracer yielded similar results to R measured by near-bottom sedimentation traps at the same locations in different years (Serruya 1977; Koren 1993; Koren and Ostrovsky 1998).

Discussion

Contribution of phototrophic organisms to sedimentary pigments above the thermocline

In shallow waters, phytoplankton are not the only primary

Fig. 4. Ratio of several chlorophyllous pigments found in bottom sediments located below the thermocline.

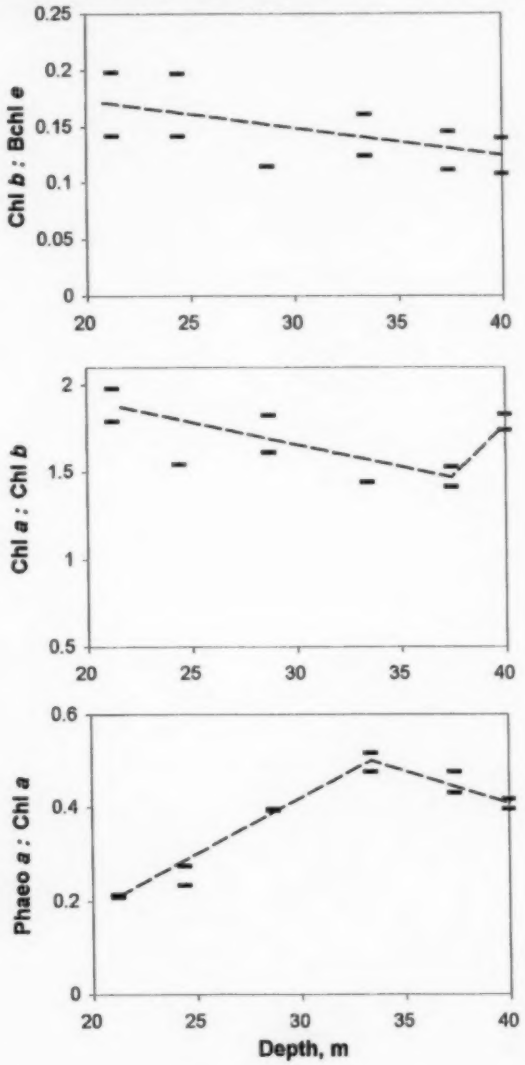

producers, and phytobenthos can be an essential contributor to newly produced OM that accumulates in sediments. Lake Kinneret phytobenthos is dominated by diatoms and accompanied mainly by cyanophytes (Serruya 1978). Chl *b* containing chlorophytes (and euglenoids) are rarely a component of the phytobenthos; hence, most of the Chl *b* found in the sediment of the shallow zone originates from cells or cell debris sinking from the epilimnetic water column. The concentration of Chl *b* (normalized to SFDM or OM) was constant down to 18 m depth, while the concentration of Chl *a* decreased from 6 to 15 m (Fig. 2). In the shallow water zone, this resulted in a sharp decrease in Chl *a* : Chl *b* with depth.

We assumed that the Chl *a* : Chl *b* of the material accumulated in the pelagic traps was representative for settled algal material of planktonic origin. Therefore, we used the

© 1999 NRC Canada

Table 1. Composition of hypolimnetic tripton and material collected in sediment traps and in the ULBS in a deepwater station positioned below the thermocline, located at the lake center (41 m depth).

Characteristic	Tripton	Trap material	Bottom sediments
OM content, %	62.5	53.7	30.4
Chl *a*, μg·mg DM^{-1}	0.345	0.281	0.145
Chl *b*, μg·mg DM^{-1}	0.079	0.117	0.098
Phaeo *a*, μg·mg DM^{-1}	0.052	0.026	0.066
Bchl *e*, μg·mg DM^{-1}	0.190	0.166	0.785
Chl *a*, μg·mg OM^{-1}	0.552	0.523	0.477
Chl *b*, μg·mg OM^{-1}	0.126	0.218	0.323
Phaeo *a*, μg·mg OM^{-1}	0.083	0.048	0.218
Bchl *e*, μg·mg OM^{-1}	0.304	0.309	2.584
Chl *a*:Chl *b*	4.38	2.41	1.48
Phaeo *a*:Chl *a*	0.15	0.09	0.46
Bchl *e*:Chl *b*	2.41	1.42	8.01

Note: Sediment traps were positioned about 2 m above the bottom for 24 h.

Fig. 5. Proportion of resuspended material (R) in the bottom sediments estimated using different tracers. □, OM content; ●, Chl *a*; △, Chl *b*.

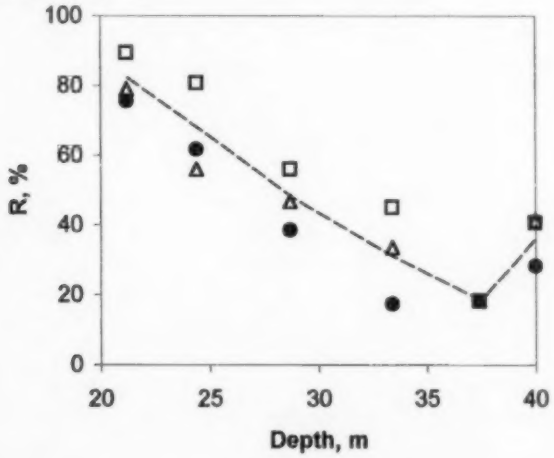

trap Chl *a*:Chl *b* (2.41) as a basis for determining Chl *a* derived from phytobenthos using the following formula:

$$\text{(3)} \quad \text{Chl } a_{\text{Benthic}} = \text{Chl } a_{\text{Total}} - \text{Chl } a_{\text{Planktonic}} = \text{Chl } a_{\text{Total}} - \text{Chl } b \times 2.41.$$

The calculated proportion of benthic-derived Chl *a* declined from 90% at 6 m to about 0% at 18 m (Fig. 6). The low proportion of planktonic components in the shallow bottom areas indicated that phytoplankton, like other light particles, could not permanently accumulate under the conditions of high turbulence prevailing in the epilimnion (Lerman and Stiller 1969). The decline in the slope of Chl a_{Benthic} ($-0.20 \cdot m^{-1}$) was lower than the light attenuation coefficient (the slope of light decline) during the 3-month period preceding our sampling (–0.33 to –0.42·m^{-1}, Y.Z. Yacobi, unpublished). The difference in slopes could be a reflection of low-light conditions inducing increase in cellular Chl *a* content (Kirk 1994) and (or) could be an indication of mechanical dispersion of benthic algae associated with heavy particles.

Fig. 6. Proportion of benthic Chl *a* in bottom sediments located above the thermocline. The calculation was based on eq. 3.

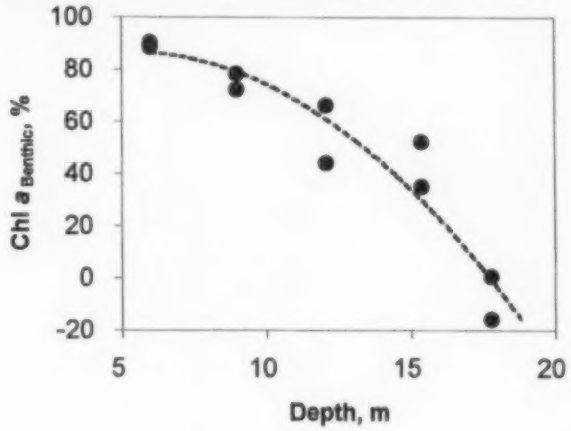

Contribution of phototrophic organisms to sedimentary OM below the thermocline

The appearance of Bchl *e* in the ULBS in October–November indicated that the collected sediments were of recent origin, as this pigment was not found during sampling done in May–June (Ostrovsky et al. 1997). Compared with previous samplings (Ostrovsky et al. 1997; Yacobi and Ostrovsky 1998), the rapid increase in concentrations of photosynthetic pigments and other organic compounds in the hypolimnetic sediments apparently resulted from a decline in the rate of OM decomposition as anoxic conditions developed (e.g., Leavitt 1993). During the period of about 4 months preceding our sampling time, 5–7 mm of the ULBS could have accumulated on the bottom at a sedimentation rate of 2–3 g DM·m^{-2}·day^{-1}, characteristic of the lake center (Klein and Koren 1998). This layer was slightly thicker than a layer that could be collected by our SCUBA sampling method (4–5 mm, Ostrovsky 1998). Thus, it can be concluded that the collected ULBS was formed within the time span of hypolimnetic anoxia.

Chl *a* based (algal) organic carbon comprised about 4–6% of the total organic carbon of bottom sediment below the thermocline, assuming that the average ratio of Chl *a* to organic carbon in algae is 1: 60. If proportions of the major photopigment to organic carbon are about the same in bacterial and algal cells, then *Chlorobium*-derived biomass was 3.2–5.4 times higher than the biomass originating directly from algal cells in hypolimnetic sediments. The higher concentration of bacterial photopigments compared with algal pigments suggested that the OM produced by epilimnetic algae was mostly decomposed within the water column and only a small fraction reached the bottom, since algal production during the summer–fall period is 1–1.5 orders of magnitude higher than photosynthetic bacterial production (Butow and Bergstein-Ben Dan 1992).

© 1999 NRC Canada

Fig. 7. Hypothetical scheme of bottom sediment formation in a stratified lake. Top: schematic presentation of suspended particle motion in a lake. Particles resuspended from the WZ are entrained by metalimnetic jets and transported towards the lake interior. The newly produced planktonic material settles down and is moved along the BBL. Bottom: the resulting distribution of sunken material on the bottom of Lake Kinneret beneath the thermocline. Two different bottom areas could be distinguished within the hypolimnion: a peripheral zone from 21 m down to 25–28 m and a central zone below 25–28 m. In the peripheral area, the decline of the resuspended fraction is more substantial than the effect of focusing, while in the central area the focusing of light particles is a dominant process in the formation of the ULBS (see text).

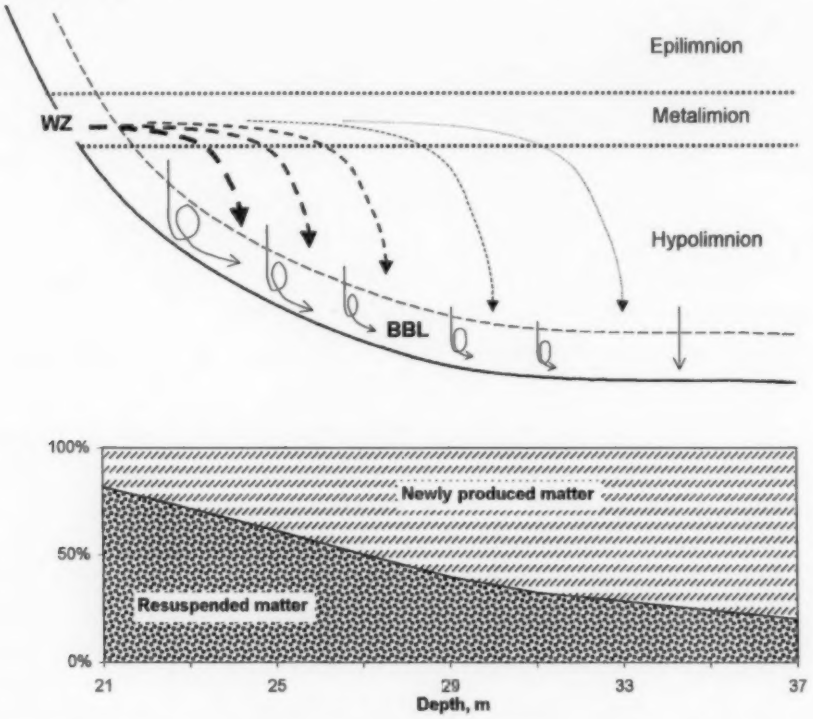

The gradual increase in the ratio of Phaeo *a* (product of Chl *a* degradation) to Chl *a* in the ULBS with bottom depth suggested that the proportion of the decomposed algal-derived fraction of the sediment slightly increased with depth. The decrease in Chl *a*:Chl *b* from the lake periphery to the lake center (34–37 m) also supports this conclusion because Chl *b* is more stable than Chl *a* (Yacobi et al. 1991). The trend in the ratio between Chl *b* (originating from the epilimnion) and Bchl *e* (originating from the metalimnion) confirmed the above conclusion, since *Chlorobium* cells remained apparently intact in the anoxic hypolimnion (no bacteriopheophytin, a degradation product of Bchl *e*, was found in notable concentrations in the sediments). However, increasing Bchl *e*:Chl *b* towards the lake center could also be due to pronounced focusing of the smaller bacterial cells.

Source of resuspended matter

The shallow zone pertaining to our sampling transect is covered primarily by stones and sand, which cannot be transported far away from the shoreline. Moreover, it is unlikely that any notable resuspension occurred in the littoral area due to surface wave action on the lee side of the lake, where the sampling transect was located. It is also unlikely that resuspension occurred in the hypolimnion, where the near-bottom current velocities did not exceed 4 $cm \cdot s^{-1}$ below 20 m depth even during the windy season of June–July (A. Nishri, Israel Oceanographic & Limnological Research, Yigal Allon Kinneret Limnological Laboratory, personal communication), because of the threshold value to induce resuspension of consolidated clayey sediments >7 $cm \cdot s^{-1}$ (e.g., Gloor et al. 1994, Bloesch 1995). The absence of resuspension of material was also confirmed by the detailed measurements of sedimentation fluxes in the hypolimnion (I. Ostrovsky, unpublished): no differences in sedimentation rates and OM content were found between near-bottom traps positioned within the turbulent BBL and traps located far above this layer.

Most probably, sediments were resuspended where metalimnetic isotherms intersect the bottom (Ostrovsky et al. 1996). In this area, breaking internal waves and seiche-related current induce various inshore phenomena, including mixing and resuspension (Imberger 1994). The center of the metalimnion–bottom interface area was situated between 15 and 19 m. Within the same depth range, we found the minimum sedimentary OM content, as calculated on a silt and clay basis. This minimal value (13.7–15.0%) was very similar to OM content (15.8 ± 1.1%) obtained for material accumulated in sediment traps positioned 1.5 m above the WZ in September–November (I. Ostrovsky and N. Koren, unpublished).

© 1999 NRC Canada

These findings suggest that the WZ was an area from which the freshly settled particles could be most easily resuspended as a result of the inshore seiche activity. Seiche-driven sediment resuspension has also been shown in other lakes of moderate depth (e.g., Chambers and Eadie 1981; Gloor et al. 1994). The high value of R obtained at the 21-m hypolimnetic station, i.e., at the peripheral zone of the hypolimnetic bottom, suggests that resuspension was vigorous.

Impact of resuspension and focusing on distribution of OM and pigments in the hypolimnion

The sharp increase in OM and photopigments with bottom depth beneath the thermocline could not be explained by horizontal changes in lake productivity because the productivity of the water column at the center is less than at the periphery (Ostrovsky et al. 1996). Also, it cannot be explained by decomposition of organic particles settled directly because at the lake center the settled particles should be more decomposed than those at the lake periphery, as their path to the bottom is longer in the former case. In contrast, the observed changes in OM and pigment composition with depth can be attributed to the impact of particles, which were resuspended and subsequently transported horizontally toward the lake center. These organic-poor particles should dilute the newly settled planktonic OM proportionally to their relative flux to a specific location on the bottom.

Our hypothesis of translocation of particles resuspended from the WZ is schematically presented in Fig. 7. These particles may be relocated by fast-moving, seiche-induced metalimnetic jets (intrusions) pumping the mixed inshore waters towards the interior. The velocity of these jets reaches 0.5 $m \cdot s^{-1}$ in Lake Kinneret (Imberger 1998). The jet-carried heavier particles quickly settle to the bottom; therefore, the vertical flux of the resuspended material declines with distance from the WZ. On the contrary, slow-sinking particles of primarily planktonic origin can be distributed equally by metalimnetic jets all over the lake. However, these particles may also be transported slowly through the sloped turbulent BBL by complicated water motions (cf. Imberger 1994), as they can remain in the turbulent layer for a relatively longer time than in quiescent water (Reynolds 1997). Slow focusing of nonresuspended particles results in an increase in the average age of particulate OM towards the lake center.

Considering the intensity of processes responsible for spatial rearrangement of OM and pigments, two hypolimnetic bottom areas may be distinguished (Figs. 3 and 7). In the peripheral area (between the WZ and 25–31 m depth), the proportion of resuspended material sharply decreased with bottom depth and the concentration of all planktonic pigments increased relative to OM (Fig. 2). In the central area, focusing of nonresuspended particles was apparently a dominant factor, as changes in pigments and OM were concurrent. These two bottom areas observed in the hypolimnion apparently reflect segregation of slow- and fast-sinking particles by different transport mechanisms: by means of metalimnetic currents and by slow directional motions via the turbulent BBL.

It would seem that the suggested approach to tracing bottom sediment formation by photopigments is useful for understanding processes of particle dynamics and transformation. The proportion of different pigments and their degradation products is indicative of particles of different origin: active algae, senescing cells, resuspended matter, etc. We believe that ongoing multidisciplinary study of particle-specific sinking velocity, decomposition rates, and turbulent properties in the water column may help to elucidate the relationships between transport processes and the fate of particles in stratified lakes.

Acknowledgements

We thank Drs. R.G. Wetzel and D. Hamilton for their valuable comments, which greatly improved the manuscript. The authors thank Ms Roberta Galili, Dr. B. Butow, and Dr. S. Schwartz for lingual corrections and J. Easton and N. Koren for assistance in carrying out the field sampling. We are grateful for the constructive criticism of two anonymous reviewers whose suggestions improved the manuscript. This research was supported by a grant from the German–Israeli Foundation (contract No. I-0416-026.08/95) and from the GSF-Forschungszentrum fuer Umwelt und Gesundheit GmbH, Neuherberg (contract No. DISUM 00024).

References

Bergstein, T., Henis, Y., and Cavari, B.Z. 1979. Investigations on the photosynthetic sulfur bacterium *Chlorobium phaeobacteroides* causing seasonal blooms in Lake Kinneret. Can. J. Microbiol. **25**: 999–1007.

Berman, T., Stone, L., Yacobi, Y.Z., Kaplan, B., Schlichter, M., Nishri, A., and Pollingher, U. 1995. Primary production and phytoplankton in Lake Kinneret: a long term record (1972–1993). Limnol. Oceanogr. **40**: 1064–1076.

Bloesch, J. 1995. Mechanisms, measurement and importance of sediment resuspension in lakes. Mar. Freshwater Res. **46**: 295–304.

Buchanan, J.B., and Kain, J.M. 1971. Measurement of the physical and chemical environment. *In* Methods for the study of marine benthos. *Edited by* N.A. Holme and A.D. McIntyre. Blackwell Scientific Publications, Oxford and Edinborough, U.K. pp. 30–58.

Butow, B., and Bergstein-Ben Dan, T. 1992. Occurrence of *Rhodopseudomonas palustris* and *Chlorobium phaeobacteroides* blooms in Lake Kinneret. Hydrobiologia, **232**: 193–200.

Chambers, R.L., and Eadie, B.J. 1981. Nepheloid and suspended particulate matter in south-eastern Lake Michigan. Sedimentology, **28**: 439–447.

Garrett, C., and Gilbert, D. 1988. Estimates of vertical mixing by internal wave reflected off a sloping bottom. *In* Small-scale turbulence and mixing in the ocean. *Edited by* J.J. Nihoul and B.M. Jamart. Elsevier, New York pp. 405–424.

Gieskes, W.W.C., and Kraay, G.W. 1986. Floristic and physiological differences between the shallow and deep nanophytoplankton community in the euphotic zone of the open tropical Atlantic revealed by HPLC analysis of pigments. Mar. Biol. **91**: 567–576.

Gloor, M., Wuest, A., and Munnich, M. 1994. Benthic boundary mixing and resuspension induced by internal seiches. Hydrobiologia, **284**: 59–68.

Hakanson, L., and Jansson, M. 1983. Principles of lake sedimentology. Springer-Verlag, New York.

© 1999 NRC Canada

Hertzig, R., Dubinsky, Z., and Berman, T. 1981. Breakdown of *Peridinium* biomass in Lake Kinneret. *In* Developments in arid zone ecology and environmental quality. *Edited by* H. Shuval. Balaban, Philadelphia, Pa. pp. 179–185.

Hurley, J.P., and Armstrong, D.E. 1990. Fluxes and transformations of aquatic pigments in Lake Mendota, Wisconsin. Limnol. Oceanogr. **35**: 384–398.

Imberger, J. 1994. Transport processes in lakes: a review article. *In* Limnology now, a paradigm of planetary problems. *Edited by* R. Margalef. Elsevier, New York.

Imberger, J. 1998. Flux path in a stratified lake: a review. Coastal Estuarine Stud. **54**: 1–18.

Kirk, J.T.O. 1994. Light and photosynthesis in aquatic ecosystems. 2nd ed. Cambridge University Press, Cambridge, U.K.

Klein, M., and Koren, N. 1998. The influence of the thermocline on sedimentation in the deep part of Lake Kinneret, Israel. Limnologica, **28**: 293–299.

Koren, N. 1993. Sedimentation rates and particle dynamics in the northern and central part of Lake Kinneret. M.S. thesis, Haifa University, Israel.

Koren, N., and Ostrovsky, I. 1998. Sedimentation in a stratified subtropical lake. *In* Water of life. XXVII SIL Congress. Societas Internationalis Limnologiae (SIL), Dublin, Ireland. p. 294. (Abstr.)

Leavitt, P.R. 1993. A review of factors that regulate carotenoid and chlorophyll deposition and fossil pigment abundance. J. Paleolimnol. **9**: 109–127.

Lemckert, C., and Imberger, J. 1998. Turbulent benthic boundary layer mixing events in fresh water lakes. Physical processes in lakes and oceans. Coastal Estuarine Stud. **54**: 503–516.

Lerman, A., and Stiller, M. 1969. Vertical eddy diffusion in Lake Tiberias. Verh. Int. Ver. Limnol. **17**: 323–333.

Nishri, A., and Koren, N. 1993. Sediment transport in Lake Kinneret. Verh. Int. Ver. Limnol. **25**: 290–292.

Ostrovsky, I. 1998. The upper-most layer of bottom sediments: sampling and artifacts. *In* Abstracts of Kinneret Symposium: Limnology and Lake Management 2000+. Israel Oceanographic and Limnological Research, Kinneret Limnological Laboratory, Tiberias, Israel. p. 24. (Abstr.)

Ostrovsky, I., Yacobi, Y.Z., Kalikhman, Y., and Walline, P. 1996. Seiche-induced mixing: its impact on lake productivity. Limnol. Oceanogr. **41**: 323–332.

Ostrovsky, I., Wynne, D., Bergstein-Ben Dan, T., Nishri, A., Li, H., Yacobi, Y.Z., Koren, N., and Parparova, R. 1997. Spatial distributions of biogeochemical parameters in surface sediments. Air Water Soil Pollut. **99**: 497–505.

Reynolds, C.S. 1997. Vegetation processes in the pelagic: a model for ecosystem theory. Excellence in Ecology No. 9. Ecology Institute, Oldendorf/Luhe, Germany.

Rowan, K.S. 1989. Photosynthetic pigments of algae. Cambridge University Press, Cambridge, U.K.

Serruya, C. 1977. Rates of sedimentation and resuspension in Lake Kinneret. *In* Interaction between sediments and freshwater. *Edited by* H.L. Golterman. Dr. W. Junk Publishers, The Hague, The Netherlands. pp. 48–56.

Serruya, C. (*Editor*). 1978. Lake Kinneret. Dr. W. Junk Publishers, The Hague, The Netherlands.

Serruya, S. 1975. Wind, water temperature and motions in Lake Kinneret: general pattern. Verh. Int. Ver. Limnol. **19**: 73–87.

Stal, L.J., van Gemerden, H., and Krumbein, W.E. 1984. The simultaneous assay of chlorophyll and bacteriochlorophyll in natural microbial communities. J. Microbiol. Methods, **2**: 295–306.

Yacobi, Y.Z., and Ostrovsky, I. 1998. Chloropigments in Lake Kinneret bottom sediments: mechanisms of spatial distribution during holomixis. *In* Abstracts of Kinneret Symposium: Limnology and Lake Management 2000+. Israel Oceanographic and Limnological Research, Kinneret Limnological Laboratory, Tiberias, Israel. p. 35. (Abstr.)

Yacobi, Y.Z., Eckert, W., Trueper, H.G., and Berman, T. 1990. High performance liquid chromatography detection of phototrophic bacterial pigments in aquatic environments. Microb. Ecol. **19**: 127–136.

Yacobi, Y.Z., Mantoura, R.F.C., and Llewellyn, C.A. 1991. The distribution of chlorophylls, carotenoids and their breakdown products in Lake Kinneret (Israel) sediments. Freshwater Biol. **26**: 1–10.

Yacobi, Y.Z., Pollinger, U., Gonen, Y., Gerhardt, V., and Sukenik, A. 1996. HPLC analysis of phytoplankton pigments from Lake Kinneret with special reference to the bloom-formidinoflagellate *Peridinium gatunense* (Dinophyceae) and chlorophyll degradation products. J. Plankton Res. **18**: 1781–1796.

© 1999 NRC Canada

Responses of rainbow trout (*Oncorhynchus mykiss*) and their prey to inorganic fertilization of an oligotrophic montane lake

N.T. Johnston, M.D. Stamford, K.I. Ashley, and K. Tsumura

Abstract: We used two montane lakes (4.5 and 7.8 ha) in a before–after control–impact pair experimental design to measure the responses of rainbow trout (*Oncorhynchus mykiss*) and their prey to 5 years of inorganic phosphorus and nitrogen (liquid ammonium polyphosphate and urea ammonium nitrate) additions. Epilimnetic total phosphorus (TP) concentration, euphotic zone chlorophyll *a* concentration, limnetic macrozooplankton biomass, and annual trout yield increased significantly in the fertilized lake. Chlorophyll *a* concentration and zooplankton biomass varied directly with epilimnetic TP. Trout yield varied as $TP^{0.5}$. Fertilization increased trout reproductive output, growth, and yield but did not alter yearling survival or the mean age of mature fish. Prey utilization by trout did not change. $\delta^{13}C$ data indicated that trout in the fertilized lake obtained 65% of their body carbon from benthic insects and 35% from zooplankton. Increased biomass of *Hesperodiaptomus* accounted for most of the zooplankton response. Benthic insect emergence decreased with increasing water depth but was greater at a given depth in the fertilized lake. Resources accounted for smaller proportions of the variance of consumer biomass with increasing trophic level.

Résumé : Dans deux lacs de montagne (4,5 et 7,8 ha), nous avons appliqué un plan d'expérience avant–après avec groupe contrôle pour mesurer les réponses de la truite arc-en-ciel (*Oncorhynchus mykiss*) et de ses proies à des ajouts de phosphore et d'azote inorganiques (polyphosphate d'ammonium liquide et nitrate d'ammonium d'urée) effectués durant 5 ans. La concentration de phosphore total (PT) épilimnétique, la concentration de chlorophylle *a* dans la zone euphotique, la biomasse de macrozooplancton limnétique et la production annuelle de truite se sont accrues significativement dans le lac fertilisé. La concentration de chlorophylle *a* et la biomasse de zooplancton ont varié en raison directe du PT épilimnétique. La production de truite a varié en fonction de $PT^{0.5}$. La fertilisation a accru le taux de reproduction, la croissance et la production des truites, mais n'a pas modifié le taux de survie des jeunes de l'année ni l'âge moyen des poissons matures. L'utilisation des proies par la truite n'a pas changé. Les données de $\delta^{13}C$ ont montré que la truite du lac fertilisé tirait 65% de son carbone corporel des insectes benthiques et 35% du zooplancton. L'accroissement de la biomasse de zooplancton était attribuable pour la plus grande part à *Hesperodiaptomus*. On a observé une baisse de l'émergence des insectes benthiques à mesure que l'eau devenait plus profonde, mais l'émergence augmentait à une profondeur donnée dans le lac fertilisé. Plus le niveau trophique était élevé, plus les proportions de la variance de la biomasse des consommateurs attribuables aux ressources étaient petites.

[Traduit par la Rédaction]

Introduction

The use of lake fertilization as a fishery management tool requires an understanding of the effects of increased productivity on the equilibrium biomass at different trophic levels in lacustrine food webs and the mechanisms responsible for observed biomass patterns. Although the productivity of lakes is largely controlled by inputs of phosphorus (Schindler 1978), empirical relationships between total phosphorus (TP) and measures of fish production (Plante and Downing 1993), fish biomass (Stockner 1987), or fish yield (Hanson and Leggett 1982) show considerable variability at a given TP value. Some of the variability results from differences in food web structure, which alter trophic dynamics and nutrient cycling (Carpenter et al. 1985). Patterns of biomass may depend on the relative influence of resources ("bottom-up" controls) and predation ("top-down" controls) in regulating animal abundance and on the constraints imposed by the stoichiometry of organisms (Andersen and Hessen 1991).

The relative importance of bottom-up and top-down controls depends partly on the efficiency with which predators exploit prey (Power 1992) and its effect on nutrient dynamics. Food chain models based on prey-dependent trophic interactions (top-down models) predict (*i*) that increasing productivity will always increase the biomass of the top predator, but that the biomass of intermediate trophic levels may increase, decrease, or remain unchanged depending on the number of trophic levels in the food chain (Oksanen et al. 1981; Ginzburg and Akçakaya 1992). Ratio-dependent

Received May 26, 1998. Accepted January 27, 1999.
J14601

N.T. Johnston,[1] M.D. Stamford,[2] K.I. Ashley, and K. Tsumura. British Columbia Ministry of Fisheries, 2204 Main Mall, University of British Columbia, Vancouver, BC V6T 1Z4, Canada.

[1]Author to whom all correspondence should be addressed. e-mail: tom.johnston@gems3.gov.bc.ca
[2]Present address: Department of Zoology, 6270 University Boulevard, University of British Columbia, Vancouver, BC V6T 1Z4, Canada.

© 1999 NRC Canada

Table 1. Physical and chemical characteristics of WTL and ETL.

Characteristic	WTL	ETL
Elevation (m)	500	460
Watershed area (ha)	50	105
Surface area (ha)	7.7	4.5
Mean depth (m)	12.5	2.9
Maximum depth (m)	34	11
Littoral area (%)	25	90
Shoreline development	1.41	1.97
pH	6.3	6.1
conductivity ($\mu S \cdot cm^{-1}$)	11	10
TP ($\mu g\ P \cdot L^{-1}$)	4.0	4.6
TN ($mg\ N \cdot L^{-1}$)	0.162	0.175
TC ($mg\ C \cdot L^{-1}$)	3.6	4.6
Alkalinity ($mg\ CaCO_3 \cdot L^{-1}$)	3.6	3.4

Note: Water chemistry data are epilimnetic geometric means over the prefertilization (1982–1989) period.

(bottom-up) models of trophic interactions (Ginzburg and Akçakaya 1992) predict (*ii*) that increased productivity will increase biomass at all trophic levels proportionately. Trophic cascades (Carpenter et al. 1985) provide strong evidence for top-down controls, while positive correlations between consumers and resources imply bottom-up regulation (McQueen et al. 1986).

A strict dichotomy between bottom-up and top-down controls is artificial, however: both operate in aquatic ecosystems (McQueen et al. 1986; Power 1992). McQueen et al. (1986) attempted an empirical synthesis of bottom-up and top-down regulation that makes a number of specific predictions: (*iii*) that the maximum biomass at each trophic level is controlled from below by nutrient availability, (*iv*) that both bottom-up and top-down effects attenuate quickly in propagating along food chains, (*v*) that the variability around bottom-up regressions can be explained by top-down effects, and (*vi*) that the relative importance of top-down effects increases in oligotrophic systems. Some observational data fit the bottom-up/top-down model (McQueen et al. 1989), but it and other models have rarely been tested by whole-ecosystem experiments. Lake fertilization experiments position whole ecosystems along productivity gradients and permit direct tests of the predictions of competing models of trophic structure.

Most fertilization studies implicitly assume bottom-up control of trophic structure, despite variable fish responses and despite the expectation that increased productivity will alter size-dependent interactions between individuals that determine survival and growth to establish a new equilibrium between nutrient supply and fish biomass. Based on previous studies, fertilization is predicted to alter fish feeding, growth, survival, fecundity, abundance, biomass, and production (Mills 1985; Mills and Chalanchuk 1987).

This study documents the responses of lacustrine rainbow trout (*Oncorhynchus mykiss*) and their prey to 5 years of increased nutrient loading. Our aims were to test the predictive relationships between productivity (nutrient concentration) and trophic-level biomass patterns listed above and to identify the changes in fish population parameters responsible for increased biomass. We monitored trout growth, reproductive allocation, recruitment to age 1, survival, abundance, and yield. We also monitored prey biomass and its utilization by the trout.

Methods

Study site

Twin Lakes are a pair of headwater lakes located in the Coast Mountains at 49°21′N, 122°15′W, about 24 km north of Mission, B.C. The small watersheds are underlain by quartz diorite bedrock that is exposed on steep hills north and south of the lakes. The surficial sediments are moderately coarse-textured glacial till and colluvium. The area has high precipitation, with mild wet winters and mild dry summers. Mean precipitation at elevations similar to Twin Lakes is above 2000 $mm \cdot year^{-1}$, occurring as rain and snow mostly between October and March. The lakes are small and oligotrophic (Table 1). They are usually ice covered from mid-December to early March. The lakes become thermally stratified soon after ice-off and remain stratified until turnover in early November. Maximum surface temperature was about 24°C. Nutrient concentrations in the two lakes were low and very similar (Table 1), but their bathymetries differed considerably. Ninety percent of the area of East Twin Lake (ETL) is littoral (depth less than 6 m), whereas only 25% of the area of West Twin Lake (WTL) is littoral. ETL receives the outflow from WTL, which has no permanent inflow. A high chute prevented the upstream movement of fish and restricted the downstream movement of marked fish from WTL to ETL to an average of $1.9\% \cdot year^{-1}$. Annual fluctuations in water levels are about 0.2–0.5 m. The lakes were without fish prior to 1982. The watersheds were logged in 1968–1969 and are regenerating with western hemlock (*Tsuga heterophylla*), amabilis fir (*Abies amabilis*), and Douglas-fir (*Pseudotsuga menziesii*). WTL has a narrow shoreline fringe of willows (*Salix* spp.) and *Vaccinium* spp., while ETL has a marshy fringe of *Sphagnum* and sedges (*Carex* spp.) as well as sparse submerged littoral macrophytes.

Experimental design and statistical procedures

We used a before–after control–impact pair (BACIP) design (Stewart-Oaten et al. 1986) to test for fertilization treatment effects (control versus the average of all fertilization treatments) and linear regression analysis to test for significant responses (slope $\neq 0$) to incremental increases in nutrient loading. We compared the mean differences between paired measurements in the control (WTL) and fertilized (ETL) lakes within the prefertilization (1982–1989) and fertilized (1990–1994) time periods with a one-tailed t test or with Tukey's HSD test following one-way ANOVA if we also had postfertilization (1995–1996) data for the variable. Years were considered to be replicates within treatment periods. We used $\log_{10}$-transformed data in our analyses to linearize relationships and stabilize variances for response variables. The transformed response variable, x, thus becomes the difference $\log_{10}(x_{\text{experimental lake}}) - \log_{10}(x_{\text{control lake}})$ in the BACIP design. Note that this is equivalent to $\log_{10}(x_{\text{experimental lake}}/x_{\text{control lake}})$. Survival and diet proportion data were arcsine square-root transformed. Statements about fertilization treatment effects refer to significant changes ($p < 0.05$) in the mean differences in transformed variables between nontreated and fertilized time periods. We estimated the magnitudes of treatment effects by back-transforming the change in mean differences in transformed response variables. We confirmed the additivity and independence assumptions of the BACIP analyses using Tukey's single degree of freedom test for nonadditivity and von Neumann's ratio test (Stewart-Oaten et al. 1986). In all cases, successive samples of differences within treatment periods were independent ($p > 0.05$) and, except for TP, effects were additive ($p > 0.05$). Additivity implies constancy of differences in the response variable and indicates that the control and treatment lakes responded similarly to background variation despite differences in lake

© 1999 NRC Canada

Table 2. Size and number of stocked rainbow trout and the effective density of all trout in ETL and WTL prior to, during, and after nutrient additions to ETL.

		ETL			WTL		
Year	Date stocked	Number	Mean weight (g)	Effective density (10^4 cm^2·ha^{-1})	Number	Mean weight (g)	Effective density (10^4 cm^2·ha^{-1})
				Prefertilization			
1982	5 Oct.	450	3.2	1.032	800	3.2	0.599
1983	8 Sept.	450	2.0	1.508	800	2.0	1.235
1984	28 May	225	10.9	1.475	400	10.9	1.152
1985	16 May	400	17.2	2.062	225	13.4	0.862
1986	15 May	225	38.5	2.393	400	38.5	1.466
1987	24 Apr.	400	10.4	2.084	225	10.4	0.773
1988	9 May	225	19.1	2.629	400	17.8	0.996
1989	9 May	400	9.7	2.162	225	9.6	0.875
				Fertilization			
1990	4 May	225	12.7	2.195	400	13.9	1.170
1991	6 May	400	11.2	3.017	225	11.4	0.796
1992	21 Apr.	225	14.0	2.334	400	14.5	0.940
1993	1 May	400	18.7	2.281	225	18.0	0.818
1994	28 Apr.	225	14.6	1.260	400	16.7	0.833
				Postfertilization			
1995	27 Apr.	400	16.2	1.277	225	15.9	0.502

Note: The effective density is ΣFL^2 for all fish known to be present in the lake at the time of stocking divided by the lake area in hectares.

morphometry. The nonadditivity of TP ($p = 0.046$) is probably incorrect because it results from the influence of a single poorly estimated point (WTL in 1989 when many TP values were below the detection limit). We tested relationships among variables with Pearson correlation coefficients, using Bonferroni-adjusted probabilities to maintain nominal α values. All statistical analyses were done with SYSTAT (Wilkinson and Hill 1994).

Fertilization treatment

We fertilized ETL from 1990 to 1994 using agricultural-grade liquid fertilizer (ammonium polyphosphate and urea ammonium nitrate mixture) with an 8.5:1 nitrogen to phosphorus atomic ratio, applied in four equal loadings at 4-week intervals between mid-May and mid-August. We sprayed a 1:1 (v/v) solution of fertilizer and lake water onto the lake surface from a single shoreline site using a portable pump and allowed wind-driven circulation to disperse the fertilizer. Circulation studies on WTL indicated that point-source application of the fertilizer would result in a rapid dispersion of the material throughout the epilimnion (Lawrence et al. 1995). We used a loading rate of 600 mg P·m^{-2}·year^{-1} in 1990 and 1991, 450 mg P·m^{-2}·year^{-1} in 1992 and 1993, and 100 mg P·m^{-2}·year^{-1} in 1994 to quantify responses as a function of phosphorus loading. The loadings spanned those used in other well-documented fertilization studies (about 100–500 mg P·m^{-2}·year^{-1}: Davies 1980; Reinertsen and Langeland 1982; Hyatt and Stockner 1985). WTL remained as an untreated control.

Two unplanned perturbations occurred during the experiment. In 1990, silvicultural thinning felled about 80% of the juvenile conifers upslope of a 100-m buffer strip around each lake. From late summer 1989 onward, both lakes were repeatedly colonized by beavers (*Castor canadensis*). Although the registered trapline owner usually removed the beavers each winter, beaver dams on the outlet streams increased summer lake levels by about 0.2 m. We believe that the thinning had no significant impact on the experiment because (*i*) the experimental design will remove perturbations that affect both lakes proportionately, (*ii*) fertilization greatly exceeded the changes in the nutrient inputs expected from silvicultural felling that left the stems in place and did not disturb the ground, and (*iii*) effects are not discernible in the control lake. For similar reasons, we believe that the intermittent occurrence of beavers had little impact on nutrient dynamics. The slight elevation in summer lake levels was well within annual fluctuations. Beaver dams did, however, influence spawning conditions in both lakes and are likely responsible for declines in the recruitment of wild fish after 1993 (see below).

Trout growth, survival, and yield

We measured fish growth, survival, and yield by stocking known numbers of marked age-0$^+$ (1982 and 1983) or age-1 (1984–1996) rainbow trout and attempting to remove the entire population at age 2 by standardized gillnetting the following spring. Table 2 gives the numbers and sizes stocked. All stocked fish were the F_1 progeny of wild parents. Although several parent stocks were used, all are from common ancestral stocks. The densities of fish stocked (30–90 fish·ha^{-1}) produced similar growth conditions in both lakes (18- to 20-cm fork length (FL) fish at age 2 in the unfertilized condition). Because interannual variation in the recruitment of wild fish may confound density effects with fertilization impacts, we varied stocking densities over a twofold range in alternate years (Table 2) to allow density effects on growth to be removed statistically (see below). We marked stocked fish with unique combinations of fin or maxilla ablation so that each cohort was identifiable by year and lake of stocking.

We estimated yield (kilograms per hectare per year) as the total wet weight of fish removed in standard gillnetting each spring from 1984 onward, prior to annual restocking. The mean interval between stocking and removal was 354 days (±3 days, $N = 11$) for yearling trout. We fished gangs of floating gill nets (each net 15.2 m long by 2.4, 4.9, or 7.6 m deep; 19-, 25-, 38-, 51-, 64-, 76-, 83-, or 102-mm stretched mesh) at fixed locations for five or six consecutive nights. Mean annual efforts were 41 net-nights·ha^{-1} in ETL and 38 net-nights·ha^{-1} in WTL, with the 38-, 51-, and 64-mm

© 1999 NRC Canada

mesh sizes accounting for about 80% of the fishing effort. Based on subsequent recoveries of known-age fish, we removed an average of 78% (±2%, $N = 22$) of the age-2 and older fish each spring. Because we removed most fish, catches in either lake typically approached an asymptote after three or four nights of fishing so that slight differences in effort have no meaningful effect on our total catches. We determined FL, wet weight, sex, maturity, and age for all fish. Mature males had enlarged testes and discharged milt under gentle pressure. Mature females had enlarged ovaries with fully developed eggs. In 1993 and 1994, we also weighed the ovaries of gravid female trout. Stocked fish were aged from their marks, while wild fish, which appeared from 1985 onward, were aged from annuli on plastic impressions of their scales at 30× magnification. In 1987, 1993, and 1994, we removed 9–15 fish during the summer for diet studies; the biomass of these removals was added to that of the following spring removal to estimate yield.

We estimated the minimum number of individuals from a given cohort of same-aged stocked or wild fish that were known to be alive at any time (MKA) as the cumulative catch of the group from that time onward. We estimated the survival to age 2 of a cohort of stocked yearling trout as the ratio of the MKA at age 2 to the number stocked.

We calculated the $(\Sigma_i \mathrm{FL}_i^2) \cdot \mathrm{ha}^{-1}$ for all fish known to be present after the spring stocking as an index of effective density. Effective density is a descriptor of the total consumptive pressure exerted by a size-structured population on its prey. Walters and Post (1993) calculated that the biomass of a prey population at equilibrium is inversely proportional to the predator's effective density and that the predator's growth is directly proportional to their prey's density. Post et al. (1999) showed that the proportion of the total variance in the growth of experimental rainbow trout populations explained by effective density was consistently higher than that explained by either numerical density or biomass. Thus, effective density is a good theoretical and empirical measure of density-mediated impacts on the growth of fish. We determined the effective density each spring from measurements of FL for the individual newly stocked fish and from the MKA and mean FL for each cohort of stocked or wild fish present at the time of stocking. Mean FL was estimated from the removal netting that immediately preceded stocking.

We compared the average effect of fertilization on trout growth in ETL against the control lake (WTL) and against ETL prior to fertilization by ANCOVA using the model

$$\log_e(W_{j,t+1}) = \mu + G_k + \beta_1 \times \log_e(W_{j,t})$$

to adjust for differences in initial size, where $W_{j,t}$ is the mean weight of a fish in cohort j in year t and G_k is the growth effect for the treatment k. The regression model is obtained by expressing the annual increment in weight between year t and year $t+1$ for a cohort as $W_{j,t+1} = W_{j,t} \times e^G$, where G is an annual growth rate, whence $\log_e(W_{j,t+1}) = \log_e(W_{j,t}) + G$. We estimated mean weights from successive spring removals for cohorts of stocked or wild trout where at least five fish were caught.

We expect G to be a function of lake productivity, fish density, and fish size. We tested the incremental impacts of fertilization on annual fish growth ($\beta_2 \neq 0$) in ETL using the regression model

$$\log_e(W_{j,t+1}) = \alpha + \beta_1 \times \log_e(W_{j,t}) + \beta_2 \times \log_e(\mathrm{TP}_t) + \beta_3 \times \mathrm{DENS}_t$$

to control for differences in fish size and density, where TP_t is the summer mean epilimnial TP concentration during year t and DENS_t is the effective fish density in the lake at the time of stocking in year t. By analogy with other nutrient–productivity relationships, we assumed that fish weight varies as a power function of TP. The specific growth rates of rainbow trout decline linearly with effective density (Post et al. 1999).

Prey abundance and trout feeding

We estimated the abundance of macrozooplankton at monthly (1987) or biweekly (1988–1995) intervals from spring to late fall by taking two (1987 and 1988) or three (1989 onward) vertical hauls over the entire water column at the deepest part of each lake using a 25-cm-diameter Wisconsin net with a 153-μm mesh size. Samples were preserved in 5% sugared formalin. We enumerated macrozooplankton by species and life stage from subsamples of known volume and measured body sizes with an ocular micrometer for up to 30 individuals of each life stage. Life stages for copepods were nauplii, copepodites, adult females, and adult males. Life stages for cladocerans were juveniles and adults. We determined total macrozooplankton biomass by halving the preserved samples with a Folsom plankton splitter, repeatedly rinsing the material with distilled water, drying overnight at 60°C, and weighing to the nearest microgram on an electrobalance. We estimated the biomass of individual species from the counts and length measurements using body length – dry weight regressions (Marmorek 1983). Biomass estimated by drying formalin-preserved samples was linearly related to that estimated from the size and abundance data ($r = 0.92$, $N = 16$, $p < 0.001$) but was generally lower.

We estimated the abundance of benthic insects by collecting emerging adults with floating traps (modified from LeSage and Harrison 1979) from mid-March to late October from 1992 to 1995. Each trap sampled 0.25 m^2. We used 14–16 traps per lake set in two (WTL) or three (ETL) transects stratified by depth so that the number of traps per depth interval was proportional to the surface area of the depth stratum. We removed emerging insects at 7-day intervals and preserved them in 80% isopropanol. We identified and counted Diptera to family and other insects to order. We estimated the biomass of each taxon emerging from each depth for the spring (March–May), summer (June–August), and fall (September–October) periods by pooling samples, rinsing the preserved insects with distilled water, drying overnight at 60°C, and weighing to the nearest milligram.

We determined prey use by trout by examining their stomach contents and by stable isotope analysis. We removed small numbers of trout from each lake at monthly intervals from April to September in 1993 and 1994 by gillnetting for 3–6 h during midday. We also used fish from our spring removal netting. We weighed and measured fish as above and then removed and preserved the stomach anterior to the pyloric sphincter in 5% formalin. We removed prey items, separated them by taxon, and rinsed them in distilled water. We then damp-dried and weighed them to the nearest milligram. We calculated mean proportions of prey taxa by weight for spring (April and May), summer (June–August), and fall (September) samples from arcsine square-root transformed data. We compared diet proportions between lakes and seasons with Pearson correlation coefficients.

We collected samples of prey organisms for stable isotope analysis from ETL at various times throughout the summers of 1992–1994. We obtained live adult insects from additional emergence traps. The insects were sorted to taxon, frozen in prerinsed glass vials, freeze-dried, and pulverized. We obtained live zooplankton from Wisconsin net hauls. The zooplankton were held overnight, sorted to species, rinsed with distilled water, and then freeze-dried and pulverized as above. Each insect or zooplankton sample comprised several to many individuals to obtain sufficient mass. We analyzed muscle tissue from 10 individual wild-origin trout (FL = 102–341 mm) from each lake caught in our 1993 spring removal netting. Fish muscle was excised from the dorsolateral portion of the left side, freeze-dried, and pulverized. The $\delta^{13}C$ and $\delta^{15}N$ values were measured at the Stable Isotope Laboratory of the Department of Earth and Ocean Sciences, University of British Columbia,

© 1999 NRC Canada

using a Prism series I triple-collector mass spectrometer (VG Isotech, Cheshire, U.K.) coupled to an NA 1500 CN analyzer. The $\delta^{15}N$ values are reported with respect to air. $\delta^{13}C$ is reported with respect to the Vienna Peedee belemnite standard. We used a two-member mixing equation (Junger and Planas 1994) to estimate the proportions of trout carbon originating from benthic and planktonic prey.

Limnology

We collected water samples for chemical analyses at irregular (1982–1985), monthly (1986, 1987, and 1996), or biweekly (1988–1995) intervals between April and November. Samples were collected at the deepest point in the lake. Epilimnetic samples were taken at a depth of 0.5 m by emersing a rinsed 2-L polyethylene bottle or a 0.25-L acid-washed glass bottle. Integrated water samples for chlorophyll *a* (Chl *a*) analyses were collected from the surface to twice the Secchi transparency depth using a 2.5-cm-diameter tube sampler. Water samples were held on ice in opaque coolers in the field, refrigerated within 6 h of collection, and processed within 24 h. All chemical analyses were done by the Environmental Laboratory, British Columbia Ministry of Environment, or its contractors and followed procedures listed in APHA (1980). Soluble reactive phosphorus (SRP) and TP were determined by the automated ascorbic acid method and nitrate nitrogen by the cadmium reduction method. Chl *a* was determined spectrophotometrically after dark acetone extraction.

We determined average spring–summer nutrient concentrations as geometric means from May to September. Where the data were left-censored, we used the maximum-likelihood method of El-Shaarawi and Dolan (1989) to estimate the geometric mean.

Results

Epilimnetic TP increased greatly in ETL during the period of fertilization (Fig. 1*a*), but dissolved inorganic nitrogen (DIN) decreased slightly and total nitrogen (TN) did not change significantly (Fig. 1*b*). SRP was generally undetectable except in ETL during fertilization where it averaged 1.1 (±0.2) $\mu g\ P \cdot L^{-1}$ for the 3 years for which mean concentrations could be estimated. TP in ETL varied directly with the fertilizer phosphorus loading (milligrams per square metre) as

$$TP = 4.69 + 0.0082 \times \text{fertilizer load}$$

$$(r^2 = 0.66,\ N = 12,\ p = 0.001).$$

Mean TP in ETL increased from 4.6 $\mu g\ P \cdot L^{-1}$ prefertilization to 8.7 $\mu g\ P \cdot L^{-1}$ during fertilization, while mean TP in the control lake varied little, from 4.0 $\mu g\ P \cdot L^{-1}$ prefertilization to 3.0 $\mu g\ P \cdot L^{-1}$ during the fertilization period. After fertilization was terminated, TP in ETL declined to 3.7 $\mu g\ P \cdot L^{-1}$, while TP in WTL averaged 2.4 $\mu g\ P \cdot L^{-1}$. Mean epilimnetic TN concentrations averaged 188 $\mu g\ N \cdot L^{-1}$ in ETL and 173 $\mu g\ N \cdot L^{-1}$ in WTL. DIN averaged 29 $\mu g\ N \cdot L^{-1}$ in ETL and 61 $\mu g\ N \cdot L^{-1}$ in WTL before fertilization and 21 and 79 $\mu g\ N \cdot L^{-1}$, respectively, during fertilization. TN:TP atomic ratios did not vary among treatment periods and averaged 74 (±6) in ETL and 123 (±14) in WTL.

Fertilization increased the euphotic zone Chl *a* concentration and the effect persisted at a lower level into the post-fertilization period (Fig. 1*c*). C• *a* in ETL increased from a mean of 1.3 $\mu g \cdot L^{-1}$ prefertilization to 6.4 $\mu g \cdot L^{-1}$ during the fertilization period and declined to 3.2 $\mu g \cdot L^{-1}$ post-fertilization, while levels in WTL remained low, at values between 0.9 and 2.2 $\mu g \cdot L^{-1}$.

The lakes had simple limnetic zooplankton communities whose prefertilization summer mean biomasses were dominated by the cladoceran *Holopedium gibberum* and the large calanoid copepod *Hesperodiaptomus kenai*. Fertilization increased the mean summer zooplankton biomass from about 0.3 to 1.5 $g \cdot m^{-2}$ with the response starting during the first summer of fertilization (Fig. 1*d*). The fertilization effect largely resulted from increased mean summer biomass of *H. kenai* and *Chaoborus* larvae (Fig. 2). The biomass of *Daphnia rosea* increased in ETL during the fertilization period, but this increase cannot be attributed directly to the fertilization treatment ($p = 0.41$) because *Daphnia* biomass in the control lake also increased (Fig. 2*b*). The smaller calanoid copepod *Leptodiaptomus tyrrelli*, which occurred only in ETL, also increased ($p = 0.003$) but was a minor component of the total biomass. Neither *D. rosea* biomass nor *H. kenai* biomass was positively correlated with mean summer Chl *a* concentration ($r = 0.65$, $N = 9$, $p_{Bonf} = 0.36$ for *D. rosea*; $r = 0.63$, $N = 9$, $p = 0.40$ for *H. kenai*).

Aquatic insect emergence during the last 3 years of the fertilization treatment averaged 5.67 (±0.92) $g \cdot m^{-2} \cdot year^{-1}$ in ETL and 0.84 (±0.09) $g \cdot m^{-2} \cdot year^{-1}$ in WTL (Fig. 1*e*). Chironomids, caddisflies, and damselflies accounted for nearly all the insect emergence and emerged at similar mean annual rates within each lake (ANOVA, $p > 0.30$) (Fig. 3), although damselfly emergence in ETL increased continuously with time ($r = 0.97$, $N = 4$, $p = 0.029$). Emergence was strongly seasonal. Chironomids emerged throughout the ice-free period but were largely concentrated into emergence peaks in early spring and midsummer, while caddisfly and damselfly emergence occurred primarily during the summer (Fig. 3). The large difference in annual emergence between the two lakes reflected differences in lake bathymetry as well as differences in productivity. Areal annual emergence declined with depth to about 10 m and was approximately constant at depths below 10 m (Fig. 4). The rate of decrease with depth was significantly less in ETL than in WTL (ANCOVA, $p_{slopes} = 0.001$). At corresponding depths, emergence was three- to four-fold greater in the fertilized lake than in the control lake.

Fertilization increased the mean yield of rainbow trout in ETL ($p = 0.024$) from 6.8 to 11.8 $kg \cdot ha^{-1} \cdot year^{-1}$ (Fig. 1*f*). Trout yield in the control lake remained unchanged at 2.8 $kg \cdot ha^{-1} \cdot year^{-1}$. Fertilization did not alter the number of fish caught ($p = 0.125$). The mean annual catch was 281 (±30) fish from ETL and 208 (±19) fish from WTL. The catch was about 55% stocked fish and 45% wild fish from both lakes during the period of fertilization. Age-2 fish comprised an average of 70% (range = 52–91%) of the yearly catches and age-3 fish comprised about 25% (range = 5–45%).

The increases in biomass that were attributable to the nutrient additions were roughly similar at all trophic levels in ETL. Average epilimnetic TP increased 2.3-fold, Chl *a* increased 2.2-fold, summer zooplankton biomass increased 3.6-fold, and trout yield increased 1.6-fold.

Mean TP concentration accounted for much of the variation in mean Chl *a* in ETL for the data from 1989 to 1996 (Fig. 5*a*). The predictive regression was

© 1999 NRC Canada

Fig. 1. Mean values of response variables in the control (WTL, triangles) and treatment (ETL, circles) lakes during nonfertilized (grey) and fertilized (black) periods. Summer average epilimnetic concentrations of (*a*) TP, (*b*) DIN (lower pair of lines) and TN (upper pair of lines), (*c*) Chl *a*, (*d*) macrozooplankton biomass, (*e*) annual insect emergence, and (*f*) annual fish yield. Fish yields are reported by year of treatment but were measured in the spring of the year following a given treatment.

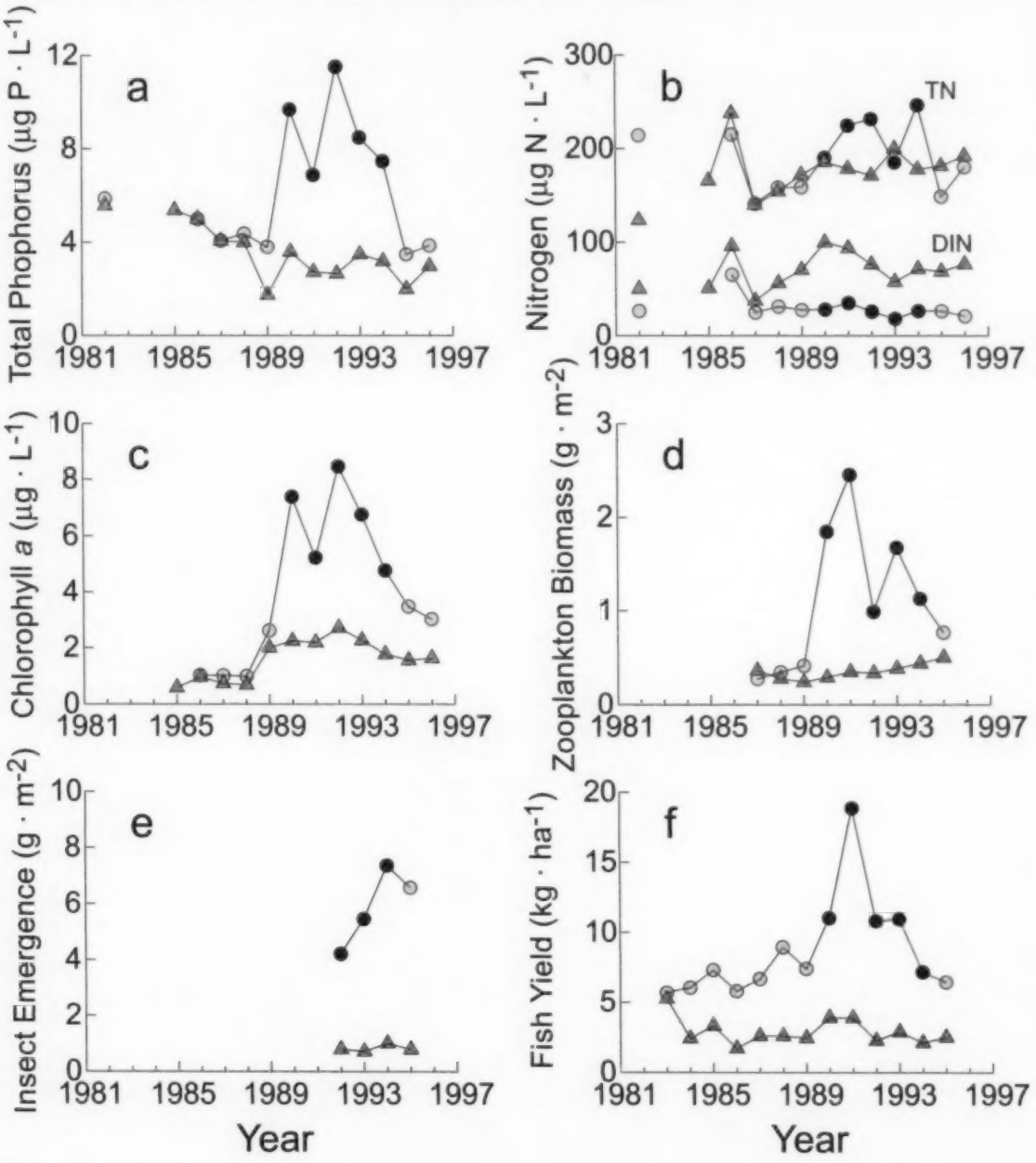

$$\log_{10}(\text{Chl } a) = -0.031 + 0.894\ (\pm 0.105) \times \log_{10}(\text{TP})$$

$$(r^2 = 0.92,\ N = 8,\ p < 0.001).$$

Chl *a* data for 1986–1988 fall well below this line and have been excluded from the regression because (*i*) the individual points are statistical outliers (studentized residuals from –7.9 to –9.5) and (*ii*) another measure of mean algal biomass, the Secchi transparency, shows a significant regression with TP ($r^2 = 0.75$, $N = 11$, $p < 0.001$) in which the 1986–1988 data fit the overall relationship, which suggests that Chl *a* was a poor estimator of algal biomass during the 1986–1988 pe-

© 1999 NRC Canada

Fig. 2. Mean (±SE) summer biomass of the dominant limnetic macrozooplankters in ETL (open bars) and WTL (black bars) (*a*) before (1987–1989) and (*b*) during (1990–1994) inorganic fertilization. BL, *Bosmina longirostris*; CH, *Chaoborus* sp.; DB, *Diaphanosoma brachyurum*; DR, *Daphnia rosea*; HG, *Holopedium gibberum*; HK, *Hesperodiaptomus kenai*.

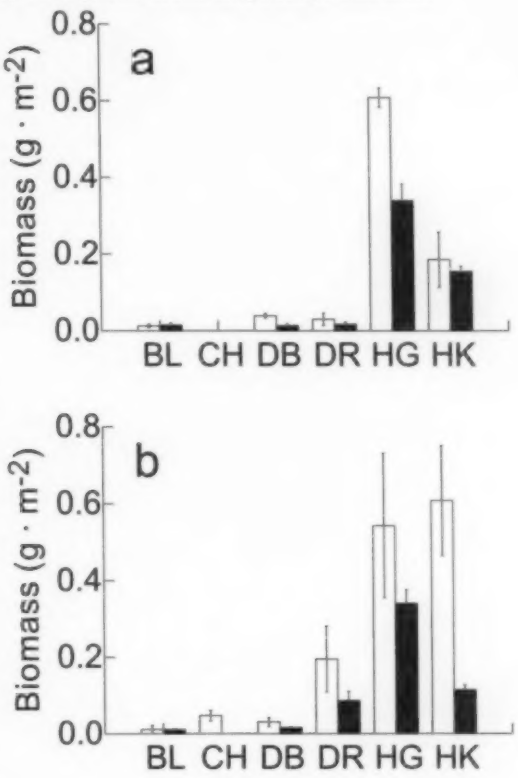

Fig. 3. Seasonal and annual mean (±SE) emergence of aquatic insects from (*a*) the control lake and (*b*) the fertilized lake during the last 3 years of fertilization, 1992–1994. Hatched bars, chironomids; black bars, caddisflies; open bars, damselflies; cross-hatched bars, other insects.

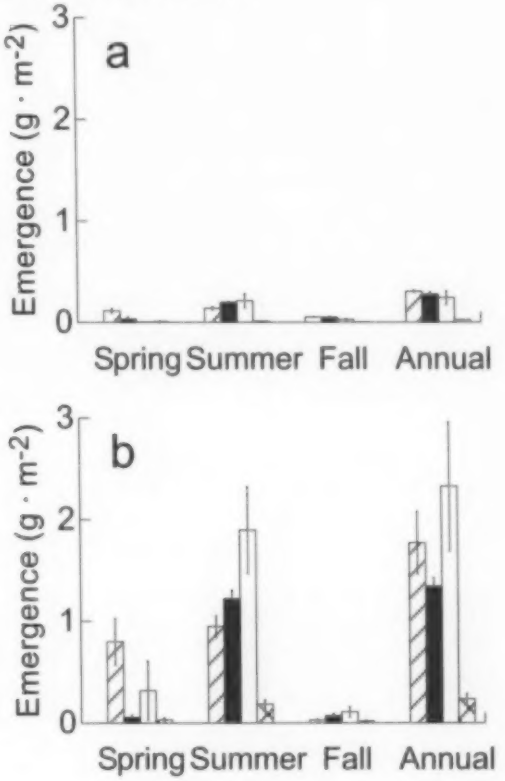

riod. If we use the relationship between Secchi depth and Chl *a* from 1989 onward to adjust the observed Chl *a* data for 1986–1988 (Fig. 5*a*), the predictive regression becomes

$$\log_{10}(\text{Chl } a) = -0.103 + 0.953\ (\pm 0.169) \times \log_{10}(\text{TP})$$
$$(r^2 = 0.78,\ N = 11,\ p < 0.001).$$

One third to one half of the interannual variation in the quantity of zooplankton and fish in the fertilized lake could be directly attributed to TP (Figs. 5*b* and 5*c*). The regressions of zooplankton biomass and fish yield on TP for ETL were

$$\log_{10}(\text{zooplankton}) = -1.049 + 1.256\ (\pm 0.455)$$
$$\times \log_{10}(\text{TP})\ (r^2 = 0.52,\ N = 9,\ p = 0.028).$$
$$\log_{10}(\text{fish yield}) = 0.546 + 0.496\ (\pm 0.250) \times \log_{10}(\text{TP})$$
$$(r^2 = 0.31,\ N = 11,\ p = 0.078).$$

Chl *a* was a good predictor of zooplankton biomass in ETL, and zooplankton biomass was a good predictor of fish yield from ETL:

$$\log_{10}(\text{zooplankton}) = -0.927 + 1.304\ (\pm 0.253)$$
$$\times \log_{10}(\text{Chl } a)\ (r^2 = 0.56,\ N = 9,\ p = 0.022).$$
$$\log_{10}(\text{fish yield}) = 0.988 + 0.318\ (\pm 0.115)$$
$$\times \log_{10}(\text{zooplankton})\ (r^2 = 0.52,\ N = 9,\ p = 0.028).$$

Insect emergence in ETL did not vary with epilimnetic Chl *a* concentration ($r = 0.84$, $N = 4$, $p = 0.156$), nor did fish yield vary with insect emergence ($r = 0.83$, $N = 4$, $p = 0.167$). Resources accounted for successively smaller variance proportions of consumers as one proceeded up the pelagic food web. The proportion of the variance of the various consumer trophic levels that was attributable to TP declined, moving from Chl *a* to zooplankton to fish (Fig. 5), and was always less than that attributable to the resource that was directly consumed.

Analogous regressions for the control lake (TP range = 3.8 μg $P \cdot L^{-1}$) were all nonsignificant ($p > 0.05$); however, extrapolations of the TP – Chl *a* and Chl *a* – zooplankton relationships for ETL encompass the WTL data.

Zooplankton biomass did not explain a significant proportion of the variation in the residuals from the TP – Chl *a* re-

© 1999 NRC Canada

Fig. 4. Depth dependence of insect emergence in the fertilized (black circles) and control (grey triangles) lakes during 1992–1995. The lines are the linear regression fits at depths above 10 m.

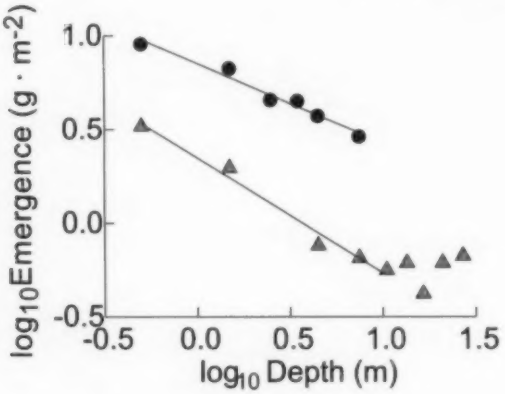

lationship (r = 0.13, N = 9, p = 0.75), nor did fish yield account for the residual variation in the Chl *a* – zooplankton relationship (r = 0.50, N = 9, p = 0.17).

The mean size of rainbow trout, adjusted for initial size 1 year earlier, increased in ETL during the fertilization period compared with WTL or to ETL prior to fertilization (Fig. 6, p_{slopes} = 0.21, $p_{intercepts}$ < 0.001). The average effect of fertilization was a 1.8-fold increase in the annual weight increment. Annual growth rates for 10-g fish increased from about 2.0 to about 2.6·year^{-1}, while those of 100-g fish increased from about 0.50 to 1.05·year^{-1}. Initial fish size and effective density significantly influenced trout size (Table 3), but the effect of TP varied by lake. Trout size increased with increasing TP in ETL but not in the control lake where the variation in TP was considerably less. Size decreased as the effective density increased, but the rate of decrease was much greater in the less-productive unfertilized lake (Table 3).

Prey consumed by rainbow trout did not differ between the fertilized and control lakes. The diets of trout in the two lakes (Fig. 7) were significantly correlated for corresponding seasons (r > 0.83, N = 10, p < 0.04). Chironomid pupae dominated trout diets in spring and fall, while zooplankton, especially cladocerans, dominated summer diets. Odonates, caddisflies, and terrestrial insects were utilized more during the summer but were also present in smaller proportions in spring and fall samples. Other prey taxa comprised only minor proportions of trout diets. Fish were not found in the stomachs.

Stable isotope analysis confirmed the pattern of prey utilization suggested by diet analysis. Mean $\delta^{13}C$ values of benthic autotrophs and planktonic particulate organic matter (POM) (phytoplankton and detritus) in ETL differed by 6‰ (Table 4). Zooplankton had $\delta^{13}C$ values greater than POM, which suggests that they fed selectively on the phytoplankton fraction of the POM. Benthic insects and fish had $\delta^{13}C$ values that were intermediate between the benthic and planktonic autotrophs. $\delta^{13}C$ values did not differ among the

Fig. 5. Dependence of consumer biomass on lake productivity in ETL during fertilized (black circles) and nonfertilized (grey circles) years. (*a*) Dependence of Chl *a* on TP; note that three statistical outliers (1986–1988, lower left) are replaced (grey squares) with Chl *a* values adjusted from the Secchi depth – Chl *a* regression; (*b*) dependence of zooplankton biomass on TP; (*c*) dependence of fish yield on TP. Data are summer means for TP, Chl *a*, and zooplankton biomasss and the annual value for rainbow trout yield. Lines are linear regressions and 95% confidence limits.

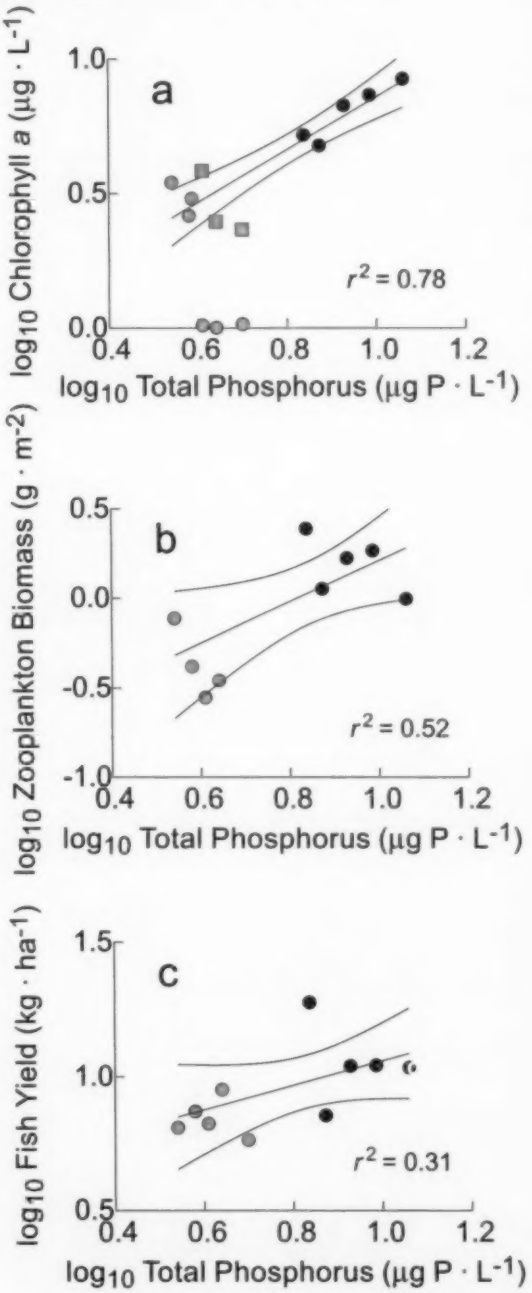

© 1999 NRC Canada

Table 3. Coefficients and summary statistics for the regression model $\log_e(W_{j,t+1}) = \alpha + \beta_1 \times \log_e(W_{j,t}) + \beta_2 \times \log_e(TP_t) + \beta_3 \times DENS_t$ relating the mean weight of an identifiable cohort of rainbow trout from spring gillnet samples in a year, $W_{j,t+1}$, to the mean weight of the cohort in the preceding spring, $W_{j,t}$, the summer mean epilimnial TP concentration during year t, TP_t, and the effective density of trout in the spring of year t, $DENS_t$.

Lake	Effect	Coefficient (±SE)	p	r^2	N
ETL	Constant, α	3.635 (±0.397)	<0.001	0.650	41
	$\log_e(W_{j,t})$	0.322 (±0.053)	<0.001		
	$\log_e(TP_t)$	0.568 (±0.142)	<0.001		
	$DENS_t$	–0.332 (±0.110)	0.005		
WTL	Constant, α	3.908 (±0.150)	<0.001	0.840	37
	$\log_e(W_{j,t})$	0.363 (±0.028)	<0.001		
	$\log_e(TP_t)$	0.039 (±0.101)	0.701		
	$DENS_t$	–0.521 (±0.137)	<0.001		

Note: Weights are in g, TP is in μg P·L^{-1}, and effective density is in 10^4 cm^2·ha^{-1}.

Fig. 6. Relationship between the mean weight of cohorts of rainbow trout in spring gillnetting samples and the mean weight of the cohort 1 year earlier from individual weights of stocked yearlings or from gillnet samples for the control (WTL, triangles) and treatment (ETL, circles) lakes in fertilized (black) and nonfertilized (grey) years. The solid lines are linear regression fits to the fertilized (upper) and all unfertilized (lower) data. Regression lines for WTL and for ETL during unfertilized years do not differ. The broken line is the 1:1 line. The weight-specific annual growth rate is the vertical distance of a point above the 1:1 line, and the mean increment in growth rate from the fertilization treatments is the vertical distance between the two regression lines.

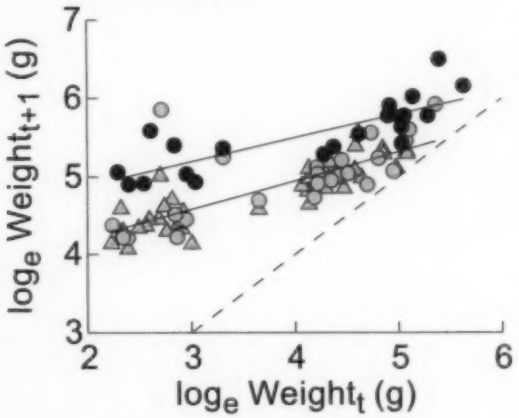

Fig. 7. Mean proportions by weight of common prey taxa in the stomachs of rainbow trout in (*a*) the control lake and (*b*) the fertilized lake during spring, summer, and fall 1993 and 1994. Taxa are chironomids (grey), odonates (checked), caddisflies, mayflies, and alderflies (black), terrestrial insects (left-hatched), unidentified insect fragments (open), cladocerans (cross-hatched), and other zooplankton (right-hatched).

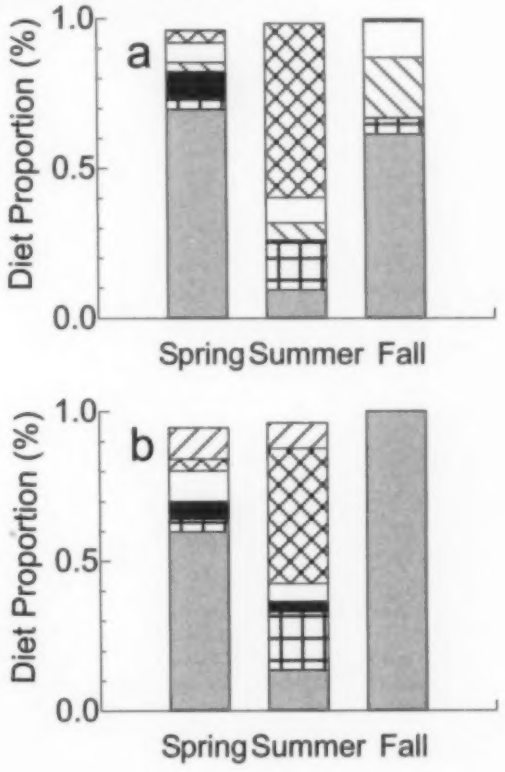

benthic insects or among zooplankton species (ANOVA, $p > 0.05$). Mean $\delta^{13}C$ values were –27.12‰ (±0.70‰, $N = 3$) for benthic insects and –33.83‰ (±0.59‰, $N = 5$) for zooplankton species. The $\delta^{15}N$ values (Table 4) indicated trophic enrichment, with trout > benthic insects or zooplankton > autotrophs. The difference in $\delta^{15}N$ values between periphyton and trout (6.4‰) in ETL suggests a trophic enrichment of about 3.2‰ per trophic step. The $\delta^{15}N$ values of benthic insects varied by only 1.3‰ among taxa, but those of zooplankton varied by 2.5‰ among species and suggested mixotrophy by *H. kenai* (Table 4), which is known to consume copepod nauplii (Olenick 1983).

If we assume benthic insects and cladocerans as the endpoints in a two-member mixing model, and a trophic enrichment of 1.1‰ per step for $\delta^{13}C$ (Peterson and Fry 1987), then rainbow trout in ETL obtained about 65% of their carbon from benthos and 35% from zooplankton. If we assume that prey in WTL had the same isotopic values as those measured in ETL, then trout in WTL obtained about 80% of their carbon from benthos and 20% from zooplankton.

© 1999 NRC Canada

Fig. 8. (*a*) Mean FL's of age-2 mature male (M_2, lower pair of lines) and age-3 mature female trout (F_3, upper pair of lines) in the control (triangles) and experimental (circles) lakes during nonfertilized (grey) and fertilized (black) periods; note that lengths are plotted by year of treatment but are measured the following spring. (*b*) Relationships between body size and ovary weight for gravid female trout from the fertilized (ETL, black circles) and control (WTL, grey triangles) lakes in 1993 and 1994; the lines are linear regression fits to the data for ETL (upper line) and WTL (lower line). (*c*) Recruitment of wild rainbow trout to age 1 by brood year in the experimental (ETL, circles) and control (WTL, triangles) lakes during nonfertilized (grey) and fertilized (black) conditions; data for brood years after 1994 (not shown) are incomplete because most fish are not caught until age 2. (*d*) Minimum survival to age 2 of stocked yearling trout in ETL (circles) and WTL (triangles) during nonfertilized (grey) and fertilized (black) years; two different stocked groups were present in 1984.

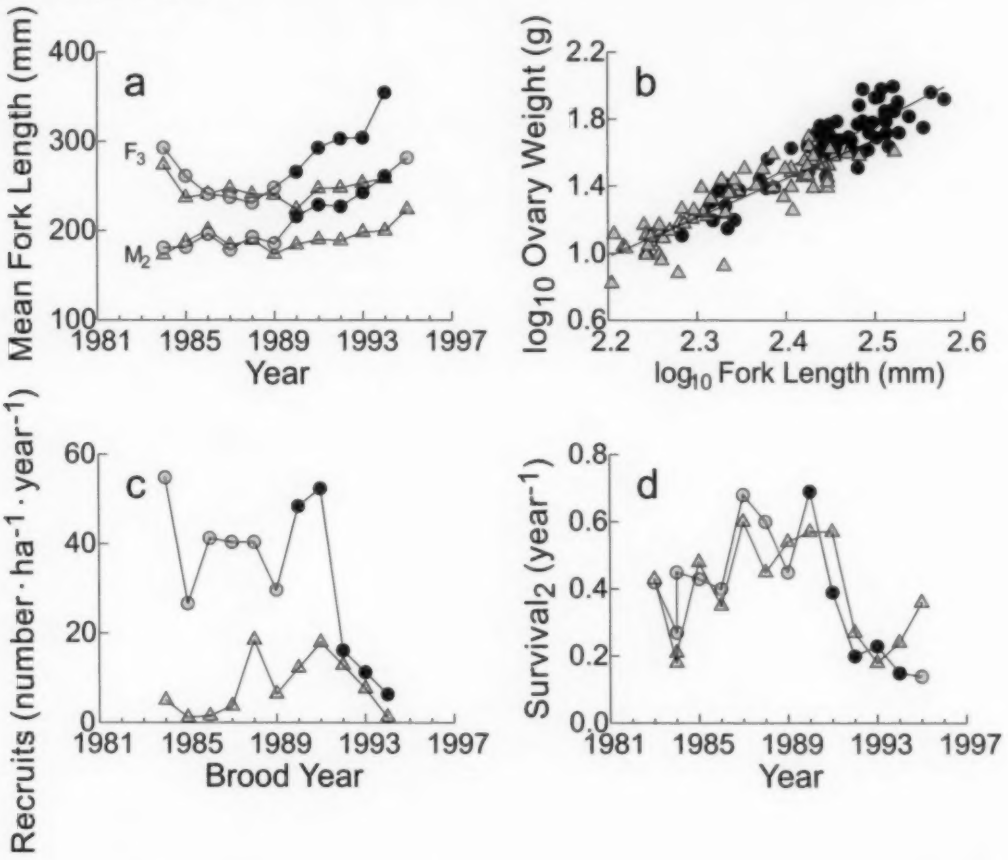

Fish demographic responses

Fertilization did not alter the ages at which trout matured (Table 5). The proportion of mature fish increased with age, but most males were mature at age 2, while most females were mature at age 3. The proportions of age-2 and age-3 females that were mature both increased slightly in ETL during fertilization compared with prefertilization ($\chi_2 = 6.4$, $p = 0.01$ and $\chi_2 = 7.2$, $p = 0.008$, respectively), but the same was true of the control lake ($\chi_2 = 7.3$, $p = 0.007$ and $\chi_2 = 5.5$, $p = 0.02$, respectively), and the proportions did not differ between the lakes during fertilization ($\chi_2 = 1.2$, $p = 0.31$ and $\chi_2 = 0.3$, $p = 0.86$, respectively). Fertilization increased the mean size of both mature age-2 males and mature age-3 females (Fig. 8*a*). Reproductive output, measured as the ovary weights of gravid female trout (Fig. 8*b*), was slightly greater in ETL during the fertilization period than for females of the same size in WTL (ANCOVA, $p_{slopes} = 0.07$, $p_{intercepts} < 0.001$). Nevertheless, the number of age-1 wild trout recruits produced per brood year (Fig. 8*c*) decreased significantly in ETL during fertilization ($p = 0.026$). The coefficient of variation of recruitment also increased in ETL during the fertilization period ($F_{4,5} = 12.54$, $p < 0.05$) but did not change in the control lake ($F_{5,4} = 1.20$, $p > 0.05$). Recruitment to age 1 in either lake was not correlated with effective density or with the abundance of large potentially predatory (FL > 25 cm) trout ($|r| < 0.3$, $N = 11$, $p > 0.8$). The survival to age 2 of stocked yearling trout varied considerably among years (Fig. 8*d*) but did not differ between prefertilization and fertilized time periods ($p = 0.17$, two-tailed). Yearling survival in either lake was not correlated with fish size, effective density, or TP ($|r| < 0.49$, $N = 10$, $p > 0.7$), but yearling survivals in ETL and WTL were

© 1999 NRC Canada

Table 4. Mean ± SE (sample size in parentheses) $\delta^{13}C$ and $\delta^{15}N$ values for biota from ETL and rainbow trout from WTL during the fertilization period.

Group	Taxon	$\delta^{13}C$ (‰)	$\delta^{15}N$ (‰)
Algae	Periphyton	–23.72±1.03 (6)	1.25±0.35 (6)
	Planktonic POM	–29.36±0.31 (2)	
Moss	*Sphagnum* sp.	–22.17±1.02 (2)	–0.61±0.12 (2)
Benthos	Chironomids	–26.99±1.18 (7)	4.64±0.35 (7)
	Caddisflies	–27.06±0.92 (4)	5.47±0.23 (4)
	Damselflies	–27.51±1.83 (3)	5.97±0.43 (2)
Zooplankton	*Daphnia rosea*	–35.58±0.34 (2)	2.61±0.59 (2)
	Holopedium gibberum	–33.83±0.46 (3)	3.65±0.29 (3)
	Hesperodiaptomus kenai	–34.16±0.85 (5)	5.19±0.27 (5)
	Diacyclops bicuspidatus	–35.56 (1)	
	Chaoborus sp.	–31.87 (1)	
Fish	Rainbow trout (ETL)	–28.28±0.49 (10)	7.67±0.29 (10)
	Rainbow trout (WTL)	–27.41±0.60 (10)	6.02±0.38 (10)

Table 5. Age distribution of female and male rainbow trout catches by maturity class in ETL (treated) and WTL (control) during prefertilization (1983–1989 treatment years) and fertilization (1990–1994) time periods.

	Prefertilization				Fertilization			
Age	ETL		WTL		ETL		WTL	
(years)	Immature	Mature	Immature	Mature	Immature	Mature	Immature	Mature
				Females				
1	24	0	0	0	55	0	30	0
2	1118	145	462	64	410	78	325	74
3	134	334	115	262	42	178	26	105
4	9	44	0	27	3	49	2	30
5	0	3	0	2	1	8	0	9
				Males				
1	11	4	2	2	28	0	20	2
2	286	691	167	428	41	323	122	304
3	45	104	45	137	12	71	14	48
4	4	5	0	13	0	5	1	7
5	0	0	0	1	0	1	0	0

strongly correlated ($r = 0.70$, $N = 14$, $p = 0.006$). The overall mean survival to age 2 of stocked yearlings was 0.38 (±0.03) ($N = 28$).

Discussion

The biomass of a population is determined by the balance between natality, growth, and mortality. These factors are strongly related to size in many fish populations. Increases in ecosystem productivity could produce complex biomass responses in size-structured populations if the outcomes of the competitive or predatory interactions that determine growth and survival depended on the sizes of individuals. Nevertheless, from previous empirical studies, we expected that rainbow trout would respond to lake fertilization by some combination of (*i*) increased growth, (*ii*) increased fecundity, (*iii*) increased survival, (*iv*) increased abundance, and (*v*) increased biomass. We observed (*i*) increased growth, (*ii*) slightly increased fecundity, (*iii*) decreased recruitment of age-1 fish, (*iv*) unchanged survival of yearling trout, (*v*) unchanged abundance, and (*vi*) increased yield when we fertilized ETL at rates between 100 and 600 mg $P \cdot m^{-2} \cdot year^{-1}$.

Fertilization increased the growth of age-1 and older trout in ETL. Fish growth increased during the first year of fertilization, varied with enrichment approximately as $TP^{0.6}$, and averaged 1.8-fold greater per year during the fertilization period. Immediate increases in growth upon enrichment are often reported for natural fish populations (Langeland 1982; Johannessen et al. 1984; Hyatt and Stockner 1985), but growth increases may lag behind enrichment (Munro 1961; Mills 1985) or not occur at all (LeBrasseur et al. 1978; Hershey 1992) depending on the factors that determine per capita food availability. It is difficult to compare growth responses

© 1999 NRC Canada

among different fertilization experiments because growth rates vary with fish size and density as well as with lake productivity (Table 3) (Langeland 1982; Hyatt and Stockner 1985). The weight increases observed in ETL are similar to those seen in fertilization experiments with comparable phosphorus loadings. The weights of stunted age-2 to age-7 Arctic char (*Salvelinus alpinus*) increased 1.2- to 1.5-fold compared with nontreated years when Lake Langvatn was fertilized at 100 and 164 mg $P \cdot m^{-2} \cdot year^{-1}$ (Langeland 1982). Sockeye salmon (*Oncorhynchus nerka*) smolt weights increased an average of 1.7-fold in lakes treated at 80–370 mg $P \cdot m^{-2} \cdot year^{-1}$ compared with untreated lakes with corresponding fish densities (Hyatt and Stockner 1985). The maximum weights of lake whitefish (*Coregonus clupeaformis*) doubled when L226NE was fertilized at 350 mg $P \cdot m^{-2} \cdot year^{-1}$ for 8 years (Mills and Chalanchuk 1988). It is possible that exploitation (78% removal) increased growth rates in our experiment, as in other exploited populations (Mills and Chalanchuk 1988), but any effect on our estimates of fertilization effects would be small. First, many of the fish that were removed would have died after spawning in the absence of any fishing. Second, we restocked similar numbers of yearlings, so the population density was not greatly affected by the fishing. Third, both the exploitation and the stocking were consistent throughout nontreated and treated periods in the experimental and control lakes. The experimental design would largely remove the influence of a consistent exploitation regime because changes in the ratio $\log_{10}(x_{experimental}/x_{control})$ were tested.

Fertilization did not increase the abundance of age-1 and older trout in our experiment. Despite a slight increase in size-adjusted ovary weight and large increases in the mean size of mature female trout, the recruitment of age-1 wild fish declined during fertilization. Our results contrast with several fertilization studies in which the survival of age-0 fish improved (LeBrasseur et al. 1978; Langeland 1982; Mills and Chalanchuk 1987) and the abundance of older fish increased. However, the abundance of slimy sculpin (*Cottus cognatus*) did not increase when a small Arctic lake was fertilized (Hershey 1992). Fertilization did not influence the survival of age-1 stocked trout in our study, nor did the survival of age-1 and older whitefish change during the fertilization of L226 (Mills and Chalanchuk 1987). These data indicate fry survival as a major determinant of the numerical responses of lacustrine fishes to enrichment.

Differences in life history may explain differing numerical responses to fertilization. Fry survival has increased during low-level enrichment in situations where fry reared in lakes and fed on zooplankton (LeBrasseur et al. 1978; Langeland 1982; Mills and Chalanchuk 1987). Recruitment in our rainbow trout populations may be largely decoupled from improved feeding conditions in a lake because trout typically spawn and rear in streams before entering the lake. It is likely that trout recruitment in ETL was limited by the very small area of suitable spawning and fry-rearing habitat in the inlet stream. The declines in recruitment seen in both ETL and WTL from the 1992 brood year onward probably resulted from flow changes in spawning habitat after beavers dammed the spawning streams. Second, the presence of larger conspecifics greatly decreases fry survival in lacustrine rainbow trout (Post et al. 1999), while agonistic interactions between fry and older year-classes are not reported for sockeye salmon and lake whitefish. The increased size of age-1 and older trout during fertilization may have reduced fry survival; however, recruitment was not correlated with the abundance of larger fish in our data.

The biomass of trout, measured as fish yield under constant fishing effort, increased an average of 1.6-fold in our experiment. Trout yield in the fertilized lake was strongly correlated with zooplankton biomass, an index of food abundance. The effect of fertilization on yield occurred through increased growth, rather than through a combination of increased growth and abundance. The increase in biomass observed in ETL was commensurate with other experiments with similar phosphorus loadings, although few studies actually report biomass. Lake whitefish biomass averaged about 1.4-fold greater in fertilized L226NE than in a control basin (Mills and Chalanchuk 1987). Sockeye salmon biomass averaged 1.7-fold greater in Great Central Lake during fertilized years (LeBrasseur et al. 1978). Lake productivity directly influenced fish biomass: fish yield varied as $TP^{0.5}$ in ETL. The dependence of yield on TP in ETL did not differ ($p = 0.28$) from the dependence of fish biomass on TP (i.e., $TP^{0.77}$) reported by Stockner (1987) for north temperate lakes.

Fertilization likely increased benthic insect production in ETL, but we lack the prefertilization data to attribute observed differences between ETL and WTL to the fertilization treatment. The emergence of benthic insects was considerably greater at corresponding depths in the fertilized ETL than in the control lake. Davies (1980) noted a similar pattern for dipteran emergence in fertilized and control lakes in northwestern Ontario. Dipteran emergence from WTL (about 0.3 $g \cdot m^{-2} \cdot year^{-1}$) was very similar to that from unfertilized lakes in the Experimental Lakes Area, and dipteran emergence from ETL (about 1.8 $g \cdot m^{-2} \cdot year^{-1}$) was similar to that from Experimental Lakes Area lakes fertilized at phosphorus loadings from 340 to 500 mg $P \cdot m^{-2} \cdot year^{-1}$ (Davies 1980). Total insect emergence was greater in our lakes, however, because caddisflies and damselflies emerged at rates similar to the dipterans. Several fertilization experiments report increased biomass or production of benthic invertebrates (Morgan 1966; Welch et al. 1988; Jorgenson et al. 1992; Clarke et al. 1997), although not invariably (Hershey 1992). Benthic invertebrate production is correlated with phytoplankton production (Davies 1980; Welch et al. 1988) and Chl *a* concentration (Rasmussen 1988). Because trout in ETL obtained two thirds of their body carbon from benthic insects, the growth response of the trout and the higher biomass of emerging benthic insects in the fertilized lake suggest bottom-up control of benthic productivity in ETL despite the absence of a statistically significant correlation between TP and annual emergence in our 4 years of data.

The limnetic community responded strongly to fertilization. Measures of both phytoplankton biomass and zooplankton biomass increased in direct proportion to TP. The Chl *a* response to increased TP in ETL, which lacked abundant (i.e., $>20 \cdot L^{-1}$) large *Daphnia*, did not differ from that reported by Mazumder (1994) for oligotrophic odd-link limnetic ecosystems ($p_{intercepts} = 0.51$, $p_{slopes} = 0.06$). Interestingly, the large mixotrophic copepod *H. kenai*, which was a minor dietary component of the trout, showed the largest

© 1999 NRC Canada

biomass increase attributable to fertilization, about threefold. Herbivorous *D. rosea*, which comprised a large part of the summer diet of trout, showed a larger biomass change in ETL (about fivefold), but the increase could not be ascribed to the fertilization treatment. Zooplankton community structure, particularly the occurrence of large cladocerans, has been suggested as a key determinant of the trophic-level biomass responses of limnetic communities to increased productivity. Mazumder (1994) observed reduced algal responses to increasing productivity in even-link ecosystems compared with odd-link systems, which fits top-down models. However, the fact that algal biomass nevertheless increased with TP for both odd- and even-link systems in his synthesis, and the widespread observations that biomass at all trophic levels increase with lake productivity, contradict the predictions of simple prey-dependent food chain models.

The responses of phytoplankton, macrozooplankton, and trout to increased nutrient loading in oligotrophic ETL indicated bottom-up control of biomass over three trophic levels. Stable isotope analyses implied that the limnetic community in ETL was functionally a three-trophic-level system. We observed proportionate increases in biomass at all three trophic levels as epilimnetic TP concentrations increased. These data were inconsistent with patterns predicted for three-link systems by simple prey-dependent models (Oksanen et al. 1981). Increased primary production in a three-level food chain will not alter the equilibrium biomass of herbivores but will increase the biomass of the carnivore level. Ratio-dependent models (Ginzburg and Akçakaya 1992) predict proportionate increases in biomass at all trophic levels in response to increased productivity. Chl *a* concentration varied directly with TP and macrozooplankton biomass varied directly with Chl *a* concentration in ETL, but trout yield varied as (zooplankton biomass)$^{0.3}$ rather than in direct proportion. Interference among predators, such as that implied by the observed effect of trout density on weight-specific growth rates adjusted for lake productivity (Table 3), will alter strict proportionality in ratio-dependent food chains (Ginzburg and Akçakaya 1992). Thus, our data generally agree with patterns predicted by ratio-dependent food chain models.

Our results do not necessarily exclude all top-down models. At least four mechanisms have been proposed that allow biomass at all trophic levels to increase with productivity under prey-dependent predation. First, McCauley et al. (1988) showed that prey and predator abundance in a two-level system can positively covary under plausible changes to a predator's functional response and density-independent death rate with increasing productivity. Second, if the predator's mortality or energetic requirements are density dependent, prey and predator abundances will covary (Mittelbach et al. 1988). Third, heterogeneity within trophic levels may also produce positively covarying abundances, as well as other abundance patterns (Abrams 1993). Finally, ontogenetic niche shifts between habitats can generate positive correlations between one life stage and its resources if density dependence operates in the other stage (Mittelbach et al. 1988).

We can reject the last three possibilities. Yearling trout survival was independent of density and so would not produce the biomass pattern observed in ETL. Heterogeneity also seems an unlikely mechanism. If we consider phytoplankton and periphyton and zooplankton and benthic insects as possible "species" pairs within successive trophic levels leading to a single top carnivore (trout), none of the possible food web configurations (Abrams 1993, his fig. 2) correctly predicts positive covariation of abundances at all three levels as productivity increases. Finally, because the recruitment of wild fish in ETL (Fig. 8*c*) was usually much lower than the numbers of yearlings stocked, we do not expect ontogenetic niche shifts (between stream-rearing fry and lake-rearing older trout) to establish strong positive covariation between fish and their resources in ETL. Other prey-dependent mechanisms remain possible. Weight-specific annual growth rates of trout were density dependent and could potentially generate covariation of resource and consumer abundance over productivity gradients. Nevertheless, bottom-up control appears to be an adequate predictor of the results of our manipulations.

Our results do not provide strong support for McQueen et al.'s (1986) empirical model of simultaneous bottom-up and top-down controls whose relative importances vary systematically with trophic level and with lake productivity. Our data support two predictions from McQueen et al.'s (1986) empirical model: (*i*) that the biomass at each trophic level is controlled from below by nutrient availability (Fig. 5) and (*ii*) that bottom-up effects attenuate quickly in propagating along food chains. The proportion of the variance in biomass or yield explained by TP decreased with increasing trophic level in ETL (r^2 = 0.78 for Chl *a*, 0.56 for zooplankton biomass, and 0.31 for trout yield), in agreement with McQueen et al.'s (1986) assertion that the strength of bottom-up controls on biomass weakens moving up a food web.

Our data contradict two of McQueen et al.'s (1986) predictions: (*i*) that the variability around bottom-up regressions can be explained by top-down effects and (*ii*) that the relative importance of top-down effects increases in oligotrophic systems. There was no evidence in our data for top-down regulation of limnetic consumer biomass by predators despite threefold variation in the effective density of fish in both the fertilized and control lakes. Predator biomass did not account for significant amounts of the residual variation about producer–consumer relationships at any trophic level. In part, the absence of predator effects on the limnetic community in ETL may reflect the importance of the benthic food chain in this ecosystem. However, other data also suggest that top-down effects are weak in oligotrophic lakes. Trophic bottlenecks may limit the impacts of some consumers on producers in oligotrophic lakes; Elser and Goldman (1991) suggested that extreme food limitation in unproductive systems prevents crustacean grazers from reaching densities at which they can control algal abundance. Our data do not agree with the hypothesis that top-down effects will be strong at the primary producer and herbivore levels in oligotrophic lakes.

In summary, variation in epilimnetic TP concentration accounted for much of the interannual variation in the biomass of phytoplankton, macrozooplankton, and rainbow trout when oligotrophic ETL was fertilized with inorganic phosphorus and nitrogen. It is likely that the biomass of benthic insects also increased, but annual insect emergence was not strongly correlated with TP, possibly because longer genera-

© 1999 NRC Canada

tion times introduced variable time lags in the aggregate response of the benthos. Average phytoplankton and zooplankton biomasses were directly proportional to average TP concentrations, but trout yield was a power function of TP. The pattern of biomass response generally agrees with that expected in donor-controlled systems and implies that predation was not a strong structuring force in this limnetic community. The same qualitative pattern of biomass responses has been observed in fertilized coastal British Columbia sockeye salmon nursery lakes (Hyatt and Stockner 1985).

Acknowledgements

A project of this duration could not be completed without the help of many people. We thank Mark Beere, Jeff Burrows, Carol Cooper, Joanne Ellis, Angelo Facchin, Theresa Godin, Ken Hall, Jeremy Hume, Carol Lamont, Bob Land, Karin Mathias, Kelsey Miller, Larry Mitchell, Bente Nielsen, Michelle Nielsen, Ross Neumann, Eric Parkinson, Morley Rempel, Megan Stirling, Itsuo Yesaki, and the staff of the Fraser Valley Trout Hatchery for technical assistance. We thank Bill Neill, Eric Parkinson, John Post, and an anonymous reviewer for their helpful comments on an earlier draft. We are grateful to the Habitat Conservation Trust Fund for financial support.

References

Abrams, P.A. 1993. Effects of increased productivity on the abundances of trophic levels. Am. Nat. **141**: 351–371.

Andersen, T., and Hessen, D.O. 1991. Carbon, nitrogen, and phosphorus content of freshwater zooplankton. Limnol. Oceanogr. **36**: 807–814.

APHA. 1980. Standard methods for the examination of water and wastewater. 15th ed. American Public Health Association, American Water Works Association, and Water Pollution Control Federation, Washington, D.C.

Carpenter, S.R., Kitchell, J.F., and Hodgson, J.R. 1985. Cascading trophic interactions and lake productivity. BioScience, **35**: 634–639.

Clarke, K.D., Knoechel, R., and Ryan, P.M. 1997. Influence of trophic role and life-cycle duration on timing and magnitude of benthic macroinvertebrate response to whole-lake enrichment. Can. J. Fish. Aquat. Sci. **54**: 89–95.

Davies, I.J. 1980. Relationships between dipteran emergence and phytoplankton production in the Experimental Lakes Area, northwestern Ontario. Can. J. Fish. Aquat. Sci. **37**: 523–533.

Elser, J.J., and Goldman, C.R. 1991. Zooplankton effects on phytoplankton in lakes of contrasting trophic status. Limnol. Oceanogr. **36**: 64–90.

El-Shaarawi, A.H., and Dolan, D.M. 1989. Maximum likelihood estimation of water quality concentrations from censored data. Can. J. Fish. Aquat. Sci. **46**: 1033–1039.

Ginzburg, L.R., and Akçakaya, H.R. 1992. Consequences of ratio-dependent predation for steady-state properties of ecosystems. Ecology, **73**: 1536–1543.

Hanson, J.M., and Leggett, W.C. 1982. Empirical prediction of fish biomass and yield. Can. J. Fish. Aquat. Sci. **39**: 257–263.

Hershey, A.E. 1992. Effects of experimental fertilization on the benthic macroinvertebrate community of an arctic lake. J. North Am. Benthol. Soc. **11**: 204–217.

Hyatt, K.D., and Stockner, J.G. 1985. Responses of sockeye salmon (*Oncorhynchus nerka*) to fertilization of British Columbia coastal lakes. Can. J. Fish. Aquat. Sci. **42**: 320–331.

Johannessen, M., Lande, A., and Rognerud, S. 1984. Fertilization of 6 small mountain lakes in Telemark, southern Norway. Verh. Int. Ver. Limnol. **22**: 673–678.

Jorgenson, J.K., Welch, H.E., and Curtis, M.F. 1992. Response of Amphipoda and Trichoptera to lake fertilization in the Canadian Arctic. Can. J. Fish. Aquat. Sci. **49**: 2354–2362.

Junger, M., and Planas, D. 1994. Quantitative use of stable carbon isotope analysis to determine the trophic basis of invertebrate communities in a boreal forest lotic system. Can. J. Fish. Aquat. Sci. **51**: 52–61.

Langeland, A. 1982. Interactions between zooplankton and fish in a fertilized lake. Holarct. Ecol. **5**: 273–310.

Lawrence, G.A., Ashley, K.I., Yonemitsu, N., and Ellis, J.R. 1995. Natural dispersion in a small lake. Limnol. Oceanogr. **40**: 1519–1526.

LeBrasseur, R.J., McAllister, C.D., Barraclough, W.E., Kennedy, O.D., Manzer, J., Robinson, D., and Stephens, K. 1978. Enhancement of sockeye salmon (*Oncorhynchus nerka*) by lake fertilization in Great Central Lake: summary report. J. Fish. Res. Board Can. **35**: 1580–1596.

LeSage, L., and Harrison, A.D. 1979. Improved traps and techniques for the study of emerging aquatic insects. Entomol. News, **90**: 65–78.

Marmorek, D. 1983. The effects of lake acidification on zooplankton community structure and phytoplankton–zooplankton interactions: an experimental approach. M.Sc. thesis, University of British Columbia, Vancouver, B.C.

Mazumder, A. 1994. Patterns of algal biomass in dominant odd- vs. even-link lake ecosystems. Ecology, **75**: 1141–1149.

McCauley, E., Murdoch, W.W., and Watson, S. 1988. Simple models and variation in plankton densities among lakes. Am. Nat. **132**: 383–403.

McQueen, D.J., Post, J.R., and Mills, E.L. 1986. Trophic relations in freshwater pelagic ecosystems. Can. J. Fish. Aquat. Sci. **43**: 1571–1581.

McQueen, D.J., Johannes, M.R.S., Post, J.R., Stewart, T.J., and Lean, D.R.S. 1989. Bottom-up and top-down impacts on freshwater pelagic community structure. Ecol. Monogr. **59**: 289–309.

Mills, K.H. 1985. Responses of lake whitefish (*Coregonus clupeaformis*) to fertilization of Lake 226, the Experimental Lakes Area. Can. J. Fish. Aquat. Sci. **42**: 129–138.

Mills, K.H., and Chalanchuk, S.M. 1987. Population dynamics of lake whitefish (*Coregonus clupeaformis*) during and after the fertilization of Lake 226, the Experimental Lakes Area. Can. J. Fish. Aquat. Sci. **44**(Suppl. 1): 55–63.

Mills, K.H., and Chalanchuk, S.M. 1988. Population dynamics of unexploited lake whitefish (*Coregonus clupeaformis*) in one experimentally fertilized and three exploited lakes. Finn. Fish. Res. **9**: 145–153.

Mittelbach, G.G., Osenberg, C.W., and Leibold, M.A. 1988. Trophic relations and ontogenetic niche shifts in aquatic ecosystems. *In* Size-structured populations. *Edited by* B. Ebenman and L. Persson. Springer-Verlag, Berlin. pp. 219–235.

Morgan, N.C. 1966. Fertilization experiments in Scottish freshwater lochs. II. Sutherland, 1954. 2. Effects on the bottom fauna. Freshwater Salmon Fish. Res. **36**: 1–19. Department of Agriculture and Fisheries for Scotland, Edinburgh.

Munro, W.R. 1961. The effect of mineral fertilizers on the growth of trout in some Scottish lochs. Verh. Int. Ver. Limnol. **14**: 718–721.

© 1999 NRC Canada

Oksanen, L., Fretwell, S., Arruda, J., and Niemela, P. 1981. Exploitation ecosystems in gradients of primary productivity. Am. Nat. **118**: 240–261.

Olenick, R.J. 1983. The effects of interspecific competition on *Diaptomus leptopus* in a montane lake: an experimental field study. Can. J. Zool. **61**: 2273–2287.

Peterson, B.J., and Fry, B. 1987. Stable isotopes in ecosytem studies. Annu. Rev. Ecol. Syst. **18**: 293–320.

Plante, C., and Downing, J.A. 1993. Relationship of salmonine production to lake trophic status and temperature. Can. J. Fish. Aquat. Sci. **50**: 1324–1328.

Post, J.R., Parkinson, E.A., and Johnston, N.T. 1999. Density-dependent processes in structured fish populations: interaction strengths in whole-lake experiments. Ecol. Monogr. **69**: 155–175.

Power, M.E. 1992. Top-down and bottom-up forces in food webs: do plants have primacy? Ecology, **73**: 733–746.

Rasmussen, J.B. 1988. Littoral zoobenthic biomass in lakes, and its relationship to physical, chemical, and trophic factors. Can. J. Fish. Aquat. Sci. **45**: 1436–1447.

Reinertsen, H., and Langeland, A. 1982. The effect of a lake fertilization on the stability and material utilization of a limnetic ecosystem. Holarct. Ecol. **5**: 311–324.

Schindler, D.W. 1978. Factors regulating phytoplankton production and standing crop in the world's freshwaters. Limnol. Oceanogr. **23**: 478–486.

Stewart-Oaten, A., Murdoch, W.W., and Parker, K.R. 1986. Environmental impact assessment: "pseudoreplication" in time? Ecology, **67**: 929–940.

Stockner, J.G. 1987. Lake fertilization: the enrichment cycle and lake sockeye salmon (*Oncorhynchus nerka*) production. *In* Sockeye salmon (*Oncorhynchus nerka*) population biology and future management. *Edited by* H.D. Smith, L. Margolis, and C.C. Wood. Can. Spec. Publ. Fish. Aquat. Sci. No. 96. pp. 198–215.

Walters, C.J., and Post, J.R. 1993. Density-dependent growth and competitive asymmetries in size-structured fish populations: a theoretical model and recommendations for field experiments. Trans. Am. Fish. Soc. **122**: 34–45.

Welch, H.E., Jorgenson, J.K., and Curtis, M.F. 1988. Emergence of Chironomidae (Diptera) in fertilized and natural lakes at Saqvaqjuac, N.W.T. Can. J. Fish. Aquat. Sci. **45**: 731–737.

Wilkinson, L., and Hill, M.A. 1994. SYSTAT for DOS version 6. SYSTAT Inc., Evanston, Ill.

© 1999 NRC Canada

von Bertalanffy growth model in a random environment

Prajneshu and R. Venugopalan

Abstract: The well-known von Bertalanffy growth model for describing age–length relationship is formulated in a randomly fluctuating environment. The fluctuations in the system are assumed to be described by a Gaussian white noise stochastic process. The resulting model, in terms of a stochastic differential equation, is solved analytically. It is shown that the probability density function of length of a fish is a Gaussian stochastic process. Finally, as an illustration, the methodology is applied to a set of pearl oyster (*Pinctada fucata* (Gould)) data.

Résumé : On a formulé dans un environnement fluctuant aléatoirement le modèle de croissance bien connu de von Bertalanffy décrivant la relation âge–longueur. On suppose que les fluctuations existant dans le système sont décrites par un processus stochastique de bruit blanc gaussien. Le modèle obtenu, qui prend la forme d'une équation différentielle stochastique, est résolu analytiquement. On montre que la densité de probabilité pour la longueur d'un poisson est un processus stochastique gaussien. Enfin, à titre d'exemple, on applique la méthode à un ensemble de données sur des huîtres perlières (*Pinctada fucata* (Gould)).

[Traduit par la Rédaction]

Introduction

The von Bertalanffy growth model (VBGM) plays a very important role in fisheries research, as is evident from the fact that, in recent years, a large number of papers have appeared in research journals dealing with its various aspects. This model, often used to describe the relationship between age and length (Xiao 1996), can be expressed as

$$(1) \qquad L(t) = L_\infty - [L_\infty - L(t_0)]e^{-k(t-t_0)}$$

where L_∞, k, and t_0 are parameters to be estimated. Although derived for a single individual, eq. 1 is widely used to model data collected from a group of animals (Watson and Turnbull 1993). The parameter L_∞ is interpreted as the maximum mean length and k is a curvature parameter that determines how fast a fish approaches its L_∞. Equation 1 is a nonlinear equation, as parameter k appears in a nonlinear manner. Xiao (1994) studied this equation in detail by assuming that L_∞ and k have the joint bivariate normal distribution. Wang et al. (1995) presented an asymptotically unbiased method for estimating the parameters L_∞ and k from tag–recapture data.

Equation 1 represents a deterministic model that implies that the future length of an animal can be predicted with certainty. However, this cannot happen in reality. Therefore, a nonlinear statistical model is formulated by adding an error term to the right-hand side of eq. 1. Venugopalan and Prajneshu (1997) compared the performance of three estimation procedures for fitting such a model, viz. linearized version of the VBGM, nonlinear estimation of the VBGM with independently and identically distributed (IID) error term, and nonlinear estimation of the VBGM with autocorrelated errors. For the data under consideration, the nonlinear estimation procedure with autocorrelated errors performed the best.

However, addition of an error term to the deterministic model may not be totally satisfactory, particularly for longitudinal data (Seber and Wild 1989). Thus, for more realistic modelling, a stochastic term describing fluctuations in the system should be added to the deterministic model and then the resulting model should be investigated. Accordingly, the present paper formulates and studies the model corresponding to eq. 1 in a random environment.

Materials and methods

Differentiating $L(t)$ in eq.(1) with respect to t yields

$$(2) \qquad dL/dt = k(L_\infty - L).$$

Let the fluctuations in the system be described by the stochastic process $F(t)$. Then, from eq. 2, the model to be considered becomes

$$(3) \qquad dL/dt = k(L_\infty - L) + F(t)$$

which is a stochastic differential equation. As the fluctuations in the system arise from variations in a large number of factors, such as temperature, their net effect may be assumed to be Gaussian by the Central Limit Theorem. Furthermore, the duration of a fluctuation is generally very short and rapid in comparison with the life span of a fish. Accordingly, the stochastic process $F(t)$ can be assumed to be a Gaussian white noise stochastic process (Karlin and Taylor 1981) with

$$(4a) \qquad E[F(t)] = 0$$

Received September 26, 1997. Accepted February 16, 1999.
J14222

Prajneshu.[1] Indian Agricultural Statistics Research Institute, New Delhi 110012, India.
R.Venugopalan. Chennai Research Centre of Central Marine Fisheries Research Institute, 68/1 and 68/4 Greams Road, Chennai 600 006, India.

[1]Author to whom all correspondence should be addressed.
e-mail: prajnesh@iasri.delhi.nic.in

© 1999 NRC Canada

(4*b*) $E[F(t_1)F(t_2)] = 2D\delta(t_1 - t_2)$

where E, D, and δ denote mathematical expectation, noise intensity, and the Dirac delta function, respectively. The dependence of the correlation function on the time difference $t_1 - t_2$ reflects the stationarity property.

A consequence of the above choice of $F(t)$ is that the solution process $L(t)$ becomes Markovian. This is of great advantage, as the theory of Markov processes is much more developed compared with that of non-Markovian processes. Our aim is to obtain the statistical characteristics for the process $L(t)$.

Mean value function

Equation 3 can be rewritten as

(5) $dL/dt = -kL(t) + R(t)$

where $R(t) = kL_\infty + F(t)$ with the solution (Appendix A)

(6) $$L(t) = e^{-kt}L(0) + \int_0^t e^{-k(t-\tau)}R(\tau)d\tau.$$

Now, $e^{-kt}L(0)$ is deterministic, but the second term on the right-hand side involves the stochastic process $R(t)$. Thus, $L(t)$ is also a stochastic process. Mathematical expectation of eq. 6 gives

(7) $$E[L(t)] = e^{-kt}L(0) + \int_0^t e^{-k(t-\tau)}E[R(\tau)]d\tau.$$

It can be easily seen that

(8) $L(0) = L_\infty - [L_\infty - L(t_0)]e^{kt_0}$, $E[R(t)] = kL_\infty$.

Substituting these expressions into eq. 7 and simplifying, we get

(9) $\mu(t) \equiv E[L(t)] = L_\infty - [L_\infty - L(t_0)]e^{-k(t-t_0)}$

which is the same as the solution of the corresponding deterministic model. This is true, since the stochastic differential equation (eq. 5) is linear. Notice that $\mu(t)$ increases with t and tends to L_∞ as $t \to \infty$.

Variance function

Writing

(10) $$Q(t) \equiv L(t) - E[L(t)] = \int_0^t e^{-k(t-\tau)}F(\tau)d\tau$$

the variance function (Appendix B) simplifies to

(11) $\sigma^2(t) \equiv E[Q^2(t)] = D(1 - e^{-2kt})/k$.

Thus, the variance function is a monotonically increasing function of t, increasing from 0 to D/k as t varies from 0 to ∞.

Probability density function

It may be noted that the last term of eq. 6 is a linear operation on the Gaussian process $R(t)$ and $e^{-kt}L(0)$ is deterministic. Consequently, $L(t)$ is a Gaussian stochastic process with its mean value function given by eq. 9 and variance function given by eq. 11. So the probability density function of $L(t)$ at age t is

(12) $$f(L(t),t) = [\sigma(t)\sqrt{2\pi}]^{-1}\exp[-\{(L(t) - \mu(t))/\sigma(t)\}^2/2],$$
$$-\infty < L(t) < \infty.$$

This implies that for every fixed value of time t, the probability density function of the random variable defined by length of a fish is a normal distribution. It may be pointed out that, theoretically, the range of a normal distribution is from $-\infty$ to $+\infty$, meaning that there is a possibility that $L(t)$ may take negative values. However, for a normal distribution, 99.73% of the area lies in the interval $(\mu - 3\sigma, \mu + 3\sigma)$ and, in practical situations, mean μ is invariably much larger than three times the standard deviation σ, i.e., $\mu - 3\sigma > 0$. Thus, for all practical purposes, the probability that $L(t)$ takes a negative value is almost zero.

The data requirement for application of the above methodology is availability of length measurements for a number of even-aged individuals at various time epochs. For each fixed time point, a random sample of individuals is selected. Thus, the same individual need not be included in the sample each time, and death of an individual between age samplings would not matter. These types of experiments are generally conducted in a hatchery or an aquaculture system. As the animals are reared from a single brood, the problem of genetic differences, which otherwise is very important, would not arise here.

As an illustration, age–length data on the Indian pearl oyster (*Pinctada fucata* (Gould)), as reported by Chellam (1988), are considered. These data, collected during April 1983 to March 1986, pertain to growth of pearl oyster from fertilization of eggs to the age of 3 years. The pearl oyster spat were produced in the hatchery of the Tuticorin Research Centre of the Central Marine Fisheries Research Institute, India. The pearl oyster spat settled to the substratum when they were around 3 mm in length. They were grown further in the nursery tanks in the hatchery, fed suitably with mixed algae until they reached a size of 5 mm. This took about 30 days. The spat were then transplanted to a farm and grown in net cages of synthetic velon screen with a mesh size of 1 mm. These nets were inserted into a retrievable bag of old fishnet, which provided protection to the spat from predation. Once the spat reached 15–20 mm, they were transferred to 40 × 40 × 15 cm box cages with webbing of about 10 mm knot to knot. Further rearing was continued in these cages. A box cage of this size can hold 125 oysters of 35–45 mm, 100 oysters of 45–55 mm, or 75 oysters of 55–70 mm. The spat spawned on 23 February 1983 were used for the growth study. Each month, they were cleaned of fouling organisms and dorsoventral measurements of sample sizes varying between 30 and 50 animals were recorded to the nearest 0.1 mm. The modal length for the oysters was calculated each month. Unfortunately, the voluminous data on individual pearl oysters were not retained. Therefore, it is not possible to recover the age–length data of individual oysters.

Results

In order to determine the age–length relationship, the probability density function $f(L(t),t)$ of the length $L(t)$ at time (t) in eq. 12 requires computation of mean value function $\mu(t)$ given by eq. 9 and variance function $\sigma^2(t)$ given by eq. 11. It may be noted that in the expression for $\mu(t)$, the parameters L_∞, $L(t_0)$, and k appear in a nonlinear manner. Therefore, the Levenberg–Marquardt nonlinear procedure, available in the Statistical Analysis System (SAS) software package, is employed for fitting purposes. Assuming an additive IID error term in eq. 9, the following parameter estimates along with their standard errors in parentheses are obtained:

(13) $\hat{L}_\infty = 78.196$ mm (0.843), $\hat{L}(t_0) = 4.966$ mm (0.650),
$\hat{k} = 0.076$/month (0.003).

However, residual analysis revealed that the assumption of independence of error terms is not satisfied, as the calculated

© 1999 NRC Canada

Table 1. Fitting of VBGM in a random environment to pearl oyster age–length data.

		$D = 0.01$				$D = 1.00$			
t	$\mu(t)$	$\sigma(t)$	$h(t)$	$\mu(t) - 3\sigma(t)$	$\mu(t) + 3\sigma(t)$	$\sigma(t)$	$h(t)$	$\mu(t) - 3\sigma(t)$	$\mu(t) + 3\sigma(t)$
1	4.51	0.14	2.93	4.10	4.91	1.36	0.30	0.42	8.59
6	27.91	0.28	1.42	27.07	28.76	2.81	0.14	19.48	36.35
16	55.06	0.35	1.15	54.01	56.10	3.48	0.11	44.61	65.50
26	67.88	0.36	1.10	66.80	68.97	3.61	0.11	57.04	78.72
36	73.94	0.36	1.10	72.85	75.03	3.64	0.11	63.01	84.87

Fig. 1. Relationship between age t and length $L(t)$ for Indian pearl oyster by VBGM in a random environment with $\hat{L}_\infty = 79.361$ mm, $\hat{L}(t_0) = 4.506$ mm, $\hat{k} = 0.075$/month, $\hat{\phi} = 0.910$, and $D = 1.00$. The solid curve depicts the mean value function, the broken curves are 99.73% confidence limits, the bell-shaped curves indicate the probability density function, and asterisks denote data points.

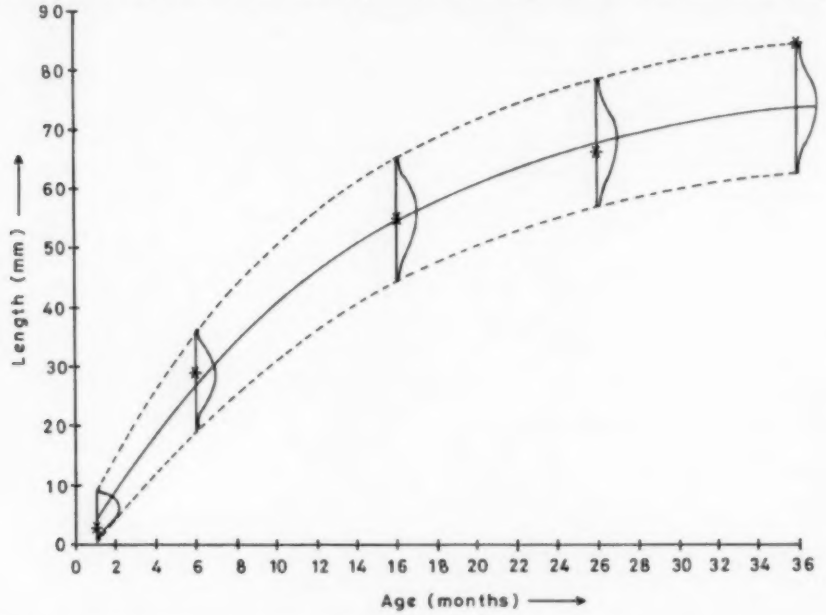

value of the test statistic Z for run test was –4.383. Further, the Durbin–Watson test statistic (Lewis-Beck 1993) given by

$$(14) \quad d = \sum_{t=2}^{n} (e_t - e_{t-1})^2 / \sum_{t=1}^{n} e_t^2$$

is found to be 0.251, indicating the possibility of autocorrelated errors of order 1. As a next step, eq. 9 is fitted under the assumption of additive error structure of the form

$$(15) \quad e_t = \varphi e_{t-1} + \varepsilon_t, \; |\varphi| < 1$$

where ϕ is the autoregressive (AR) parameter and ϵ_t are IID. This implies that, apart from random fluctuations, size at a particular time epoch is directly proportional to the size at the immediate past time epoch. Employing the %AR Macro facility available with the SAS/ETS (SAS Institute Inc. 1990) software package, the following estimates of the parameters along with their standard errors in parentheses are obtained:

$$(16) \quad \hat{L}_\infty = 79.361 \text{ mm } (2.221), \; \hat{L}(t_0) = 4.506 \text{ mm } (0.533),$$
$$\hat{k} = 0.075/\text{month } (0.005), \; \hat{\phi} = 0.910 \; (0.098).$$

Again, carrying out residual analysis, it is observed that neither the assumption of independence (calculated value of $Z = 0.0$) nor that of normality of error terms (Shapiro–Wilk test statistic value = 0.980) is violated.

To compute variance function $\sigma^2(t)$ from eq. 11, an estimate of parameter D is also required. A prerequisite for this is availability of all the raw data on individual pearl oysters for each time epoch. However, as mentioned earlier, these data cannot be recovered. Under these circumstances, the only solution seems to be to compute various relevant statistics for different values of D. Specifically, the estimates of $\mu(t)$, $\sigma^2(t)$, lower and upper limits of the 99.73% confidence interval, viz. $(\mu(t) \pm 3\sigma(t), \mu(t) + 3\sigma(t))$, and height at mode, viz. $h(t) = (\sigma(t)\sqrt{2\pi})^{-1}$, are computed for various values of D. However, to save space, estimates of these parameters for only two values of D, viz. $D = 0.01$ and $D = 1.00$, are presented in Table 1 for selected values of t. It may be noted that $\mu(t)$ is independent of D, while $\sigma(t)$ increases as D increases. The minimum value of D for which all the data

© 1999 NRC Canada

points are within the 99.73% confidence limits is found to be 0.034. To get a visual idea, the fitted VBGM in a random environment for the pearl oyster data is presented in Fig. 1.

Discussion

The relationship between age and length of a fish is usually described by the deterministic VBGM. Generally, the assumption of an additive error term is made and parameters of the model are estimated by employing nonlinear estimation procedures such as the Levenberg–Marquardt procedure. However, this approach may seem reasonable with cross-sectional data in which a single size measurement is taken on each individual or experimental unit. Nonetheless, growth data are often collected longitudinally and size measurements are taken on the same individual or a group of individuals as time progresses. Thus, for longitudinal growth models, explaining scatter by simply tacking a random error term onto the deterministic growth equation is inappropriate.

An attractive alternative approach is to regard growth as an incremental process in which the current environmental conditions affect the current increment in size. To account for the random environmental variations, a stochastic process, with suitable assumptions, is added to the right-hand side of the differential equation model. The resultant model may thus be expressed in terms of a stochastic differential equation. The present work is probably the first application of this type of model in fisheries in which the complete temporal development is obtained. It may act as a springboard for other applications of stochastic processes to fisheries modelling. More specifically, exact expressions are worked out for the mean value function, variance function, and probability density function of the VBGM in a random environment. In general, the mean value function and solution of the corresponding deterministic model will be different; however, for a linear stochastic differential equation model, the two will be the same. An added advantage of the approach followed in this paper is that additional information about variability and even the probability density function of the underlying process is obtained. Thus the present approach provides a fuller description of the system but at the expense of more difficult calculations.

Unfortunately, due to nonavailability of all the raw data, full impact of the methodology could not be realized for the illustration considered in this paper. More precisely, the fourth parameter of the model, viz. D, representing noise intensity, could not be estimated properly. Accordingly, the importance of retaining the complete data for ongoing experiments is being emphasized to the fisheries biologists here. Only after that, attempts would be made for developing efficient procedures for estimating parameter D. One possibility is to try a maximum likelihood parameter search approach in order to obtain the best fit for all four parameters.

In the model discussed in this paper, the noise term is assumed to be "white", whose correlation function is expressible in terms of a Dirac delta function. This implies that the sample paths of the process are very irregular and totally without memory and fluctuate with infinite rapidity. Nevertheless, white noise is a very useful mathematical idealization for describing random influences that fluctuate rapidly and hence are virtually uncorrelated for different instants of time. In a biological system in which the random environmental fluctuations do not occur with great rapidity, in comparison with the time scale of population growth, the noise term should be "coloured", i.e., the noise may have an arbitrary correlation time. Work is in progress to study the effect of coloured noise with an exponential correlation function for the VBGM and the results will be published elsewhere.

Acknowledgements

We are grateful to the referees for their valuable suggestions that led to substantial improvement in the quality of the paper.

References

Chellam, A. 1988. Growth and biometric relationship of pearl oyster *Pinctada fucata* (Gould). Indian J. Fish. **35**: 1–6.

Karlin, S., and Taylor, H.M. 1981. A second course in stochastic processes. Academic Press, New York.

Lewis-Beck, S.M. 1993. Regression analysis. Sage Publication, Inc., Newbury Park, Calif.

SAS Institute Inc. 1990. SAS/ETS users' guide, version 6, edition 4. SAS Institute Inc., Cary, N.C.

Seber, G.A.F., and Wild, C.J. 1989. Nonlinear regression. John Wiley & Sons, New York.

Venugopalan, R. and Prajneshu. 1997. von Bertalanffy growth model with autocorrelated errors. Indian J. Fish. **44**: 63–67.

Wang, Y.G., Thomas, M.R., and Somers, I.F. 1995. A maximum likelihood approach for estimating growth from tag–recapture data. Can. J. Fish. Aquat. Sci. **52**: 252–259.

Watson, R.A., and Turnbull, C.T. 1993. Migration and growth of two tropical panaeid shrimps within Torres Strait, northern Australia. Fish. Res. **17**: 353–368.

Xiao, Y. 1994. von Bertalanffy growth models with variabililty in, and correlation between, K and L_∞. Can. J. Fish. Aquat. Sci. **51**: 1585–1590.

Xiao, Y. 1996. How does somatic growth rate affect otolith size in fishes? Can. J. Fish. Aquat. Sci. **53**: 1675–1682.

Appendix A. Solution of the stochastic differential equation

The stochastic differential equation (eq. 5) is

$$\text{(A1)} \quad dL/dt = -kL(t) + R(t).$$

To solve this stochastic differential equation, we use the Laplace transformation approach. The advantage of this approach is that the stochastic differential equation is transformed into an algebraic equation that can be easily solved. Denote the Laplace transform by inserting a bar and replacing the argument t by s. Thus, the Laplace transform of $L(t)$ is

© 1999 NRC Canada

(A2) $\bar{L}(s) = \int_0^\infty e^{-st} L(t)dt,\ s > 0.$

It can be easily seen that the Laplace transform of dL/dt is $s\bar{L}(s) - L(0)$. Taking the Laplace transform of eq. A1, we get

(A3) $s\bar{L}(s) - L(0) = -k\bar{L}(s) + \bar{R}(s)$

which implies that

(A4) $\bar{L}(s) = (s + k)^{-1}[L(0) + \bar{R}(s)]$.

Laplace inversion, on using the Convolution Theorem, yields

(A5) $L(t) = e^{-kt}L(0) + \int_0^t e^{-k(t-\tau)}R(\tau)d\tau.$

Appendix B. Determination of the variance function

Using eq. 12:

(B1) $E[Q(t_1)Q(t_2)] = \int_0^{t_1}\int_0^{t_2} e^{-k(t_1+t_2-\tau-\tau')}E[F(\tau)F(\tau')]d\tau d\tau'.$

Application of eq. 4*b* yields

$$E[Q(t_1)Q(t_2)] = \int_0^{t_1}\int_0^{t_2} e^{-k(t_1+t_2-\tau-\tau')}2D\delta(\tau-\tau')d\tau d\tau' = 2D\int_0^{t_2} e^{-k(t_1+t_2-2\tau)}d\tau, \text{ assuming } t_1 > t_2.$$

Therefore, the variance function $\sigma^2(t)$ is

$$\sigma^2(t) \equiv V[L(t)] = E[Q^2(t)] = 2D\int_0^t e^{-2k(t-\tau)}d\tau$$

which, on simplification, gives

(B2) $\sigma^2(t) = D(1 - e^{-2kt})/k.$

© 1999 NRC Canada

Contrasting patterns of productivity and survival rates for stream-type chinook salmon (*Oncorhynchus tshawytscha*) populations of the Snake and Columbia rivers

Howard A. Schaller, Charles E. Petrosky, and Olaf P. Langness

Abstract: The effects of increasing hydropower development and operation appear extremely important in the decline and near extripation of stream-type chinook salmon (*Oncorhynchus tshawytscha*) stocks of the upper Columbia and Snake rivers. We evaluated temporal and spatial patterns of productivity and survival rates (for index stocks from the Snake, upper Columbia, and lower Columbia regions) to determine the cause of dramatic declines of the upriver stocks. This evaluation tested hypotheses about nonstationarity (changes over time in average productivity) in the Ricker recruitment function caused by changes in the physical environment. Individual stocks showed recent declines in indicators of productivity and survival rate; however, the comparisons indicate that upriver stocks showed greater declines coincident with the development and operation of the hydropower system. Evidence from the aggregate run indicates that declines over the last 50 years were quite abrupt and corresponded to construction and completion of the hydropower system.

Résumé : L'accroissement du développement et de l'exploitation de l'hydro-électricité semble jouer un rôle très important dans le déclin et la disparition presque complète des stocks de quinnat (*Oncorhynchus tshawytscha*) de type dulcicole dans le cours supérieur du Columbia et la Snake. Nous avons évalué les profils temporels et spatiaux de la productivité et du taux de survie (pour des stocks indicateurs des régions de la Snake, du haut Columbia et du bas Columbia) pour déterminer la cause des déclins marqués des stocks d'amont. Pour cette évaluation, on a testé des hypothèses concernant la non-stationnarité (changements temporels dans la productivité moyenne) dans la fonction de recrutement de Ricker causée par les changements dans le milieu physique. Les stocks individuels ont connu des déclins récents selon les indicateurs de la productivité et du taux de survie, mais les comparaisons montrent que les stocks d'amont ont connu des déclins plus importants par suite du développement et de l'exploitation du réseau hydro-électrique. Les données sur la remonte totale montrent que les déclins des 50 dernières années ont été assez abrupts et ont suivi la construction et la finalisation du réseau hydro-électrique.

[Traduit par la Rédaction]

Introduction

Snake River spring and summer (stream-type) chinook salmon (*Oncorhynchus tshawytscha*) populations have declined dramatically with the completion of the Federal Columbia River Power System (FCRPS). They have been listed as threatened under the Endangered Species Act (ESA) since 1992. Under the ESA, the National Marine Fisheries Service (NMFS) is charged with developing and implementing management plans to ensure survival and recovery of the listed salmon populations. The NMFS 1995–1998 Biological Opinion on operation of the FCRPS (NMFS 1995) created a process called PATH (plan for analyzing and testing hypotheses). The first phase of PATH is retrospective and involves explicitly stating hypotheses about the distribution of mortality over the life cycle, evaluating strengths and weaknesses of supporting evidence, and testing those alternative hypotheses that have significant management implications.

We describe a quantitative approach to test for nonstationarity (change over time in average productivity) in recruitment functions due to physical change in the environment. We applied this approach to spawner (parents) and recruit (progeny) information from populations of spring and summer chinook of the Columbia River basin. We provided spatial contrast by using replicate index stocks from three different regions of the basin (which presently experience very different conditions during their juvenile migrations through the FCRPS) for spatial contrast. Our work is based on a unique spatial and temporal contrast of stock performance, which evaluates hypotheses about causes of decline for Snake River populations.

The focus of this analysis is on spawner and recruitment information rather than on simple escapement trends. The productivity and survival rate indices are more robust mea-

Received March 11, 1998. Accepted February 12. 1999.
J14489

H.A Schaller.[1] Oregon Department of Fish and Wildlife, 2501 SW First Avenue, P.O. Box 59, Portland, OR 97207, U.S.A.
C.E. Petrosky. Idaho Department of Fish and Game, 600 S Walnut Avenue, P.O. Box 25, Boise, ID 83707, U.S.A.
O.P. Langness. Washington Department of Fish and Wildlife, 2108 Grand Boulevard, Vancouver, WA 98661, U.S.A.

[1]Author to whom all correspondence should be addressed.
e-mail: howard.schaller@state.or.us

© 1999 NRC Canada

Fig. 1. Distribution of index stocks of spring and summer chinook. Mainstem dams: Bonneville (BON), The Dalles (TDA), John Day (JDA), and McNary (MCN) on the lower Columbia River, Ice Harbor (IHR), Lower Monumental (LMN), Little Goose (LGS), Lower Granite (LGR), Hells Canyon (HC), Oxbow (OX), and Brownlee (BR) on the Snake River, and Priest Rapids (PRD), Wanupum (WMD), Rock Island (RIS), Rocky Reach (RRH), Wells (WEL), Chief Joseph (CHJ), and Grand Coulee (GRC) on the upper Columbia River.

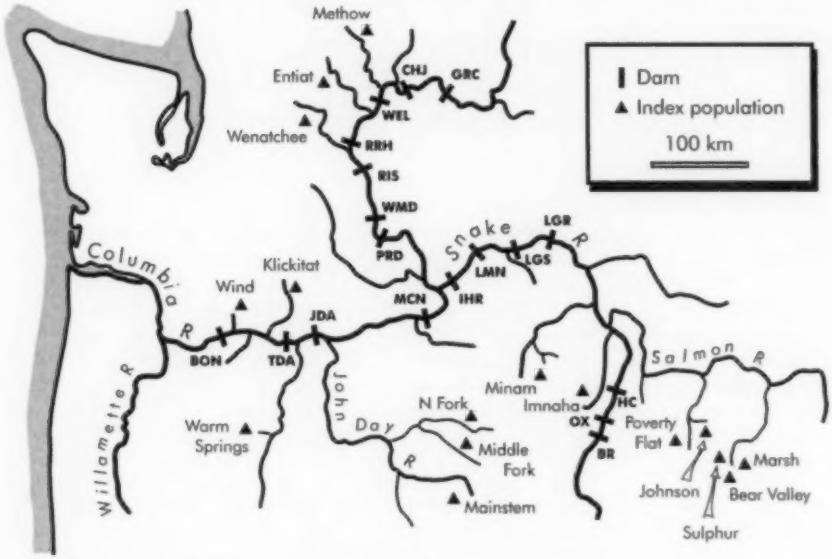

sures of stock performance because they account directly for several factors that may confound simple escapement measures. The productivity and survival rate indices account for hatchery fish, age composition of returns, variable harvest mortality rates and adult passage survival rates, and density dependence.

We evaluated the following sets of alternative hypotheses for stream-type chinook.

Hypothesis 1*a*: Productivity (Ricker *a* from ln(*R*/*S*) versus *S*) has shown similar responses over time between upriver stocks and downriver stocks. **Hypothesis 1*b***: Productivity declined more over time for upriver stocks, which were most affected by hydropower development, than for downriver stocks.

Hypothesis 2*a*: Survival rate indices (ln[(observed *R*/*S*)/(predicted *R*/*S*)]) have shown similar responses over time between upriver stocks and downriver stocks. **Hypothesis 2*b***: Survival rate indices declined more and become more variable for upriver stocks, which were most affected by hydropower development, than for downriver stocks.

Hypothesis 3*a*: Productivity and survival rate of the upriver run of Columbia River wild spring chinook have been in a long-term decline since escapements were first measured (1939). **Hypothesis 3*b***: Declines in productivity and survival rate of upriver runs of Columbia River wild spring chinook over the past 50 years corresponded to construction and completion of the FCRPS.

Methods

Index stocks

Four groups of naturally reproducing stocks are used in this analysis: Snake River spring and summer chinook, upper Columbia River spring chinook, lower Columbia River spring chinook, and the aggregate upriver run of spring chinook.

Index stocks were grouped geographically to reflect similar potential impacts from hydropower development and operation. All stocks in the analysis are classified as upriver runs (ODFW and WDFW 1995) because they originate from upriver of Bonneville Dam (Fig. 1), east of the Cascade Mountain Range. Upriver spring chinook adults enter the mouth of the Columbia River in March through May, and summer chinook adults enter the river in June and July (ODFW and WDFW 1995). Spawning takes place primarily in August through September. All stocks are stream-type chinook (Healy 1991), producing yearling smolts that migrate seaward in the spring (primarily April and May).

The aggregate upriver run of wild spring chinook consists of all wild spring chinook that originate upriver of Bonneville Dam, including all spring chinook stocks in this analysis. This aggregate run provides indices of productivity and survival rates over a much longer time series than is possible for the individual index stocks.

Spawning and rearing habitat factors would be expected to contribute to productivity and survival rate variability within regions. A broad mix of habitat condition exists within each of the three regions (Table 1), and significant effects of habitat degradation predate most of the time series (Fulton 1968; Beamesderfer et al. 1997).

The Snake River region in this analysis includes streams in Idaho and Oregon, upriver of Lower Granite Dam (Fig. 1). The seven Snake River stocks are from four subbasins and occupy a wide range of tributary habitat condition (Table 1) from wilderness (Minam and Sulphur) to heavily impacted (Poverty Flat and Bear Valley).

The upper Columbia region was defined as the Columbia River upriver of the confluence with the Snake River (Fig. 1). The three upper Columbia stocks represent three subbasins and occupy tributaries that have sustained moderate habitat impacts (Table 1).

The lower Columbia region was defined in this analysis as the Columbia River downriver of the Snake River confluence to

© 1999 NRC Canada

Table 1. Summary of years of data and attributes of index populations of wild spring and summer chinook.

Region, subbasin, population	Run	Years of data	Dams passed	Completion of last dam	Habitat quality	Hatchery influence	Year of first hatchery program
Snake							
Middle Fork Salmon							
Bear Valley	Spring	1957–1995	8	1975	Poor	Low	na
Marsh	Spring	1957–1995	8	1975	Good	Low	na
Sulphur	Spring	1957–1995	8	1975	Good	Low	na
South Fork Salmon							
Poverty Flat	Summer	1957–1995	8	1975	Poor	Moderate	1980
Johnson	Summer	1957–1995	8	1975	Fair	Moderate	1980
Grande Ronde							
Minam	Spring	1954–1995	8	1975	Good	Moderate	1986
Imnaha							
Mainstem	Spring/summer	1949–1995	8	1975	Good	Moderate	1982
Upper Columbia							
Methow							
Mainstem	Spring	1960–1995	9	1968	Fair	Moderate	1941
Entiat							
Mainstem	Spring	1955–1995	8	1968	Fair	Moderate	1942
Wenatchee							
Mainstem	Spring	1958–1995	7	1968	Fair	Moderate	1899
Lower Columbia							
John Day							
Mainstem	Spring	1959–1995	3	1968	Fair	Low	na
Middle Fork	Spring	1959–1995	3	1968	Poor	Low	na
North Fork	Spring	1959–1995	3	1968	Good	Low	na
Deschutes							
Warm Springs	Spring	1969–1995	2	1957	Fair	Moderate	1958
Klickitat							
Mainstem	Spring	1966–1995	1	1938	Fair	Moderate	1950
Wind							
Mainstem	Spring	1970–1995	1	1938	Good	High	1938
Upriver aggregate	Spring	1939–1995	Variable	Variable	Variable	Variable	Variable

Note: Imnaha data are for 1949–1950 and 1952–1995.

Bonneville Dam (Fig. 1). The six lower Columbia stocks are from four subbasins and occupy a wide range of tributary habitat condition (Table 1) from wilderness (North Fork John Day) to significantly impacted (Middle Fork John Day). Note that only the three John Day River stocks had sufficient pre-1970 spawner–recruit data to use in the productivity and survival rate analyses. Data from the other three stocks were incorporated in escapement comparisons.

Hatchery factors would also be expected to contribute to productivity and survival rate variability within regions. In the early years, wild fish predominated the aggregate Columbia River spring chinook run (Fig. 2*a*), with most of the production from the Snake and upper Columbia regions (Fulton 1968). The proportion of hatchery fish in the total run has increased with time, primarily from programs to compensate for loss of fish production due to hydropower development. The potential influence of hatchery programs ranges widely between stocks within each region (Table 1). Stocks with no anadromous fish hatchery programs within their subbasin are the three Middle Fork Salmon River stocks (Snake region) and the three John Day River stocks (lower Columbia region).

The estimates of recruits used in hypothesis testing explicitly take into account the tributary and mainstem Columbia River harvest rates. Historically, upriver spring and summer chinook supported substantial commercial and sport fisheries and Tribal commercial, ceremonial, and subsistence fisheries in the mainstem Columbia River (ODFW and WDFW 1995) and sport and Tribal fisheries in the tributaries (Beamesderfer et al. 1997). The mainstem harvest rates were cut back dramatically as runs declined in the mid-1970's for spring chinook and in the late 1960's for summer chinook (Fig. 2*b*). These harvest rates have remained at low levels. Snake River wild stocks last supported tributary harvest in 1978. In contrast, the index stocks below the Snake River confluence (lower Columbia River stocks) in this analysis (Wind, Klickitat, Warm Springs, and John Day rivers) have continued to support tributary sport and Tribal fisheries (Beamesderfer et al. 1997).

Ocean harvest rates are very small for stream-type chinook originating above Bonneville Dam, estimated at less than 1% based on a near absence of coded-wire tag (CWT) recoveries from ocean fishery mark recovery programs (Berkson 1991). For instance, only 62 marked stream-type chinook were recovered in ocean fisheries out of 2.1 million CWT marks released from Snake and lower Columbia region hatcheries in release years 1983–1990 (Pacific States Marine Fisheries Commission data). This is in stark contrast with much higher ocean recoveries and harvest rates for Columbia

© 1999 NRC Canada

Fig. 2. (*a*) Run size of upriver aggregate spring chinook (wild and hatchery components) to the Columbia River mouth and (*b*) mainstem harvest rates (combined commercial, tribal, and sport) for Columbia River and Snake River spring and summer chinook index stocks, 1939–1995.

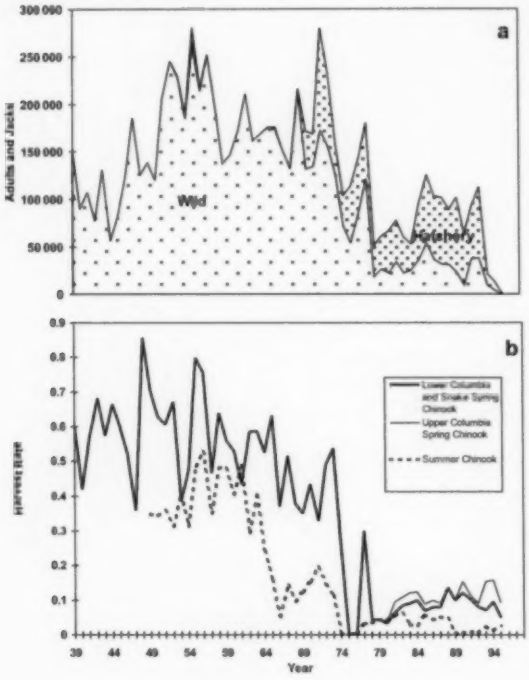

River basin ocean-type (fall) chinook. Both stream-type and ocean-type chinook are sampled by the same ocean recovery program.

The stocks from the three regions have experienced different juvenile migration conditions, due to mainstem hydropower development and operations. The maximum number of dams that Snake River and upper Columbia River chinook salmon encounter during migration has increased to eight and nine dams, respectively (Fig. 3*a*; Table 1). In contrast, the most dams encountered by lower Columbia River stocks are three. The completion dates for the final dam faced by stocks from the three regions are 1975 for Snake, 1968 for upper Columbia, and 1968 for lower Columbia (Table 1). Survival rates of smolts decreased as dams and reservoirs were built (Raymond 1988). To circumvent mortality of juveniles, most Snake River juveniles arriving at the dams have been collected at either Lower Granite Dam or Little Goose Dam since 1977 and transported by barge or truck for release below Bonneville Dam (Mundy et al. 1994). A fraction of juveniles arriving at McNary Dam from both the upper Columbia and Snake regions have been transported since 1979. None of the lower Columbia stocks are collected and transported.

One effect of increased impoundment has been to decrease water velocity and thus slow outmigration of fish from upriver areas (Raymond 1979, 1988; Berggren and Filardo 1993). Water velocity is generally expressed as the average time that it takes a water particle to travel through a river reach (water travel time). Average historic water travel times (in days and by region) for the juvenile mainstem migration period (April 16 – May 31) are depicted in Fig. 3*b*. The river reaches representing the three regions are the head of Lower Granite Reservoir to Bonneville Dam for the Snake region, the mouth of the Methow River to Bonneville Dam for the upper Columbia region, and the mouth of the John Day River to

Fig. 3. (*a*) Maximum number of hydroelectric dams and (*b*) average annual water travel time experienced by spring and summer chinook yearling outmigrants from stocks representing the three regions of the interior Columbia River basin, 1932–1995 (E. Weber, Columbia River Inter-Tribal Fish Commission, personal communication (e-mail: webe@critfc.org)), and (*c*) upriver passage survival rates (average ± SE) of adult spring and summer chinook salmon from stocks representing the three regions of the interior Columbia River basin, 1954–1969, 1970–1974, and 1975–1995 (Beamesderfer et al. 1997).

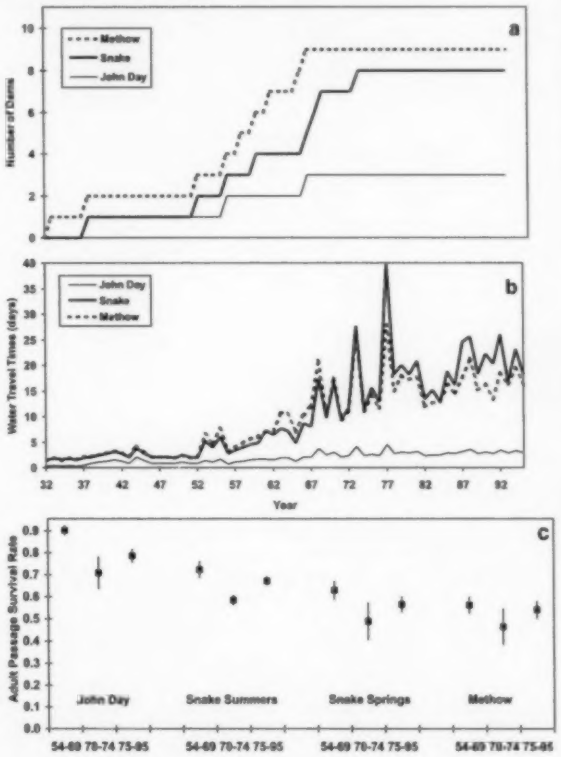

Bonneville Dam for the lower Columbia region. These data were provided by the Columbia River Inter-Tribal Fish Commission (E. Weber, Columbia River Inter-Tribal Fish Commission, personal communication (e-mail: webe@critfc.org)). Prior to Bonneville Dam completion in 1938, water travel time consistently averaged less than 3 days for the Snake and upper Columbia regions. Prior to 1968 when John Day Dam was completed, water travel time for these upriver regions generally averaged less than 10 days, with the earlier years averaging less than 5 days. Since completion of the final dams, average water travel times have been highly variable and have generally exceeded 2 weeks. In contrast, average water travel times for the lower Columbia region, while somewhat elevated, have remained under 5 days. The annual survival rates of Snake River stocks for brood years 1975–1986 were correlated with water travel times (Petrosky and Schaller 1992).

Hydropower development in the basin has also reduced the survival of mature fish returning to spawn. Adult passage survival rates (Beamesderfer et al. 1997) were generally similar during the pre-1970 and post-1974 periods, with a notable decline during the transition period (Fig. 3*c*). The estimates of recruits used in hypothesis testing explicitly take into account the adult passage survival rates.

© 1999 NRC Canada

Spawning escapement trends

Time trends of spawning escapement were compared graphically among and within the geographic stock groups, and limitations of these comparisons were identified. These spawning escapement measures include both natural origin fish and, where applicable, hatchery fish spawning in the wild. All years of escapement data were standardized by dividing each year's value by the average escapement computed from all available years through 1995. Caution is needed when comparing escapement trends because of the following limitations: (*i*) a lack of accounting for density dependence, (*ii*) exclusion of harvest and adult passage mortality, both of which have varied considerably through time and across stocks, and (*iii*) a general lack of accounting of hatchery spawner contributions or of direct effects of hatchery operations (natural brood stock removal or adult outplants).

Spawners and recruits

We developed estimates of spawners and recruits for each of the index stocks; the data sources, run reconstruction methods, and results are documented in Beamesderfer et al. (1997). Spawners (returning fish with greater than 1 year of ocean residence) were independently estimated for each index area based on expanded ground and aerial redd counts or live fish and carcass counts. Recruits were measured to the mouth of the Columbia River and included jacks (precocious males that return after 1 year of ocean residence). We expanded age-structured spawners into recruitment by accounting for prespawning survival, tributary harvest, mainstem harvest, and adult passage losses at the dams. Computation of the recruits for different stocks relied on both unique and shared survival rates. In streams where hatchery fish spawned with natural fish, the hatchery contribution was estimated and subtracted from total recruits. Any natural-origin fish taken as brood stock were counted as natural recruits. Estimated numbers of spawners for index stocks included any hatchery strays or outplants. That is, the spawner estimates included all fish spawning in the wild, and recruits counted only those of natural origin. The numbers of age-structured wild spring chinook in the upriver aggregate run were estimated at Bonneville Dam by expanding hatchery rack returns for adult passage survival, harvest, and prespawning mortality rates back to Bonneville Dam and subtracting the expanded hatchery estimate from the total Bonneville count (Beamesderfer et al. 1997). The run reconstruction methods for the aggregate upriver spring chinook run expand numbers of wild spring chinook recruits to the Columbia River mouth for mainstem harvest rates of upriver spring chinook below Bonneville Dam (ODFW and WDFW 1995).

Time periods

For each index stock, spawner and recruit data were classified into two primary time periods (and a transition period), defined by FCRPS development and operations affecting the threatened Snake River index stocks. The first period, pre-1970 brood years, was prior to completion of the last two Snake River dams. All mainstem dams in the upper Columbia River migration corridor were completed and fully operational by 1969. The second primary period, post-1974 brood years, was marked by the initiation of mass transportation of smolts around the Snake River dams and gradual passage improvements. Upper Columbia River stocks were also influenced by incremental system improvements in this period and by transportation from McNary Dam since 1979. The transition period, 1970–1974 brood years, was a period of construction and changing operations in the Snake River that caused extremely high levels of atmospheric gas supersaturation in high-flow years (Raymond 1979).

Productivity and survival rates

Productivity and survival rate indices were estimated for different periods and stocks throughout the Columbia River Basin. Productivity is defined as the natural log of the ratio of recruits to spawners in the absence of density-dependent mortality (Neave 1953). Spawner (S) and recruit (R) data can be fit to the Ricker (1975) recruitment function:

$$(1) \qquad R = e^{a} S e^{-\beta S}.$$

The a and β parameters are typically estimated by the log transformation of eq. 1. Productivity is typically measured as the intercept, or Ricker a. The Ricker recruitment function exhibited a better fit to our first period data than a Beverton–Holt function.

Survival rate indices provide a time series of density-independent mortality estimates through deviations of observed R/S from those predicted by the fitted stock–recruitment function for a specified time period. Survival rate indices were expressed as the natural log of the ratio of observed R/S to the predicted R/S. The natural log of these ratios transforms the differences, such that they tend to be normally distributed (Peterman 1981).

Spawner–recruitment analysis normally assumes that the average spawner–recruitment relationship does not change over time. Often the spawner–recruitment curve will indeed change (nonstationarity) due to physical change in the environment or change in stock structure (Walters 1987; Hilborn and Walters 1992).

We tested for evidence of nonstationarity in the recruitment functions caused by physical change in the migratory habitat (due to hydroelectric development). Large changes in density-independent mortality (caused by change in the physical environment) within a time series of spawner–recruitment data would cause nonstationary behavior in the recruitment function. We used two methods, suggested by Walters (1987), to detect if a systematic change in the spawner–recruitment relationships took place associated with this dramatic change in the physical environment: (*i*) covariance analysis of data in time blocks associated with the physical change and (*ii*) evaluation of time series of recruitment model deviations.

We relied primarily on the analysis of multiple index stocks to address potential nonstationarity due to changes over time in the aggregate stock structure. Using an aggregation of stocks in spawner–recruitment analysis has the potential to overestimate productivity if stock structure changes. This nonstationarity in spawner–recruitment relationships could occur if the less productive stocks made a smaller contribution to the aggregate over time, due to an increasing level of density-independent mortality (e.g., dam passage mortality, incidental fishing mortality). Common patterns in productivity and survival rates between index stocks and an aggregate run would suggest that nonstationary behavior in the aggregate recruitment function was not primarily due to changes in aggregate stock structure.

A lack of contrast in spawner abundance could give a distorted picture of average recruitment rates, with productivity being overestimated at low stock sizes (Walters 1990). To provide a large contrast in spawner abundance, we fit spawner and recruit data for the longest available time series (with a period effect).

The hypothesis testing of productivity in this paper was primarily concerned with estimating the relative change in spawner–recruitment functions between time periods and among geographic regions of the interior Columbia River basin. In hypothesis testing of survival rates, the deviation from the average spawner–recruitment relationship was of primary importance to the analyses, and estimation of average parameter values was secondary, consistent with the approach of Hilborn and Walters (1992). All statistical tests were performed at an α level of 0.05.

Hypothesis 1. Productivity changes

We evaluated whether productivity declined more for upriver stocks (which were most affected by the hydrosystem) in the post-

© 1999 NRC Canada

1974 period than for downriver stocks. We would expect a temporal change in the density-independent mortality, such as that imposed by hydroelectric development and operation, to be reflected primarily in the intercept (Ricker a) rather than in the slope (β) of the regressions. Therefore, hypothesis 1 was tested with analysis of covariance (ANCOVA) using the SAS (1993) general linear model (GLM) procedure to examine differences between the two periods for the intercept (Ricker a value) of the relationship of $\ln(R/S)$ versus S:

$$(2) \qquad \ln(R_{i,j}/S_{i,j}) = \tau_i + a - \beta(S_{i,j} - \bar{S}..) + \varepsilon_{i,j}$$

where τ_i is the class effect (period), a is the overall intercept, β is the overall slope, $\varepsilon_{i,j}$ is the normally distributed residual, i is the class (period), j is the observation

First, the assumption of homogeneity of slopes was tested for significant interaction between treatment (period) and the covariate (spawners). Then, ANCOVA was run to estimate the period effect on the $\ln(R/S)$, taking into account spawning level. The measure of productivity by period was estimated using $\tau_i + a$ from the ANCOVA results (eq. 2). This is equivalent to the Ricker a parameter by period assuming a common slope (β) over periods.

Hypothesis 2. Survival rate changes

We tested whether survival rates declined more and became more variable for upriver stocks (which were most affected by the hydrosystem) in the post-1974 period than for downriver stocks. Survival rate indices provide a time series of density-independent mortality estimates through deviations of observed R/S from those predicted by the fitted stock–recruitment function for a specified time period. The deviations, or survival rate indices, were expressed as ln[(observed R/S)/(predicted R/S)], where predicted values were based on fits to data from different time periods. This approach, using the deviations as an index of survival rate, is similar to approaches in Hilborn and Walters (1992, fig. 7.2.1), Peterman (1981), and Peterman et al. (1998).

We tested for changes in survival rates between regions using two indices. Survival rate index 1 (SRI-1) represented the deviation of post-1974 observations from pre-1970 predicted values based on the ANCOVA fit of eq. 2, and SRI-2 represented the deviation of pre-1970 observations from the post-1974 predicted values from the same ANCOVA fit. Attributes of SRI-1 and SRI-2 include the assumption of a common β between periods (i.e., temporal changes are explained by density-independent factors, τ_i and a) and use of the three John Day River stocks to represent the lower Columbia region. The use of SRI-1 and SRI-2 was consistent with our expectation that effects of hydropower development and operation would impose additional density-independent mortality on upriver stocks.

Period differences in survival rate indices (SRI-1 and SRI-2) were tested between stock groups from different regions with one-way classification analysis of variance (ANOVA) under the GLM procedure of SAS (1993). The GLM procedure was used because of unequal sample sizes between categories (regions). Differences in survival rate indices among the Snake, upper Columbia, and lower Columbia regions were then compared using Bonferroni's multicomparison test (SAS 1993), fixed to a prescribed experimentwise error rate of $\alpha = 0.05$. Bonferroni's pairwise procedure is the most appropriate test when making only a small number of comparisons (Milliken and Johnson 1984).

The hypothesis that survival rates became more variable for upriver stocks in the recent period was examined using F tests of survival rate variance of the two periods. The survival rate variance for the pre-1970 period was calculated using the SRI-1 for that period. The survival rate variance for the post-1974 period was calculated using the SRI-2 for that period.

Hypothesis 3. Long-term changes in aggregate upriver run

We evaluated whether the aggregate upriver spring chinook run has been in long-term decline since escapements were first measured (1939) or whether declines in productivity and survival rates were more associated with completion of the FCRPS during the 1970's. Data were categorized for these hypotheses by decade: 1939–1949, 1950–1959, 1960–1969, 1970–1979, and 1980–1990. The ANCOVA was run using the SAS GLM procedure to examine differences between the five periods in the relationship of $\ln(R/S)$ versus S. The covariance model for this test is also represented by eq. 2. The assumption of homogeneity of slopes was first tested for significant interaction between treatment (period) and the covariate (spawners). Then, ANCOVA was run to estimate the effect of period on $\ln(R/S)$, taking into account spawning level. The least squares means test was used in the ANCOVA (with homogenous slopes) to compare the period effect on productivity (Freund et al. 1986).

In addition, ANCOVA was run for the pre-1970 and post-1974 periods to parallel the individual index stocks analysis. The assumption of homogeneity of slopes was tested as described above.

For the aggregate upriver spring chinook run, SRI-1 represented the deviation of post-1974 observations from pre-1970 predicted values based on the ANCOVA fit of eq. 2, and SRI-2 represented the deviation of pre-1970 observations from the post-1974 predicted values from the same ANCOVA fit. SRI-1 and SRI-2 for the aggregate upriver spring chinook run were plotted and compared for the brood years 1939–1990.

Results

Spawning escapement trends

Patterns of standardized escapements for Snake River stocks exhibited a similar trend of decline, which was particularly noticeable by the mid-1970's (Fig. 4*a*). Before 1970, Snake River stock escapements ranged from 33 to 541% of their average escapement level. After 1974, escapements ranged from 0 to 184%. All Snake River stocks experienced severely depressed returns in 1994 and 1995.

Standardized escapements for upper Columbia River stocks exhibited a similar trend of decline, beginning in the late 1960's (Fig. 4*b*). Before 1970, escapements ranged from 32 to 337% of their average escapement level. After 1974, escapements ranged from 1 to 161%. Like the Snake River stocks, the upper Columbia River stocks experienced severely depressed returns in 1994 and 1995.

Standardized escapements for the lower Columbia River stocks were quite variable and appeared to show no trend during the past three decades (Fig. 4*c*). Before 1970, escapements ranged from 5 to 234% of their average escapement level. After 1974, escapements in the lower Columbia River index stocks ranged from 9 to 506%.

Escapements for the upriver aggregate run showed a weak upward trend up through the mid-1970's, at which time a major decline was evident (Fig. 2). Before 1970, escapements ranged from 29 to 227% of their average escapement level. After 1974, escapements ranged from 6 to 189%. The upriver run experienced severely depressed returns in 1994 and 1995.

Hypothesis 1. Productivity changes

The majority of index stocks exhibited a decrease in productivity from the pre-1970 period to the post-1974 period;

© 1999 NRC Canada

Fig. 4. Spawner escapements of spring and summer chinook index stocks, standardized to their average escapements (computed for all available brood years through 1990) and plotted on a natural logarithm scale, for the (*a*) Snake, (*b*) upper Columbia, and (*c*) lower Columbia regions. MIN, Minam; IMN, Imnaha; BVE, Bear Valley; MAR, Marsh; SUL, Sulphur; POV, Poverty Flat; JON, Johnson; WEN, Wenatchee; ENT, Entiat; MET, Methow; WIN, Wind; KLI, Klickitat; WS, Warm Springs; JDMA, mainstem John Day; JDMI, Middle Fork John Day; JDNG, North Fork John Day. ln(0) values plotted as 0.01.

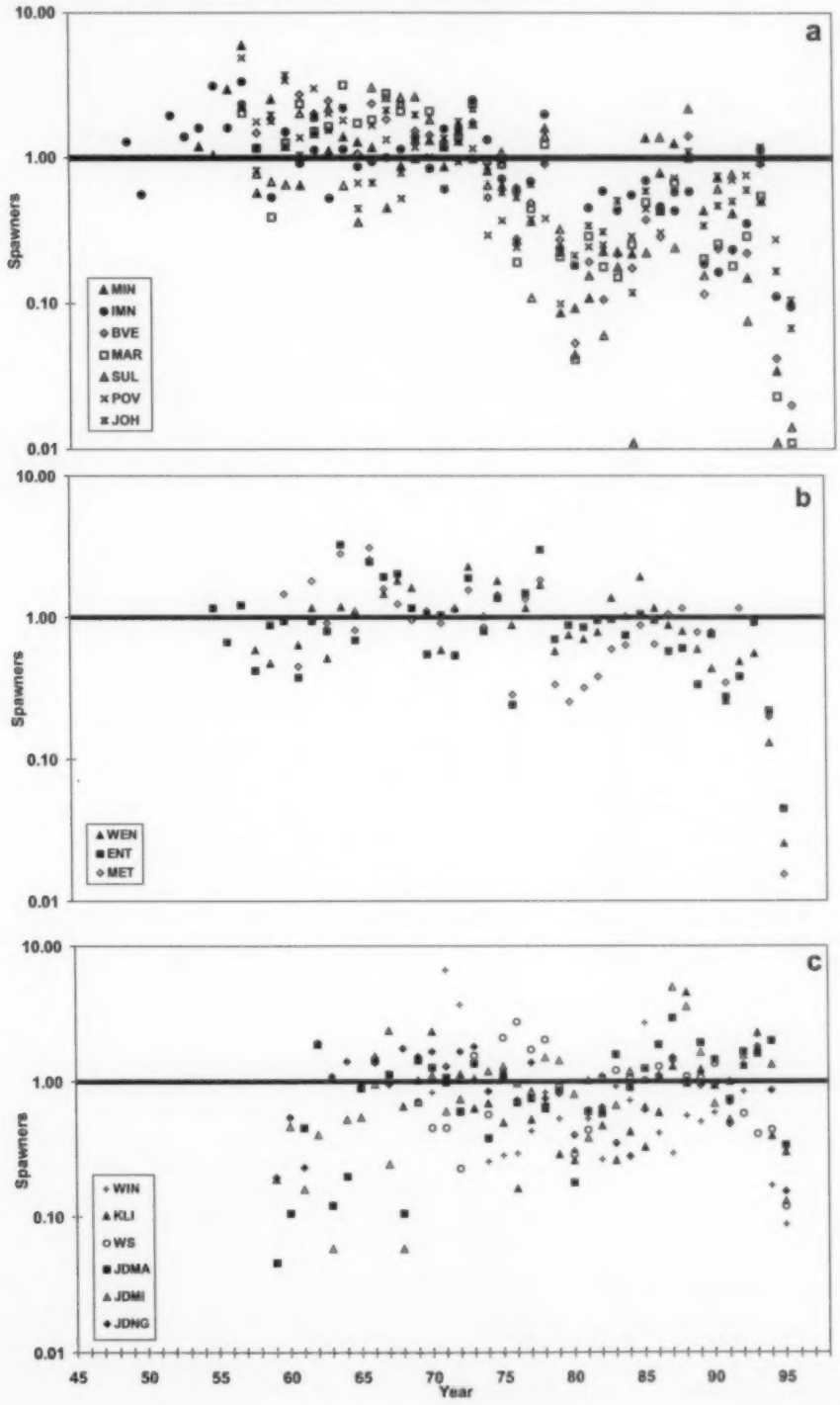

© 1999 NRC Canada

Table 2. ANCOVA results for Ricker recruitment functions using period (treatment) and spawners (covariate) for spring/summer chinook index stocks from the Snake, upper Columbia, and lower Columbia regions and upriver aggregate run.

Region, subbasin	Index stock	Intercept $\tau_1 + a$, pre-1970	Intercept $\tau_2 + a$, post-1974	$\tau_1 - \tau_2$	Intercept H_0: $\tau_1 = \tau_2$, p	SE (τ)	Slope β	Slope H_0: $\beta \leq 0$, p	R^2	Homogeneity of slope, p
Snake										
Middle Fork Salmon	Bear Valley	3.3707	0.7611	2.6096	0.0016	0.7397	0.001309	0.0214	0.36	0.2785
	Marsh	3.7245	0.7134	3.0110	0.0001	0.6464	0.002933	0.0047	0.46	0.1325
	Sulphur	3.3884	0.8709	2.5175	0.0002	0.5818	0.003535	0.0034	0.44	0.5176
South Fork Salmon	Poverty Flat	1.4731	0.7851	0.6880	0.1125	0.4189	0.000368	0.1503	0.10	0.1700
	Johnson	2.1315	0.6829	1.4486	0.0016	0.4123	0.001952	0.0239	0.32	0.5915
Imnaha	Mainstem	2.1318	0.6869	1.4450	0.0001	0.2394	0.000662	0.0002	0.53	0.8842
Grande Ronde	Minam	2.5967	0.6230	1.9737	0.0001	0.4011	0.001556	0.0004	0.49	0.0079
Upper Columbia										
Methow	Mainstem	3.3043	1.6028	1.7014	0.0001	0.3417	0.000725	0.0003	0.56	0.2099
Entiat	Mainstem	2.5445	1.0778	1.4667	0.0001	0.2603	0.002014	0.0009	0.58	0.2398
Wenatchee	Mainstem	2.3930	0.4544	1.9387	0.0001	0.3520	0.000208	0.1661	0.55	0.0684
Lower Columbia										
John Day	Mainstem	2.2200	1.6027	0.6174	0.0188	0.2451	0.003279	0.0001	0.66	0.3814
	Middle Fork	1.7562	1.3519	0.4043	0.2742	0.3613	0.001680	0.0010	0.52	0.0451
	North Fork	2.8774	1.4983	1.3792	0.0001	0.1926	0.000874	0.0001	0.75	0.6614
Upriver aggregate		2.0562	0.4085	1.6477	0.0001	0.1333	0.000016	0.0001	0.79	0.1651

however, the upriver stocks showed greater declines. The ANCOVA tests for differences between periods (pre-1970 and post-1974), in the relationship of $\ln(R/S)$ versus S, were significant for 11 of the 13 stocks tested (Table 2). The two exceptions were Poverty Flat and Middle Fork John Day River. It should be noted that degraded spawning and rearing habitats for these two stocks had shown gradual improvements since the late 1960's and 1970's. In all cases the productivity ($\tau_i + a$) dropped from the pre-1970 period to the post-1974 period (Table 2). Overall, productivity declined more between periods in the Snake River and the upper Columbia River stocks than in the lower Columbia River stocks (Table 2). The average decline in productivity from the pre-1970 period to the post-1974 period was 1.96 in the Snake River stocks, 1.7 in the upper Columbia River stocks, and 0.8 in the lower Columbia River stocks. These reductions in productivity were approximately equal to a decrease in recruits per spawner (in the absence of density dependence) of seven for Snake River stocks, six for upper Columbia River stocks, and two for lower Columbia River stocks. The assumption of a common β between periods (homogeneity of slopes) was plausible for the majority of stocks, since the probability values for the treatment (period) by covariate (spawners) interaction were not significant for 11 of 13 stocks tested (Table 2). Furthermore, the two stocks with significant interactions (Minam and Middle Fork John Day) were from different regions. Because there was no apparent regional pattern to the interactions, the ANCOVA was applied to all the stocks.

Hypothesis 2. Survival rate changes

The pattern of survival rates as measured by SRI-1 (ANCOVA estimate for the pre-1970 brood years) for Snake River and upper Columbia River stocks exhibited a marked decline in the post-1974 brood years (Figs. 5*a* and 5*b*), except for Poverty Flat, which had no apparent pattern. The pattern of SRI-1 for lower Columbia River stocks exhibited little to no decline (Fig. 5*c*). Patterns for SRI-2 were very similar to those for SRI-1, except for the change in scale of the survival rate index (not shown; see Fig. 7 for example).

The survival rate declines were significantly greater, over time, for upriver stocks than for downriver stocks. The means for SRI-1 for the Snake, upper Columbia, and lower Columbia regions were –1.95, –1.70, and –0.80, respectively. For SRI-1, a larger negative value indicated a greater decline from the pre-1970 brood years. The means for the SRI-2 are nearly identical to SRI-1 means except for having opposite signs (Table 3). There were significant regional differences in mean survival rates ($F = 17.03$ and $p < 0.0001$ for SRI-1; $F = 23.96$ and $p < 0.0001$ for SRI-2) (Table 3).

© 1999 NRC Canada

Fig. 5. Deviations of ln[(observed *R/S*)/(predicted *R/S*)] from ANCOVA fit to the pre-1970 period (SRI-1) for the (*a*) Snake, (*b*) upper Columbia, and (*c*) lower Columbia regions, brood years 1949–1990. Abbreviations as described in Fig. 4.

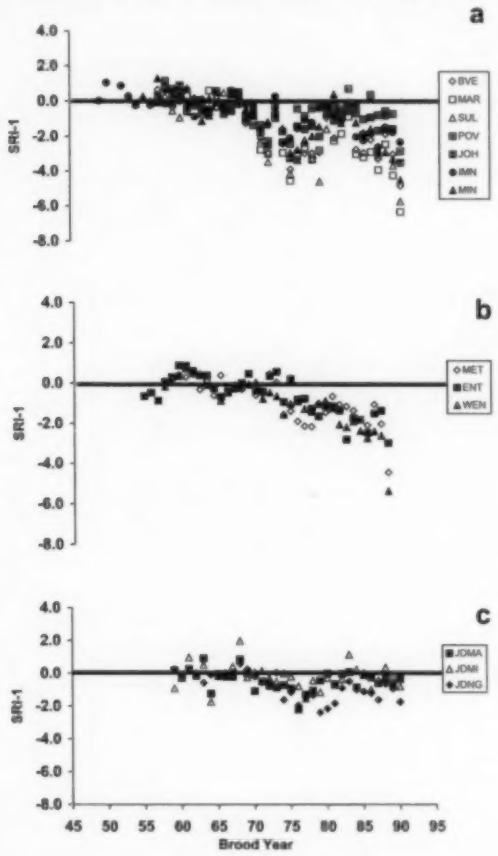

The multiple comparison tests for SRI-1 and SRI-2 indicated no significant difference between Snake and upper Columbia stocks (Table 3). There were significant differences between Snake and lower Columbia stocks and between upper Columbia and lower Columbia stocks (Table 3). The Snake and upper Columbia survival rates declined more over time than lower Columbia indices, as indicated by SRI-1 and SRI-2 (Table 3).

The survival rates of Snake and upper Columbia region stocks became more variable in the post-1974 period than in the pre-1970 period (Table 4). The variance of survival rate indices increased significantly in the post-1974 period for six of 10 Snake and upper Columbia region stocks (Table 4). For the lower Columbia region stocks, variance of survival rate indices increased significantly for one and decreased significantly for another.

Hypothesis 3. Long-term changes in aggregate upriver run

The aggregate upriver run of wild spring chinook for the pre-1970 brood years exhibited higher ln(*R/S*) at *S* than for the 1970–1990 brood years, when escapement levels were fairly similar (Fig. 6). The pre-1970 relationship of ln(*R/S*) versus *S* appeared relatively linear over a long time series (1939–1969). This aggregate wild run, during the pre-1970 brood years, maintained high levels of escapement during a period of substantial harvest rates (Fig. 2). The ln(*R/S*) at *S* of the aggregate upriver run declined after 1969 (Fig. 6). Spawner numbers decreased, even with large reductions in harvest rates. The same temporal pattern was also evident in ln(*R/S*) versus *S* plots for the individual index stocks in the Snake River and upper Columbia River regions (Schaller et al. 1996). These patterns of ln(*R/S*) versus *S* are indicative of a shift in density-independent mortality in the later period.

The productivity of the upriver aggregate run did not exhibit a significant decline until the post-1970 decades. The difference in productivity ($\tau_i + a$) among decades (1939–1949, 1950–1959, 1960–1969, 1970–1979, and 1980–1990) was significant (Table 5). The productivity estimates for the first three decades were 1.93, 2.04, and 1.86. The productivity estimates for the 1970's and 1980's decreased to 0.69 and 0.42. The analysis indicated no significant differences among productivity values for the first three decades (LSMEAN, Table 5). The results indicated a significant difference between the 1970's productivity and those for each of the first three decades and between the 1980's productivity and those for each of the first three decades. The productivity values did not differ significantly between the 1970's and 1980's. The probability value for the treatment (period) by covariate (spawners) interaction was not significant (Table 5), so the assumption of a common β among decades was plausible.

The productivity estimate of the upriver aggregate declined from 2.06 in the pre-1970 period to 0.41 in the post-1974 period (Table 2). The probability value for the treatment (period) by covariate (spawners) interaction was not significant (Table 2).

The survival rates of the upriver aggregate run exhibited a sharp reduction, beginning in the early 1970's. The pattern of SRI-1 (fit to the pre-1970 brood years) for the aggregate upriver run of wild spring chinook exhibited no apparent trend for the pre-1970 brood years (Fig. 7*a*); the post-1970 survival rate indices exhibited a declining pattern. The same pattern was evident for SRI-2 (Fig. 7*b*).

Discussion

We analyzed a wide range of Snake River, upper Columbia River, and lower Columbia River wild spring and summer chinook index stocks to evaluate hypotheses concerning change in productivity and survival rates. The differences in productivity and survival rates between upriver (Snake River and upper Columbia River regions) and downriver (lower Columbia River region) stream-type chinook stocks coincided in space and time with development and operation of the hydropower system. Based on these comparisons of the productivity and survival rate indices among stocks, the effects of increasing hydropower development and operation appear extremely important in the decline of upriver stocks and near extirpation of Snake River spring and summer chinook. The escapement trend comparisons, while less robust measures of stock performance, are consistent with this conclusion.

© 1999 NRC Canada

Table 3. Results of tests for regional differences in survival rate indices.

Parameter, attribute	SRI-1	SRI-2
Productivity estimated from brood years	1949–1969	1975–1990
Comparison brood years	1975–1990	1949–1969
Estimated change in survival rate indices by region		
Snake	–1.9511	1.9222
Upper Columbia	–1.7022	1.6832
Lower Columbia	–0.8003	0.8004
ANOVA, H_0: no region differences in mean survival rate indices		
F	17.03	23.96
p	<0.0001	<0.0001
Reject H_0	Yes	Yes
Pairwise difference		
Snake – upper Columbia	–0.2489	0.2390
Snake – lower Columbia	–1.1509	1.1218
Upper Columbia – lower Columbia	–0.9020	0.8829
Multicomparison test, reject H_0: no significant pairwise region differences		
Snake – upper Columbia	No	No
Snake – lower Columbia	Yes	Yes
Upper Columbia – lower Columbia	Yes	Yes

Table 4. Results of F tests for change in variance between periods based on SRI-1 and SRI-2.

Region, subbasin	Index stock	Variance of pre-1970 deviations	Variance of post-1974 deviations	F	df1, df2	$p > F$	Direction of change
Snake							
Middle Fork Salmon	Bear Valley	0.3015	4.5062	14.95	11, 14	0.000035	+
	Marsh	0.2162	8.2398	38.11	11, 14	0.000000	+
	Sulphur	0.1502	10.6512	70.93	11, 13	0.000000	+
South Fork Salmon	Poverty Flat	0.6414	0.8798	1.37	11, 14	0.302874	0
	Johnson	0.4481	1.0433	2.33	11, 14	0.082588	0
Imnaha	Mainstem	0.3669	0.8152	2.22	18, 14	0.067463	0
Grande Ronde	Minam	0.6393	7.5784	11.86	14, 14	0.000019	+
Upper Columbia							
Methow	Mainstem	0.1541	0.4919	3.19	8, 14	0.051982	0
Entiat	Mainstem	0.4334	1.4469	3.34	13, 14	0.018239	+
Wenatchee	Mainstem	0.2430	0.8537	3.51	10, 14	0.025912	+
Lower Columbia							
John Day	Mainstem	0.4396	0.2607	1.69	9, 14	0.183621	0
	Middle Fork	3.7356	1.0344	3.61	9, 14	0.015747	–
	North Fork	0.1049	0.3408	3.25	9, 14	0.040506	+

Note: Negative or positive direction of change based on significance at $\alpha = 0.05$.

The empirical evidence from spawner and recruit data supported the hypothesis that productivity declined more for those stocks most affected by hydropower development, while lower river stocks have remained relatively stable. All index stocks compared showed some decline in productivity between the pre-1970 and post-1974 periods (non-stationarity). However, productivity estimates declined more in the Snake River and upper Columbia River than in the lower Columbia River.

Available spawner and recruit data from throughout the interior Columbia River basin also supported the hypothesis that survival rate declined and became more variable for those stocks most affected by hydropower development, while lower river stocks have remained relatively stable. All index stocks compared showed some decline in survival rate indices between the pre-1970 and post-1974 periods. However, survival rate, as measured by deviations from recruitment function fit to pre-1970 and post-1974 brood year data, declined significantly more in the Snake and upper Columbia rivers than in the lower Columbia River. The lack of significant interaction between the Ricker β and the period effect implies that the survival rate declines were primarily due to increases in density-independent mortality, consistent with our expectation about the FCRPS. In addition, similar

© 1999 NRC Canada

Fig. 6. ln(*R*/*S*) versus *S* for upriver wild aggregate spring chinook, brood years 1939–1990.

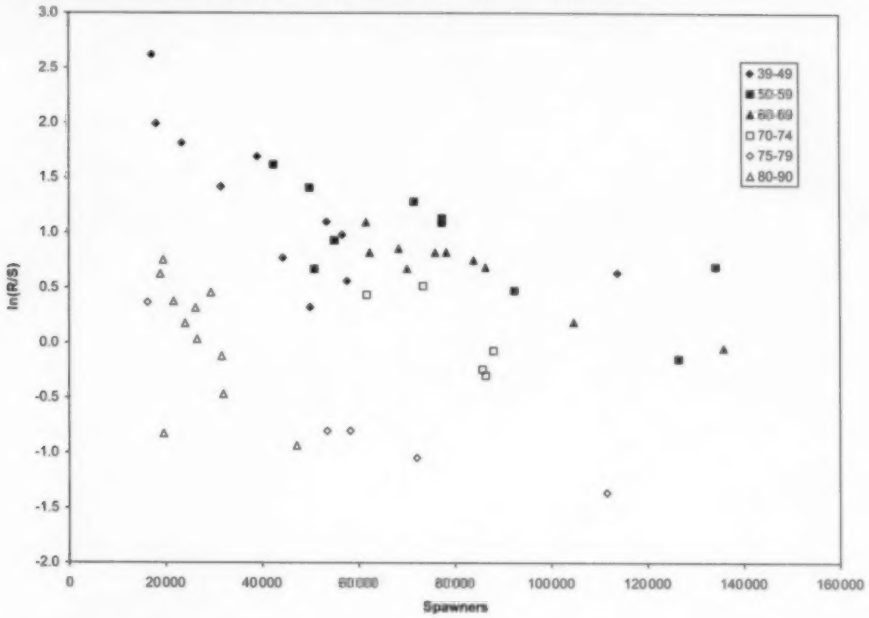

Table 5. ANCOVA for Ricker recruitment functions using period (treatment) and spawners (covariate) for the upriver aggregate wild spring chinook run, 1939–1990 brood years.

Period	Intercept $\tau_i + a$	SE	Intercept H_0: $\tau_i = \tau_j$, p	Slope β	Slope H_0: $\beta \leq 0$, p	R^2	Homogeneity of slope, p
Overall	0.4231	0.1577	0.0001	0.000014	0.0001	0.71	0.4826
1939–1949	1.9263	0.2033					
1950–1959	2.0380	0.2455					
1960–1969	1.8601	0.2537					
1970–1979	0.6903	0.2349					
1980–1990	0.4231						

Results of least squares means tests for differences between periods: t for H_0: LSMEAN(i) = LSMEAN(j)/$p > t$

	1939–1949	1950–1959	1960–1969	1970–1979	1980–1990
1939–1949	1				
1950–1959	0.6138	1			
1960–1969	0.7705	0.3934	1		
1970–1979	0.0001	0.0001	0.0001	1	
1980–1990	0.0001	0.0001	0.0001	0.2612	1

Note: Periods represented decades, with 1939 and 1990 brood years incorporated into the nearest decadal interval.

results were obtained when slopes were allowed to vary by period (i.e., tests of residuals based on log transformation of eq. 1; Schaller et al. 1996).

Spawner and recruit data of the aggregate upriver run of wild spring chinook for brood years 1939–1990 provided little or no evidence of a long-term, gradual decline in productivity and survival rate. Rather, the analyses provided support for the hypothesis that the productivity and survival rate of upriver spring chinook remained fairly stable from early hydropower development (1939) until the era of major hydropower development (about 1970), when major declines began. ANCOVA and least squares means tests found no differences in productivity estimates among the periods 1939–1949, 1950–1959, and 1960–1969. Productivity estimates from the periods 1970–1979 and 1980–1990 were significantly less than those from any of the early periods. This aggregate provides a longer time series of *R*/*S* data than any of the index stocks. The indices of climate change over the Pacific Ocean, which Beamish et al. (1997) linked to sockeye salmon (*Oncorhynchus nerka*) production, varied widely from 1939 to 1970. Interestingly, the productivity of the aggregate remained fairly stable through these decades and then decreased coincident with the period of major hydropower development and operation and similar to productivity changes of the upper basin index stocks. Plots of survival rate indices for the aggregate upriver run also indicated that the major declines in survival rate began about 1970.

We conclude that the dams had a major effect on the de-

© 1999 NRC Canada

Fig. 7. Deviations of ln[(observed *R/S*)/(predicted *R/S*)] from ANCOVA fit to (*a*) pre-1970 data (SRI-1) and (*b*) post-1974 data (SRI-2) for upriver aggregate spring chinook, brood years 1939–1990.

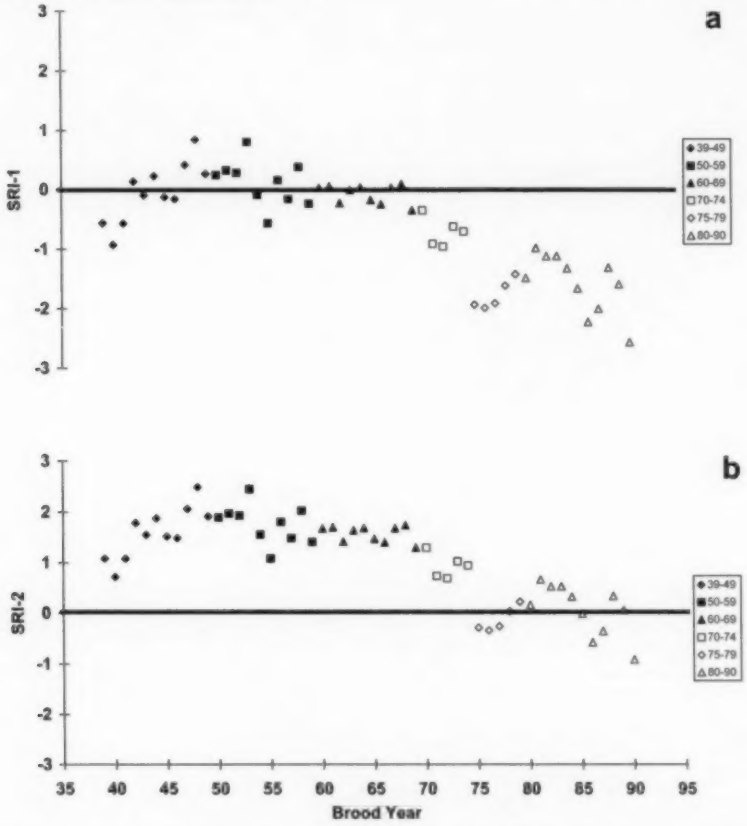

cline of upriver stocks. Our results provide evidence that productivity and survival rates declined more for upriver stocks than for downriver stocks. This differential decline coincided with the development and operation of the FCRPS. As discussed below, we see little evidence of an alternative systematic stressor that selected against upriver stocks, coincident with the declines and unrelated to the hydropower system. Estuary and early ocean conditions do not appear to exert a systematically different effect on survival of stream-type chinook stocks from upriver regions of the interior Columbia River basin. Climatic influences appear to affect populations on large geographic scales. The stocks contrasted in our analysis are similar in life history and overlap in time and space during their early ocean residence (and beyond). Finally, we see little evidence that hatchery, spawning, and rearing habitat or harvest factors could explain the spatial and temporal patterns of stock performance.

Evidence that oceanic influences on salmon populations operate on broad regional scales supports the stock comparison approach within the interior Columbia River basin. Deriso et al. (1996) found evidence of a common year effect for our index stocks of stream-type chinook from the Snake River and lower Columbia River regions. Such a common year effect is consistent with other literature. Beamish and Bouillon (1993) provided evidence that indices of climate over the North Pacific Ocean may play an important role in catch (an index of abundance) of different species of salmon originating over a wide geographic range. Bradford (1994) found common year-to-year trends in spawning escapements of stream-type chinook stocks from widely separated streams of the Fraser River, B.C. Adkison et al. (1996) found that productivity (*R/S*) covaried among sockeye stocks from the Bristol Bay region, Alaska. Peterman et al. (1998) presented evidence that large-scale environmental processes can strongly influence survival rates (residuals from spawner–recruitment relationships) of sockeye on broad regional scales (i.e., Bristol Bay and Fraser River). Their results suggested that, within each of these broad regions, common environmental processes influenced survival rates but that these processes were distinct for the stocks of each region. Furthermore, year of ocean entry appeared to determine variability in survival rate for Bristol Bay sockeye (Peterman et al. 1998).

There are several lines of evidence suggesting that the interior Columbia River basin stream-type chinook stocks are exposed to similar estuary and ocean conditions, particularly during the critical first year. Current hypotheses regarding ocean survival of Pacific salmon generally focus on the juveniles' critical first months at sea (Pearcy 1992), where juveniles of these index stocks are most likely to overlap in time and space. Of the lower Columbia River stocks in this

© 1999 NRC Canada

analysis, at least the John Day River and Warm Springs River spring chinook smolt timing appears very similar to that of Snake River spring and summer chinook. Smolts of these lower Columbia River, Snake River, and upper Columbia River stocks migrate through the mainstem to the estuary primarily in late April and May (Mains and Smith 1964; Raymond 1979; Lindsay et al. 1986, 1989; Hymer et al. 1992). Year-class strength for these spring and summer chinook is apparently established, for the most part, within the first year in the ocean, as evidenced by the ability of fishery managers to predict subsequent adult escapements from jack counts (e.g., Fryer and Schwartzberg 1993).

Since Columbia River basin stream-type chinook share a common estuary and nearshore ocean environment through a critical life stage and have overlapping distributions in later ocean residence, it seems very unlikely that differential estuary and ocean conditions could explain systematic differences in stock survival. Such a factor seemingly would have to operate on later life stages, after juveniles have dispersed from near the Columbia River mouth. Ocean distributions of upriver and downriver stream-type chinook are not well known because ocean recoveries of CWT-marked stream-type chinook have been infrequent. However, the few recaptures (62 recoveries) of 2.1 million tagged smolts released over 8 years from hatchery stocks in both the Snake River (21 recoveries) and lower Columbia River (41 recoveries) were widely scattered from California to Alaska ocean fisheries (Pacific States Marine Fisheries Commission, unpublished data). Finally, the productivity and survival rates of the aggregate spring chinook run, which is weighted heavily by Snake and upper Columbia stocks (Fulton 1968), were relatively stable from 1939 until the era of major hydropower development. It is difficult to imagine an oceanic phenomenon that would have systematically depressed upriver stocks, coincident with, and unrelated to, development of the hydropower system.

It is noteworthy that even the lower Columbia stocks have been affected by hydropower and that a portion of their recent decline may be hydropower related, rather than environmental. John Day River stocks, in particular, were likely subjected to a higher smolt passage mortality at John Day Dam relative to other stocks passing the dam between 1968 and 1984 (Lindsay et al. 1986). Development of the Canadian storage projects in the upper Columbia River in the mid-1970's and hydrosystem regulation have reduced flows during the spring smolt migration for all stream-type chinook (Raymond 1988). Since Columbia River basin stream-type chinook share a common lower river migratory corridor and estuary, changes that may have occurred due to the development of storage projects in the mid-1970's are unlikely to account for the differential decline in productivity and survival rates between the upriver and downriver index stocks.

In order for hatchery, habitat, and harvest factors to have caused the temporal and spatial differences that we observed in stock performance, those factors would also have had to show temporal and spatial differences. Hatchery releases have increased in the post-1974 period for all regions. However, there was little indication that stock performance declined more in index areas directly influenced by hatchery releases. In fact, the Middle Fork Salmon River stocks, which had no direct hatchery releases, showed larger declines in productivity than the other Snake River stocks that had hatchery fish runs. Hatchery programs are for the most part mitigation for hydropower, and therefore, any influences are hard to separate from hydropower impacts. For most index stocks, habitat conditions have been relatively stable over the period of study. Where habitat conditions have changed over time (Poverty Flat and Middle Fork John Day River), we observed improving conditions, which would not induce declines in stock performance. A broad range of habitat conditions were represented in each region, so spatial differences in habitat factors are unlikely to account for differential stock performances. Petrosky and Schaller (1996) did not find decreases in productivity and survival rates (where recruits were measured as smolts entering the hydrosystem during 1964–1995) that could explain the overall decline in Snake River stream-type chinook. We can draw some inferences about harvest impacts by examining the harvest data that we used to adjust recruits. Harvest rates were drastically reduced in response to declines in upriver stream-type chinook abundance. Furthermore, given that the upriver spring chinook stocks share common fisheries (except for some additional tributary harvest in the lower Columbia River stocks), it seems unlikely that differential harvest rates could explain systematic differences in stock performance. We conclude that factors other than hydropower development have not played a significant role in differential decline in performance between upriver and downriver stocks.

Certain concepts and approaches in this paper have applicability to an adaptive management strategy and associated monitoring and evaluation program being considered under the ESA for Snake River and Columbia River spring, summer, and fall chinook and steelhead (*Oncorhynchus mykiss*). Criteria need to be established in terms important to stock survival and recovery. A basinwide monitoring and evaluation program involving index population response needs to be established and tied to those criteria. The spawner and recruit information that we developed for this paper (Beamesderfer et al. 1997) should be continued and augmented with population response data. A core set of information, such as the age, sex, and size composition of escapements and hatchery/wild accounting, coupled with estimates of catch in intercepting fisheries, allows managers to estimate the productivity of individual stocks and to track changes in stock productivity and survival rate over time. Such information, if available for stocks in different geographic areas, would allow managers to understand how healthy stocks perform under natural variations and to better interpret performance of damaged stocks, allowing the design of effective recovery plans.

Fish population responses to recovery actions should be assessed in terms of smolt-to-adult and adult-to-adult survival rates that are sufficiently high for short-term preservation and ultimate recovery and rebuilding. While use of survival rate criteria is key to sound resource decisions, natural variability of survival rates may confound interpretation of responses to management actions. An experimental design for management actions should enable managers to (*i*) test whether treatments produce repeatable effects in situations with similar conditions, (*ii*) distinguish treatment

© 1999 NRC Canada

effects from natural variation, (*iii*) estimate the variance associated with various parameters, and (*iv*) test significance (McAllister and Peterman 1992). Finally, future management actions need to deviate substantially from status quo operations so that experimental designs could be able to distinguish among competing hypotheses for salmon population survival and recovery.

The PATH process was initiated to assist regional fish managers in making long-term hydrosystem management decisions, which need to ensure survival and recovery of Snake River chinook and sockeye. Key to salmon recovery and rebuilding plans will be a determination of whether adequate survival can be attained with existing measures, such as collection and transportation of smolts, or whether other actions will be necessary, including restoring portions of the natural migration corridor. These analyses indicate that mainstem measures to date, including smolt collection and transportation in the Snake River, have not mitigated adequately for hydropower impacts on these stocks. The threatened Snake River spring and summer chinook and depressed upper Columbia River spring chinook have exhibited considerably greater declines in productivity and survival rate in recent years (even with those mitigation measures) than stocks whose migration corridor has been impacted by considerably fewer dams and reservoirs.

Acknowledgments

We thank J. Collie, R. Peterman, C. Walters, and P. Wilson for their helpful review comments on earlier versions of this paper and two anonymous reviewers who provided constructive comments. This study was funded by the U.S. Department of Energy, Bonneville Power Administration contract No. 96BI90134.

References

Adkison, M.D., Peterman, R.M., LaPointe, M.L., Gillis, D.M., and Korman, J. 1996. Alternative models of climate effects on sockeye salmon productivity in Bristol Bay, Alaska, and Fraser River, British Columbia. Fish. Oceanogr. **5**: 137–152.

Beamesderfer, R.C.P., Schaller, H.A., Zimmerman, M.P., Petrosky, C.E., Langness, O.P., and LaVoy, L. 1997. Spawner–recruit data for spring and summer chinook salmon populations in Idaho, Oregon, and Washington. *In* Plan for analyzing and testing hypotheses (PATH): report of retrospective analysis for fiscal year 1997. *Compiled and edited by* D.R. Marmorek and C. Peters. ESSA Technologies Ltd., Vancouver, B.C.

Beamish, R.J., and Bouillon, D.R. 1993. Pacific salmon production trends in relation to climate. Can. J. Fish. Aquat. Sci. **50**: 1002–1016.

Beamish, R.J., Neville, C.M., and Cass, A.J. 1997. Production of Fraser River sockeye salmon (*Oncorhynchus nerka*) in relation to decadal-scale changes in the climate and the ocean. Can. J. Fish. Aquat. Sci. **54**: 543–554.

Berggren, T.J., and Filardo, M.J. 1993. An analysis of variables influencing the migration of salmonids in the Columbia River Basin. North Am. J. Fish. Manage. **13**: 48–63.

Berkson, J. 1991. Coded wire tag analysis on Snake River spring, summer, and fall chinook. Letter dated February 19, 1991, to the National Marine Fisheries Service for Endangered Species Act record. Columbia River Inter-Tribal Fisheries Commission, Portland, Oreg.

Bradford, M.J. 1994. Trends in abundance of chinook salmon (*Oncorhynchus tshawytscha*) of the Nechako River, British Columbia. Can. J. Fish. Aquat. Sci. **51**: 965–973.

Deriso, R., Marmorek, D., and Parnell, I. 1996. Retrospective analysis of passage mortality of spring chinook of the Columbia River. *In* Plan for analyzing and testing hypotheses (PATH): final report of retrospective analysis for fiscal year 1996. *Compiled and edited by* D.R. Marmorek and 21 coauthors. ESSA Technologies Ltd., Vancouver, B.C.

Freund, R.J., LiHell, R.C., and Spector, P.C. 1986. SAS system for linear models. SAS Institute, Inc., Cary, N.C.

Fryer, J.K., and Schwartzberg, M. 1993. Age and length composition of Columbia Basin spring and summer chinook salmon at Bonneville Dam in 1992. CRITFC Tech. Rep. 93-3. Columbia River Inter-Tribal Fisheries Commission, Portland, Oreg.

Fulton, L.A. 1968. Spawning areas and abundance of chinook salmon (*Oncorhynchus tshawytchsa*) in the Columbia River Basin — past and present. U.S. Dep. Interior Fish Wildl. Serv. Spec. Sci. Rep. Fish. 571.

Healy, M. 1991. Life history of chinook salmon. *In* Pacific salmon life histories. *Edited by* C. Groot and L. Margolis. University of British Columbia Press, Vancouver, B.C. pp. 313–391.

Hilborn, R., and Walters, C.J. 1992. Quantitative fisheries stock assessment: choice, dynamics & uncertainty. Chapman and Hall, New York.

Hymer, J.A., Pettit, R., Wastel, M., Hahn, P., and Hatch, K. 1992. Stock summary reports for Columbia River anadromous salmonids. Vol. IV. Washington. Coordinated information system. Prepared for U.S. Department of Energy, Bonneville Power Administration, Portland, Oreg. Project 88-108. Contract DE-FC79-89BP94402.

Lindsay, R.B., Knox, W.J., Flesher, M.W., Smith, B.J., Olsen, E.A., and Lutz, L.S. 1986. Study of wild spring chinook salmon in the John Day River system. Oregon Department of Fish and Wildlife 1985 Final Report. Prepared for U.S. Department of Energy, Bonneville Power Administration, Portland, Oreg. Project 79-4. Contract DE-AI79-83BP39796.

Lindsay, R.B., Jonasson, B.C., Schroeder, R.K., and Cates, B.C. 1989. Spring chinook salmon in the Deschutes River, Oregon. Oreg. Dep. Fish Wildl. Inf. Rep. 89-4.

Mains E.M., and Smith, J.M. 1964. The distribution, size, time and current preferences of seaward migrant chinook salmon in the Columbia and Snake rivers. Wash. Dep. Fish. Res. Pap. 3. pp. 5–43.

McAllister, M.K., and Peterman, R.M. 1992. Decision analysis of a large-scale fishing experiment designed to test for a genetic effect of size-selective fishing on British Columbia pink salmon (*Oncorhynchus gorbuscha*). Can. J. Fish. Aquat. Sci. **49**: 1305–1314.

Milliken, G.A., and Johnson, D.A. 1984. Analysis of messy data. Vol.1. Designed experiments. Lifetime Learning Publications, Belmont, Calif.

Mundy, P.R., Neeley, D., Steward, C.R., Quinn, T.P., Barton, B.A., Williams, R.N., Goodman, D., Whitney, R.R., Erho, M.W., and Botsford, L.W. 1994. Transportation of juvenile salmonids from hydroelectric projects in the Columbia River Basin; an independent peer review. Final Report. U.S. Fish and Wildlife Service, Portland, Oreg.

Neave, F. 1953. Principles affecting the size of pink and chum salmon populations in British Columbia. J. Fish. Res. Board Can. **9**: 450–491.

© 1999 NRC Canada

NMFS (National Marine Fisheries Service). 1995. Biological opinion: reinitiation of consultation on 1994–1998 operations of the Columbia River power system and juvenile transportation program in 1994–1998. Endangered Species Act, section 7 consultation. NMFS, Portland, Oreg.

ODFW and WDFW (Oregon Department of Fish and Wildlife and Washington Department of Fish and Wildlife). 1995. Status report: Columbia River fish runs and fisheries, 1938–94. Oregon Department of Fish and Wildlife, Portland, Oreg.

Pearcy, W.G. 1992. Ocean ecology of North Pacific salmonids. University of Washington Press, Seattle, Wash.

Peterman, R.M. 1981. Form of random variation in salmon smolt-to-adult relations and its influence on production estimates. Can. J. Fish. Aquat. Sci. **38**: 1113–1119.

Peterman, R.M., Pyper, B.J., Lapointe, M.F., Adkison, M.D., and Walters, C.J. 1998. Patterns of covariation in survival rates of British Columbian and Alaskan sockeye salmon (*Oncorhynchus nerka*) stocks. Can. J. Fish. Aquat. Sci. **55**: 2503–2517.

Petrosky, C.E., and Schaller, H.A. 1992. A comparison of productivities for Snake River and Lower Columbia River spring and summer chinook stocks. Proceedings of Salmon Management in the 21st Century: Recovering Stocks in Decline. 1992 Northeast Pacific Chinook and Coho Workshop. American Fisheries Society, Idaho Chapter, Boise, Idaho.

Petrosky, C.E., and Schaller, H.A. 1996. Evaluation of productivity and survival rate trends in freshwater spawning and rearing life stage for Snake River spring and summer chinook *In* Plan for analyzing and testing hypotheses (PATH): final report of retrospective analysis for fiscal year 1996. *Compiled and edited by* D.R. Marmorek and 21 coauthors. ESSA Technologies Ltd., Vancouver, B.C.

Raymond, H.L. 1979. Effects of dams and impoundments on migrations of juvenile chinook salmon and steelhead from the Snake River, 1966–1975. Trans. Am. Fish. Soc. **90**: 58–72.

Raymond, H.L. 1988. Effects of hydroelectric development and fisheries enhancement on spring and summer chinook salmon and steelhead in the Columbia River Basin. North Am. J. Fish. Manage. **8**:1–24.

Ricker, W.S. 1975. Computation and interpretation of biological statistics of fish populations. Bull. Fish. Res. Board Can. 191.

SAS. 1993. SAS/STAT users guide, version 6, edition 4. Vol. 2. SAS Institute, Inc., Cary, N.C.

Schaller, H., Petrosky, C., and Langness, O. 1996. Contrasts in stock recruitment patterns of Snake and Columbia River spring and summer chinook. *In* Plan for analyzing and testing hypotheses (PATH): final report of retrospective analysis for fiscal year 1996. *Compiled and edited by* D.R. Marmorek and 21 coauthors. ESSA Technologies, Ltd., Vancouver, B.C.

Walters, C.J. 1987. Nonstationarity of production relationships in exploited populations. Can. J. Fish. Aquat. Sci. **44**(Suppl. 2): 156–165.

Walters, C.J. 1990. A partial bias correction factor for stock–recruitment parameter estimation in the presence of autocorrelated environmental effects. Can. J. Fish. Aquat. Sci. **47**: 516–519.

© 1999 NRC Canada

Patterns of covariation in length and age at maturity of British Columbia and Alaska sockeye salmon (*Oncorhynchus nerka*) stocks

Brian J. Pyper, Randall M. Peterman, Michael F. Lapointe, and Carl J. Walters

Abstract: We examined patterns of covariation in age-specific adult body length and in mean age at maturity among 31 sockeye salmon (*Oncorhynchus nerka*) stocks from western Alaska to southern British Columbia. Positive covariation in body length was prevalent across stocks of all regions (e.g., correlations (r) from 0.2 to 0.6), suggesting either that growth periods critical to final body length of sockeye salmon occur while ocean distributions of these stocks overlap or that large-scale environmental processes influence these stocks similarly while they do not overlap. We also found stronger covariation among body length of stocks within regions (r from 0.4 to 0.7), indicating that unique regional-scale processes were also important. Mean age at maturity also showed positive covariation both among and within regions, but correlations were weaker than those for length. We also examined patterns of covariation between length and mean age at maturity and between these variables and survival rate. Although length and mean age at maturity were negatively correlated, there was little evidence of covariation between these variables and survival rate, suggesting that environmental processes that influence marine survival rates of sockeye salmon are largely different from those affecting size and age at maturity.

Résumé : Nous avons examiné les profils de covariation de la longueur selon l'âge des adultes et de l'âge moyen à la maturité chez 31 stocks de saumon rouge (*Oncorhynchus nerka*) répartis de l'ouest de l'Alaska au sud de la Colombie-Britannique. On a observé une covariation positive de la longueur corporelle dans les stocks de toutes les régions (r = 0,2 à 0,6), ce qui laisse penser que les périodes de croissance qui déterminent la longueur corporelle finale des saumons rouges ont lieu quand les distributions océaniques de ces stocks se chevauchent, ou que des processus environnementaux à grande échelle ont des effets similaires sur ces divers stocks en l'absence de chevauchement. Nous avons aussi observé une covariation plus forte des longueurs corporelles dans les stocks à l'intérieur des régions (r = 0,4 à 0,7), ce qui indique que des processus régionaux particuliers étaient aussi importants. L'âge moyen à la maturité a aussi montré une covariation positive tant d'une région à l'autre qu'à l'intérieur des régions, mais les corrélations étaient plus faibles que pour la longueur. Nous avons aussi examiné les profils de covariation entre la longueur et l'âge moyen à la maturité, et entre ces variables et le taux de survie. Tandis que la longueur et l'âge moyen à la maturité étaient négativement corrélés, il ne semblait pas y avoir une covariation évidente entre ces variables et le taux de survie, ce qui laisse penser que les processus environnementaux qui influent sur les taux de survie du saumon rouge sont nettement différents de ceux qui déterminent la taille et l'âge à la maturité.

[Traduit par la Rédaction]

Introduction

Harvestable biomass for a given stock of sockeye salmon (*Oncorhynchus nerka*) is influenced by year-to-year variation in three recruitment processes: survival rate from eggs to adults, somatic growth rate (reflected by body size at maturity), and age at maturity. Although survival rates are typically the largest source of variation, variability in body size and age at maturity can also be important. For instance, interannual variability in size and age at maturity of sockeye salmon can affect the tonnage and economic value of catches, reproductive success of spawners (Healey 1987), and forecasts of available biomass (e.g., Fried and Yuen 1987). Furthermore, understanding more about what causes variation in size and age at maturity may be important for forecasting the effects of climate change on these variables (e.g., Hinch et al. 1995) or for evaluating and designing enhancement strategies (Peterman 1991).

Research has shown that variability in both size and age at maturity of sockeye salmon is affected by parental mechanisms (genetic and maternal effects) as well as environmental processes. For instance, Ricker (1972) and Wood and Foote (1996) documented genetic effects on growth rate and age at maturity, while Bilton (1970) and Bradford and Peterman (1987) demonstrated nongenetic maternal effects on age at maturity. Genetic effects also create the possibility that

Received August 28, 1998. Accepted February 16, 1999. J14774

B.J. Pyper, R.M. Peterman,[1] and M.F. Lapointe.[2] School of Resource and Environmental Management, Simon Fraser University, Burnaby, BC V5A 1S6, Canada.
C.J. Walters. Fisheries Centre, University of British Columbia, Vancouver, BC V6T 1Z4, Canada.

[1]Author to whom all correspondence should be addressed. e-mail: peterman@sfu.ca
[2]Present address: Pacific Salmon Commission, 600-1155 Robson St., Vancouver, BC V6E 1B5, Canada.

© 1999 NRC Canada

size-selective fishing might influence size and age at maturity over time; however, there is little evidence of such effects in sockeye salmon (Ricker 1982, 1995). In addition, environmental factors are also known to affect body size and age at maturity. For example, researchers have shown that adult body size of Bristol Bay (Alaska) and British Columbia sockeye salmon stocks is affected by ocean abundances of competing sockeye salmon stocks and oceanographic conditions such as sea surface temperature (Rogers 1980, 1984, 1987; Peterman 1984; Rogers and Ruggerone 1993; McKinnell 1995; Cox and Hinch 1997).

Although previous studies of size and age at maturity identified some important environmental sources of variation, they did not address two important questions. First, what are the spatial scales over which environmental processes affect size and age at maturity of sockeye salmon? Are they specific to stocks in a region or do they affect stocks throughout the northeastern Pacific Ocean? Second, to what extent do environmental processes simultaneously influence the three components of recruitment of sockeye salmon biomass: size at maturity, age at maturity, and survival rate?

Thus, our first objective was to identify spatial and temporal characteristics of environmental processes that drive variation over time in size and age at maturity of sockeye salmon. To do this, we used a comparative, multistock approach similar to that used in a companion paper (Peterman et al. 1998) on patterns of covariation in survival rates of sockeye salmon stocks. Here, we examine patterns of covariation in size and age at maturity for sockeye salmon stocks over a wide geographical area from western Alaska to southern British Columbia: Bristol Bay, Upper Cook Inlet, Copper River, central British Columbia (Skeena River and Nass River stocks), and Fraser River, B.C.

Our comparative analysis was based on "natural experiments" created by the different durations and extent of spatial overlap during ocean migrations of various cohorts of these stocks. Alternative hypotheses about ocean distributions of stocks and spatial scales of environmental processes lead to different predictions for patterns of covariation. For instance, one hypothesis is that size at maturity is primarily determined by unique, regional-scale environmental processes that influence growth when stocks of a given region (e.g., Bristol Bay stocks or Fraser River stocks) share distributions that are distinct from stocks of other regions. If this hypothesis is true, we expect to find positive covariation in body size among stocks within each region but not among stocks of different regions. Alternatively, if, during growth periods critical to final body size, stocks of different regions share ocean distributions or are jointly influenced by large-scale processes, then we expect to find positive covariation in body size both among regions and within regions. Analogous hypotheses and associated predictions apply to age at maturity.

Our second objective was to examine patterns of covariation between size and age at maturity and between each of these components of recruitment and the survival rates of Peterman et al. (1998). We examined across-component correlations because environmental processes such as favorable ocean conditions for growth may simultaneously affect more than one component of recruitment. The extensive data set (up to 41 years, 31 stocks) available for sockeye salmon allowed a unique examination of such relationships.

Methods

Data

Juvenile sockeye salmon usually rear one or two winters in freshwater lakes and then migrate to the ocean where they spend two or three winters before returning to their natal streams to spawn. We use European age designations where, for example, 1.2 represents a sockeye salmon that spent one winter in a lake and two winters in the ocean before maturing. This corresponds to age 4_2 in the Gilbert–Rich notation, and 2.2 corresponds to 5_3 (see Burgner 1991 for age designations).

Length at a given age

We used 72 time series of length at age data as indices of somatic growth rate for 31 sockeye salmon stocks or stock complexes (i.e., sockeye salmon returning to a river or lake system, which could comprise various spawning populations). For Bristol Bay sockeye salmon, we used mean lengths (mideye to fork) of age 1.2, 1.3, 2.2, and 2.3 female spawners for eight stocks (Egegik, Igushik, Kvichak, Naknek, Nuyakuk, Togiak, Ugashik, and Wood River) over return years 1957–1997 (up to 1988 for Nuyakuk; B. Cross, Alaska Department of Fish and Game, Anchorage, Alaska, personal communication). For the Upper Cook Inlet stock, we examined eight time series consisting of mean lengths (mideye to fork) of age 1.2, 1.3, 2.2, and 2.3 spawners (weighted average of both sexes) of the Kasilof and Kenai rivers over return years 1967–1997 (D. Waltemyer, Alaska Department of Fish and Game, Soldotna, Alaska, personal communication). Three time series were examined for the Copper River stock, consisting of mean lengths (mideye to fork) of age 1.2, 1.3, and 2.3 females harvested in Copper River District drift gillnet fisheries over return years 1968–1997 (J. Wilcock, Alaska Department of Fish and Game, Cordova, Alaska, personal communication). For the Skeena River stock, time series were calculated for age 1.2 and 1.3 female spawners over return years 1964–1997 by averaging (using standardized residuals) mean lengths (nose to fork) from four escapement sites (Fulton River, Pinkut Creek, and the two Fulton River spawning channels; D. Plotnikoff, Department of Fisheries and Ocean, Vancouver, B.C., personal communication). For Fraser River sockeye salmon, we examined 27 time series consisting of mean lengths (nose to hypural plate) of age 1.1 male spawners (jacks) of five stocks (Birkenhead, Cultus, Chilko River, Gates, and Weaver) over return years 1951–1997, mean lengths of age 1.2 female spawners of 20 stocks (Lower Adams, Birkenhead, Bowron, Chilko River, Cultus, Early Stuart, Fennel, Gates, Upper Horsefly, the Middle and Tachie River populations of the Late Stuart stock, Nadina, Pitt, Portage, Raft, Scotch, Seymour, Lower Shuswap, Stellako, and Weaver) over return years 1952–1997, and mean lengths of age 1.3 female spawners of two stocks (Birkenhead and Pitt) over return years 1953–1997 (J. Woodey, Pacific Salmon Commission, Vancouver, B.C., personal communication).

Mean age at maturity

We computed 32 time series of mean ocean age at maturity using recruitment data (catch plus escapement) described in Peterman et al. (1998). For each available brood year, we calculated mean ocean age separately for age 1.*x* recruits (i.e., all recruits that spent one winter in a lake) and age 2.*x* recruits. Sufficient data were available to calculate mean age of 1.*x* and 2.*x* recruits for nine Bristol Bay stocks (those noted previously plus the Branch stock) over brood years 1952–1991 (up to 1982 for Nuyakuk), the Upper Cook Inlet stock over brood years 1968–1991, the Copper

© 1999 NRC Canada

River stock over brood years 1961–1991, and the Nass River stock over brood years 1967–1991. Because Skeena River recruits were predominantly age 1.*x*, mean age was calculated only for recruits of this freshwater age group over brood years 1948–1992. In contrast with the more northern stocks examined, recruits of Fraser River stocks were predominantly age 1.2, with few 1.1, 1.3, or 2.*x* adults. Thus, we calculated mean age of 1.*x* recruits for only seven stocks (Birkenhead, Bowron, Chilko, Pitt, Raft, Stellako, and Weaver), which had at least 10% of age 1.*x* recruits other than age 1.2, over brood years 1948–1992.

Indices of survival rate

Indices of survival rate were developed by Peterman et al. (1998). These consisted of (*i*) residuals from the best-fit Ricker model (referred to here as spawner-to-recruit survival rates) for nine Bristol Bay stocks, the Cook Inlet, Copper, Nass, and Skeena stocks, and 16 Fraser River stocks, (*ii*) marine survival rates (i.e., smolt-to-adult survival rate) for four Bristol Bay stocks (Egegik, Kvichak, Ugashik, and Wood), the Skeena stock, and one Fraser River stock (Chilko), and (*iii*) "aggregated" spawner-to-recruit survival rates for Bristol Bay and Fraser River computed by averaging across their nine and 16 stocks, respectively (see Peterman et al. 1998 for details).

Statistical analysis

Autocorrelation and time trends

Positive autocorrelation and time trends were present in many of the time series of length, mean age, and survival rate. This indicates that low-frequency (i.e., slowly changing) variability is an important feature of these data. However, in standard inference tests of correlations, autocorrelation and time trends increase the chance that statistically significant but spurious correlations will occur (i.e., Type I error rates will be greater than the specified alpha). Thus, fisheries researchers often remove autocorrelation or time trends from data before computing and testing correlations (e.g., Thompson and Page 1989). Unfortunately, if low-frequency sources of variability are also sources of real covariation among data, then their removal can greatly reduce that covariation and the statistical power to detect it (Pyper and Peterman 1998). In other words, much of the "signal", or evidence of an environmental process experienced in common by different sockeye salmon stocks, might be lost.

We therefore used two approaches to examine correlations. First, we computed correlations using the original time series and based significance tests on the method recommended by Pyper and Peterman (1998), which adjusts degrees of freedom to account for autocorrelation. This test procedure is effective at maintaining Type I error rates near the specified alpha when autocorrelated data can be represented by simple, stationary time series models; however, it may not completely guard against spurious correlations caused by independent time trends. Thus, *P* values reported here may overstate significance levels in some cases. Our second approach was to first-difference the time series (subtract each data point from the next) and recompute correlations. First-differencing is often an effective method for removing positive autocorrelation and time trends from data (Thompson and Page 1989). Furthermore, when real covariation is largely due to low-frequency sources of variability, first-differencing is particularly effective at removing that covariation (Pyper and Peterman 1998). Thus, first-differencing allowed us to quantify the potential importance of low-frequency sources of covariation. For example, if correlations are systematically reduced after first-differencing, this provides evidence that slow-changing processes may be an important and shared source of variation in the data.

In addition, in some analyses described below, we compared correlations between data series at two or more time lags. However, if a real correlation exists at a given lag between two autocorrelated time series, large but spurious correlations are expected at adjacent time lags (Jenkins and Watts 1968). The test procedure described by Pyper and Peterman (1998) is not appropriate in this case. Again, a standard recommendation is to remove autocorrelation from data before computing correlations at multiple time lags (Jenkins and Watts 1968). To remove autocorrelation for these analyses, we used prewhitening (i.e., fitting an appropriate time series model to the data and using the residuals to compute correlations) rather than first-differencing because in some cases, first-differencing produced negative autocorrelation, which also creates problems when testing correlations at multiple lags.

Average correlations and combining groups of time series

To simplify presentation of results, we report average correlations for some groups of comparisons. These averages were calculated using the Fisher *z* transform of each correlation coefficient to normalize them (Zar 1984). In addition, for some analyses, we combined length or mean age data from stocks within regions into single time series, referred to as "aggregated" data series. These aggregated series were computed by first standardizing each stock-specific time series to have zero mean and unit variance and then averaging values across stocks within a region for a given year. Such aggregated data series will better depict the variability that is shared by a group of stocks (Thompson and Page 1989).

Patterns of covariation in length at age

To test the previously stated hypotheses about environmental sources of variation in adult size, we examined patterns of covariation among length at age data both within and between regions. We calculated Pearson product-moment correlation coefficients for pairwise comparisons among the 72 time series of lengths, aligned to have the same return year (year in which they returned to their natal streams), giving a total of 2556 (i.e., $(N^2 - N)/2$) comparisons. Length series were aligned to have return years in common because recent research suggests that interannual variability in body size of recruits is largely determined by growth in their final year at sea (Rogers and Ruggerone 1993; McKinnell 1995).

We used principal components analysis (PCA) to further examine spatial and temporal covariation among lengths. Our purpose here was to reduce patterns of variability shared by each age class and region to a few defining time series (principal components (PC's)). For this analysis, we used region-specific aggregated lengths at age, computed across stocks in the Bristol Bay, Cook Inlet, and Fraser River regions, because these aggregated lengths should better depict the signal common to stocks in each region. Stock-specific lengths at age were used for the Copper and Skeena stocks to represent these two geographically distinct regions. We restricted this analysis to those years for which data were available for all length series and examined unrotated PC's with eigenvalues greater than 1 (Pielou 1977). To examine the importance of low-frequency sources of variability, we repeated the correlation analyses using first-differenced data.

Causes of patterns of covariation in length at age: conditions in early or late marine life?

Rogers and Ruggerone (1993) and McKinnell (1995) suggested the importance of late marine life in determining adult length. However, it is conceivable that interannual variability in adult length might also be heavily influenced by conditions during early marine life (e.g., first year at sea), when growth in length is proportionally the greatest (reviewed by Burgner 1991). The relative importance of early versus late marine life can be examined using lengths of fish with different ocean ages. For example, age *x*.2 and *x*.3 fish that enter the ocean in the same calendar year (referred to as ocean-entry year (OEY)) are at sea together during their first

© 1999 NRC Canada

Fig. 1. Summary of stock-specific, pairwise correlations among lengths of Bristol Bay (BB), Cook Inlet (CK), Copper River (CP), Skeena River (SK), and Fraser River (FR) stocks by age group (1.2, 1.3, etc.). For all comparisons involving Bristol Bay, Cook Inlet, and Fraser River stocks, cells in the matrix show average correlations. For example, the r of 0.29 for BB(1.2) versus SK(1.2) is the average of the eight sample correlations between the Skeena 1.2 length series and the 1.2 length series for the eight Bristol Bay stocks. Levels of shading, defined in the legend, reflect different ranges of correlations.

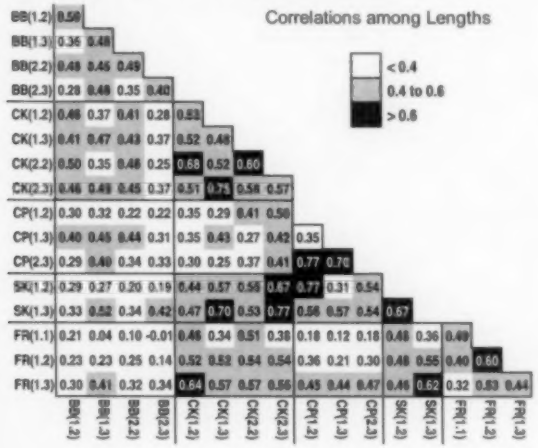

2 years but do not share their final year at sea. In comparison, the final year is shared by age groups that return in the same year (see life history time lines in Peterman 1985). Thus, to examine the importance of early versus late marine life (i.e., final year at sea), we compared correlations among lengths of fish with different ocean ages using data aligned by OEY with correlations between these lengths aligned by return year. We made these comparisons using aggregated length series for a given region to limit the influence of measurement error. Because lengths were autocorrelated and correlations were computed at two time lags (i.e., OEY and return year), we computed correlations using both prewhitened data and original data to help discern between real and spurious correlations.

Patterns of covariation in mean age at maturity

To examine within-region and between-region patterns of covariation in mean age at maturity, we used analyses similar to those used for length. Correlations were calculated for pairwise comparisons among the 32 time series of mean age, aligned by OEY, giving 496 comparisons. Time series for age 1.x and 2.x fish were aligned by OEY because research suggests that environmental processes influence age at maturity of sockeye salmon during their early marine life (i.e., first 2 years in the ocean; Peterman 1985). Aggregated mean ages were computed for Bristol Bay and Fraser River stocks, respectively. We used these aggregates along with mean ages for the Cook, Copper, Nass, and Skeena stocks in a PCA. To examine the importance of low-frequency sources of variability, we repeated the correlation analyses using first-differenced data.

Patterns of covariation across the three components of sockeye salmon recruitment

To determine whether similar environmental processes influenced each of the three components of recruitment biomass of sockeye salmon, within-stock correlations were examined for the following comparisons: (*i*) length versus mean age, (*ii*) length versus survival rate, and (*iii*) mean age versus survival rate. Time series were aligned where covariation might be expected due to shared environmental influences (discussed in detail below). We repeated these comparisons using aggregated lengths, mean ages, and survival rates of the Bristol Bay, Cook Inlet, and Fraser River regions, where applicable.

Fig. 2. Histograms of correlations between lengths of age 1.2 sockeye salmon for comparisons (A) among Bristol Bay stocks (all 28 correlations positive; 23 significant at $P < 0.05$), (B) among Fraser River stocks (all 190 correlations positive; 161 significant), and (C) between Bristol Bay and Fraser River stocks (136 of 160 correlations positive; 25 significant positive correlations). Averages of these three sets of correlations are shown in Fig. 1. Open bars represent negative correlations; solid bars are positive correlations.

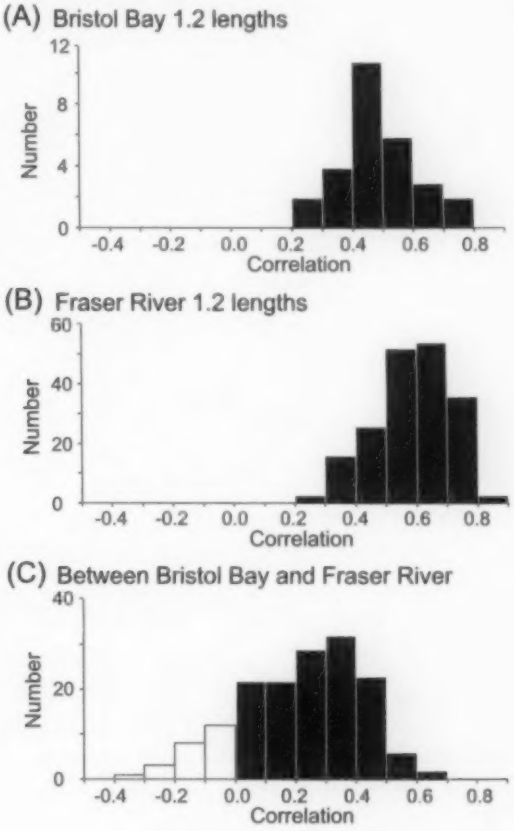

Results and discussion

Length at a given age

There was widespread positive covariation among the 72 body length time series, aligned by return year, both across stocks and across ages (Fig. 1). Of the 2556 correlations, 2335 were positive (43%, or 1006, of these were significant at $P < 0.05$) and only 221 were negative (with just three significant). The average of all correlations was 0.37.

These correlations provide strong evidence of positive covariation between regions as well as distinct patterns of

© 1999 NRC Canada

Fig. 3. Time series of region-specific lengths at age for various sockeye salmon stocks. Regional aggregated lengths (e.g., aggregated across the eight Bristol Bay 1.2 data series) are shown for Bristol Bay, Cook Inlet, and Fraser River stocks, whereas standardized lengths at age are given for the Copper River and Skeena River stocks.

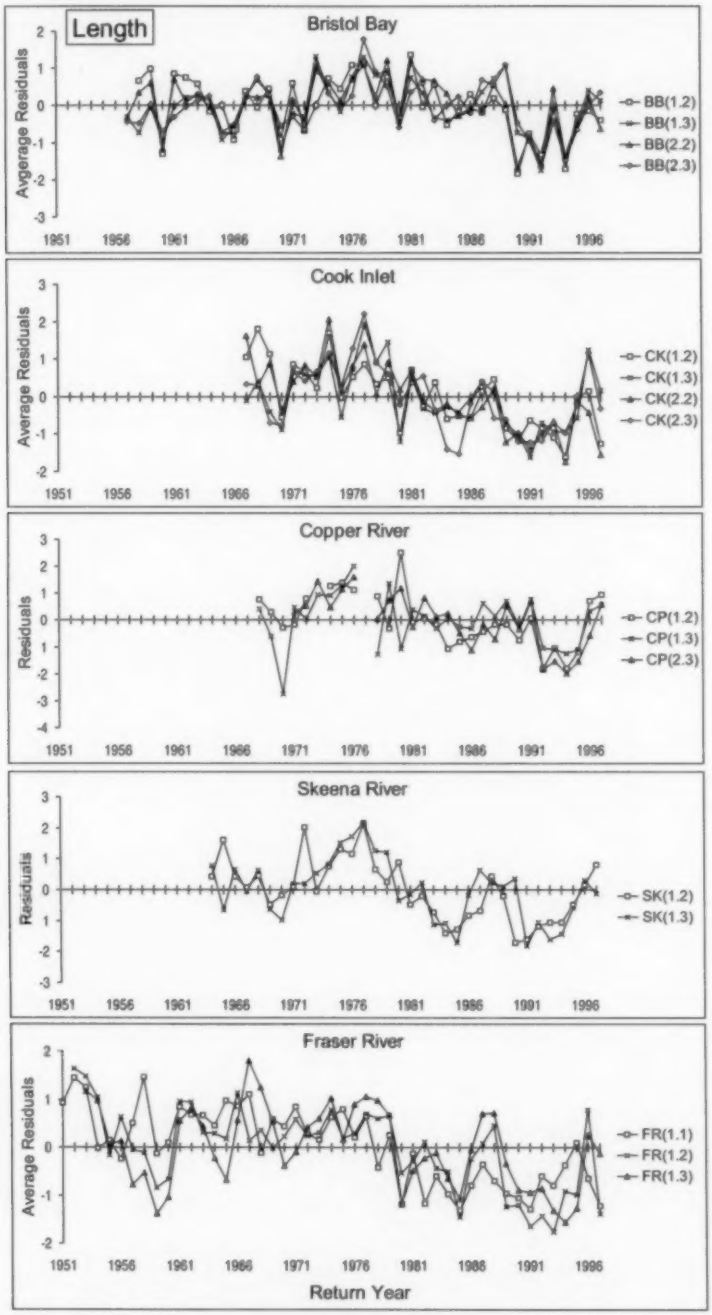

covariation within regions. The first is indicated by the predominance of positive correlations among lengths of stocks from different regions (e.g., Cook Inlet versus Fraser River; Fig. 1). Evidence of additional within-region covariation is provided by the generally larger correlations among lengths of stocks in the same region (e.g., larger correlations within Bristol Bay than between Bristol Bay and other regions; Fig. 1). This different strength of within-region and between-region covariation was most obvious among Bristol Bay and Fraser River sockeye salmon, for which we had data from

© 1999 NRC Canada

Fig. 4. Correlations (loadings) between the 16 length data series in Fig. 3 and the time series (scores) of the second and third principal components of the body length PCA. Regions or stocks are identified along with age designations (1.2, 2.3, etc.).

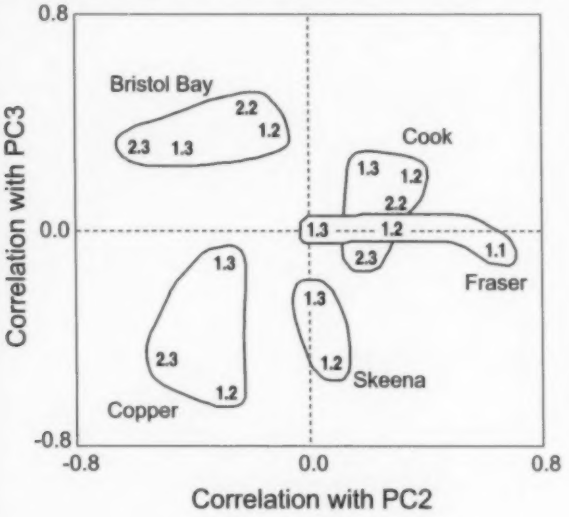

numerous stocks. For example, there was a tendency toward strong positive correlations among the eight Bristol Bay 1.2 length series (average $r = 0.50$; Fig. 2A) and among the 20 Fraser 1.2 data (average $r = 0.60$; Fig. 2B) but weaker, yet still predominantly positive, correlations between 1.2 lengths from these two geographically distinct regions (average $r = 0.23$; Fig. 2C). In general, the percent variation in length shared by stocks in the same region (27%; based on average $r = 0.52$ from Fig. 1) was about twice that shared by stocks from different regions (16%; based on average $r = 0.41$ from Fig. 1).

Combining length at age series within the Bristol Bay, Cook Inlet, and Fraser River regions, respectively, was very effective at increasing the signal shared among ages and regions (Fig. 3). Correlations among these regional aggregates were considerably greater than the average stock-specific correlations (Fig. 1) for all combinations of age class and region. For example, within Bristol Bay, correlations between aggregated lengths of age 1.2 and 2.2 fish and between aggregated lengths of age 1.3 and 2.3 fish were 0.87 and 0.93, respectively. By comparison, the average stock-specific correlation among lengths was only 0.48 in both cases (Fig. 1).

PCA of the 16 regional length series (Fig. 3) defined the temporal characteristics of variation shared among regions and also more clearly identified region-specific patterns. For return years 1971–1997 (i.e., years where data were available for all regions), the PCA yielded three PC's with eigenvalues greater than 1, accounting for 58.5, 11.0, and 9.6% of the total variance, respectively. The time series (scores) of the dominant component, PC1, had an obvious declining trend from 1971 to 1997 ($P < 0.001$; linear regression with autocorrelated error), which is also evident in the regional length data (Fig. 3). All 16 length series correlated strongly with PC1 (range 0.61–0.88), suggesting that much of the covariation among lengths of Alaska and British Columbia sockeye salmon resulted from a similar declining trend over this period. In addition, the PCA revealed distinct region-specific sources of variation in length at age over this period (Fig. 4).

Analyses using first-differenced data support the suggestion from the PCA that slowly changing, low-frequency patterns of variability, such as the declining time trends noted above, were important sources of covariation among lengths of stocks. After autocorrelation and time trends in the 72 stock-specific length series were removed by first-differencing, widespread positive covariation was still evident both within and between regions. However, correlations were consistently and often substantially lower than those computed using the original data. The average of the 2556 correlations was reduced from 0.37 to 0.23, the number of negative correlations increased from 211 to 578, and the number of significant ($P < 0.05$) positive correlations decreased from 1026 to 745. Thus, there is little evidence that the general patterns of covariation in lengths could be solely a spurious result of unrelated time trends; instead, to the extent that the observed covariation in length at age of sockeye salmon arises from shared processes, such processes appear to be largely characterized by low-frequency patterns of variability.

The correlation analysis and PCA thus support hypotheses that environmental processes similarly affect adult length of sockeye salmon stocks both among different regions and within regions. The distinct within-region patterns of covariation in length (Figs. 1, 2, and 4) may have a simple explanation. These patterns likely reflect differences in ocean distributions of fish from each region and subsequent differences in growth conditions that they experience. In particular, ocean distributions of maturing sockeye salmon from each region become increasingly distinct in their final few months at sea (French et al. 1976). At this time, sockeye salmon are feeding and growing at high rates (Ricker 1976), creating the potential for much interannual variation in final body size to be determined during this short period. Many of the distinct patterns of within- versus between-region covariation are consistent with differences in spatial distributions (Figs. 1 and 4). For example, covariation in length was weakest between Bristol Bay and Fraser River sockeye salmon (Fig. 1), which have spawning grounds that are separated by the greatest distance (about 2400 km).

There are two plausible explanations whereby environmental processes could produce positive covariation in body size among stocks from different regions. Stocks may have similar geographical distributions when interannual variability in growth rate is most strongly determined, or stocks may have different distributions at such times but experience similar large-scale environmental conditions. There is some evidence for both possibilities. Regarding the first hypothesis, tagging studies (e.g., French et al. 1976) show that ocean distributions of sockeye salmon from Alaska and British Columbia overlap considerably in space and time in the Gulf of Alaska. Thus, the degree of covariation between lengths of stocks from different regions may reflect the extent to which stocks share similar distributions and hence growth conditions. Further support for this mechanism is provided by clear evidence of the effect on body size of competitive interactions among stocks from different regions (Peterman 1984; McKinnell 1995). Also, total ocean abundances of

© 1999 NRC Canada

Table 1. Correlations between aggregated lengths at age aligned by ocean-entry year or by return year.

	Ocean-entry year		Return year	
Age groups compared	Original data	Prewhitened data	Original data	Prewhitened data
Bristol Bay				
1.2 vs. 1.3	0.22	0.09	0.64	0.67
1.2 vs. 2.3	0.35	0.22	0.54	0.54
2.2 vs. 1.3	0.21	–0.06	0.80	0.85
2.2 vs. 2.3	0.36	0.09	0.69	0.72
Cook Inlet				
1.2 vs. 1.3	0.24	–0.06	0.65	0.70
1.2 vs. 2.3	0.29	–0.15	0.63	0.56
2.2 vs. 1.3	0.34	–0.07	0.62	0.57
2.2 vs. 2.3	0.50	–0.06	0.67	0.53
Fraser River				
1.1 vs. 1.2	0.66	0.19	0.67	0.34
1.1 vs. 1.3	0.47	0.09	0.44	0.36
1.2 vs. 1.3	0.61	0.00	0.77	0.71

Note: For each alignment, correlations were calculated using the original data as well as data prewhitened to remove autocorrelation.

Fig. 5. Summary of correlations among mean age at maturity of Bristol Bay (BB), Cook Inlet (CK), Copper River (CP), Nass River (NS), Skeena River (SK), and Fraser River (FR) stocks. Average correlations are shown for all comparisons involving Bristol Bay and Fraser River stocks. Levels of shading, defined in the legend, reflect different ranges of correlations.

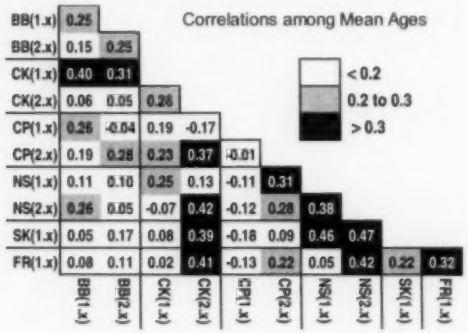

sockeye salmon increased substantially after the mid-1970's (Rogers 1987; Bigler et al. 1996), so the declining trends in body size common to sockeye salmon from each region (Fig. 3) may be evidence of increased competition.

The second explanation for covariation across different regions is also plausible because physical and biological variables are known to vary coherently over large areas of the northeastern Pacific Ocean. For example, beginning in the mid-1970's, persistent and large-scale decreases in sea surface temperatures in the central North Pacific were recorded along with increases in coastal ocean temperatures (McLain 1984) and changes in other physical and biological variables (e.g., Venrick et al. 1987; Brodeur and Ware 1992; Graham 1994). Therefore, stocks from different regions may have been exposed to similar growth conditions despite having different distributions during periods critical to determining adult size.

However, it is also possible that between-region covariation in lengths, in particular the covariation arising from similar declining trends, was due in part to coinciding but unrelated processes acting independently within different regions. For example, the persistent changes in ocean temperatures noted above were coincident with long-term increases in sockeye salmon abundance for the Bristol Bay, Cook Inlet, and Fraser River regions. It is currently unclear to what extent such variables may be important, region-specific determinants of adult body size.

In addition to distinct within- and between-region patterns of covariation in length, there is also some evidence of differences among age classes. For between-region comparisons involving Bristol Bay sockeye salmon, correlations were generally greater for older age classes (e.g., *x*.3) of Fraser stocks and the Skeena stock (Fig. 1). The result for the Skeena stock is consistent with tagging data reviewed by McKinnell (1995), which showed that age 1.2 Skeena sockeye salmon were distributed farther east in the Gulf of Alaska than age 1.3 fish. This could reduce similarity with Bristol Bay stocks in environmental conditions, including the degree of competition with other sockeye salmon in the Gulf of Alaska. Analogous age-specific distributional differences for Fraser River sockeye salmon may also account for the greater degree of covariation between lengths of older age classes of Fraser River fish and lengths of Bristol Bay stocks (Fig. 1).

Causes of patterns of covariation in length at age: conditions in early or late marine life?

In the above analyses, length series were aligned by return year under the assumption that interannual variability was primarily determined by growth conditions during the final year at sea (Rogers and Ruggerone 1993; McKinnell 1995). However, growth in length of sockeye salmon is proportionally greatest during their first year at sea. If early marine growth is an important determinant of final body length, there should be positive covariation in length among sockeye salmon that entered the ocean in the same year (i.e., had the same OEY and therefore experienced similar growth conditions during their early marine life) but that returned in different years (e.g., as *x*.2 and *x*.3 recruits).

© 1999 NRC Canada

Fig. 6. Histograms of correlations between mean ages of 1.*x* sockeye salmon for comparisons (A) among Bristol Bay stocks (35 of 36 correlations positive; 12 significant at $P < 0.05$), (B) among Fraser River stocks (20 of 21 correlations positive; six significant), and (C) between Bristol Bay and Fraser River stocks (49 of 63 correlations positive; none significant). Averages of these three sets of correlations are shown in Fig. 5. Open bars represent negative correlations; solid bars are positive correlations.

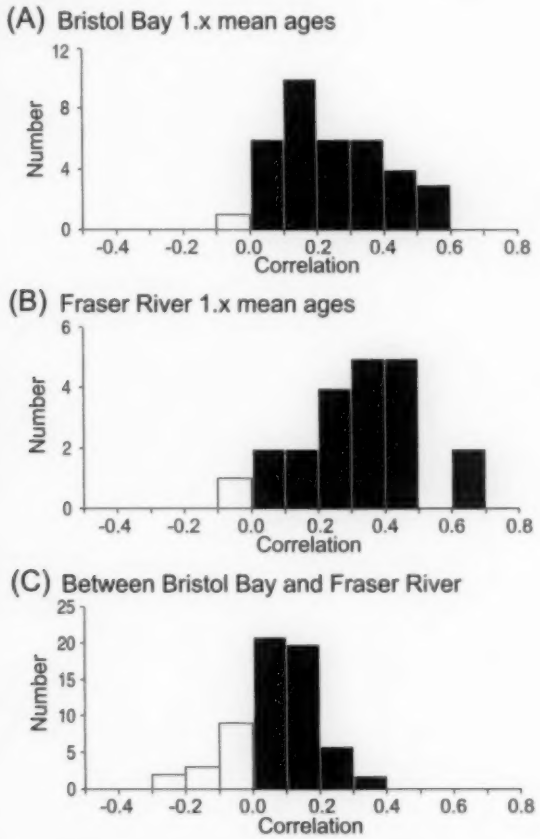

However, after possible confounding effects of autocorrelation were removed by prewhitening, there was little evidence of such covariation. Comparisons among aggregated lengths for the Bristol Bay, Cook Inlet, and Fraser River regions showed moderate positive correlations among the original (autocorrelated) lengths when aligned by OEY but weak or negative correlations among prewhitened lengths (Table 1). In contrast, when length series were aligned by return year, there were large positive correlations among original data for each region, and prewhitening made little difference to these comparisons (Table 1). These results suggest that the moderate positive correlations in the original data, when aligned by OEY, were due to a combination of autocorrelation and real covariation driven by processes operating primarily during the final year at sea rather than early ocean life. These findings are consistent with other analyses (Rogers and Ruggerone 1993; McKinnell 1995) and imply that interannual variability in growth conditions during early marine life is not nearly as important a determinant of interannual variation in final sockeye salmon body length as is variability in conditions during late marine life.

Mean age at maturity

Correlations among the 32 time series of mean age at maturity, aligned by OEY, showed evidence of weak but predominantly positive covariation both within and between regions (Fig. 5). Although the average of the 496 correlations was only 0.17, 66 of 394 positive correlations were significant ($P < 0.05$), while none of 102 negative correlations was significant. Correlations among stocks of different regions were mostly positive, except those involving Copper River 1.*x* mean age (Fig. 5). Distinct within-region patterns of covariation were evident for comparisons among mean age series of the Bristol Bay and Fraser River regions, where we had data for several stocks. Mean ages tended to be positively correlated among stocks within those regions, with little evidence of positive covariation between the two regions (e.g., Fig. 6). In general, the proportion of variation shared among stocks, either within or between regions, was 10% or less.

Time trends were also an important source of covariation in mean age at maturity (Fig. 7). Aggregated Fraser 1.*x* mean age showed a clear shift towards older ages beginning with the 1979 OEY. There was also a tendency towards greater mean age for both aggregated Bristol Bay age groups, Cook Inlet 2.*x*, and Nass and Skeena age groups beginning in the early 1980's (Fig. 7). These shared trends were reflected by the PCA of the 10 regional mean age series (Fig. 7), which yielded four PC's with eigenvalues greater than 1, explaining 33.1, 18.3, 12.9, and 10.7% of the variance, respectively. Although the analysis did not yield a substantial simplification of the data, PC1 was moderately to strongly correlated (0.38–0.73) with all 10 mean age series except Copper River 1.*x* ($r = -0.29$). Moreover, the time series (scores) of PC1 had an increasing trend from OEY 1971 to 1994 ($P < 0.001$; linear regression with autocorrelated error), suggesting that much of the covariation among sockeye salmon stocks from Alaska and British Columbia was due to a shared trend toward greater mean age at maturity over this two-decade period.

Repeating the correlation analysis and PCA using first-differenced data confirmed the importance of low-frequency sources of covariation. For example, after first-differencing, the average correlation computed among the seven Fraser River mean age series was 0.13, compared with 0.32 for the original data. Furthermore, when the PCA was repeated using first-differenced data, there was no longer a clear dominant PC. Thus, after positive autocorrelation and time trends were removed from the data, there was little evidence of large-scale covariation in mean age at maturity across all regions. This supports the interpretation, as with length data, that long-term, slowly changing conditions account for a large portion of the shared variation in age at maturity of these stocks.

The tendency toward positive covariation between regions suggests that age at maturity of sockeye salmon from Alaska and British Columbia was in part influenced by similar environmental processes. However, such processes appear to account for only a small portion of the total variation (Fig. 5).

© 1999 NRC Canada

Fig. 7. Time series of region-specific mean age at maturity for various sockeye salmon stocks. Regional aggregated mean ages (e.g., aggregated across the nine Bristol Bay 1.*x* data series) are shown for Bristol Bay and Fraser River stocks, whereas standardized mean ages at maturity are given for the Cook Inlet, Copper River, Nass River, and Skeena River stocks.

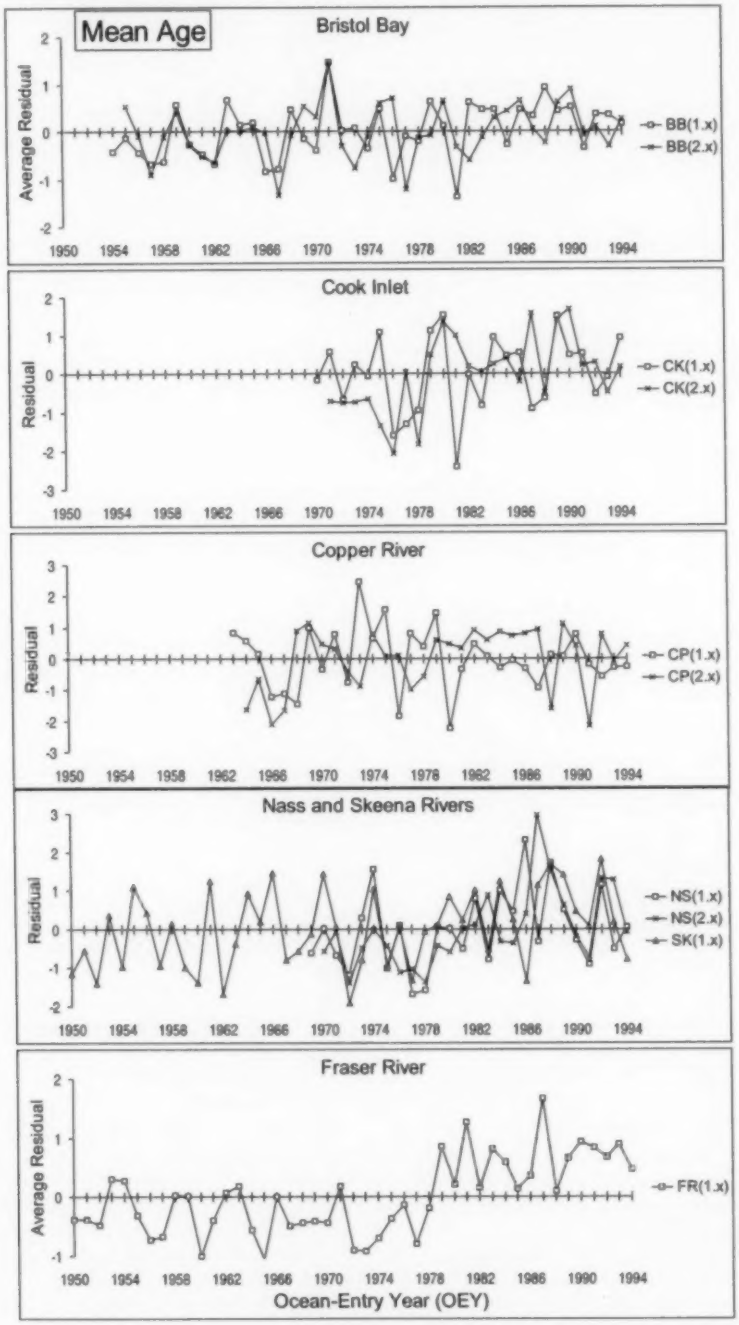

As we discussed for length, covariation between regions may reflect either similarities in ocean distributions during periods critical to determining age at maturity or large-scale environmental conditions that influenced fish with different distributions in similar ways. Likewise, the general across-region increases in mean age during the 1980's may be related to coincident increases in ocean abundances of sockeye salmon, as suggested by Bigler et al. (1996), or to the mid-1970's shift in ocean conditions in the North Pacific.

Regional-scale environmental processes also had a nota-

© 1999 NRC Canada

Table 2. Correlations between length and mean age at maturity for comparisons within stocks and for comparisons between regional aggregates.

	Comparisons within stocks		Comparisons between aggregates	
	RY = OEY + 1	RY = OEY + 2	RY = OEY + 1	RY = OEY + 2
Length (1.1) vs. mean age (1.*x*)				
Fraser River	–0.29	–0.17	–0.73*	–0.66*
Length (1.2) vs. mean age (1.*x*)				
Bristol Bay	–0.21	–0.04	–0.39*	–0.23
Cook Inlet	–0.11	–0.01	–0.13	–0.01
Copper River	0.47	0.01		
Skeena River	–0.17	–0.36		
Fraser River	–0.28	–0.33	–0.58*	–0.61*
Length (1.3) vs. mean age (1.*x*)				
Bristol Bay	–0.02	–0.05	–0.16	–0.07
Cook Inlet	–0.27	0.03	–0.32	0.03
Copper River	0.07	0.45		
Skeena River	–0.34	–0.27		
Fraser River	–0.28	–0.22	–0.44*	–0.50*
Length (2.2) vs. mean age (2.*x*)				
Bristol Bay	–0.14	–0.13	–0.27	–0.10
Cook Inlet	–0.49	–0.53	–0.58	–0.56
Length (2.3) vs. mean age (2.*x*)				
Bristol Bay	–0.07	–0.01	–0.18	0.05
Cook Inlet	–0.58	–0.45	–0.61*	–0.47
Copper River	0.02	0.05		

Note: Two alternative lags for comparing lengths and mean age were examined: (*i*) return year (RY) of length data aligned to match the ocean-entry year (OEY + 1) of mean age data and (*ii*) RY = OEY + 2. Averages of within-stock correlations are shown for the Bristol Bay, Cook Inlet, and Fraser River regions.

*Significant correlations ($P < 0.05$) for comparisons between aggregates.

ble effect on interannual variation in age at maturity. The predominance of positive correlations within regions is consistent with Peterman's (1985) findings for Bristol Bay sockeye salmon stocks, which were based only on data through the 1980 return year. Although patterns of positive covariation in age at maturity found here were stronger within the Bristol Bay and Fraser regions than between them (e.g., Fig. 6), and generally greater among the neighboring (point of ocean entry 60 km apart) Nass and Skeena stocks (Fig. 5), correlations were generally weak. This suggests that most of the temporal variability in mean age was related to unique factors influencing individual stocks. Such factors likely include genetic (Ricker 1972) and other parental effects (Bilton 1970; Bradford and Peterman 1987), stock-specific environmental effects, as well as measurement error in data.

Covariation across the three components of sockeye salmon recruitment

The above patterns of covariation in size and age at maturity and those for survival rates of sockeye salmon stocks (Peterman et al. 1998) provide evidence of the spatial scales over which environmental processes affect these variables. In addition, by examining patterns of covariation across these components of recuitment, we can make further general inferences about the extent to which ocean conditions may simultaneously drive interannual variability in each component.

For comparisons between length and mean age, we might expect negative covariation if marine conditions favorable for growth resulted in both greater length at maturity and younger mean age at maturity (e.g., Bilton et al. 1982; Wood and Foote 1996). As discussed above, interannual variation in adult length of sockeye salmon appears to be largely determined by conditions during the final year at sea. In contrast, environmentally induced variation in age at maturity likely occurs within the first 2 years of marine life, although the exact period is unclear (Peterman 1985). To address the main possibilities, we correlated length and mean age data at two lags. First, return year of length data was lagged to match the OEY + 1 year of mean age data (i.e., lengths of adults returning in the summer of 1980, for example, are aligned with the mean age data of smolts that enter the ocean in the spring of 1979, so that for their entire first year at sea, smolts are in the ocean along with returning adults). Second, return year was lagged to match OEY + 2 years (for their first 2 years at sea, smolts overlap with returning adults). To simplify the analysis, age 1.*x* lengths were correlated with age 1.*x* mean ages, and similarly for age 2.*x* indices.

For most regions, we found moderate negative correlations between length and mean age within stocks and between regional aggregates at both lags examined (Table 2). These results were not surprising because opposite time trends were observed in length and mean age series for many Alaska and British Columbia stocks (Figs. 3 and 7). Perhaps the best evidence of the coherence between size and age of adults was shown for Fraser River stocks, which exhibited abrupt shifts toward smaller length beginning in the 1980 return year (Fig. 3) and greater mean age in the 1979

© 1999 NRC Canada

OEY (Fig. 7). Correlations computed using prewhitened data did not help identify a critical lag. These correlations were generally negative at both lags and were much weaker than those among the original data series. Thus, while it was not possible to determine at which point during marine life the lengths and mean age share similar influences, it was clear that opposite time trends in these recruitment variables were the primary source of negative correlations.

Favorable ocean conditions for growth may also be associated with increased marine survival rates for sockeye salmon, with effects on survival rate likely to occur during the first year at sea. Thus, for comparisons among lengths and survival rates (marine, stock–recruit, and aggregate stock–recruit indices of survival rate), we aligned data series so that return year for lengths was the same as the OEY for survival rates. Results were similar when return year was aligned with the OEY + 1 year. For most regions, there was no evidence of either positive or negative covariation among lengths and survival rates. An exception was Bristol Bay stocks, for which within-stock correlations between length and stock–recruit survival rates (which had more years of data than marine survival rates) were positive in 28 of 32 cases (four length series for each of eight stocks). However, these correlations were generally weak (average $r = 0.18$; three positive correlations significant at $P < 0.05$). The four correlations among Bristol Bay aggregates of survival rate and length were also weak (average $r = 0.24$; none significant). The weak and inconsistent associations between length and survival rate suggest that different processes drive interannual variability in these components of recruitment. This conclusion is further supported by evidence that environmental processes influence these two variables at different spatial scales. Length shows much stronger between-region positive covariation (e.g., Fig. 2C) than survival rate (e.g., fig. 1C of Peterman et al. 1998); the latter only shows within-region positive covariation.

Finally, negative covariation between survival rate and mean age at maturity might be expected as a result of processes in early marine life, where conditions favoring growth might lead to higher survival rates and lower mean age. However, correlations among mean age and survival rate aligned by OEY of smolts were weak with no tendency toward negative or positive values. For example, the average of the 32 within-stock correlations (13 of which were negative) was 0.02. Similar correlations were found when OEY of mean age data was lagged either 1 or 2 years ahead of OEY for survival rates. Thus, there appears to be little association between environmental processes determining interannual variability in survival rates and those affecting mean age at maturity, although such relationships may be masked by measurement error or parental effects on mean age.

Conclusions

This paper on length and age at maturity and the Peterman et al. (1998) paper on survival rate report different patterns of covariation over space for each of these three variables. Adult length of sockeye salmon tends to be positively correlated among stocks across different regions and most strongly correlated among stocks within regions. Mean age at maturity shows similar but much weaker correlations than for length data. In contrast, survival rates show positive covariation within regions but no covariation between regions (Peterman et al. 1998). These differences in patterns of covariation imply that to some extent, each of these components of recruitment is affected by environmental processes that operate at different spatial scales. Therefore, future models for forecasting annual salmon abundance (reflecting survival rates and changing age at maturity schedules) or body size should be based on appropriate measures of environmental conditions that reflect this information about spatial scales. For instance, instead of using sea surface temperatures averaged over the entire northeastern Pacific Ocean as an independent variable in a model to forecast variability in survival rates, a regional measure would be more appropriate. However, both large-scale and regional-scale measures of ocean conditions may be useful for forecasting changes in body length.

Acknowledgments

We are extremely grateful to the numerous biologists and technicians in various management agencies who gathered and processed the lengthy time series of data analyzed here. Without those people, this research would not have been possible. We also thank the people named in the Methods section for providing data and Don Rogers and an anonymous referee for their helpful reviews. Michael Bradford and Chris Wood provided very useful comments on a draft manuscript. Funding was provided by grants to R.M. Peterman from the Ocean Production Enhancement Network (one of Canada's Networks of Centres of Excellence) and the Natural Sciences and Engineering Research Council of Canada.

References

Bigler, B.S., Welch, D.W., and Helle, J.J. 1996. A review of size trends among North Pacific salmon (*Oncorhynchus* spp.). Can. J. Fish. Aquat. Sci. **53**: 455–465.

Bilton, H.T. 1970. Maternal influences on the age at maturity of Skeena River sockeye salmon (*Oncorhynchus nerka*). Fish. Res. Board Can. Tech. Rep. No. 167.

Bilton, H.T., Alderdice, D.F., and Schnute, J.T. 1982. Influence of time and size of release of juvenile coho salmon (*Oncorhynchus kisutch*) on returns at maturity. Can. J. Fish. Aquat. Sci. **39**: 426–447.

Bradford, M.J., and Peterman, R.M. 1987. Maternal size effects may explain positive correlations between age at maturity of parent and offspring sockeye salmon (*Oncorhynchus nerka*). *In* Sockeye salmon (*Oncorhynchus nerka*) population biology and future management. *Edited by* H.D. Smith, L. Margolis, and C.C. Wood. Can. Spec. Publ. Fish. Aquat. Sci. No. 96. pp. 90–100.

Brodeur, R.D., and Ware, D.M. 1992. Long-term variability in zooplankton biomass in the subarctic Pacific Ocean. Fish. Oceanogr. **1**: 32–38.

Burgner, R.L. 1991. Life history of sockeye salmon. *In* Pacific salmon life histories. *Edited by* C. Groot and L. Margolis. University of British Columbia Press, Vancouver, B.C. pp. 1–117.

Cox, S.P., and Hinch, S.G. 1997. Changes in size at maturity of Fraser River sockeye salmon (*Oncorhynchus nerka*) (1952–

© 1999 NRC Canada

1993) and associations with temperature. Can. J. Fish. Aquat. Sci. **54**: 1159–1165.

French, R., Bilton, H., Osaka, M., and Hartt, A. 1976. Distribution and origin of sockeye salmon (*Oncorhynchus nerka*) in offshore waters of the North Pacific Ocean. Int. North Pac. Fish. Comm. Bull. No. 34.

Fried, S.M., and Yuen, H.J. 1987. Forecasting sockeye salmon (*Oncorhynchus nerka*) returns to Bristol Bay, Alaska: a review and critique of methods. *In* Sockeye salmon (*Oncorhynchus nerka*) population biology and future management. *Edited by* H.D. Smith, L. Margolis, and C.C. Wood. Can. Spec. Publ. Fish. Aquat. Sci. No. 96. pp. 273–279.

Graham, N.E. 1994. Decadal-scale climate variability in the tropical and North Pacific during the 1970s and 1980s: observations and model results. Clim. Dyn. **10**: 135–162.

Healey, M.C. 1987. The adaptive significance of age and size at maturity of female sockeye salmon (*Oncorhynchus nerka*). *In* Sockeye salmon (*Oncorhynchus nerka*) population biology and future management. *Edited by* H.D. Smith, L. Margolis, and C.C. Wood. Can. Spec. Publ. Fish. Aquat. Sci. No. 96. pp. 110–117.

Hinch, S.G., Healey, M.C., Diewert, R.E., Thomson, K.A., Hourston, R., Henderson, M.A., and Juanes, F. 1995. Potential effects of climate change on marine growth and survival of Fraser River sockeye salmon. Can. J. Fish. Aquat. Sci. **52**: 2651–2659.

Jenkins, G.M., and Watts, D.G. 1968. Spectral analysis and its applications. Holden-Day, San Francisco, Calif.

McKinnell, S. 1995. Age-specific effects of sockeye abundance on adult body size of selected British Columbia sockeye stocks. Can. J. Fish. Aquat. Sci. **52**: 1050–1063.

McLain, D.R. 1984. Coastal ocean warming in the North Pacific, 1976–83. *In* The influence of ocean conditions on the production of salmonids in the North Pacific. *Edited by* W.G. Pearcy. Oregon State University Press, Corvallis, Oreg. pp. 61–86.

Peterman, R.M. 1984. Density-dependent growth in early ocean life of sockeye salmon (*Oncorhynchus nerka*). Can. J. Fish. Aquat. Sci. **41**: 1825–1829.

Peterman, R.M. 1985. Patterns of interannual variation in age at maturity of sockeye salmon (*Oncorhynchus nerka*) in Alaska and British Columbia. Can. J. Fish. Aquat. Sci. **42**: 1595–1607.

Peterman, R.M. 1991. Density-dependent marine processes in North Pacific salmonids: lessons for experimental design of large-scale manipulations of fish stocks. ICES Mar. Sci. Symp. **192**: 69–77.

Peterman, R.M., Pyper, B.J., Lapointe, M., Adkison, M.D, and Walters, C.J. 1998. Patterns of covariation in survival rates of British Columbia and Alaskan sockeye salmon (*Oncorhynchus nerka*) stocks. Can. J. Fish. Aquat. Sci. **55**: 2503–2517.

Pielou, E.C. 1977. Mathematical ecology. John Wiley & Sons, New York.

Pyper, B.J., and Peterman, R.M. 1998. Comparison of methods to account for autocorrelation in correlation analyses of fish data. Can. J. Fish. Aquat. Sci. **55**: 2127–2140.

Ricker, W.E. 1972. Hereditary and environmental factors affecting certain salmonid populations. *In* The stock concept in Pacific salmon. *Edited by* R.C. Simon and P.A. Larkin. H.R. MacMillan Lectures in Fisheries, University of British Columbia, Vancouver, B.C. pp. 19–60.

Ricker, W.E. 1976. Review of the rate of growth and mortality of Pacific salmon in salt water, and noncatch mortality caused by fishing. J. Fish. Res. Board Can. **33**: 1483–1524.

Ricker, W.E. 1982. Size and age at maturity of British Columbia sockeye salmon (*Oncorhynchus nerka*) in relation to environmental factors and the fishery. Can. Tech. Rep. Fish. Aquat. Sci. No. 1115.

Ricker, W.E. 1995. Trends in the average size of Pacific salmon in Canadian catches. *In* Climate change and northern fish populations. *Edited by* R.J. Beamish. Can. Spec. Publ. Fish. Aquat. Sci. No. 121. pp. 596–602.

Rogers, D.E. 1980. Density-dependent growth of Bristol Bay sockeye salmon. *In* Salmonid ecosystems of the North Pacific. *Edited by* W.J. McNeil and D.C. Himsworth. Oregon State University Press, Corvallis, Oreg. pp. 267–283.

Rogers, D.E. 1984. Trends in abundance of northeastern Pacific stocks of salmon. *In* The influence of ocean conditions on the production of salmonids in the North Pacific. *Edited by* W.G. Pearcy. Oregon State University Press, Corvallis, Oreg. pp. 100–127.

Rogers, D.E. 1987. Pacific salmon. *In* The Gulf of Alaska: physical environment of biological resources. *Edited by* D.W. Wood and S.T. Zimmerman. U.S. Government Printing Office, Washington, D.C. pp. 461–476.

Rogers, D.E., and Ruggerone, G.T. 1993. Factors affecting marine growth of Bristol Bay sockeye salmon. Fish. Res. **18**: 89–103.

Thompson, K.R., and Page, F.H. 1989. Detecting synchrony of recruitment using short, autocorrelated time series. Can. J. Fish. Aquat. Sci. **46**: 1831–1838.

Venrick, E.L., McGowan, J.A., Cayan, D.A., and Hayward, T.L. 1987. Climate and chlorophyll *a* long-term trends in the central North Pacific Ocean. Science (Washington, D.C.), **238**: 70–72.

Wood, C.C., and Foote, C.J. 1996. Evidence of sympatric genetic divergence of anadromous and nonanadromous morphs of sockeye salmon (*Oncorhynchus nerka*). Evolution, **50**: 1265–1279.

Zar, J.H. 1984. Biostatistical analyses. Prentice-Hall, Englewood Cliffs, N.J.

© 1999 NRC Canada

Effect of solar ultraviolet radiation (280–400 nm) on the eggs and larvae of Atlantic cod (*Gadus morhua*)

France Béland, Howard I. Browman, Carolina Alonso Rodriguez, and Jean-François St-Pierre

Abstract: In the Gulf of St. Lawrence, Canada, solar ultraviolet B radiation (UV-B, 280–320 nm) penetrates a significant percentage of the summer mixed-layer water column: organisms residing in this layer, such as the eggs of Atlantic cod (*Gadus morhua*), are exposed to UV-B. In outdoor exposure experiments, Atlantic cod eggs were incubated in the presence versus the absence of UV-B and (or) UV-A (320–400 nm). We tested two hypotheses: H_1, UV-B induces mortality in Atlantic cod eggs, and H_2, UV-A either exacerbates or mitigates any such UV-B-induced mortality. Hypothesis H_1 was supported: there was a significant mortality effect on Atlantic cod eggs exposed to UV-B at the surface and at a depth of 50 cm. Hypothesis H_2 was not supported: there was no effect of UV-A. These experiments indicate that Atlantic cod eggs present in the first metre of the water column (likely only a small percentage of the total egg population) are susceptible to UV-B. However, UV-B must be viewed as only one among many environmental factors that produce the very high levels of mortality typically observed in the planktonic early life stages of marine fishes.

Résumé : Dans le golfe du Saint-Laurent (Canada), le rayonnement solaire ultraviolet B (UV-B, 280–320 nm) pénètre une partie importante de la couche de mélange estivale. Les organismes présents dans cette partie, comme les oeufs de morue franche (*Gadus morhua*), se trouvent exposés aux UV-B. Dans des essais extérieurs d'exposition, des oeufs de morue franche ont été incubés en étant exposés ou non aux UV-B et (ou) aux UV-A (320–400 nm). Nous avons testé deux hypothèses : H_1, les UV-B entraînent une mortalité chez les oeufs de morue franche, et H_2, les UV-A accentuent ou atténuent l'éventuel effet létal des UV-B sur les oeufs. L'hypothèse H_1 a été corroborée : on a observé une mortalité significative des oeufs exposés aux UV-B à la surface et à une profondeur de 50 cm. L'hypothèse H_2 a été rejetée : les UV-A n'avaient pas d'effet. Ces expériences montrent que les oeufs de morue franche présents dans le premier mètre de la colonne d'eau (qui ne constituent probablement qu'un faible pourcentage de la population totale d'oeufs) sont sensibles aux UV-B. Cependant, les UV-B ne sont qu'un des nombreux facteurs environnementaux responsables des très forts taux de mortalité habituellement observés chez les premiers stades planctoniques des poissons marins.

[Traduit par la Rédaction]

Introduction

The work of Marinaro and Bernard (1966), Pommeranz (1974), and Hunter et al. (1979, 1982) provided clear evidence of the detrimental effect of solar ultraviolet B radiation (UV-B, 280–320 nm) on the planktonic early life stages of fishes. Hunter et al. (1979), working with the eggs and larvae of northern anchovy (*Engraulis mordax*) and chub mackerel (*Scomber japonicus*), reported that exposure to surface levels of UV-B could be lethal. Significant sublethal effects were also reported: lesions in the brain and retina and reduced growth rate. The study concluded that up to 13% of the annual production of northern anchovy larvae could be lost as a result of UV-B-related mortality (Hunter et al. 1982). In the time since these results were published, very little additional information has been generated for the effects of UV-B on ichthyoplankton (but see Malloy et al. 1997; Williamson et al. 1997; Vetter et al. 1999). The goal of this study was to evaluate the effects of UV (280–400 nm) on the eggs and larvae of Atlantic cod (*Gadus morhua*).

Since 1981, levels of solar UV-B incident at the earth's surface have increased significantly at midlatitudes of the Northern and Southern hemispheres (Kerr and McElroy 1993). These increases in UV-B are linked to reductions of stratospheric ozone (Kerr and McElroy 1993). A growing number of studies indicate that UV-B, at current levels, is

Received June 2, 1998. Accepted February 10, 1999.
J14618

F. Béland and C.A. Rodriguez. Département d'Océanographie, Université du Québec à Rimouski, 300, allée des Ursulines, C.P. 3300, Rimouski, QC G5L 3A1, Canada, and Department of Fisheries and Oceans, Maurice Lamontagne Institute, Division of Ocean Sciences, 850 Route de la Mer, Mont-Joli, QC G5H 3Z4, Canada.
H.I. Browman[1] **and J.-F. St-Pierre.** Department of Fisheries and Oceans, Maurice Lamontagne Institute, Division of Ocean Sciences, 850, route de la Mer, Mont-Joli, QC G5H 3Z4, Canada.

[1]Author to whom all correspondence should be addressed. Current address: Institute of Marine Research, Austevoll Aquaculture Research Station, N-5392 Storebø, Norway. e-mail: howard.browman@imr.no

© 1999 NRC Canada

harmful to aquatic organisms and may reduce the productivity of marine ecosystems (Häder et al. 1995; Häder 1997). Such UV-B-induced reductions in productivity have been reported for phytoplankton, heterotrophs, and zooplankton, the key intermediary levels of marine food chains (Häder 1997). Analogous studies on fish eggs and larvae, although rare, indicate that exposure to levels of UV-B currently incident at the earth's surface results in higher mortality, which may lead to poorer recruitment to adult populations (Pommeranz 1974; Hunter et al. 1982; Williamson et al. 1997).

The few analagous studies on UV-A (320–400 nm) have yielded mixed results. While the role of UV-A in inducing photorepair of DNA damage is well documented (e.g., Mitani et al. 1996), only a small number of studies have reported deleterious effects (e.g., Winckler and Fidhiany 1996*a*, 1996*b*; Bass and Sistrun 1997; Williamson et al. 1997).

In early summer, the mixed layer in the northern Gulf of St. Lawrence and Labrador Shelf comprises the upper 0–15 m of the water column and is separated from an intermediate layer of colder water (<1°C) by a sharp thermocline (Petrie et al. 1988; Therriault 1991). This underlying cold water, and the steep density gradient associated with it, effectively confines biological productivity to the much warmer surface mixed layer (Therriault 1991). Measurements of the diffuse attenuation coefficients for UV-B at various locations in the Gulf of St. Lawrence indicate maximum 10% depths (the depth to which 10% of the surface energy penetrates at a given wavelength) of 3–4 m at a wavelength of 310 nm (Kuhn et al. 1999). UV-A penetrates these waters to even greater depths: 10% depths of 7–10 m were observed at a wavelength of 360 nm (Kuhn et al. 1999). These depths represent a significant percentage of the summer mixed-layer water column. UV-B-induced damage to the DNA of fish eggs and larvae has been detected in samples collected from depths of up to 20 m (Malloy et al. 1997; Vetter et al. 1999). Thus, the early life history stages of the crustacean and fish species that are present in the shallow mixed layer of the water column in this geographic region may be susceptible to UV-B.

The reproductive season for Atlantic cod in the Gulf of St. Lawrence begins early in the spring (April) and continues through midsummer (July) (Ouellet et al. 1997). Spawning occurs in deep water (>200 m), and Atlantic cod eggs, which are typically positively buoyant, ascend to the surface mixed layer over a period of 2–10 days (Solemdal and Sundby 1981; Anderson and de Young 1995; Ouellet 1997). A significant proportion of all Atlantic cod eggs present in the water column occur in the 0- to 25-m depth stratum off the Newfoundland Shelf (Anderson and de Young 1995), off Greenland and Labrador (Brander 1994), on southern Georges Bank (Lough et al. 1996), and in the northern Gulf of St. Lawrence (Ouellet 1997). However, it is also possible for eggs to become trapped at density barriers (such as the thermocline), and these eggs would likely never reach the surface (Ouellet 1997). Nonetheless, when wind speed is low, the highest egg concentrations are observed in the upper 0–10 m of the water column (Solemdal and Sundby 1981). The early larval stages are also typically present and often even closer to the surface (Anderson and de Young 1995).

Following from the hydrographics of this region, and given the planktonic character of the early life stages of Atlantic cod and many other fish and crustacean species, this system offers an appropriate opportunity to assess the impacts of UV on temperate-latitude marine ecosystems. As one step towards meeting this goal, we undertook a series of experiments in which Atlantic cod eggs were incubated under the sun, with and without the UV-B and (or) UV-A wavebands, in outdoor exposures. We tested two hypotheses: H_1, UV-B has a negative impact on Atlantic cod egg survival, and H_2, UV-A either exacerbates or mitigates any such UV-B-induced mortality. The results of these experiments are reported here.

Materials and methods

Animal husbandry

Fertilized Atlantic cod eggs were obtained from a broodstock maintained at the Maurice Lamontagne Institute. Male–female pairs were kept in separate tanks outfitted with egg collectors (see Dutil et al. (1998) for complete details). Thus, the source of the eggs used in the UV-B exposure experiments was known.

Egg production by these fish occurred several weeks later into the spring–summer than is the case for wild populations in this geographic region. Thus, in our August and September experiments, Atlantic cod eggs were exposed to solar UV-B slightly later in the season than they would be in the wild. However, daily exposure to UV-B was similar in all experiments (with the possible exception of that on 2–12 September) (see Fig. 3*a*). This strongly supports the validity of our results within a realistic ecological framework for the Atlantic cod spawning cycle in this geographic region.

Fertilized eggs were incubated in the dark at 6 ± 1°C in 60-L black round-bottom basins (the indoor rearing basins). Eggs were removed from these basins immediately prior to an exposure experiment. To minimize the risk of bacterial contamination, newly collected eggs were disinfected by immersion in a solution of 1% Aquiodyne (Aquipro, St-Apollinaire, Que.) after which they were thoroughly rinsed in seawater. Further, at the time the eggs were transferred to the incubation tanks, they were treated with an antibiotic solution (0.075 g streptomycin·L^{-1} and 0.01 g penicillin·L^{-1}). The bottom of the basin was cleaned and the seawater renewed each day.

General protocols and experimental design

Exposures to UV-B commenced about 4 days postfertilization, since Atlantic cod eggs are released at depth and will not be exposed to UV-B until they reach the surface layer several days later. The time required for Atlantic cod eggs to reach the surface is highly variable; therefore, the choice of a 4-day delay in beginning the exposures was arbitrary. At this point in development, embryos had reached stages 14–18. All developmental stage numbers referred to in the text are those described by Friðgeirsson (1978). This index of development is nonlinear; there are more discrete stages early in embryonic development than later. Thus, stage 14–18 embryos have not reached the halfway point of the embryonic period (which consists of a total of 32 stages).

Eggs were removed from the indoor rearing basins using a glass pipette (disinfected prior to each use) and placed into quartz tubes 10 cm long with an inner diameter of 2.2 cm (Quartz Scientific, Fairport Harbour, Ohio). One end of these tubes was sealed with a rubber stopper that had a small central hole. The hole was covered with 470-μm Nitex™. The other end of the tube was sealed with Nitex™. This arrangement allowed water to circulate in the tubes during the exposure experiments: removal of the rubber stopper

© 1999 NRC Canada

Fig. 1. (*a*) Irradiance delivered to the Quartz, Mylar, and OP-2 spectral exposure treatments under which Atlantic cod eggs were incubated in an outdoor reservoir. Also presented is spectral irradiance measured just below the surface and at 50 cm depth in the outdoor reservoir under cloudless skies on 5 August 1996 at 13:05 EDT outside the Maurice Lamontagne Institute, Mont-Joli, Qué., Canada (48°38′25.9′′N, 68°09′21.0′′W). (*b*) Spectral irradiance (in the UV) at the surface and at 50 cm depth in the outdoor reservoir (from Fig. 1*a*). Note that irradiance is now plotted on a common log scale and that the units have changed from mW to W.

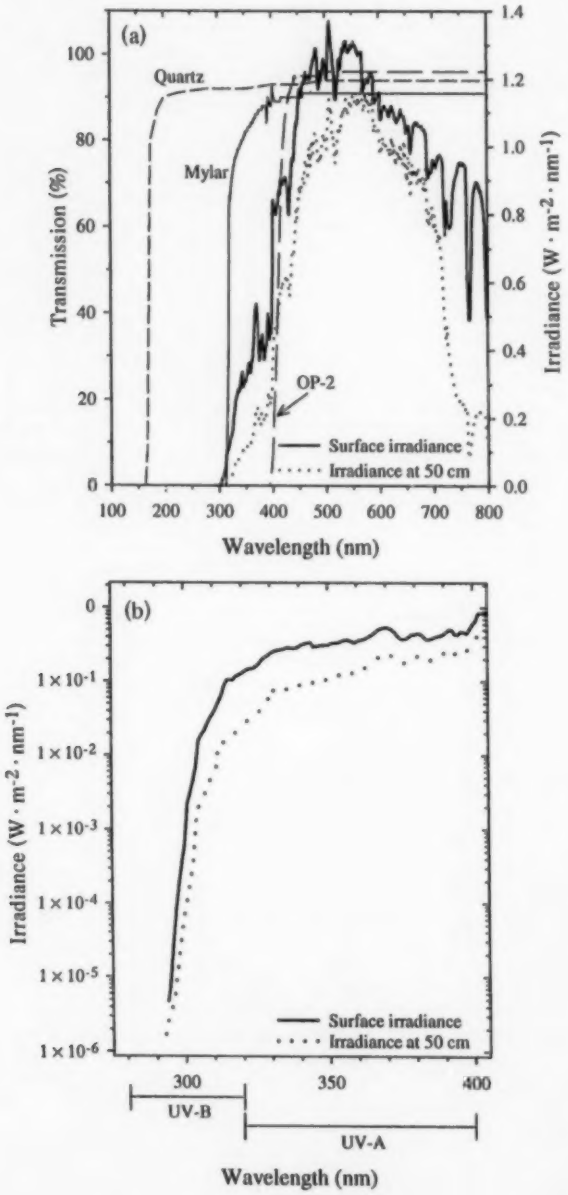

permitted access to the contents. About 100 eggs (range 90–141) were placed into each quartz tube.

The quartz tubes filled with Atlantic cod eggs were immersed in a seawater reservoir (the outdoor reservoir) located on the grounds of the Maurice Lamontagne Institute (48°38′25.9′′N, 68°09′21.0′′W). The reservoir was made of gray double-walled polyethylene and contained 1.08 m^3 of finely filtered seawater (renewed each hour) drawn from the St. Lawrence estuary. The water intake pipe at the Maurice Lamontagne Institute, and the source of water for the experimental reservoir, is located 100 m offshore at a depth of 15 m. The physical characteristics of the water at this location are unstable: they are affected by the tides and by freshwater runoff from nearby streams. Thus, the salinity and temperature in the reservoir were variable.

Five experiments were conducted: the first between 10 and 20 July 1996, the second between 27 July and 6 August 1996, the fourth between 19 and 29 August 1996, and the fifth between 2 and 12 September 1996. The results of the third experiment in the series are not presented because all of the eggs, in all of the treatments, died soon after being placed in the outdoor reservoir.

Tubes were suspended underwater, at depths of 3 and 50 cm, under three light regimes as follows. (*i*) UV-B + UV-A + PAR (photosynthetically active radiation, 400–700 nm): eggs in this treatment (Quartz), incubated in quartz tubes, were exposed to the complete solar spectrum. (*ii*) UV-A + PAR: in this treatment (Mylar), UV-B was excluded by wrapping the quartz tubes with Dupont 0.05-mm-thick type D Mylar®. (*iii*) PAR only (OP-2): UV-A and UV-B were eliminated by placing the quartz tubes under a 3-mm-thick piece of the acrylic sheet material OP-2® (Cyro Industries). There was no OP-2 treatment in experiment 1 because we had not yet received the material from the manufacturer. The spectral irradiance measured under these materials verified their effectiveness in producing the desired exposure treatment (Fig. 1*a*). There were a total of 42 quartz tubes in each experiment (except for experiment 1, in which there were 28): seven for each light regime at each of the two depths. Incubations were run for 10 days.

Physical variables

The temperature (degrees Celsius) and salinity (precision salinity units) of the water in the outdoor reservoir was recorded during each day of the experiments using a conductivity/salinity/temperature probe (model 130, Orion Research Inc., Beverly, Mass.).

Spectral irradiance was measured, at both incubation depths, using an OL754-O-PMT scanning spectroradiometer equipped with a submersible detector (OL-86T-WP) (Optronic Laboratories, Orlando, Fla.). This instrument provides spectroradiometric data from 250 to 800 nm, with a resolution of 1 nm. Spectral transmission profiles for the screening materials used in the exposure experiments were also measured with this instrument.

Wavelength-specific diffuse attenuation coefficients ($K_{d\lambda}$) were derived from the spectral irradiance scans made at the two incubation depths. Ten percent depths for the UV waveband were calculated from these $K_{d\lambda}$ values. These calculations are detailed in Kuhn et al. (1999).

Data on total daily UV-B energy delivered to the earth's surface at this location were obtained using a Brewer MKIII double monochromator spectrophotometer (Sci-Tec Instruments Inc., Saskatoon, Sask.) deployed on the roof of the Maurice Lamontagne Institute. Brewer data were not available for all days because of instrument malfunction.

Biological variables

Atlantic cod eggs become opaque shortly after dying, making it possible to census mortality by visual inspection. Thus, the number of dead eggs in each of the incubation tubes was counted daily throughout each experiment. To minimize handling, dead eggs

© 1999 NRC Canada

Fig. 2. Ten percent depths (the depth to which 10% of the surface energy penetrates at a given wavelength), plotted on a common log scale, for the water in the outdoor reservoir on the south shore of the St. Lawrence estuary (49°05′35″W, 67°05′83″N; see Station R5 on the map in Kuhn et al. 1999) and in the Gulf of St. Lawrence at a location near Atlantic cod spawning sites (49°07′25″W, 59°50′53″N; see Station S27 on the map in Kuhn et al. 1999).

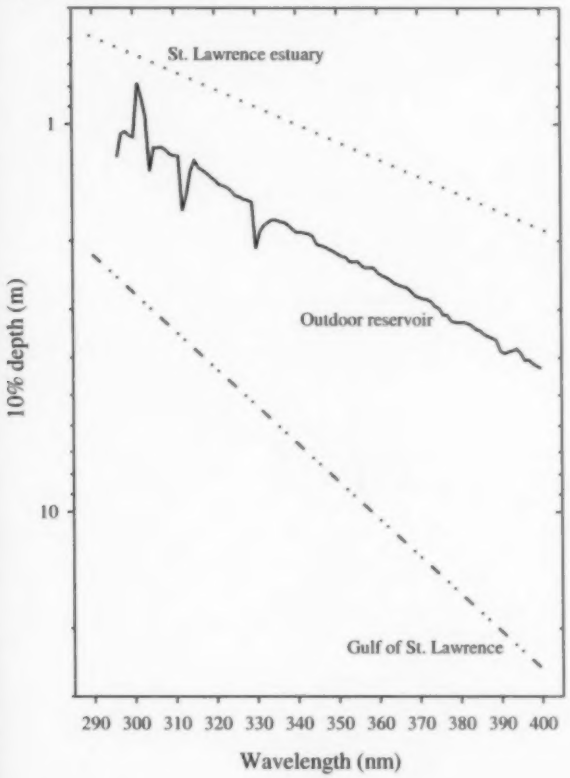

were not removed from the tubes until the end of the experiment. Tubes were retrieved from the outdoor reservoir at the end of each experiment and their content, live and (or) dead eggs and larvae, was examined under a binocular microscope. Hatching success, for experiments 4 and 5 only, was expressed as a percentage of the total number of eggs originally placed in each vial.

Live larvae, retrieved from the tubes at the end of experiments 4 and 5, were placed in petri plates in a temperature-controlled room at 6°C under a 12 h light :12 h dark photoperiod. Images of these yolk-sac larvae (n = 1–12), from the different light treatments and depths, were photographed or videotaped 24 h later. Yolk-sac larvae from the indoor rearing basin (the source of the eggs in each of these experiments) were also examined. Larvae were positioned on their left side. These images were used to quantify (*i*) standard length and (*ii*) the degree of corporeal pigmentation (the surface area covered with pigment as a function of the total surface area, excluding the eye and digestive system). These measurements were made using a Bioquant System IV imaging system (R&M Biometrics Inc., Nashville, Tenn.).

The progress of embryonic development was followed in experiments 1 and 2. Four or five eggs were removed every day from two of the vials in each treatment and at both depths. Embryos were viewed under a dissecting microscope and their developmental stage was determined following the numerical descriptive system proposed by Friðgeirsson (1978).

Statistical analysis

Cumulative mortality of Atlantic cod eggs was derived from the daily counts of dead eggs in each tube. These data were $\log(x)$, $\arcsin\sqrt{x}$, or $1/\sqrt{x}$ transformed to obtain homogeneity of variance and normally distributed error terms (Sokal and Rohlf 1994). A two-factor repeated measures design ANOVA was performed on the transformed data to determine the overall effect of spectral treatment and depth on egg mortality. A Tukey–Kramer multiple comparisons test was performed (on cumulative mortality) when the ANOVA identified a statistically discernible effect. This allowed determination of which treatments differed from one another. The Tukey–Kramer test could not be applied to experiment 1 because it requires a minimum of three levels and there were only two in that experiment, Quartz and Mylar.

Larval corporeal pigmentation, standard length, and hatching success data were $\log(x)$, $\sqrt{x}$, or power transformed (as necessary) before being evaluated by single-factor ANOVA (Sokal and Rohlf 1994). Data for larvae from the indoor rearing basins were not included in these analyses because they were not held under the same conditions as those exposed outdoors.

Results

Spectral irradiance

The PAR spectral irradiance delivered to the tubes in the outdoor reservoir was similar at both depths (Fig. 1*a*). However, irradiance in the UV waveband was several times higher at the surface than at 50 cm (Fig. 1*b*). Longer-wave radiation (>700 nm) was also rapidly attenuated (Fig. 1*a*).

The 10% depth for UV in the outdoor reservoir was about 1 m at 300 nm, 1.5 m at 320 nm, and 4.25 m at 400 nm (Fig. 2). Since the water in the reservoir was finely filtered, these 10% depths were greater than those for waters on the south shore of the St. Lawrence estuary (49°05′35″W, 67°05′83″N; see Station R5 on the map in Kuhn et al. 1999) (Fig. 2). However, 10% depths in the Gulf of St. Lawrence, at a location near Atlantic cod spawning sites, were higher than those in the reservoir (49°07′25″W, 59°50′53″N; see Station S27 on the map in Kuhn et al. 1999) (Fig. 2).

Egg mortality

The cumulative mortality of Atlantic cod eggs incubated at the surface was highest in the Quartz treatment on most days (Fig. 3). Although less pronounced, this was also true at 50 cm; at this incubation depth, eggs in the Quartz treatment died at a higher rate (Fig. 3*b*). Within any given treatment, cumulative mortality was generally lower at 50 cm depth than at the surface. In two of the experiments, cumulative mortality in the Quartz treatment at 50 cm depth was similar to that in the surface groups that were not exposed to UV-B (Mylar and OP-2) (Fig. 3, 19–29 August experiment). These differences were statistically discernible (Tables 1 and 2).

Developmental stage, hatching success, and larval viability

The progress of embryonic development was unaffected by spectral treatment, at either incubation depth (Table 3). By the end of the experiments, almost all embryos had reached embryonic stage 32 (the last embryonic stage before

© 1999 NRC Canada

Fig. 3. Percent cumulative mortality (mean ± SE) in Atlantic cod eggs incubated outside the Maurice Lamontagne Institute, Mont-Joli, Qué., Canada (48°38′25.9″N, 68°09′21.0″W) between 10 July and 12 September 1996. Incubations were carried out at two depths: (*a*) just below the surface and (*b*) 50 cm depth. Superimposed on the left-hand panels is the daily UV-B integrated irradiance (vertical bars). Superimposed on the right-hand panels are the salinity (precision salinity units) and temperature of the water in the outdoor reservoir throughout the experiments.

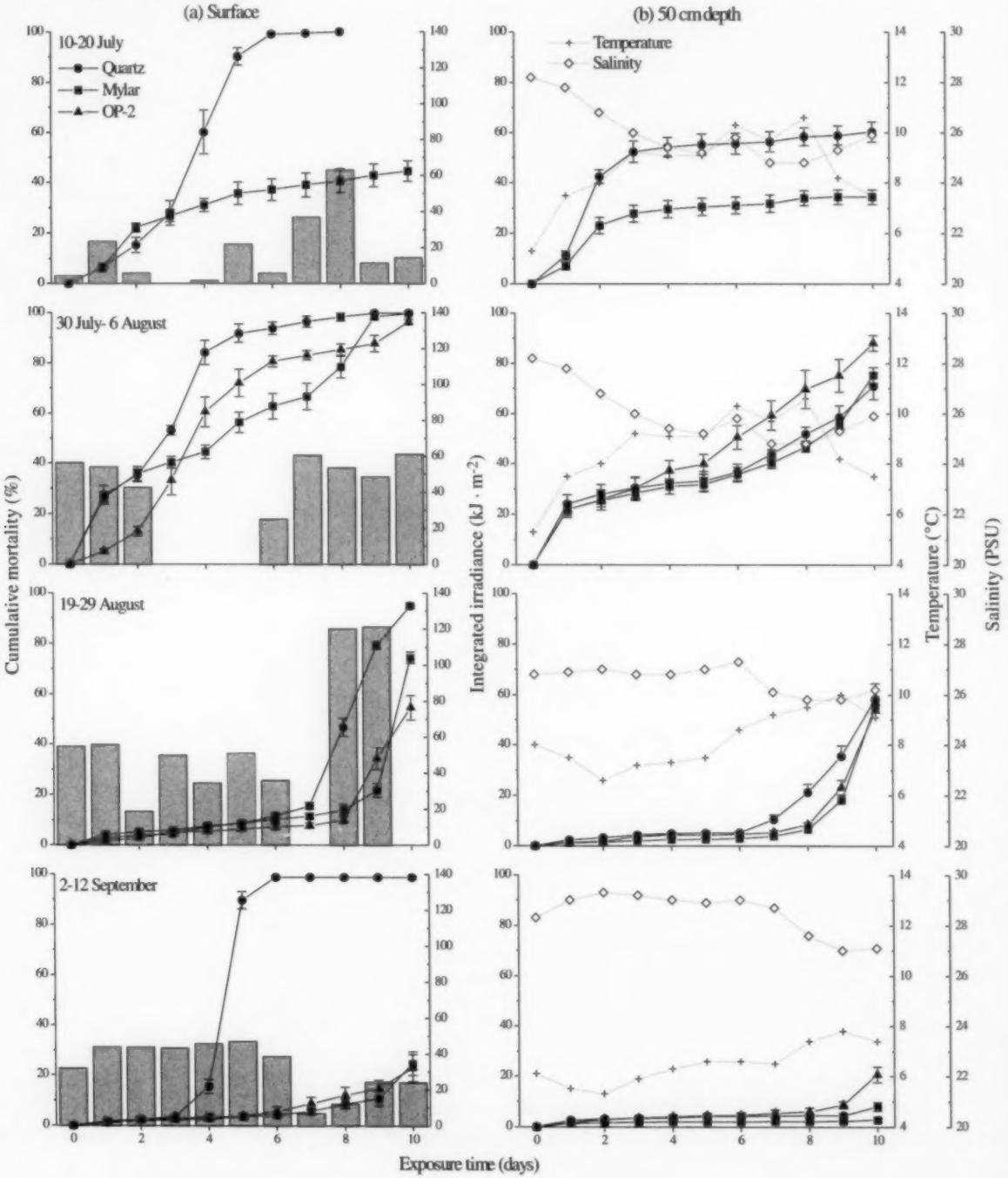

© 1999 NRC Canada

Table 1. Summary of the two-factor repeated measures design ANOVA's performed on the cumulative mortality of Atlantic cod eggs.

Selection	Experiment	Source(s)	df error	*Fs*	*p*
Entire experiment	1	Spectral exposure	24	53.735	<0.001
		Depth	24	2.054	0.165
	2	Spectral exposure	34	15.902	<0.001
		Depth	34	209.513	<0.001
	4	Spectral exposure	35	9.480	0.001
		Depth	35	31.940	<0.001
	5	Spectral exposure	36	9.662	<0.001
		Depth	36	14.640	<0.001
Surface	1	Spectral exposure	12	34.464	<0.001
	2	Spectral exposure	16	32.173	<0.001
	4	Spectral exposure	18	6.295	0.008
	5	Spectral exposure	18	9.291	0.002
50 cm	1	Spectral exposure	12	22.016	0.001
	2	Spectral exposure	18	7.016	0.006
	4	Spectral exposure	17	7.229	0.005
	5	Spectral exposure	18	4.128	0.033
Quartz	1	Depth	12	2.519	0.138
	2	Depth	12	266.260	<0.001
	4	Depth	12	5.961	0.031
	5	Depth	12	19.845	0.001
Mylar	1	Depth	12	0.645	0.437
	2	Depth	12	56.646	<0.001
	4	Depth	12	34.315	<0.001
	5	Depth	12	5.531	0.037
OP-2	1	Depth	na	na	na
	2	Depth	10	10.305	0.009
	4	Depth	11	2.948	0.114
	5	Depth	12	0.109	0.747

Note: The ANOVA's test for the overall effect of spectral exposure treatment, and depth, on egg mortality. The spectral exposures were UV-B + UV-A + PAR (Quartz), UV-A + PAR (Mylar), and PAR (OP-2). Incubation depths were surface and 50 cm. na, not available.

hatching), but most never hatched (Table 4). Hatching success was highest in the OP-2 treatment (Tables 4 and 5). Those larvae that did hatch were moribund and died soon after exiting the egg.

Corporeal pigmentation and standard length

Neither corporeal pigmentation nor the standard length of larvae was affected by spectral exposure, at either depth (Tables 4 and 5).

Discussion

Direct effects of UV-B

Egg mortality

Atlantic cod embryos exposed to UV-B (Quartz treatment) exhibited higher cumulative mortality than those shielded from UV-B (Mylar and OP-2 treatments). UV-B-induced mortality at the surface was virtually 100%, while that at 50 cm depth was less severe. The mechanism of this mortality appears to be direct damage to the DNA molecule (Kouwenberg et al. 1999).

Mortality of yellow perch (*Perca flavescens*) eggs, incubated in situ at various depths and with spectral exposure treatments similar to those reported here, was very high (>95%), even at depths up to 0.8 m (Williamson et al. 1997). Observations from the few other studies on UV-B-induced mortality in fish eggs are also consistent with our results (Marinaro and Bernard 1966; Pommeranz 1974; Hunter et al. 1982).

Several studies report on negative effects of UV-A: hatching success in the Japanese medaka (*Oryzias latipes*) is adversely affected by UV-A exposure (Bass and Sistrun 1997), long exposures to UV-A had negative effects on the metabolic performance and survivorship of the convict cichlid *Cichlasoma nigrofasciatum* (Winckler and Fidhiany 1996*a*, 1996*b*), and in situ exposure to UV-A induced elevated mortality in yellow perch eggs (Williamson et al. 1997). In the experiments reported here, Atlantic cod eggs were not negatively affected by exposure to UV-A: there were no clear dif-

© 1999 NRC Canada

Table 2. Summary of the Tukey–Kramer multiple comparisons tests on the cumulative mortality of Atlantic cod eggs.

			Exposure (days)									
Experiment	Depth	Spectral exposure	1	2	3	4	5	6	7	8	9	10
2	Surface	Quartz	a	a	b	b	b	b	b	b	a	a
		Mylar	a	a	a	a	a	a	a	a	a	a
		OP-2	b	b	a	a	a	a	a	a	b	b
	50 cm	Quartz	a	a	a	a	a	a	a	ab	ab	a
		Mylar	a	a	a	a	a	a	a	a	a	a
		OP-2	a	a	a	a	a	b	b	b	b	a
4	Surface	Quartz	a	a	a	a	a	a	a	a	a	a
		Mylar	b	a	a	a	a	ab	a	b	b	b
		OP-2	ab	a	a	a	a	b	b	b	c	c
	50 cm	Quartz	a	a	a	a	a	a	a	a	a	a
		Mylar	a	a	b	b	b	b	b	b	b	a
		OP-2	a	a	ab	ab	ab	ab	ab	b	ab	a
5	Surface	Quartz	a	a	a	a	a	a	a	a	a	a
		Mylar	a	a	a	b	b	b	b	b	b	b
		OP-2	a	a	a	b	b	b	b	b	b	b
	50 cm	Quartz	a	a	a	a	a	a	a	a	a	a
		Mylar	a	a	a	a	a	a	a	a	b	b
		OP-2	a	a	a	a	a	a	a	a	a	a

Note: This test identifies under which spectral exposures cumulative mortality was different on each day (within a single depth). The same letter in any given column indicates that there is no discernible difference between those treatments at that depth and on that day. A different letter indicates a discernible difference. The spectral exposures were UV-B + UV-A + PAR (Quartz), UV-A + PAR (Mylar), and PAR (OP-2).

Table 3. Embryonic development of Atlantic cod during 10-day exposures to solar radiation.

			Exposure (days)										
Experiment	Depth	Light regime	0	1	2	3	4	5	6	7	8	9	10
1	Surface	Quartz	14	18	21	24	24	28	ad	ad	ad	ad	ad
		Mylar	14	18	21	24	24	28–30	30	31	32	32	32, hatching
	50 cm	Quartz	14	18	21	24	24	30	30–31	31–32	32	32	32, hatching
		Mylar	14	18	21	24	24	30	30	31–32	32	32	32, hatching
2	Surface	Quartz	18	21	24	26	na	na	na	na	32	32	ad
		Mylar	18	21	24	27–28	29	30	30–31	31	32	32	ad
		OP-2	18	21	24	26–27	30	30	30	31	32	32	32, hatching
	50 cm	Quartz	18	21	24	26	30	30	31–32	32	32	32	32, hatching
		Mylar	18	21	24	28	30	30	31	32	32	32, hatching	32, hatching
		OP-2	18	21	24	28	30	30	31	32	32	32, hatching	32, hatching

Note: Measurements were made for embryos incubated under three spectral exposures, UV-B + UV-A + PAR (Quartz), UV-A + PAR (Mylar), and PAR (OP-2), and at two depths, surface and 50 cm. ad, all dead; na, not available.

ferences in mortality, rate of development, pigmentation, or size in the UV-A + PAR treatment relative to the PAR-only treatment (OP-2). This result is consistent with other experiments, conducted at a higher spectral resolution (three discrete spectral treatments within the UV-A waveband as opposed to the one presented here), on UV-induced mortality in Atlantic cod eggs: there was no clear negative effect of UV-A (Kouwenberg et al. 1999). Further experiments on the role of UV-A and visible light are required to resolve this issue.

Mortality in the treatments that were not exposed to UV was high, but egg mortality in the indoor rearing basins, in which the source egg populations were maintained throughout these experiments, was also high. Nonetheless, some discussion of the elevated mortality exhibited by all of the treatment groups (in all but the last experiment) is necessary.

Fluctuations in water temperature and salinity might have influenced Atlantic cod egg mortality during these experiments. However, mortality of Atlantic cod eggs incubated at 5 and 10°C (Hunt von Herbing and Boutilier 1996) or between 2 and 12°C (Laurence and Rogers 1976) was not discernibly different. The temperatures to which Atlantic cod eggs were exposed in the current experiments fall within this range (Fig. 3). Further, development of Atlantic cod eggs is apparently normal at salinities above 11 precision salinity units (Westin and Nissling 1991). Thus, it is unlikely that

© 1999 NRC Canada

Table 4. Corporeal pigmentation, standard length, and hatching success of Atlantic cod larvae hatched from eggs exposed to solar radiation for 10 days and at two depths.

		Experiment 4		Experiment 5	
Variable	Spectral exposure	Surface	50 cm	Surface	50 cm
Corporeal igmentation (%)	Quartz	na	19.0±5.6 (5)	na	26.1±1.7 (5)
	Mylar	na	23.4±3.1 (9)	na	24.4±3.2 (11)
	OP-2	17.6±9.9 (2)	17.8±4.7 (2)	28.5±5.4 (11)	22.9±2.2 (12)
	Indoor basin	16.8±2.6 (12)		13.3±3.9 (12)	
Standard length (mm)	Quartz	na	3.8±0.2 (5)	na	3.8±0.1 (5)
	Mylar	na	3.9±0.1 (9)	na	3.8±0.2 (11)
	OP-2	3.4±0.3 (2)	3.1±0.1 (2)	3.6±0.1 (11)	3.7±0.1 (12)
	Indoor basin	3.8±0.2 (12)		4.5±0.1 (12)	
Hatching success (%)	Quartz	0.0	1.13±0.45	0.0	2.03±0.55
	Mylar	0.88±0.35	5.91±0.67	0.0	5.76±0.86
	OP-2	17.97±2.32	7.76±0.78	8.39±1.89	7.64±1.38

Note: The spectral exposures were UV-B + UV-A + PAR (Quartz), UV-A + PAR (Mylar), and PAR (OP-2). Also reported are values for larvae hatched in the indoor rearing basins. Values are means ± SE (*n* in parentheses). na, not available.

Table 5. Summary of the single-factor ANOVA's performed on corporeal pigmentation, standard length, and hatching success of Atlantic cod larvae.

Variable	Experiment	Depth	Spectral exposure	df error	*Fs*	*p*
Corporeal pigmentation	4	50 cm	Quartz, Mylar	12	1.271	0.282
	5	Surface, 50 cm	OP-2	21	0.772	0.390
	5	50 cm	Quartz, Mylar, OP-2	25	0.262	0.772
Standard length	4	50 cm	Quartz, Mylar	12	0.566	0.466
	5	Surface, 50 cm	OP-2	21	0.490	0.491
	5	50 cm	Quartz, Mylar, OP-2	25	0.902	0.418
Hatching success	4	50 cm	Quartz, Mylar, OP-2	17	18.767	<0.001
	5	50 cm	Quartz, Mylar, OP-2	18	12.033	<0.001

Note: The ANOVA's test for the overall effect of spectral exposure treatment, or depth, on these variables. The spectral exposures were UV-B + UV-A + PAR (Quartz), UV-A + PAR (Mylar), and PAR (OP-2).

temperature or salinity alone would have caused the mortality observed. Other factors (bacterial or viral infection, high light intensity (across the entire spectrum), poor egg group quality, or some synergy among all of these) may have been responsible for the non-UV-B-related mortality observed.

Since all of the tubes in each of the experiments were incubated under the same water quality conditions, any differences in mortality were most likely the result of the spectral exposure treatments. Thus, the high mortality exhibited by many of the treatments does not obviate the conclusion that UV-B negatively affects Atlantic cod eggs: the UV-B-exposed group had the highest cumulative mortality, or reached 100% mortality soonest, in all of the experiments (Fig. 3).

Corporeal pigmentation and standard length

Melanosome dispersion in northern anchovy larvae exposed to UV-B was more pronounced than in those groups shielded from UV-B (Hunter et al. 1979). Further, UV-B-exposed larvae were darker than larvae reared indoors. These observations were interpreted as a shielding response that would protect the larva's tissues from damage due to absorption of high-energy UV-B photons (Hunter et al. 1979). Melanin content in the epidermis of juvenile hammerhead sharks increased in response to the higher levels of solar radiation to which they are exposed when they migrate to the near-surface waters of Hawaii (Lowe and Goodman-Lowe 1996). It appears, therefore, that pigments play an important photoprotective role in aquatic vertebrates, as they do in zoolankton (Dey et al. 1988). Despite this, there was no discernible effect of UV-B exposure on the pigmentation of Atlantic cod larvae in our experiments. This was most likely due to the small number of larvae that survived the experiments: given the small sample sizes, it is not possible to say definitively that UV-B exposure does not affect corporeal pigment coverage in Atlantic cod larvae.

There was no consistent difference in the size of Atlantic cod larvae reared under the different spectral exposures. This is contrary to the observations of Hunter et al. (1979), who reported that UV-B-exposed northern anchovy larvae were smaller than those shielded from UV-B. However, as was the case for pigment content, the small numbers of larvae available to be measured prevent any definitive conclusion.

Indirect effects of UV-B

Indirect effects of UV-B on Atlantic cod early life stages, and other ichthyoplankton, are also possible. UV-B can be a potent immunosuppressive agent in adult fishes (Salo et al. 1998); it is not yet known whether this is also true for em-

© 1999 NRC Canada

bryos or larvae. For species that spawn in the surface layer, UV-B may affect sperm quality (Don and Avtalion 1993; Valcarcel et al. 1994). There is also the potential effect of UV-B on food availability: the protozoan and zooplankton prey of fish larvae are also negatively affected by UV-B (e.g., Karanas et al. 1981; Chalker-Scott 1995; Häder et al. 1995; Williamson et al. 1997). Further, food quality might be negatively impacted by UV-B. For example, UV-B exposure reduces the omega-3 fatty acid content of some microalgae (Wang and Chai 1994). Fish larvae require these fatty acids in their diets and obtain them from the zooplankton that they ingest, zooplankton that themselves take up these fatty acids from the microalgae upon which they graze. One of the microalgal fatty acids that is negatively influenced by UV-B exposure, docosahexaenoic acid (Wang and Chai 1994), also appears to be important for normal visual and behavioural development in fish larvae (Bell et al. 1995; Masuda et al. 1998). All such indirect effects have yet to be evaluated; these will be a focus of our future efforts.

Ecological context

The experiments reported here indicate that Atlantic cod eggs, at least those present in the first metre of the water column, are susceptible to UV-B. The 10% depths for UV penetration in the outdoor reservoir were less than those for regions of the Gulf of St. Lawrence where Atlantic cod spawn (Fig. 2). This suggests that the impact of UV-B reported here is an underestimate of that which would be observed in the wild. This conclusion, however, must be carefully qualified.

Although the available information on the vertical distribution of Atlantic cod eggs in this region is limited, it appears that most are not present in the upper 4 m of the water column (Ouellet 1997). Even if most Atlantic cod eggs were present in the 10- to 15-m-deep mixed layer of the northern Gulf of St. Lawrence water column, they would be in circulation and their daily residence time in the upper 4 m would depend on meteorological and hydrographic conditions (among other things; see Solemdal and Sundby 1981). Short residence times, which appear likely, would further reduce the population-level impact of UV-B on Atlantic cod eggs.

A more complete quantitative assessment of direct UV-B effects on the population dynamics of Atlantic cod early life stages requires further information and analysis. Specifically: (*i*) detailed vertical distribution of eggs in the mixed layer of the water column (with high resolution in the upper 10 m), (*ii*) surface UV-B irradiance during the spawning period and subsurface spectral irradiance for waters supporting such eggs (see Kuhn et al. 1999), (*iii*) a biological weighting function, which explicitly considers the possibility of photorepair (and therefore the absence of reciprocity), for the effect of UV-B on Atlantic cod egg mortality (see Kouwenberg et al. 1999), and (*iv*) a model to predict the vertical position of passive particles (such as eggs) in the mixed layer and particularly their daily residence time near the surface under various meteorological and hydrographic conditions. All of these components would have to be incorporated into a broader simulation model that would provide an assessment of UV-B effects on a population of eggs distributed (and circulating) throughout the mixed layer (e.g., Neale et al. 1998). We are currently developing such a model for Atlantic cod eggs.

Finally, although UV-B can have negative impacts on ichthyoplankton populations, it must be viewed as only one among many environmental factors that produce the very high levels of mortality typically observed in the planktonic early life stages of marine fishes.

Acknowledgments

We are grateful for the assistance of the following colleagues: Marise Bélanger, Chris Hazzi, Pierre Joly, Juliana Kouwenberg, Penny Kuhn, and Jeffrey Runge. The biological impacts components of this project were supported by grants in aid of research from the Department of Fisheries and Oceans, the St. Lawrence Vision 2000 Program, and the Natural Sciences and Engineering Research Council of Canada (NSERC) to H.I. Browman and Jeffrey A. Runge. The optical and meteorological components were supported from these sources and also by grants in aid of research from Environment Canada's Atmospheric Environment Program to Bruce McArthur. F. Béland was supported by a postgraduate stipend from an NSERC operating grant to H.I. Browman.

References

Anderson, J., and de Young, B. 1995. Application of a one-dimensional model to vertical distributions of cod eggs on the northeastern Newfoundland Shelf. Can. J. Fish. Aquat. Sci. **52**: 1978–1989.

Bass, E.L., and Sistrun, S.N. 1997. Effect of UV-A radiation on development and hatching success in *Oryzias latipes*, the Japenese medaka. Bull. Environ. Contam. Toxicol. **59**: 537–542.

Bell, J.G., Batty, R.S., Dick, J.R., Fretwell, K., Navarro, J.C., and Sargent, J.R. 1995. Dietary deficiency of docosahexaenoic acid impairs vision at low light intensities in juvenile herring (*Clupea harengus* L.). Lipids, **26**: 565–573.

Brander, K.M. 1994. Spawning and life history information for North Atlantic cod stocks. ICES Coop. Res. Rep. No. 205.

Chalker-Scott, L. 1995. Survival and sex ratios of the intertidal copepod, *Tigriopus californicus*, following ultraviolet-B (290–320 nm) radiation exposure. Mar. Biol. **123**: 799–804.

Dey, D.B., Damkaer, D.M., and Heron, G.A. 1988. UV-B dose/dose-rate responses of seasonally abundant copepods of Puget Sound. Oecologia, **76**: 321–329.

Don, J., and Avtalion, R.R. 1993. Ultraviolet irradiation of tilapia spermatozoa and the Hertwig effect: electron microscopic analysis. J. Fish Biol. **42**: 1–14.

Dutil, J.-D., Castonguay, M., Hammill, M.O., Ouellet, P., Lambert, Y., Chabot, D., Browman, H., Gilbert, D., Fréchet, A., Gagné, J.-A., Gascon, D., and Savard, L. 1998. Environmental influences on the productivity of cod stocks: some evidence for the northern Gulf of St. Lawrence, and requireu changes in management practices. DFO Atl. Fish. Res. No. 98/18.

Friðgeirsson, E. 1978. Embryonic development of five species of gadoid fishes in Iceland waters. Rit Fiskideildar, Reykjavik.

Häder, D.P. 1997. Effects of ozone depletion on aquatic ecosystems. R.G. Landes Company, Austin, Tex.

Häder, D.P., Worrest, R.C., Kumar, H.D., and Smith, R.C. 1995. Effects of increased solar ultraviolet radiation on aquatic ecosystems. Ambio, **24**: 174–180.

Hunter, R.J., Taylor, J.H., and Moser, H.G. 1979. Effect of ultraviolet irradiation on eggs and larvae of the northern anchovy,

© 1999 NRC Canada

Engraulis mordax, and the Pacific mackerel, *Scomber japonicus*, during the embryonic stage. Photochem. Photobiol. **29**: 325–338.

Hunter, R.J., Kaupp, S.E., and Taylor, J.H. 1982. Assessment of effects of UV radiation on marine fish larvae. *In* The role of solar ultraviolet radiation in marine ecosystems. *Edited by* Calkins J. Plenum Press, New York. pp. 459–493.

Hunt von Herbing, I., and Boutilier, R.G. 1996. Activity and metabolism of larval Atlantic cod (*Gadus morhua*) from Scotian Shelf and Newfoundland source populations. Mar. Biol. **124**: 607–617.

Karanas, J.J., Worrest, R.C., and Dyke, H.V. 1981. Impact of UV-B radiation on the fecundity of the copepod *Acartia clausii*. Mar. Biol. **65**: 125–133.

Kerr, J.B., and McElroy, C.T. 1993. Evidence for large upward trends of ultraviolet-B radiation linked to ozone depletion. Science (Washington, D.C.), **262**: 1032–1034.

Kouwenberg, J.H.M., Browman, H.I., Cullen, J.J., Davis, R.F., St-Pierre, J.-F., and Runge, J.A. 1999. Biological weighting of ultraviolet (280–400 nm) induced mortality in marine zooplankton anf fish. I. Atlantic cod (*Gadus morhua* L.) eggs. Mar. Biol. In press.

Kuhn, P., Browman, H.I., St-Pierre, J.-F., and McArthur, B. 1999. Penetration of ultraviolet radiation in the waters of the estuary and Gulf of St. Lawrence. Limnol. Oceanogr. **44**: 710–716.

Laurence, G.C., and Rogers, C.A. 1976. Effects of temperature and salinity on comparative embryo development and mortality of Atlantic cod (*Gadus morhua* L.) and haddock (*Malanogrammus aeglafinus* L.). J. Cons. Cons. Int. Explor. Mer, **36**: 220–228.

Lough, R.G., Caldarone, E.M., Rotunno, T.K., Broughton, E.A., Burns, B.R., and Buckley, L.J. 1996. Vertical distribution of cod and haddock eggs and larvae, feeding and condition in stratified and mixed waters on southern Georges Bank, May 1992. Deep-Sea Res. II, **43**: 1875–1904.

Lowe, C., and Goodman-Lowe, G. 1996. Suntanning in hammerhead sharks. Nature (Lond.), **383**: 677.

Malloy, K.D., Holman, M.A., Mitchell, D., and William Detrich, H. 1997. Solar UV-B-induced DNA damage and photoenzymatic DNA repair in antarctic zooplankton. Proc. Natl. Acad. Sci. U.S.A. **94**: 1258–1263.

Marinaro, J., and Bernard, M. 1966. Contribution à l'étude des oeufs et des larves pélagiques de poissons méditerranés. I. Notes préliminaires sur l'influence létale du rayonnement solaire sur les oeufs. Pelagos, **6**: 49–55.

Masuda, R., Takeuchi, T., Tsukamoto, K., Ishizaki, Y., Kanematsu, M., and Imaizumi, K. 1998. Critical involvement of dietary docosahexaenoic acid in the ontogeny of schoolong behaviour in the yellowtail. J. Fish Biol. **53**: 471–484.

Mitani, H., Uchida, N., and Shima, A. 1996. Induction of cyclobutane pyrimidine dimer photolyase in cultured fish cells by UVA and blue light. Photochem. Photobiol. **64**: 943–948.

Neale, P.J., Davis, R.F., and Cullen, J.J. 1998. Interactive effects of ozone depletion and vertical mixing on photosynthesis of Antarctic phytoplankton. Nature (Lond.), **392**: 585–589.

Ouellet, P. 1997. Characteristics and vertical distribution of Atlantic cod (*Gadus morhua*) eggs in the northern Gulf of St. Lawrence, and the possible effect of cold water temperature on recruitment. Can. J. Fish. Aquat. Sci. **54**: 211–223.

Ouellet, P., Lambert, Y., and Castonguay, M. 1997. Spawning of Atlantic cod (*Gadus morhua*) in the northern Gulf of St. Lawrence: a study of adult and egg distributions and characteristics. Can. J. Fish. Aquat. Sci. **54**: 198–210.

Petrie, B., Akenhead, S., Lazier, J., and Loder, J. 1988. The cold intermediate layer on the Labrador and northeast Newfoundland shelves, 1978–1986. NAFO Sci. Counc. Stud. **12**: 547–569.

Pommeranz, T. 1974. Resistance of plaice eggs to mechanical stress and light. *In* The early life history of fish. *Edited by* J.H.S. Blaxter. Springer-Verlag, New York. pp. 397–416.

Salo, H.M., Aaltonen, T.M., Markkula, S.E., and Jokinen, E.I. 1998. Ultraviolet B irradiation modulates the immune system of fish (*Rutilus rutilus*, Cyprinidae). I. Phagocytes. Photochem. Photobiol. **67**: 433–437.

Sokal, R.R., and Rohlf, F.J. 1994. Biometry. The principles and practice of statistics in biological research. W.H. Freeman and Company, San Francisco, Calif.

Solemdal, P., and Sundby, S. 1981. Vertical distribution of pelagic fish eggs in relation to species, spawning behavior and wind conditions. ICES CM 1981/G:77.

Therriault, J.-C. 1991. The Gulf of St. Lawrence: small ocean or big estuary? Can. Spec. Publ. Fish. Aquat. Sci. No. 113.

Valcarcel, A., Guerrero, G., and Maggese, M.C. 1994. Hertwig effect caused by UV-irradiation of sperm of the catfish, *Rhamdia sapo* (Pisces, Pimelodidae), and its photoreactivation. Aquaculture, **128**: 21–28.

Vetter, R.D., Kurtzman, A.L., and Mori, T. 1999. Diel cycles of DNA damage and repair in eggs and larvae of northern anchovy, *Engraulis mordax*, exposed to solar ultraviolet radiation. Photochem. Photobiol. **69**: 27–33.

Wang, K.S., and Chai, T. 1994. Reduction in omega-3 fatty acids by UV-B irradiation in microalgae. J. Appl. Phycol. **6**: 415–421.

Westin, L., and Nissling, A. 1991. Effects of salinity on spermatozoa motility, percentage of fertilized eggs and egg development of Baltic cod (*Gadus morhua*), and implications for cod stock fluctuations in the Baltic. Mar. Biol. **108**: 5–9.

Williamson, C.E., Metzgar, S.L., Lovera, P.A., and Moeller, R.E. 1997. Solar ultraviolet radiation and the spawning habitat of yellow perch, *Perca flavenscens*. Ecol. Appl. **7**: 1017–1023.

Winckler, K., and Fidhiany, L. 1996*a*. Significant influence of UV-A on the general metabolism in the growing cichlid fish, *Cichlasoma nigrofasciatum*. J. Photochem. Photobiol. B. Biol. **33**: 131–135.

Winckler, K., and Fidhiany, L. 1996*b*. Combined effects of constant sublethal UV-A irradiation and elevated temperature on the survival and general metabolism of the convict-cichlid fish, *Cichlasoma nigrofasciatum*. Photochem. Photobiol. **63**: 487–491.

© 1999 NRC Canada

Floating, switching, or nonswitching as different behaviours when Arctic char (*Salvelinus alpinus*) are visiting two feeding tanks

Eva Brännäs and Torleif Eriksson

Abstract: The following questions were addressed. Will individual Arctic char (*Salvelinus alpinus*) differ in their visiting strategies when given a choice between two feeding tanks? If so, will the choice of strategy depend on individual characteristics (size) and will it affect their success (growth)? Further, will their allocation of visits to the two feeding tanks correspond to the food ratio? The passages between the nonfeeding tank and the two equally rich feeding tanks were recorded for four separate groups during a 3-week period. In an additional study, a single group was continuously monitored for 5 months using the same setup, but the feed ratio between the two feeding tanks was changed. Certain individuals in both studies consistently visited the same feeding tank (nonswitchers) and these were the most successful ones in terms of growth rate. Other individuals either kept visiting both tanks (switchers) or spent most of their time in the nonfeeding tank (floaters). These behaviours were applied by individuals that had a lower growth rate and are therefore likely to have lower competitive ability or feeding motivation. No significant difference in initial weight between the behavioural categories was found in either of the two studies. In the four-group study, the proportion of visits into the two feeding tanks matched the food ratio among the switchers only and the distribution of the groups failed to match the food ratio. In the single-group study, the group distributed according to the food ratio (ideal free distribution) if they were given sufficient time to learn the quality of the patches. A change in the relative food ratio caused the switchers and floaters to alter their visiting behaviour, always favouring the more profitable tank, whereas the nonswitchers continued to visit the same tank.

Résumé : Nous avons voulu répondre aux questions suivantes. Est-ce que les ombles chevaliers (*Salvelinus alpinus*) adopteront différentes stratégies de visite si on leur donne le choix entre deux bassins d'alimentation? Si oui, est-ce que le choix de stratégie dépendra de caractéristiques individuelles (taille) et aura un impact sur leur condition (croissance)? De plus, est-ce que la répartition de leurs visites entre les deux bassins d'alimentation correspondra au ratio alimentaire? Les passages entre le bassin sans aliments et les deux bassins renfermant des ressources alimentaires identiques ont été enregistrés pour quatre groupes distincts durant trois semaines. Dans une autre expérience, on a surveillé en continu durant cinq mois un groupe unique dans le même dispositif, sauf que le ratio d'aliments entre les deux bassins d'alimentation avait été changé. Dans les deux expériences, certains individus ont constamment visité le même bassin d'alimentation, et ces individus ont montré le meilleur taux de croissance. D'autres individus ont visité tour à tour les deux bassins d'alimentation ou ont passé le plus clair de leur temps dans le bassin sans aliment. Ces derniers comportements ont été observés chez des individus qui avaient un taux de croissance moins élevé et qui sont donc probablement moins aptes à la compétition ou moins motivés à s'alimenter. Dans les deux expériences, on n'a observé aucune différence significative dans les poids initiaux des individus des diverses catégories comportementales. Dans l'expérience des quatre groupes, la proportion de visites dans les deux bassins d'alimentation ne correspondait au ratio alimentaire que dans le cas des individus qui visitaient les deux bassins, et la distribution des groupes ne correspondait pas au ratio alimentaire. Dans l'expérience du groupe unique, le groupe se distribuait selon le ratio alimentaire (distribution libre idéale) si on donnait aux individus un temps d'apprentissage suffisant pour l'évaluation des réserves alimentaires. Un changement dans le ratio alimentaire relatif faisait en sorte que les individus qui visitaient les deux bassins et ceux qui demeuraient le plus souvent dans le bassin sans aliment modifiaient leur comportement de visite, toujours en faveur du bassin le plus profitable, tandis que ceux qui visitaient toujours le même bassin d'alimentation continuaient de visiter ce même bassin.

[Traduit par la Rédaction]

Received September 26, 1997. Accepted February 5, 1999.
J14220

E. Brännäs[1] and T. Eriksson. Department of Aquaculture, Swedish University of Agricultural Sciences, S-901 83, Umeå, Sweden.

[1]Author to whom all correspondence should be addressed. e-mail: eva.brannas@vabr.slu.se

© 1999 NRC Canada

Introduction

The way in which Arctic char (*Salvelinus alpinus*) utilise temporary feeding habitats is typical of opportunistic species (reviewed by Johnson 1980). According to Näslund (1990) and Näslund et al. (1993), individuals in a Swedish landlocked Arctic char population showed one of two migrating strategies: some temporarily changed habitats during the summer, while others remained in their home habitat. There is, however, little knowledge if individual characteristics such as competitive ability, size, or others determine an Arctic char's choice of strategy and the subsequent effect of this strategy on growth. Available field data indicate that individuals that shift habitats tend to have a lower condition factor than nonmigrating fish before the migration period in early summer, but eventually gain by a faster growth rate in the temperate rich habitat compared with those individuals that remain in the home lake (Näslund 1990). Slaney and Northcote (1974) suggested that it is likely that less competitive fish face limited access to resources, which could explain why they accept the cost of migrating to potentially better feeding habitats.

In experimental studies on fish, individual differences in sampling behaviour are also found. For instance, when food is released on each side of an aquarium, groups of sticklebacks display two strategies (Milinski 1984). At first, they all sample on both sides, but soon, some individuals remain feeding on one side of the aquarium. These individuals have greater feeding success than the other fish that continue to sample both patches. Similarly, individual cichlids differ in patch-switching frequency, with the high-frequency switchers having a lower feeding rate than the low-frequency switchers (Godin and Keenleyside 1984). In addition, Talbot and Kramer (1986), who analysed the distribution of guppies in a more complex system consisting of five feeding patches surrounded by nonfeeding areas, found that 50% of the fish, which they defined as floaters, remained in nonfeeding areas. The floaters had a lower mean weight than those individuals found in the feeding patches (Talbot 1983).

The aim of this study was to test the hypothesis that individuals in groups of Arctic char apply different strategies when utilising two different feeding patches and that the strategy that an individual applies depends on its ability to compete for and utilise the food resources. Groups of Arctic char reared in captivity typically develop pronounced dominance hierarchies that result in measurable growth variations (Jobling 1995). In this study, the individual visits of Arctic char to two different well-delimited feeding areas were continuously monitored using a passive integrated transponder (PIT) system, their behaviour was analysed with respect to different strategies used, and success was measured by growth rate.

In addition, we focused on the correspondence between the feeding patch distribution of the behavioural categories and the relative profitability of the two feeding tanks. When predicting and (or) measuring the distribution of animals within patchy feeding habitats, ideal free distribution (IFD) models are often applied. These models have succeeded in predicting the distribution of groups between food patches of different profitability in short-term experiments where the patches are on opposite sides of an aquarium (reviewed by Sutherland 1996). However, the distribution of fish groups between feeding patches in more complex systems and over longer periods is less well known.

Material and methods

The visiting activity into two feeding tanks with respect to individual differences in strategy was analysed using data from a previous study, which was designed to evaluate the use of multitank systems for rearing Arctic char (Brännäs 1998). In this previous study, four replicate groups were continuously monitored for 3 weeks each at constant food and environmental conditions. Also, results from a long-term study were included in the analysis where a single group was monitored for 5 months under natural photoperiod and ambient temperature and with monthly changes in feed ratio between the two feeding areas. The purpose of the second study was to test the application of regression models for individual data in single groups (included in the results). These models will be applied to forthcoming field studies on the partial migration in Arctic char using the PIT tag system. The differences in abiotic factors (e.g., constant conditions in the four-group study and ambient condition in the single-group study) in the two studies were not deliberately chosen but depended on changing conditions in the experimental facility.

Experimental animals and setup

Hatchery-reared Arctic char from a landlocked population in Lake Rensjön, central Sweden, were used in both experiments. The hatchery-reared fish originated from wild-caught parents. The Arctic char were transferred from the hatchery to the laboratory at least 3 months prior to the respective experiment. Fish from each experiment were reared as a single group in a tank (1 × 1 × 0.9 m) receiving water at a flow rate of 12 L/min. Fish density during this rearing period was 30–40 kg/m^3, during which fish in the single-group study were maintained under a natural photoperiod, while fish in the four-group study were reared under a constant 12 h light : 12 h dark photoperiod. This difference was unavoidable due to changes in the experimental facilities over the course of the two studies. The Arctic char were fed standardised rations of commercial pellets based on fish size and water temperature and had no prior experience with the three-tank system. The fish were anaesthetised with phenoxyethanol when handled for tagging and weighing purposes.

Three tanks connected by fibreglass tubes (length 0.38 m, diameter 0.2 m) constituted the experimental system. The largest tank, in which no food was presented, was 2 × 2 × 0.65 m and was connected to two smaller feeding tanks (Tanks 1 and 2, 1 × 1 × 0.9 m). Movements of individual fish in and out of the feeding tanks were monitored using a PIT registration system. Antennas were placed close to the ends of the connecting tubes to ensure that a passage was registered only when a fish left the tube. Each time a PIT tag came within 200 mm of an antenna, it was activated, and a tag-specific, 10-digit hexadecimal identification number was stored in a computer. Details of the registration system are given in Prentice et al. (1990) and the use of PIT tags in behavioural studies is described in Brännäs et al. (1994).

The setup was located at the Marine Research Centre along Bothnian Bay (63°35′N, 19°50′E). Brackish (3–4‰) water was supplied to the two feeding tanks (flow rate 10 L/min). From here, the water flowed via connecting tubes into the bigger tank and left through a central drain outlet. The water level was kept at 45 cm.

Four-group experiment

The fish in the four-group experiment were exposed to a constant artificial day length of 12 h of light and 12 h of dark with lights on at 08:00 h and to a constant water temperature of 10 ±

© 1999 NRC Canada

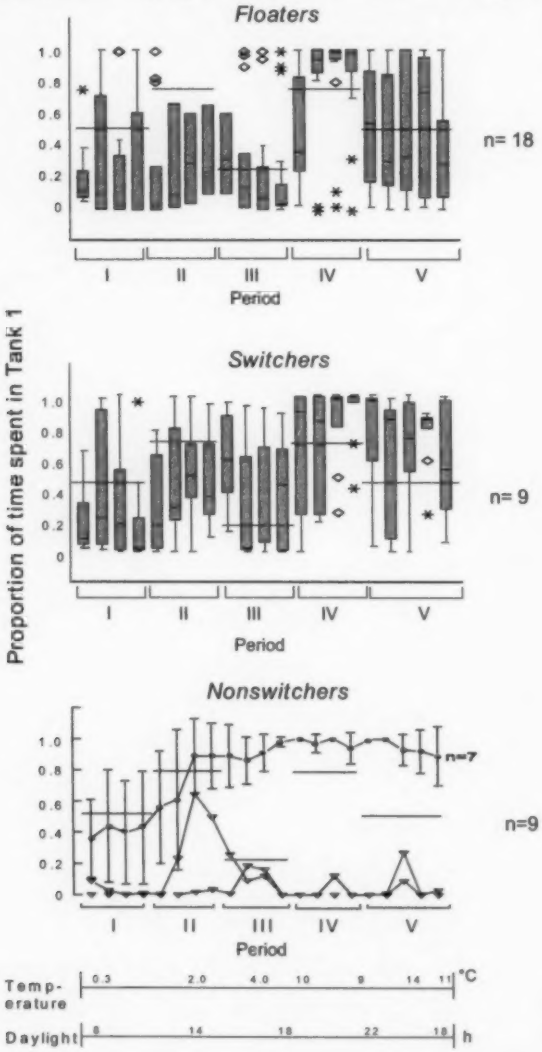

Fig. 1. Temporal variation in Tank 1 proportions of total time spent in feeding tanks by a single group during 5 months where the individuals were classified as floaters, switchers, or nonswitchers based on their behaviour. During periods I–V, the Tank 1/(Tank 1 + Tank 2) food level ratio was 0.5/0.5, 0.75/0.25, 0.25/0.75, 0.75/0.25, and 0.5/0.5, respectively. Box plots represent the distribution of individual Tank 1 proportions of total duration in food tanks for switchers and floaters. The corresponding proportions are given as single values for nonswitchers. Data from each feeding period are divided into four subperiods (8–10 days). Solid horizontal lines indicate feeding levels in Tank 1. The medians divide the bars, and asterisks and circles represent outliers. Annual fluctuations in temperature and daylength are given at the bottom of the figure.

1°C. Fluorescent lamps in the ceiling 3 m above the tanks were the only light source and gave an evenly distributed light of about 5.2 μeinsteins/m^2 just above the water surface. Three weeks before the start of each replicate round, 40 individuals were selected. PIT tags were then injected into their body cavity and they were acclimatised to the temperature conditions in a separate fish-rearing tank of the type in which they had been raised. The initial temperature ranged from 0.3°C in January through April (groups 1 and 2) to 5°C in May (group 3) and 7°C in June (group 4). The period of gradual temperature increase lasted 7 days at 0.3°C, 3 days at 5°C, and 1 day at 7°C. After the acclimatisation period, the weight of each fish was registered. The Arctic char were then put into the large nonfeeding tank and registrations were started. Since the replications were carried out in succession and all fish came from the same population, mean weights generally increased. Increases in mean start weight were 21.1 ± 7 g in group 1, 20.5 ± 6.3 g in group 2, 40.2 ± 10.9 g in group 3, and 51.2 ± 15.8 g in group 4. During the registration period, the fish were fed a daily ration of dry food equal to 0.8% of the total fish wet weight.

The daily ration was divided equally between the two feeding patches. Automatic feeders supplied the food in equal aliquots 12 times a day each hour from 08:00 to 20:00. Movements of all fish between tanks were registered for 3 weeks before the fish were collected and weighed again to determine their individual growth rates. During the registration period, two Arctic char died in group 1, one in group 2, none in group 3, and one in group 4. These individuals were excluded from the study; thus, data from 156 Arctic char were used in the analysis.

Single-group experiment

During the course of the experiment, the fish in the single-group experiment were exposed to natural variations in day length and water temperature with the only source of light coming from the windows. In February, when the experiment was started, the initial water temperature was 0.3°C. The temperature started to increase in April and reached a maximum of 14.8°C in August. The day length increased steadily from 7 h in February to 22 h in June and then decreased to 19 h in August (Fig. 1). Fish ranging from 155 to 170 mm in length and from 33.4 to 67.5 g (mean ± SD 46.8 ± 8.2 g) in weight were selected. A PIT tag was injected into the body cavity of each fish 1 month before starting the experiment. Then, the registration started after putting the 36 fish into the larger nonfeeding tank on February 23. Movements of the Arctic char were continuously monitored for 5 months, i.e., until August 5. The two feeding tanks were initially equal in terms of the relative profitability of foraging in them. The total dry weight of food supplied increased from 0.4%/fish wet weight in February to 0.9% in August. At intervals of 4–5 weeks thereafter, the Tank 1 to Tank 2 food level ratio was changed from 0.5:0.5 to 0.75:0.25 to 0.25:0.75 to 0.75:0.25 and back to 0.5:0.5 again (Fig. 1). The total daily amount of food was equally distributed among 10 feeding periods that occurred synchronously in the two tanks. Feeding periods were distributed uniformly in time between dawn and sunset, following the natural photoperiod; thus the feeding interval ranged from 65 min in February to a maximum of 143 min by the end of June. Weight and length measurements on each fish were collected at the start and the end of the experiment and, on one occasion, at the start of period IV during the course of the experiment.

Data management and statistical analyses

Growth rate was used as a measure of individual success in competing for food. The measure used was $gw = 100(\ln w_2 - \ln w_1)/$ number of days, where w_2 is the final weight and w_1 the initial weight. Jobling et al. (1989) found a strong linear correlation between the amount of food eaten (using X-ray analysis) and growth rate in Arctic char. The sequence in which signals are received from antennas surrounding the connecting tube can be analysed to determine whether a given fish was entering or leaving one of the feeding tanks. The software allows the total time spent in each feeding tank and the total number of visits to be calculated for each individual. Visits to feeding tanks that lasted less than 10 s

© 1999 NRC Canada

Fig. 2. Box plots representing the distribution of individual Tank 1 proportions of total duration in food tanks for floaters and switchers. The corresponding proportions are given as single values for nonswitchers. The 3-week registration periods of groups 1–4 are divided into the first and second 10-day period. The proportions are pooled for four replicate groups and divided into three behavioural categories: floaters, switchers, and nonswitchers.

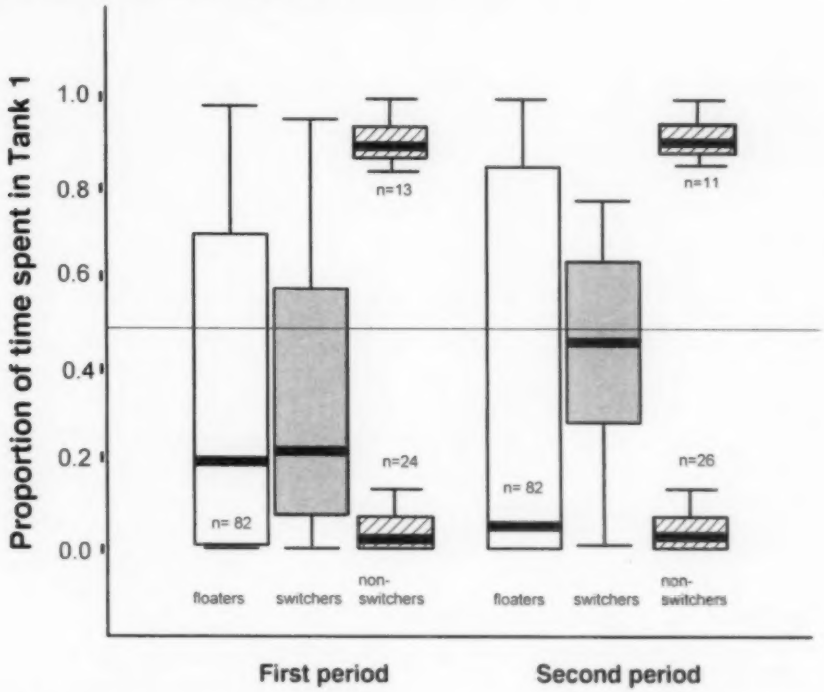

were deleted because it is unlikely that food would have been obtained in a visit of such short duration.

The impact of patch quality on the proportion of time spent in Tank 1 or on the number of visits to Tank 1 was tested on accumulated 8- to 10-day visiting data, corresponding to each point on the x value in Figs. 1 and 2. A conventional test of the proportion (Wonnacott and Wonnacott 1972) was made on the mean values in the four-group experiment. The test is $(P - \alpha)/(\alpha(1 - \alpha)/n^{1/2})$, where α is 0.5 and P is the observed proportion.

In the single-group experiment the impact of food ratio on the distributions of the duration and frequency of visits between the two feeding tanks was analysed as repeated measurements on individual fish. We used two different regression models for the longitudinal data: a duration model and a frequency (count data) model. With the duration model, we tested the hypothesis that the food ratio and duration of visits in the two feeding tanks were related, and with the count data model the relationship between food ratio and frequency of visits was tested. The response of each fish to a change in food ratio was analysed. In each model, individual differences were taken into account by using fixed effects for each fish. In this way, individual differences due to size and other factors could be accounted for.

The duration model has the form

$$(1) \qquad \ln t_{ij} = a_i + \beta_1 \text{food}_{ij} + \beta_2 \text{period}_{ij} + \beta_3 \text{ within period}_{ij} + e_{ij}$$

where subscript i refers to fish i and subscript j to the jth duration of that fish. The fixed effect a_i is different for every fish and shifts the regression planes up or down the $\ln t_{ij}$ dimension. If the food ratio is increased by 1% from a value of 1, the average duration will change by β_1%.

The count data model is of the negative binomial type. The mean λ_{ij} of fish i in subperiod j satisfies

$$(2) \qquad \ln \lambda_{ij} = a_i + \beta_1 \text{food}_{ij} + \beta_2 \text{period}_{ij} + \beta_3 \text{within period}_{ij}.$$

The β_1 parameter can be interpreted in analogy with the duration model. The Limdep program (Limited Dependent software, Econometric Software Inc.) was used for estimating and testing both models.

Relationships between the different variables were analysed by using linear regressions for continuous data and one-way ANOVA or a Kruskall–Wallis test for normally distributed and skew-grouped data, respectively. These analyses were made in SPSS.

Results

General visiting pattern

The proportion of the total study period spent in the two feeding tanks ranged from 0 to 62% for individual fish in the four-group study and from 8 to 58% in the single-group study (Fig. 3). Only one individual (in group 4) never visited the feeding tanks. All other Arctic char made visits that lasted for more than 10 s. The longest single visit made by an individual to one of the feeding tanks was 144 h in the four-group study and 94 h in the single-group study. The relationship between total number of visits and total time (in

© 1999 NRC Canada

Fig. 3. Total time that each individual spent in feeding Tanks 1 + 2. Groups 1–4 were continuously monitored for 3 weeks, while the single group was monitored for 5 months.

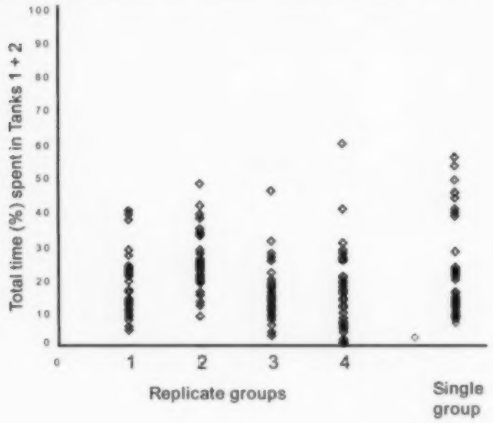

Table 1. Mean, median, and SD of the proportion of total individual duration of time spent in Tank 1/(Tank 1 + Tank 2).

		First period			Second period		
Group	*n*	Mean	Median	SD	Mean	Median	SD
1	38	0.78*	0.75	0.15	0.36*	0.20	0.35
2	39	0.31*	0.26	0.21	0.48^{ns}	0.48	0.31
3	40	0.17*	0.02	0.26	0.31*	0.13	0.35
4	39	0.19*	0.04	0.29	0.29*	0.10	0.35

Note: The 3-week registration periods of groups 1–4 are divided into first and second 10-day periods. Difference significant (*$p < 0.05$) and not significant (ns, $p > 0.05$) between the proportion of visits and a 0.5:0.5 food proportion in Tanks 1 and 2 (Wonnacott and Wonnacott (1972) test of proportion).

seconds) spent in Tank 1 + Tank 2 was significantly positive ($y = 279.28x + 222\,141$; $r^2 = 0.14$, $p < 0.05$, $n = 155$) in the four-group study and nonsignificant ($p > 0.05$, $n = 36$) in the single-group study. No difference was found between groups in the four-group study or between periods in the single-group study when these were analysed separately. Thus, no individuals monopolised any of the feeding tanks in terms of spending most of their time (defined by >80% of total experimental time) in there. In such a case, a negative relationship between total time and number of visits would have been found. Individual variation in the total number of visits to Tank 1 + Tank 2 ranged from 0 to nearly 1000 during the 3-week study and from 480 to 28 800 in the 5-month study.

In the four-group study, the proportions of individual data from groups 1–4 on the total time spent in the Tank 1 (Table 1) and the total number of visits to Tank 1 (Table 2) are summarised for the first and second 10-day periods. During both periods and in all replicate groups (except the proportion of duration during the second period), the proportion of duration and frequency of visits differed significantly ($p < 0.05$, Wonnacott and Wonnacott (1972) test of proportion) from a 0.5:0.5 food ratio. In all groups, except group 1 during the first 10 days, there was a preference for visiting Tank 2.

In the single-group study, the regression models on longitudinal data give significant positive relationships between

Table 2. Mean, median, and SD of the proportion of the frequency of individual visits to Tank 1/(Tank 1 + Tank 2).

		First period			Second period		
Group	*n*	Mean	Median	SD	Mean	Median	SD
1	38	0.45*	0.45	0.14	0.27*	0.14	0.26
2	39	0.24*	0.17	0.18	0.38*	0.33	0.25
3	40	0.18*	0.10	0.19	0.38*	0.30	0.34
4	39	0.22*	0.13	0.24	0.34*	0.33	0.30

Note: The 3-week registration periods of groups 1–4 are divided into first and second 10-day periods. Difference significant (*$p < 0.05$) between the proportion of visits and a 0.5:0.5 food proportion in Tanks 1 and 2 (Wonnacott and Wonnacott (1972) test of proportion).

Table 3. Estimated effects (β_1) of food ratio on cumulative visit duration and the frequency of visits in two feeding tanks by all individuals in the single-group study and by switchers and floaters only.

	Total	Tank 1	Tank 2
Duration			
All individuals ($n = 36$)	0.673	0.661	0.713
Switchers and floaters ($n = 28$)	0.694	0.713	0.822
Frequency			
All individuals ($n = 36$)	0.536	0.535	0.816
Switchers and floaters ($n = 28$)	0.541	0.445	0.896

Note: All estimates are significant ($p < 0.05$) in regression models for individual data.

the food ratio and the individual total visit duration as well as frequency of visits in the two feeding tanks (Table 3). Both variables are a sum for each 10-day period, corresponding to each box in Fig. 1. When the effect of tank is tested separately, it is found that the effect of food ratio is lower in Tank 1 than in Tank 2.

Distribution of floaters, switchers, and nonswitchers

The general level of tank-visiting activity and preferred tank varied considerably. Arctic char were classified into one of three categories modified from the studies by Milinski (1984), Godin and Keenleyside (1984), and Talbot and Kramer (1986): (*i*) those that spent most of their time in the nonfeeding tank (floaters), (*ii*) active visitors that showed no preference for either of the feeding tanks (switchers), and (*iii*) active visitors that showed a clear preference for one of the tanks (nonswitchers). The classification process worked as follows. Active visitors were defined as those plotting out in the upper half of each plot in Fig. 3 in the four-group study. For these individuals, the daily proportion of time spent in Tank 1 was plotted, and Arctic char with values of <0.2 and >0.8 during the second half of the registration period were classified as nonswitchers and those with proportions of visits in Tank 1 between 0.2 and 0.8 were classified as switchers. The remaining individuals were defined as floaters (Table 4).

The proportion data in the four-group study were pooled (excluding group 1 during the first period, which appeared different compared with the other replicates) and divided into three behavioural categories as described above (Fig. 2). The distributions of floaters and switchers in terms of proportion of time that they spent in Tank 1 are presented as

© 1999 NRC Canada

Table 4. Number of individuals in each group in the two selected categories where the switchers category showed low visit activity and (or) visited both feeding tanks and the nonswitchers category showed high visit activity and preference for visiting one of the feeding tanks.

	Group			
Category	1	2	3	4
Switchers	9	12	8	8
Nonswitchers	8	7	12	10
Floaters	21	20	20	21

Note: The remaining individuals were defined as floaters.

box plots. However, as the nonswitchers' proportions of duration in the two tanks are limited to ≥ 0.8 and ≤ 0.2, these distributions are presented as two plots, the upper for values ≥ 0.8 and the lower for values ≤ 0.2. During the first period, all three behavioural categories showed a preference for Tank 2 and all proportions of total duration differed significantly from the 0.5:0.5 food ratio ($p < 0.05$, Wonnacott and Wonnacott (1972) test of proportion). This preference lasted during the second period for floaters and nonswitchers ($p < 0.05$, Wonnacott and Wonnacott (1972) test of proportion), while the switchers distributed their duration of visits in equal proportion between the two feeding tanks, not significantly different from the food ratio ($p > 0.05$, Wonnacott and Wonnacott (1972) test of proportion). In accordance, a corresponding test of proportion of visit frequency into the feeding tanks gave no significant difference from food ratio for the switchers and only during the second period ($p > 0.05$, Wonnacott and Wonnacott test (1972) of proportion), while all other proportions were significantly different ($p < 0.05$, Wonnacott and Wonnacott (1972) test of proportion). Thus, only those Arctic char that were classified as switchers utilized the two feeding tanks according to the food ratio and only during the second 10-day period. Both floaters and nonswitchers spent the most time in and made more frequent visits to Tank 1.

In a similar way, the proportion of time spent in Tank 1 for each individual fish was plotted for each 10-day period in the single-group study. The fish were then categorised as floaters, switchers, or nonswitchers according to the classification used in the four-group study. The distribution of individuals between the two feeding tanks in the single-group study is illustrated by the total time spent in Tank 1, where each box or single plot summarises the individual distribution of proportions during 8–10 days (Fig. 1). The proportions of floaters ($n = 18$) and switchers ($n = 9$) in Tank 1/(Tank 1 + Tank 2) are plotted as box plots and the proportions of nonswitchers ($n = 9$) are plotted as single values (Tank 1) and mean values (Tank 2) for nonswitchers ($n = 9$). During the first feeding period, when the food ratio was 0.5:0.5, there was a preference to visit Tank 2 by all behavioural groups. During the second feeding period, with a food ratio of 0.75:0.25, the median visit ratios were closer to an equal distribution in the two tanks. In periods III and IV, when the temperature increased rapidly, the median time ratios matched the food ratios better. Thus, the overall trend in the results indicates that the floaters and switchers switched to the tank with the most food when the food ratios were changed. The regression analyses of longitudinal data gave an increased significant positive relationship between the food ratio and the individual total visit duration as well as the frequency of visits to the two feeding tanks by all individuals after exclusion of the nonswitchers (Table 3). Thus, in the single-group study, the match between food ratio and proportion of time in and frequency of visits to the feeding tanks reflected the switchers' and floaters' change in preference to that for the most profitable tank.The nonswitchers consistently preferred the same tank regardless of its relative profitability. Again, there was a skewed distribution in the number of nonswitchers between the two feeding tanks. Seven Arctic char preferred Tank 2, while only two favoured Tank 1.

Activity and growth depending on behavioural categories

The activity level differed significantly between the groups ($F_3 = 38.97$, $p < 0.001$, one-way ANOVA) in the four-group study and subsequently a comparison of the total number of visits into the feeding tanks made by individual fish of the three behavioural categories were tested within groups. One-way ANOVA gave no significant difference among the floaters', switchers', and nonswitchers' total frequency of visits to the feeding tanks in three of the four replicate groups ($p < 0.05$). In group 2, the nonswitchers had a significantly higher visiting frequency than the switchers and floaters ($F_2 = 7.28$, $p = 0.002$, one-way ANOVA). In the single-group study, there was no difference in the total number of visits made by individual fish depending on the behavioural category that they were classified as ($p > 0.05$, one-way ANOVA).

At the start of the experiment, there was no significant difference ($p > 0.05$, one-way ANOVA) in weight among the floaters, switchers, and nonswitchers in any of the groups in the four-group study. Accordingly, no significant difference in initial weight was found in the single-group study ($p > 0.05$, one-way ANOVA) (Fig. 4).

The performances of floaters, switchers, and nonswitchers were compared by means of growth rate in the four-group study, since initial weights of the groups were different and weight increase was uses as comparison in the single-group study. An analysis based on the pooled data showed that nonswitchers grew significantly faster than switchers and floaters ($\chi^2 = 10.17$, $p = 0.006$, Kruskall–Wallis test), while no difference was found between the last two categories ($p > 0.05$, Mann–Whitney U test) (Fig. 5). In the single-group study, a significant difference was found in June ($\chi^2 = 11.56$, $p = 0.003$, Kruskall–Wallis test) and at the end of the experiment ($\chi^2 = 14.57$, $p = 0.001$, Kruskall–Wallis test) in weight of the behavioural categories. Separate Mann–Whitney U tests of paired categories gave no significant difference in weight between switchers and floaters ($p > 0.05$) on any of these occasions. (Fig. 4).

Discussion

The two experiments used in this analysis differed in both environmental and feeding conditions. We assumed that these differences in day length and temperature do not affect the occurrence of different behavioural strategies, although the difference in temperature may affect the total growth rate

© 1999 NRC Canada

Fig. 4. Box plots showing the weight distributions of floaters (n = 18), switchers (n = 9), and nonswitchers (n = 9) in the single-group study at the start in February, in June, and at the end of the experiment in August. Differences were assessed statistically with the Mann–Whitney U test.

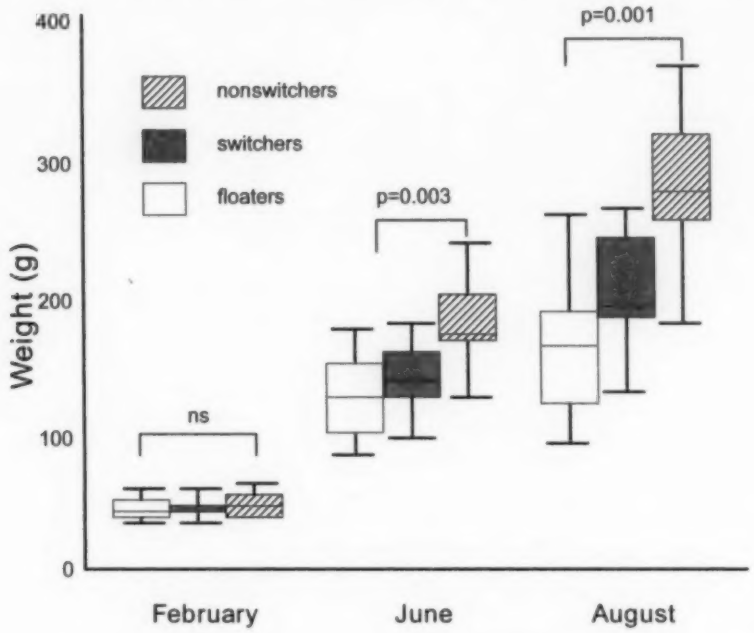

Fig. 5. Box plots of growth rate during 21 days for floaters, switchers, and nonswitchers from groups 1–4 (pooled data). Differences were assessed statistically with the Mann–Whitney U test. ns, not significant.

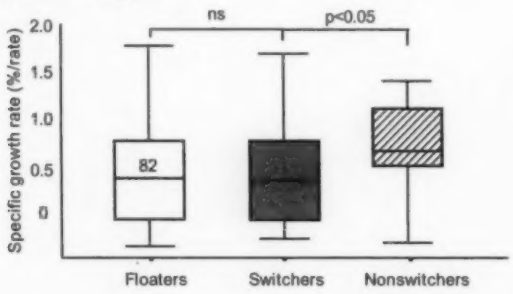

in the two studies. Also, earlier studies of ours showed that the growth rate of Arctic char reared in tanks at 0°C as well as at 10°C is unaffected by photoperiod (E. Brännäs et al., unpublished results).

Thus, based on their visiting activity and preference for one of the feeding tanks, different behavioural categories were recognised in both the single-group and the four-group studies. We classified the individuals into three types according to a combination of definitions from earlier experimental studies where mainly two behavioural categories were described at a time. Behaviours such as low- and high-frequency switchers were defined in experimental studies on distribution of fish groups between feeding patches in sticklebacks (Milinski 1984) and cichlids (Godin and Keenleyside 1984). In these experiments the two feeding patches represented two sides of an aquarium where the feeding commenced. The distribution of guppies by Talbot and Kramer (1986) was studied in a system with five feeding patches surrounded by a well-defined nonfeeding area where a "floating" behaviour was described in some guppies as opposed to individuals that spent more time in the feeding patches. No individual recognition was done in Talbot and Kramer's (1986) study where the more actively feeding individuals could be recognised as switchers or nonswitchers.

In Milinski's (1984) experiment on sticklebacks, the nonswitchers first decided which side of the tank to forage in and then remained there for the duration of the trial, which lasted only a few minutes. However, in our longer experimental trials, rather than remaining in their "chosen tank", the nonswitching individuals made frequent visits into and out of the feeding tanks but always directed their feeding tank visits to the same one. In fact, PIT tag data revealed that no fish actually monopolised a feeding tank by spending most of their time in there. Instead, the frequency of movements back and forth between tanks did not differ significantly between nonswitchers and switchers. The difference was that the switchers directed their visits to both feeding tanks. In experimental trials where groups of goldfish were given a choice between two unequal feeding patches, individuals that had located the best patch still kept sampling in the poor patch (Pitcher and Magurran 1983). A flexible sampling behaviour, e.g., sampling different patches even though the present feeding patch provides sufficient food, has great adaptive value in fish (Dill 1983). Without making such periodic sampling forays, the fish has no way of knowing whether any of the surrounding patches have become richer than the one being used. However, in contrast with the

© 1999 NRC Canada

goldfish experiment, the nonswitching Arctic char did not sample the alternative patch when they left their preferred patch. Instead, they limited their excursion to the larger nonfeeding patch. The differences in results between studies could have been due in part to the different experimental setups used. When a fish leaves a feeding patch, it is more likely to turn up in the alternative patch if kept in a small aquarium than if kept in a feeding tank system like the one used in the Arctic char experiment.

The switching and floating behaviour was applied by individuals that had a lower growth rate and were therefore likely to have lower competitive ability compared with those individuals that applied a nonswitching behaviour. There are probably differences between nonswitchers and switchers in the motivation for sampling alternative patches. Successful individuals (nonswitchers) may have a lower motivation for sampling new areas than the less successful ones (switchers), as they do well enough when feeding in the feeding tank they favour. The switchers, on the other hand, presumably had a lower competitive ability, as they grew slower and had to sample both feeding tanks to increase their chances of finding food. In accordance, sticklebacks that fed on just one side of an aquarium had greater feeding success than individuals that kept sampling on both sides (Milinski 1984).

In addition, the nonswitching fish in the single-group experiment were able to compete successfully for food in a given feeding patch regardless of whether it contained 75% of the food in the two tanks or only 25%. The less successful switchers mainly visited the patch where the chance of gaining food was highest, i.e., the tank with 75% of the food. Nonswitching individuals were apparently satisfied to visit just one of the feeding patches, and their visits to the central nonfeeding tank were probably for reasons other than food sampling. For instance, such forays could have been made to join other individuals that formed shoals in the larger tank. Barber et al. (1995) demonstrated that individual minnows and threespine sticklebacks alternate between joining shoals when satiated and foraging on their own when hungry.

The Arctic char classified as floaters because of their generally low visiting activity into the feeding tanks may be a reflection of an altogether lower feeding motivation in these individuals. Appetite in part appears to be governed by metabolic rate, which was found to be strongly related to social status in juvenile Atlantic salmon (Metcalfe et al. 1995). Dominant individuals have a higher metabolic rate compared with subordinate ones and may therefore be "driven" to feed more often due to higher maintenance requirements (Metcalfe et al. 1995).

In Lake Visjön, in central Sweden, part of the Arctic char population migrates to a smaller lake, where they spend the summer, and return home in autumn. The smaller, shallower lake has a higher productivity (from human activities) than the larger, deeper home lake but freezes solid in winter. Migrating individuals initially tend to have a lower condition factor than individuals that remain in the large lake throughout the year (Näslund 1990). Partial migration has been found in an Arctic char population both with and without interspecific competition (I. Näslund, personal communication). In a laboratory experiment, Näslund (1991) found that swimming activity of Arctic char was higher in groups fed reduced rations than in groups fed in excess. In accordance with the behavioural strategies found in the laboratory, successful competitors in wild populations of Arctic char may do well enough by applying a nonswitching strategy and foraging in their home lake. On the other hand, less competitive individuals may face the choice of taking the risk of finding (switching to) new, temporary richer habitats, and a population with partial migration occurs, as suggested by Slaney and Northcote (1974). No behavoiur corresponding to a floating, less active strategy has been described in available field studies. If these individuals have a lover motivation for feeding compared with the migrating and nonmigrating individuals, they are likely to stay in their home lake as poor competitors.

The benefits of applying a switching or nonswitching strategy depend on the situation. In the Lake Visjön system, migrants initially have a lower condition factor but grow faster than nonmigrants (Näslund et al. 1993), while the nonswitchers perform better under the experimental conditions. The situation is much more complex in a natural environment where both migration related costs and benefits in terms of a richer feeding habitat determine which strategy will be most successful. In addition, if patch profitability changes frequently in the short term (as often happens in nature) the switchers may do better, since they sample more often (Warburton 1990). A similar situation occurs when an animal's choice of a particular habitat or feeding patch is dependent on variation in food intake rate. If the mean intake rate is sufficient, the animal avoids feeding patches with a high variance in productivity (reviewed by Stephens and Krebs 1986). Such patches may, however, be more desirable if the intake rate of the animal does not meet its daily food needs.

In the four-group experiment, the switchers' proportion of frequency as well as duration in the feeding tanks matched the food ratio during the second 10-day period. Individuals assigned to the other two behavioural categories visited one of the feeding tanks more often and spent a longer time there than in the alternative feeding tank. In the single-group experiment, the distributions were skewed to start with, but for the 5-month period as a whole, there was a significant correspondence between patch visitation time/number of visits and the relative profitability of the two feeding patches, even when all individuals were included in the regression analysis. It was, however, the switchers and floaters that began to favour the most profitable patch when the relative proportion of food was changed. This change in tank utilisation did not start during the first period, probably because the initial temperature was so low. At a low temperature, feeding activity is generally suppressed, so any differences in food supply are of little relevance. The Arctic char is, however, well adapted to high altitudes, where it feeds and grows quite well at temperatures as low as 0.3°C (Brännäs and Wiklund 1992). When the temperature started to rise, the switch from a less to a more profitable patch required at least 10 days in the single-group study. Thus, in situations where the difference in patch quality is more difficult to determine, floaters and switchers will input-match their visit activity in two feeding tanks provided they are given sufficient time.

IFD models are the most common types of model used to

© 1999 NRC Canada

predict the distribution of animals among different habitats (Sutherland 1996). To describe situations where groups of fish are scrambling for drifting prey, Sutherland and Parker (1985) and Parker and Sutherland (1986) developed the "continuous-input" IFD model, which is a modified version of the original IFD model presented by Fretwell and Lucas (1969). Both models predict that individuals can maximise their gain by distributing themselves according to the proportions of food available in the patches. In our Arctic char experiments, daily visual observations suggested that the situation was close to a continuous-input scenario. There were some accumulations of food in the afternoon but never in the mornings, which excludes a long-term accumulation of food. The IFD models also assume that the level of competition is high and that all individuals have perfect knowledge of patch quality. Small groups of fish did, indeed, distribute themselves according to the model's predictions in cases where food was continuously delivered on two sides of a partition in an aquarium (Milinski 1979, 1984; Godin and Keenleyside 1984). However, the distribution of guppies showed a poor fit to an IFD scenario in a situation where the feeding patches were in separate compartments within a large tank, making knowledge concerning the relative quality of the patches more difficult to gain (Talbot and Kramer 1986). In our study, the experimental setup that was closest to an IFD scenario, where the proportion of food differs between the patches, was the single-group study were the food ratio was changed at regular intervals. The allocation of visits to the two feeding tanks of the whole group did indeed match an IFD scenario throughout the 5-month registration period.

Use of the IFD model (continuous input) as a general tool with the wrong assumptions to predict animal distributions has, however, been thoroughly criticised (Milinski 1994; Tregenza 1994). A number of modifications have already been made including dominance, despotism, and other types of interference (as reviewed by Sutherland and Parker 1985; Milinski and Parker 1991; Kacelnik et al. 1992; Sutherland 1996). Modifications are also needed to account for systems where the feeding patches are less likely to occur within perception distance including the role of information (Abrahams 1986). In such situations, longer periods of observation are required in an experimental context before distribution stabilises and effects of different behaviours can be distinguished.

The overuse of one of the tanks may have been an effect of shoaling when the fish were faced with the new three-tank environment. Fish that forage in shoals find food easier and can spend more time feeding but also face the cost of competing with other members of the group (Pitcher and Parish 1993). Such fish are faced with making a trade-off between the positive and negative effects of feeding in a larger group. Group feeding offers increased safety but results in increased interference as well. The best strategy to adopt when foraging in large lakes, which are the main habitats of Arctic char, is shoaling behaviour (Johnson 1980). The overuse of one feeding tank resulted in greater competition for food, in which case, an increase in visits to the alternative tank would be expected. The preferred tank was always directed eastward and reotactic behaviour might have influenced the choice of habitat. Arctic char exhibit a pronounced preference for swimming either against or with the water current depending on the season (Linnér et al. 1990). In the single-group experiment, the direction of the tanks was identical, but there was a minor difference in light conditions because the light came from the windows, making the condition more variable depending on the light influx.

In conclusion, individuals in groups of Arctic char apply different behavioural strategies when given a choice of utilising alternative feeding habitats. Similar to the behaviour found in partially migrating wild populations of Arctic char, the most successful individuals mainly utilise or stay in one habitat. The switching, or probably the migratory behaviour, in the wild is applied by less competitive individuals, who may do better in a temporary rich feeding habitat. Only in the single-group study did the fish distribute according to the food ratio (IFD) if they were given sufficient time to learn the quality of the patches. It was the switchers and floaters that altered their visiting behaviour after a change in the relative food ratio, always favouring the more profitable tank, while the nonswitchers continued to visit the same tank.

Acknowledgements

We thank three anonymous referees for their helpful and thorough comments. This work was supported by grants from the Swedish Council for Forestry and Agricultural Research.

References

Abrahams, M.V. 1986. Patch choice under perceptual constraints: a cause for deviations from an ideal free distribution. Behav. Ecol. Soc. **19**: 409–415.

Barber, I., Huntingford, F.A., and Crompton, D.W.T. 1995. The effect of hunger and cestode parasitism on the shoaling decisions of small freshwater fish. J. Fish Biol. **47**: 524–536.

Brännäs, E. 1998. Individual variation in distribution, activity and growth rate of Arctic charr kept in a three-tank system. J. Fish Biol. **53**: 795–807.

Brännäs, E., and Wiklund, B.-S. 1992. Low temperature growth potential of Arctic charr and rainbow trout. Nord. J. Freshwater Res. **67**: 77–81.

Brännäs, E., Lundqvist, H., Prentice, E., Schmitz, M., Brännäs, K., and Wiklund, B.-S. 1994. Use of the passive integrated transponder (PIT) in a fish identification and monitoring system for fish behavioural studies. Trans. Am. Fish Soc. **123**: 395–401.

Dill, L.M. 1983. Adaptive flexibility in the foraging behaviour of fishes. Can. J. Fish. Aquat. Sci. **40**: 398–408.

Fretwell, S.D., and Lucas, H.L. 1969. On territorial behaviour and other factors influencing habitat distribution in birds. I. Theoretical development. Acta Biotheor. **19**: 16–36.

Godin, J.-G.J., and Keenleyside, M.H.A. 1984. Foraging on patchily distributed prey by a cichlid fish (Teleosti, Cichlidae): a test of the ideal free distribution theory. Anim. Behav. **32**: 120–131.

Jobling, M. 1995. Feeding in charr in relation to aquaculture. Nord. J. Freshwater Res. **71**: 102–112.

Jobling, M., Baardvik, B.M., and Jørgensen, E.H. 1989. Investigation of food growth relationships of Arctic charr, *Salvelinus alpinus* L., using radiography. Aquaculture, **81**: 367–372.

Johnson, L. 1980. The Arctic charr, *Salvelinus alpinus*. *In* Charrs, salmonid fishes of the genus *Salvelinus*. *Edited by* E.K. Balon. Dr. W. Junk Publishers, The Hague, The Netherlands. pp. 15–98.

© 1999 NRC Canada

Kacelnik, A., Krebs, J.R., and Bernstein, C. 1992. The ideal free distribution and predator–prey population. Trends Ecol. Evol. **7**: 50–55.

Linnér, J., Brännäs, E., Wiklund, B.-S. and Lundqvist, H. 1990. Diel and seasonal locomotor activity patterns in Arctic charr, *Salvelinus alpinus* (L). J. Fish Biol. **37**: 675–685.

Metcalfe, N.B., Taylor, A.C., and Thorpe, J.E. 1995. Metabolic rate, social status and life-history strategies in Atlantic salmon. Anim. Behav. **49**: 431–436.

Milinski, M. 1979. An evolution stable feeding strategy in sticklebacks. Z. Tierpsychol. **51**: 36–40.

Milinski, M. 1984. Competitive resource sharing: an experimental test of a learning rule for ESSs. Anim. Behav. **32**: 233–242.

Milinski, M. 1994. Ideal free theory predicts more than only input matching — a critique of Kennedy and Gray's review. Oikos, **71**: 163–170.

Milinski, M., and Parker, G.A. 1991. Competition for resources. *In* Behaviour ecology: an evolutionary approach. Vol. 3. *Edited by* J.R. Krebs and N.B. Davies. Blackwell Scentific Publications, Oxford, U.K. pp. 137–168.

Näslund, I. 1990. The development of regular seasonal habitat shifts in a landlocked Arctic charr, *Salvelinus alpinus* L., population. J. Fish Biol. **36**: 401–414.

Näslund, I. 1991. Effects of temperature, season and feeding conditions on the rheotactic behaviour of two stocks of landlocked Arctic charr. Nord. J. Freshwater Res. **66**: 108–114.

Näslund, I., Milbrink, G., Eriksson, L.O., and Holmgren, S. 1993. Importance of habitat productivity differences, competition and predation for the migratory behaviour of Arctic charr. Oikos, **66**: 538–546.

Parker, G.A., and Sutherland, W.J. 1986. Ideal free distribution when individuals differ in competitive ability: phenotype-limited ideal free models. Anim. Behav. **34**: 1222–1242.

Pitcher, T.J., and Magurran, A.E. 1983. Shoal size, patch profitability and information exchange in foraging goldfish. Anim. Behav. **31**: 546–555.

Pitcher, T.J., and Parrish, J.K. 1993. Teleost foraging: facts and theories. *In* The behaviour of teleost fishes. *Edited by* T.J. Pitcher. Croom-Helm, London, U.K. pp. 253–284.

Prentice, E.F., Flagg, T.A., McCutcheon, C.S., and Brastov, D.F. 1990. PIT tag monitoring system for hydroelectrical dams and fish hatcheries. Trans. Am. Fish. Soc. Symp. **7**: 323–334.

Slaney, P.A., and Northcote, T.G. 1974. Effect of prey abundance on density and territorial behavior of young rainbow trout (*Salmo gairdneri*) in laboratory stream channels. J. Fish. Res. Board Can. **31**: 1201–1209.

Stephens, D.W., and Krebs, J.R. 1986. Foraging theory. Princeton University Press, Princeton, N.J.

Sutherland, W.J. 1996. From individual behaviour to population ecology. Oxford University Press, U.K.

Sutherland, W.J., and Parker, G.A. 1985. The distribution of unequal competitors. *In* Behavioural ecology: ecological consequences of adaptive behaviour. *Edited by* R.M. Sibly and R.H. Smith. Blackwell Scientific Publications, Oxford, U.K. pp. 255–274.

Talbot, A. 1983. A test of habitat selection theory using response of guppies, *Poecilia reticulata* (Pisces: *Poeciliidae*), to food and oxygen availability. M.S. thesis, McGill University, Montreal, Que.

Talbot, A.J., and Kramer, D.L. 1986. Effects of food and oxygen availability on habitat selection by guppies in a laboratory environment. Can. J. Zool. **64**: 88–93.

Tregenza, T. 1994. Common misconceptions in applying the ideal free distribution. Anim. Behav. **47**: 485–487.

Warburton, K. 1990. The use of local landmarks by foraging goldfish. Anim. Behav. **40**: 500–505.

Wonnacott, T.H., and Wonnacott, R.J. 1972. Introductory statistics for business and economics. John Wiley & Sons, Inc., New York.

© 1999 NRC Canada

BUGS in Bayesian stock assessments

Renate Meyer and Russell B. Millar

Abstract: This paper illustrates the ease with which Bayesian nonlinear state–space models can now be used for practical fisheries stock assessment. Sampling from the joint posterior density is accomplished using Gibbs sampling via BUGS, a freely available software package. By taking advantage of the model representation as a directed acyclic graph, BUGS automates the hitherto tedious calculation of the full conditional posterior distributions. Moreover, the output from BUGS can be read directly into the software CODA for convergence diagnostics and statistical summary. We illustrate the BUGS implementation of a nonlinear nonnormal state–space model using a Schaefer surplus production model as a basic example. This approach extends to other assessment methodologies, including delay difference and age-structured models.

Résumé : Le présent article montre la facilité avec laquelle des modèles d'espace d'états Bayesiens non linéaires peuvent maintenant être utilisés dans l'évaluation des stocks de pêche. On échantillonne des unités dans la fonction de densité a posteriori conjointe en utilisant la méthode d'échantillonnage de Gibbs avec BUGS, un logiciel facilement disponible. En tirant avantage de la représentation du modèle sous la forme d'un graphe acyclique orienté, BUGS automatise le calcul jusqu'ici fastidieux des distributions conditionnelles a posteriori complètes. De plus, le produit de BUGS peut être lu directement dans le logiciel CODA pour établir un diagnostic de convergence et un sommaire statistique. Nous illustrons l'application d'un modèle d'espace d'états non linéaire et non normal en utilisant, à titre d'exemple, un modèle de production excédentaire de Schaefer. Cette approche peut être étendue à d'autres méthodes d'évaluation, notamment aux modèles à différences retardées et aux modèles structurés selon l'âge.

[Traduit par la Rédaction]

Introduction

State–space models are among the most powerful tools for dynamic modeling and forecasting (Fahrmeir and Tutz 1994). They have started to enjoy an increasing popularity in fisheries stock assessment (Sullivan 1992; Pella 1993; Gudmundsson 1994; Schnute 1994; Freeman and Kirkwood 1995; Kinas 1996; Reed and Simons 1996; Meyer and Millar 1999; Millar and Meyer 1999*a*) because they can realistically account for both measurement and process error. However, unrealistic assumptions such as linearity of state transitions and Gaussian error distributions are imperative for maximum likelihood estimation via Kalman filtering and have limited the number of fisheries models that can be fit within the classical/frequentist paradigm.

Meyer and Millar (1999) explained how delay difference and surplus production models can be cast into the framework of state–space modeling. They demonstrated a fully Bayesian approach using Gibbs sampling for posterior computation following Carlin et al. (1992). In contrast with the classical approach, the Bayesian approach can easily handle realistic distributional assumptions as well as nonlinearities in state and observation equations. The papers by Millar and Meyer (1999*a*) and Meyer and Millar (1999) provide the underlying theory of fitting Bayesian state–space surplus production and delay difference models, respectively.

Here, we report on significant progress made in facilitating the routine implementation that may have a revolutionary effect on Bayesian stock assessment in everyday practice. This is achieved through BUGS (Bayesian inference using Gibbs sampling), a recently developed software package (Spiegelhalter et al. 1996) by the Medical Research Council Biostatistics Unit, Institute of Public Health, Cambridge, England. BUGS samples from the joint posterior distribution by using the Gibbs sampler (Gilks et al. 1996), i.e., by cyclically sampling from each of the full conditionals. For reviews on BUGS the reader is referred to Thomas et al. (1992), Gilks et al. (1994), and Gentleman (1997). BUGS is available free of charge from http://www.mrc-bsu.cam.ac.uk/bugs/Welcome.html for the operating systems UNIX, LINUX, and Windows, among others. It comes with complete documentation and two example volumes. These examples demonstrate the variety of complex models (random effects, generalized linear, proportional hazards, latent variable, and frailty models) amenable to a Bayesian analysis via BUGS. We will show that nonlinear non-Gaussian state–space models can be added to this list.

In nonlinear non-Gaussian state–space models the full conditional distributions required for Gibbs sampling are typically not log-concave. Both Meyer and Millar (1999) and Millar and Meyer (1999*a*) implemented the Gibbs sampler in C code, using the C subroutines ARS (Gilks and Wild 1992) and ARMS (Gilks et al. 1995) to sample from univariate log-concave and non-log-concave full conditional distributions, respectively. This, however, required the explicit derivation "by hand" of the full conditional distribution of each parameter in the model, a nontrivial, substantial,

Received September 18, 1998. Accepted February 19, 1999. J14789

R. Meyer[1] **and R.B. Millar.** Department of Statistics, University of Auckland, Private Bag 92019, Auckland, New Zealand.

[1]Author to whom all correspondence should be addressed. e-mail: meyer@stat.auckland.ac.nz

© 1999 NRC Canada

Table 1. Catch (1000's t) and CPUE (kg/100 hooks) data for South Atlantic albacore from Polacheck et al. (1993).

Year	Catch	CPUE
1967	15.9	61.89
1968	25.7	78.98
1969	28.5	55.59
1970	23.7	44.61
1971	25.0	56.89
1972	33.3	38.27
1973	28.2	33.84
1974	19.7	36.13
1975	17.5	41.95
1976	19.3	36.63
1977	21.6	36.33
1978	23.1	38.82
1979	22.5	34.32
1980	22.5	37.64
1981	23.6	34.01
1982	29.1	32.16
1983	14.4	26.88
1984	13.2	36.61
1985	28.4	30.07
1986	34.6	30.75
1987	37.5	23.36
1988	25.9	22.36
1989	25.3	21.91

and tedious task that may deter the practical stock assessment scientist from fitting these models. We explain how BUGS alleviates this chore by making use of conditional independence assumptions in the model that are graphically represented by a directed acyclic graph (DAG). Moreover, the new version 0.6 of BUGS contains a method to sample from any not necessarily log-concave full conditional density. This makes it now possible to fit nonlinear non-Gaussian state–space models.

The paper is organized as follows. In the first section, we briefly describe a biomass dynamics model, the Schaefer surplus production model, that is the most commonly used non-age-structured model in practical stock assessments. This simple, parsimonious model was chosen for illustrative purposes. We use the same catch–effort data set on South Atlantic albacore (*Thunnus alalunga*) as in Millar and Meyer (1999*a*) and in Polacheck et al. (1993). In the second section, we put this surplus production model into the context of nonlinear, non-Gaussian state–space methodology. This model is then represented as a DAG in the third section. In the subsequent sections, we explain how this DAG assists the model's implementation in BUGS and how to perform convergence diagnostics using CODA (Best et al. 1995).

The problem

The data available for stock assessment purposes quite often consist of a time series of annual catches C_t, $t = 1,..., N$, and relative abundance indices I_t, $t = 1,..., N$, such as research survey catch rates or catch-per-unit-effort (CPUE) indices from commercial fisheries. For example, Table 1 gives a historical data set of catch–effort data of South Atlantic albacore from 1967 to 1989. Age composition data are not available for this stock. This data set has previously been analysed by Polacheck et al. (1993) and Yeh et al. (1991). Objectives include the estimation of the size of the stock at the end of 1989 and management parameters such as the maximum surplus production (MSP), the biomass at which MSP occurs (B_{MSP}), and the optimal effort (E_{MSP}), the level of commercial fishing effort required to harvest MSP when the stock is at B_{MSP}.

When only catch–effort data are available, biomass dynamics models are the primary assessment tools for many fisheries (Hilborn and Walters 1992). They relate the current biomass to previous biomass plus terms for growth and recruitment minus terms for natural mortality and catch. Surplus production models aggregate terms for recruitment, growth, and natural mortality into one term for "surplus production" so that the biomass dynamics equations can be written in the form (Polacheck et al. 1993)

$$(1) \qquad B_t = B_{t-1} + g(B_{t-1}) - C_{t-1}$$

where B_t, C_t, and $g(B_t)$ denote biomass at the start of year t, catch during year t, and the surplus production function, respectively. The surplus production function is usually assumed to be nonnegative with $g(0) = g(K) = 0$, where K is the carrying capacity (corresponding to the level of the stock biomass at equilibrium prior to commencement of the fishery). The Schaefer (1954) form of the surplus production function is

$$(2) \qquad g(B_{t-1}) = rB_{t-1}\left(1 - \frac{B_{t-1}}{K}\right)$$

Substituting eq. 2 into eq. 1 gives a parsimonious model describing the annual biomass dynamics transitions with just the two parameters r, the intrinsic growth rate, and K:

$$(3) \qquad B_t = B_{t-1} + rB_{t-1}\left(1 - \frac{B_{t-1}}{K}\right) - C_{t-1}.$$

Note that the annual catch is treated as a fixed constant. A common, although simplifying assumption is that the relative abundance index is directly proportional to the biomass, i.e.:

$$(4) \qquad I_t = qB_t$$

with catchability parameter q.

For the Schaefer surplus production model, the maximum surplus production MSP = $rK/4$ occurs at $B_{MSP} = K/2$. When the biomass indices are CPUE's from commercial fishing, then eq. 4 gives $MSP/E_{MSP} = qK/2$ and thereby the optimal effort is $E_{MSP} = r/2q$.

For a more detailed discussion on surplus production models, the interested reader is referred to Hilborn and Walters (1992, chap. 8), Polacheck et al. (1993), Millar and Meyer (1999*a*), and references therein.

Bayesian nonlinear state–space model

Polacheck et al. (1993) compared three commonly used statistical techniques for fitting the model defined by eqs. 3

© 1999 NRC Canada

and 4: process error models, observation error models, and equilibrium models. None of these is capable of incorporating uncertainty present in both equations: natural variability underlying the annual biomass dynamics transitions (process error) and uncertainty in the observed abundance indices due to measurement and sampling error (observation error). This is possible, however, using a state–space model, as shown in Meyer and Millar (1999) and Millar and Meyer (1999*a*). State–space models (see Meyer and Millar 1999 and references therein) relate time series observations $\{I_t\}$ to unobserved "states" $\{B_t\}$ through a stochastic observation model for I_t given B_t. The states are assumed to follow a stochastic transition model. Equations 3 and 4 are the deterministic versions of the stochastic state and observation equations. We assumed lognormal error structures and used a reparametrization ($P_t = B_t/K$) by expressing the annual biomass as a proportion of carrying capacity as in Millar and Meyer (1999*a*) to speed mixing (i.e., sampling over the support of the posterior distribution) of the Gibbs sampler. The state equations are rewritten as

$$(5)\quad P_1|\sigma^2 = e^{u_1}$$
$$P_t|P_{t-1}, K, r, \sigma^2 = (P_{t-1} + rP_{t-1}(1 - P_{t-1}) - C_{t-1}/K)e^{u_t}, \quad t = 2,\ldots,N$$

and the observation equations are

$$(6)\quad I_t|P_t, q, \tau^2 = qKP_te^{v_t}, \quad t = 1,\ldots,N$$

where u_t are iid normal with mean 0 and variance σ^2 and v_t are iid normal with mean 0 and variance τ^2. Here, $X|Y$ denotes the conditional distribution of X given Y.

A fully Bayesian model consists of the joint prior distribution of all unobservables, here the five parameters K, r, q, σ^2, and τ^2 and the unknown states $P_1,\ldots, P_N$, and the joint distribution of the observables, here the relative abundance indices $I_1,\ldots, I_N$. Bayesian inference is then based on the posterior distribution of the unobservables given the data. In the sequel, we will denote the probability density function of a parameter θ by $p(\theta)$. We assume that the parameters K, r, q, σ^2, and τ^2 are independent a priori. By a successive application of Bayes' theorem and conditional independence of subsequent states, the joint prior density is given by

$$(7)\quad p(K, r, q, \sigma^2, \tau^2, P_1,\ldots, P_N) = p(K)p(r)p(q)p(\sigma^2)p(\tau^2)p(P_1|\sigma^2) \times \prod_{i=2}^{N} p(P_t|P_{t-1}, K, r, \sigma^2).$$

A noninformative prior is chosen for q. Prior distributions for K, r, σ^2, and τ^2 are specified using biological knowledge and inferences from related species and stocks as discussed in Millar and Meyer (1999*a*):

$$K \sim \text{lognormal}(\mu_K = 5.04,\ \sigma_K = 0.5162)$$

$$r \sim \text{lognormal}(\mu_r = -1.38,\ \sigma_r = 0.51)$$

$$p(q) \propto 1/q$$

$$\sigma^2 \sim \text{inverse-gamma}(3.79,\ 0.0102)$$

$$\tau^2 \sim \text{inverse-gamma}(1.71,\ 0.0086).$$

For general guidelines on the choice of prior distributions for parameters in stock assessment models, the reader is referred to Punt and Hilborn (1997).

Because of the conditional independence assumption of the relative abundance indices given the unobserved states, the sampling distribution is

$$(8)\quad p(I_1,\ldots, I_N|K, r, q, \sigma^2, \tau^2, P_1,\ldots, P_N) = \prod_{t=1}^{N} p(I_t|P_t, q, \tau^2).$$

Then, by Bayes' theorem, the joint posterior distribution of the unobservables given the data, $p(K, r, q, \sigma^2, \tau^2, P_1,\ldots, P_N|I_1,\ldots, I_N)$, is proportional to the joint posterior distribution of all unobservables and observables:

$$(9)\quad p(K, r, q, \sigma^2, \tau^2, P_1,\ldots, P_N, I_1,\ldots, I_N) = p(K)p(r)p(q)p(\sigma^2)p(\tau^2)p(P_1|\sigma^2) \times \prod_{i=2}^{N} p(P_t|P_{t-1}, K, r, \sigma^2) \prod_{t=1}^{N} p(I_t|P_t, q, \tau^2)$$

i.e., the product of eqs. 7 and 8, the product of prior and sampling distribution. Thus, the joint distribution (eq. 9) is the crucial one for subsequent Bayesian inference.

Model representation as DAG

Now let us step back and look at a graphical representation of the fully Bayesian model. This abstraction has the advantage that we can concentrate on the essential model structure without getting bogged down by all the details about densities. For any year t, let us represent all unobservables (K, r, q, σ^2, τ^2, P_t) and observables (I_t) as ellipses and constants (C_t) as rectangles. A way to express the conditional independence assumptions is by drawing solid arrows between nodes (see Fig. 1). (By analogy, a graphical representation can be drawn for the node P_1 whose state equation is different from that of the nodes P_t, $t = 2,\ldots, N$; see eq. 5.) Hollow arrows go to deterministic nodes, which are logical functions of other nodes. The logarithm of the conditional median of P_t, Pmed[t], is an example of a deterministic node, as it is a function of the nodes K, r, C_{t-1}, and P_{t-1}.

This renders a model representation as a DAG, as all edges in the graph are directed and there are no cycles because of the conditional independence assumptions. Let V denote the set of all nodes in the graph. Direct predecessors of a node $v \in V$ are called "parents" and direct offspring the "children". The solid arrows indicate that *given its parent nodes*, each node v is independent of all other nodes except descendants of v. For instance, if we are in year t and know the biomass in year $t - 1$ and the values of the parameters r, K, and σ^2, then our belief in P_t is independent of the biomass in previous years 1 to $t - 2$ and the data of all other years except the current relative abundance index I_t.

It is then easy to construct the joint probability distribution of all stochastic nodes using the graphical description of the conditional independence assumptions:

© 1999 NRC Canada

Fig. 1. Representation of the surplus production model as a DAG.

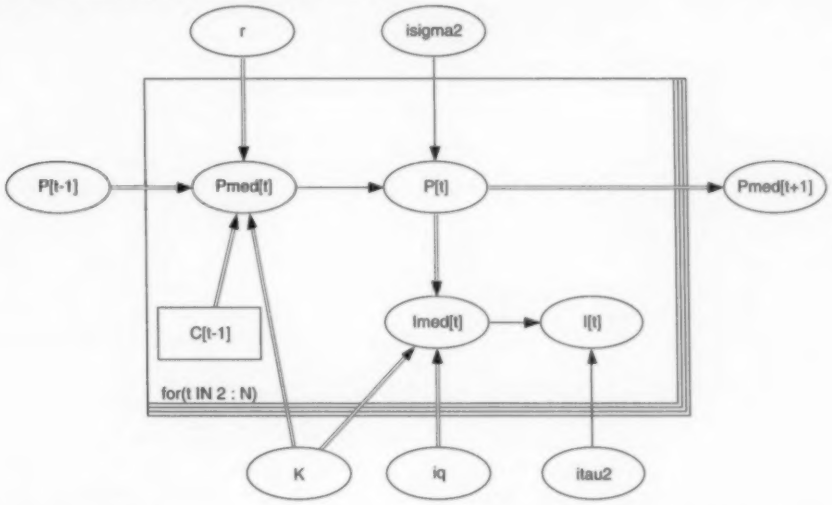

$$(10) \quad p(V) = \prod_{v \in V} p(v \mid \text{parents}(v)).$$

For our specific surplus production model, eq. 10 is the graph-theoretical version of eq. 9. In this way, the DAG (Fig. 1) assists in constructing the full Bayesian model. For further reading on conditional independence graphs and graphical chain models, the interested reader is referred to Wermuth and Lauritzen (1990).

Bayesian inference using BUGS

Let V_u denote the subset of unobservable nodes and V_o the subset of observable nodes. Once $p(V)$ has been obtained from eq. 10, a general technical difficulty encountered in any application of Bayesian inference is calculating the high-dimensional integral necessary to find the normalization constant in the posterior distribution of the unobservables given the data:

$$(11) \quad p(V_u \mid V_o) \frac{p(V_u, V_o)}{p(V_o)} = \frac{p(V)}{\int p(V_u, V_o)\, dV_u}.$$

In our specific example, this would require an $(N + 5)$-dimensional integration, as we have to integrate over the unobservables K, r, q, σ^2, τ^2, P_1,..., P_N. Calculating the marginal posterior distribution of any variable would require a subsequent $(N + 4)$-dimensional integration. High-dimensional integration problems can be solved via Markov chain Monte Carlo (MCMC) as reviewed in Gilks et al. (1996). The Gibbs sampler, a special MCMC algorithm, generates a sample from the posterior eq. 11 by iteratively sampling from each of the univariate full conditional posterior distributions as explained in Meyer and Millar (1999). These univariate full conditional posterior distributions $p(v|V \setminus v)$, for $v \in V_u$, can be easily constructed from the joint posterior distribution $p(V)$ in eq. 10 by picking out those terms that depend on v:

$$(12) \quad p(v \mid V \setminus v) \propto p(v \mid \text{parents}(v)) \times \prod_{v \in \text{parents}(w)} p(w \mid \text{parents}(w)).$$

This is facilitated by the graphical representation (Fig. 1), as the full conditional posterior distribution of any node v depends only on its parents, children, and coparents. For instance, if $v = P_t$, then the full conditional posterior distribution of P_t, $p(P_t|K, r, q, \sigma^2, \tau^2, P_1,..., P_{t-1}, P_{t+1}, P_N, I_1,..., I_N)$, is proportional to

$$p(P_t \mid P_{t-1}, K, r, \sigma^2) \times p(P_{t+1} \mid P_t, K, r, \sigma^2) \times p(I_t \mid P_t, q, \tau^2).$$

Here, the dependence of the deterministic nodes Pmed[t] and Imed[t] as logical functions of P_t, r, K, and q has been resolved. In this way, BUGS exploits the representation of the model as a DAG for constructing these full conditional posterior distributions for all unobservable nodes. Once this is accomplished, it uses certain sophisticated sampling methods to sample from these univariate densities. BUGS contains a small expert system for choosing the best sampling method. The first choice is to identify conjugacy, where the full conditional reduces analytically to a well-known distribution, and to sample accordingly. If the density is not conjugate but turns out to be log-concave, it employs the adaptive rejection sampling (ARS) algorithm (Gilks and Wild 1992). If the density is not log-concave, BUGS uses a Metropolis–Hastings (MH) step. The MH algorithms differ across the various BUGS versions and platforms. The current UNIX version 0.6 uses the Griddy–Gibbs sampler as developed by Ritter and Tanner (1992). More efficient MH implementations currently under development include slice sampling (Neal 1997) for variables with a restricted range and adaptive techniques (Gilks et al. 1998) for variables with unrestricted range. A first version has been released under WinBUGS, the BUGS version for the Windows 95 operating system.

Model implementation in BUGS

For a typical BUGS run using the UNIX version 0.6, four different files have to be specified: (*i*) the data are entered in a file with extension .dat, here called tuna.dat, (*ii*) initial val-

© 1999 NRC Canada

ues for all unobservables needed to start the Gibbs sampler are in a .in file, here surplus.in, (*iii*) the file that contains the model descriptions has the .bug extension, here surplus.bug, and (*iv*) the commands for running BUGS that control the number of sampled values, which parameters to monitor, and so on go into the surplus.cmd file; in WinBUGS, these commands are options in various menus. These four files are listed in the Appendix.

The data file can be either in rectangular format like tuna.dat or in SPLUS format as in tuna_S.dat.

The format of the initial value file follows that of the data file, here, for instance, surplus.in in SPLUS format. If initial values for parameters are not given in the initial value file, then values will be generated by forward sampling from the prior distributions specified in the model.

The DAG representation of our model not only serves BUGS-internal purposes but can assist us in specifying our model in the BUGS language. The file containing the model specification, surplus.bug, consists of two sections: the declarations and the model description. The declaration part specifies the name of the model, which nodes are constants (rectangles), and which nodes are stochastic (ellipses) and gives the names of the files containing the data and initial values. The model description forms a declarative representation of the fully Bayesian model. It is enclosed in curly brackets {...}. This is a translation of the graphical model into BUGS syntax. Each statement consists of a relationship of two kinds: ~, which means "is distributed as" and substitutes the solid arrows, and <-, which means "is to be replaced by" and substitutes the hollow arrows. Quantities on the left of a ~ are stochastic; those on the left of <- are deterministic. In general, each quantity should appear once and only once on the left-hand side of a statement. The order of the expressions within a pair of braces is irrelevant.

WinBUGS even has an option Doodle that allows the user to specify the model graphically by drawing a DAG. It uses a hyperdiagram approach to add extra information to the graph to give a complete model specification. DoodleBUGS then writes the corresponding model in BUGS syntax to a file.

Note that BUGS uses a nonstandard parametrization of distributions in terms of the precision (1/variance) instead of the variance. For example, a lognormal distribution denoted by dlnorm(v, φ^2) has density function

$$\int(x|\mathrm{v},\varphi^2)=\sqrt{\frac{\tau}{2\pi}}\frac{1}{x}e^{-\frac{1}{2}(\log x-\mathrm{v})^2\varphi^2}$$

Thus, we need the nodes isigma2 and itau2. BUGS does not permit an expression to be used as a parameter of a distribution, and hence, we need the deterministic nodes Pmed[t] and Imed[t]. BUGS only allows use of proper prior distributions. The noninformative distribution for q is improper, however. Therefore, we use a gamma(0.001, 0.001) prior for the inverse of q, which is practically equivalent to $p(q) \propto 1/q$. Furthermore, we have to restrict the ranges of those nodes with non-log-concave full conditional distributions by specifying lower and upper bounds using the I(lower, upper) function. This is not necessary in the WinBUGS version because of the adaptive MH algorithm.

It is very easy to obtain posterior samples of the management parameters MSP and E_{MSP}, which are functions of the parameters K, r, and q, simply by adding these deterministic nodes MSP and EMSP to the BUGS code (see file surplus.bug in the Appendix). The same holds for predictions like the depletion P_{1990} and total biomass B_{1990} in the year 1990.

Finally, the file surplus.cmd compiles the BUGS commands in surplus.bug, generates an initial 25 000 iterations (the so-called "burn-in" period), monitors every specified parameter for the next 225 000 iterations, stores every 25th value, and calculates summary statistics of the sampled values for each specified parameter. Our preference is to submit these commands as a batch job by using the command backbugs "surplus.cmd" with session output automatically directed to the bugs.log file. Alternatively, BUGS can be run interactively by using the command bugs. This run took 90 min on a 233-MHz laptop.

BUGS generates five files after completion as follows.

(*i*) The file bugs.log contains the BUGS code (surplus.bug) that was used, any error messages, the running time, and the requested summary statistics of the marginal posterior distribution of each parameter. The posterior summaries from this file are listed in the Appendix. Note that the results from fitting this surplus production model are presented and discussed in detail in Millar and Meyer (1999*a*).

(*ii*) The file bugs.out contains two columns. The first column gives the iteration number and the second column gives the corresponding sampled value.

(*iii*) The file bugs.ind tells you which line of the bugs.out file corresponds to which monitored variable. Here, lines 1–9000 of bugs.out are samples from variable K, lines 9001 – 18 000 are samples from variable r, and so on.

(*iv*) The file bugs1.out contains the results of the stats command in a rectangular format suitable for reading into statistical packages for producing graphs, tables, etc. The 10 columns contain the summary statistics mean, SD, observed lower percentile being reported (default 2.5%), observed lower percentile, observed upper percentile being reported, observed upper percentile (default 97.5%), median, number of iterations, start iteration, and finish iteration.

(*v*) The file bugs1.ind contains the node names for the variables listed and the corresponding row number in the bugs1.out file.

Whenever one employs MCMC methods to sample from the posterior distribution, a question of extreme importance is "has the chain converged to its target distribution?" Convergence diagnostics is still an area of active research. A recent review on methods used for establishing whether an MCMC algorithm has converged, i.e., whether its output can be regarded as samples from the target distribution of the Markov chain, has been done by Cowles and Carlin (1996). Some of these methods are implemented in the software CODA (Best et al. 1995), a menu-driven collection of SPLUS functions for analysing the output obtained by BUGS. Besides trace plots and the usual tests for convergence, CODA calculates statistical summaries of the posterior distributions and kernel density estimates. CODA is

© 1999 NRC Canada

Fig. 2. Kernel density estimates (solid lines) of the posterior distribution of various model and management parameters. Proper prior densities are given by the broken lines.

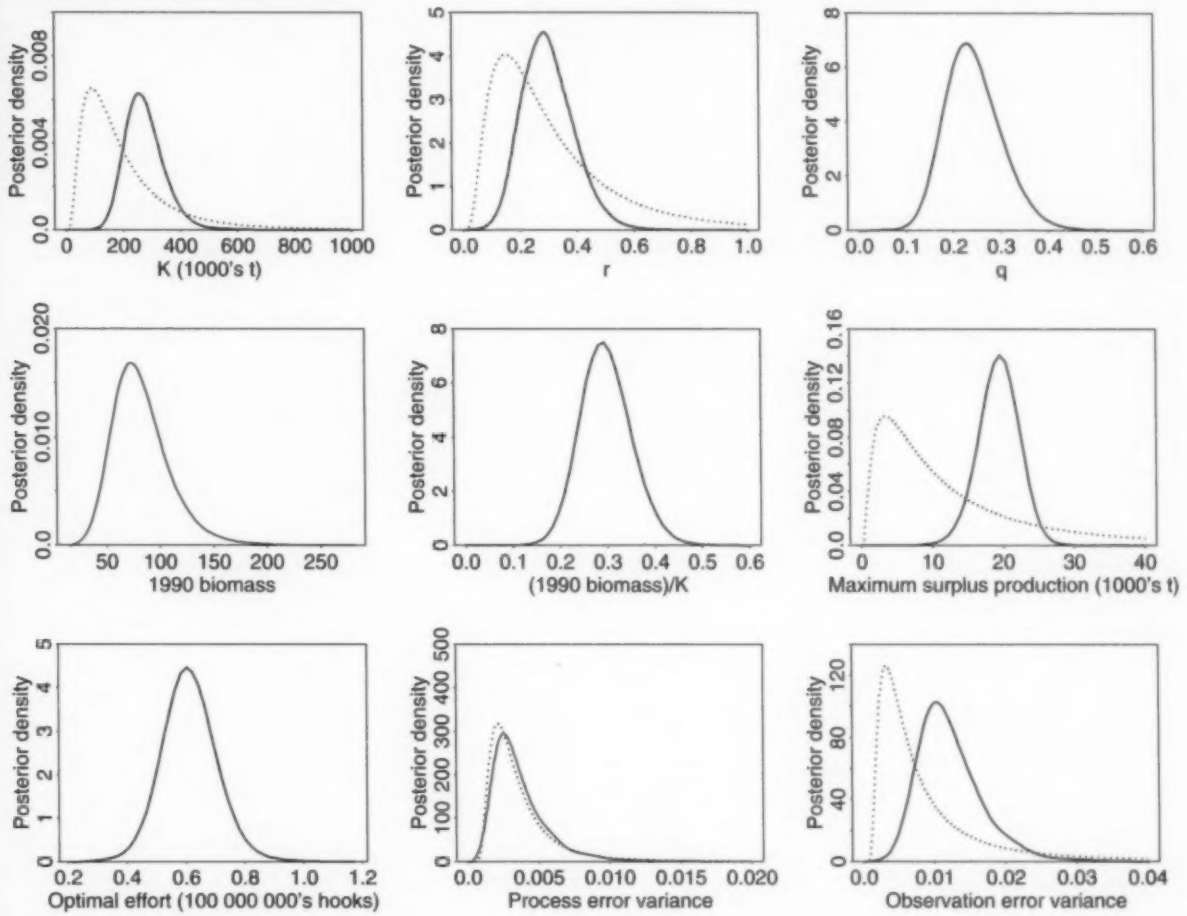

being maintained and distributed by the same research group responsible for BUGS.

CODA can be used to automatically generate trace plots and kernel density plots of model parameters based on the samples stored in the file bugs.out and the information provided in bugs.ind. Kernel estimates of the posterior densities of the parameters K, r, q, B_{1990}, P_{1990}, MSP, E_{MSP}, σ^2, and τ^2 are shown in Fig. 2, together with their respective prior densities. From the kernel density estimates, one can see that the posterior modes of K, r, and q are similar to the maximum likelihood estimates obtained by Polacheck et al. (1993) under the observation error model. This may hold in general when priors are diffuse and the observation error variance (τ^2 has posterior mean of 0.012) is substantially larger than the process error variance (σ^2 has posterior mean of 0.0031). Table 2 compares the posterior means of the parameters K, r, q, B_{1990}, P_{1990}, MSP, and E_{MSP} with the observation error and process error estimates of Polacheck et al. (1993).

Extensive convergence diagnostics for this chain were calculated using the CODA software of Best et al. (1995). All parameters passed the Heidelberger and Welch stationarity and halfwidth tests. Geweke's Z scores do not fall within the extreme tails of a standard normal distribution, suggesting that the chain fully converged. The Raftery and Lewis convergence diagnostics (estimating the 2.5th percentile up to an accuracy of 0.02 with probability 0.9) confirmed that the thinning, burn-in period, and sample size were sufficient.

We noted a strong dependency of the mixing behaviour of the chains on the specification of bounds for each parameter with non-log-concave full conditional posterior. The tighter those bounds, the faster the convergence due to the Griddy–Gibbs sampler used in the implementation of the MH step that is necessary to sample from non-log-concave full conditional posteriors. We therefore conclude that slow convergence of the MCMC chains generated by BUGS is an initial impediment that will be overcome with more efficient MH implementations like those based on slice sampling and adaptive techniques that are currently being developed and implemented.

As to the practical limitations in the number of parameters, an age-structured sequential population analysis applied

© 1999 NRC Canada

Table 2. Comparison of estimates of a number of management parameters: maximum likelihood estimates obtained by Polacheck et al. (1993) using observation error and process error models, respectively, and posterior means obtained by applying a Bayesian state–space model.

Parameter	Observation error model	Process error model	State–space model
K (1000's t)	239.6	153.4	279.8
r	0.328	0.620	0.293
$q \times 10^4$	26.71	43.72	23.89
B_{1990}	75.51	50.04	83.97
P_{1990}	0.315	0.326	0.297
MSP (1000's t)	19.65	23.78	19.26
E_{MSP}	61.4	70.9	60.86

to northern Atlantic cod (*Gadus morhua*) data that included about 200 unknowns is the most sophisticated model that we have yet fitted using BUGS (Millar and Meyer 1999*b*). This is basically at the current limit of computational practicability. Runs were prohibitively slow, taking 3 h on a 233-MHz laptop to compute 15 000 iterations of the Gibbs sampler. This, however, should only be a transient curb, as continuous algorithmic improvements in the BUGS software are enhancing its performance and capabilities.

Discussion

BUGS provides a means for a Bayesian analysis of the most complex fisheries models such as fully age-structured models (Millar and Meyer 1999*b*) and fully Bayesian hierarchical random effects models for stock–recruitment data (Liermann and Hilborn 1997) and for tackling the important Bayesian hierarchic metaanalysis problems identified in the "future directions" of Hilborn and Liermann (1998). BUGS will have considerable implications for the day-to-day practice of the fisheries stock assessment scientist. He/she can concentrate on the essential realistic modeling of data and of prior knowledge, handing over the mathematical intricacies of model fitting to a software package. Because prior and sampling distributions can be easily modified without having to recalculate full conditional distributions, the scientist's time is freed up to experiment with different scenarios — a hitherto far too time-consuming procedure.

The recent evolution in Bayesian computation and software within the last few years parallels and outperforms in some ways the development seen over the last decades of *frequentist* software packages based on maximizing the likelihood function. Once stable numerical routines for nonlinear optimization (like the Newton–Raphson algorithm) had been developed, these were implemented as modules in software packages (like SAS, GLIM, or SPLUS) for maximizing the likelihood function. Fitting a complicated model became possible for the statistical layperson just by running a certain DATA and PROC step in SAS, for instance. Knowledge about mathematical differentiation and optimization was no longer required.

The inevitable difficulty in calculating the high-dimensional integrals necessary for the determination of posterior probability distributions has hindered routine *Bayesian* data analysis. For scientists applying Bayesian inference, a good grasp of numerical and Monte Carlo integration techniques has been essential. Until recently, all applications have involved writing one-off computer code in low- or intermediate-level languages such as C or Fortran. Even with reliable MCMC subroutines like the MH algorithm and the Gibbs sampler to overcome the multidimensional integrations, writing and debugging a specific program would have taken anything from a few days to several weeks. A subsequent modification of the program, perhaps an extension of the model or an application to a different data set, might well have taken several hours. So Bayesian computations were previously impractical when compared with model fitting in SAS or SPLUS for which model specification may take just a few minutes and modifications may take just a few seconds. Therefore, the Bayesian software package BUGS has been developed with the Gibbs sampler and MH algorithms as building blocks. Instead of having to choose the right PROC in SAS for the problem at hand, with different commands and options for each procedure, the user of BUGS only has to specify prior and sampling distributions for his/her model. In this respect, the Bayesian software package BUGS is considerably more flexible, general, and user friendly. Moreover, as demonstrated in the context of state–space models, the Bayesian approach in conjunction with the Gibbs sampler is capable of handling far more complex models than the classical approach.

The progress made in Bayesian computation via MCMC methods has already revolutionized many scientific disciplines and provided solutions to problems that were hitherto considered computationally intractable. The routine implementation of Bayesian inference that is now possible will "almost surely" have an impact on fisheries stock assessment.

Despite the immense promise of this new Bayesian approach via Gibbs sampling, the reader should also be aware of potential pitfalls with the Bayesian paradigm and the use of MCMC techniques for posterior computation. Playing devil's advocates, we will point some of them out. One of the most controversial issues in Bayesian inference is the specification of prior distributions. An overview of selection of prior distributions by formal rules is given in Kass and Wasserman (1996) and guidelines on prior specification in fisheries stock assessment models are given in Punt and Hilborn (1997). A sensitivity analysis that explores how much the posterior inferences change when other prior distributions are assumed should always accompany a Bayesian data analysis. Basic techniques for model checking by comparing data with posterior predictive distributions and using

© 1999 NRC Canada

Bayes factors are given in Gelman et al. (1996). Despite the ease with which MCMC techniques can be employed using BUGS, a number of subtleties remain, such as assessing convergence, using parameter transformations to reduce posterior correlations and thereby enhance the mixing of the chains, the choice of starting values, and computing simulation standard errors. These are topics of active current research. An article giving advice and guidance to novice users of MCMC that addresses these topics is Kass et al. (1998). We caution against the noninformed use of BUGS, as against any other statistical software package, whether Bayesian or frequentist, and end with the warning issued on the title page of the BUGS manual, "Beware — Gibbs sampling can be dangerous!".

References

Best, N.G., Cowles, M.K., and Vines, S.K. 1995. CODA manual version 0.30. Medical Research Council Biostatistics Unit, Institute of Public Health, Cambridge, England.

Carlin, B.P., Polson, N.G., and Stoffer, D.S. 1992. A Monte Carlo approach to nonnormal and nonlinear state–space modeling. J. Am. Stat. Assoc. **87**: 493–500.

Cowles, M.K., and Carlin, B.P. 1996. Markov chain Monte Carlo convergence diagnostics: a comparative review. J. Am. Stat. Assoc. **91**: 883–904.

Fahrmeir, L., and Tutz, G. 1994. Multivariate statistical modelling based on generalized linear models. Springer, New York.

Freeman, S.N., and Kirkwood, G.P. 1995. On a structural time series method for estimating stock biomass and recruitment from catch and effort data. Fish. Res. **22**: 77–98.

Gelman, A., Carlin, J.B., Stern, H.S., and Rubin, R.B. 1996. Bayesian data analysis. Chapman and Hall, London, U.K.

Gentleman, R. 1997. A review of BUGS: Bayesian inference using Gibbs sampling. Chance, **10**: 48–51.

Gilks, W.R., and Wild, P. 1992. Adaptive rejection sampling for Gibbs sampling. Appl. Stat. **41**: 337–348.

Gilks, W.R., Thomas, A., and Spiegelhalter, D.J. 1994. A language and program for complex Bayesian modelling. Statistician, **43**: 169–178.

Gilks, W.R., Best, N.G., and Chan, K.K.C. 1995. Adaptive rejection Metropolis sampling within Gibbs sampling. Appl. Stat. **44**: 455–472.

Gilks, W.R., Richardson, S., and Spiegelhalter, D.J. 1996. Markov chain Monte Carlo in Practice. Chapman and Hall, London, U.K.

Gilks, W.R., Roberts, G.O., and Sahu, S.K. 1998. Adaptive Markov chain Monte Carlo through regeneration. MCMC preprint server (http:/www.stats.bris.ac.uk/MCMC/).

Gudmundsson, G. 1994. Time series analysis of catch-at-age observations. Appl. Stat. **43**: 117–126.

Hilborn, R., and Liermann, M. 1998. Standing on the shoulders of giants: learning from experience in fisheries. Rev. Fish Biol. Fish. **8**: 1–11.

Hilborn, R., and Walters, C.J. 1992. Quantitative fisheries stock assessment: choice, dynamics and uncertainty. Chapman and Hall, New York.

Kass, R.E., and Wasserman, L. 1996. The selection of prior distributions by formal rules. J. Am. Stat. Assoc. **91**: 1343–1370.

Kass, R.E., Carlin, B.P., Gelman, A., and Neal, R.M. 1998. Markov chain Monte Carlo in practice: a roundtable discussion. Am. Stat. **52**: 93–100.

Kinas, P.G. 1996. Bayesian fishery stock assessment and decision making using adaptive importance sampling. Can. J. Fish. Aquat. Sci. **53**: 414–423.

Liermann, M., and Hilborn, R. 1997. Depensation in fish stocks: a hierarchic Bayesian meta-analysis. Can. J. Fish. Aquat. Sci. **54**: 1976–1983.

Meyer, R., and Millar, R.B. 1999. Bayesian stock assessment using a state–space implementation of the delay difference model. Can. J. Fish. Aquat. Sci. **56**: 37–52.

Millar, R.B., and Meyer, R. 1999*a*. Nonlinear state–space modeling of fisheries biomass dynamics using Metropolis–Hastings within Gibbs sampling. Tech. Rep. STAT9901. Department of Statistics, University of Auckland, Auckland, N.Z.

Millar, R.B., and Meyer, R. 1999*b*. Bayesian state–space modeling of age-structured data: fitting the model is just the beginning. Tech. Rep. STAT9902. Department of Statistics, University of Auckland, Auckland, N.Z.

Neal, R.M. 1997. Markov chain Monte Carlo methods based on "slicing" the density function. Tech. Rep. No. 9722. Department of Statistics, University of Toronto, Toronto, Ont.

Pella, J.J. 1993. Utility of structural time series models and the Kalman filter for predicting consequences of fishery actions. *In* Proceedings of the International Symposium on Management Strategies for Exploited Fish Populations. *Edited by* G. Kruse, D.M. Eggers, R.J. Marasco, C. Pautzke, and T.J. Quinn II. Alaska Sea Grant College Program Rep. 93-02. University of Alaska, Fairbanks, Alaska. pp. 571–593.

Polacheck, T., Hilborn, R., and Punt, A.E. 1993. Fitting surplus production models: comparing methods and measuring uncertainty. Can. J. Fish. Aquat. Sci. **50**: 2597–2607.

Punt, A.E., and Hilborn, R. 1997. Fisheries stock assessment and decision analysis: the Bayesian approach. Rev. Fish Biol. Fish. **7**: 35–63.

Reed, W.J., and Simons, C.M. 1996. Analyzing catch–effort data by means of the Kalman filter. Can. J. Fish. Aquat. Sci. **53**: 2157–2166.

Ritter, C., and Tanner, M.A. 1992. Facilitating the Gibbs sampler: the Gibbs stopper and the Griddy–Gibbs sampler. J. R. Stat. Soc. Ser. B (Methodol.), **59**: 291–317.

Schaefer, M.B. 1954. Some aspects of the dynamics of populations important to the management of commercial marine fisheries. Inter-Am. Trop. Tuna Comm. Bull. **1**: 27–56.

Schnute, J.T. 1994. A general framework for developing sequential fisheries models. Can. J. Fish. Aquat. Sci. **51**: 1676–1688.

Spiegelhalter, D.J., Thomas, A., Best, N., and Gilks, W.R. 1996. BUGS 0.5, Bayesian inference using Gibbs sampling. Manual version ii. Medical Research Council Biostatistics Unit, Institute of Public Health, Cambridge, England.

Sullivan, P.J. 1992. A Kalman filter approach to catch-at-length analysis. Biometrics, **48**: 237–257.

Thomas, A., Spiegelhalter, D.J., and Gilks, W.R. 1992. BUGS: a program to perform Bayesian inference using Gibbs sampling. *In* Bayesian statistics 4. *Edited by* J.M. Bernardo, J.O. Berger, A.P. Dawid, and A.F.M. Smith. Oxford University Press, Oxford, U.K. pp. 837–842.

Wermuth, N., and Lauritzen, S.L. 1990. On substantive research hypothesis, conditional independence graphs and graphical chain models (with discussion). J. R. Stat. Soc. Ser. B (Methodol.), **52**: 21–72.

Yeh, S.-Y., Tsou, T.-S., and Liu, H.-C. 1991. Assessment of the South Atlantic albacore resource by using surplus production models, 1976–1988. Collect. Vol. Sci. Pap. ICCAT, **39**: 166–170.

© 1999 NRC Canada

Appendix

tuna.dat

```
15.9 61.89
25.7 78.98
28.5 55.59
23.7 44.61
25.0 56.89
33.3 38.27
28.2 33.84
19.7 36.13
17.5 41.95
19.3 36.63
21.6 36.33
23.1 38.82
22.5 34.32
22.5 37.64
23.6 34.01
29.1 32.16
14.4 26.88
13.2 36.61
28.4 30.07
34.6 30.75
37.5 23.36
25.9 22.36
25.3 21.91
```

tuna_S.dat

```
list(C=c(15.9,25,7,...,25.3), I=c(61.89,78.98,...,21.91))
```

surplus.in

```
list(P=c(0.99,0.98,0.96,0.94,0.92,0.90,0.88,0.86,0.84,0.82,
0.80,0.78,0.76,0.74,0.72,0.70,0.68,0.66,0.64,0.62,0.60,0.5
8,0.56),
r=0.8, K=200, iq=5, isigma2=100, itau2=100)
```

surplus.bug

```
model surplusproduction;
const N=23;
var C[N], I[N], Imed[N], P[N], Pmed[N],
r, K, q, iq, sigma2, isigma2, tau2, itau2, MSP, EMSP,
P1990, B1990;
data C, I in "tuna.dat";
inits in "surplus.in";
{

# prior distribution of K: lognormal with 10% and 90%
quantile at 80 and 300
K ~ dlnorm(5.042905,3.7603664)I(10,1000);

# prior distribution of r: lognormal with 10% and 90%
quantile at 0.13 and 0.48
r ~ dlnorm(-1.38,3.845)I(0.01,1.2);

# prior distribution of q: instead of improper (prop. to 1/q)
use just proper IG
iq ~ dgamma(0.001,0.001)I(0.5,100);
q <- 1/iq;

# prior distribution of sigma2: inv. gamma with 10% and
90% qu. at 0.04 and 0.08
isigma2 ~ dgamma(3.785518,0.010223);
sigma2 <- 1/isigma2;

# prior distribution of tau2: inv. gamma with 10% and
90% qu. at 0.05 and 0.15
itau2 ~ dgamma(1.708603,0.008613854);
tau2 <- 1/itau2;

# (conditional) prior distribution of Ps (from state equa-
tions):
Pmed[1] <- 0;
P[1] ~ dlnorm(Pmed[1],isigma2) I(0.001,2.0)
for (t in 2:N) { Pmed[t] <- log(P[t-1] + r*P[t-1]*(1-P[t-1])
- C[t-1]/K);
P[t] ~ dlnorm(Pmed[t],isigma2)I(0.001,2.0) }

# sampling distribution:
for (t in 1:N) { Imed[t] <- log(q*K*P[t]);
I[t] ~ dlnorm(Imed[t],itau2);
}

# further management parameters and predictions:
MSP <- r*K/4;
EMSP <- r/(2*q);
P1990 <- P[N]+r*P[N]*(1-P[N]) -C[N]/K;
B1990 <- P1990*K;
}
```

surplus.cmd

```
compile("surplus.bug")
update(25000)
monitor(K,25)
monitor(r,25)
monitor(q,25)
monitor(sigma2,25)
monitor(tau2,25)
monitor(P[],25)
monitor(P1990,25)
monitor(B1990,25)
monitor(MSP,25)
monitor(EMSP,25)
update(225000)
stats(K)
stats(r)
stats(q)
stats(sigma2)
stats(tau2)
stats(P[])
stats(P1990)
stats(B1990)
stats(MSP)
stats(EMSP)
q()
```

© 1999 NRC Canada

bugs.log

Bugs > stats(K)

	mean	sd	2.5% :97.5% CI	median	sample
	2.798E+2	6.307E+1	1.826E+2 4.251E+2	2.709E+2	9000

Bugs > stats(r)

	mean	sd	2.5% : 97.5% CI	median	sample
	2.928E–1	8.663E–2	1.436E–1 4.793E–1	2.869E–1	9000

Bugs > stats(q)

	mean	sd	2.5% : 97.5% CI	median	sample
	2.389E–1	5.694E–2	1.434E–1 3.627E–1	2.344E–1	9000

Bugs > stats(sigma2)

	mean	sd	2.5% : 97.5% CI	median	sample
	3.100E–3	1.894E–3	1.133E–3 7.826E–3	2.601E–3	9000

Bugs > stats(tau2)

	mean	sd	2.5% : 97.5% CI	median	sample
	1.215E–2	4.422E–3	5.731E–3 2.270E–2	1.137E–2	9000

Bugs > stats(P[])

	mean	sd	2.5% : 97.5% CI	median	sample
[1]	1.018E+0	5.432E–2	9.165E–1 1.133E+0	1.015E+0	9000
[2]	9.959E–1	7.436E–2	8.741E–1 1.171E+0	9.874E–1	9000
[3]	8.807E–1	6.579E–2	7.646E–1 1.025E+0	8.755E–1	9000
.					
.					
.					
[22]	3.543E–1	3.603E–2	2.910E–1 4.324E–1	3.519E–1	9000
[23]	3.282E–1	4.014E–2	2.557E–1 4.136E–1	3.255E–1	9000

Bugs > stats(P1990)

	mean	sd	2.5% : 97.5% CI	median	sample
	2.973E–1	4.654E–2	2.123E–1 3.955E–1	2.946E–1	9000

Bugs > stats(B1990)

	mean	sd	2.5% : 97.5% CI	median	sample
	8.397E+1	2.579E+1	4.457E+1 1.441E+2	8.017E+1	9000

Bugs > stats(MSP)

	mean	sd	2.5% : 97.5% CI	median	sample
	1.926E+1	2.412E+0	1.401E+1 2.354E+1	1.944E+1	9000

Bugs > stats(EMSP)

	mean	sd	2.5% : 97.5% CI	median	sample
	6.086E–1	8.770E–2	4.382E–1 7.903E–1	6.079E–1	9000

© 1999 NRC Canada

Fecundity and duration of egg incubation for multiparous female snow crabs (*Chionoecetes opilio*) in the fjord of Bonne Bay, Newfoundland

Michel Comeau, Michel Starr, Gérard Y. Conan, Guy Robichaud, and Jean-Claude Therriault

Abstract: Multiparous female snow crabs (*Chionoecetes opilio*) were collected by trap and *Nephrops* trawl in the fjord of Bonne Bay, Newfoundland, between April 1988 and August 1992 to study the fecundity and embryonic development. A relationship was established between the color of the egg mass and embryonic development. Fecundity was positively correlated with carapace width. A female of 67 mm carapace width can produce up to about 54 000 eggs. Egg mortality over the incubation period could reach 21%, being greater in larger females. Based on the bimodal distributions of embryonic developmental stages observed in the study, the female reproductive cycle was determined as 2 years and females probably only hatch two broods in their lifetime. Eggs hatch mainly in May and June.

Résumé : Des femelles multipares du crabe des neiges (*Chionoecetes opilio*) ont été capturées à l'aide de casiers et un chalut *Nephrops* dans le fjord de Bonne Bay, Terre-Neuve, entre avril 1988 et septembre 1992 afin d'étudier la fécondité et le développement embryonnaire. Une relation a été trouvée entre la couleur de la masse d'oeuf et le développement embryonnaire. La fécondité est positivement corrélées avec la largeur de la carapace. Une femelle d'une taille de 67 mm largeur de la carapace peut produire 54 000 oeufs. La mortalité des oeufs au cours de l'incubation pourrait atteindre 21%; étant plus élevée pour les femelles de grande taille. Basé sur les distributions bimodales des stages de développement embryonnaire observés dans l'étude, le cycle reproducteur des femelles est approximativement de deux ans et les femelles ne libèrent probablement que deux portées au cours de leur vie. L'éclosion des oeufs a lieu surtout en mai et juin.

Introduction

In the past, the egg incubation period for snow crab (*Chionoecetes opilio*) was believed to be about 1 year (Ito 1963; Watson 1969) or 1.5 years (Kon 1974*b*). However, recent studies conducted in Japan (Kanno 1987) and in the Gulf of St. Lawrence (Mallet et al. 1993; Sainte-Marie 1993) suggested that the female reproductive cycle may be 2 years. Furthermore, the reproductive cycle may be 1 year in one area and 2 years in another area due to temperature and (or) other environmental parameters (Mallet et al. 1993; Sainte-Marie 1993). This reproductive cycle could influence the reproductive potential of different stocks.

Gaining a better understanding of the snow crab reproductive cycle is important for this fishery. Maturity is reached for both male and female snow crabs after a terminal molt over a wide range of ages and sizes (Yoshida 1941; Ito 1963; Watson 1970; Conan and Comeau 1986; Comeau and Conan 1992; Sainte-Marie and Hazel 1992). Females mate for the first time shortly after their terminal molt while the carapace is still soft (Watson 1969) and the next mating occurs shortly before or immediately after the hatching of the eggs (Conan and Comeau 1986). Female snow crabs may also produce more than one viable brood from spermatophores stored in their spermatheca (Sainte-Marie and Carrière 1995) without mating. Females extruding eggs for the first time immediately after molting and repeat spawners with hard-shell carapace are termed primiparous and multiparous, respectively.

A male-directed fishery can affect the reproductive potential of females (McMullen and Yoshihara 1971; Smith and Jamieson 1991). As fewer mature males become available for mating due to fishing, multiparous females would have to rely on old stored ejaculates in their spermathecae for egg fertilization. Laboratory studies on Tanner crab (*Chionoecetes bairdi*) showed that females using old stored spermatophores to fertilize their eggs have a lower fecundity than females that have recently mated (Paul 1984). For *C. opilio*, Sainte-Marie and Carrière (1995) found that fe-

Received August 28, 1998. Accepted February 10, 1999. J14772

M. Comeau[1] **and G. Robichaud.** Department of Fisheries and Oceans, Science Branch, Gulf Fisheries Centre, P.O. Box 5030, Moncton, NB E1C 9B6, Canada.
M. Starr and J.-C. Therriault. Ministère des Pêches et des Océans, Région Laurentienne, Institut Maurice-Lamontagne, Division de la Productivité des Océans, C.P. 1000, Mont-Joli, QC G5H 3Z4, Canada.
G.Y. Conan.[2] Department of Fisheries and Oceans, Marine Biology Research Laboratory, Université de Moncton, Moncton, NB E1A 3E9, Canada.

[1]Author to whom all correspondence should be addressed. e-mail: comeaum@mar.dfo-mpo.gc.ca
[2]Present address: 5 Halifax Street, St. John's, NF E1A 2P6, Canada.

© 1999 NRC Canada

males can effectively fertilize a second clutch of eggs from stored ejaculate but warned that their laboratory findings cannot be indiscriminately extrapolated to the field, due firstly to the importance of interannual sperm storage and secondly to a 2-year reproductive cycle instead of the 1-year cycle from their experiment. Thus, fishing could reduce the fecundity of females and (or) increase egg mortality by reducing the number of mature males.

The objectives of the present study are to examine the reproductive cycle and fecundity of multiparous female snow crabs from an unexploited stock located in the fjord of Bonne Bay, northeast Gulf of St. Lawrence, and to compare these results with published data from exploited stocks in the northwest and southwest Gulf of St. Lawrence.

Materials and methods

Study site and field sampling

Female snow crabs were sampled during spring and summer between April 1988 and August 1992 in the fjord of Bonne Bay, Newfoundland (49°32′N, 57°56′W). Detailed information on the study site is provided in Comeau et al. (1998). An important feature of the fjord is the shallow sill at its entrance that appears to restrict adult movements in or out, and there is no known concentration of snow crabs in the Gulf near Bonne Bay. Furthermore, during the time of the study, snow crabs were not commercially exploited in Bonne Bay, and thus may show characteristics of a stock in its pristine state, prior to any commercial fishing. Small conical traps (base diameter 115 cm, height 62 cm, opening 51 cm) covered with a 2.0-cm-mesh net were used to collect females at depths ranging from 90 to 130 m on the steep slope and the flat muddy bottom. A Bay of Biscay *Nephrops* 25-m headrope otter trawl with 2.5-cm-mesh codend was also used to collect females on the flat muddy bottom. The trawl has a heavy chain footrope and is designed to capture crustaceans semiburied in the mud.

Biological parameters

The following characteristics of all mature females collected were recorded from live specimens prior to preservation: carapace width (CW), exoskeleton condition, color of the eggs under the abdomen, and presence of new and (or) old grasping marks on the pereiopods (as an index of mating embrace). CW measurements were made to the nearest 0. 1 mm using a caliper. The average color and condition of the egg mass were divided into six categories: bright orange, orange, brown (developing eyed eggs), black (eyed eggs), empty eggshells mixed or not with black eggs, and degenerating eggs. The color standardization was done on fresh egg samples using the Pantone® Color Formula Guide 1000 (Pantone, Inc., Carlstadt, NJ 07072-3098, U.S.A.). Criteria used to describe the exoskeleton condition are detailed in Comeau et al. (1998). In this study, newly molted primiparous (first spawners) females, characterized by a clean soft-shell or clean hard-shell condition and newly spawned eggs under the abdomen, were not considered. These females were excluded from this study because of the uncertainty of their time of spawning, which is probably before multiparous (repeat spawners) females in Bonne Bay (Comeau et al. 1991). Also, the larger size of their eggs (Sainte-Marie 1993), which could influence embryo development, could have biased our estimation of the duration of egg development.

Subsamples of eggs, still attached to the abdomen of females, were fixed in 4% buffered formalin in seawater and were used to determine the embryonic developmental stage as described by Kon (1974*b*). Eggs from inside the brood were detached and placed in a dye solution (green light at 1% dilution) to enhance details of the embryo for stereomicroscopic observations at 16 and 40× magnification. Empty eggshells were classified as Stage 7, as they were often associated with eyed eggs. Degenerated eggs, associated with dirty soft (senile) females, were discarded.

To establish the fecundity of multiparous females, 70 clutches of eggs were randomly selected from the trawling survey done on September 10, 1991. At the laboratory, the preserved clutches of eggs were separated based on embryonic developmental stage, dried for 48 h at 80°C, and weighed to the nearest 10^{-5} g. For each brood, a subsample of 250 eggs was dried for 48 h at 80°C and weighed to the nearest 10^{-5} g. Fecundity was determined as the ratio of the total dry weight of the brood to the dry weight of the 250-egg subsamples.

Statistical methods

The squared residual of the regression lines of the number of eggs and the CW was tested for homogeneity (F test). Because of heterogeneity ($p < 0.05$), the comparison of regression lines was done graphically using the ellipses of joint confidence limits for slopes and elevations (y-intercept). In this comparison, the regression lines are significantly different ($p < 0.05$) if the ellipses do not intersect.

Results

Seasonal changes in color of the egg mass

A total of 6868 mature females, with a mean size of 67 mm CW (ranging from 37 to 90 mm CW) were sampled from April 1988 to August 1992 (Table 1). Orange eggs were observed in all samples (Fig. 1). Females with orange eggs were observed simultaneously with females having well-developed eggs, females with empty eggshells and (or) remains of a previous brood, and females with bright orange eggs in the spring samples from March to June (Fig. 1). The presence of bright orange eggs was observed in May 1991 and June of every year except for 1992, which is probably due to the low number of females sampled in that particular year (Fig. 1). Females observed in May 1991 with bright orange eggs, sometimes with eggs not yet attached to the pleopods, were only observed on two occasions (May 29 and 31, 1991). Consequently, spawning (extrusion of a new brood) of multiparous females in Bonne Bay probably occurs between the end of May and mid-June. Thereafter, no females with either bright orange eggs, black eggs, or empty eggshells were observed. Brown eggs were only observed in late summer in September 1991 and August 1992 concurrently with females carrying orange eggs (Fig. 1).

Description and seasonal changes in embryonic development

A total of 912 mature females with eggs were examined to determine the embryonic development of the eggs. All the developmental stages described by Kon (1974*b*) were observed in Bonne Bay with the exception of Stage 5, which was too difficult to distinguish from late Stage 4.

A strong relationship was observed between embryonic development and the color of the eggs (Table 2). The bright orange color of the eggs is observed in early Stage 1 (cell cleavage stage) immediately after fertilization. At late Stage 1, the color of the eggs becomes orange and remains that color until early Stage 4. By late Stage 4, the color of the eggs gradually changes to brown and the abdomen bulges as the brood increases in volume and is easily visible from the

© 1999 NRC Canada

Table 1. Number of mature multiparous snow crab females sampled by traps and trawls between 1988 and 1992 in Bonne Bay.

Year	Gear used	March	April	May	June	July	Aug.	Sept.
1988	Trap		143	369	526	474	176	
	Trawl					151		
1989	Trap			187	102	18		160
	Trawl					236		
1990	Trap					5		
	Trawl				638	655		
1991	Trap		10	215	62			
	Trawl			666	1186			132
1992	Trap	6			8			
	Trawl						743	

Fig. 1. Percentage of multiparous snow crab females with eggs at different embryonic developmental stages in Bonne Bay from April 1988 to August 1992. The total number of females sampled appears above the bars. Solid, bright orange eggs; cross-hatching, orange eggs; horizontal hatching, brown eggs; vertical hatching, black eggs; open, empty eggshells mixed or not with black eggs; checkered, degenerating eggs.

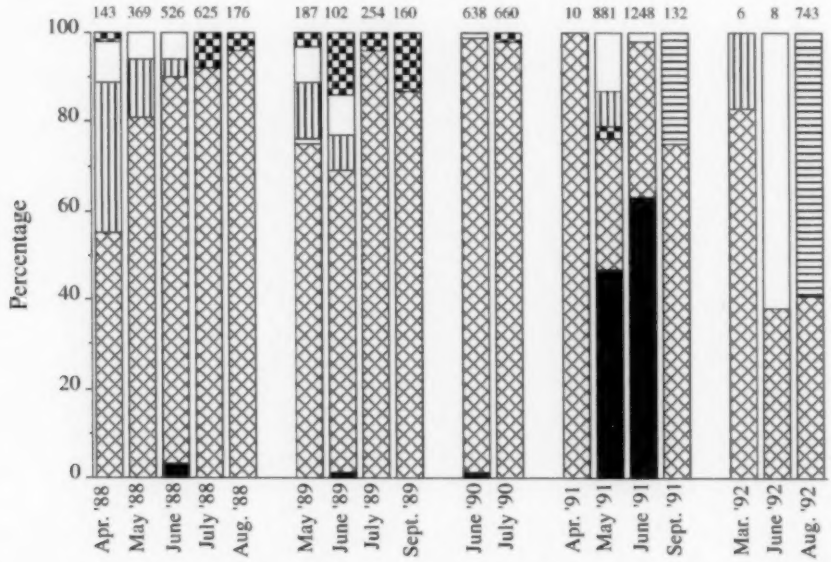

side. In Stage 6, the eggs are dark in color (black), due mainly to the pigmentation of the eyes and the chromatophores. Stage 7 is the hatching stage: the egg is black and a well-formed larva can be observed inside the eggshell.

On the basis of embryonic development, two groups of females can be distinguished at any given time between March and September (Table 3). Between March and June, females with embryonic developmental Stage 7 (hatching) and Stage 1 (eggs being spawned) were observed simultaneously with females in Stage 3 (nauplius stage) and early Stage 4. During July and August, females in Stage 4 and Stage 1 were observed simultaneously. In September, females in embryonic developmental early Stage 2 (gastrula) were observed with females in late Stage 4 (metanauplius).

In 1991, the percentage of females in their second year of egg development was about 26%, as the orange eggs (Stage 3 and early Stage 4) observed in spring developed to brown eggs (late Stage 4) by September (Tables 3 and 4). In 1991, 83% (1129/1362) had mated or were involved in a mating courtship embrace, as identified by the new grasping mark in the spring of either black (late Stage 7), hatched, or bright orange (early Stage 1) eggs.

Size–fecundity relationship

Fecundity was positively correlated with carapace size (Fig. 2*a*). A significant difference ($p < 0.05$) was observed between the size–fecundity relationships of orange (Stage 2) and brown eggs (late Stage 4), as determined from the non-intersection of the ellipses of joint confidence limits for slopes and elevations (*y*-intercept). The difference was greater for larger females.

Discussion

Reproductive cycle

Based on egg color observations and embryonic develop-

© 1999 NRC Canada

Table 2. Relationship between Kon's (1974*b*) embryonic developmental stages and egg color for snow crab females collected in Bonne Bay.

Embryonic developmental stage	Egg color[a]	Observations
Early 1	Bright orange (021C)	Egg cleavage stage; immediately after fertilization of the egg to about the 64- or 128-cell stage of the cell division; at the earliest stage the eggs are not yet attached with a stem on the pleopods; abdomen covers the entire brood
Late 1	Orange (151C)	Egg cleavage stage; no appearance of a blastopore; abdomen covers the entire brood
2	Orange (151C)	Gastrula stage; abdomen covers the entire brood
3	Orange (151C)	Nauplius stage; abdomen covers the entire brood
Early 4	Orange (151C)	Volume of the brood increased; some eggs are visible on the front
Late 4	Brown (144C)	Formation of the metanauplius; abdomen is bulged and the eggs are visible on the side
5	—	Not observed in the Bonne Bay samples
6	Black	Eggs dark; pigmentation of the compound eyes and chromatophores can be observed
7	Black	Eggs dark; hatching stage; well-formed larvae can be observed

[a]Color standardization using the Pantone® Color Formula Guide 1000 (Pantone, Inc., Carlstadt, NJ 07072-3098, U.S.A.).

Table 3. Percentage of multiparous snow crab females with eggs at different embryonic developmental stages in Bonne Bay from April 1988 to August 1992.

			Embryonic developmental stage								
Year	Month	Number	Early 1	Late 1	2	3	Early 4	Late 4	5	6	7
1988	April	55				66				29	5
	May	57		16		40	28				16
	June	73	14	21		27	26				12
	July	114		43		13	44				
	August	43		22	24		54				
1989	May	63		51		24					25
	June	27		37		33					30
	July	20		90	10						
	September	25			100						
1990	June	106		41		53					6
	July	61		31	16	15	38				
1991	April	10				100					
	May	55	46	18		22					14
	June	60	50	25		25					
	September	70			76			24			
1992	March	6					83				17
	June	8					38				62
	August	59			34		17	49			

Note: A description of the embryonic developmental stages is outlined in Table 2.

ment, our study suggests that multiparous female snow crabs in Bonne Bay have a 2-year reproductive cycle. Females with recently fertilized eggs (early Stage 1), hatching eggs (late Stage 7), and middevelopment eggs (early Stage 3) were observed simultaneously in the spring. By September, the newly extruded eggs (Stage 1) developed to the gastrula stage (Stage 2) and the middevelopment eggs (Stage 3) developed to brown eggs (late Stage 4). The observation of bimodal distributions of the embryonic developmental stage suggests that the incubation period of multiparous female eggs in Bonne Bay is 2 years.

Data from recent studies carried out on heavily exploited stocks in the Gulf of St. Lawrence and in Japan corroborate our findings of a 2-year reproductive cycle for multiparous females. In the southwestern Okhotsk Sea (Japan), Kanno (1987) reported that female snow crabs have a reproductive cycle of 2 years based on a gonad index showing bimodal distribution. In a study conducted at various locations in the southwestern Gulf of St. Lawrence, Mallet et al. (1993) suggested a 2-year reproductive cycle for female snow crabs based on the histology of the gonads, the development of the embryo, and the color of the eggs. Sainte-Marie (1993) also indicated that female snow crabs from Baie Sainte-Marguerite located on the northwestern Gulf of St. Lawrence had a 2-year reproductive cycle based on ovarian condition and weight, color of the eggs, and quantitative analyses of spermathecal contents. Furthermore, Sainte-Marie (1993) estimated that the maturation of the ovaries and brood lasted 27 months for primiparous and 24 months for multiparous females. These results and ours therefore suggest that a 2-year reproductive cycle is characteristic of the female snow crab life cycle and is not related to fishing pressure.

In Japan, Kon (1974*b*) estimated a 1-year duration of embryonic development based on laboratory rearing at temperatures ranging from 4.5 to 5.5°C. He estimated the duration

© 1999 NRC Canada

Table 4. Percentages of multiparous snow crab females collected by trawl in Bonne Bay in spring (May–June) and September 1991 with new grasping marks on the walking legs, indicating possible mating, in relation to the color of the eggs.

	Total no. females examined	Eggs		Females with new grasping marks (%)
		Color	%	
Spring (May–June)	1852	Bright orange	63	89
		Orange	26	29
		Brown	<1	0
		Black	3	27
		Empty eggshell	7	60
		Degenerated	<1	0
September	132	Orange	75	85
		Brown	25	36

of the first stage of development at 28 days and the second and third stages at 74 and 27 days, respectively. Stages 4–7 were estimated to take a total of 194 days. Our observations from the wild in Bonne Bay suggest a 2-year cycle at temperatures ranging from –1 to 1°C (Starr et al. 1994). Our estimates are about twice that calculated by Kon (1974*b*) for Stages 4–7 and three times that for Stages 1–3. As will be discussed later, temperature and other environmental factors observed in a natural environment, often not reproducible in the laboratory, are important controlling factors for the incubation period of the eggs and may explain the differences observed between aquarium and field studies. For example, a major difference in the duration of egg development between Kon's (1974*b*) aquarium estimates and ours is the slowing down of the embryonic development at very early stages, especially at the gastrula stage (Stage 2). Such a diapause early in the incubation period has already been reported by Sainte-Marie (1993) and for other brachyurans by Wear (1974) (*Hyas coarcticus* and *Corystes cassivelaunus*) and Peterson (1995) (*Hyas araneus*). Compared with other spider crabs, which have incubation periods varying between 3 and 11 months (Hartnoll 1963; Wear 1974), female snow crabs have possibly one of the longest reproductive cycles currently known for majid crabs.

The 2-year reproductive cycle and the diapause observed for female snow crabs may be related to the low temperature regime found in the natural habitat. Mallet et al. (1993) mentioned that the 2-year cycle that they observed in the southwestern Gulf of St. Lawrence may only be valid for that location, as females remain year-round in a water layer with temperatures ranging from –1 to +1°C. They also suggested that egg development may benefit from a higher temperature regime as females move up to shallower waters in certain locations such as Bonne Bay (Conan and Comeau 1986; Hooper 1986; Comeau et al. 1991; Comeau and Conan 1992) and Baie Sainte-Marguerite (Sainte-Marie and Hazel 1992) and shorten the incubation period of the eggs from 2 years to 1 year. Mallet et al. (1993) based this assumption on the fact that females from the Gulf of St. Lawrence, with a reproductive cycle of 2 years in nature, could complete their egg development in 1 year if they were placed in a temperature above 2°C. A similar temperature-dependent egg incubation period has also been observed by

Fig. 2. Linear relationship between the natural logarithm (ln) of the number of eggs and the CW of multiparous snow crab females. Predictive regression equations were fitted to multiparous females with orange and brown eggs from (*a*) Bonne Bay in 1991 (circles, orange eggs (n = 53); squares, brown eggs (n = 17)) and (*b*) Bonne Bay and Baie des Chaleurs (data from Baie des Chaleurs were taken from Conan et al. 1989).

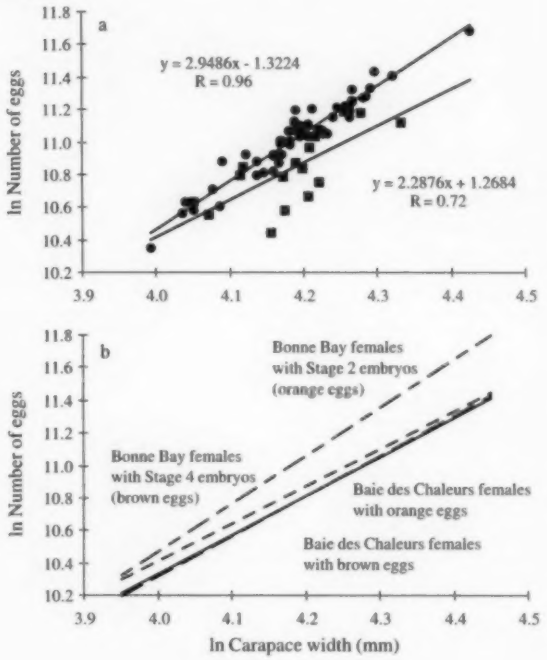
a
y = 2.9486x - 1.3224
R = 0.96
y = 2.2876x + 1.2684
R = 0.72
ln Number of eggs
b
Bonne Bay females with Stage 2 embryos (orange eggs)
Bonne Bay females with Stage 4 embryos (brown eggs)
Baie des Chaleurs females with orange eggs
Baie des Chaleurs females with brown eggs
ln Number of eggs
ln Carapace width (mm)

Sainte-Marie and Carrière (1995) and a related cold-water majid crab (*H. araneus*) (Petersen 1995) from laboratory studies. Although a 1-year reproductive cycle was observed in aquarium studies, females in nature do not seem to take advantage of a higher temperature regime as they move up to shallow waters in the spring during mating (Sainte-Marie's 1993; this study). In Bonne Bay, for instance, females observed in shallow waters, where water temperature may occasionally reach 5°C in early June, are almost exclusively females in the mating courtship embrace (precopulatory embrace, Conan and Comeau 1986) with hatching eggs (Stage 7) or early Stage 1 eggs (Comeau et al. 1991). Solitary females are seldom observed at temperatures above 1°C (Comeau et al. 1991). Females that were sampled on the slope for this study were captured at a depth of 90 m and more, where temperatures ranged from –1 to 0°C year-round (Comeau et al. 1991; Starr et al. 1994). However, Sainte-Marie and Gilbert (1998) proposed that a warming trend in the cold intermediate layer over the entire snow crab habitat would shorten the incubation time from 2 years to 1 year, as observed in 1996–1997 in Baie Sainte-Marguerite. Although temperature may be an important environmental factor influencing the incubation period of the eggs, other factors such as dissolved oxygen may also play a role in the development of the embryos.

© 1999 NRC Canada

The color of the eggs was found to be as good an indicator of embryonic development as the system proposed by Kon (1974*b*) (Table 2). Although the color of the eggs is less accurate, especially in the summer (July–August) when late Stage 1 and Stage 3 (both characterized by orange eggs) are found simultaneously, it can be used as an alternative to Kon's (1974*b*) egg staging by stereomicroscope.

Indication of mating

Grasping marks identify multiparous females that were potentially participating in spring mating. Grasping marks are left when the male grasps the pereiopods of the female with his propodite during the mating courtship embrace (Comeau and Conan 1992). During the 1991 spring trawl survey, 83% of females with old eggs (Stage 7) or newly extruded eggs (Stage 1) had new grasping marks compared with 29% for females with Stage 3 and early Stage 4 eggs, indicating that a large number of females with old (hatching) or newly extruded eggs were involved in the act of mating. Although 29% of females with Stage 3 and early Stage 4 eggs (middevelopment) had grasping marks, they should not be considered as involved in mating, as they will not spawn for another year. Thus, the percentage of multiparous females involved in the act of mating could be determined by the presence of new grasping marks in spring and the color of the eggs (bright orange or hatching eggs) and (or) the embryonic development of the embryo (either Stage 1 or Stage 7). The fact that not all gravid multiparous females appear to have mated recently may be due to the use of stored spermatophores in their spermatheca to inseminate the new brood (Watson 1970, 1972; Sainte-Marie 1993; Sainte-Marie and Carrière 1995). Alternatively, it may indicate that some females mated without injury (Donaldson and Adams 1989).

Fecundity

In Bonne Bay, females with well-developed eggs have fewer eggs than those with newly extruded eggs. Our results indicate that egg mortality over the incubation period could reach 21% for large females (75 mm CW). Similarly, Kon (1974*a*) in Japan, Conan et al. (1989) in the southern Gulf of St. Lawrence, and Elner and Gass (1984) in Cape Breton suggested egg loss during incubation. These results contrast with those reported by Sainte-Marie (1993) in Baie Sainte-Marguerite, northwestern Gulf of St. Lawrence, who indicated no significant egg mortality over time for primiparous and multiparous females.

Because the egg developmental stage has a significant effect on the estimates of fecundity, it must be taken into consideration when establishing a size–fecundity relationship. In Baie des Chaleurs, Conan et al. (1989) indicated that the number of eggs for multiparous females (size ranging from 55 to 85 mm CW) ranged between 31 000 and 90 500 for orange eggs and between 31 000 and 88 800 for brown eggs (Fig. 2*b*). The results of the present study show that the number of orange eggs (Stage 2) of large females (85 mm CW) is actually higher (116 000) for the females from Bonne Bay, indicating a higher fecundity for newly extruded eggs. However, this higher fecundity for large females in Bonne Bay seems to be balanced by a higher egg mortality, which may result from a variety of processes such as predation, parasitism (Brattey et al. 1985), abrasion, unfertilized eggs, or developmental failure (Elner and Beninger 1995). Thus, our final estimate (88 500) for females with brown eggs is comparable with what was found by Conan et al. (1989). The number of eggs of smaller females (55 mm CW) from Bonne Bay (31 500) is comparable with what was estimated by Conan et al. (1989) in Baie des Chaleurs. Egg loss for smaller females was not observed in Bonne Bay, suggesting that egg loss is proportionately greater for large females. A similar relationship has been reported by Kon (1974*a*) and Elner and Gass (1984). Comparison with other published results is difficult, as many did not differentiate the egg developmental stage (Watson 1969; Haynes et al. 1976; Thompson 1979; Davidson et al. 1985) or had poor fecundity relationships due to low correlation coefficients (Elner and Gass 1984).

Implication to the fishery

For management and industry, one of the most important questions is the impact of the fishery on the population reproductive potential. Since females are protected from harvesting, the reproductive potential of the resource has been hypothesized to be unaffected by the commercial removal of males only. However, McMullen and Yoshihara (1971) and Smith and Jamieson (1991) indicated that a reduction in fecundity could result from a reduction in the availability of suitable mates in crustacean populations subjected to high male fishing mortality. For snow crab, a reduction of suitable males, either by natural or fishing mortality, can be counteracted by an increased reliance of females on stored spermatophores (Sainte-Marie 1993; Elner and Beninger 1995; Sainte-Marie and Carrière 1995). Long-term monitoring of exploited and unexploited populations is necessary to evaluate the impact of a fishery on the populations' reproductive potential. To date, our data indicate no major impact of fishery on female snow crab fecundity.

A 2-year reproductive cycle has important implications for management of this recruitment-based fishery. Based on isotopic aging techniques, the life expectancy of female snow crabs in Bonne Bay is about 5 years (Comeau et al. 1991; G.Y. Conan, unpublished data) after their terminal molt. Consequently, as mentioned by Sainte-Marie (1993), a female can probably only hatch two broods in its lifetime. Assuming that the fecundity of primiparous females is about 20% less than that of multiparous females (Sainte-Marie 1993), the lifetime fecundity of an average female of 67 mm CW from Bonne Bay would be a little less than 100 000 eggs. This estimate is at least half of what was previously estimated. In terms of fishery management, females would only participate twice in the recruitment process and not every year for 4–5 years as was originally thought. Thus, to trace the fluctuations in recruitment back to parental stocks and to develop a sound yield per recruit model, it is important to identify the timing of egg production and the reproductive cycle of both primiparous and multiparous females. In view of these new findings, statements based on a 1-year female reproductive cycle that high egg production has not either translated into high recruitment levels into the fishery (Elner and Beninger 1989) or ensured stock stability (Bailey and Elner 1989) have to be reassessed.

Further studies on the effect of the percentage of male removals (exploitation level) on the potential of egg produc-

© 1999 NRC Canada

tion would be needed in order to achieve a better understanding of stock fluctuation in relation to female fecundity.

Acknowledgments

The authors wish to thank R. Bannister, B. Comeau, A. Jones, G. Paulin, M. Wen, and the crew of the CSS *Opilio* for technical assistance in the field. Special thanks to Y. Chiasson, K.G. Davidson, and Drs. M. Chadwick, M. Moriyasu, and T.W. Sephton for critically reviewing the manuscript. Logistic and financial support of M. Starr was provided by the Gulf and Québec regions, now renamed the Maritimes and Laurentien regions, respectively, of the Department of Fisheries and Oceans through the NSERC/DFO visiting fellowship program.

References

Bailey, R.F.J., and Elner, R.W. 1989. Northwest Atlantic snow crab fisheries: lessons in research and management. *In* Scientific approaches to management of shellfish resources. *Edited by* J.F. Caddy. John Wiley & Sons, New York. pp. 261–280.

Brattey, J., Elner, R.W., Uhazy, L.S., and Bagnall, A.E. 1985. Metazoan parasites and commensals of five crab (Brachyura) species from eastern Canada. Can. J. Zool. **63**: 2224–2229.

Comeau, M., and Conan, G.Y. 1992. Morphometry and gonad maturity of male snow crab, *Chionoecetes opilio*. Can. J. Fish. Aquat. Sci. **49**: 2460–2468.

Comeau, M., Conan, G.Y., Robichaud, G., and Jones, A. 1991. Life history patterns and population fluctuations of snow crab (*Chionoecetes opilio*) in the fjord of Bonne Bay on the west coast of Newfoundland, Canada — from 1983 to 1990. Can. Tech. Rep. Fish. Aquat. Sci. No. 1817.

Comeau, M., Conan, G.Y., Maynou, F., Robichaud, G., Therriault, J.-C., and Starr, M. 1998. Growth, spatial distribution and abundance of the benthic stages of the snow crab *Chionoecetes opilio* in Bonne Bay, Newfoundland, Canada. Can. J. Fish. Aquat. Sci. **55**: 262–279.

Conan, G.Y., and Comeau, M. 1986. Functional maturity and terminal molt of male snow crab, *Chionoecetes opilio*. Can. J. Fish. Aquat. Sci. **43**: 1710–1719.

Conan, G.Y., Moriyasu, M., Maynard, D.R., and Chiasson, Y. 1989. Factors influencing egg production in decapod Crustacea with two case studies: *Chionoecetes opilio* and *Homarus americanus* in the Gulf of St. Lawrence. Int. Counc. Explor. Sea C.M. 1989/Mini 04.

Davidson, K., Roff, J.C., and Elner, R.W. 1985. Morphological, electrophoretic and fecundity characteristics of Atlantic snow crab, *Chionoecetes opilio*, and implications for fisheries management. Can. J. Fish. Aquat. Sci. **42**: 474–482.

Donaldson, W.E., and Adams, A.E. 1989. Ethogram of behavior with emphasis on mating for the Tanner crab *Chionoecetes bairdi* Rathbun. J. Crustacean Biol. **9**: 37–53.

Elner, R.W., and Beninger, P.G. 1989. Comment on functional maturity in small male crab (*Chionoecetes opilio*): sizing up the evidence. Can. J. Fish. Aquat. Sci. **46**: 2037–2039.

Elner, R.W., and Beninger, P.G. 1995. Multiple reproductive strategies in snow crab, *Chionoecetes opilio*: physiological pathways and behavioral plasticity. J. Exp. Mar. Biol. Ecol. **193**: 94–112.

Elner, R.W., and Gass, C. 1984. Observations on the reproduction condition of female snow crabs from N.W. Cape Breton Island, November 1983. Can. Atl. Fish. Sci. Adv. Comm. Res. Doc. 84/14.

Hartnoll, R.G. 1963. The biology of Manx spider crabs. Proc. Zool. Soc. Lond. **141**: 423–496.

Haynes, E., Karinen, J.F., Watson, J., and Hopson, D.J. 1976. Relation of number of eggs and length to carapace width in the brachyuran crabs *Chionoecetes bairdi* and *C. opilio* from the southwestern Bering Sea and *C. opilio* from the Gulf of St. Lawrence. J. Fish. Res. Board Can. **33**: 2592–2595.

Hooper, R.G. 1986. A spring breeding migration of the snow crab, *Chionoecetes opilio* (O. Fabr.), into shallow water in Newfoundland. Crustaceana, **50**: 257–264.

Ito, K. 1963. A few studies on the ripeness of eggs of Zuwai-gani, *Chionoecetes opilio*. Bull. Jpn. Sea Reg. Fish. Res. Lab. **11**: 65–76. (Translated from Japanese; Fish. Res. Board Can. Transl. Ser. 1117.)

Kanno, Y. 1987. Reproductive ecology of tanner crab in the southwestern Okhotsk Sea. Nihon Suisan Gakkaishi, **53**: 733–738.

Kon, T. 1974*a*. Fisheries biology of the Japanese Tanner crab — VI. On the number of ovarian eggs and eggs held on the pleopods. Bull. Jpn. Soc. Sci. Fish. **40**: 465–469.

Kon, T. 1974*b*. Fisheries biology of the Tanner crab, *Chionoecetes opilio* — VII. Changes of the external morphogenesis in the process of the embryonic development. Aquaculture, **23**: 103–110.

Mallet, P., Conan, G.Y., and Moriyasu, M. 1993. Periodicity of spawning and duration of incubation time for *Chionoecetes opilio* in the Gulf of St. Lawrence. Int. Counc. Explor. Sea C.M. 1993/K:26.

McMullen, J.C., and Yoshihara, H.T. 1971. Deposition of unfertilized eggs in unmated king crabs, *Paralithodes camtschatica* (Tilesius). Trans. Am. Fish. Soc. **100**: 583–584.

Paul, A.J. 1984. Mating frequency and viability of stored sperm in the tanner crab *Chionoecetes bairdi* (Decapoda, Majidae). J. Crustacean Biol. **4**: 375–381.

Petersen, S. 1995. The embryonic development of *Hyas araneus* L. (Decapoda, Majidae): effects of temperature. Sarsia, **80**: 193–198.

Sainte-Marie, B. 1993. Reproductive cycle and fecundity of primiparous and multiparous female snow crab, *Chionoecetes opilio*, in the northwest Gulf of St. Lawrence. Can. J. Fish. Aquat. Sci. **50**: 2147–2156.

Sainte-Marie, B., and Carrière, C. 1995. Fertilization of the second clutch of eggs of snow crab, *Chionoecetes opilio*, from females mated once or twice after their molt to maturity. Fish. Bull. U.S. **93**: 759–764.

Sainte-Marie, B., and Gilbert, G. 1998. Possible effects of changes in CIL temperature and thickness on population dynamics of snow crab, *Chionoecetes opilio*, in the Gulf of Saint Lawrence. DFO Can. Stock Assess. Sect. Res. Doc. 98/38.

Sainte-Marie, B., and Hazel, F. 1992. Moulting and mating of snow crab, *Chionoecetes opilio* (O. Fabricius), in shallow waters of the northwestern Gulf of Saint Lawrence. Can. J. Fish. Aquat. Sci. **49**: 1282–1293.

Smith, B.D., and Jamieson, G.S. 1991. Possible consequences of intensive fishing for males on the mating opportunities of Dungeness crabs. Trans. Am. Fish. Soc. **120**: 650–653.

Starr, M., Therriault, J.-C., Conan, G.Y., Comeau, M., and Robichaud, G. 1994. Larval release in a sub-euphotic zone invertebrate triggered by sinking phytoplankton particles. J. Plankton Res. **16**: 1137–1147.

Thompson, R.J. 1979. Fecundity and reproductive effort in the blue mussel (*Mytilus edulis*), the sea urchin (*Strongylocentrotus droebachiensis*), and the snow crab (*Chionoecetes opilio*) from populations in Nova Scotia and Newfoundland. J. Fish. Res. Board Can. **36**: 955–964.

Watson, J. 1969. Biological investigations on the spider crab *Chionoecetes opilio*. Can. Fish. Rep. **13**: 24–47.

© 1999 NRC Canada

Watson, J. 1970. Maturity, mating and egg laying in the spider crab, *Chionoecetes opilio*. J. Fish. Res. Board Can. **27**: 1607–1616.

Watson, J. 1972. Mating behavior in the spider crab, *Chionoecetes opilio*. J. Fish. Res. Board Can. **29**: 447–449.

Wear, R.G. 1974. Incubation in British decapod Crustacea, and the effects of temperature on the rate of success of embryonic development. J. Mar. Biol. Assoc. U.K. **54**: 745–762.

Yoshida, H. 1941. On the reproduction of useful crabs in North Korea. Suisan Kenkyushi, **36**: 116–123.

© 1999 NRC Canada

Spawning season influences on commercial catch rates: computer simulations and *Plectropomus leopardus*, a case in point[1]

Elizabeth Fulton, David Kault, Bruce Mapstone, and Marcus Sheaves

Abstract: Spatial and temporal closures of sections of the marine environment are proposed frequently as fishery management devices, particularly when specific areas, such as spawning aggregations, can be identified. The ultimate effectiveness of spawning area closures is unknown, as spawning-related determinants of catch rate have not been studied. A simulation model, based on existing biological and fisher information, was constructed to examine the most important determinants of the spawning season catch rates using the protogynous aggregative spawner *Plectropomus leopardus* (Family Serranidae, Subfamily Epinephelinae) as a test case. Model output indicated that spawning season catches rose as long as catchability of spawners was equal to or greater than that of nonspawners. Greatest increases in catch were produced by fish moving from habitats inaccessible to fishers into regularly fished locations during migrations to spawning aggregations. Elevated catches were not simply dependent on the targeting of aggregations by fishers. Small-scale spatial closures around spawning aggregation sites would not be sufficient to protect the spawning stock of fish such as *P. leopardus*, but larger scale closures during the spawning season may be useful even when fishers are not targeting spawning aggregations.

Résumé : À titre de mesures de gestion, on propose fréquemment d'interdire l'exploitation des espèces marines dans des secteurs donnés ou durant certaines périodes, surtout dans certains secteurs particuliers comme ceux où les animaux se rassemblent pour se reproduire. L'efficacité réelle des fermetures des zones de reproduction est inconnue étant donné que les facteurs liés à la reproduction déterminant le taux de capture n'ont pas été étudiés. On a élaboré un modèle de simulation, fondé sur les données biologiques et les données de la pêche, pour étudier les facteurs déterminants les plus importants agissant sur les taux de capture durant la saison de reproduction en prenant pour exemple *Plectropomus leopardus* (famille Serranidae, sous-famille Epinephelinae), une espèce protogyne qui se rassemble au moment de la reproduction. Les résultats du modèle ont montré que les prises durant la saison de reproduction ont augmenté aussi longtemps que la capturabilité des géniteurs était égale ou supérieure à celle des non-géniteurs. Les plus forts accroissements des prises ont été observés quand les poissons passaient d'habitats inaccessibles aux pêcheurs à des zones régulièrement exploitées durant les migrations vers les lieux de rassemblement où les poissons se reproduisent. Les fortes prises n'étaient pas simplement liées au fait que les pêcheurs ciblaient les rassemblements. Des fermetures de petits secteurs autour des lieux de rassemblement ne suffiraient pas à protéger le stock de géniteurs de poissons comme *P. leopardus*, mais des fermetures de plus grands secteurs durant la saison de reproduction pourraient être utiles, même quand les pêcheurs ne visent pas les rassemblements de géniteurs.

[Traduit par la Rédaction]

Introduction

Over a century of fisheries science and spectacular fisheries collapses has emphasised that biological information alone is not enough to successfully manage a fishery (Hilborn and Walters 1992). An understanding of fishing practices and the dynamic responses of fish and fishers to changing fishing pressures and conditions is required before management can produce truly sustainable fishery systems (Hilborn 1985; Allen and McGlade 1986).

One of the most profitable ways of integrating existing knowledge of a system is through simulation modelling (Rjinsdorp and Pastoors 1995). This technique allows for the consideration of dynamic responses under differing conditions, but it also highlights the areas of information on which outcomes are most sensitively dependent and any

Received June 17, 1998. Accepted January 22, 1999.
J14658

E. Fulton[2] and M. Sheaves. Department of Marine Biology, James Cook University of North Queensland, Townsville QLD 4811, Australia.
D. Kault. Department of Mathematics and Statistics, James Cook University of North Queensland, Townsville QLD 4811, Australia.
B. Mapstone. CRC Reef Research Centre, James Cook University of North Queensland, Townsville QLD 4811, Australia.

[1]A publication of the Effects of Line Fishing Project, CRC Reef, Australia.
[2]Author to whom all correspondence should be addressed. e-mail: beth.fulton@marine.csiro.au

© 1999 NRC Canada

shortfalls in data or understanding. These attributes make simulation modelling an ideal tool for fisheries science. Without at least a basic understanding of the behaviours of both fish and fisher, however, management strategies and tactics cannot be evaluated fully, even with well-considered models.

Spatial and temporal closures have become an integral part of fisheries management (Attwood et al. 1997). If closures do not actually protect the target stock, or modify fishing practices, however, then they are essentially ineffectual and potentially very costly because resources are wasted maintaining something of little or no use, and if the stock collapses, economic losses will occur. For example, area closures of spawning sites to protect the spawning stock may prove futile if fishers can circumvent spatial closures by targeting fish migrating to and from these locations. Moreover, closures of any form will be of little value if the overall harvest is not reduced as a result of closure. With regard to stock size, spawning season closures are unlikely to be any more effective than closures at other times, if the harvest landed during the spawning season was no greater than that landed during any other part of the year. This could conceivably occur if aggregations of spawning fish could not be reliably located, if the catchability of spawning fish was consistently lowered, or if general catch rates fell as individuals migrated away from home sites to the aggregation sites (Mapstone et al. 1996*a*). Clearly, research into the area of catch rate determinants and the targeting of spawning aggregations is required before firm judgements can be made about the utility of spawning season closures as a management strategy.

In those fisheries where there is some understanding of the effects on the stock of fishing aggregations, most studies have concentrated on the biology of the fish and made inferences from there, rather than specifically considering the dynamic interactions of fisher and fish. In this study, we explored the interaction between fish and fishers and how they were affected by aggregative spawning behaviour of the fish, using a typical reef line fishery as the empirical vehicle for the work. The Great Barrier Reef (GBR) line fishery for the common coral trout (*Plectropomus leopardus*) is a potentially useful case through which to examine spawning season influences on catch rates. The targeting of spawning aggregations of this protogynous hermaphrodite has become a topic of interest for the management, fishing, and public bodies of the GBR, and spawning season closures have been suggested as a potential management option (QFMA 1996). The effectiveness of such a scheme is largely unknown, however, as there is scant information about the degree to which spawning aggregations are targeted or the benefits or disadvantages accruing from targeting spawning aggregations. The simulation model discussed in this paper provides an example of the way in which considering the mechanics of fishing can give some insight into the determinants of catch rates during the spawning season and, thus, the utility of closure management strategies.

Background to the case study

Coral trout are large, long-lived predatory groupers with few natural predators. They usually grow to a maximum of about 65 cm (Brown et al. 1994), reach 14–18 years of age in the waters of the GBR (Ferreira and Russ 1994), and exhibit a relatively low annual natural mortality rate of about 17% (Mapstone et al. 1996*b*). Coral trout are also relatively sedentary during the nonspawning season (Davies 1996; Mapstone et al. 1996*b*). Home sites of about 2 km^2 are frequented for periods of at least 4–5 months (Samoilys 1997), and tagging studies have shown that interreefal movement of coral trout is negligible (Davies 1996).

Coral trout are protogynous hermaphrodites that aggregate to spawn (Samoilys and Squire 1994). They have been observed aggregating at densities ranging from 37.06 to 75.29 fish/km^2, which represents a 9.5- to 19.5-fold increase in density over the nonspawning period (M.A. Samoilys, unpublished data). There may be six or more spawning aggregations of coral trout per 2.5 km^2 of reef (Zeller 1998). Spawning individuals aggregate during the late afternoons of 4 or 5 days either side of the new moons during late spring – early summer, and spawning occurs at dusk (Samoilys and Squire 1994). Aggregations disperse during the early morning (M.A. Samoilys, unpublished data), although some fish that have travelled a long distance (>1.5 km) to reach an aggregation will remain in the area for several days (Zeller 1998). There is no record of spawning away from spawning aggregations.

Plectropomus species make up the single largest component of the landed catch in the GBR line fishery (Mapstone et al. 1996*a*). Coral trout consistently made up 35–45% of the catch of about 2800–3700 t of fish landed by the commercial line fleet each year between 1989 and 1994 (Mapstone et al. 1996*a*).

The GBR line fishery operates via a system of primary vessels and associated tender vessels (dories). The dories are typically 4–5 m long and powered by outboard motors (Mapstone et al. 1996*a*). Each primary vessel typically has between one and six dories, although the majority of the most active primary vessels in the GBR line fishery have three or four dories. The primary vessels move between reefs on a daily basis, but most of the fishing is done from the dories, which roam each reef once it has been reached (Mapstone et al. 1996*a*). Before commencing fishing, a fisher anchors at a coral outcrop (bombie) where the tide is pushing onto the reef and about which bait fish aggregate. Handlines (50–150 lb (23–68 kg)) are used with a 7–10/O hook.

Between 1989 and 1994, about 16 000 – 18 500 primary vessel days of fishing effort occurred per year (Mapstone et al. 1996*a*), 70% of which was allocated to targeting coral trout. A seasonal peak in both catch and effort coincides with the spawning period of the coral trout (Mapstone et al. 1996*a*). One possible interpretation of this pattern is that fishers actively concentrate their effort during the spawning season, although other explanations also exist. For example, skippers may purposefully avoid unfavourable weather conditions in the summer and winter months by concentrating their effort in the calmer spring months.

The widespread use of GPS navigation systems provides the opportunity for fishers to return to aggregation sites that have been identified in the past. Varying accounts have been given by commercial fishers as to the benefit of targeting aggregations: some reported large catches, whereas others

© 1999 NRC Canada

found no clear advantage, as they had difficulty in predicting where aggregations occur (Mapstone et al. 1996*a*).

Present management strategies on the GBR include a limited-entry licensing scheme, minimum legal size limits, and area closures (via the reef zoning imposed by the Great Barrier Reef Marine Park Authority) (QFMA 1996), although the latter is not explicitly intended for fishery management (GBRMPA Act 1975). Concerns remain that these measures are not sufficient to ensure a sustainable fishery based on coral trout (QFMA 1996).

Methods

We used a two-stage model of the behaviour of coral trout and the fishers targeting them to explore the implications of fishing spawning aggregations. A general overview of this model is given first. A more detailed explanation of the model's basic structure then follows. Finally, scenarios used to examine the more speculative or sensitive dynamics are outlined.

Model outline

There are two ways of conceptualising a fishery, such as the GBR line fishery, which spans a matrix of fishing habitats. The first focuses on the traditional source of fisheries data, a boat's recorded catch as it moves from spot to spot. The second is the sum of a reef's (habitat's) losses as it is visited by a procession of boats. Ultimately, the totals on both sides must match, but the way in which the numbers track through time and what this implies about the underlying responses and impacts do not have to correspond. Thus, to allow for a more complete evaluation of the mechanics and consequences of fishing, both sides of the fish–fisher process were monitored. This was achieved by following the output of two forms of the simulation model. One form followed a single boat fishing four reefs over a 4-day period. The second form of the model followed the cumulative effect of different vessels fishing a single reef over 4 days. Both forms utilised the same reef geometry and covered the same range of fish behaviour. The patterns produced by the simulations that followed a boat visiting a new reef each day were weaker than those from the simulations following a single reef for 4 days, but they did match and thus, only the latter will be considered for the remainder of this discussion.

The simulations involved a hypothetical reef 5 km long and 2.5 km wide (Fig. 1). The reef was grided into 50 × 50 m cells. These cells were the scale at which movement and fishing occurred.

Simulations were run under spawning and nonspawning conditions. There was a single fundamental difference between these two conditions. Under spawning conditions, a percentage of fish were in the spawning state and behaved accordingly. This typically involved changes in their range of movements, some degree of aggregating behaviour, and the likelihood of them taking a bait.

Fish movement followed a "directed random walk" in that the route had to be within set bounds, but the timing of each step taken depended on a set of random numbers. Nonspawning fish were restricted to their three-cell-long (150 m) home sites whereas spawning fish moved from their home site to the closest spawning site. Potential spawning sites were at fixed locations (Fig. 1). As the initial location and the spawning condition of a fish were both random, not all potential spawning locations were actually used in every run of the simulation under spawning conditions.

Behaviour of fishers was mimicked as accurately as possible. Four dorymen fished the reef at any one time. They were placed at random at one of up to 185 potential fishing sites and from there systematically searched the potential sites for productive fishing locations. Fishers did not fish outside the predetermined fishing sites, as they represented hydrographic features that fishers use as cues to locate fishing sites. It was not possible for two or more fishers to occupy the same site (cell) at the same time, but they could be in adjacent cells. Thus, the potential for limited aggregative predatory behaviour by the fishers existed. Fishers would not remain on a fishing site if they had caught fewer than three fish during the previous time step (which represented 10 min). There was a movement penalty imposed if the distance between fishing sites was >50 m. In such cases, fishers could not fish for between one and three time steps (depending on the distance to be covered), as that time was taken up by movement and anchoring. Known gear saturation levels meant that fishers could not catch more than five fish in a single step.

There were two sessions fished per simulated day. Each of these sessions lasted 24 time steps (4 h), after which the fishing sites and other tidal and daily components were adjusted for the next session. The fishing sites were session dependent, as they changed with the tide; thus, there were two possible sets per day: one in the morning and one in the afternoon (Fig. 1).

A few potential aggregation sites coincided with potential fishing sites. The rate at which fishers encountered a spawning aggregation site was modified by manipulating the degree to which spawning and fishing sites overlapped, so that the effect of fishing aggregations could be investigated. A high rate of coincidence between fishing sites and spawning sites would be functionally equivalent to active, although imperfect, targeting of aggregations by fishers.

Model structure and assumptions

In this section, each step in the simulation will be explained in order of occurrence. The parameters used in the model and a brief description of the reasoning behind their use can be found in Table 1. Any expression that is not easily justified within the format of Table 1 will be discussed during the appropriate step. Figure 2 is a flow diagram of the model.

Step 1. Fisher creation and placement

Each fisher was allocated a fishing ability and randomly placed onto one of the morning set of fishing locations. Fishers' ability only affected their capability of landing a fish. All fishers were equally adept at finding fishing sites, as they all had a perfect knowledge of the potential fishing sites of the reef. This perfect knowledge of fishing locations implies very rapid learning or considerable previous experience of the reef. Admittedly, the omniscience employed in the simulation will not always be the case. However, skilled fishers do quickly identify viable fishing locations in areas they have never visited before, and experienced fishers, who have targeted the same sites over many years, do build extensive information bases. It was in an effort to capture these features that the simulated fishers were given perfect knowledge of fishing locations. Short-term learning (based on the site of the previous day's successes) was not included, however, as primary vessels do not remain on a reef for more than 1 day; thus the fishers must rely on their long-term experience alone.

Step 2. Fish creation and placement

The number of fish per cell was determined and then each was allocated a home site (centred on the current cell), a size and corresponding weight, and a spawning condition (which was dependent on size and the spawning scenario under consideration). The size of the spawning population proved to be the most difficult facet of the model. Calculations, based on existing work by Samoilys and Squire (1994), suggested that only 6–10% of the population on a reef aggregated to spawn. Accordingly, in many of the simulations, 6–10% of the fish were chosen, at random, to be spawners. However, the inclusion of alternative scenarios was necessary, as it would be highly atypical of a reef fish to have such a small spawn-

© 1999 NRC Canada

Fig. 1. Schematic representation of the simulated reef (Lachlan Reef). The darkened areas represent areas inhospitable to fish, as they represent those areas of the reef that are often exposed, at least at low tide. Note that the reef was broken up into a 5000-cell grid (each cell representing a 50 × 50 m square) (this grid is not shown on the diagrams) and that the reef is not drawn to scale. (*a*) Fish's perspective. The small areas with solid outlines represent potential aggregation sites that are included in every scenario, and those with dotted outlines are only present in some scenarios. The potential aggregation sites varied in size from two to four cells. Only the outline of the entire area of each aggregation site is shown; the individual cells within each aggregation site are not indicated. The number of potential aggregations was set to match the range seen in the field. The locations are representative of those on an average reef. (*b*) Fisher's perspective. The shaded areas represent the general locations of potential fishing sites for the morning sessions, and the striped areas are the approximate positions of the afternoon fishing sites. Solid outlines indicate areas included in every simulation, and dotted outlines indicate selective inclusion. The potential fishing sites varied in size from two to 17 cells. Only the outline of the entire area of each fishing site is shown; the individual cells within each fishing site are not indicated. The locations are determined by hydrodynamics and are representative of those on an average reef.

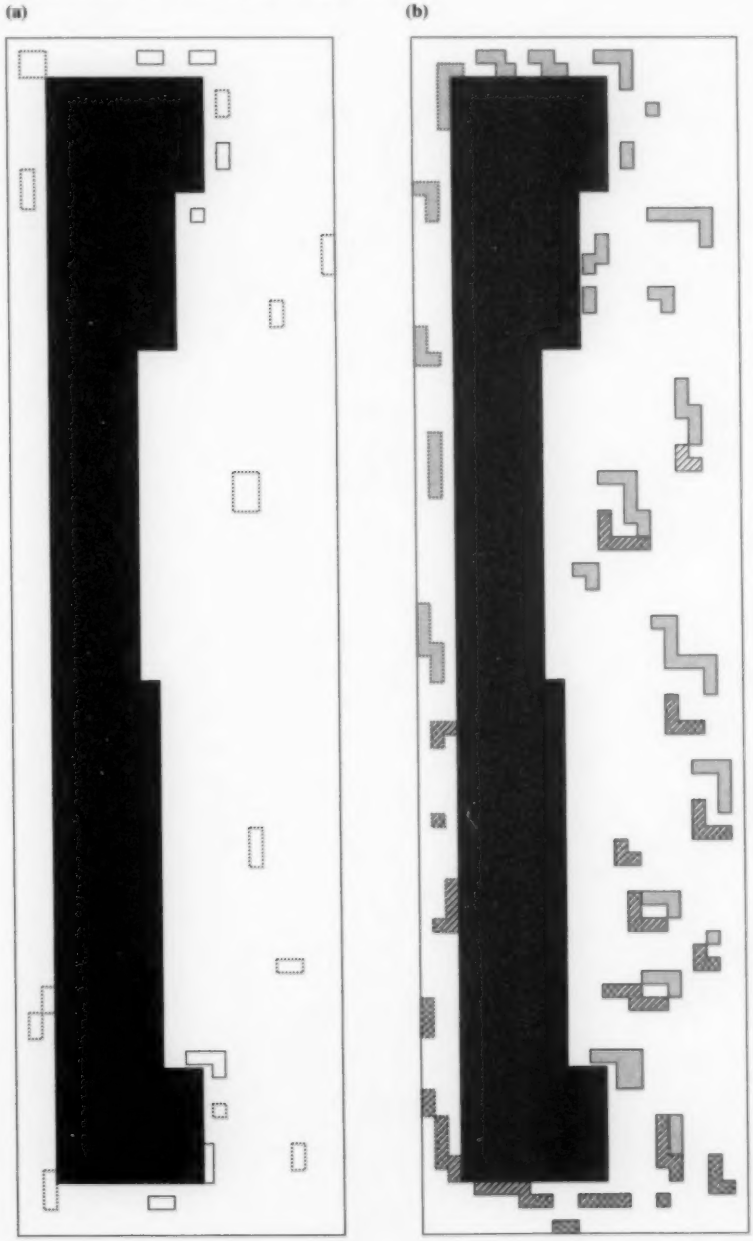

© 1999 NRC Canada

Table 1. List of the parameters used in the model, their values, the reasoning behind their form, and the source of any data or information used.

Step	Parameter	Value	Reasoning	Source(s)
1	Fishing ability of fisher j on day i	$a_{ij} \sim U(0.5, 1)$	A differential in behaviour, ability, and haul exists (which mirrors those observed in other fisheries). The range 0.5–1 was chosen as commercial fishers are being modelled. Thus, 0–1 was inappropriate, as fishers in the lower half of the range would either rapidly increase their skill by accumulating experience or slip from the industry if their performance persisted below an adequate level	Hilborn 1985; Hilborn and Ledbetter 1985; Allen and McGlade 1986; Abrahams and Healey 1990; Thorlindsson 1994
2	Number of fish per grid cell k at time $t = 0$	$n_{k,0} \sim U(0, 19)$	The range of numbers and average densities on the simulated reef agreed with nonspawning field observations	Samoilys 1997; Beinssen 1989
2	Fork length (cm) of fish u in cell k	$l_{uk} \sim N(39.659, 61.732)$ OR $l_{uk} \sim N(36.662, 48.177)$	The first distribution was used in the majority of the scenarios and came from data from both reefs that are currently closed to commercial fishing and reefs open to fishing. A scenario, considering the effect of intensive fishing pressure in the past, was run using the second distribution, which was based on data solely from reefs open to fishing	ELF Program, Collaborative Research Centre for the Ecologically Sustainable Development of the GBR, unpublished data
2	Weight (kg) of fish u in cell k	$w_{uk} = 7.978 \times 10^{-6} \times l_{uk}^{3.17}$	Three curves are given in publications (from reefs along the length of the GBR). This was the intermediate curve of the three	Brown et al. 1994
2	Catchability of nonspawner nu in cell k	$q_{nuk} \sim U(0, 1)$ (in most scenarios; see text for exception)	There is not enough available information to construct any other distribution. q_{nuk} is allocated on the first and third days	Frequency of gut renewal based on St. John 1995
2	Catchability of spawner su in cell k	$q_{suk} \sim U(0, 1)$ $q_{suk} \sim N_T(0, 0.05)$ $q_{suk} \sim N_T(1, 0.05)$	There is no available information, so a range of distributions were used to try and cover (*i*) no change, (*ii*) a lack of interest in food, and (*iii*) belligerence	
3	Session length	4 h	The session length is representative of what occurs in the fishery	Mapstone et al. 1996*a*
3	Trip length	4 days	Trip length is less than a week, so that demographic changes (e.g., natural mortality, growth, and recruitment) of the fish population are negligible and there is little chance of significant changes in fish behaviour, as aggregative spawning activities occur for at least a week	Samoilys and Squire 1994; Brown et al. 1994
3*a*	Gear selectivity for fish of size l_{uk}	$s_{lu} = [1 + \exp(-b'(l_{uk} - l'_{sm}))]^{-1}$ where $b' = 0.52691$, $l'_{sm} = 31.55$	Curve estimated from data collected by the ELF Project using the method of Punt et al. (1996), where b' is an index of the width of the curve and l_{sm} indicates the point where the selectivity = 0.5	E. Fulton, unpublished work
3*a*	Probability of capture of fish u in cell k at time t on day i	$c_{ukti} = q_{uk}a_{ij}s_{lu}$	—	—
3*a*	Probability of mortality due to capture and release (for undersize fish u in cell k)	$m_{uk} = 0.05$	Not all individuals will survive the trauma of capture and release, so there must be an undersize mortality. A 5% hooking mortality was based on observed mortality rates for other serranid species caught using similar gear	Muoneke and Childress 1994; Wilson and Burns 1996

© 1999 NRC Canada

Table 1 (*concluded*).

Step	Parameter	Value	Reasoning	Source(s)
3*b*	Probability of spawner movement (*sm*) at time *t*	$P_i(sm) = 0$ if already at its designated spawning site; $= 1 - \left\lvert \frac{L_i - 10t}{k_i - k_{spawn}} \right\rvert$ otherwise, where L_i is time (minutes) that all fish must be present at aggregation site, k_i is current location at time t, k_{spawn} is location of spawning site ($k_i - k_{spawn}$ is remaining distance to spawning site)	It has been observed that spawning fish reach aggregation sites in the afternoon of each day and that fish move to the aggregation site closest to their home site. Consequently, probabilities and movement rules incorporated these restrictions	Zeller 1998
3*b*	Probability of nonspawner movement (*nmk*) at time *t*	$P(nmkt) = P$(nonspawner is in cell k at time t) $= P$(move to k at t| at $(k-1)$ at $(t-1)) \times P$(at $(k-1)$ at $(t-1)) + P$(stay at k for t| at k at $(t-1)) \times P$(at k at $(t-1)) + P$(move to k at t| at $(k+1)$ at $(t-1)) \times P$(at $(k+1)$ at $(t-1)) = 0.07$	Nonaggregating coral trout are relatively sedentary over short periods of time; thus, they are restricted to their three square home sites. Fish movement over their home site was unpredictable and sporadic, as in nature. Low probability of movement at any one time, as great periods of each day are spent in one (unpredictable) spot	Samoilys 1997

Note: Time t refers to time step t and not a time in minutes and N_T stands for a truncated normal distribution.

Fig. 2. Schematic diagram of the model's framework and flow.

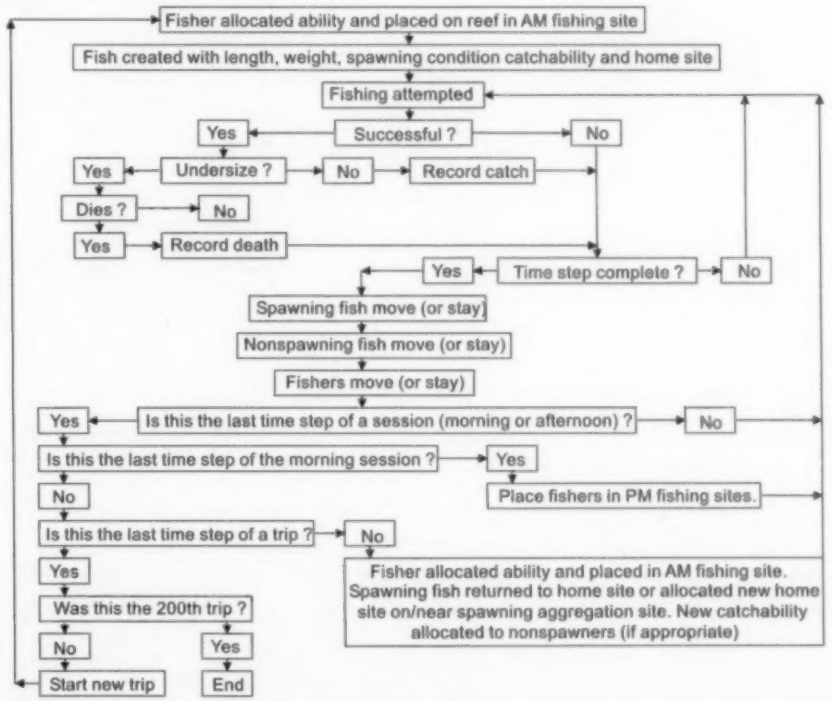
Fisher allocated ability and placed on reef in AM fishing site
Fish created with length, weight, spawning condition catchability and home site
Fishing attempted
Successful ?
Yes
No
Undersize ?
Yes
No
Record catch
Dies ?
Yes
No
Record death
Time step complete ?
Yes
No
Spawning fish move (or stay)
Nonspawning fish move (or stay)
Fishers move (or stay)
Is this the last time step of a session (morning or afternoon) ?
Yes
No
Is this the last time step of the morning session ?
Yes
No
Place fishers in PM fishing sites.
Is this the last time step of a trip ?
No
Yes
Fisher allocated ability and placed in AM fishing site. Spawning fish returned to home site or allocated new home site on/near spawning aggregation site. New catchability allocated to nonspawners (if appropriate)
Was this the 200th trip ?
No
Yes
Start new trip
End

ing population (Schultz and Warner 1991) and because >75% of the fish collected during spawning seasons had ripe gonads (S Adams, CRC Reef Research Centre, c/o James Cook University, Townesville, Queensland, Australia, 4811, personal communication; Effects of Line Fishing (ELF) Project, unpublished data). Thus, a set of scenarios was run where all adult fish spawned, but the percentage forming aggregations was scenario dependent. These will be outlined below. All spawners had to be more than

© 1999 NRC Canada

26 cm in fork length, as this was the minimum size of first spawning observed in the field (Brown et al. 1994).

Each fish was also allocated a catchability (represented by a likelihood of taking a bait). In the scenarios discussed here, nonspawning fish had a constant catchability (which was reallocated on the third day). The effects of spawning on catchability are unknown, and so, three catchability distributions (cases) were used. The first case represented no difference between the spawning and nonspawning fish. The others reflected when spawners were more or less catchable than nonspawners.

Step 3. Fishing, movement, and updating

This step was repeated for 192 time steps, which represented 4 days of fishing with two 4-h sessions (24 time steps) a day.

Step 3a. Fishing: If there was a fish at the same location as a fisher and the gear saturation limit had not been reached, then fishing was attempted. The program calculated the selectivity of the gear for a fish of the size of the one encountered. The probability of capture was determined and compared with a random number, $\sim U(0, 1)$. If the random number was less than the probability of capture, the fish was caught.

The gear used by commercial fishers does allow for the capture of undersize individuals (fish <38 cm total length). These individuals cannot be legally retained and must be released, a rule employed in the simulation. Not all of these discards will survive due to hooking-related trauma, and the resulting number of undersize deaths was recorded in the simulation output. Any fish that were discarded and survived could not be recaptured for the rest of that time step. However, they could be caught on any subsequent time step. Long-term hook avoidance was not included in the model, as little is known about it for coral trout, and what is known suggests that hunger, not learned behaviour such as gear avoidance, drives catchability.

Step 3b. Movement: The movements of fish to spawning aggregation sites followed the form of a directed random walk. If a generated random number was less than the probability of movement, then the fish moved one step along a predetermined path; otherwise, it did not move during that time step. Spawning fish appear to use reef contours as their guide to aggregation sites (L. Squire, P.O. Box 5N, North Cairns, Queensland, Australia, 4870, personal communication), and so the model had aggregating fish following set routes.

A restricted random walk was employed to simulate the movement regime of nonaggregating trout. A random number, $\sim U(0, 1)$, was generated, and depending on its value the fish would remain in place or move to an adjacent cell within the bounds of its home site. No fish, whether spawning or not, could leave the reef.

Like other predators and foragers, fishers do not remain on a fishing site if catch rates are too low. Thus, a simulated fisher moved to the next fishing site if the fisher had caught less than three fish in the last time step. Comparisons made between the time spent on fishing sites by simulated and real fishers (C.R. Davies and B. Mapstone, unpublished data) indicated that the distribution of time spent on fishing sites produced by the model was realistic. Fishers always moved straight to the closest unoccupied fishing site, although they did not revisit a site they had already fished during the current session.

Step 3c. Updating: At the completion of each morning session (time steps 24, 72, 120, and 168), the reef was set up for the afternoon session by randomly placing the fishers onto a fishing site from the afternoon set of fishing locations (Fig. 1). At the end of each day (time steps 48, 96, and 144), the reef was set up for a new fishing day. Fishers were randomly placed into morning sites and allocated a new fishing ability. Fish catchability changes were also completed and adjustments were made to the movement behaviour of some of the spawning fish. Fish that had moved ≤1.5 km to reach the aggregation site were returned to their home sites whereas fish that had moved >1.5 km remained within a 50-m radius of the aggregation site for the rest of the simulation.

Scenarios

To ensure that the model was fairly robust to the accuracy of the assumptions underlying its formulation, mechanics to which the model was relatively sensitive, and particularly unnecessary or speculative dynamics, were not included in the foundations of the model discussed above. Rather, scenarios capturing different sets of dynamics were used to posit contrasts. These contrasts allowed for a comparison of catches taken under a wide range of circumstances, but where only one aspect of the simulation varied at a time. Quite a range of scenarios were employed. However, modifications such as alternate catchability distributions and an increased number of potential aggregation sites in alternate positions (dotted sites in Fig. 1*a*) made little, if any, difference to the results. As a consequence, only a subset of the scenarios will be discussed here. Similarly, synergistic effects of various factors will not be discussed here, as it was apparent that any synergisms that did exist simply gave stronger examples of the dynamics produced when the factors were considered separately.

The set of simulations within a scenario included the three catchability regimes for the spawning fish, mentioned above. They also covered the fishing alternatives of high and low aggregation encounter rates (AER) by fishers. All scenarios were run under spawning and nonspawning conditions. The list of scenarios discussed here and the catchability cases employed are given in Table 2. The actual contrasts performed and the areas of interest covered by the contrasting of these scenarios can be found in Table 3.

Basic scenario (Base)

The basic scenario used only those sites (fishing or aggregation) that have solid outlines in Fig. 1. When run under spawning conditions, only 6–10% of the population spawned. This basic set acted comparatively like a control, and all results from all alternative scenarios were compared with its output.

All adults spawn (ASAA and AS6A)

There were two scenarios in which all adults spawned. In the first of these, all spawners also moved; movements on this scale have not been observed in coral trout, although they have been observed in other species. In the other scenario the case was considered where 6–10% of the sexually mature fish aggregated, even though all fish spawned, a more plausible situation based on field observations. The nonspawning conditions of these scenarios were identical to those of the basic scenario.

Intensive exploitation in the past (PExp)

There was one scenario that used an alternative size distribution of fish (Table 1) to represent reefs that had been previously heavily exploited.

Fishing windward reef face (ACFR and AAFR)

Lastly, there were two scenarios that dealt with the relatively unusual case of fishers fishing the steep weather faces of reefs. This practice usually occurs only under very favourable weather conditions, if at all. The first scenario only had extra fishing sites on the front corners, while the second had them dotted along the entire windward face of the reef.

Analysis

Daily catches from the model were compared with those from compulsory logbook data from the GBR line fishery to check that

© 1999 NRC Canada

Table 2. Scenario – catchability case combinations, run to investigate the fishing process, that are discussed in the text.

	Scenario (code)					
					Fishers could access more of the front of the reef	
Modifications made	Basic (Base)	All adult fish spawned and aggregated (ASAA)	All adult fish spawned, but only 6–10% aggregated (AS6A)	Previous intensive exploitation (PExp)	Access windward corners (ACFR)	Access all windward side (AAFR)
Spawners and nonspawners are identical	Y	Y	Y	Y	Y	Y
Spawners ~ $N_T(0, 0.05)$	Y		Y	Y		Y
Spawners ~ $N_T(1, 0.05)$	Y		Y	Y		Y

Note: All of these combinations were run with high and low aggregation encounter rates. The cells with a Y indicate the combinations run. N_T stands for a truncated normal distribution.

Table 3. By contrasting the scenarios, certain topics could be more thoroughly investigated. Cross reference the two scenarios of interest and consider the cell's contents. In the lower half of the table, a Y indicates that the contrast was performed during the study. In the upper half of the table, the cell's contents briefly describe the areas of interest covered by the contrast.

Sensible contrasts	Areas explored by contrasts					
	Base	ASAA	AS6A	Pexp	ACFR	AAFR
Base		Effect of complete behavioural changes by entire adult population, effect of the degree of spawner movement (number involved), and effect of removal of a guaranteed supply of unaffected (nonspawning) fish	Effect of aggregation spawning (effect of removal of a guaranteed supply of unaffected (nonspawning) fish)	Effect of fishing with respect to all the other factors' effects	Effect of increased access (with limitations)	Effect of increased access (unrestricted)
ASAA	Y	—	Effect of the degree of spawner movement (number involved)	As above	Effects of availability (access to fish and fish presence)	
AS6A	Y	Y	—	As above	Effect of spawning-induced catchability changes versus effect of generally increased access	
PExp	Y	Y	Y	—	Effect of fishing with respect to all the other factors' effects	
ACFR	Y	Y	Y	Y	—	Effect of the degree of increased access
AAFR	Y	Y	Y	Y	Y	

Note: Scenarios: Base, basic (unmodified) scenario; ASAA, all adult fish spawned and all aggregated; AS6A, all adult fish spawned, but only 6–10% aggregated; PExp, previous intensive exploitation; ACFR, fishers could access the corners of the front of the reef; AAFR, fishers could access all of the front of the reef.

the simulations were producing realistic results. Dory-level catch records are not currently reported for the commercial fishery. Thus the total daily catches taken by the four simulated dories were lumped and compared with that of the fishery on the basis of catch per primary vessel.

Differences between the mean catch in the basic scenario and each of the other scenarios were compared to determine which factors most affected catch. Means of the spawning season catches and nonspawning season catches from the same scenario were compared to consider how key factors of each scenario acted within the spawning season.

Results

The codes given for the scenarios in Tables 2–5 are used in the description of the results.

Match to logbook data

None of the simulated catches were outside the range of catches reported in the compulsory fishing logbooks (Mapstone et al. 1996*a*). Most of the catches from the simulations lay between the upper and lower quartiles of the actual com-

© 1999 NRC Canada

Table 4. Percentage increase above the baseline catch (mean nonspawning season catch from the basic scenario) of the mean spawning season catch for each scenario × catchability case × aggregation encounter rate combination run following one reef for 4 days.

	Catchability case					
	S = NS		S > NS		S < NS	
Scenario	HAER	LAER	HAER	LAER	HAER	LAER
Base	6.12	4.18	8.77	6.90	–3.76	–3.34
ASAA	–16.53	–19.14	—	—	—	—
AS6A	3.66	2.88	46.62	44.47	–75.04	–75.07
PExp	–32.32	–35.05	–29.61	–31.73	–38.39	–38.56
ACFR	3.17	0.15	5.67	1.32	–3.44	–4.57
AAFR	7.78	6.29	—	—	—	—

Note: The observed standard errors associated with these percentages range in size from 0.55–1.9. Scenarios: Base, basic (unmodified) scenario; ASAA, all adult fish spawned and all aggregated; AS6A, all adult fish spawned, but only 6–10% aggregated; PExp, previous intensive exploitation; ACFR, fishers could access the corners of the front of the reef; AAFR, fishers could access all of the front of the reef. Catchability cases: S = NS, no difference between the catchability of spawning and nonspawning fish; S > NS, spawning fish more likely to bite; S < NS, spawning fish less likely to bite. Aggregation encounter rates: HAER, high aggregation encounter rate; LAER, low aggregation encounter rate.

mercial catches. A few of the catches taken in scenarios ASAA (when all adults spawned and aggregated) and PExp (when there had been previous intensive exploitation) fell below the lower quartile of the logbook data, while some of the catches from the other scenarios lay above the upper quartile of the logbook data. Overall, the catches taken in the simulation were representative of those landed in the GBR line fishery.

Patterns produced by the simulations

Four main patterns were apparent. Firstly, if spawning fish had a catchability as great as, or greater than, that of nonspawners, then catches were substantially higher during the spawning season. Secondly, a high AER did not substantially increase catch beyond the base spawning season level, although "targeting" influenced catch rates more when catchability was not altered by spawning condition. Thirdly, the change in the level of catch was greatest when more of the population spawned, as a greater proportion of the fish encountered by the fishers was affected by spawning-induced catchability changes. Lastly, as a larger percentage of the population was undersize in the scenarios mimicking previous exploitation, fewer legal size fish were caught under these conditions. Thus, catches (by weight) taken in these scenarios were consistently lower than the catches observed in the other scenarios.

Catch by weight

Table 4 presents, as a percentage, the changes from the baseline catch (mean nonspawning season catch from the basic scenario) of the mean spawning season catch for each scenario × catchability case × AER combination run. In contrast, Table 5 presents, as a percentage, the changes in mean catch observed from the nonspawning to the spawning season simulation runs for each scenario × catchability case × AER combination considered.

If spawning reduced catchability, then catches by weight were no different from those of nonspawning periods regardless of the AER or scenario employed. If spawning fish were more catchable than nonspawners, then fishing during the spawning season increased the catch by weight by 2.0–8.1% in most scenarios and 44.1% in scenario AS6A (when all adult fish spawned, but only 6–10% aggregated). This represented a magnitude of change 2–55 times greater than that produced by a higher AER. In the scenarios where fishers could fish the windward reef face, the overall catch in either season was higher than that taken when only fishing the leeward reef face, suggesting that availability and catch were directly related. Notably, increases in catch during the spawning season were smaller when fishing was allowed along the windward face. This was because the fishers had greater access to the fish at all times and did not have to rely so heavily on migration of spawners to aggregation sites to increase the availability of fish. These results suggested that elevated catches may be the result of increased availability of fish during migrations in the spawning season.

When there was no spawning-induced change in catchability, catch by weight was marginally higher if AER was high. However, the magnitude of the increase was about 2.4 times smaller, on average, than that produced by simply fishing during the spawning season, which caused a 1.6–4.1% increase in catch in every scenario, except the hypothetical scenario where all fish spawned and moved (ASAA), where catch fell by 19.9%.

A fall in catch in ASAA initially seems counterintuitive, as one would expect to see an increase in catch if aggregations were larger and all adult fish became more available as they migrated to the spawning locations. In an attempt to discover why catches had fallen, the dory-level output was considered. Apparently the drop in total catch seen when all the fish spawned and aggregated was due to the inability of the fishers who found aggregations, or migration routes, to compensate for those who found few, if any fish, off spawning sites. This was most clearly illustrated by considering the range in landed catch by the dories under the different spawning strategies. The greatest range in catch taken by the fishers on a single day, when 6–10% of the population spawned and aggregated, was 81 kg, with most of the catches taken on a single day differing by <30 kg. When the entire adult population spawned, but only 6–10% aggregated, the greatest range in catches taken in a single day rose to 89 kg, but most catches were still within 40 kg of one another. The greatest range in catches taken on the same day, when the entire population spawned and aggregated, peaked

© 1999 NRC Canada

Table 5. Percentage increase in mean catch observed from the nonspawning to the spawning season simulation runs for each scenario × catchability case × aggregation encounter rate combination considered following one reef for 4 days.

	Catchability case					
	S = NS		S > NS		S < NS	
Scenario	HAER	LAER	HAER	LAER	HAER	LAER
Base	5.98	4.05	8.75	6.89	–3.89	–3.46
ASAA	–17.29	–19.88	—	—	—	—
AS6A	4.14	3.36	46.25	44.10	–74.62	–74.65
PExp	5.93	1.66	11.43	8.07	–3.33	–3.59
ACFR	5.83	2.74	4.51	1.95	–3.72	–4.84
AAFR	3.19	1.77	—	—	—	—

Note: The observed standard errors associated with these percentages range in size from 0.53–1.53. Scenarios: Base, basic (unmodified) scenario; ASAA, all adult fish spawned and all aggregated; AS6A, all adult fish spawned, but only 6–10% aggregated; PExp, previous intensive exploitation; ACFR, fishers could access the corners of the front of the reef; AAFR, fishers could access all of the front of the reef. Catchability cases: S = NS, no difference between the catchability of spawning and nonspawning fish; S > NS, spawning fish more likely to bite; S < NS, spawning fish less likely to bite. Aggregation encounter rates: HAER, high aggregation encounter rate; LAER, low aggregation encounter rate.

at 191 kg, with most catches from the same day differing by >75 kg.

Comparison of the mean catch by primary vessel indicated that the catch (kilograms) taken in scenario PExp (where reefs had been previously exploited) was consistently ~34% lower than that of any other scenario, except AS6A. The spawning season catch taken in scenario AS6A was strongly affected by the catchability of the spawners: if spawners had a higher catchability, catch rose by ~45% whereas it dropped by 75% if they were less likely than nonspawners to bite.

Thus, inspection of the means indicated three things. Firstly, AER did not substantially alter the levels or patterns of catch produced by the other two factors. Secondly, catch was consistently higher in the spawning season, provided the fish were biting. Lastly, previous exploitation and the percentage of the population affected by spawning-induced behavioural changes can have substantial impacts on catch.

Number of fish captured

Inspection of the mean number of fished landed indicated that the numbers taken were usually 3–6% higher in the spawning season, although the mean dropped by 17% during the spawning season in scenario ASAA (when all fish spawned and aggregated). This drop was caused by the same set of circumstances that reduced total catch by weight taken in ASAA during the spawning season. Fewer fish were captured in scenario PExp (where reefs had been previously exploited), regardless of spawning state. The number of fish taken in PExp was 6.6–42% lower than the numbers captured in any of the other scenarios. Thus, catch by weight was lower in scenario PExp beacause fewer fish were landed, and not only because the average size of fish had been decreased by previous exploitation.

Number of undersize deaths

The mean number of undersize fish killed as a result of fishing increased by about 3–10% in the spawning season for all scenarios except ASAA, where it increased by 18.6%. The number of deaths of undersize fish was consistently 19–25% higher in scenario PExp than in any other scenario, regardless of season. Thus, the number of undersize deaths observed was proportional not only to the total catch but also to the percentage of the entire population made up of undersize fish (which was greater in previously exploited populations).

Discussion

The simulation model identified two crucial points: (*i*) that the existence of spawning season behavioural changes and the size of the adult population affected by them had a substantial impact on total catch by commercial fishers and (*ii*) that the targeting of spawning aggregations by fishers had a smaller impact on observed catch than did the general increase in availability of fish, produced by increased movements, during spawning.

The sensitivity of the catch rates to changes in catchability and the proportion of the population spawning clearly signifies the importance of these factors. However, little is known about these facets of the biology of coral trout or many of the other target species of the world's fisheries. Detailed investigations of the patterns and shifts in catchability of spawning fish are required to field test the conclusions drawn about spawning season catches and catchability cases employed by the simulations.

It may seem obvious that catches will be greater when catchability is greater. However, for fish that move to aggregation sites to spawn, it is not clear whether changes in catchability alone ultimately determine changes in spawning season catch rates. Even when catchability is unchanged or increased during spawning, catches could fall if the aggregation sites, or migration routes, cannot be found consistently, or if catches made at these locations do not compensate for the loss of fish at fishing sites that do not coincide with aggregation sites or migration routes. This is exactly what was observed in the pattern of catches produced by the hypothetical scenario ASAA (where all fish spawned and moved).

Targeting spawning aggregations, such as those formed by coral trout, by commercial fishers has been identified as an area of concern by scientists (Brown et al. 1994), management bodies (QFMA 1996), and fishers alike (Mapstone et

© 1999 NRC Canada

al. 1996*a*). Consideration of the fate of other fisheries, both trawl and line fisheries, in which spawning aggregations have been targeted justifies this concern, as those fisheries are typified by stock declines and fishery collapses (Hilborn and Walters 1992; Aguilar-Perera and Aguilar-Dàvila 1996). The results of this study, however, suggest that targeting spawning aggregations may play a secondary role in the elevation of commercial catches, especially for targets of hook and line fisheries, such as coral trout. Increased catches during the spawning season were not principally dependent on the targeting of aggregation sites. Clearly, a fundamental mechanism existed that produced this clear signal despite the interference introduced by scenario modifications.

The interaction of the movement patterns of the fishers and the aggregating fish leads to increased catches. Fishers could fish as normal and still record higher catches if several of the sites they regularly identified as suitable fishing sites happened to coincide with the routes fish followed to aggregations sites, even if aggregation sites did not overlap with fishing sites. Ultimately, catch rates rose because fish, which had home sites in areas that fishers did not usually access, became available to fishers as they migrated to the spawning sites. Hence, increased availability of fish during the spawning season was likely to be the main dynamic increasing catches.

Increased catches resulting from increased availability are not an unusual phenomenon in fisheries or ecology in general. The salmon fisheries of the North Pacific are built upon the increased availability of salmon during the spawning run (Hilborn and Ledbetter 1979), just as the lion *Panthera leo* relies on the increased availability of migratory zebra (*Equus burchelli*) to increase its catch at certain times of the year (Mills and Shenk 1992). Furthermore, the results from the simulations run in this project suggest that natural refuges and availability may play critical roles in even the most simple spatially distributed predator–prey relationships.

As yet, there is no record of commercial fishers in the GBR line fishery consciously taking advantage of increased densities of fish moving along migration routes. However, the practice was the mainstay of the Australian trawl fisheries for *Rexea solandri* (Blackburn 1979) and *Panulirus ornatus* (Skewes et al. 1994), both of which are now closed. Globally, fishing spawning migrations is a lucrative business, as it supports the temperate salmonoid fisheries and is also beginning to become widespread in the tropics. For example, fishers in Mexico have started targeting migration routes of the Nassau grouper (*Epinephelus striatus*) now that the actual aggregation sites are closed to fishing (Aguilar-Perera and Aguilar-Dàvila 1996). Because fishers may maintain pressure on a stock by changing from targeting spawning aggregations to targeting migration routes, small-scale spatial closures are unlikely to be sufficient protection for species such as coral trout that migrate to specific aggregation sites to spawn. Extensive temporal closures or large spatial closures would be more appropriate management actions for such species.

One ancillary benefit in using simulation modelling is that it considers the mechanics of the system free of the expense or confounding factors that make field studies difficult. As a consequence, modelling can indicate the existence of effects that may otherwise be neglected. Undersize mortality is a topic that is largely ignored in models and management (Myers et al. 1997). The fact that in the simulations discussed here the number of undersized deaths caused by fishing was equivalent to the catch of another active (but unreported) dory suggests that ignoring undersize mortality may be a perilous act. With a modest hooking mortality of 5% (which is probably an underestimate), fishing mortality rose by up to 25%, although this rise may have been smaller if long-term hook avoidance by discarded fish had been included. Perhaps the most worrying facet of the undersize deaths was that they increased if there had been intensive exploitation previously. It is not uncommon for large proportions of fished stocks to be undersize (Myers et al. 1997), and as a result, undersize mortality will be greater than in a less harvested stock. Thus, fishing has a twofold impact on the ability of a population to withstand exploitation: it not only removes the large spawners, but it also substantially increases the mortality of those juveniles and smaller adults who may have replaced the larger individuals. Unfortunately, this second impact has long gone unaccounted for and is only recently being suggested as a possible cause of some of this century's most spectacular fishery collapses (Myers et al. 1997).

Fishing will reduce the reproductive potential of any fished stock by removing spawner biomass and reducing average fish size (Coleman et al. 1996), and fishing spawning aggregations would increase the pace of this process. Denying fishers access to aggregations would appear to be the logical solution. Without knowledge of the true nature of the determinants of catch rates, the blind application of such solutions may prove ineffective. However, field research to address some of the key issues in devising sound management strategies to protect spawning fishes is likely to be expensive and take a long time, leaving the spawning stocks vulnerable for prolonged periods. We have illustrated the utility of computer simulations based on limited field data to examine scenarios for the harvest of spawning fishes. The simulations allowed us to identify key properties of the short-term interactions between spawning fishes and harvesters and point to the areas in which the simulations were most in need of field data. Other, equally important, areas would no doubt be identified by simulations structured to consider longer term dynamics that would be impacted upon by demographic changes and density-dependent changes in resources.

Our work suggests that spawning season closures will only help to alleviate fishing pressure on a stock if the following conditions are satisfied: (*i*) the behaviour of spawning fish does not make them less vulnerable to fishing, something we often know little about, and (*ii*) the spatial and temporal scale of any closures must incorporate spawning migrations and not just spawning itself, as both events represent points at which stock accessibility may be increased.

Acknowledgments

The work discussed in this paper was completed as part of an honours degree at James Cook University of North Queensland. Funding was provided by the Cooperative Research Centre for the Ecologically Sustainable Development of the Great Barrier Reef and the Departments of Marine Biology

© 1999 NRC Canada

and Mathematics and Statistics of James Cook University. We would like to thank all those researchers who shared their unpublished data and personal observations.

References

Abrahams, M.V., and Healey, M.C. 1990. Variation in the competitive abilities of fishermen and its influence on the spatial distribution of the British Columbia salmon troll fleet. Can. J. Fish. Aquat. Sci. **47**: 1116–1121.

Aguilar-Perera, A., and Aguilar-Dàvila, W. 1996. A spawning aggregation of Nassau grouper *Epinephelus striatus* (Pisces: Serranidae) in the Mexican Caribbean. Environ. Biol. Fishes, **45**: 351–361.

Allen, P.M., and McGlade, J.M. 1986. Dynamics of discovery and exploitation: the case of the Scotian Shelf groundfish fisheries. Can. J. Fish. Aquat. Sci. **43**: 1187–1200.

Attwood, C.G., Harris J., and Williams, A. 1997. International experience of marine protected areas with relevance for South Africa. *In* Towards a new policy on marine protected areas for South Africa. *Edited by* Marine Reserves Task Group. S. Afr. Network Coastal Oceanic Res. Occas. Rep. No. 2.

Beinssen, K. 1989. Results of the Boult Reef replenishment area study. Report to the Department of Conservation, Parks and Wildlife, Australia. (Available from the Department of Environment, P.O. Box 155, Brisbane Albert Street, Queensland, Australia, 4002.)

Blackburn, M. 1979. The gemfish, *Rexea solandri* (Cuvier and Valenciennes): distribution and length. Report to the Division of Fisheries and Oceanography, CSIRO Cronulla No. 103. (Available from Library, G.P.O. Box 1538, Hobart, Tasmania, Australia, 7001.)

Brown, I.W., Doherty, P., Ferreira, B., Keenan, C., McPherson, G., Russ, G., Samoilys, M., and Sumpton, W. 1994. Growth, reproduction and recruitment of Great Barrier Reef food fish stocks. Report to FR and DC, project No. 90/18. (Available from Fisheries Research and Development Corporation, P.O. Box 222, Deakin West, ACT, Australia, 2600.)

Coleman, F.C., Koenig, C.C., and Collins, L.A. 1996. Reproductive styles of shallow-water groupers (Pisces: Serranidae) in the eastern Gulf of Mexico and the consequences of fishing spawning aggregations. Environ. Biol. Fishes, **47**: 129–141.

Davies, C.R. 1996. Inter-reef movement of the common coral trout, *Plectropomus leopardus*. Report to the Great Barrier Reef Marine Park Authority. (Available from Great Barrier Reef Marine Park Authority, P.O. Box 1379, Townsville, Queensland, Australia, 4810.)

Ferreira, B.P., and Russ, G.R. 1994. Age validation and estimation of growth rate of the coral trout, *Plectropomus leopardus* (Lacepede 1802), from Lizard Island, Northern Great Barrier Reef. Fish. Bull. U.S. **92**: 46–57.

GBRMPA Act. 1975. Government Printers, Canberra. (Available from Great Barrier Reef Marine Park Authority, P.O. Box 1379, Townsville, Queensland, Australia, 4810.)

Hilborn, R. 1985. Fleet dynamics and individual variation: why some people catch more fish than others. Can. J. Fish. Aquat. Sci. **42**: 2–13.

Hilborn, R., and Ledbetter, M. 1979. Analysis of the British Columbia salmon purse-seine fleet: dynamics and movement. J. Fish. Res. Board Can. **36**: 384–391.

Hilborn, R., and Ledbetter, M. 1985. Determinants of the catching power in the British Columbia purse seine fleet. Can. J. Fish. Aquat. Sci. **42**: 51–56.

Hilborn, R., and Walters, C.J. 1992. The dynamics of fishing fleets. Quantitative fisheries stock assessment: choice, dynamics and uncertainty. Chapman and Hall, New York.

Mapstone, B.D., McKinlay, J.P., and Davies, C.R. 1996*a*. A description of the commercial reef line fishery logbook data held by the Queensland Fisheries Management Authority. Report to the Queensland Fisheries Management Authority, Brisbane, Australia. (Available from Queensland Fisheries Management Authority, P.O. Box 344, Fortitude Valley, Queensland, Australia, 4006.)

Mapstone, B.D., Campbell, R.A., and Smith, A.D.M. 1996*b*. Design of experimental investigations of the effects of line and spear fishing on the Great Barrier Reef. CRC Reef Res. Cent. Tech. Rep. No. 7, CRC Reef Research Centre, Townsville, Queensland, Australia. (Available from CRC Reef Research Centre, c/o James Cook University, Townsville, Queensland, Australia, 4811.)

Mills, M.G.L., and Shenk, T.M. 1992. Predator–prey relationships: the impact of lion predation on wildebeest and zebra populations. J. Anim. Ecol. **61**: 693–702.

Muoneke, M.I., and Childress, W.M. 1994. Hooking mortality: a review for recreational fisheries. Rev. Fish. Sci. **2**: 123–156.

Myers, R.A., Hutchings, J.A., and Barrowman, N.J. 1997. Why do fish stocks collapse? The example of cod in Atlantic Canada. Ecol. Appl. **7**: 91–106.

Punt, A.E., Pulfrich, A., Butterworth, D.S., and Penney, A.J. 1996. The effect of hook size on the size-specific selectivity of hottentot *Pachymetopon blochii* (Val.) and on yield per recruit computation. S. Afr. J. Mar. Sci. **17**: 155–172.

QFMA. 1996. Queensland Fisheries Management Authority Discussion Pap. No. 2. Queensland tropical coral reef fish species. Reef Fish Management Advisory Committee, Brisbane, Australia. (Available from Queensland Fisheries Management Authority, P.O. Box 344, Fortitude Valley, Queensland, Australia, 4006.)

Rjinsdorp, A.D., and Pastoors, M.A. 1995. Modelling the spatial dynamics and fisheries of North Sea plaice (*Pleuronectes platessa* L.) based on tagging data. ICES J. Mar. Sci. **52**: 963–980.

Samoilys, M.A. 1997. Movement in a large predatory fish: coral trout, *Plectropomus leopardus* (Pisces: Serranidae), on Heron Reef, Australia. Coral Reefs, **16**: 151–158.

Samoilys, M.A., and Squire, L.C. 1994. Preliminary observations on the spawning behaviour of coral trout, *Plectropomus leopardus* (Pisces: Serranidae), on the Great Barrier Reef. Bull. Mar. Sci. **54**: 332–342.

Schultz, E.T., and Warner, R.R. 1991. Phenotypic plasticity in life-history traits of female *Thalassoma bifasciatum* (Pisces: Labridae): 2. Correlation of fecundity and growth rate in comparative studies. Environ. Biol. Fishes, **30**: 333–344.

Skewes, T.D., Pitcher, C.R., and Trendall, J.T. 1994. Changes in the size structure, sex ratio and molting of a population of ornate rock lobsters, *Panulirus ornatus*, caused by an annual maturation molt and migration. Bull. Mar. Sci. **54**: 38–48.

St. John, J. 1995. Feeding ecology of the coral trout, *Plectropomus leopardus* (Serranidae), on the Great Barrier Reef, Australia. Ph.D. thesis, Department of Marine Biology, James Cook University, Townsville, Queensland, Australia. (Available from Library, James Cook University, Townsville, Queensland, Australia, 4811.)

Thorlindsson, T. 1994. Skipper science: a note on the epistemology of practice and the nature of expertise. Sociol. Q. **35**: 329–345.

Wilson, R.R., and Burns, K.M. 1996. Potential survival of released groupers caught deeper than 40 m based on shipboard and in

© 1999 NRC Canada

situ observations, and tag–recapture data. Bull. Mar. Sci. **58**: 234–247.

Zeller, D.C. 1998. Spawning aggregations: patterns of movement of the coral trout *Plectropomus leopardus* (Serranidae) as determined by ultrasonic telemetry. Mar. Ecol. Prog. Ser. **162**: 253–263.

© 1999 NRC Canada

Limnological succession in reservoirs: a paleolimnological comparison of two methods of reservoir formation

Roland I. Hall, Peter R. Leavitt, Aruna S. Dixit, Roberto Quinlan, and John P. Smol

Abstract: Analysis of diatoms, algal pigments, and chironomids in sediment cores from two otherwise similar prairie reservoirs demonstrated that differences in reservoir formation (river valley impoundment versus lake inundation) and hydrological regime (variable versus stable water level) resulted in distinct patterns of aquatic community change. Lake Diefenbaker, a 500-km^2 reservoir created by damming the South Saskatchewan River in 1968, experiences water level fluctuations of 6 m·year^{-1}. In contrast, impoundment of Buffalo Pound Lake in 1952 flooded a natural lake, raised mean water levels ~2.0 m, and reduced water level fluctuations from ~3 to <1 m·year^{-1}. Comparison of fossil records showed that reservoir formation did not inevitably lead to eutrophication. Lake Diefenbaker exhibited typical reservoir ontogeny with three trophic periods, including an initial ~4-year period of eutrophy, a decade of mesotrophy, and a gradual shift to modern productive conditions. Planktonic taxa dominated diatom communities at all times, whereas benthic chironomid and algal remains were rare. In contrast, pigment analyses suggested that phytoplankton standing crops declined after impoundment in Buffalo Pound Lake but that chironomid and macrophyte populations expanded. Such site specificity in trophic development appears to result from differences in the extent of inundation (500 versus ~5 km^2) and the magnitude of subsequent water level fluctuations (6.3 versus <1 m).

Résumé : L'analyse des diatomées, des pigments algaux et des chironomides dans des carottes de sédiments de deux réservoirs de prairie semblables par ailleurs montre que les différences dans la formation des réservoirs (endiguement de rivière dans une vallée ou inondation d'un lac) et le régime hydrologique (niveau de l'eau variable ou stable) ont donné des profils distincts de changement dans les communautés aquatiques. Au lac Diefenbaker, un réservoir de 500 km^2 créé par l'endiguement de la rivière Saskatchewan Sud en 1968, on observe des fluctuations du niveau de l'eau de 6 m·an^{-1}. Par contre, l'endiguement du lac Buffalo Pound en 1952 a agrandi ce lac naturel et élevé le niveau moyen de l'eau d'environ 2,0 m tout en réduisant les fluctuations du niveau d'environ 3 m·an^{-1} à moins de 1 m·an^{-1}. La comparaison des registres fossiles a montré que la formation d'un réservoir ne conduit pas nécessairement à une eutrophisation. On a observé au lac Diefenbaker une ontogénie typique de réservoir avec trois périodes trophiques, soit une période initiale d'eutrophie de 4 ans environ, une décennie de mésotrophie et un passage graduel aux conditions actuelles de productivité. Les taxons planctoniques ont dominé les communautés de diatomées en tout temps, tandis que les chironomides benthiques et les restes d'algues étaient rares. Par ailleurs, les analyses des pigments permettent de penser que les populations de phytoplancton ont décliné après l'endiguement du lac Buffalo Pound, mais que les populations de chironomides et de macrophytes se sont accrues. Les différences dans le développement trophique de ces deux réservoirs semble résulter des différences dans l'étendue de l'inondation (500 km^2 contre environ 5 km^2) et dans l'amplitude des fluctuations subséquentes du niveau de l'eau (6,3 m contre moins de 1 m).

[Traduit par la Rédaction]

Introduction

According to a widely accepted paradigm, reservoirs often pass through a series of changes in aquatic productivity and community composition following impoundment (Rodhe 1964; Ostrofsky and Duthie 1978; Thornton et al. 1990). Initially, production of phytoplankton (Chamberlain 1972), crustaceans (Rodhe 1964), benthic invertebrates (Nursall 1952), and fish (Baxter 1977) may increase for between 5 and 20 years, depending on the biomass of flooded terrestrial material, the magnitude of water level changes, as well as other factors (Kimmel et al. 1990). This period of trophic

Received February 11, 1998. Accepted December 18, 1998.
J14443

R.I. Hall[1] and P.R. Leavitt. Limnology Laboratory, Biology Department, University of Regina, Regina, SK S4S 0A2, Canada. **A.S. Dixit, R. Quinlan, and J.P. Smol.** Paleoecological Environmental Assessment and Research Laboratory (PEARL), Department of Biology, Queen's University, Kingston, ON K7L 3N6, Canada.

[1]Author for all correspondence at the following address: Climate Impacts Research Centre (CIRC) and Department of Environmental Health, Umeå University, Abisko Scientific Research Station, Box 62, S-981 07 Abisko, Sweden. After Sept. 1, 1999, Department of Biology, University of Waterloo, Waterloo, ON N2L 3G1, Canada.

© 1999 NRC Canada

upsurge is often followed by a variable period (3–30 years) of reduced production of benthic invertebrates and fish (Lindström 1973), although less is known of patterns of algal production (Donar et al. 1996) and trends in nutrient fluxes and periphytic community change (Thornton et al. 1990). In some reservoirs, fish production may gradually increase during a third interval (e.g., Lindström 1973), but the long-term impacts of inundation on reservoir biogeochemistry and biotic composition of other trophic levels remain poorly understood.

In the absence of changes in external loads, temporal patterns of reservoir production result from changes in nutrient biogeochemistry associated with flooding. For example, initial increases in plankton growth arise due to leaching of soluble nutrients from flooded soil, erosion of newly formed shorelines, and decomposition of inundated vegetation (Ostrofsky and Duthie 1978; Kennedy and Walker 1990). Oxygen consumption during vegetation decomposition can induce deepwater anoxia, further increasing nutrient flux from sediments (Kennedy and Nix 1987). Zoobenthos often increases due to rapid immigration to newly submerged vegetation, high fecundity, and tolerance to low oxygen tensions (Baxter 1977). Increased fish production has been linked to abundant invertebrate and zooplankton food supplies as well as to cover for young fish provided by submerged vegetation (Thornton et al. 1990). However, continued erosion of shorelines rapidly buries submerged organic substrates (Nursall 1952), reduces oxygen demand and nutrient release (Kennedy and Nix 1987), reduces benthic communities (Popp and Hoagland 1995) in favour of planktonic assemblages, and lowers fish production (Baxter 1977; Thornton et al. 1990).

This paradigm of reservoir ontogeny was developed mainly from observations of valley reservoirs that convert riverine environments into lakes (Baxter 1977), but it does not always describe accurately the responses of reservoirs that are formed by flooding a preexisting lake (Hecky et al. 1984; Campbell et al. 1998). In fact, typical responses of biota can be muted or even reversed in flooded lakes, especially when impoundment causes only a small increase in lake level or when operations maintain relatively stable water levels (Hecky et al. 1984). For example, production did not increase in several biotic communities following impoundment of Southern Indian Lake that raised mean water levels by 3 m, increased lake area by 21%, and maintained annual water level fluctuations at <1 m (Hecky et al. 1984). Instead, phytoplankton production was suppressed by light limitation from suspended sediments (Hecky and Guildford 1984), zooplankton abundance declined due mainly to lower water temperatures and phytoplankton abundance (Patalas and Salki 1984), and macrobenthos biomass increased only slightly in response to the low-level flooding (Wiens and Rosenberg 1984). Such divergent responses suggest there are fundamental differences in the processes that regulate development of biotic communities in reservoirs formed by raising water levels in an extant lake versus de novo flooding of a river valley.

Differences in area of flooded land, shoreline development (the ratio of surface area to shoreline length), and magnitude of water level fluctuations may be important determinants of divergent patterns that occur during development of lake and valley reservoirs. Shoreline development and the area of flooded land are usually much greater in new reservoirs than in impounded lakes, leading to elevated nutrient releases from shoreline erosion, vegetation decomposition, and leaching of solutes that fuel the initial trophic upsurge (Baxter 1977; Thornton et al. 1990). Additionally, because river valleys are generally steeper than lake catchments, valley reservoirs can be operated over a greater range of water levels, as required for their role as hydroelectric and flood control utilities. The magnitude of water level fluctuations not only affects the supply of nutrients and organic and inorganic materials via erosion of shorelines (Baxter 1977) but also regulates pelagic communities (Naselli-Flores and Barone 1997) and determines the presence or absence of littoral communities (Rodhe 1964). Critical assessment of the role of these factors on valley versus lake reservoirs has been hampered by a lack of long-term data encompassing the full sequence of development in most reservoirs (Popp and Hoagland 1995). Additionally, site-specific factors such local soil characteristics, permafrost, terrestrial vegetation, and reservoir stratification have complicated direct comparisons of ontogeny among regions (Hecky et al. 1984).

In this study, we used a multiple-indicator paleolimnological approach to investigate changes in algal and invertebrate communities following formation and operation of two different prairie reservoirs. Lake Diefenbaker was created by flooding a river valley, whereas Buffalo Pound Lake was formed by impounding the outflow of a shallow lake. These reservoirs are located within 50 km of each other and have similar climate, vegetation, land use, geology, soils, and topography. Present limnological conditions in Lake Diefenbaker and Buffalo Pound Lake are typical of those seen in other prairie impoundments in western Canada (reviewed in Mitchell and Prepas 1990). In the absence of long-term historical water quality and limnological data, we used paleolimnology to quantify past changes in algal and benthic invertebrate communities. Previous studies have shown that organismal remains are often well preserved in reservoir sediments and that analysis of fossils provides detailed information on both pelagic and littoral habitats (Prat and Daroca 1983; Donar et al. 1996). Because soils, climate, topography, vegetation, land use, and potential colonists differed little among sites (Graham 1997; Hall et al. 1999), comparison of Diefenbaker and Buffalo Pound reservoirs allowed tests of the hypothesis that differences in the temporal sequence of production and species replacement should reflect mainly physical factors associated with variable flooding and hydrologic regimes (i.e., area inundated, water level change).

Materials and methods

Study sites

Lake Diefenbaker and Buffalo Pound Lake are reservoirs located at the headwaters of the Qu'Appelle River drainage system in southern Saskatchewan (Fig. 1). While there are no major point sources of nutrients to the reservoirs, over 95% of the ~50 000-km^2 drainage area is composed of agricultural fields (wheat, barley, canola) and pastures (cattle, swine). Regional climate is subhumid continental with annual moisture deficits of ~40 cm, short warm

© 1999 NRC Canada

Fig. 1. Drainage basin of the Qu'Appelle Valley, indicating lakes and reservoirs (black areas) and urban centres (squares). Modified from Hall et al. (1999).

Table 1. Physical characteristics of Lake Diefenbaker and Buffalo Pound Lake and mean values of selected water column chemical and biological characteristics during June–August 1994.

Variable	Units	Lake Diefenbaker	Buffalo Pound Lake
Latitude	N	51°07′	50°39′
Longitude	W	106°38′	105°30′
Elevation	m a.s.l.	552	509.3
Surface area	km^2	500	29.1
Mean depth	m	33	3
Maximum depth	m	62	5.5
Relative depth	%	0.24	0.09
Total capacity	$m^3 \times 10^6$	9400	87.5
Conductivity	$\mu S \cdot cm^{-1} \pm 1$ SD	380±16	482±24
pH	±1 SD	7.8±0.7	8.4±0.6
Dissolved C	$mg \cdot L^{-1} \pm 1$ SD	6.3±5.8	13.4±3.6
Dissolved N	$\mu g \cdot L^{-1} \pm 1$ SD	205±86	499±24
Dissolved P	$\mu g \cdot L^{-1} \pm 1$ SD	93±71	185±124
Total N : total P	±1 SD	3.1±2.6	3.4±2.2
Chlorophyll *a*	$\mu g \cdot L^{-1} \pm 1$ SD	4.9±3.9	6.3±3.2
% N_2-fixing cyanobacteria	Mean (range)	17.2 (7–32)	17.4 (4–26)
% cyanobacteria	Mean (range)	17.2 (7–32)	33.1 (13–46)

Note: N_2-fixing cyanobacteria and total cyanobacteria expressed as percentage of total algal biovolume. Modified from Hall et al. (1999).

summers (105 frost-free days; July mean temperature 19°C), and cold winters (January mean temperature –16°C). Reservoirs are ice-covered from November to late-April. Hydrology is highly variable and spring runoff dominates annual discharge (Allan and Kenney 1978). Both reservoirs have low relative depth (i.e., ratio of maximum depth as a percentage of the mean lake diameter at the surface <0.3%) and do not stratify thermally (Table 1).

Lake Diefenbaker was formed in November 1967 with completion of the Gardiner and Qu'Appelle dams on the South Saskatchewan River valley, Saskatchewan (Environment Canada 1988). Reservoir formation inundated ~500 km^2 of unimproved, mainly treeless prairie grassland. Full storage capacity, 9.4×10^9 m^3, was first reached in 1968 (Fig. 2*a*). Annual water level changes average 6.3 m (1968–1994; range = 2–10 m), with high levels in autumn and low levels in late winter. Resulting shoreline erosion has created a littoral zone composed primarily of sand and rock with little organic sediment and few macrophytes.

Buffalo Pound Lake is the main source of water for the cities of Regina and Moose Jaw and was converted to a reservoir by damming the lake's outlet in 1952. Impoundment raised maximum wa-

© 1999 NRC Canada

Fig. 2. Minimum, maximum, and mean (hatches) bank-full water levels in (*a*) Lake Diefenbaker (A. Banga, Saskatchewan Water Corp., Moose Jaw, Sask., unpublished data) and (*b*) Buffalo Pound Lake. Water levels in Buffalo Pound Lake were directly measured (1941 to present; vertical solid lines) by Saskatchewan Water Corp., computed from hydrometric data and depth–capacity relationships (1911–1941; broken lines) (Durrant 1958), or estimated from correlations between precipitation and lake level (1904–1911; broken lines) (Durrant 1958). (*c*) Annual volume of water discharged from South Saskatchewan River and Lake Diefenbaker to Buffalo Pound Lake (1958–1995; solid line) and withdrawn from Buffalo Pound Lake at the water treatment plant (1955–1995; broken line).

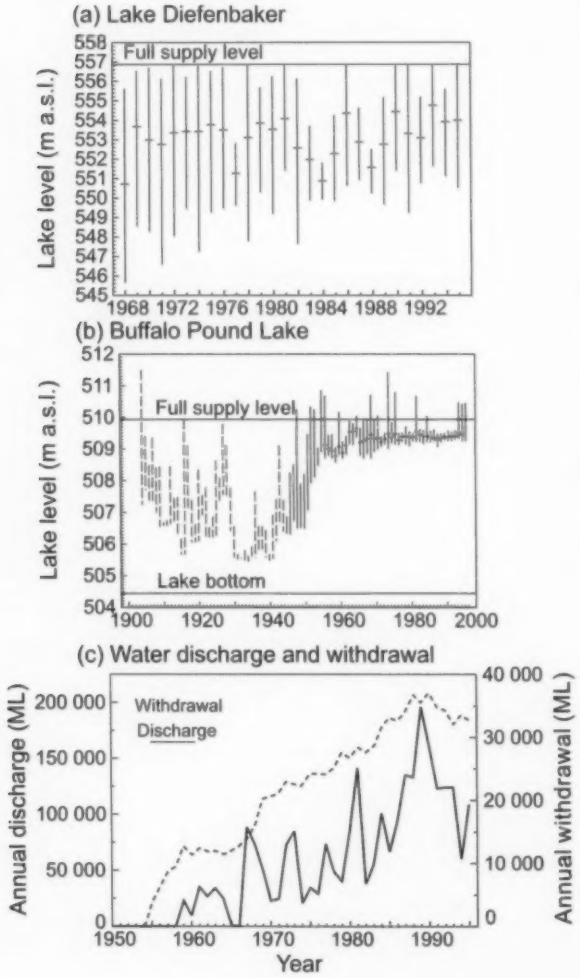

ter levels by ~2.0 m and flooded the western valley, creating a shallow, weeded area of 5 km^2. Reservoir formation raised seasonal minimum and maximum water levels but reduced annual water level fluctuations to <1 m in most years (Fig. 2*b*).

Before 1958, Buffalo Pound Lake drained only the headwater reach of the Qu'Appelle Valley and did not receive water from the South Saskatchewan drainage system. Since 1958, water has been diverted into Buffalo Pound Lake directly from the South Saskatchewan River (1958–1963) and via Lake Diefenbaker (since 1968) in order to maintain water quality and storage capacity (Figs. 1 and 2*c*). Discharge from the South Saskatchewan River to Buffalo Pound Lake was low prior to 1958–1968 because water was pumped mechanically over the natural drainage divide. Construction of a canal in 1960 bypassed the shallow wetland (Eyebrow Lake; Fig. 1), minimized evaporative losses, and increased flow volumes by ~60% (Wiens 1987). Discharge volumes further increased after Lake Diefenbaker was formed, leading to stable water levels and improved water quality in Buffalo Pound Lake (Figs. 2*b* and 2*c*; Table 2). Salinity declined from 644 mg total dissolved solids·L^{-1} (1959–1968) to 433 mg total dissolved solids·L^{-1} (1988–1994), with a shift in ionic composition from predominantly Na^+ and SO_4^{2-} to Ca^+ and HCO_3^-. Nutrient concentrations also declined and cyanobacterial blooms were reduced after 3–4 years (Hammer 1973). These changes were also accompanied by obvious but unquantified increases in macrophyte populations (Hammer 1973).

Algal community composition is similar between the two reservoirs and biomass is distributed evenly among green algae (*Chlorella vulgaris*, *Cosmarium* spp., *Scenedesmus* spp., *Pediastrum boryanum*, *Staurastrum* spp.), diatoms (*Fragilaria crotonensis*, *Tabellaria flocculosa*, *Aulacoseira ambigua*), chrysophytes (*Dinobryon sociale*), dinoflagellates (*Ceratium hirundinella*), cryptophytes (*Cryptomonas erosa*, *Rhodomonas minuta*) and cyanobacteria (*Anabaena* spp., *Microcystis*, *Oscillatoria*, *Aphanizomenon*) (Graham 1997). Cyanobacteria often contribute a greater proportion of biomass in Buffalo Pound Lake than in Lake Diefenbaker, particularly during late summer (Table 1). Crustacean zooplankton are similar between reservoirs and include cladocerans *Daphnia galeata mendotae*, *Daphnia retrocurva*, and *Diaphanosoma birgei*. The copepod *Diacyclops thomasi* is one of the most abundant zooplankton in Lake Diefenbaker (30–70 individuals·L^{-1}), whereas the predaceous cladoceran *Leptodora kindtii* can reach high densities in Buffalo Pound Lake (>2 individuals·L^{-1}). Fish communities of both lakes include planktivorous cisco (*Coregonus artedi*), yellow perch (*Perca flavescens*), and white sucker (*Catostomus commersoni*) as well as predaceous northern pike (*Esox lucius*) and walleye (*Stizostedion vitreum*).

Field and laboratory methods

In March 1995, a 18.5-cm-long sediment core was retrieved from 28 m depth in Lake Diefenbaker north of the Qu'Appelle dam (51°05.5′N, 106°36.5′W) using standard freeze-coring procedures (Leavitt and Findlay 1994). The frozen core was quartered lengthwise, cleaned by removing the outermost 5 mm using a wood-plane, and slowly thawed and dewatered in the dark before sectioning. A 31-cm-long core was retrieved from the deepwater region (4.6 m) of Buffalo Pound Lake (50°41.7′N, 105°34.3′W) in July 1996 using a Glew gravity corer (Hall and Smol 1992). The core was sectioned at the lakeside. In both cases, the upper sediments (0–15 cm depth) were sectioned into 5-mm intervals, while deeper samples were sectioned every 1 cm. All samples were flushed with N_2 gas and frozen (–20°C) in the dark until analysis of sedimentary remains.

Freeze-dried sediments (48 h, 0.01 Pa) from Buffalo Pound Lake were analyzed for ^{210}Pb content by Chalk River Laboratories, Atomic Energy of Canada Limited, using alpha spectrometry. Sediment age (years BP) was calculated using the constant rate of supply model and the computer program of Binford (1990). The chronology of the Lake Diefenbaker core was not determined radiometrically. Instead, core chronology was estimated from known stratigraphic markers. For example, the 18-cm-deep contact be-

© 1999 NRC Canada

Table 2. Total dissolved solids and mean concentration (relative proportions in parentheses) of major ions in Buffalo Pound Lake before (1959–1968) and after (1988–1994) water diversion from Lake Diefenbaker.

Variable	Units	1959–1968	1988–1994
Total dissolved solids	$mg \cdot L^{-1}$	644	443
Ca^{2+}	$mg \cdot L^{-1}$ (%)	41 (21.0)	43.8 (43.1)
Mg^{2+}	$mg \cdot L^{-1}$ (%)	32 (27.1)	19.5 (19.2)
K^{+}	$mg \cdot L^{-1}$ (%)	17 (4.5)	3.8 (3.7)
Na^{+}	$mg \cdot L^{-1}$ (%)	106 (47.4)	34.5 (34.0)
CO_3^{2-}	$mg \cdot L^{-1}$ (%)	28 (9.6)	2.7 (0.9)
HCO_3^{-}	$mg \cdot L^{-1}$ (%)	105 (34.4)	199.4 (66.4)
Cl^{-}	$mg \cdot L^{-1}$ (%)	42 (12.1)	9.6 (3.2)
SO_4^{2-}	$mg \cdot L^{-1}$ (%)	206 (43.9)	88.6 (29.5)

Note: Data for 1959–1969 from Hammer (1973) and for 1988–1994 from the Buffalo Pound Water Treatment Plant (City of Regina, unpublished data).

tween dark brown lacustrine sediment and black granular soil indicated the onset of reservoir sedimentation in 1968, while the uppermost sediment sample was assumed to represent 1994. The presence of uniform, visible laminae between the surface and 13-cm-deep sediment suggested that sediment age could be estimated by linear interpolation of the sediment depth and average lacustrine sedimentation rate.

Microscope slides for diatom analyses were prepared using standard techniques (Hall and Smol 1992). For each sample, a minimum of 500 diatom valves were identified using an Olympus BHS microscope (1000× magnification; numerical aperture = 1.40). Species were enumerated along transects to determine relative community composition (percentage of diatom sum), as described in Hall et al. (1999).

Sedimentary pigments were extracted, filtered, and dried under N_2 gas following Leavitt and Findlay (1994). Pigments identified included carotenoids characteristic of total algae (β-carotene), cryptophytes (alloxanthin), siliceous algae and dinoflagellates (fucoxanthin), mainly diatoms (diatoxanthin), cyanobacteria (echinenone), colonial cyanobacteria (myxoxanthophyll), and N_2-fixing cyanobacteria (aphanizophyll). Isomeric carotenoids from green algae (lutein) and cyanobacteria (zeaxanthin) were inseparable on our high-performance liquid chromatography system and are presented together. Similarly, carotenoids from *Aphanizomenon* (aphanizophyll), *Anabaena* (4-ketomyxoxanthophyll), and the Oscillatoriaceae (oscillaxanthin) were incompletely resolved and were presented as aphanizophyll (Leavitt and Findlay 1994). Chlorophyll *a* represented total algae, whereas chlorophyll *b* was used to independently quantify changes in chlorophytes. Pheophorbide *a*, a derivative of chlorophyll *a* produced during ingestion of algae by aquatic grazers, was used as an index of herbivory (Leavitt 1993). Pigment concentrations were expressed as nanomoles of pigment per gram of organic matter, following estimation of organic content by weight loss-on-ignition at 500°C. Calibration of annual fossil records against 20 years of phytoplankton data indicates that organic matter specific concentrations are significantly correlated with water column standing crops of most major algal groups (Leavitt and Findlay 1994; Leavitt et al. 1997).

Sediments from Buffalo Pound Lake also included pigments characteristic of environments with high ultraviolet (UV) irradiance (Leavitt et al. 1997). These pigments are produced by benthic algae when exposed to UV radiation and exhibit sedimentary concentrations that are correlated with the depth of penetration of UV radiation within lakes. Concentrations of UV radiation specific compounds were quantified assuming structural and light extinction characteristics similar to the carotenoid lutein (Leavitt et al. 1997). We expressed fossil UV pigment concentrations as a percentage of the sum of indicator carotenoid pigments (alloxanthin, lutein–zeaxanthin, diatoxanthin) so that the resulting UV index varied as a function of UV radiation, independent of algal abundance (Leavitt et al. 1997).

Chironomid analyses were performed as described in Hall et al. (1999). Briefly, chironomid remains were isolated from sediments after deflocculation in warm 8–10% KOH. Head capsules retained on 95-μm Nitex mesh were sorted at 50× magnification, mounted in Euparol onto microscope slides, and identified at 100–1000× magnification. Densities of chironomid remains were too low in sediments from Lake Diefenbaker to permit detailed taxonomic analyses, and only total concentrations are reported.

Numerical analyses

Stratigraphic zones were determined by constrained cluster analysis of sedimentary diatom, pigment, and chironomid profiles and scaled by Euclidean distance. Pigment concentrations required square root transformation to provide normal error distribution (Jongman et al. 1995), whereas diatom and chironomid percent abundances were not transformed.

Results

Sediment accumulation rate

The core from Lake Diefenbaker consisted of 18 cm of lacustrine sediment overlying black, granular, soil-like material. Alternating uniform black and tan laminae were apparent in the upper 13 cm of lacustrine sediments and appeared to be composed of shoreline mineral material interspersed with darker organic matter. The presence of regular laminae and a uniform organic matter profile (6.8 ± 0.4%) indicated that sediment deposition was highly predictable. As a consequence, the mean linear sedimentation rate (0.69 $cm \cdot year^{-1}$) could be used as a chronological reference.

Activity of ^{210}Pb in Buffalo Pound Lake declined with sediment depth but in a nonmonotonic fashion (Fig. 3). In general, ^{210}Pb activities were low but similar to those at other sites in Saskatchewan (Hall et al. 1999). Supported ^{210}Pb activity (background levels, or ^{210}Pb activity derived from in situ decay of ^{238}U daughter products, 0.03 $Bq \cdot g^{-1}$) was almost an order of magnitude lower than surface values, although activities were relatively constant in the upper 8 cm. In general, dry mass accumulation rates were higher during ca. 1930–1955 and ca. 1968–1990 than during other periods (Fig. 3*c*). Organic content varied only slightly (10–14% of dry mass).

Lake Diefenbaker

Diatoms

Diatoms were well preserved at all sediment depths and consisted of three distinct communities based on constrained cluster analysis (Fig. 4*a*). The first assemblage commenced with reservoir formation in 1968, persisted until ca. 1975, and was initially composed of *Stephanodiscus niagarae* and *Stephanodiscus parvus*, with subsequent increases of *Cyclotella bodanica* v. *lemanica* and *Cyclotella michiganiana*. The second distinct assemblage (ca. 1975–1986) was characterized by declines in *Stephanodiscus* and *Cyclotella* species in favour of *Tabellaria flocculosa* str. IIIp, *Fragilaria croto-*

© 1999 NRC Canada

Fig. 3. Results of analysis of ^{210}Pb and loss-on-ignition in sediments from Buffalo Pound Lake including (*a*) total ^{210}Pb activity versus sediment depth, (*b*) ^{210}Pb-estimated sediment age versus burial depth, (*c*) estimated sediment age versus cumulative dry mass, and (*d*) estimated sediment age versus organic matter content (% weight loss-on-ignition).

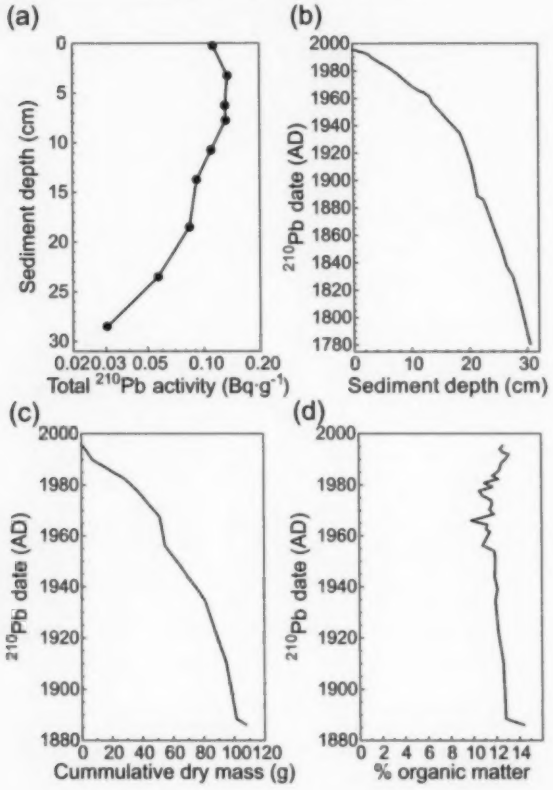

nensis, and *Aulacoseira ambigua*. Finally, *Tabellaria flocculosa* str. IIIp declined and assemblages became dominated by *Aulacoseira ambigua* after ca. 1986.

Pigments

Fossil pigment analyses indicated that algal assemblages in Lake Diefenbaker were diverse (Fig. 4*b*), with similar concentrations of pigments from cyanobacteria (echinenone, myxoxanthophyll), N_2-fixing cyanobacteria (aphanizophyll), diatoms (diatoxanthin, fucoxanthin), and cryptophytes (alloxanthin). Overall, there were few directional trends in total algal standing crop, as inferred from ubiquitous, chemically stable β-carotene (Fig. 4*b*). However, pigment composition changed after ca. 1985 when concentrations of chlorophyll *a* (all algae), chlorophyll *b* (greens), fucoxanthin (primarily diatoms), and cyanobacterial carotenoids (myxoxanthophyll, aphanizophyll, echinenone) all increased two- to 10-fold. Although these patterns were consistent with postdepositional degradation of labile pigments (e.g., fucoxanthin, chlorophyll *a*), similar stratigraphies were recorded for chemically stable carotenoids (e.g., alloxanthin, diatoxanthin, aphanizophyll, echinenone).

Chironomids

Concentrations of chironomid remains were low at all sediment depths (<15 head capsules·g wet sediment^{-1}) and prevented reliable analysis of taxonomic composition (Fig. 4*c*). In general, total chironomid remains increased from trace levels to ~10 head capsules·g wet sediment^{-1} ~5 years after reservoir formation. Concentrations then declined to low levels (1–3 head capsules·g wet sediment^{-1}) until ca. 1986, after which abundance increased to a corewide maximum in 1992 (13 head capsules·g wet sediment^{-1}).

Buffalo Pound Lake

Diatoms

Diatoms were poorly preserved below 10 cm depth (ca. 1970) but were abundant and well preserved in the upper sediments (Fig. 5*a*). Assemblages deposited ca. 1970–1990 consisted mainly of periphytic taxa, with the epiphyte *Cocconeis placentula* comprising ~50% of all diatoms. Other common periphyton included *Amphora inariensis*, *Amphora libyca*, *Fragilaria brevistriata*, and several *Nitzschia* taxa. After ca. 1990, periphytic taxa were replaced by eutrophic planktonic species including *Cyclotella* cf. *atomus*, *Cyclostephanos* cf. *tholiformis*, *Asterionella formosa*, *Diatoma tenue*, and *Stephanodiscus niagarae*.

Pigments

Sedimentary pigment assemblages were composed primarily of compounds characteristic of cyanobacteria (myxoxanthophyll, aphanizophyll, echinenone), diatoms (diatoxanthin), cryptophytes (alloxanthin), and green algae (chlorophyll *b*). Constrained cluster analysis identified four periods of different pigment composition (Fig. 5*b*). First, basal sediments were characterized by gradually declining concentrations of most pigments ca. 1880–1950. This initial period also exhibited high relative abundances of UV-absorbing pigments and low concentrations of pigments produced by herbivory (pheophorbide *a*). The second period (ca. 1950–1970) was characterized by more rapid declines in β-carotene, alloxanthin, and the UV index but not in other pigments. Concentrations of most pigments increased during the third period (ca. 1970–1990), especially those of β-carotene, fucoxanthin, diatoxanthin, and cyanobacterial pigments (myxoxanthophyll, aphanizophyll, echinenone). During this period, the grazing indicator pigment (pheophorbide *a*) reached maximum values coincident with loss of UV index pigments. Finally, concentrations of β-carotene, fucoxanthin, aphanizophyll, echinenone, and chlorophyll *a* have doubled since 1990, while concentrations of the grazing indicator have declined by 50%.

Chironomids

Sedimentary chironomid assemblages were composed of taxa characteristic of productive waters with high plant biomass (Fig. 6). For example, deepwater taxa tolerant of anoxic waters (*Chironomus* spp.) were common throughout the past 200 years as were plant-associated and predacious littoral chironomids. Constrained cluster analysis identified four taxonomic assemblages. Preagricultural communities (ca. 1780–1860) were characterized by low total densities, constant *Chironomus* abundance, and subtle changes in litto-

© 1999 NRC Canada

Fig. 4. Fossil stratigraphy from Lake Diefenbaker. (*a*) Diatoms; (*b*) algal pigments; (*c*) chironomids. Zonation determined by constrained cluster analysis (CONISS) using Euclidean distances (TSS, total sum of squares).

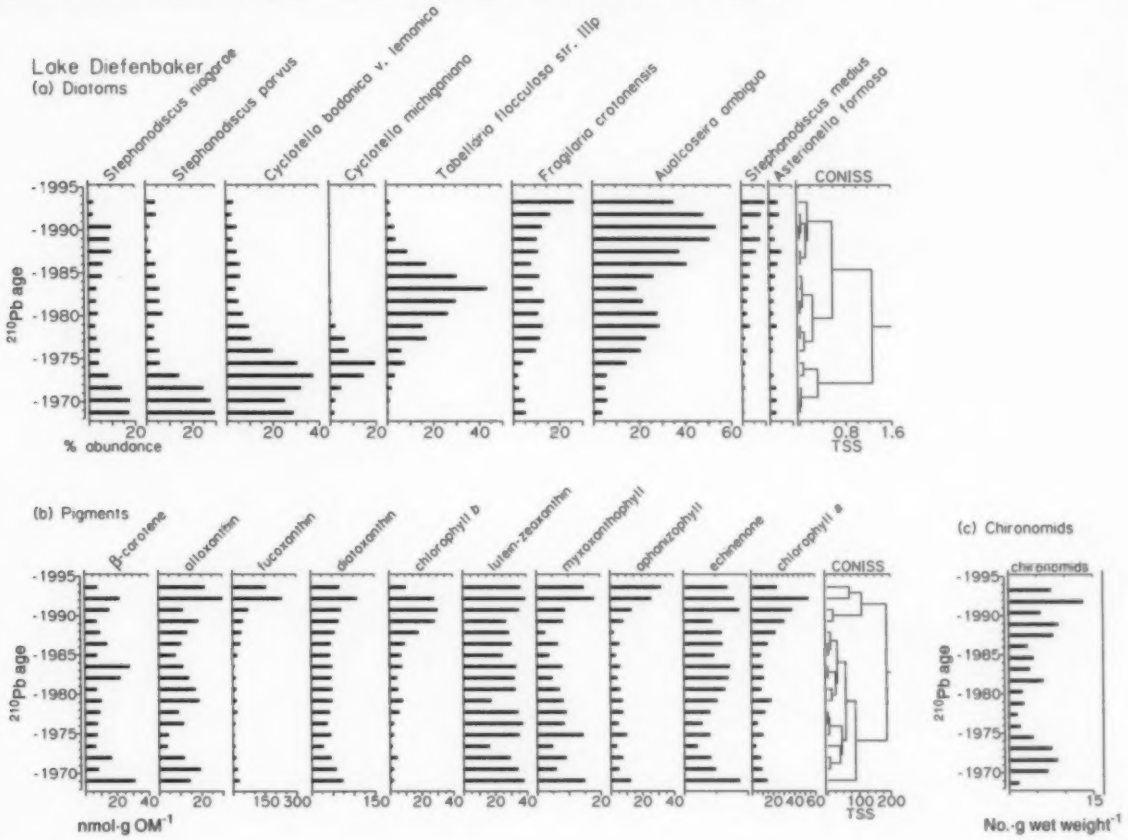

ral taxa, with slow losses of *Glyptotendipes* and *Cricotopus/Orthocladius* in favour of a more diverse assemblage (Fig. 6*a*). The second zone was defined by sharp increases in *Chironomini* sp. 1 and *Procladius* ca. 1860 combined with later increases in *Chironomus* ca.1870–1930. The third distinct assemblage was evident between 1940 and 1980 and was defined by high relative abundance of littoral *Tanytarsus* and *Procladius*, declining *Chironomus* and *Chironomini* sp. 1 densities, and increases in minor taxa (e.g., *Endochironomus*, *Corynoneura/Thiennemanniella*, *Parachironomus*). Finally, post-1980 communities were identified by historical minima in *Chironomus* and reciprocal increases in most other taxa.

Changes in chironomid densities generally corresponded to documented historical changes in lake level (Fig. 6*b*). For example, low water levels (1.5–2 m maximum depth) during the drought years 1930–1940 (Fig. 2*b*) coincided with increased densities of the littoral *Tanytarsus* (Fig. 6). Similarly, reservoir formation in 1952 was accompanied by elevated mean densities and temporal variability of several taxa, including *Tanytarsus*, *Cryptochironomus*, *Cladopelma*, *Parachironomus*, *Endochironomus*, and *Corynoneura/Thienemanniella*. Finally, diversion of water from Lake Diefenbaker after 1968 was accompanied by reductions in chironomid concentrations to values comparable with those that existed prior to reservoir formation.

Discussion

Patterns of biological communities and water quality change varied substantially between the two reservoirs despite similarities in local geology, vegetation, soils, land use, and climate. For example, Lake Diefenbaker exhibited three distinct periods of production, corresponding to an initial 4-year increase in pelagic production, >10 years of oligotrophication, and a modern return to productive conditions. This pattern is typical of newly formed dryland reservoirs (Baxter 1977; Ostrofsky and Duthie 1978). In contrast, phytoplankton abundance decreased after impoundment of Buffalo Pound Lake, indicating that reservoir formation does not invariably lead to eutrophication (Thornton et al. 1990). Below, we discuss the major limnological changes that occurred during development of each reservoir and then compare reservoir responses to identify how differences in the method of formation and water level regulation may have influenced reservoir ontogeny.

© 1999 NRC Canada

Fig. 5. Fossil stratigraphy from Buffalo Pound Lake. (*a*) Diatoms; (*b*) algal pigments. Horizontal dashed lines indicate onset of European-style agriculture in 1890, dam construction in 1952, and onset of water diversion from Lake Diefenbaker in 1968. Zonation calculated as in Fig. 4.

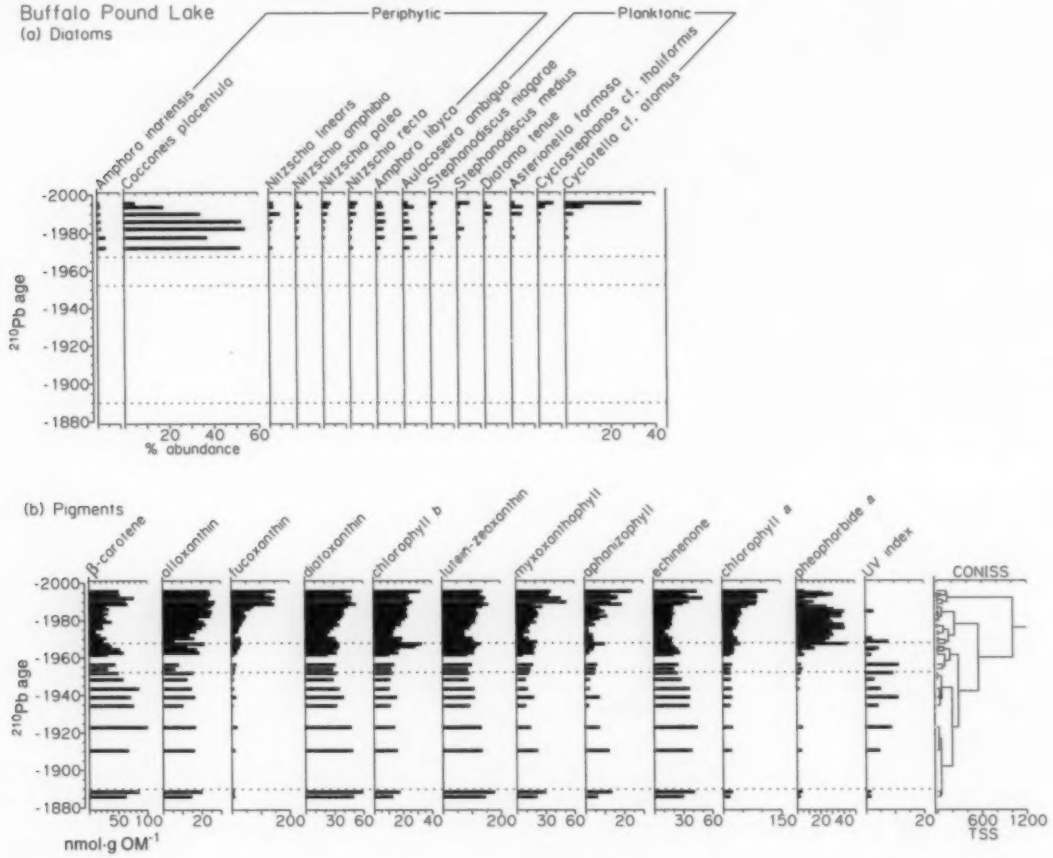

Lake Diefenbaker

Analysis of fossil communities suggested that Lake Diefenbaker has experienced three main periods of different aquatic communities and production since its formation in 1967. The period immediately following reservoir formation (ca. 1968–1975) was characterized by an initial increase in trophic status, followed by a rapid shift to less productive conditions. Initial diatom assemblages (ca. 1968–1972) consisted of relatively large populations of *Stephanodiscus niagarae* and *Stephanodiscus parvus* (Fig. 4), which are reliable indicators of eutrophic conditions (Hall and Smol 1992). Additionally, pigment analyses indicated that cyanobacteria (as echinenone, myxoxanthophyll) were an important component of algal communities at this time, including N_2-fixing taxa (as aphanizophyll) that presently predominate in nutrient-rich prairie lakes (Hammer 1973; Graham 1997). Elevated abundances of benthic chironomids during this period are also consistent with high algal deposition and abundant submerged herbaceous vegetation immediately following inundation (Prat and Daroca 1983; Popp and Hoagland 1995). Similar patterns are observed in most newly formed reservoirs, where nutrients from flooded soils and erosion of littoral zone materials stimulate phytoplankton growth and promote eutrophic conditions (Chamberlain 1972; Holz et al. 1997). Additionally, eutrophic conditions may have been enhanced by increased water residence times during reservoir filling that could minimize losses of nutrients and plankton via washout (Campbell et al. 1998). After ca. 1972, however, aquatic communities shifted towards more oligotrophic diatoms (e.g., *Cyclotella* spp., 10–12 μg $P \cdot L^{-1}$; Hall and Smol 1992), lower chironomid densities, and comparatively stable abundances of fossil pigments (Fig. 4).

Changes after ca. 1972 signaled a shift to a period of reduced reservoir production that lasted at least 10 years (ca. 1975–1986). Diatom assemblages became dominated by *Tabellaria flocculosa* str. IIIp, *Fragilaria crotonensis*, and *Aulacoseira ambigua* (Fig. 4*a*), taxa indicative of less productive lake conditions (Hall and Smol 1992). Similarly, concentrations of chironomids and fossil pigments remained relatively low and constant during this time (Fig. 4). Overall, the data are consistent with maintenance of moderate trophic status (1975–1986) during a period of trophic suppression (sensu Ostrofsky and Duthie 1978).

Declines in internal nutrient supply may have contributed to lower overall aquatic production in Diefenbaker reservoir

© 1999 NRC Canada

Fig. 6. Stratigraphy of fossil chironomids from Buffalo Pound Lake expressed as (*a*) percent abundance, including the ratio of percent pelagic taxa to percent littoral taxa, and (*b*) concentrations. Horizontal dashed lines as defined in Fig. 5 and zonation calculated as in Fig. 4.

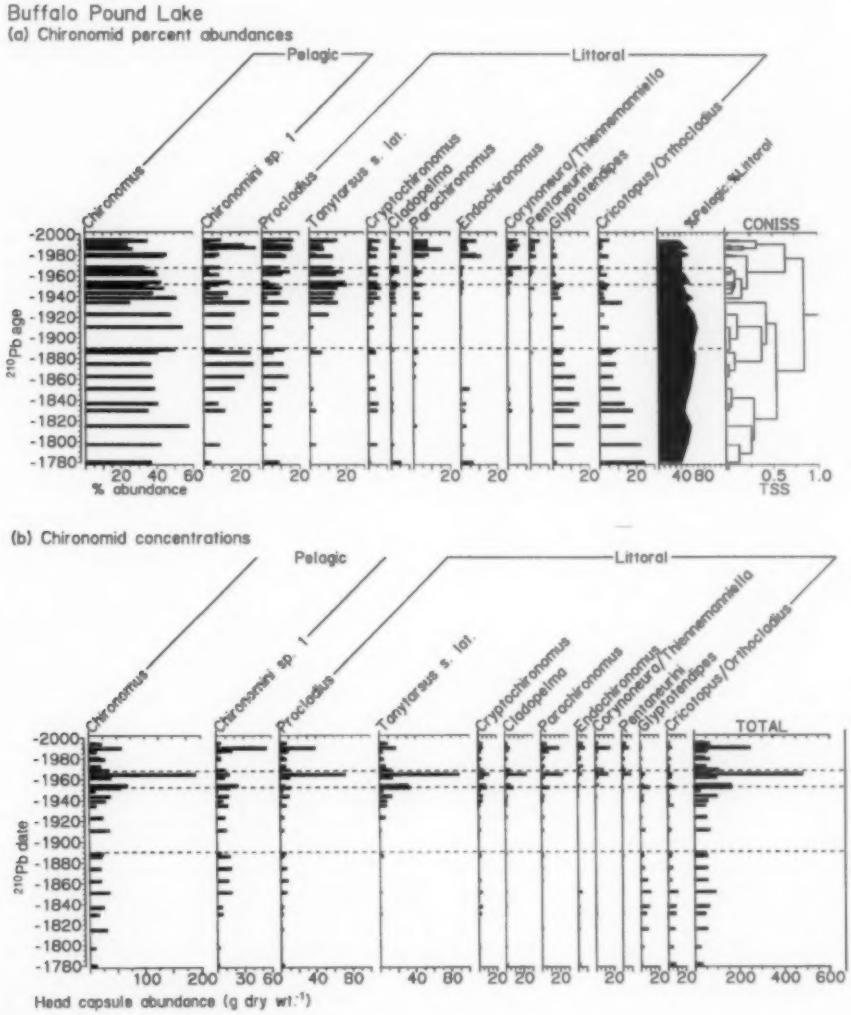

between ca. 1975 and 1986. We infer that aquatic production was mainly from pelagic biota, as indicated by the near absence of littoral and benthic diatoms, low densities of chironomids, and abundant pigments from taxa with largely planktonic habits (cryptophytes, N_2-fixing cyanobacteria; Fig. 4). Low production of benthic and littoral biota is not surprising considering the relatively great depth of Lake Diefenbaker (mean depth 33 m), lack of woody vegetation as substrate, high littoral erosion (Environment Canada 1988), and substantial water level changes that reduce availability of suitable habitats for benthic and periphytic biota. The relative paucity of benthic communities in Lake Diefenbaker, therefore, indicates that the oligotrophication seen following 1972 did not arise from elimination of benthic production, as occurs in other reservoirs (Baxter 1977). Also, because agricultural fertilizer use did not decrease during 1972–1986 (Korol and Girard 1996), we further infer that changes in external nutrient loads could not account for the observed trophic suppression (cf. Ostrofsky and Duthie 1978). Instead, declines in primary production were likely due to reduced nutrient flux from sediments following permanent burial of organic materials by eroded mineral matter from lakeshores (e.g., Nursall 1952; Lindström 1973) and depletion of soil leachate pools and reduced mineralization of submerged terrestrial plants (Baxter 1977). Additionally, lower production and sedimentation of phytoplankton likely decreased resource flux to benthic habitats, leading to observed declines in chironomid abundance (Fig. 4*c*), as seen in other reservoirs (Prat and Daroca 1983). Finally, habitat losses due exposure and increased erosion during low water levels may have suppressed chironomid populations, as has been observed in montane reservoirs of western Canada (e.g., Nursall 1952; Geen 1974).

Paleolimnological evidence suggests that the trophic status

© 1999 NRC Canada

of Lake Diefenbaker has increased since ca. 1986 (Fig. 4). Elevated abundance of *Aulacoseira ambigua* at the expense of *Tabellaria flocculosa* str. IIIp demonstrates increased nutrient flux and productivity (Hall and Smol 1992), while concomitant increases in pigments from chlorophytes (chlorophyll *b*), filamentous cyanobacteria (myxoxanthophyll), N_2-fixing cyanobacteria (aphanizophyll), and diatoms (diatoxanthin, fucoxanthin) and elevated chironomid densities all suggest more productive conditions. Parallel increases of chemically stable (e.g., alloxanthin, diatoxanthin, aphanizophyll, echinenone) and relatively labile pigments (fucoxanthin, chlorophyll *a*) suggest that stratigraphic patterns were produced by increased algal standing crops rather than by diagenetic processes (Leavitt 1993). These inferred increases in trophic status are consistent with occasional historical measurements that document an increase in summer mean phosphorus concentration from ~24 $\mu g\ P \cdot L^{-1}$ in 1984 to 93 $\mu g\ P \cdot L^{-1}$ in 1994 (Table 1) (Environment Canada 1988; Graham 1997). Similarly, planktonic chlorophyll increased from ~1 $\mu g \cdot L^{-1}$ in 1984 (Environment Canada 1988) to over 5 $\mu g \cdot L^{-1}$ in 1994 (Table 1). Interestingly, land use practices that regulate external loads (e.g., cattle, fertilization) have not increased since 1986 (Korol and Girard 1996, Hall et al. 1999). Consequently, we infer that either internal nutrient supply has increased or recent fish farms may have contributed to higher lake productivity during the past decade. Presently, we cannot distinguish between these explanations.

Buffalo Pound Lake

Prior to reservoir formation in 1952, Buffalo Pound Lake was a shallow prairie lake (1–4 m deep) that experienced annual water level changes of 1–3 m in most years (Fig. 2*b*). Paleolimnological analyses indicate that biological communities and aquatic production were relatively stable before impoundment, characterized by high algal production, low herbivore activity, and high penetration of UV radiation. Although concentrations of pigments from filamentous (myxoxanthophyll) and N_2-fixing (aphanizophyll) cyanobacteria declined gradually during this period, possibly as the lake recovered from land disturbance by ancestral Europeans (Hall et al. 1999), both total cyanobacteria (echinenone) and total algal standing crops (β-carotene) did not change markedly (Fig. 5*b*). Similarly, chironomid abundance and community composition were relatively unchanged, with roughly equal representation of littoral and pelagic taxa (Fig. 6). The high proportion of cyanobacteria (myxoxanthophyll, aphanizophyll, echinenone) is typical of productive prairie lakes (Hammer 1973; Graham 1997).

Sediments deposited before impoundment (ca. 1880–1950) contained low concentrations of pheophorbide *a*, suggesting either that herbivores were scarce or that algae were not easily ingested during natural lake conditions. Although we did not directly measure the abundance of zooplankton in this study, high proportions of pigments from large filamentous cyanobacteria (aphanizophyll, myxoxanthophyll) suggest that algal inedibility could have contributed to low rates of herbivory. Regardless of the mechanisms involved, the low abundance of pheophorbide *a* shows that herbivory was not a strong control of algal abundance before impoundment.

Relatively high exposure to UV radiation may have favoured filamentous cyanobacteria and reduced grazing prior to impoundment in 1952. Throughout the preinundation period, sediments of Buffalo Pound Lake contained significant concentrations of UV-absorbing pigments characteristic of shallow lakes (<5 m average depth) with low concentrations (<2 $mg \cdot L^{-1}$) of UV-absorbing dissolved organic matter (DOM) (Leavitt et al. 1997). These pigments are derivatives of scytonemin, a photoprotectant compound produced by benthic cyanobacteria in response to damaging levels of UV radiation (Garcia-Pichel and Castenholtz 1991). Surveys of clear, shallow lakes in the Canadian Rocky Mountains and boreal forest demonstrate that the ratios of UV-absorbing pigments to carotenoids are linearly correlated with the depth of penetration of UV radiation within the lake (Leavitt et al. 1997). In general, this indicator ratio was substantially lower in Buffalo Pound Lake (<10%) than in highly transparent alpine lakes (50–100%) and probably reflects the relatively great concentrations of DOM in the water column (Table 1). Nevertheless, biotic exposure to UV radiation is greater in Buffalo Pound Lake than in most boreal lakes because the DOM of prairie lakes is often colourless and lacks UV-absorbing aromatic constituents (Curtis and Adams 1995; P.R. Leavitt et al., unpublished data). UV radiation has been shown to inhibit herbivores (Bothwell et al. 1994) and favour UV-tolerant cyanobacteria (Vinebrooke and Leavitt 1999) in other clear systems.

Dam construction in 1952 raised the mean depth of Buffalo Pound Lake ~2 m relative to levels in the 1930's, stabilized water levels, and was associated with substantial changes in algal and invertebrate communities (Figs. 2*b*, 5, and 6). Algal production often increases in newly constructed reservoirs (e.g., Baxter 1977; Thornton et al. 1990) and in newly flooded lakes which experience substantial water level fluctuations (Rodhe 1964). By contrast, concentrations of β-carotene (total algae) and alloxanthin (cryptophytes) declined ca. 50% after dam construction at Buffalo Pound (Fig. 5*b*) when water levels stabilized, shoreline erosion was reduced, and nutrient regeneration presumably declined relative to the preimpoundment period. These findings are consistent with those from Southern Indian Lake (a subarctic lake–reservoir; Hecky et al. 1984) and indicate that reservoir formation does not necessarily lead to increased algal production, especially when low-level flooding does not greatly alter nutrient supplies. Interestingly, reservoir formation in Buffalo Pound Lake was associated with increased abundances of chironomids, particularly the littoral *Tanytarsus* taxa (Fig. 6*b*). Although this pattern is typical of new reservoirs (Nursall 1952), in Buffalo Pound Lake, it was not coupled to increases in algal production or herbivorous zooplankton (as pheophorbide *a*; Fig. 5*b*). Instead, we conclude that reduced fluctuations in water level and littoral erosive forces, rather than increased food supply, stimulated benthic production by enhancing stability of sedimentary environments and increasing availability of littoral and macrophyte habitats.

Increased discharge from Lake Diefenbaker after 1968 (Fig. 2*c*) coincided with prolonged reductions in algal standing crops and further expansion of macrophyte populations in Buffalo Pound Lake (Figs. 5 and 6). Concentrations of many fossil pigments reached historical minima during the

© 1999 NRC Canada

1970's (Fig. 5*b*). At the same time, diatom preservation dramatically improved (see below) and assemblages were composed mainly of the epiphyte *Cocconeis placentula*. Similarly, increased relative abundance of plant-associated chironomids *Parachironomus*, *Endochironomus*, and *Corynoneura/Thienemanniella* indicated an expansion of macrophyte populations. These findings agree with historical data that documented declines in cyanobacterial blooms, increased light penetration, and a major expansion of macrophytes 3–4 years after diversion (Hammer 1973).

Improved diatom preservation after ca. 1970 likely resulted from reduced salinity and altered brine composition following diversion of Lake Diefenbaker water into Buffalo Pound Lake. For example, fragments of diatom frustules were routinely observed in sediments deposited during 1880–1970 and the carotenoid diatoxanthin (Leavitt 1993) was common, indicating that diatoms were present but that preservation was poor. Historical records show that salinity declined from 644 to 443 $mg \cdot L^{-1}$ and brine composition shifted from dominance by Na_2SO_4 to $CaHCO_3$ immediately after diversion (Table 2; Hammer 1973). While diatom preservation is not usually altered by this magnitude of change in salinity (Cumming and Smol 1993), experimental studies have shown that calcium carbonate brines foster better preservation of siliceous frustules than do sodium brines (Flower 1993).

Finally, water diversion and increased macrophyte abundance after 1968 resulted in reduced penetration of UV radiation and increased herbivory (as pheophorbide *a*) in Buffalo Pound Lake (Fig. 5*b*). Following sustained diversion of water from Lake Diefenbaker (Fig. 2*c*), concentrations of UV pigments declined to trace levels and often became absent from the sedimentary record (Fig. 5*b*). This pattern is consistent with reduced penetration of UV radiation due to both increased water depth (1952–1970) and elevated concentrations of UV-absorbing DOM from expanding macrophyte beds. Additionally, planktivore populations would be expected to increase with development of macrophytes, both because of reduced UV penetration and because migratory invertebrates use shallow plant communities as refugia from visually orienting predators (e.g., Lauridsen et al. 1996). Overall, pigment-inferred phytoplankton biomass was low throughout the period of elevated grazing indicator (1970–1990) either because intense grazing pressure by herbivores reduced algal standing crops or because macrophytes outcompeted algae for available nutrients, such as seen in many European shallow lakes (see Mortensen et al. 1994).

Identification of factors regulating reservoir development

Comparison of multidecade paleoecological records from Lake Diefenbaker and Buffalo Pound Lake provided a unique opportunity to compare mechanisms that regulate community ontogeny and production following formation of reservoirs by de novo flooding and lake inundation. Previous studies variously suggested that reservoir development is controlled by site-specific factors related to external nutrient flux (e.g., Ostrofsky and Duthie 1978; Hecky et al. 1984), in-lake processes that influence nutrient regeneration (e.g., Kennedy and Walker 1990; Schaus et al. 1997), and their interactions. External processes include such variables as area of land inundated (Kimmel et al. 1990), shoreline and soil erosion (Kennedy and Walker 1990), presence of permafrost (Hecky et al. 1984), composition of terrestrial vegetation (Baxter 1977; Holz et al. 1997), flushing rates (Campbell et al. 1998) and land use practises (e.g., agriculture) and climatic variation among regions (e.g., temperature; Patalas and Salki 1984). In contrast, internal nutrient flux is regulated by thermal structure and development of deepwater anoxia (Kennedy and Nix 1987), sedimentation rates (Nursall 1952), and nutrient recycling by biota (Schaus et al. 1997). Although it is difficult to unambiguously assign causation based on paleoecological records alone, comparison among sites allows some assessment of the relative importance of factors regulating reservoir development.

External factors related to local topography, soils, geology, vegetation, land use, and climate are unlikely to have produced the observed differences in reservoir production and ontogeny following inundation. Buffalo Pound and Diefenbaker reservoirs are located <50 km apart in the semiarid, mixed-grass prairie of south-central Saskatchewan (Fig. 1). Both lakes lie in broad glacial outwash valleys formed by the meltwaters of the Wisconsinan ice sheet (Christiansen 1960) and are underlain by cretaceous marine sedimentary bedrock (Bearpaw formation) covered with thick glacial till and predominantly dark brown chernozemic soils (Acton et al. 1998). Over 95% of each catchment is used for the production of cereal crops and livestock, mainly without the use of additional fertilizer or irrigation (Hall et al. 1999). There are no major urban centres within the effective drainage of each reservoir. Consequently, while catchment characteristics or external nutrient loading is known to cause differences in trophic ontogeny among other reservoirs (Ostrofsky and Duthie 1978; Thornton et al. 1990), these factors do not appear to have been active in the Qu'Appelle drainage.

Internal factors related to stratification and fish-mediated nutrient cycling do not appear to have caused observed differences in reservoir development. Low relative depths (sensu Wetzel 1983) are characteristic of all Qu'Appelle Valley water bodies (0.09–0.55%; Hall et al. 1999), and neither reservoir exhibits pronounced thermal stratification (Graham 1997). Although Lake Diefenbaker is polymictic, patterns of community change were typical of thermally stratified reservoirs formed on drylands (Ostrofsky and Duthie 1978; Prat and Daroca 1983; Kennedy and Nix 1987; Marsicano et al. 1995; Donar et al. 1996) and demonstrated that the occurrence of an initial trophic upsurge and suppression was independent of thermal stratification. In contrast, unstratified Buffalo Pound Lake became less productive after flooding. In addition, because both lakes have similar pelagic fish communities (*Esox lucius*, *Stizostedion vitreum*, *Coregonus arteri*, *Perca flavescens*) and because benthic detritivores that consume sediments and release nutrients (Schaus et al. 1997) are common at both sites (e.g., *Catostomus commersoni*; Saskatchewan Environment and Resource Management, unpublished data), differences in fish community composition were unlikely to have caused variations in trophic ontogeny among reservoirs.

Instead, differences in the extent of inundation may partly account for variation in the response of aquatic biota in Lake Diefenbaker and Buffalo Pound Lake to reservoir formation.

© 1999 NRC Canada

The prevailing reservoir paradigm predicts that release of bioavailable nutrients from flooded vegetation and soils leads to an initial eutrophication of reservoirs, the magnitude of which depends on the area of land inundated and the volume of eroded shoreline (Ostrofsky and Duthie 1978; Thornton et al. 1990). Consistent with this hypothesis, flooding of Lake Diefenbaker submerged 500 km^2 of valley grassland, created a lake with high shoreline development (Fig. 1; Wetzel 1983), increased erosion rates to 1–3 $m \cdot year^{-1}$, and resulted in a rapid increase in aquatic production during the first 4 years of lake existence (Fig. 4). In contrast, conversion of Buffalo Pound Lake into a reservoir inundated ~5 km^2 of valley bottom, had little effect on shoreline development based on aerial photographs (1945–1995; R.I. Hall et al., unpublished data), and was recorded by a ~50% decline in algal, but not invertebrate, production (Figs. 5 and 6). Instead, these latter patterns are consistent with the observation that aquatic biota exhibit little response to modest changes in lake levels during flooding (Hecky et al. 1984; Wiens and Rosenberg 1984).

The magnitude of water level fluctuations following reservoir formation also may have played an important role in the ontogeny of reservoir communities (Rodhe 1964; Naselli-Flores and Barone 1997). For example, mean annual water levels in Lake Diefenbaker vary by >6 m (Fig. 2) and result in a broad littoral zone composed of sand and rocks, with few macrophytes or benthic communities. In addition, shoreline erosion rates of 1–3 $m \cdot year^{-1}$ and ice scouring due to winter drawdown (Environment Canada 1988) prevent development of littoral communities. Under these conditions, aquatic production in Lake Diefenbaker appears restricted to pelagic communities. In contrast, stabilization of water levels following impoundment of Buffalo Pound Lake (Fig. 2) permitted growth of extensive macrophyte beds (Hammer 1973) and development of littoral- and macrophyte-associated chironomid fauna. Because shallow lakes such as Buffalo Pound Lake permit penetration of light to most of the lake bottom, macrophytes can rapidly colonize nearshore and open-water habitats once water levels are stable (Mortensen et al. 1994).

In conclusion, comparison of paleoecological records from reservoirs formed by de novo flooding and by lake inundation reveals that reservoir ontogeny does not inevitably lead to eutrophication, as is commonly believed (Baxter 1977; Ostrofsky and Duthie 1978; Thornton et al. 1990). Comparison of algal and invertebrate fossil records demonstrates that oligotrophication can arise from increased lake level stability, reduced erosion, and complex ecological interactions among phytoplankton, grazers, and macrophyte populations. In addition, variations in community composition through time are sensitive to the area of land flooded and subsequent changes in hydrologic regimes which influence nutrient supply and ecological interactions among algae, invertebrates, and fish.

Acknowledgements

This project was funded by a Natural Sciences and Engineering Research Council of Canada (NSERC) strategic grant to J.P. Smol and P.R. Leavitt. R.I. Hall was partly funded by the Environment and Space Research Institute (MRI) and the Climate Impacts Research Centre (CIRC), Sweden, via structural grants from the European Union. Chris Teichreb performed high-performance liquid chromatography and loss-on-ignition analyses, Mark Graham enumerated phytoplankton and zooplankton, and Linda Kimpe prepared diatom slides. We thank Alex Banga (Saskatchewan Water Corp.) for hydrology and water level records from Lake Diefenbaker, Joe Bergman (Buffalo Pound Water Administration Board) for water chemistry and withdrawal records from Buffalo Pound Lake, and officials at the Hydrology Division, Prairie Farm Rehabilitation Administration (Agriculture Canada, Regina office), for historical lake levels in Buffalo Pound Lake. Norman Yan, Rolf Vinebrooke, Owen Lind, and an anonmymous reviewer provided helpful comments.

References

Acton, D.F., Padbury, G.A., and Stushnoff, C.T. 1998. The ecoregions of Saskatchewan. Canadian Plain Research Centre, Regina, Sask.

Allan, R.J., and Kenney, B.C. 1978. Rehabilitation of eutrophic Prairie lakes. Verh. Int. Ver. Limnol. **20**: 214–224.

Baxter, R.M. 1977. Environmental effects of dams and impoundments. Annu. Rev. Ecol. Syst. **8**: 255–283.

Binford, M.W. 1990. Calculation and uncertainty analysis of ^{210}Pb dates for PIRLA project lake sediment cores. J. Paleolimnol. **3**: 253–267.

Bothwell, M.L., Sherbot, D.M.J., and Pollack, C.M. 1994. Ecosystem response to solar ultraviolet-B radiation: influence of trophic-level interactions. Science (Washington, D.C.), **265**: 97–100.

Campbell, C.E., Knoechel, R., and Copeman, D. 1998. Evaluation of factors related to increased zooplankton biomass and altered species composition following impoundment of a Newfoundland reservoir. Can. J. Fish. Aquat. Sci. **55**: 230–238.

Chamberlain, L.L. 1972. Primary productivity in a new and an older California reservoir. Calif. Fish Game, **58**: 254–267.

Christiansen, E.A. 1960. Geology and ground-water resources of the Qu'Appelle area, Saskatchewan. Geology Division Report No. 1, Saskatchewan Research Council, Saskatoon, Sask.

Cumming, B.F., and Smol, J.P. 1993. Development of diatom-based salinity models for paleoclimate research from lakes in British Columbia (Canada). Hydrobiologia, **269/270**: 179–196.

Curtis, P.O., and Adams, H.E. 1995. Dissolved organic matter quantity and quality from freshwater and saline lakes in east-central Alberta. Biogeochemistry, **36**: 125–138.

Donar, C.M., Neely, R.K., and Stoermer, E.G. 1996. Diatom succession in an urban reservoir system. J. Paleolimnol. **15**: 237–243.

Durrant, E.F. 1958. Buffalo Pound Lake: a compilation of information extracted from several reports published by the Hydrology Division, P.F.R.A. Report by Agriculture Canada, Prairie Farm Rehabilitation Administration, Regina, Sask.

Environment Canada. 1988. Lake Diefenbaker and Upper South Saskatchewan River water quality study. Report WQ 111, Environment Canada, Burlington, Ont.

Flower, R.J. 1993. Diatom preservation: experiments and observations on dissolution and breakage in modern and fossil material. Hydrobiologia, **269/270**: 473–484.

Garcia-Pichel, F., and Castenholtz, R.W. 1991. Characterization and biological implications of scytonemin, a cyanobacterial sheath pigment. J. Phycol. **27**: 345–409.

© 1999 NRC Canada

Geen, G.H. 1974. Effects of hydroelectric development in western Canada on aquatic ecosystems. J. Fish. Res. Board Can. **31**: 913–927.

Graham, M.D. 1997. Omnivory and selective feeding by zooplankton along a lake production gradient: complementary ^{15}N isotope and gut pigment analysis. M.Sc. thesis, Biology Department, University of Regina, Regina, Sask.

Hall, R.I., and Smol, J.P. 1992. A weighted-averaging regression and calibration model for inferring total phosphorus concentration from diatoms in British Columbia (Canada) lakes. Freshwater Biol. **27**: 417–434.

Hall, R.I., Leavitt, P.R., Dixit, A.S., Quinlan, R., and Smol, J.P. 1999. Effects of agriculture, urbanization and climate on water quality in the northern Great Plains. Limnol. Oceanogr. **44**: 739–756.

Hammer, U.T. 1973. Eutrophication and its alleviation in the upper Qu'Appelle River system, Saskatchewan. *In* Proceedings of the Symposium on Lakes of Western Canada. University of Alberta Press, Edmonton, Alta. pp. 352–368.

Hecky, R.E., and Guildford, S.J. 1984. Primary productivity of Southern Indian Lake before, during, and after impoundment and Churchill River diversion. Can. J. Fish. Aquat. Sci. **41**: 591–604.

Hecky, R.E., Newbury, R.W., Bodaly, R.A., Patalas, K., and Rosenberg, D.M. 1984. Environmental impact prediction and assessment: the Southern Indian Lake experience. Can. J. Fish. Aquat. Sci. **41**: 720–732.

Holz, J.C., Hoagland, K.D., Spawn, R.L., Popp, A., and Andersen, J.L. 1997. Phytoplankton community response to reservoir aging, 1968–92. Hydrobiologia, **346**: 183–192.

Jongman, R.H.G., ter Braak, C.J.F., and van Tongeren, O.F.R. 1995. Data analysis in community and landscape ecology. Cambridge University Press, Cambridge, U.K.

Kennedy, R.H., and Nix, J. (*Editors*). 1987. Proceedings of the DeGray Lake Symposium. Tech. Rep. E-87-4, U.S. Army Engineer Waterways Experiment Station, Vicksburg, Miss.

Kennedy, R.H., and Walker, W.W. 1990. Reservoir nutrient dynamics. *In* Reservoir limnology: ecological perspectives. *Edited by* K.W. Thornton, B.L. Kimmel, and F.E. Payne. John Wiley & Sons, New York. pp. 109–132.

Kimmel, B.L., Lind, O.T., and Paulson, L.J. 1990. Reservoir primary production. *In* Reservoir limnology: ecological perspectives. *Edited by* K.W. Thornton, B.L. Kimmel, and F.E. Payne. John Wiley & Sons, New York. pp. 133–194.

Korol, M., and Girard, L. 1996. Canadian fertilizer consumption, shipments and trade, 1994/5. Agriculture and Agri-Foods Canada, Farm Input Markets Unit, Policy Branch, Ottawa, Ont.

Lauridsen, T.L., Pedersen, L.J., Jeppesen, E., and Søndergaard, M. 1996. The importance of macrophyte bed size for cladoceran composition and horizontal migration in a shallow lake. J. Plankton Res. **18**: 2283–2294.

Leavitt, P.R. 1993. A review of factors that regulate carotenoid and chlorophyll deposition and fossil pigment abundance. J. Paleolimnol. **9**: 109–127.

Leavitt, P.R., and Findlay, D.L. 1994. Comparison of fossil pigments with 20 years of phytoplankton data from eutrophic Lake 227, Experimental Lakes Area, Ontario. Can. J. Fish. Aquat. Sci. **51**: 2286–2299.

Leavitt, P.R., Vinebrooke, R.D., Donald, D.B., Smol, J.P., and Schindler, D.W. 1997. Past ultraviolet radiation environments in lakes derived from fossil pigments. Nature (Lond.), **388**: 457–459.

Lindström, T. 1973. Life in a lake reservoir. Ambio, **2**: 145–153.

Marsicano, L.J., Hartranft, J.L., Siver, P.A., and Hamer, J.S. 1995. An historical account of water quality changes in Candlewood Lake, Connecticut, over a sixty year period using paleolimnology and ten years of monitoring data. Lake Reservoir Manage. **11**: 15–28.

Mitchell, P., and Prepas, E. 1990. Atlas of Alberta lakes. University of Alberta Press, Edmonton, Alta.

Mortensen, E., Jeppesen, E., Søndergaard, M., and Kamp-Nielson, L. (*Editors*). 1994. Nutrient dynamics and biological structure in shallow freshwater and brackish lakes. Kluwer Academic Publishers, Dordrecht, The Netherlands.

Naselli-Flores, L., and Barone, R. 1997. Importance of water-level fluctuation on population dynamics of cladocerans in a hypertrophic reservoir (Lake Arancio, south-west Sicily, Italy). Hydrobiologia, **360**: 223–232.

Nursall, J.R. 1952. The early development of a bottom fauna in a new power reservoir in the Rocky Mountains of Alberta. Can. J. Zool. **30**: 387–409.

Ostrofsky, M.L., and Duthie, H.C. 1978. An approach to modelling productivity in reservoirs. Verh. Int. Ver. Limnol. **20**: 1562–1567.

Patalas, K., and Salki, A. 1984. Effects of impoundment and diversion on the crustacean plankton of Southern Indian Lake. Can. J. Fish. Aquat. Sci. **41**: 613–637.

Popp, A., and Hoagland, K.D. 1995. Changes in benthic community composition in response to reservoir aging. Hydrobiologia, **306**: 159–171.

Prat, N., and Daroca, M.V. 1983. Eutrophication process in Spanish reservoirs as revealed by biological records in profundal sediments. Hydrobiologia, **103**: 153–158.

Rodhe, W. 1964. Effects of impoundment on water chemistry and plankton in Lake Ransaren (Swedish Lappland). Verh. Int. Ver. Limnol. **15**: 437–443.

Schaus, M.H., Vanni, M.J., Wissing, T.E., Bremigan, M.T., Garvey, J.E., and Stein, R.A. 1997. Nitrogen and phosphorus excretion by detritivorous gizzard shad in a reservoir ecosystem. Limnol. Oceanogr. **42**: 1386–1397.

Thornton, K.W., Kimmel, B.L., and Payne, F.E. (*Editors*). 1990. Reservoir limnology: ecological perspectives. John Wiley & Sons, New York.

Vinebrooke, R., and Leavitt, P.R. 1999. Differential responses of littoral communities to ultraviolet radiation in an alpine lake. Ecology, **80**: 223–237.

Wetzel, R.G. 1983. Limnology. 2nd ed. W.B. Saunders Co., Philadelphia, Pa.

Wiens, A.P., and Rosenberg, D.M. 1984. Effect of impoundment and river diversion on profundal macrobenthos of Southern Indian Lake, Manitoba. Can. J. Fish. Aquat. Sci. **41**: 638–648.

Wiens, L.H. 1987. The South Saskatchewan – Qu'Appelle diversion: history and future prospects. *In* Proceedings of the Symposium on Interbasin Transfer of Water: Impacts and Future Needs for Canada. *Edited by* W. Nicholaichuk and F. Quinn. Symposium No. 1, National Hydrology Research Institute, Saskatoon, Sask. pp. 105–119.

© 1999 NRC Canada

Comparison of activity rates of 1+ yellow perch (*Perca flavescens*) from populations of contrasting growth rates using underwater video observations

N. Aubin-Horth, J. Gingras, and D. Boisclair

Abstract: We compared the stereocinematographic (SCG) method to estimate activity rates of yellow perch (*Perca flavescens*) with the more traditional bioenergetic approach. We also compared activity rates of perch from two populations with contrasting growth rates to test the hypothesis that fish with lower growth rates are characterized by higher activity rates. We attempted to corroborate the SCG method by comparing values of energetic costs obtained with observations of fish movements with estimates obtained using the difference between field-derived consumption and growth rates (bioenergetic method). Independent estimates of consumption and activity rates were obtained for Lakes Hertel (average growth = 172 J·day^{-1}) and Memphremagog (average growth = 595 J·day^{-1}). Daily consumption rates averaged 720 J·day^{-1} in Lake Hertel and 1457 J·day^{-1} in Lake Memphremagog. SCG and bioenergetic methods provided similar activity estimates for Lake Hertel (<2.5% difference) and diverged by 0.4–82% for Lake Memphremagog depending on initial values of fish weight or consumption inputted in the bioenergetic equation. Regardless of the method employed, activity rates of fish from Lake Hertel were proportionally higher (24% of consumption rates) than those from Lake Memphremagog (on average 13% of consumption rates). Our work supported the suggestion that populations with slower growth rates may be associated with proportionally higher activity rates.

Résumé : Nous avons comparé la méthode stéréocinématographique (SCG) pour estimer les taux d'activité de perchaudes (*Perca flavescens*) avec l'approche plus traditionnelle de la bioénergétique. Nous avons aussi comparé les taux d'activité de perchaudes provenant de deux populations ayant des taux de croissance contrastants pour vérifier l'hypothèse selon laquelle les poissons ayant des taux de croissance plus faibles sont caractérisés par des taux d'activité plus élevés. Nous avons tenté de corroborer la méthode SCG en comparant les valeurs de coûts énergétiques obtenus à l'aide d'observations des mouvements de poissons à des estimés obtenus en utilisant la différence entre les taux de consommation et de croissance dérivés de données de terrain (méthode bioénergétique). Des estimés indépendants de consommation et d'activité ont été obtenus pour les lacs Hertel (croissance moyenne = 172 J·jour^{-1}) et Memphrémagog (croissance moyenne = 595 J·jour^{-1}). Les taux journaliers de consommation valaient en moyenne 720 J·jour^{-1} pour le lac Hertel et 1 457 J·jour^{-1} pour le lac Memphrémagog. La méthode SCG et l'approche bioénergétique ont fourni des estimés similaires d'activité pour le lac Hertel (<2,5% différence) et divergeaient de 0,4%–82% pour le lac Memphrémagog, dépendant des valeurs initiales de masse de poisson ou de consommation utilisées dans l'équation bioénergétique. Peu importe la méthode employée, les taux d'activité des poissons du lac Hertel étaient proportionnellement plus élevés (24% du taux de consommation) que ceux du lac Memphrémagog (en moyenne 13% du taux de consommation). Notre étude supporte l'hypothèse selon laquelle les populations ayant des taux de croissance plus faibles peuvent être associées avec des taux d'activité proportionnellement plus élevés.

Introduction

Bioenergetic models have been used as a framework to forecast the potential influence of changes in environmental conditions on different characteristics of freshwater communities (Stewart et al. 1981; Schindler et al. 1993; Bevelhimer and Adams 1993; LaBar 1993; Krohn et al. 1997). Fish growth and consumption rates have often been the subject of bioenergetic modeling (Eby et al. 1995; Rudstam et al. 1995; Salonen et al. 1996). These variables, combined with values of fish abundance, define the productivity of fish populations and the intensity of the predation pressure im-

Received March 27, 1998. Accepted February 26, 1999.
J14519

N. Aubin-Horth,[1] J. Gingras, and D. Boisclair.[2] Département de sciences biologiques, Université de Montréal, C.P. 6128, Succursale Centre-ville, Montréal, QC H3C 3J7, Canada.

[1]Present address: Centre interuniversitaire de recherche sur le saumon atlantique (CIRSA), Département de biologie, Université Laval, Cité universitaire, Québec, QC G1K 7P4, Canada.
[2]Author to whom all correspondence should be addressed. e-mail: daniel.boisclair@umontreal.ca

© 1999 NRC Canada

posed by fish on their prey community. Fish growth and productivity are of interest because they determine the value of a fish population for fisheries purposes. Foraging intensity on lower trophic levels and its effect on invertebrate communities have been assumed to represent a key component of trophic interactions, particularly in lakes (Carpenter et al. 1996; Proulx et al. 1996).

The quality of the predictions made by bioenergetic models has been argued to depend on numerous assumptions and on the reliability of submodels developed to adequately represent metabolic rates in the field (Hansen et al. 1993; Ney 1993). Activity rates may be the least understood component of fish bioenergetic models (Lucas et al. 1991; Hewett and Johnson 1992). Suggestions that activity may represent a large and variable component of fish energy budgets (Boisclair and Leggett 1989*c*) have further emphasized the possibility that inappropriate assumptions regarding activity costs may affect the predictions made by bioenergetic models (Kitchell et al. 1977; Madon and Culver 1993; Rowan and Rasmussen 1996). One key implication of this proposition is that activity rates may contribute to explaining the range of growth rates observed under natural conditions (Minton and McLean 1982; Koch and Wieser 1983; Boisclair and Leggett 1989*c*). It can therefore be hypothesized that there may be a negative relationship between fish growth and activity rates (Boisclair and Leggett 1989*c*).

With the exception of enclosure experiments (Boisclair 1992*b*; Boisclair and Sirois 1993; Sirois and Boisclair 1995; Marchand and Boisclair 1998) and telemetry (Lucas et al. 1991; Demers et al. 1996; Briggs and Post 1997), fish activity rates are generally quantified using the difference between estimates of consumption and growth rates (Boisclair and Leggett 1989*c*; Madon and Culver 1993; Rowan and Rasmussen 1996). This strategy prevents the analysis of relationships between different components of fish energy budgets under natural conditions, since these are not statistically independent. However, recent studies indicate that underwater videocamera observations may allow one to obtain accurate and independent estimates of activity rates for littoral fish (Trudel and Boisclair 1996).

The objectives of our study were to (*i*) compare in situ activity rates of yellow perch (*Perca flavescens*) estimated using underwater videocameras with values obtained using the bioenergetic approach and (*ii*) compare activity rates of fish from two populations with contrasting growth rates to test the hypothesis that fish with lower growth rates are characterized by higher activity rates.

Material and methods

Species and lakes studied

We sampled age 1+ yellow perch from Lakes Hertel (45°32′N 73°09′W) and Memphremagog (45°12′N, 75°13′W) in the Eastern Townships region of Quebec. Perch aged 1+ were selected for our work because they are an abundant component of the fish communities in the study area and are largely limited to the littoral zone of lakes (Scott and Crossman 1973). This allowed us to collect an appropriate number of samples to estimate growth and food consumption rates. The high abundance of 1+ perch was also expected to facilitate the filming of a sufficient number of fish movements. Furthermore, we expected that fish size differences between lakes would be minimized by focusing on a young age-class. The lakes sampled were selected on the basis of known differences in perch growth rates (Boisclair and Leggett 1989*a*). Fish and invertebrate communities and limnological characteristics of the two lakes sampled have been described by Boisclair and Leggett (1989*b*) and Rasmussen (1988, 1993). Mean water temperature ranged from 19 to 25°C (Lake Hertel) and from 17 to 23°C (Lake Memphremagog) during sampling.

Sampling

The sampling schedule involved three visits of three consecutive days to each lake. Each visit to a lake is hereafter referred to as a sampling period. Sampling periods were initiated at 11- to 18-day intervals between June and August 1995 (Julian days 171–215). Fish were sampled to estimate growth, consumption, and activity rates on each day of a given sampling period. This strategy was adopted to ensure that our data would adequately reflect potential day-to-day variations in consumption and activity rates (Trudel and Boisclair 1993, 1996).

Growth rates

On each sampling day, 10 perch of a length expected to correspond to age 1+ fish were collected at 4- to 8-h intervals using a 40 × 2 m seine (mesh size = 0.2 cm). This sampling schedule was used to match the requirements to estimate prey consumption rates (see Consumption rates below). On the first and last sampling periods, 5–15 additional perch in the same size range were frozen in the field and kept to quantify their energetic content in the laboratory. Each fish was killed immediately following capture from an overdose of a fish anaesthetic (2-phenoxyethanol, 1 $mL \cdot L^{-1}$). However, fish kept for calorimetric analyses were killed by suffocation to avoid the potential effect of our anaesthetic on fish energetic content. All perch were measured (± 0.1 cm) and weighed (± 0.01 g wet) in the field. Calorimetry of 1+ perch was performed using a microbomb calorimeter. These fish were homogenized individually using a Cyclone sample mill. Energetic content of each fish was determined in triplicate. The age of the perch used for growth and calorimetry estimation was determined using their scales. These procedures, after the exclusion of a few 2+ fish, resulted in 40 estimates of total length and mass (wet and dry; 60°C for 24 h) of 1+ perch for any given sampling day and 5–15 estimates of energetic content for the first and last sampling period. These data were also used to quantify wet to dry weight ratios and length–weight relationships of 1+ perch.

The numerical density of 1+ perch in the littoral zone (fish per cubic metre) was estimated in each sampling period by performing a total of 16 seine hauls per lake. The volume of the littoral zone sampled by each haul was determined using the geometric formulae of a truncated cylinder to account for variations of slopes of the littoral zone among sampling sites.

Consumption rates

Consumption rates of 1+ perch were estimated for each sampling day by combining information on variations of fish digestive tract contents and gastric evacuation rates (Eggers 1977; Boisclair and Leggett 1988). Fish collected at 4- to 8-h intervals during the sampling for growth were dissected within 3 h of capture to estimate the complete digestive tract contents (CDTC) of individuals (60°C for 24 h; ± 0.0001 g dry). This procedure, after the exclusion of a few 2+ fish, resulted in 40 estimates of CDTC for each sampling day. The sampling interval and number of fish used to estimate ration were selected on the basis of previous studies that suggested that the sampling of 10 fish at 8-h intervals was sufficient to estimate daily consumption rates of fish (Boisclair and Leggett 1988). Energetic content of the food consumed by fish was estimated in triplicate by pooling the prey found in the digestive tract of all age 1+ perch sampled within a given sampling period.

© 1999 NRC Canada

Evacuation rates of 1+ perch were estimated once for each combination of sampling period and lake using the decrease in digestive tract contents of fish collected in the lake near their peak of digestive tract contents (Boisclair and Leggett 1988).

Activity rates

Activity rates are hereafter used to represent exclusively the cost of performing external movements. Estimation of fish activity rate was achieved using the stereocinematographic (SCG) method (Ménard 1991; Boisclair 1992*a*). This method involves the filming of fish under field situations with pairs of underwater videocameras. Each pair of cameras allows the estimation of a series of *x,y,z* coordinates for each fish moving within the volume under observation. In our study, fish were observed using two pairs of cameras. Each pair of cameras was mounted on a metal support and anchored 10–12 m apart in the littoral zone of the lake the evening before the beginning of a sampling period. Scuba divers installed a pair of cameras at 1 m and another pair at 2 m below the water surface. Both camera systems were about 0.3 m from the bottom of the lakes. Fish were filmed during five 1-h periods on each sampling day (beginning at 6:00, 11:00, 14:00, 17:00, and 19:00). Seining, required to estimate growth or consumption rates and fish abundance, was never performed within 10 m of the videocamera systems. Furthermore, seining was always done within 1 h after a filming period.

Computations

Growth rates

Growth rates were estimated on a weight (grams wet per day) and an energetic basis (joules per day). Growth was calculated as the difference between the geometric mean weight or energetic content value of 1+ perch at the beginning and at the end of the study divided by the total sampling interval.

Consumption rates

Mean daily ration (D_i, grams dry per day) was determined using the Eggers model (1977) as modified by Boisclair and Leggett (1988). Cumulative seasonal consumption (D_T, joules) was estimated by summing the product of daily ration values and prey energetic content (joules per gram dry) for the time interval covered by our sampling. Values of D_i between sampling periods were obtained by linear interpolation. The 95% CI's associated with our values of daily and seasonal consumption rates were estimated using Monte Carlo simulations (described in detail by Trudel and Boisclair 1993).

Activity rates

The series of *x,y,z* Cartesian coordinates of the head and the tail of fish were used to estimate the swimming characteristics of fish and the size of the fish observed. The computations to obtain these variables from *x,y,z* coordinates have been described in detail by Ménard (1991), Boisclair (1992*a*), and Boisclair and Tang (1993), who also validated the use of this method in laboratory and enclosure experiments. In summary, the coordinates of the position of a given fish at two consecutive seconds permitted the estimation of fish swimming speed (centimetres per second). Speeds slower than 0.5 $cm \cdot s^{-1}$ were excluded from further analysis because such speeds are expected to be associated with negligible energy expenditure (Krohn and Boisclair 1994). The coordinates of the head and the tail of a fish at a given instant were used to estimate its length. When fish were observed for more than 1 s, fish length was taken as the mean length estimated during the time of observation. Perch of a length outside the range known to correspond to age 1+ for that species at the time of the filming (see Growth rates under Sampling above) were excluded from our analysis. The number of movements performed by fish during a given hour (number of swimming seconds (SS) per cubic metre per hour) was calculated as the total number of seconds that perch of a length within the expected range of 1+ were observed swimming. When more than one 1+ perch was seen swimming in the image during a given second, SS for that second was taken as the total number of 1+ perch seen swimming. Fish orientation and distribution within the volume sampled by our videocameras (e.g., fish directly facing the cameras or hiding part of another fish) did not always allow us to estimate their position as *x,y,z* Cartesian coordinates. In these cases, swimming characteristics were not taken but the time spent swimming by these fish was included in our SS values.

Cumulative seasonal activity (A_T, joules) was determined by adding mean daily activity rate values (A_D, joules per fish per day). The A_D values for days between sampling periods were determined by linear interpolation. The A_D was defined as the quantity of energy spent swimming by an average individual fish during 1 day and was estimated as the sum of the mean hourly activity rates (A_F, joules per fish per hour). Our filming schedule allowed us to estimate five values of A_F. Hourly activity rates between filming hours were estimated by linear interpolation. The cameras we used did not allow clear images of fish movements at night. This represents a limitation of the method that we used and of our study. We attempted to minimized the impact of this problem by using the characteristics of a significant positive relationship between fish hourly activity rates and consumption rates (Boisclair 1992*b*). The intercept of this relationship suggests that activity rates are close to zero when no food is consumed. Since, in our study, we observed that 1+ perch did not consume a significant quantity of food during the night, we assumed that activity rates at night were also negligible.

We could not obtain one A_F for each combination of filming hour (H), sampling day, and sampling period because, on some occasions, we could only estimate a few swimming speeds for a specific H of a given day. We therefore estimated only one A_F per hour H for each sampling period. Our A_F values should therefore be taken as hourly activity rates of 1+ perch at hour H averaged over the three consecutive days of a given sampling period. Similarly, our estimates of A_D should be taken as daily activity rates averaged over three consecutive days.

The A_F was obtained by dividing the total energy spent for activity per cubic metre per hour (A_H, joules per cubic metre per hour) by the average numerical density of age 1+ perch (fish per cubic metre). The A_H was calculated as

$$(1) \qquad A_H = \frac{E_H}{V \cdot pU}$$

where E_H is the sum of the swimming costs obtained for three consecutive days at hour H using fish for which swimming characteristics could be estimated (joules per hour), V is the sum of the volumes sampled by the two pairs of videocameras (cubic metres) for three consecutive days at hour H, and pU the proportion of SS effectively used to estimate swimming speeds at hour H for a given sampling period. Steps required to estimate these variables have been described by Trudel and Boisclair (1996).

These computations were used to estimate fish activity rates for all days and lakes except for the first sampling period in Lake Memphremagog. On this occasion, manipulations of the cameras caused a drifting of the relative positions of their optical axes that prevented us from performing a proper calibration. This situation allowed us to approximate the number of movements performed by fish but not to estimate fish length or swimming speeds. However, as suggested by Trudel and Boisclair (1996), hourly activity rates may be more directly related to the number of SS than to fish swimming speed per se. We therefore circumvented the lack of precise values of speed by assessing the existence of a relationship between hourly activity rates and the number of SS observed. Such

© 1999 NRC Canada

Fig. 1. Mean yellow perch mass for the three sampling periods for Lakes Hertel (solid circles) and Memphremagog (open circles). The 95% CI's associated with these values are represented by the vertical lines.

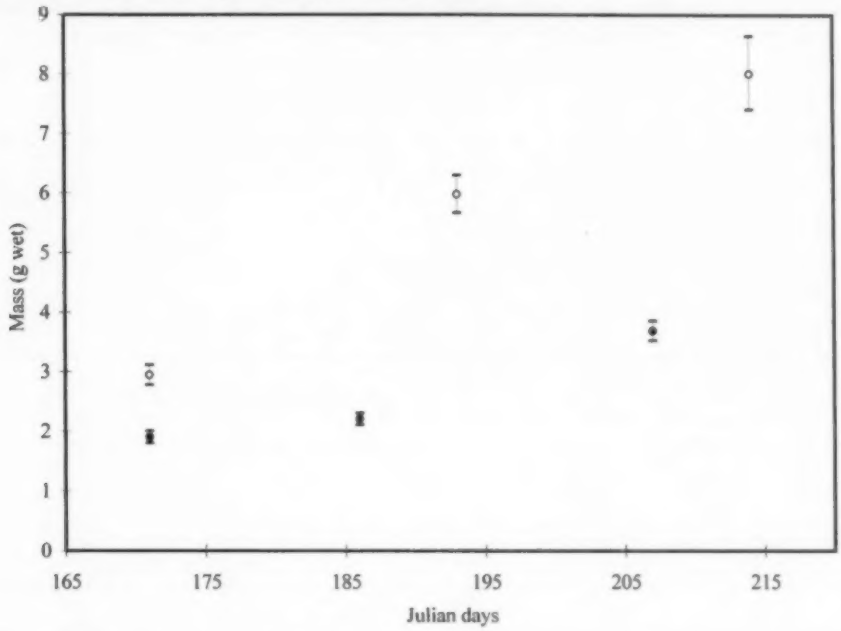

a relationship could be (and eventually was; see Results) used to estimate a series of hourly activity rates for the first sampling period of Lake Memphremagog. The 95% CI's of our activity rates were estimated using the bootstrap method (Sokal and Rohlf 1995).

Bioenergetic modeling

Bioenergetic modeling was performed to compare our estimates of activity rates with values obtained by difference using the bioenergetic equation and to compare our field-derived consumption rates with predictions of the model. These comparisons were made with the computer version of the bioenergetic model developed by Kitchell et al. (1977). Model parameters corresponded to the values suggested by Hewett and Johnson (1992), except for the intercept of the relationship between respiration rate, fish weight, and water temperature. This intercept was modified because the original respiration model was developed using respiration rates obtained for fed fish allowed to swim freely in rectangular respirometers (Solomon and Brafield 1972). Under these conditions, respiration rates comprise costs of digestion and activity rates displayed by fish under laboratory conditions. Hence, activity rates estimated by difference (activity = consumption – [growth + respiration + excretion + egestion]) using the original respiration model may be underestimated and may be inappropriate for comparisons with the net activity values obtained during our study. We evaluated the proportion of oxygen consumption due to activity rates in the respiration values of Solomon and Brafield (1972) by comparing their results with those obtained by Mann (1965). Mann (1965) conducted a series of experiments with perch of a size range identical to that used by Solomon and Brafield (1972). Perch respiration was estimated under rapid and slow current speeds (no data on absolute speeds were provided in the paper). Respiration data suggest that oxygen consumption by fish in rapid currents is similar to that predicted by the model of Solomon and Brafield (1972) (and used in the model of Kitchell et al. 1977). Furthermore, Mann (1965) noted that respiration in slow currents was 42% lower than that in fast currents. We take this comparison as an indication that at least 42% of the respiration estimates predicted using the parameters suggested by Hewett and Johnson (1992) represent net activity costs. Fish used by Mann (1965) and by Solomon and Brafield (1972) had been fed a few hours before the respirometry experiments. Hence, heat increment (costs of digestion) may also be included in the respiration rates obtained by both authors. Heat increment has been suggested to represent 15–23% of the respiration rates that presumably represented standard metabolic rate in these studies. Hence, it can be expected that actual standard metabolic rate may be 57–65% lower than the values proposed by Solomon and Brafield (1972). Similarly, analysis performed by Trudel and Boisclair (1994) suggested that the intercept of the respiration rate model for northern redbelly dace (*Phoxinus eos*) should be decreased by 60% to account for the fraction of oxygen consumption caused by activity rates and heat increment during respirometry experiments. This correction allowed them to estimate activity rates using a bioenergetic model that were on average within 7.4% of values obtained using videocameras. We therefore decreased the intercept of the respiration model suggested by Hewett and Johnson (1992) by 60% (RA = 0.00432). The bioenergetic model was inputted with our estimates of fish weight, perch and prey energetic content, and water temperature.

Results

Growth rates

The mean weight of 1+ perch increased from 1.9 to 3.7 g wet in Lake Hertel and from 2.9 to 8.0 g wet in Lake Memphremagog (Fig. 1). Mean fish weight varied significantly among sampling periods and between populations (Table 1). The interaction term was also significant, supporting the apparent divergence of mass trajectories in the two study lakes (Fig. 1). Seasonal mean growth rates of 1+ perch

© 1999 NRC Canada

Table 1. Statistics of the variability between lakes and among sampling periods in yellow perch weight, yellow perch energetic content, CDTC, and prey energetic content.

		F	df	*p*
Weight	Lake	1545.06	1,608	<0.0001
	Sampling period	719.2	2,608	<0.0001
	Interaction	11.43	2,608	<0.0001
Perch energetic content	Lake	11.40	1,75	<0.001
	Sampling period	1.84	1,75	>0.1
	Interaction	2.917	1,75	>0.09
CDTC	Lake	228.4	1,573	<0.0001
	Sampling period	48.7	2,573	<0.0001
	Interaction	73.1	2,573	<0.0001
Prey energetic content	Lake	0.79	1,6	>0.4
	Sampling period	0.56	1,6	>0.4
	Interaction	1.05	1,6	>0.3

Table 2. Seasonal mean rate and partitioning of energy acquired via consumption (*C*) among growth (*G*), activity (*A*), standard metabolism (*R*), and heat increment, fecal, and urinary losses (HI, *F*, *U*) for the whole sampling period.

	C (J·day^{-1})	*G* (J·day^{-1})	*A* (J·day^{-1})	*R* (J·day^{-1})	HI, *F*, *U* (J·day^{-1})	Total (%)
Lake Hertel	720	172	172	104	277	
% of energy budget		23.9	23.9	14.4	38.5	100.7
Lake Memphremagog	1327	595	182	190	507	
% of energy budget		44.8	13.7	14.3	38.2	111.1

ranged from 0.05 (Lake Hertel) to 0.11 g wet·day^{-1} (Lake Memphremagog).

Mean energetic content of 1+ perch, between the beginning and end of our sampling, was relatively constant in Lake Hertel (18 782 – 18 715 J·g dry^{-1}) but tended to increase in Lake Memphremagog (19 406 – 20 461 J·g dry^{-1}). Mean energetic content of 1+ perch varied significantly between populations but not among sampling periods. The interaction term was not significant (Table 1). A sum of squares simultaneous test procedure (Sokal and Rohlf 1995, p. 254) was used to make a posteriori multiple comparisons. This test was selected because it is particularly appropriate to compare means obtained using unequal sample sizes. These comparisons indicated that the energetic content of 1+ perch from Lakes Hertel and Memphremagog was not statistically different at the beginning of the season (sum of squares among = 0.1965, critical sum of squares = 1.6479, $p > 0.05$). However, significant between-lake differences were found at the end of our sampling ($p < 0.05$). Seasonal mean growth rates on an energetic basis were 3.5 times faster in Lake Memphremagog (595 J·day^{-1}) than in Lake Hertel (172 J·day^{-1}) (Table 2).

Consumption rates

Variations of the CDTC of 1+ perch indicated the presence of significant diel feeding cycles for seven of the eight daily surveys performed in Lake Hertel ($0.0001 < p < 0.002$) and for five of the nine sampling days realized in Lake Memphremagog ($0.001 < p < 0.02$). CDTC of 1+ perch was highest at 14:00 for 75% of the surveys performed in Lake Hertel (0.037 g dry) and for 55% of the sampling days in Lake Memphremagog (0.110 g dry). CDTC of 1+ perch from a given lake did not vary significantly among days of specific sampling periods ($0.06 < p < 0.8$) except during the third sampling period in Lake Hertel. CDTC displayed significant variations among sampling periods and between lakes. The interaction term was also significant (Table 1). A posteriori comparisons indicated that there was no statistically significant difference between the CDTC values of Lakes Hertel and Memphremagog at the beginning of the sampling (sum of squares among = 2.21×10^{-5}, critical sum of squares = 3.13×10^{-4}, $p > 0.05$).

Prey energetic content ranged from 18 414 (June) to 18 803 J·g dry^{-1} (August) in Lake Hertel and from 18 606 to 16 081 J·g dry^{-1} in Lake Memphremagog. Prey energetic content did not vary among sampling periods or between lakes. The interaction term was not significant (Table 1).

Evacuation rates ranged from 0.15 to 0.26·h^{-1} in Lake Hertel and from 0.13 to 0.19·h^{-1} in Lake Memphremagog. These values did not vary significantly (analysis of covariance, $F_{5,21} = 1.08$, $p > 0.05$). Mean daily ration ranged from 0.024 to 0.054 g dry·day^{-1} in Lake Hertel and from 0.028 to 0.132 g dry·day^{-1} in Lake Memphremagog (Fig. 2). The 95% CI represented, on average, 24 and 26% of the mean daily ration of fish from Lakes Hertel and Memphremagog, respectively.

We noted that growth rates estimated for 1+ perch from Lake Memphremagog during the first sampling period represented, on average, 129% of the energetic value of the quantity of food consumed by these fish (Fig. 3*b*). This observation may suggest that (*i*) our estimates of initial fish size in Lake Memphremagog are underestimated (which would inflate our growth rates between the first and second sampling periods) and (or) (*ii*) our values of ingestion rates during the first sampling period at Lake Memphremagog are underestimated. An underestimation of initial mean fish weight by 1.4 g (from our original estimate of 2.9 g wet to a corrected 4.3 g wet) would render values of gross growth efficiency (GGE) for the first sampling period similar to those obtained for the two other sampling periods in Lake

© 1999 NRC Canada

Fig. 2. Mean yellow perch daily ration estimated with field-derived values for the three sampling periods for Lakes Hertel (solid circles) and Memphremagog (open circles). The 95% CI's associated with these values are represented by the vertical lines.

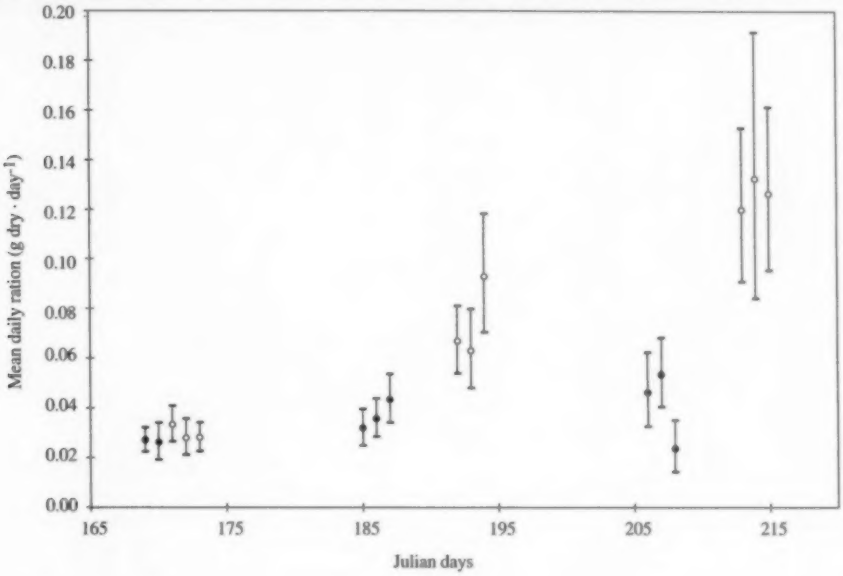

Memphremagog. Alternatively, our estimates of daily consumption rates during the first sampling period would have to be underestimated 2.6-fold (from our original value of 0.03 g dry·day^{-1} to 0.08 g dry·day^{-1}) to achieve comparable GGE. We have no basis for determining the relative role played by the two potential sources of error (initial fish weight and initial daily ration) on the unrealistic values of GGE obtained in Lake Memphremagog during the first sampling period. Therefore, our original (2.9 g wet) and corrected values of initial mean fish weight (4.3 g wet) are hereafter adopted as representing a probable range of mean weight during the first sampling period in Lake Memphremagog. Similarly, the most probable range of daily ration during the first sampling period in Lake Memphremagog is taken as 0.03–0.08 g dry·day^{-1}. These values are hereafter referred to as original and corrected initial mean fish weight and daily ration (IDR_o and IDR_c). Hence, on a seasonal basis, growth represented 24% of the energy consumed by 1+ perch in Lake Hertel (Fig. 3*a*). Corresponding values for fish from Lake Memphremagog ranged from 33% (using IDR_o and corrected value of initial mean fish weight) to 45% (using IDR_o and original value of mean fish weight) depending on the variables taken to estimate GGE (Fig. 3*b*). Daily ration averaged 720 J·day^{-1} in Lake Hertel and 1327–1587 J·day^{-1} in Lake Memphremagog (Table 2). Cumulative seasonal consumption (±95% CI) was 26 636 J ± 13% in Lake Hertel (from Julian day 171 to 207) and 58 314 J ± 7% in Lake Memphremagog (from Julian day 171 to 215 using IDR_o). Cumulative seasonal consumption estimated for Lake Memphremagog using IDR_c was 69 744 J. Consequently, despite errors that may affect our values of initial fish weight or ingestion rates in Lake Memphremagog, our original interpretation that fish growth, consumption, and growth efficiency were higher in this lake than in Lake Hertel remains.

Activity rates

Swimming speeds estimated for 1+ perch observed in Lake Hertel ranged from 0.9 to 32.3 cm·s^{-1} and had a geometric mean of 11.0 cm·s^{-1}. The range (2.2 and 32.6 cm·s^{-1}) and the overall geometric mean (11.7 cm·s^{-1}) of the speed obtained for perch in Lake Memphremagog were within 7.6% of the values found in Lake Hertel. Swimming speeds were ln transformed prior to analysis to correct for the lack of normality of the samples. Normality of the distribution of the ln-transformed samples was verified with a Kolmogorov–Smirnov test. Swimming speeds did not vary significantly between lakes but displayed statistically significant differences between sampling periods. The interaction term was not significant (Table 3), indicating that speed tended to follow similar seasonal trajectories for the two lakes studied. The speeds observed corresponded to values ranging from 0.14 to 6.4 fish body lengths (BL)·s^{-1}) for Lake Hertel and from 0.5 to 4.7 BL·s^{-1} for Lake Memphremagog. Relative swimming speed did not vary significantly between lakes but presented statistically significant differences among sampling periods. The interaction term was also significant (Table 3).

The number of movements performed by 1+ perch ranged from 0 to 366 SS·m^{-3}·h^{-1} in Lake Hertel and from 0 to 163 SS·m^{-3}·h^{-1} in Lake Memphremagog. The mean number of movements performed by 1+ perch in Lake Hertel (31 SS·m^{-3}·h^{-1}) was four times larger than that observed in Lake Memphremagog (7 SS·m^{-3}·h^{-1}). The number of movements was ln transformed prior to analysis to correct for the lack of normality of the samples. The mean number of movements varied significantly between lakes but not among sampling periods. The interaction term was not significant (Table 3).

There was a 1.6-fold difference in average numerical density of age 1+ perch between Lakes Memphremagog (0.0124 fish·m^{-3}) and Hertel (0.0195 fish·m^{-3}). This difference could

© 1999 NRC Canada

Fig. 3. Absolute yellow perch consumption rate (broken line) and growth rate (solid line) for the whole sampling period for (*a*) Lake Hertel and (*b*) Lake Memphremagog. Diamonds represent field-derived values of consumption.

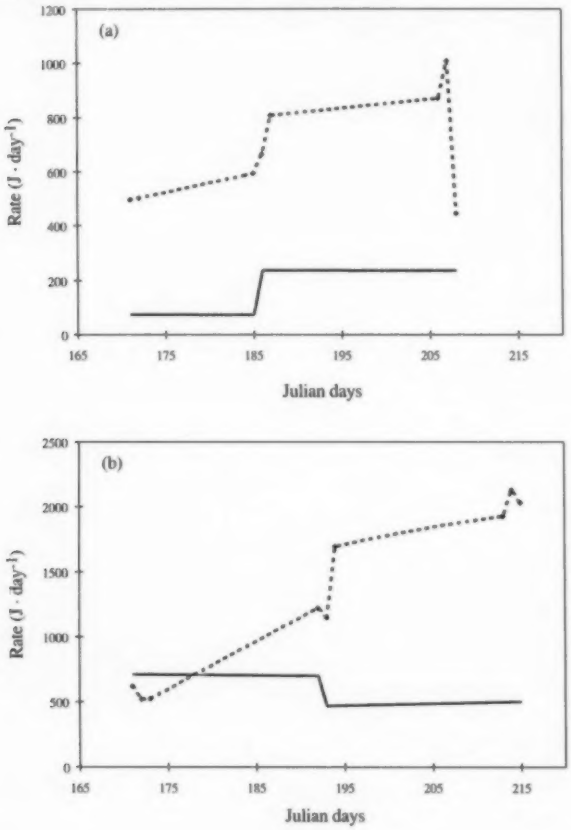

therefore be responsible for the higher number of movements observed in Lake Hertel. The mean number of movements of 1+ perch corrected for their density ranged from 565 SS·1+ perch^{-1}·h^{-1} in Lake Memphremagog to 1590 SS·1+ perch^{-1}·h^{-1} in Lake Hertel. The number of movements corrected for perch density varied significantly between lakes but not among sampling periods. The interaction term was not significant (Table 3).

Mean hourly activity rates (A_F) ranged from 1.67 to 36.4 J·fish·h^{-1} in Lake Hertel and from 3.77 to 38.9 J·fish·h^{-1} in Lake Memphremagog. The 95% CI associated with these values represented, on average, 30 and 49% of the respective means. There was no significant relationship between mean hourly activity rates and mean swimming speed during that hour (Pearson correlation test: Hertel, $r = 0.04$, $p > 0.8$; Memphremagog, $r = 0.002$, $p > 0.9$). Total energy spent for activity (A_H) was positively related to the number of movements performed by fish in Lakes Hertel ($r = 0.78$, $p < 0.005$) and Memphremagog ($r = 0.815$, $p < 0.007$). A regression analysis was performed using number of movements and A_H values from both lakes ($y = 0.4902x$; $r^2 = 0.71$, $p < 0.0001$). This relationship was used to predict a series of hourly activity rates, and hence of mean daily activity rate (A_D), for the first sampling period in Lake Memphremagog when perch SS, but no speed, could be quantified. Mean daily activity rates ranged from 45.6 to 252.0 J·fish·day^{-1} in Lake Hertel and between 6.3 and 326.6 J·fish·day^{-1} in Lake Memphremagog. The 95% CI associated with these values represented, on average, 16 and 35% of the mean value, respectively (Fig. 4). Cumulative seasonal activity rate (A_T) was 6335 J in Lake Hertel and 8022 J in Lake Memphremagog (on average, 172 and 182 J·day^{-1}, respectively) (Table 2). On a seasonal basis, activity rates represented 24% of the energy budget of fish from Lake Hertel (Table 2). Corresponding values for 1+ perch from Lake Memphremagog ranged from 12% (using IDR_c) to 14% (using IDR_o).

Bioenergetic modeling

Seasonal cumulative activity rate determined by difference using a bioenergetic model inputted with our original values of growth and consumption rates was 6192 J in Lake Hertel. This estimate was within 2.5% of the value obtained using SCG (6335 J). For Lake Memphremagog, three series of bioenergetic simulations were performed. First, the model was inputted with our original values of fish weight (and hence growth) and ingestion. Second, activity rates were obtained using corrected values of fish weight and our original estimates of ingestion. Third, we used our original values of fish weight but the corrected values of ingestion rates. Based on our original values of growth and consumption rates, seasonal cumulative activity rates of 1+ perch from Lake Memphremagog represented 1424 J. Corresponding values obtained using either our corrected fish weight or corrected daily ration estimates were 7988 and 8055 J, respectively. These simulations suggest that the difference between activity values obtained using a bioenergetic model and the SCG method (8022 J) ranges from 0.4 to 82% depending on the assumption adopted during the modeling exercise.

If real activity rates were closer to bioenergetic model estimates than to SCG method estimates, activity for fish from Lakes Hertel and Memphremagog would represent 23 and 2%, respectively, of the seasonal consumption. Seasonal activity multipliers (ACTM = activity + standard metabolism/standard metabolism) estimated using our modified version of the model for standard metabolism and the SCG method ranged from 2.0 for 1+ perch from Lake Memphremagog to 2.6 for fish from Lake Hertel. The ACTM value estimated by difference using the bioenergetic model based on our original values of growth and consumption rates represented 1.17 for Lake Memphremagog and 2.6 for Lake Hertel.

Discussion

The strategy that we adopted to validate the use of the SCG method to estimate fish activity cost was to compare results obtained using this approach with those of the more common bioenergetic equation (activity = consumption – growth – metabolism). While we agree that convergence to a given result by two independent approaches does not constitute a validation per se, we believe that it nevertheless improves the probability that results obtained are accurate. In this context, our analyses indicate that both methods converge to provide similar activity rates for 1+ perch from

© 1999 NRC Canada

Fig. 4. Mean daily activity (A_D) of 1+ yellow perch estimated with the SCG method for Lakes Hertel (solid circles) and Memphremagog (open circles). The 95% CI's associated with these values are represented by the vertical lines except for the data point of the first sampling period in Lake Memphremagog where it was omitted for clarity.

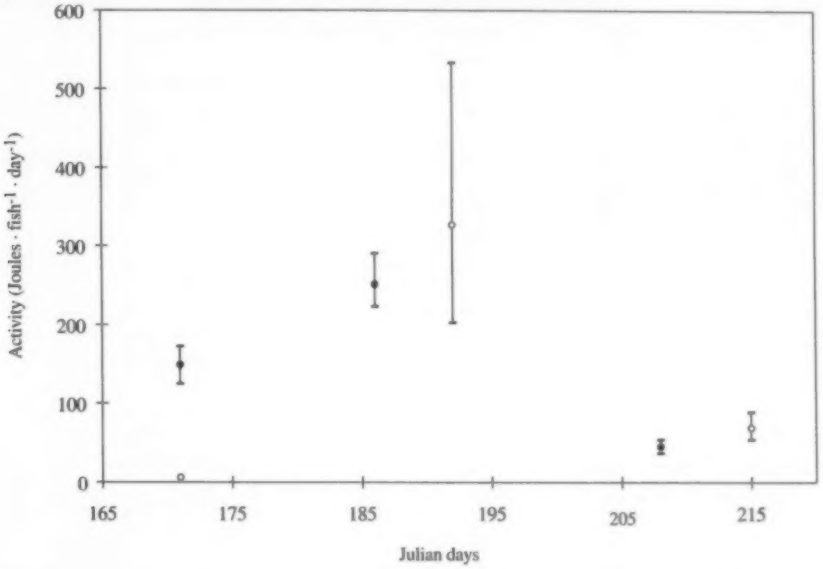

Table 3. Statistics of the variability between lakes and among sampling periods in swimming characteristics of 1+ yellow perch.

		F	df	*p*
Swimming speed (cm·s^{-1})	Lake	2.10	1,258	>0.1
	Sampling period	11.54	1,258	<0.001
	Interaction	1.09	1,258	>0.29
Swimming speed (BL·s^{-1})	Lake	0	1,258	>0.9
	Sampling period	10.99	1,258	<0.001
	Interaction	11.52	1,258	<0.001
SS·m^{-3}·h^{-1}	Lake	12.98	1,143	<0.0001
	Sampling period	0.22	2,143	>0.8
	Interaction	0.45	2,143	>0.6
SS·1+ perch^{-1}·h^{-1}	Lake	9.78	1,143	<0.002
	Sampling period	0.16	2,143	>0.8
	Interaction	0.45	2,143	>0.6

Lake Hertel (within 2.5%) but may diverge by as little as 0.4 and by as much as 82% for fish from Lake Memphremagog depending on the values inputted during computations.

The discrepancy between activity estimates obtained for Lake Memphremagog may be caused by errors in estimates of fish weight or consumption rates (that could affect activity values obtained using the bioenergetic approach) at the beginning of our sampling season. Our calculations indicate that an underestimation of initial mean fish weight and initial ingestion rates by 46 and 151%, respectively, can explain the difference between activity rates obtained following bioenergetic and SCG methods in Lake Memphremagog. Individual growth rate estimated using the mean weight of age 1+ perch for the first and second sampling periods in Lake Memphremagog could also be biased by size-selective mortality. Mean individual growth rate could be overestimated if predators consistently consumed the smaller individuals of the population during this period (Sogard 1997). In a laboratory experiment on conspecific predation (Post and Evans 1989), adult yellow perch (230–270 mm total length) selected small individuals (52–59 mm total length) over large individuals (66–73 mm total length) in more than 80% of the experiments. It could be hypothesized that this type of situation may have occurred in Lake Memphremagog. In this lake, size variations were always larger than in Lake Hertel (Fig. 1), a condition necessary for the occurrence of detectable size-selective mortality (Sogard 1997).

The difference observed between activity costs determined using both methods may not be caused only by inaccurate estimation of initial fish weight or ingestion in Lake Memphremagog but also by errors associated with the SCG method. The quality of the activity values obtained using the SCG method depends on the accuracy of five estimates: (*i*) the position of objects or fish in space at any

© 1999 NRC Canada

given moment, (*ii*) the predicted costs of performing movements for a given combination of mass and speed, (*iii*) the predicted costs of activity using the number of movements performed as the independent variable, (*iv*) the number of movements observed, and (*v*) the density of 1+ perch in the littoral zone. The error associated with the position, and hence with fish length, speed, and the volume sampled by the cameras, has been shown by Boisclair (1992*a*) to average 4.5% of the mean. Furthermore, the 95% CI around the mean prediction of the empirical model used to estimate the costs of performing movement from swimming speed and mass was evaluated to represent on average 24% of the predicted mean (Boisclair and Tang 1993). Because the magnitude of error on estimates of position and on the predictions by the Boisclair and Tang (1993) model is similar for both lakes, these errors may not explain the substantial difference in activity rates found only in Lake Memphremagog. The lack of speed estimates in the first sampling period in Lake Memphremagog forced the use of a relationship between fish movements (SS) and and total energy spent for activity (A_H). The 95% CI associated with the mean activity value predicted using this relationship represented between 30 and 32% of the mean. Mean daily activity for the first sampling period estimated using this method represented 6.3 J·day^{-1}. Using the lower or the upper 95% CI of activity during the first sampling period to estimate seasonal activity changes the cumulative activity costs by only 21 J (<0.3% of our original value). The estimation of the absolute number of movements of 1+ perch seen in the cameras required a direct count of fish. We assessed the precision of our estimates of SS by having two different observers analyzing 15 h of recorded video. The maximum difference between counts of SS by two observers was 5%. The accuracy of fish density values used with the SCG method is important for transforming activity costs per unit volume into activity rates per fish. If the method used to obtain this value underestimated actual fish density in the immediate surroundings of the cameras, activity per individual fish would be overestimated. The density of age 1+ perch in Lake Memphremagog that would be necessary to explain the difference between activity estimated with the bioenergetic and the SCG methods is equal to 0.074 fish·m^{-3}, which is 600% times greater than the original value estimated for that lake. We have no absolute rationale to evaluate the net effect of the potential sources of error. However, the relative magnitude of the errors described above and the biological uncertainty associated with GGE's of 129% during the first sampling period in Lake Memphremagog suggest that errors in growth or initial ingestion rates may be the most probable cause of discrepancy between activity rates obtained using both methods in this lake.

Our analyses suggest that two populations characterized by a twofold difference in mean weight and a 3.5-fold difference in growth rates (joules per day) may have very similar mean activity rates (within 6% in joules per day). This situation represents a proportionally higher energetic burden on the population from Lake Hertel, particularly since these fish also had average consumption rates 1.8-fold lower than those in Lake Memphremagog. These values can be interpreted from two perspectives. First, our data support the hypothesis that higher growth rates in Lake Memphremagog may be related to higher consumption rates in this lake. It is interesting to note, however, that we found no significant difference between consumption rates of fish from both lakes when their respective mean weights were closest (first sampling period). Second, our values are consistent with the hypothesis that allocation of energy towards activity rates may have a significant negative effect on growth rates of fish from Lake Hertel. The SCG method suggests that seasonal activity rates represent 24% of the energy budget of 1+ perch in Lake Hertel. Considering the error that may have occurred in ingestion rates during the first sampling period, activity estimated with the SCG method may range between 12 and 14% of seasonal consumption for fish from Lake Memphremagog. Our results therefore suggest that perch from Lake Hertel use about twice as much of their energy budget in activity expenditures than perch from Lake Memphremagog. The additional 10–12% of the energy budget allocated to activity in Lake Hertel corresponds to at least 50–60% of the observed difference in growth efficiency between populations. While the uncertainty around our estimates for Lake Memphremagog during the first sampling period does not allow us to draw more precise conclusions, it appears realistic to interpret that both consumption and activity rates have a marked influence on growth and that neither variable should be ignored in explaining growth patterns.

Bioenergetic models have often been used to assess the interaction among growth, consumption, and activity rates. In particular, bioenergetic models have been used to estimate consumption rates using field-derived growth rates and assumptions regarding fish activity rates. Bioenergetic models often represent activity rates as a multiple of standard metabolism. In our study, values of ACTM ranged from 2.0 for 1+ perch from Lake Memphremagog to 2.6 for fish from Lake Hertel. For comparative purposes, ACTM calculated using our estimates of activity rates (SCG method) and the original model of standard metabolism (Kitchell et al. 1977) would range from 1.4 (Lake Memphremagog) to 1.7 (Lake Hertel). These differences in ACTM values suggest that the use of constant ACTM for a series of lakes could potentially bias estimates of fish consumption rates obtained using bioenergetic models. To illustrate this, we estimated seasonal consumption rates of 1+ perch in Lake Hertel with a bioenergetic model implemented with an ACTM of 1.17 (a value corresponding to seasonal activity estimated by difference in Lake Memphremagog) instead of 2.6. Seasonal consumption estimates predicted using this approach were 34% lower than our original value. This result suggests that the use of a constant ACTM for different populations may affect the validity of consumption estimates obtained with a bioenergetic model.

Our study supports the hypothesis that populations with slower growth rates may be associated with proportionally higher activity rates. However, our initial expectation was that by selecting populations that maximized growth differences for the southeastern region of Quebec, we would also maximize the range of ACTM obtained. Our results are inconsistent with this expectation, since, in our study, ACTM varied only 20–25% between lakes (depending on the standard metabolic rate model used), while Boisclair and Leggett (1989*c*) found at least a fourfold difference in

© 1999 NRC Canada

ACTM in this area. After the initiation of our study, Boisclair and Rasmussen (1996) produced an analysis that may provide a rationale for this situation. Activity rates have been argued to depend on fish density and prey abundance and size composition (Boisclair and Leggett 1989*c*; Sirois and Boisclair 1995; Marchand and Boisclair 1998). We do not have the data to test the effect of any of these variables. However, following a reanalysis of the data collected by Boisclair and Leggett (1989*a*, 1989*b*, 1989*c*) and Rasmussen (1988, 1993), Boisclair and Rasmussen (1996) suggested that activity rates may be most directly influenced by fish weight (ACTM increased with fish weight) and by water transparency (ACTM increased with water transparency as measured using Secchi depth). Interestingly, the range of mean fish weight (2.8–5.5 g wet) and the range of mean water transparency (3.5–4.2 m) covered by our study are small, and for fish weight, the range stands outside that used by Boisclair and Rasmussen (1996) to develop their model (fish weight: 6–35 g wet; Secchi depth: 1–6 m). As a consequence, the range of ACTM found in our study (1.4–1.7 using the original model of standard metabolic rate) does not overlap with that predicted for Lakes Hertel and Memphremagog by the model of Boisclair and Rasmussen (1996) (0.7–1.2; also developed using the original model of standard metabolic rate). However, both our data and the predictions of the model of Boisclair and Rasmussen (1996) indicate that ACTM for 1+ perch from Lakes Hertel and Memphremagog should be relatively small. Expectations are that with a wider range of water transparency, a wider range of ACTM could also be observed. This may suggest that the range of ACTM observed in our study may not represent the full range found under field situations and that the consequences of among-lake variations in ACTM on predictions by bioenergetic models as revealed by our analysis may underestimate reality.

Acknowledgments

We thank Jean-Christophe Guay, Nathalie Gaudreau, Stéphane Comeau, Isabelle St-Onge, Patrick Lafrance, Martin Bellavance, and Valérie Lapointe for their help in the field and in the laboratory. Funding for this research was provided by a Natural Sciences and Engineering Research Council of Canada research grant, a FCAR-Nouveau chercheur and a FCAR-Equipe grant to Daniel Boisclair. Nadia Aubin-Horth was supported by a postgraduate scholarship from FCAR and La Fondation J.A. Paulhus.

References

Bevelhimer, M.S., and Adams, S.M. 1993. A bioenergetic analysis of diel vertical migration by kokanee salmon, *Oncorhynchus nerka*. Can. J. Fish. Aquat. Sci. **50**: 2336–2349.

Boisclair, D. 1992*a*. An evaluation of the stereocinematographic method to estimate fish swimming speed. Can. J. Fish. Aquat. Sci. **49**: 523–531.

Boisclair, D. 1992*b*. Relationship between feeding and activity rates for actively foraging juvenile brook trout (*Salvelinus fontinalis*). Can. J. Fish. Aquat. Sci. **49**: 2566–2573.

Boisclair, D., and Leggett, W.C. 1988. An in situ experimental evaluation of the Elliott and Persson and the Eggers models for estimating fish daily ration. Can. J. Fish. Aquat. Sci. **45**: 138–145.

Boisclair, D., and Leggett, W.C. 1989*a*. Among-population variability of fish growth: I. Influence of the quantity of food consumed. Can. J. Fish. Aquat. Sci. **46**: 457–467.

Boisclair, D., and Leggett, W.C. 1989*b*. Among-population variability of fish growth: III. Influence of fish community. Can. J. Fish. Aquat. Sci. **46**: 1539–1550.

Boisclair, D., and Leggett, W.C. 1989*c*. The importance of activity in bioenergetics model applied to actively foraging fishes. Can. J. Fish. Aquat. Sci. **46**: 1859–1867.

Boisclair, D., and Rasmussen, J.B. 1996. Empirical analysis of the influence of environmental variables associated with lake eutrophication on perch growth, consumption and activity rates. Ann. Zool. Fenn. **33**: 507–515.

Boisclair, D., and Sirois, P. 1993. Testing assumptions of fish bioenergetics models by direct estimation of growth, consumption, and activity rates. Trans. Am Fish. Soc. **122**: 784–796.

Boisclair, D., and Tang, M. 1993. Empirical analysis of the influence of swimming pattern on the net energetic cost of swimming in fishes. J. Fish Biol. **42**: 169–183.

Briggs, C.T., and Post, J.R. 1997. Field metabolic rates of rainbow trout estimated using electromyogram telemetry. J. Fish Biol. **51**: 807–823.

Carpenter, S.R., Kitchell, J.F., Cottingham, K.L., Schindler, D.E., Christensen, D.L., Post, D.M., and Voichick, N. 1996. Chlorophyll variability, nutrient input, and grazing — evidence from whole-lake experiments. Ecology, **77**: 725–735.

Demers, E., McKinley, R.S., Weatherley, A.H., and McQueen, D.J. 1996. Activity patterns of largemouth and smallmouth bass determined with electromyogram biotelemetry. Trans. Am. Fish. Soc. **125**: 434–439.

Eby, L.A., Rudstam, L.G., and Kitchell, J.F. 1995. Predator responses to prey population dynamics — an empirical analysis based on lake trout growth rates. Can. J. Fish. Aquat. Sci. **52**: 1564–1571.

Eggers, D.M. 1977. Factor in interpreting data obtained by diel sampling of fish stomachs. J. Fish. Res. Board Can. **34**: 290–294.

Hansen, M.J., Boisclair, D., Brandt, S.B., Hewett, S.W., Kitchell, J.F., Lucas, M.C., and Ney, J.J. 1993. Applications of bioenergetics models to fish ecology and management: where do we go from here? Trans. Am. Fish. Soc. **122**: 1019–1030.

Hewett, S.W., and Johnson, B.L. 1992. A generalized bioenergetics model of fish growth for microcomputers. Tech. Rep. WIS-SG-87-245, University of Wisconsin Sea Grant Institute, Madison, Wis.

Kitchell, J.F., Stewart, D.J., and Weininger, D. 1977. Applications of a bioenergetics model to yellow perch (*Perca flavescens*) and walleye (*Stizostedion vitreum vitreum*). J. Fish. Res. Board Can. **34**: 1922–1935.

Koch, F., and Wieser, W. 1983. Partitioning of energy in fish: can reduction of swimming activity compensate for the cost of production? J. Exp. Biol. **107**: 141–146.

Krohn, M., and Boisclair, D. 1994. Use of a stereo-video system to estimate the energy expenditure of free-swimming fish. Can. J. Fish. Aquat. Sci. **51**: 1119–1127.

Krohn, M., Reidy, S., and Kerr, S. 1997. Bioenergetic analysis of the effects of temperature and prey availability on growth and condition of northern cod (*Gadus morhua*). Can. J. Fish. Aquat. Sci. **54**(Suppl. 1): 113–121.

LaBar, G.W. 1993. Use of bioenergetics models to predict the effects of increased lake trout predation on rainbow smelt following sea lamprey control. Trans. Am. Fish. Soc. **122**: 942–950.

© 1999 NRC Canada

Lucas, M.C., Priede, I.G., Armstrong, J.D., Gindy, A.N.Z., and DeVera, L. 1991. Direct measurements of metabolism, activity and feeding behavior of pike, *Esox lucius* L., in the wild, by the use of heart rate telemetry. J. Fish Biol. **39**: 325–345.

Madon, S.P., and Culver, D.A. 1993. Bioenergetics model for larval and juvenile walleyes: an in situ approach with experimental ponds. Trans. Am. Fish. Soc. **122**: 797–813.

Mann, K.H. 1965. Energy transformations by a population of fish in the river Thames. J. Anim. Ecol. **34**: 253–275.

Marchand, F., and Boisclair, D. 1998. The influence of fish density on energy allocation pattern of juvenile brook trout (*Salvelinus fontinalis* Mitchill). Can. J. Fish. Aquat. Sci. **55**: 796–805.

Ménard, C. 1991. Utilisation de la vidéo pour mesurer les poissons in situ. Mémoire de maîtrise, Université de Montréal, Montréal, Qué.

Minton, J.W, and Mclean, R.B. 1982. Measurements of growth and consumption of sauger (*Stizostedion canadense*): implication for fish energetics studies. Can. J. Fish. Aquat. Sci. **39**: 1396–1403.

Ney, J.J. 1993. Bioenergetics modeling today: growing pains on the cutting edge. Trans. Am. Fish. Soc. **122**: 736–748.

Post, J.R., and Evans, D.O. 1989. Experimental evidence of size-dependent predation mortality in juvenile yellow perch. Can. J. Zool. **67**: 521–523.

Proulx, M., Pick, F.R., Mazumder, A., Hamilton, P.B., and Lean, D.R.S. 1996. Effects of nutrients and planktivorous fish on the phytoplancton of shallow and deep aquatic systems. Ecology, **77**: 1556–1572.

Rasmussen, J.B. 1988. Littoral zoobenthic biomass in lakes, and its relationship to physical, chemical, and trophic factors. Can. J. Fish. Aquat. Sci. **45**: 1436–1447.

Rasmussen, J.B. 1993. Patterns in the size structure of littoral zone macroinvertebrate communities. Can. J. Fish. Aquat. Sci. **50**: 2192–2207.

Rowan, D.J., and Rasmussen, J.B. 1996. Measuring the bioenergetic cost of fish activity in situ using a globally dispersed radiotracer (^{137}Cs). Can. J. Fish. Aquat. Sci. **53**: 734–745.

Rudstam, L.G., Peppard, P.E, Fratt, T.W., Bruesewitz, R.E., Coble, D.W., Copes, F.A., and Kitchell, J.F. 1995. Prey consumption by the burbot (*Lota lota*) population in Green Bay, Lake Michigan, based on a bioenergetic model. Can. J. Fish. Aquat. Sci. **52**: 1074–1082.

Salonen, S., Helminen, H., and Sarvala, J. 1996. Feasibility of controlling coarse fish populations through pike perch (*Stizostedion lucioperca*) stocking in Lake Köyliönjärvi, SW Finland. Ann. Zool. Fenn. **33**: 451–457.

Schindler, D.E., Kitchell, J.F., He, X., Carpenter, S.R., Hodgson, J.R, and Cottingham, K.L. 1993. Food web structure and phosphorus cycling in lakes. Trans. Am Fish. Soc. **122**: 756–773.

Scott, W.B., and Crossman, E.J. 1973. Freshwater fishes of Canada. Bull. Fish. Res. Board. Can. No. 184.

Sirois, P., and Boisclair, D. 1995. The influence of prey biomass on activity and consumption rates of brook trout. J. Fish Biol. **46**: 787–805.

Sogard, S.M. 1997. Size-selective mortality in the juvenile stage of teleost fishes: a review. Bull. Mar. Sci. **60**: 1129–1157.

Sokal, R.R., and Rohlf, F.J. 1995. Biometry: The principles and practice of statistics in biological research. 3rd ed. W.H. Freeman and Company, New York.

Solomon, D.J., and Brafield, A.E. 1972. The energetics of feeding, metabolism and growth of perch (*Perca fluviatilis* L.). J. Anim. Ecol. **41**: 699–718.

Stewart, D.J., Kitchell, J.F., and Crowder, L.B. 1981. Forage fishes and their salmonid predators in Lake Michigan. Trans. Am. Fish. Soc. **110**: 751–763.

Trudel, M., and Boisclair, D. 1993. An in situ evaluation of the day to day variation in the quantity of food consumed by fish. Can. J. Fish. Aquat. Sci. **50**: 2157–2165.

Trudel, M., and Boisclair, D. 1994. Seasonal consumption by dace (*Phoxinus eos* × *P. neogaeus*): a comparison between field and bioenergetic model estimates. Can. J. Fish. Aquat. Sci. **51**: 2558–2567.

Trudel, M., and Boisclair, D. 1996. Estimation of fish activity costs using underwater video cameras. J. Fish Biol. **48**: 40–53.

© 1999 NRC Canada

Habitat factors controlling Pacific herring (*Clupea pallasi*) egg loss in Prince William Sound, Alaska

Christopher N. Rooper, Lewis J. Haldorson, and Terrance J. Quinn, II

Abstract: Recruitment for many marine fishes is believed to be determined at an early life history stage. Pacific herring (*Clupea pallasi*) spawn in the intertidal and shallow subtidal zones and have a demersal egg stage that is susceptible to egg removals during incubation. Data were collected by the Alaska Department of Fish and Game in four years in Prince William Sound, Alaska, to identify important factors contributing to egg removals. We constructed analysis of variance models based on physical and biological variables to determine which environmental factors control egg loss rates. The habitat variables examined at each study transect were depth, wave exposure, north–south location, substrate, vegetation, mean bird abundance, abundance of loose eggs, and fish predation. Depth of spawn was the primary factor determining egg loss. Cumulative time of air exposure over incubation was substituted into the model for depth. Using the model, the total estimated egg loss from spawning to hatching ranged from 67 to 100% with an average of 75% (SE = 3.3%) in 1995. Eggs were originally deposited from 4 to –6 m depth relative to mean low water. The majority of eggs that remained in the spawning beds to hatching were deposited from 1 to –4 m depth. Egg removals due to avian predation were probably responsible for extreme egg loss rates at shallow depths.

Résumé : Chez de nombreuses espèces de poissons marins, le recrutement semble déterminé dans les premiers stades de développement. Le hareng du Pacifique (*Clupea pallasi*) fraye dans la zone intertidale et dans la zone infratidale peu profonde, et ses oeufs démersaux peuvent disparaître durant l'incubation. L'Alaska Department of Fish and Game a recueilli durant quatre ans des données dans le golfe du Prince-William, en Alaska, pour établir les facteurs importants responsables de la disparition d'oeufs. Nous avons construit des modèles d'analyse de variance fondés sur des variables physiques et biologiques pour établir quels facteurs environnementaux déterminent les taux de perte d'oeufs. Les variables de l'habitat qui ont été prises en considération dans chaque transect de l'étude sont les suivants : la profondeur, l'exposition aux vagues, la localisation selon l'axe nord–sud, le substrat, la végétation, l'abondance moyenne des oiseaux, l'abondance des oeufs libres et la prédation par les poissons. La profondeur à laquelle la fraye était effectuée était le principal facteur déterminant la perte d'oeufs. La durée cumulative de l'exposition à l'air durant l'incubation a été substituée dans le modèle pour la profondeur. Au moyen du modèle, on a estimé la perte totale d'oeufs depuis la fraye jusqu'à l'éclosion à 67 à 100%, avec une perte moyenne de 75% (E.-T. = 3,3%) en 1995. Les oeufs étaient au départ pondus à une profondeur de 4 à –6 m par rapport au niveau moyen des basses eaux. La majorité des oeufs qui sont demeurés dans les frayères jusqu'à l'éclosion avaient été pondus à une profondeur de 1 à –4 m. Les taux de perte d'oeufs extrêmes aux faibles profondeurs étaient probablement attribuables à la prédation par les oiseaux.

[Traduit par la Rédaction]

Introduction

Explaining recruitment fluctuations is a central problem in fisheries science (Sissenwine 1984). Dramatic recruitment fluctuations in some marine fish are thought to be related to mortality in early life history stages (Hjort 1914). Hypotheses based on a variety of mechanisms have been advanced to explain recruitment fluctuations (Cushing 1975; Lasker 1975; Sinclair 1988; Bailey and Houde 1989). Clupeid fishes are especially susceptible to dramatic fluctuations in population abundance over both long and short time periods (Cushing 1971; Soutar and Isaacs 1974). Pacific herring (*Clupea pallasi*) show strong linkages of recruitment to environmental conditions such as sea surface temperature, regardless of the mechanism (Hay and Kronlund 1987; Wespestad 1991; Schweigert 1995; Zebdi and Collie 1995).

Although egg mortality has not been directly correlated with adult recruitment for most fish species (Peterman et al. 1988; Pepin and Myers 1991; Bradford 1992), egg survival does determine the number of potential recruits to later life history stages. The demersal egg stage of Pacific herring may be especially vulnerable to mortality because they incubate for long periods in shallow locations. Predators can feed for an extended period on eggs and may exhibit a numerical response to the food source. Eggs can also be sus-

Received June 11, 1998. Accepted February 26, 1999.
J14646

C.N. Rooper,[1] L.J. Haldorson,[2] and T.J. Quinn, II. Juneau Center for Fisheries and Ocean Sciences, University of Alaska–Fairbanks, 11120 Glacier Hwy, Juneau AK 99801, U.S.A.

[1]Present address: School of Fisheries, University of Washington, Box 357980, Seattle WA 98195, U.S.A.
[2]Author to whom all correspondence should be addressed. e-mail: ffljh@aurora.alaska.edu

© 1999 NRC Canada

Fig. 1. Map of Prince William Sound, Alaska, showing egg loss study transects. Year and transect number are indicated, e.g., 95-6 refers to transect No. 6 in 1995.

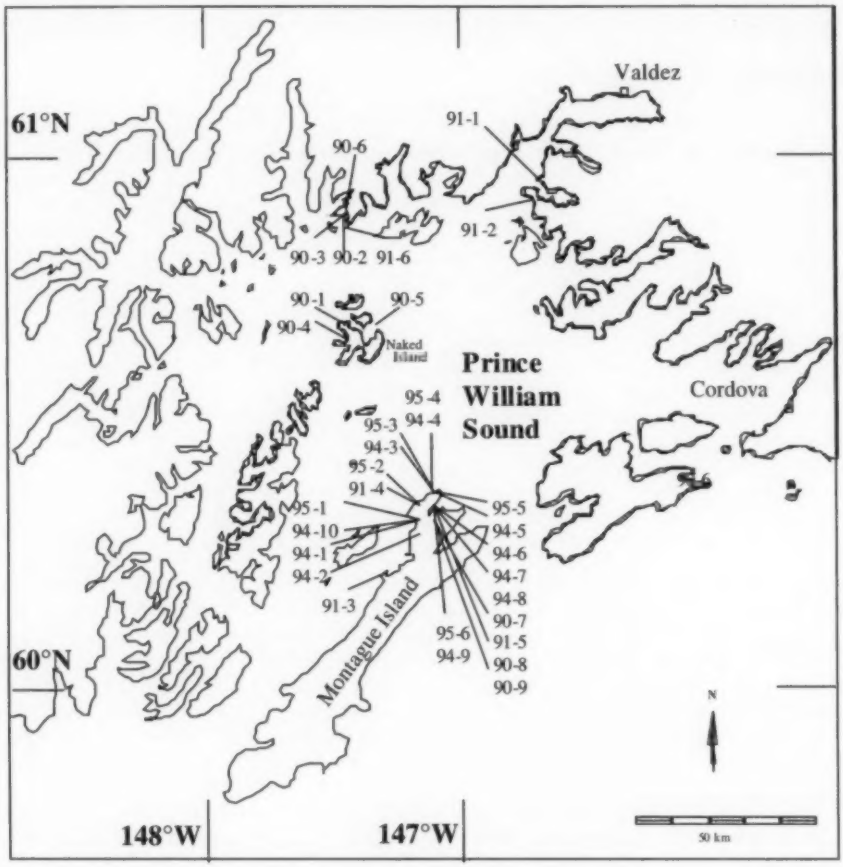

ceptible to harsh environmental conditions because they are unable to move from the spawning beds.

Pacific herring spawn in intertidal and shallow subtidal habitats and have a demersal egg stage that usually lasts from 14 to 21 days. Studies have documented large proportions of herring eggs lost due to the physical action of waves (Hart and Tester 1934; Hay and Miller 1982). Significant egg loss in the intertidal zone has also been attributed to avian predation (Cleaver and Franett 1946; Outram 1958; Steinfeld 1971; Haegele and Schweigert 1989; Haegele and Schweigert 1991). Subtidally, predation by marine mammals (Haegele and Schweigert 1989), fishes (Palsson 1984; Rooper 1996), and invertebrates (Haegele and Schweigert 1989; Haegele 1993) have been implicated as sources of herring egg loss.

Accurate estimation of herring spawning biomass has been identified as a source of error in management of herring stocks where biomass is estimated from egg deposition (Haegele and Schweigert 1991; Zheng et al. 1993). Development of a site-specific estimate of egg loss may improve the estimates of adult herring biomass by reducing the error in estimating total egg deposition.

Substantial interest in the herring stock of Prince William Sound, Alaska, was generated after the 1989 *Exxon Valdez* oil spill and a population crash in 1994 (Funk 1994). Large-scale investigations of the herring population were initiated, of which this study was one. The objective of our study was to determine how habitat affects the egg stage of herring, and thus the potential number of recruits to later life stages. We hypothesized that exposure to waves and high levels of predation would increase egg loss. We then developed a statistical model for predicting egg loss based on environmental variables and estimated the total loss of eggs from the spawning beds using the model.

Methods

Egg loss was estimated for Prince William Sound Pacific herring in four years: 1990, 1991, 1994, and 1995. Alaska Department of Fish and Game personnel collected data at 31 transects within herring spawning beds from four different locations (Fig. 1). Transect location was randomly chosen in the first year of the study; in subsequent years, transect locations were chosen to be as near as possible to the original transects. Exact placement of subsequent years' transects at the original sites was hampered by the year-to-year variation in egg deposition, in that spawn was not always found at some of the original locations. The data consisted of visual estimates by SCUBA divers of the number of eggs within 0.1-m^2 quadrats. Each quadrat was a square constructed of plastic

© 1999 NRC Canada

Fig. 2. Schematic of an egg loss transect showing the quadrat diagram and corresponding spawn deposition transect. A two by five grid of 0.1-m^2 quadrats is represented; within the frame the five sampled quadrats are indicated by an X. These frames were permanently established at specified depth strata for each egg loss transect as indicated by the arrows. Also shown is the placement of a spawn deposition transect adjacent to the egg loss quadrat frames.

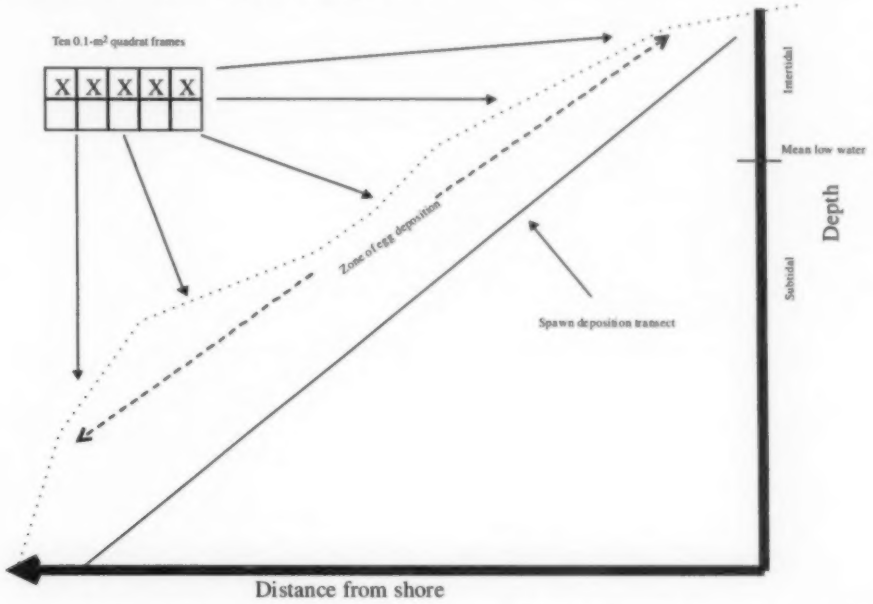

tubing with sides of 32 cm. Ten quadrats in a two by five grid were permanently established at specified depth strata for each egg loss transect (except in 1990 when a leadline was used to mark quadrat placement sites). Egg counts were visually estimated for the same one of the two rows of five quadrats at each visit (Fig. 2). This method ensured that eggs were counted at the same specific location throughout the incubation period. Egg abundance was estimated at intervals of 3–7 days at each transect during incubation, and these estimates were calibrated for each diver (Biggs-Brown and Baker 1993) before data analysis was undertaken.

Factorial analyses

Seven combinations of data in time and space were modeled using analysis of variance: data from the four individual years, 1990 and 1991 combined, 1994 and 1995 combined, and all years combined at Montague Island. Montague Island in south Prince William Sound was the only location where herring eggs were found in all years of the study. Each transect was classified by wave exposure into two categories: within an embayment or on a headland. Transects were also classified by location, either in the northern half of the sound or in the southern half. Transects were classified into four substrate types: rocky, boulder, sand, or mud. Within transects, each quadrat was classified according to its dominant vegetation species, depth, and the cumulative time that the quadrat was exposed to air during incubation. In the analyses, depth was a categorical rather than a continuous variable. In Prince William Sound the mean tidal range is 3.7 m, and time of air exposure over incubation was calculated from a tide program (Tide1, Micronautics Inc., P.O. Box 1017, Rockport, ME 04856, U.S.A.). In 1994 and 1995, mean bird abundance of all species and mean abundance of glaucous-winged gulls calculated from observations of U.S. Forest Service personnel at the transects (M.A. Bishop and P. Green, USFS-CRDI, P.O. Box 1460, Cordova, AK 99574, U.S.A., unpublished data) were used in the model. In 1994, cumulative loose eggs were estimated by divers at each transect and were also used in the models. In 1995, an index of fish abundance from gillnet sampling was used to classify the transects for model construction (Rooper 1996). Data for some of these variables were not available for modeling in some years due to inadequate data collection or lack of replication (Table 1).

Our models of egg loss assume that a constant proportion of eggs were lost over time. If N_t is the number of eggs at day t, N_0 is the number of eggs initially deposited at spawning, and Z is the instantaneous egg loss rate, then

$$(1) \qquad N_t = N_0 e^{-Zt} e^{\varepsilon}$$

where ε is a random error term with mean zero and constant variance. By taking the natural log of both sides of this equation, the instantaneous egg loss rate may be calculated by linear regression of the transformed egg counts against time.

Modeling of the effects of environmental variables was carried out using the egg loss rates (Z). Egg loss rates were dependent variables in analysis of variance models where

$$(2) \qquad Z = \mu + \alpha_i + \beta_j + \lambda_k + (\alpha\beta)_{ij} + \ldots + \varepsilon$$

Independent variables were the habitat classifications, predation variables, depth, and year. Factorial analyses of these variables were performed, sequentially removing insignificant factors ($p > 0.05$). In most cases the resulting models explained a significant portion of the variability in egg loss rates.

Because the time of air exposure of the eggs is a function of depth, these two variables were not used simultaneously. A separate set of factorial analyses were performed on the egg loss rates using air exposure as a covariate in place of depth. Air exposure models were then compared with depth models using an F test (Schnute 1981), and the results of all factorial analyses of the seven data sets were then compared to determine the best model for herring egg loss.

© 1999 NRC Canada

Table 1. Summary of habitat variables available for classification of data from each year of the Prince William Sound egg loss study.

	1990	1991	1994	1995
Depths (m)	–9.2, –4.6, –1.5, 0, 0.3, 1.5	–4.6, –1.5, 0, 0.3, 1.5	–3.1, –0.9, –0.6, 0, 0.6, 0.9	–1.5, –0.3, 0, 0.3, 0.9, 1.5
Time of air exposure	X	X	X	X
Wave exposure	X	X	X	X
Location	X	X		
Year	X	X	X	X
Substrate	X		X	
Kelp type	X	X	X	X
Mean bird abundance			X	X
Mean gull abundance			X	X
Cumulative loose eggs			X	
Fish index				X

Note: Data available for factorial analysis are indicated by an X; missing values indicate that no data were collected regarding that variable.

Estimation of total egg removals

To accurately describe the depth distribution and total abundance of spawn, a spawn deposition transect was placed at the same location as each egg loss transect in 1995. Spawn deposition transects provided a systematic estimation of egg density across the spatial distribution of eggs; detailed methods for spawn deposition transects in Prince William Sound can be found in Biggs and Funk (1988). Divers counted eggs in 0.1-m^2 quadrats at 5-m intervals along each transect extending perpendicular from the beach, continuing past the depth at which no more eggs were observed (Fig. 2). In 1995, these surveys occurred one time only from 4 to 7 days after spawn was initially laid down. The egg loss model from factorial analysis was used to calculate the total number of eggs initially deposited at these spawn deposition transects, as well as the number of eggs retained in the beds until hatching. The equation for estimating egg loss rate (Z) that resulted from factorial analysis (explained below) was

$$(3) \qquad Z = 0.052357 + 0.000601 \cdot AE$$

where AE is the cumulative time of air exposure during incubation. The initial number of eggs deposited, N_0, is estimated by

$$(4) \qquad N_0 = N_t e^{Zt} e^{\varepsilon}$$

where t is the number of days from spawning to the survey. The estimated number of eggs at the time of the hatching is then calculated from eq. 1, where t is the length of the incubation period at the transect. The method for estimating standard errors for the percentage of eggs lost during incubation is developed in the Appendix.

Results

Factorial analyses

Estimated egg loss rates (Z) ranged from –0.112 to 0.263 among the 31 study transects. Variation in egg counts by divers was high and may explain increasing egg counts over time at some depths within transects. An example of changing egg density over time is shown in Fig. 3 for transect 95-1; the slope of the regression line in each graph represents egg loss rate for each depth at the transect. Factorial analyses of the egg loss rates resulted in a variety of significant factors in the seven data sets. Interannual variability in egg loss rates was clearly evident (Table 2), and in all years the majority of regressions for calculating egg loss rates were significant ($p < 0.05$). Lack of replication over some variables necessitated using subsets of the data in the modeling.

In 1990 the factorial model contained three terms: north–south location, wave exposure, and depth (Table 3). The average egg loss rate at southern transects in 1990 was 0.125 (SE = 0.022), while the average in the north was only 0.019 (SE = 0.015). At wave-exposed transects, the average egg loss rate was 0.091 (SE = 0.027), slightly higher than at protected transects, 0.070 (SE = 0.022). Egg loss increased at shallower depths. The factorial analysis model in 1991 contained two significant habitat variables: depth and wave exposure (Table 3). At wave-protected transects, the average egg loss rate was 0.074 (SE = 0.015), whereas at wave-exposed transects, the average was –0.018 (SE = 0.010). Egg loss rates were inversely related to depth; higher egg loss rates occurred at shallower depths. The factorial analysis model for 1994 data contained only two significant terms: depth and the depth × average bird abundance interaction (Table 3). Egg loss rates decreased at deeper depths, and higher bird abundance was associated with higher egg loss rates at shallower depths. Factorial analysis of the 1995 egg loss rates led to a model containing only the depth term (Table 3). Again, egg loss rates were higher at shallower depths.

Factorial analysis of the combined 1990 and 1991 data resulted in a model containing the year × location interaction term, year, location, wave exposure, and depth (Table 4). Depth and the interaction term accounted for the most variability in egg loss rates, suggesting that these two were the most important factors affecting egg loss in 1990 and 1991. The significance of the interaction term implies that location had different effects on egg loss in the individual years. Egg loss rates were higher in the south in 1990, and egg loss rates were higher in the north in 1991. The average egg loss rate was higher at shallower depths; the egg loss rate was also higher for protected transects (0.079, SE = 0.012) than for exposed transects (0.021, SE = 0.018). The factorial analysis model for 1994 and 1995 combined included only the depth term and is consistent with the previous analyses, in that higher egg loss occurred at shallower depths (Table 4). Factorial analysis of the Montague Island data from

© 1999 NRC Canada

Fig. 3. Estimated egg density through incubation at transect 95-1 on Montague Island in 1995. Plots of egg density through time are shown for each of the six depths sampled at the transect; plots of egg density data over time are shown for each depth. Depths are (A) 1.5 m, (B) 0.9 m, (C) 0.3 m, (D) 0.0 m, (E) –0.3 m, and (F) –1.5 m relative to mean low water. The slope of the regression line in each plot is the estimate of the egg loss rate for that depth at transect 95-1.

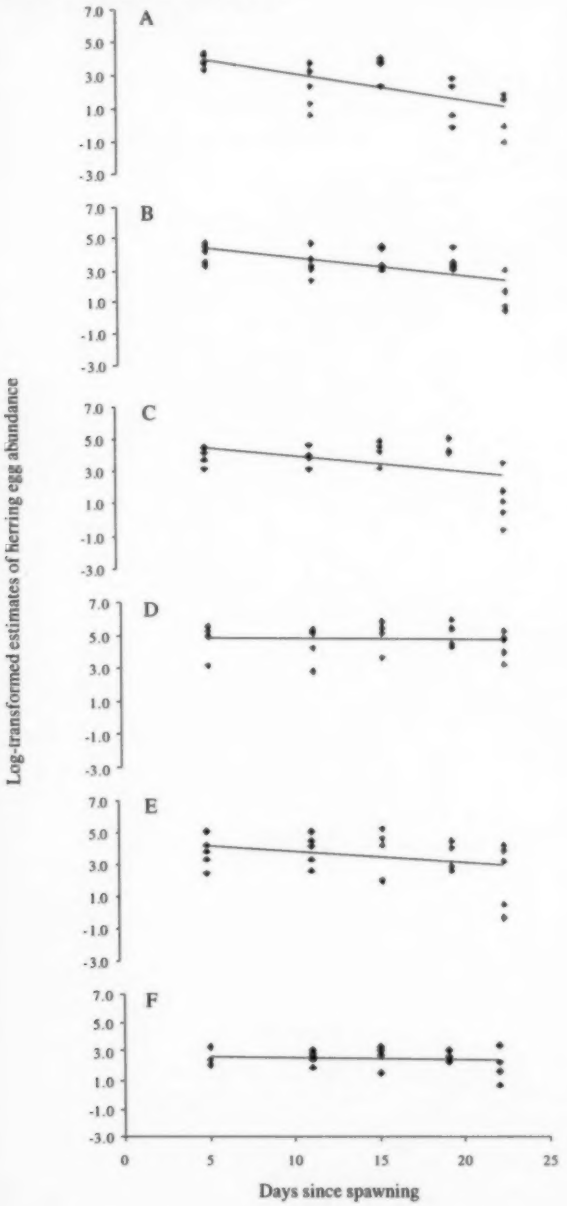

all years resulted in a model containing three significant terms: depth, wave exposure, and year, with depth explaining the majority of the variation in egg loss rates (Table 4). The average egg loss rate for the Montague Island data was higher in areas protected from waves (0.116, SE = 0.015) than in exposed areas (0.071, SE = 0.012). Montague Island had the highest egg loss in 1990 (0.154, SE = 0.029), and 1991 had the lowest egg loss (0.003, SE = 0.015). At shallower depths, egg loss rates were again higher.

In summary, depth was the most important variable affecting egg loss, since it was included in all factorial analyses (Table 5). Egg loss rates were higher at shallower depths in all cases. Wave exposure was significant in four of the seven data sets, and egg loss rates were higher in protected areas than in exposed areas for all analyses except 1990. Interannual variability was important in models with combined data. The results of F tests to determine if depth models were significantly different from air exposure models are given in Table 6, and the relationship between time of air exposure and depth is shown in Fig. 4. Over five of the seven data sets, air exposure models were not significantly different from depth models. From a statistical perspective, air exposure models are more parsimonious than depth models. Air exposure models replace the categorical depth variable with a continuous air exposure variable, so degrees of freedom in the model are increased by the number of depth categories minus 1 for the air exposure variable.

Estimation of total egg removals

We used the 1995 air exposure model parameters (eqs. 1, 3, and 4) to calculate egg counts at the initial spawning and the number of eggs surviving to hatch (Fig. 5). Eggs deposited at depths below –3.5 m were not exposed to air during incubation; thus, AE = 0 for these eggs. In 1995 the beginning of spawning ranged from April 27 to April 29, with spawning at most transects beginning on April 28. The time from the beginning of spawning to the spawn deposition survey ranged from 4 to 7 days. The time from spawning to hatching in 1995 ranged from 21 to 22 days. The percentage of eggs lost over the entire incubation period ranged from 67.40% at subtidal depths to an asymptote at 100% at the shallower depths (Fig. 6). The average percentage of eggs lost over the incubation period was 74.70% (SE = 3.31%). Based on the original egg distribution, the majority of eggs that remained in the spawning beds until hatching were deposited in the region between 1 and –4 m relative to mean low water (Fig. 7).

Discussion

Results of egg loss modeling indicated that depth of spawn was the most consistent variable determining egg loss in Prince William Sound. Cumulative time of air exposure over incubation was found to be a reasonable substitute for depth in the models. Other variables were important in some models and are discussed below. When the egg loss model was applied to 1995 egg deposition data, almost three quarters of the eggs initially deposited were lost over incubation. Egg loss was higher at shallower depths, and most eggs remaining in the spawning beds until hatching were deposited at intermediate depths.

An important assumption of this analysis is that eq. 1 is an accurate representation of egg loss over time. The equation assumes that a constant proportion of eggs are lost throughout the incubation period and divergence of egg loss

© 1999 NRC Canada

Table 2. Summary of egg loss rates (Z) in each year of the Prince William Sound egg loss study.

Year	No. transects	n	Mean Z	SE	Range	Proportion significant ($p < 0.05$)
1990	9	41	0.076	0.011	0.244 to –0.025	0.63
1991	6	26	0.042	0.013	0.263 to –0.059	0.58
1994	10	30	0.096	0.012	0.242 to –0.112	0.90
1995	6	32	0.096	0.011	0.231 to –0.007	0.66

Note: The total number of quadrat frames for all transects in a year is given by n. Lack of replication in some categories of habitat classifications necessitated the use of data subsets in factorial analyses; therefore, Tables 2–4 may have differing values of n. The proportion of significant log-transformed egg abundance versus time regressions used to calculate egg loss rates is also shown.

Table 3. Summary of egg loss models resulting from factorial analyses of Prince William Sound egg loss rates for each year.

Data set	n	Term	Sum of squares	df	p	R^2
1990	21	Location	0.057	1	0.000	0.854
		Wave exposure	0.016	1	0.005	
		Depth	0.042	5	0.005	
		Error	0.019	13		
1991	26	Depth	0.025	4	0.036	0.653
		Wave exposure	0.049	1	0.000	
		Error	0.040	20		
1994	30	Depth × bird abundance	0.060	5	0.001	0.756
		Depth	0.050	5	0.002	
		Bird abundance	0.002	1	0.234	
		Error	0.029	18		
1995	32	Depth	0.067	5	0.001	0.539
		Error	0.057	26		

Note: Due to lack of replication in some variables in some years, subsets of data were used in these analyses.

Table 4. Summary of egg loss models resulting from factorial analysis of combined Prince William Sound data sets.

Data set	n	Term	Sum of squares	df	p	R^2
1990 and 1991	51	Year × location	0.046	1	0.000	0.734
		Depth	0.054	5	0.000	
		Wave exposure	0.036	1	0.000	
		Location	0.025	1	0.001	
		Year	0.009	1	0.034	
		Error	0.077	41		
1994 and 1995	41	Depth	0.076	8	0.001	0.524
		Error	0.069	32		
Montague Island	59	Depth	0.098	9	0.000	0.715
		Year	0.068	3	0.000	
		Wave exposure	0.018	1	0.005	
		Error	0.091	45		

Note: Due to lack of replication in some variables in some years and data combinations, subsets of data were used in these analyses.

from the pattern described by the model would present problems for our analyses. Although there was much variation in the visual estimates of egg abundance by divers (Fig. 3), the majority of the regressions of log-transformed egg counts against time used to calculate egg loss rates were significant (Table 2). This variation may have introduced some error into our estimation of egg loss rates, but the significance of the regressions indicated that the underlying model was reasonably accurate in representing egg loss over time.

Some major differences in egg loss between the first two years of the study and the last two years are evident from the models. These differences may have been due to the high

© 1999 NRC Canada

Table 5. Summary of important habitat variables for each data set modeled.

Data set	Depth	Wave exposure	Other
1990	X	X	Location
1991	X	X	
1994	X		Mean bird abundance
1995	X		
1990 and 1991	X	X	Year, location
1994 and 1995	X		
Montague Island	X	X	Year

Note: X denotes that the variable was significant in the model resulting from factorial analyses of egg loss rates.

egg biomass in the early years as opposed to later years after the population crash. In 1994 and 1995, spawning occurred only in the southern half of the sound, confounding year effects. Location was significant in 1990, and differences in physical and biological regimes between the north and south sounds may be responsible for the observed differences in egg loss rates. The model for Montague Island transects included data from all years, and in it, year was significant. Thus, it seems that interannual variability and spatial differences can be important in determining egg loss. Some of these interannual differences in egg loss rates are probably an artifact of the study design. Depths sampled varied from year to year, and transect locations also varied from year to year. For example, transect locations on Montague Island were all on the east side in 1990 and were spread throughout the island in 1991. These differences may provide an alternative explanation of some of the interannual differences in egg loss rates found in the modeling.

The wave exposure variable produced a very interesting result in that egg loss was consistently higher at protected transects than at exposed transects. Only in 1990 was egg loss higher at exposed areas, and in that year the wave-exposed category was represented by only one transect. Lower egg loss in exposed areas is highly counterintuitive and may reflect the presence of an undiscovered process driving egg loss in protected areas. Wave sensor data at three egg loss transects in 1995 suggest that there can be site-specific storm events leading to extreme egg losses that may not be detected on a larger scale (Rooper 1996). It is possible that predation may also be higher in protected areas, since it may be easier for predators to feed in the calmer water of bays than in more energetic areas. However, bird abundance was lower at protected transects than at exposed transects. Egg density was also lower in protected areas, although the difference was not significant.

Both substrate type and kelp type were found to be insignificant in all the models of egg loss rates. Substrates other than rocky were not well represented in most years, so replication was not sufficient to provide robust analyses. Of the covariate terms used in the modeling (average bird abundance, average gull abundance, fish predation index, and cumulative loose eggs), only bird abundance was significant, and only in 1994, when increased bird abundance resulted in higher egg loss rates at shallower depths. Mean bird abundance was highly variable among transects, ranging from two to 886 in 1994 and from zero to 221 in 1995. Fish abundance was less variable, with catches ranging from zero to six fish per gillnet set (Rooper 1996). The reason for the lack of significance of bird predation in the 1995 model may lie in the choice of predator indices used in egg loss modeling. For modeling, the average abundance of predators was used as a covariate; however, this failed to account for the total abundance of spawn at the egg loss transect. The consumption of eggs by a lesser number of predators at a transect with low egg density could result in a higher egg loss rate than the consumption by many predators at a transect with large numbers of eggs, confounding our results. This pattern of consumption and egg density may also explain higher egg loss rates found in protected areas, since egg abundance and bird abundance were lower at protected transects.

It is apparent that depth is the most important variable affecting egg loss. Depth was included in all factorial analyses of egg loss and was the predominant variable in the models of 1994 and 1995 data. Based on the results from the F test and model comparisons, air exposure is a good substitute for depth, reducing the number of parameters estimated without significantly decreasing the efficiency of the model. The air exposure model may also a more biologically realistic representation of the causes of egg loss, since it is probably more closely related to processes such as predation than is a categorical depth variable. The most abundant predators at egg loss transects, glaucous-winged gulls, fed primarily on eggs located in the intertidal zone as they were exposed by the tides. Thus, the model of egg loss recommended by this study is a linear model based on the time of air exposure over the incubation period. The range of the total percentage of eggs lost over incubation according to the 1995 model (67.4–100%) is slightly higher than the range found by Biggs-Brown and Baker (1993) of 50.4–91.2% in Prince William Sound. Other ranges of egg loss from Pacific herring spawning beds are from 56 to 99% for Barkeley Sound, British Columbia (Outram 1958), and from 46 to 92% for Strait of Georgia, British Columbia (Haegele and Schweigert 1991). The results of our model are quite similar to these studies of egg loss, and all studies have found that extremely high egg loss occurs at the shallowest depths.

The results of this study indicate that most of the eggs that remain in the spawning beds until hatching are deposited in a range of depths from 1 to –4 m (Fig. 7). The cause for higher egg loss at depths above mean low water is presumed to be predation. Results of the U.S. Forest Service study of egg consumption by bird species indicate that avian predators, primarily glaucous-winged gulls, may be responsible for removals of large amounts of spawn (27% of the total spawn deposited over all depths, M.A. Bishop and P. Green, USFS-CRDI, P.O. Box 1460, Cordova, AK 99574, U.S.A., unpublished data). Two species of hexagrammid fishes may remove from 4.1 to 7.3% of total spawn as well (C.N. Rooper, unpublished data). Predation by glaucous-winged gulls is more intense in the intertidal zone when herring eggs are exposed or covered by shallow water. Conversely, predation by fishes is expected to be stronger in the subtidal zone. Wave exposure can also be important, at least on fine temporal and spatial scales. Egg removal during a storm event at an exposed transect in 1995 was estimated at 74% of the total spawn at the transect (Rooper 1996). Other

© 1999 NRC Canada

Table 6. Results of F tests comparing the significance of models with depth and models with air exposure.

Data set	RSS_{depth}	RSS_{air}	df_{depth}	df_{air}	F	p
1990	0.019	0.038	13	17	3.25	0.012
1991	0.040	0.043	20	23	0.50	0.939
1994	0.032	0.103	19	27	5.27	0.000
1995	0.057	0.064	26	30	0.80	0.718
1990 and 1991	0.077	0.085	41	45	1.06	0.417
1994 and 1995	0.069	0.080	32	39	0.73	0.820
Montague Island	0.091	0.105	45	53	0.87	0.689

Note: RSS, residual sum of squares error, df, residual degrees of freedom. The full model (with depth) was tested against a reduced model (with air exposure) to determine significant differences between the two (Schnute 1981).

Fig. 4. Relationship of air exposure to depth showing cumulative time of air exposure over incubation at egg loss transects as a function of depth relative to mean low water.

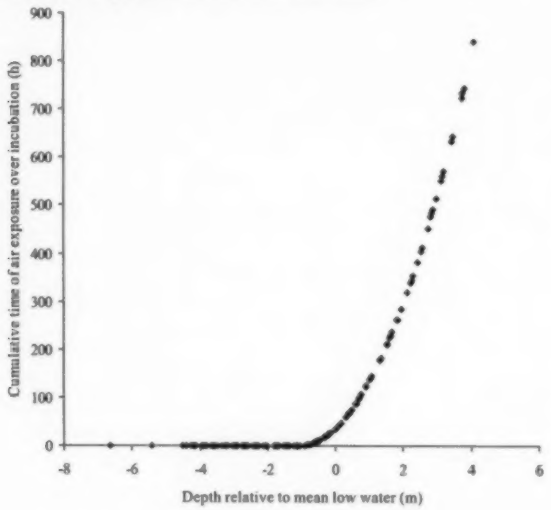

Fig. 5. Egg loss rates versus air exposure in 1995 and the best fitting linear regression model.

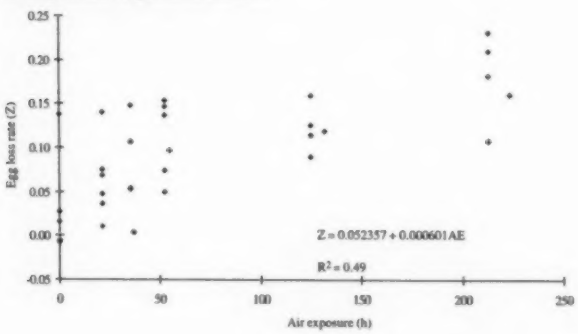

studies have also documented site-specific losses of large proportions of eggs due to storms (26%, Hart and Tester 1934; 40%, Hay and Miller 1982). The effect of wave exposure on egg loss should also vary with depth, with wave action removing more eggs in the lower intertidal zone than in the subtidal zone.

The results of this study show that the amount of time that

Fig. 6. Percentage of eggs lost during egg incubation for spawn deposition transects in 1995 as predicted by the egg loss model.

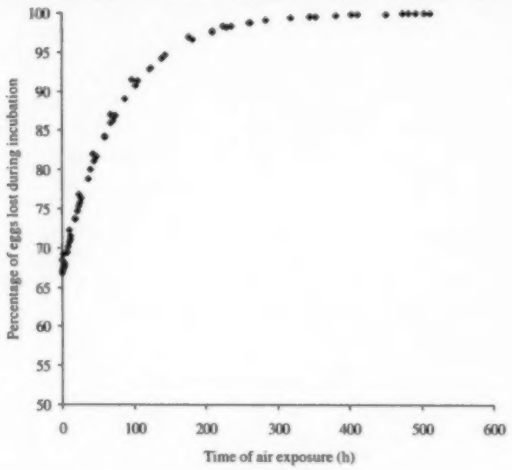

Fig. 7. Depth distribution of egg density observed at the time of the survey and the estimated density of eggs initially spawned and the density remaining until hatching in 1995 as predicted by the egg loss model.

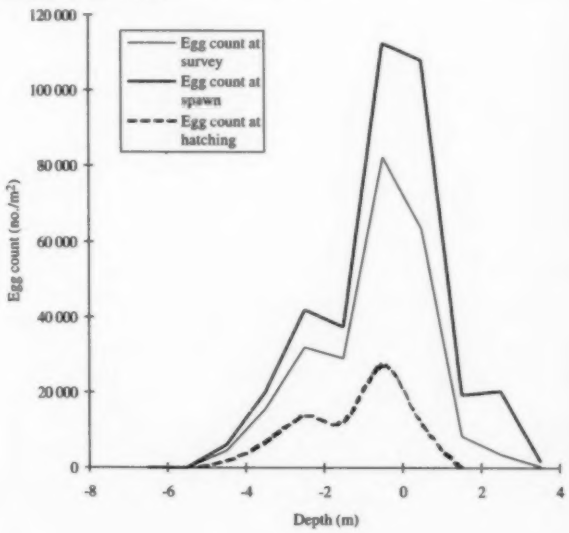

© 1999 NRC Canada

eggs are exposed to air may be important in regulating how susceptible the eggs are to mechanisms such as predation and wave action and may be used as a proxy for these processes. In other studies, bird exclusion experiments in the intertidal zone have resulted in estimates of egg loss due to birds of 96.7% (Cleaver and Franett 1946), 30–55% (Outram 1958), and 70% (Steinfeld 1971). These studies did not estimate intertidal egg loss due to other predators such as invertebrates or fishes. Together, these results indicate that the depth where eggs are spawned may be important to the retention of eggs in the spawning beds until hatching. Eggs spawned in the upper intertidal zone may have little or no chance of being retained in the spawning beds until hatching, while eggs spawned subtidally have a lower chance of being lost (around 70%). Egg mortality studies in Prince William Sound indicate that mortality may be high at both the shallowest and deepest depths where spawn is observed (E.D. Brown and E.M. Debevic, Institute of Marine Science, School of Fisheries and Ocean Sciences, University of Alaska–Fairbanks, Fairbanks, AK 99775-6100, U.S.A., personal communication). Some authors speculate that spawn in the upper range of the tidal zone may benefit from increased temperatures during incubation (Jones 1972). This would reduce the incubation period and increase survival to the larval stage. Therefore, spawning at intermediate depths would reduce egg losses due to predation but increase survival rates by reducing incubation times. The upper limit of egg deposition may thus be regulated by egg loss due to predation. The lower limit may be set by mortality related to factors other than egg loss, such as the length of incubation due to temperature, that are as yet unexplained.

Acknowledgments

We thank John Wilcock, Alaska Department of Fish and Game, for providing the data set used in egg loss models and Evelyn Brown, University of Alaska Fairbanks, for her support throughout the study. We thank MaryAnne Bishop and Patrick Green of the U.S. Forest Service Copper River Delta Institute for providing the data on avian predators. Dr. Loveday Conquest, Kevin Brink, Heather Caffoe, Michael Etnier, Nancy Gove, Nicolle Mode, Chris Shuck, and Marianne Turley provided a very helpful statistical review of our manuscript. Funds for this study were provided by the Exxon Valdez Trustee Council through the Alaska Department of Fish and Game, Herring Natal Habitats project No. 95166.

References

Bailey, K.M., and Houde, E.D. 1989. Predation on eggs and larvae of marine fishes and the recruitment problem. Adv. Mar. Biol. **25**: 1–83.

Biggs, E.D., and Funk, F. 1988. Pacific herring spawning ground surveys for Prince William Sound, 1988, with historic overview. Regional Inf. Rep. 2C88-07, Alaska Department of Fish and Game, Anchorage, Alaska.

Biggs-Brown, E.D., and Baker, T.T. 1993. Estimates of egg loss for Pacific herring in Prince William Sound, 1990–1991. NRDA Damage Assessment, Fish/Shellfish Study 11. Alaska Department of Fish and Game, Anchorage, Alaska.

Bradford, M.J. 1992. Precision of recruitment predictions from early life stages of marine fishes. Fish. Bull. U.S. **90**: 439–453.

Cleaver, F.C., and Franett, D.M. 1946. The predation by sea birds upon the eggs of the Pacific herring (*Clupea pallasi*) at Holmes Harbor during 1945. Wash. State Dep. Fish. Biol. Rep. 46B.

Cushing, D.H. 1971. The dependence of recruitment on parent stock in different groups of fishes. J. Cons. Cons Int. Explor. Mer, **33**: 340–362.

Cushing, D.H. 1975. Marine ecology and fisheries. Cambridge University Press, Cambridge, U.K.

Funk, F. 1994. Preliminary summary of 1994 Alaska herring roe fisheries. Regional Inf. Rep. 5J94-20, Alaska Department of Fish and Game, Juneau, Alaska.

Haegele, C.W. 1993. Seabird predation of Pacific herring, *Clupea pallasi*, spawn in British Columbia. Can. Field-Nat. **107**: 73–82.

Haegele, C.W., and Schweigert, J.F. 1989. Egg loss from Pacific herring spawns in Barkeley Sound in 1988. Can. MS Rep. Fish. Aquat. Sci. No. 2037.

Haegele, C.W., and Schweigert, J.F. 1991. Egg loss in herring spawns in Georgia Strait, British Columbia. Proceedings of the International Herring Symposium, Anchorage, Alaska, October 23–25, 1990. University of Alaska–Fairbanks, Fairbanks, Alaska.

Hart, J.L., and Tester, A.L. 1934. Quantitative studies on herring spawning. Trans. Am. Fish. Soc. **64**: 307–313.

Hay, D.E., and Kronlund, A.R. 1987. Factors affecting the distribution, abundance and measurement of Pacific herring (*Clupea harengus pallasi*) spawn. Can. J. Fish. Aquat. Sci. **44**: 1181–1194.

Hay, D.E., and Miller, C.C. 1982. A quantitative assessment of herring spawn lost by storm action in French Creek, 1980. Can. MS Rep. Fish. Aquat. Sci. No. 1636.

Hjort, J. 1914. Fluctuations in the great fisheries of Europe. Rapp. P.-v. Réun. Cons. Int. Explor. Mer, **20**:1–13.

Jones, B.C. 1972. Effect of intertidal exposure on survival and embryonic development of Pacific herring spawn. J. Fish. Res. Board Can. **29**: 1119–1124.

Lasker, R. 1975. Field criteria for survival of anchovy larvae: the relation between inshore chlorophyll maximum layers and successful first feeding. Fish. Bull. U.S. **73**: 453–462.

Outram, D.M. 1958. The magnitude of herring spawn losses due to bird predation on the west coast of Vancouver Island. Fish. Res. Board Can. Pac. Biol. Stn. Prog. Rep. No. 111. pp. 9–13.

Palsson, W.A. 1984. Egg mortality upon natural and artificial substrata within Washington State spawning grounds of Pacific herring (*Clupea harengus pallasi*). M.S. thesis, University of Washington, Seattle, Wash.

Pepin, P., and Myers, R.A. 1991. Significance of egg and larval size to recruitment variability of temperate marine fish. Can. J. Fish. Aquat. Sci. **48**: 1820–1828.

Peterman, R.M., Bradford, M.J., Lo, N.C.H., and Methot, R.D. 1988. Contribution of early life stages to interannual variability in recruitment of northern anchovy (*Engraulis mordax*). Can. J. Fish. Aquat. Sci. **45**: 8–16.

Rooper, C.N. 1996. Physical and biological factors affecting Pacific herring egg loss in Prince William Sound, Alaska. M.Sc. thesis, University of Alaska–Fairbanks, Fairbanks, Alaska.

Schnute, J. 1981. A versatile growth model with statistically stable parameters. Can. J. Fish. Aquat. Sci. **38**: 1128–1140.

Schweigert, J.F. 1995. Environmental effects on long-term population dynamics and recruitment to Pacific herring (*Clupea pallasi*) populations in southern British Columbia. *In* Climate change and northern fish populations. *Edited by* R.J. Beamish. Can. Spec. Publ. Fish. Aquat. Sci. No. 121. pp. 569–583.

Seber, G.A.F. 1982. The estimation of animal abundance and related parameters. Oxford University Press, New York.

© 1999 NRC Canada

Sinclair, M. 1988. Marine populations. Washington Sea Grant Program, Seattle, Wash.

Sissenwine, M.P. 1984. Why do fish populations vary? *In* Exploitation of marine communities. *Edited by* R. May. Springer-Verlag, Berlin. pp. 59–94.

Soutar, A., and Isaacs, J.D. 1974. Abundance of pelagic fish during the 19th and 20th centuries as recorded in anaerobic sediment of the Californias. Fish. Bull. U.S. **72**: 257–273.

Steinfeld, J.D. 1971. Distribution of Pacific herring spawn in Yaquina Bay, Oregon, and observations on mortality through hatching. M.Sc. thesis, Oregon State University, Corvallis, Oreg.

Wespestad, V.G. 1991. Pacific herring population dynamics, early life history, and recruitment variation relative to eastern Bering Sea oceanographic factors. Ph.D. dissertation, University of Washington, Seattle, Wash.

Zebdi, A., and Collie, J.S. 1995. Effect of climate on herring (*Clupea pallasi*) population dynamics in the Northeast Pacific Ocean. *In* Climate change and northern fish populations. *Edited by* R.J. Beamish. Can. Spec. Publ. Fish. Aquat. Sci. No. 121. pp. 277–290.

Zheng, J., Funk, F.C., Kruse, G.H., and Fagen, R. 1993. Evaluation of threshold management strategies for Pacific herring in Alaska. Proceedings of the International Symposium on Management Strategies for Exploited Fish Populations, Anchorage, Alaska, October 21–24, 1992. University of Alaska–Fairbanks, Fairbanks, Alaska.

Appendix

The percentage of eggs lost per day and its variance were estimated by incorporating information from both the egg loss model and the spawn deposition surveys. In spawn deposition surveys, density estimates (d_i) are obtained uniformly every 5 m. Variance estimates $SE^2(d_i)$ are obtained from diver calibrations. First the egg loss rate Z_i for each egg density estimate from spawn deposition surveys was predicted from eq. 2 with estimated variance

$$SE^2(Z_i) = s^2_{ylx}\left[1 + \frac{1}{n} + \frac{(AE_i - \overline{AE})^2}{\sum(AE_i - \overline{AE})^2}\right]$$

where s^2_{ylx} is the mean squared error from the egg loss rate regression, n is the regression sample size, AE_i is the amount of air exposure from the spawn deposition site, and $\overline{AE}$ is the mean hours of air exposure from the egg loss study sites. Then the estimated relative change in egg abundance per day (r_i) for each spawn deposition location was

$$r_i = 1 - e^{-Z_i}$$

with estimated variance from the delta method (Seber 1982) of

$$SE^2(r_i) = (1 - r_i)^2 SE^2(Z_i).$$

The mean egg loss percentage per day, $\bar{r}$, was then obtained as the average across spawn deposition sites weighted by density:

$$\bar{r} = \sum\left(\frac{d_i}{d}\right) r_i$$

with estimated variance from the delta method for the variance of a product of two variables

$$SE^2(\bar{r}) = \sum\left[\left(\frac{d_i}{d}\right)^2 SE^2(r_i) + r_i^2 SE^2\left(\frac{d_i}{d}\right)\right]$$

where d is equal to the total of all eggs counted and d and r are assumed to be independent and

$$SE^2\left(\frac{d_i}{d}\right) = \left(\frac{d_i}{d}\right)^2\left[CV^2(d_i) + CV^2(d) - 2\left(\frac{d_i}{d} CV^2(d_i)\right)\right]$$

obtained from the delta method for variance of a quotient of two variables, where CV is the coefficient of variation.

© 1999 NRC Canada

ASSIGNMENT OF COPYRIGHT

Ms. No. _____

To: NATIONAL RESEARCH COUNCIL OF CANADA ("NRC") Research Press

From: _____

_____

_____

_____

(name and address of author signing this form)

This refers to the manuscript entitled: _____

_____

written by myself and the following additional author(s): _____

_____

for publication in: _____

1. I declare that the list of authors fairly conforms to academic conventions about who should be listed. I declare that the manuscript, or its equivalent, has not been submitted for publication elsewhere. If it is accepted for publication by the National Research Council of Canada, I will ensure that it, or its equivalent, is not submitted for publication elsewhere.

2. I declare that I am (check ONE):

☐ (a) the sole owner of the copyright relating to the manuscript,	and →	I **assign** to NRC the entire copyright.
☐ (b) a part owner of the copyright, in conjunction with interests held by co-authors or their employers,	and →	I **assign** to NRC my entire interest in the copyright, and I expect the co-authors to also sign a form like this one.
☐ (c) an agent of my employer with authority to assign the copyright owned by the employer, who is: _____,	and →	I **assign** to NRC, on behalf of my employer, my employer's entire interest in the copyright relating to the manuscript, and I expect the co-authors to also sign a form like this one.
☐ (d) a public servant in Canada (federal, provincial or territorial) or the United Kingdom, so that the copyright is owned by Her Majesty,	and →	I have obtained the approval of my employer, according to the terms of my employment, to grant NRC **non-exclusive permission** to publish the manuscript and administer the copyright.
☐ (e) a public servant of the United States of America, and subject to the law that creates no U.S. copyright for the manuscript,	and →	I **assign** to NRC, on behalf of my employer, my employer's entire interest in any copyright that may exist outside the U.S., and I expect the co-authors to sign a form like this one.

3. I understand that my submission of this document does not guarantee publication, and that publication will not occur until **all authors** have provided a copyright transfer. If the manuscript is not published within 2 years after I sign this, the assignment is revoked.

Signed at _____ on _____

(City and Province/State) (Date)

_____

(Signature)

[Standard NRC form; alterations not acceptable.]

Comments on Copyright Transfer
(with extracts from the *Copyright Act*, Revised Statutes of Canada 1985, chapter C-42, as amended)

The publisher is not permitted to publish the manuscript without permission or an assignment of ownership of copyright. For greatest flexibility, and to be prepared to deal with future uses of the published material, the publisher requires ownership.

The owner may assign the right, but that assignment must be in writing:

13.(4) The owner of the copyright in any work may assign the right, either wholly or partially, and either generally or subject to territorial limitations, and either for the whole term of the copyright or for any other part thereof, and may grant any interest in the right by licence, but no assignment or grant is valid unless it is in writing signed by the owner of the right in respect of which the assignment or grant is made, or by his duly authorized agent.

The owner may be the author, but in many cases, the owner is the author's employer:

13.(3) Where the author of a work was in the employment of some other person under a contract of service or apprenticeship and the work was made in the course of his employment by that person, the person by whom the author was employed shall, in the absence of any agreement to the contrary, be the first owner of the copyright, but where the work is an article or other contribution to a newspaper, magazine or similar periodical, there shall, in the absence of any agreement to the contrary, be deemed to be reserved to the author a right to restrain the publication of the work, otherwise than as part of a newspaper, magazine or similar periodical.

The only exception to taking ownership arises when the manuscript is covered by Crown copyright owned by a Canadian government.

12. Without prejudice to any rights or privileges of the Crown, where any work is, or has been, prepared or published by or under the direction or control of Her Majesty or any government department, the copyright in the work shall, subject to any agreement with the author, belong to Her Majesty and in that case shall continue for the remainder of the calendar year of the first publication of the work and for a period of fifty years following the end of that calendar year.

Governments, and in particular the federal government, do not have a simple mechanism for assigning ownership of this particular type of Crown asset. Therefore, when an author is a public servant so that there is Crown copyright in the manuscript, a simple permission to use is acceptable to the publisher, if it is granted by a person with appropriate authority.

CESSION DU DROIT D'AUTEUR

Document n° _____

Au : CONSEIL NATIONAL DE RECHERCHES DU CANADA («CNRC») - Presses scientifiques

De : _____

_____

_____

_____

(nom et adresse de l'auteur qui signe le présent formulaire)

La présente cession porte sur le document intitulé : _____

_____

rédigé par moi, en collaboration avec l'auteur/les auteurs suivant(s) : _____

_____

aux fins de publication dans : _____

1. Je déclare que la liste des auteurs ci-dessus respecte les pratiques usuelles de rédaction savante quant aux personnes dont le nom doit être cité. Je déclare que le document ou son équivalent n'a pas été soumis à quelque autre organisme aux fins de publication. Si le CNRC accepte de publier le document, je m'assurerai que celui-ci ou son équivalent n'est soumis à aucun autre organisme aux fins de publication sans en obtenir la permission préalable du CNRC.

2. Je déclare être (UN SEUL choix) :

☐ (a)	le seul titulaire de droit d'auteur afférent au document,	et →	je **cède** le droit d'auteur intégral au CNRC.
☐ (b)	un titulaire partite du droit d'auteur, de concert avec des coauteurs ou leurs employeurs,	et →	je **cède** ma part du droit d'auteur au CNRC et m'attends à ce que les coauteurs signent une entente comparable.
☐ (c)	un agent de mon employeur ayant l'autorité de céder le droit d'auteur appartenant à l'employeur, nommément : _____,	et →	je **cède** au CNRC, au nom de mon employeur, la part entière du droit d'auteur afférent au document appartenant à mon employeur, et m'attends à ce que les coauteurs signent une entente comparable.
☐ (d)	un fonctionnaire du Canada (fédéral, provincial ou territorial) ou du Royaume-Uni, donc le droit d'auteur appartient à Sa Majesté,	et →	j'ai obtenu de mon employeur, en vertu de mes conditions d'emploi, l'autorisation d'accorder au CNRC la **permission non exclusive** de publier le document et de gérer le droit d'auteur.
☐ (e)	un fonctionnaire des États-Unis d'Amérique, donc sujet à la loi qui n'associe aucun droit d'auteur américain au document,	et →	je **cède** au CNRC, au nom de mon employeur, la part entière de quelque droit d'auteur en vigueur ailleurs qu'aux É.-U. appartenant à mon employeur, et m'attends à ce que les coauteurs signent une entente comparable.

3. Je comprends que la soumission du document ne garantit aucunement sa publication et que la publication ne pourra être réalisée tant que **tous les auteurs** n'auront pas signé une cession du droit d'auteur. Si le document n'est pas publié dans les deux années suivant ma signature des présentes, la cession sera automatiquement révoquée.

Signé à _____, le _____

(ville et province/état) (date)

_____

(signature)

[Formulaire normalisé du CNRC; aucune modification permise]

Commentaires sur la cession du droit d'auteur
(accompagnés d'extraits de la *Loi sur le droit d'auteur,* Lois révisées du Canada 1985, chapitre C-42 modifié)

L'éditeur ne peut publier un document sans la permission ou une cession du droit d'auteur. Pour des raisons de souplesse et en vue de l'utilisation future du document publié, l'éditeur doit devenir titulaire du droit d'auteur.

Le titulaire peut céder le droit, mais cette cession doit être faite par écrit :

13.(4) Le titulaire du droit d'auteur sur une oeuvre peut céder ce droit, en totalité ou en partie, d'une façon générale, ou avec des restrictions territoriales, pour la durée complète ou partielle de la protection; il peut également concéder, par une licence, un intérêt quelconque dans ce droit; mais la cession ou la concession n'est valable que si elle est rédigée par écrit et signée par le titulaire du droit qui en fait l'objet, ou par son agent dûment autorisé.

Le titulaire peut être l'auteur, mais dans plusieurs cas, le titulaire est l'employeur de l'auteur:

13.(3) Lorsque l'auteur est employé par une autre personne en vertu d'un contrat de louage de service ou d'apprentissage, et que l'oeuvre est exécutée dans l'exercice de cet emploi, l'employeur est, à moins de stipulation contraire, le premier titulaire du droit d'auteur; mais lorsque l'oeuvre est un article ou un autre contribution, à un journal, à une revue ou à un périodique du même genre, l'auteur, en l'absence de convention contraire, est réputé posséder le droit d'interdire la publication de cette oeuvre ailleurs que dans un journal, une revue ou un périodique semblable.

La seule exception dans la cession du droit d'auteur est lorsque le document est associé au droit d'auteur de la Couronne, qui appartient au gouvernement du Canada .

12. Sous réserve de tous les droits ou privilèges de la Couronne, le droit d'auteur sur les oeuvres préparées ou publiées par l'entremise, sous la direction ou la surveillance de Sa Majesté ou d'un ministère du gouvernement, appartient, sauf stipulation conclue avec l'auteur, à Sa Majesté et, dans ce cas, il subsiste jusqu'à la fin de la cinquantième année suivant celle de la première publication de l'oeuvre.

Les gouvernements, en particulier le gouvernement fédéral, ne disposent pas d'un mécanisme simple de cession de droit d'auteur pour ce genre de biens de la Couronne. C'est pourquoi lorsqu'un auteur est un fonctionnaire et que, par conséquent, le droit d'auteur appartient à la Couronne, une simple permission d'usage est suffisante pour l'éditeur, pour autant que celle-ci ait été octroyée par une personne jouissant de l'autorité nécessaire pour ce faire.

Perspectives on Canadian Marine Fisheries Management

L.S. Parsons and/et W.H. Lear
(*Editors/Directeurs scientifiques*)

446 pages
Hardcover/Édition reliée
November/Novembre1993
ISBN 0-660-15003-4
ISSN 0706-6503
NRC/CNRC 36176
$55.00/55,00 $

This volume, Canadian Bulletin of Fisheries and Aquatic Sciences 226, is a collection of 15 articles describing management approaches in different fisheries arising from the diversity and complexity of Canada's marine fisheries. Visit http://www.nrc.ca/cisti/journals/books/perspe_e.html at the NRC Research Press Web site to view the Table of Contents.

On décrit dans ce document, le Bulletin canadien des sciences halieutiques et aquatiques 226 (un recueil des 15 articles), des approches de gestion de diverses pêches axées sur la diversité et la complexité des pêches maritimes canadiennes. Visitez http://www.nrc.ca/cisti/journals/books/perspe_f.html au site Web des Press scientifiques du CNRC pour consulter la table des matières.

To order copies of this publication/Pour commander des exemplaires de ce livre

- Telephone: (613) 993-0151
- Fax: (613) 952-7656
- Mail orders: Monograph Orders, NRC Research Press, National Research Council Canada, Ottawa, Ontario K1A 0R6, Canada
- Internet e-mail: research.journals@nrc.ca
- World Wide Web: http://www.nrc.ca/cisti/journals/formmono.html

Canadian customers please add 7% GST. Orders from Quebec add a further 6.5% QST to the total price including GST. Make cheque or money order payable to "Receiver General for Canada, credit NRC". Note that for all orders outside Canada, rates are in U.S. Dollars. All sales are final.

- Téléphone : (613) 993-0151
- Télécopieur : (613) 952-7656
- Par la poste : Monographies, Presses scientifiques du CNRC, Conseil national de recherches Canada, Ottawa (Ontario) K1A 0R6, Canada
- Courrier électronique : research.journals@nrc.ca
- World Wide Web : http://www.nrc.ca/cisti/journals/formmofr.html

Les clients canadiens doivent ajouter la TPS de 7 %. Les clients du Québec doivent ajouter 6,5 % de TVQ au montant total, une fois la TPS additionnée. Libellez le chèque ou le mandat à l'ordre du «Receveur général du Canada, au crédit du CNRC». Pour les clients non canadiens, les prix sont en dollars américains. Aucun remboursement.

Please send me ____ copies of/Veuillez me faire parvenir ____ exemplaire(s) de *Perspectives on Canadian Marine Fisheries Management.*

NRC Research Press

Monograph Program

Presses scientifiques du CNRC

Programme de monographies

NRC·CNRC

PLEASE PRINT/LETTRES MOULÉES

☐ Payment enclosed/Paiement inclus ☐ Charge to/Imputer à ☐ Visa ☐ MasterCard

Account number/ N° de compte | | | | | | | | | | | | | | | | Expiry date/ Date d'expiration ____

Name/Nom

Signature/Signature

Address/Adresse

City/Ville Province/Province

Postal code/Code postal Country/Pays

Telephone/Téléphone Fax/Télécopieur

e-mail/Courrier électronique Date of order/Date de la commande

Guide to the Parasites of Fishes of Canada. Part IV. Trematoda

David I. Gibson

373 pages
Softcover/Édition brochée
March/mars 1996
ISBN 0-660-16403-5
ISSN 0706-6481
NRC/CNRC 40083
$42.95/42,95 $
Canadian Special Publication of Fisheries and Aquatic Sciences/ Publication spéciale canadienne des sciences halieutiques et aquatiques 124

More than 80 keys leading to the identification of more than 220 species of trematode parasites of Canadian fishes and diagnoses of more than 80 family–group taxa and 130 genera are given. Each genus is illustrated. For each species a Canadian host list, locality data, and any relevant remarks are included. Visit http://www.nrc.ca/cisti/journals/40083/133to136.html at the NRC Research Press Web to view a short chapter of this book.

On retrouve plus de 80 clefs qui permettent d'identifier quelque 220 espèces de trématodes parasites des poissons du Canada et la description de plus de 80 taxums de famille/groupe et de 130 genres. Chaque genre y est illustré. À chaque espèce sont associées des données sur l'emplacement et des remarques particulières. Visitez http://www.nrc.ca/cisti/journals/40083/f133to6.html au site Web des Presses scientifiques du CNRC pour afficher un court chapitre du livre.

To order copies of this publication/Pour commander des exemplaires de ce livre

- Telephone: (613) 993-0151
- Fax: (613) 952-7656
- Mail orders: Monograph Orders, NRC Research Press, National Research Council Canada, Ottawa, Ontario K1A 0R6, Canada
- Internet e-mail: research.journals@nrc.ca
- World Wide Web: http://www.nrc.ca/cisti/journals/formmono.html

Canadian customers please add 7% GST. Orders from Quebec add a further 6.5% QST to the total price including GST. Make cheque or money order payable to "Receiver General for Canada, credit NRC". Note that for all orders outside Canada, rates are in U.S. dollars. All sales are final.

- Téléphone : (613) 993-0151
- Télécopieur : (613) 952-7656
- Par la poste : Monographies, Presses scientifiques du CNRC, Conseil national de recherches Canada, Ottawa (Ontario) K1A 0R6, Canada
- Courrier électronique : research.journals@nrc.ca
- World Wide Web : http://www.nrc.ca/cisti/journals/formmofr.html

Les clients canadiens doivent ajouter la TPS de 7 %. Les clients du Québec doivent ajouter 6,5 % de TVQ au montant total, une fois la TPS additionnée. Libellez le chèque ou le mandat à l'ordre du «Receveur général du Canada, au crédit du CNRC». Pour les clients non canadiens, les prix sont en dollars américains. Aucun remboursement.

Please send me ____ copies of/Veuillez me faire parvenir ____ exemplaire(s) de *Guide to the Parasites of Fishes of Canada: Part IV. Trematoda.*

NRC Research Press

Monograph Program

Presses scientifiques du CNRC

Programme de monographies

NRC·CNRC

PLEASE PRINT/LETTRES MOULÉES

☐ Payment enclosed/Paiement inclus ☐ Charge to/Imputer à ☐ Visa ☐ MasterCard

Account no./ Nº de compte | | | | | | | | | | | | | | | | Expiry date/ Date d'expiration_____

Name/Nom

Signature/Signature

Address/Adresse

City/Ville Province/Province

Postal code/Code postal Country/Pays

Telephone/Téléphone Fax/Télécopieur

e-mail/Courrier électronique Date of order/Date de la commande

Howard A. Schaller, Charles E. Petrosky, and Olaf P. Langness	**1031–1045**	Contrasting patterns of productivity and survival rates for stream-type chinook salmon (*Oncorhynchus tshawytscha*) populations of the Snake and Columbia rivers
Brian J. Pyper, Randall M. Peterman, Michael F. Lapointe, and Carl J. Walters	**1046–1057**	Patterns of covariation in length and age at maturity of British Columbia and Alaska sockeye salmon (*Oncorhynchus nerka*) stocks
France Béland, Howard I. Browman, Carolina Alonso Rodriguez, and Jean-François St-Pierre	**1058–1067**	Effect of solar ultraviolet radiation (280–400 nm) on the eggs and larvae of Atlantic cod (*Gadus morhua*)
Eva Brännäs and Torleif Eriksson	**1068–1077**	Floating, switching, or nonswitching as different behaviours when Arctic char (*Salvelinus alpinus*) are visiting two feeding tanks
Renate Meyer and Russell B. Millar	**1078–1087**	BUGS in Bayesian stock assessments
Michel Comeau, Michel Starr, Gérard Y. Conan, Guy Robichaud, and Jean-Claude Therriault	**1088–1095**	Fecundity and duration of egg incubation for multiparous female snow crabs (*Chionoecetes opilio*) in the fjord of Bonne Bay, Newfoundland
Elizabeth Fulton, David Kault, Bruce Mapstone, and Marcus Sheaves	**1096–1108**	Spawning season influences on commercial catch rates: computer simulations and *Plectropomus leopardus*, a case in point
Roland I. Hall, Peter R. Leavitt, Aruna S. Dixit, Roberto Quinlan, and John P. Smol	**1109–1121**	Limnological succession in reservoirs: a paleolimnological comparison of two methods of reservoir formation
N. Aubin-Horth, J. Gingras, and D. Boisclair	**1122–1132**	Comparison of activity rates of 1+ yellow perch (*Perca flavescens*) from populations of contrasting growth rates using underwater video observations
Christopher N. Rooper, Lewis J. Haldorson, and Terrance J. Quinn, II	**1133–1142**	Habitat factors controlling Pacific herring (*Clupea pallasi*) egg loss in Prince William Sound, Alaska

National Research Council Canada
Ottawa, Canada K1A 0R6

Conseil national de recherches Canada
Ottawa, Canada K1A 0R6

Postage paid at Ottawa
Publications mail
Registration No. 1240579

Port payé à Ottawa
Poste-publication
Enregistrement n° 1240579

Canadian Journal of Fisheries and Aquatic Sciences

Volume 56, Number 6, June 1999

Journal canadien des sciences halieutiques et aquatiques

Volume 56, numéro 6, juin 1999

W.J. Fletcher and Neil R. Sumner	**907–914**	Spatial distribution of sardine (*Sardinops sagax*) eggs and larvae: an application of geostatistics and resampling to survey data
F. Richard Hauer, Geoffrey C. Poole, John T. Gangemi, and Colden V. Baxter	**915–924**	Large woody debris in bull trout (*Salvelinus confluentus*) spawning streams of logged and wilderness watersheds in northwest Montana
John R. Sibert, John Hampton, David A. Fournier, and Peter J. Bills	**925–938**	An advection–diffusion–reaction model for the estimation of fish movement parameters from tagging data, with application to skipjack tuna (*Katsuwonus pelamis*)
Brett B. Roper and Dennis L. Scarnecchia	**939–946**	Emigration of age-0 chinook salmon (*Oncorhynchus tshawytscha*) smolts from the upper South Umpqua River basin, Oregon, U.S.A.
D.T. Nolan, P. Reilly, and S.E. Wendelaar Bonga	**947–959**	Infection with low numbers of the sea louse *Lepeophtheirus salmonis* induces stress-related effects in postsmolt Atlantic salmon (*Salmo salar*)
Barry D. Smith	**960–972**	A probabilistic analysis of decision-making about trip duration by Strait of Georgia sport anglers
Masayuki Noto and Ichiro Yasuda	**973–983**	Population decline of the Japanese sardine, *Sardinops melanostictus*, in relation to sea surface temperature in the Kuroshio Extension
Laurent Dagorn and Pierre Fréon	**984–993**	Tropical tuna associated with floating objects: a simulation study of the meeting point hypothesis
J.P. Mallet, S. Charles, H. Persat, and P. Auger	**994–1000**	Growth modelling in accordance with daily water temperature in European grayling (*Thymallus thymallus* L.)
I. Ostrovsky and Y.Z. Yacobi	**1001–1010**	Organic matter and pigments in surface sediments: possible mechanisms of their horizontal distributions in a stratified lake
N.T. Johnston, M.D. Stamford, K.I. Ashley, and K. Tsumura	**1011–1025**	Responses of rainbow trout (*Oncorhynchus mykiss*) and their prey to inorganic fertilization of an oligotrophic montane lake
Prajneshu and R. Venugopalan	**1026–1030**	von Bertalanffy growth model in a random environment

Continued on inside back cover / Suite au verso

Canada

Printed in Canada by / Imprimé au Canada par
University of Toronto Press Inc.
Typesetting by / Typographie par
NRC Research Press / Presses scientifiques du CNRC

0706-652X(199906)56:6;1-P